Chemical Proteomic Methods to Investigate Cysteine Post-Translational Modifications

Julia A. Falco

A dissertation

submitted to the faculty of

the department of chemistry

in partial fulfillment

of the requirements for the degree of

Doctor of Philosophy

Boston College
Morrissey College of Arts and Sciences
Graduate School

January 2023

Chemical Proteomic Methods to Investigate Cysteine Post-Translational Modifications

Julia A. Falco

Advisor: Eranthie Weerapana, Ph.D.

Abstract

Functional cysteine residues within proteins often serve as active sites for nucleophilic or redox catalysis, ligands for metal binding, structural disulfides, and are susceptible to modifications. Post-translational modifications on functional cysteine residues play various roles in regulating proteins, altering activity, localization, or cellular signaling. Such modifications arise endogenously in response to reactive oxygen species or reactive nitrogen species, respectively termed protein oxidation or protein *S*-nitrosation. These modifications play a role in numerous biological processes, and have implications in neurodegenerative disorders and cancers. Using chemical proteomic methods developed in our lab, specifically isotopic Tandem Orthogonal Proteolysis - Activity Based Protein Profiling (isoTOP-ABPP), we identify functional cysteines within a proteome and characterize proteins that undergo redox post-translational modifications on cysteines. I have particularly focused on *S*-nitrosation mediated by the novel transnitrosation donor *S*-nitroso-coenzyme A (CoA-SNO), as well as the functional characterization of nitrosation on specific target proteins involved in various metabolic processes: phosphofructokinase (PFKP), ATP citrate synthase (ACLY), and ornithine aminotransferase (OAT). In addition, I have studied the redox regulation of the

human ribonuclease inhibitor protein (RI) to elucidate the mechanism of protein oxidation and inactivation. Lastly, I have used chemical proteomic tools to interrogate reactive cysteines in the apicomplexan parasite, *Toxoplasma Gondii,* for prioritization of targets for drug discovery.

TABLE OF CONTENTS

LIST OF TABLES

Table A2-2 Ranking cysteines by sensitivity to untreated control. 509 cysteine containing peptides from MCF7 cell lysate were reported with R values. R value is the average heavy:light ratio from two individual datasets.

Table A2-3 Ranking cysteines by sensitivity to GSNO. 1038 cysteine containing peptides from MCF7 cell lysate were reported with R values. R value is the average heavy:light ratio from two individual datasets.

Table A2-4 Ranking cysteines by sensitivity to PAPA NONOate. 985 cysteine containing peptides from MCF7 cell lysate were reported with R values. R value is the average heavy:light ratio from two individual datasets.

Table A2-5 Comparing cysteine sensitivity to CoA-SNO, GSNO, and PAPA NONOate. 429 cysteine containing peptides were identified in all 3 datasets with a corresponding *R* value. *R* value is the average heavy:light ratio from two individual datasets.

Table A3-1 Proteins identified with OAT immunoprecipitation. R values indicicate light:heavy ReDiMe ratios normalized to the reported OAT R value and averaged across two datasets. Considered peptides were required to have a SEM < 30%.

Table A5-1 Reactive cysteines in *T. gondii*. Displayed are average R values ±RSD for 1018 IA-alkyne labelled peptides averaged across 2 MS runs with RSD < 50%. (*) indicates probe-modified residue within the peptide sequence.

Table A5-2 Highly reactive cysteines identified in *T. gondii*. Shown are final R values for 102 peptides with R values < 3, representing 130 modified cysteines. Labeled cysteines are indicated by asterisks (*) within the grouped peptide sequence.

LIST OF FIGURES

Chapter 1

Chapter 2

Figure 2-1 Production of *S*-nitroso-coenzyme A (CoA-SNO) is achieved via reaction of equimolar coenzyme A (CoA) and sodium nitrate ($NaNO_2$) under acidic conditions.

Figure 2-2 Competitive cysteine-profiling strategy to quantify sensitivity to transnitrosation. MCF7 cell lysates are treated with transnitrosation donor (CoA-SNO) or the control buffer (0.5 M HCl), followed by cysteine alkylation with iodoacetamide-alkyne, copper catalyzed click chemistry (CuAAC) with a light (CoA-SNO treated) or heavy (control) Azo tag, combination of samples, streptavidin enrichment, trypsin digestion, sodium dithionite cleavage from beads, and subsequent LC/LC-MS/MS analysis to identify and quantify the IA-probe reactive cysteine residues in each sample. A loss in cysteine reactivity is reflected in an increasing heavy:light ratio (*R*), and is indicative of transnitrosation donor mediated *S*-nitrosation or other resulting cysteine modification**.**

Figure 2-3 Identifying cysteines sensitive to CoA-SNO mediated transnitrosation. **(A)** Heavy:light ratios (*R*) are shown for 789 cysteine residues identified in response to CoA-SNO treatment (n=2). **(B)** representative extracted ion chromatograms and isotopic envelopes (light = red; heavy = blue) are shown for three cysteine residues with low, moderate, and high sensitivity to CoA-SNO. Ratio values are averaged across the different charge states identified, but displayed chromatograms are for a single representative charge state.

Figure 2-4 Heavy:light ratios (*R*) are shown for 509 cysteine residues identified in an untreated vs untreated control sample (n=2).

Figure 2-5 Structures of NO donors and heavy:light ratios (*R*) shown for **(A)** 1038 cysteine residues identified in GSNO treated MS analysis (n=2). Inset displays 50 most sensitive cysteines to GSNO treatment **(B)** 985 cysteine residues identified in PAPA NONOate treated MS sample (n=2). Inset displays 50 most sensitive cysteines to PAPA NONOate treatment. Previously annotated sites of nitrosation shown in yellow.

Figure 2-6 Assessing target selectivity of CoA-SNO. **(A)** Heatmap comparing the sensitivity of 489 individual cysteine residues to each of the NO donors: CoA-SNO, GSNO, and PAPA NONOate. Darker blue indicates higher sensitivity to the corresponding NO donor. **(B)** Extracted ion chromatograms display cysteines with differential sensitivity to the various NO donors, with Cys 329 CTSD being highly sensitive to CoA-SNO, GSNO, and PAPA NONOate and Cys 845 ACLY being highly sensitive to CoA-SNO, but insensitive to GSNO or PAPA NONOate.

Figure 2-7 Overlap of cysteine containing proteins highly sensitive to CoA-SNO, GSNO, and PAPA NONOate. Out of the top 50 cysteine containing

Chapter 4

Figure 5-3 (A) Highly reactive cysteine-containing genes with functional annotations for three gene ontology categories; molecular function, biological process and subcellular localization. **(B)** Enrichment analysis of functional annotations in annotated genes containing highly electrophile-sensitive cysteines relative to the *T. gondii* genome. Fold change is plotted (purple bar) against statistical significance (black dot) determined from a two-tailed Fisher's exact test. Figure adapted from Benns *et al*.

LIST OF ABBREVIATIONS

Standard 3-letter and 1-letter codes are used for the 20 natural amino acids.

ABPP	activity-based protein profiling
ACLY	ATP citrate synthase
ADP	adenine diphosphate
AKR1A1	aldo-keto reductase 1 A1
AKT	protein kinase B
AMP	adenosine monophosphate
ATP	adenosine triphosphate
ARG	arginase
BCL2	B-cell lymphoma-2
BST	biotin switch technique
BTD	benzathione dioxide
CASP3	caspase-3
CAT	catalase
CBR1	carbonyl reductase 1
cDNA	complementary DNA
cGMP	cyclic guanosine monophosphate

CoA	coenzyme A
CoA-SNO	*S*-nitroso-coenzyme A
CORe	CRISPR-based oligo recombineering
CTSD	cathepsin D
CuAAC	copper-catalyzed azide-alkyne cycloaddition
Cyt *c*	cytochrome *c*
DAB	denaturing alkylation buffer
DMSO	dimethyl sulfoxide
DTT	dithiothreitol
DTPA	diethylenetriaminepentaacetic acid
EDTA	ethylenediaminetetraacetic acid
EGF	epidermal growth factor
EGFR	epidermal growth factor receptor
ER	endoplasmic reticulum
ESI	electrospray ionization
ETC	electron transport chain
F1,6P	fructose-1,6-phosphate
F6P	fructose-6-phosphate
FAD	flavin adenine dinucleotide
FBS	fetal bovine serum
FDR	false discovery rate
FMN	flavin mononucleotide
GAPDH	glyceraldehyde-3-phosphate dehydrogenase

Gpx	glutathione peroxidase
GSH	glutathione (reduced)
GO	gene ontology
GSA	glutamate-5-semialdehyde
GSNO	*S*-nitrosoglutathione
GSNOR	*S*-nitrosoglutathione reductase
GSSG	glutathione (oxidized)
HADH2	3-hydroxyacyl-CoA dehydrogenase type 2
HCD	high-energy collision dissociation
HEN	HEPES, EDTA, neocuproine buffer
HEPES	4-(2-hydroxyethyl)-1-piperazineethanesulfonic acid
IA	iodoacetamide
IAA	iodoacetamide alkyne
IC50	half maximal inhibitory concentration
ICAT	isotope coded-affinity tagging
IP	immunoprecipitation
isoTOP-ABPP	isotopic tandem orthogonal proteolysis – activity-based protein profiling
iTOCR	isotopic tagging of oxidized and reduced cysteines
iTRAQ	isobaric tags for relative and absolute quantitation
Keap1	kelch-like ECH-associated protein 1
LC-MS	liquid chromatography-mass spectrometry
LDE	lipid derived electrophile
LMW-SNO	low molecular weight *S*-nitrosothiol

MAHMA NONOate	methylamine hexamethylene methylamine diazenium diolate
MAPK	mitogen activated kinase
MeCN	acetonitrile
MMTS	methyl methanethiosulfonate
MOI	multiplicity of infection
MS	mass spectrometry
NADH	nicotinamide adenine dinucleotide (reduced)
NADPH	nicotinamide-adenine-dinucleotide phosphate
NEM	N-ethylmaleimide
NO	nitric oxide
NOS	nitric oxide synthase
NOX	nicotinamide-adenine-dinucleotide phosphate oxidase
OAT	ornithine aminotransferase
ODC1	ornithine decarboxylase 1
Orn	ornithine
OxICAT	oxidative isotope-coded affinity tagging
P5C	pyroline-5-carboxylate
PAPA NONOate	propylamine propylamine diazenium diolate
PBS	phosphate buffered saline
PD	proteome discoverer
PDB	protein databank
PDI	protein disulfide isomerase
PFK	phosphofructokinase

PFKP	phosphofructokinase, platelet type
PI3K	phosphoinositide 3-kinase
PKM2	pyruvate kinase M2
PLP	pyridoxal-5-phosphate
PPI	protein-protein interaction
Prx	peroxiredoxin
PSM	peptide spectral match
PTEN	phosphatase and tensin homologue
PTM	post-translational modification
ReDiMe	reductive dimethylation
RI	ribonuclease inhibitor
RNA	ribonucleic acid
RNase	ribonuclease
RNS	reactive nitrogen species
ROS	reactive oxygen species
SCX	strong cation exchange
SD	standard deviation
SDS	sodium dodecyl sulfate
SDS-PAGE	sodium dodecyl sulfate – polyacrylamide gel electrophoresis
sGC	soluble guanylate cyclase
SNO	*S*-nitrosothiol
SNO-DIGE	*S*-nitrosothiol difference gel electrophoresis
SNO-RAC	*S*-nitrosothiol resin assisted capture

SOD	superoxide dismutase
Srx	sulfiredoxin
TCA	trichloroacetic acid
TCEP	tris(2-carboxyethyl)phosphine
TEAB	triethylammonium bicarbonate
Tm	melting temperature
Trx	thioredoxin
TrxR	thioredoxin reductase
TXPTS	tris (4,6-dimethyl-3-sulfonatophenyl) phosphine trisodium salt hydrate
UniProt	universal protein resource
WT	wild type

ACKNOWLEDGEMENTS

First and foremost, I would first like to thank my advisor, Professor Eranthie Weerapana. I thank you for your unwavering mentorship, support, and advice. I will always admire the dedication you have to your work and your lab, and your innovative approach to scientific problems. The years I have spent working in your lab have transformed me into a better scientist, coworker, friend, and person. I would also like to thank my thesis committee members, Jia Niu and Abhishek Chatterjee, I truly appreciate your help and guidance over the years.

Thank you to all my collaborators. Especially Dr. Sarah Wynia-Smith and Dr. Brian Smith at Medical College of Wisconsin, who helped me put the pieces together of the CoA-SNO project. I am thankful for all of the insightful discussions and your expertise in *S*-nitrosation and the biotin-switch assays! I would also like to thank our collaborators Professor Bo Li, Professor Matthew A. Child, Professor Marc-Jan Gubbels, and Professor Ronald T. Raines and their lab members with whom I have had the pleasure to work on such diverse projects.

I am extremely thankful to the past and present members of the Weerapana lab who I have had the pleasure of working beside. Lisa, Kyle, Masahiro, Tyler, Jenny, Rebecca, Aaron, Emma, Dan, Eleni, Ben, Sarah C., Qianni, Angela, Sarah M., Avinash, and Madison – you all have been wonderful colleagues and friends over the years,

and I sincerely enjoyed my time working with you all. I am thankful for all of your guidance and helpful discussions. A special thanks to Tyler, Dan, and Jenny for training me when I started in the lab and for your constant mentorship and willingness to help. Sarah C., thank you for always being such a good friend, for showing up for me in hard times and for being there to laugh and sing/dance during the good times.

Thank you to the Boston College Chemistry Department staff: Dale, Lynne, Leah, Lori, Ian, Dumazo, Steve, Tim, and Bob. You all are wonderful people and the ongoing research at BC could not happen without you. I always enjoyed our conversations and appreciated your constant help.

Lastly, thank you to all my family and friends who have continuously supported me. To my parents, Debra and James, thank you for setting me up for a successful and happy life. Your love, support, and the sacrifices made for our family have meant the world to me. To my sisters, Natalie and Gina, and their families, thank you for being a constant source of joy and peace, and for reminding me what life is truly about. Thank you to my grandparents, uncle Doug, and the Bock family for being such an important part of my life. To my life partner, Peyton, I would not be here without you. Thank you for being by my side and doing life with me. I am thankful for your love every single day. Thank you for always listening, for pushing me and helping me grow, and for believing in me. Thank you for carrying me through some incredibly challenging moments, yet always helping me to see the beauty of this life.

1.0 INTRODUCTION TO CYSTEINE POST-TRANSLATIONAL MODIFICATIONS

1.1 PROPERTIES OF CYSTEINE

Cysteine is a highly conserved amino acid with numerous functional roles within a complex proteome. Functional cysteines serve as active sites for nucleophilic or redox catalysis, ligands for metal binding, structural disulfides, and sites of allosteric regulation[1]. These functionalities arise from the unique physiochemical properties of cysteine residues. The cysteine thiol group has a large atomic radius of sulfur (1.27 Å) and the low dissociation energy of the S-H bond 82 kcal/mol), making it more acidic and nucleophilic compared to the hydroxyl group on serine[2,3]. The pKa of a cysteine thiol is typically ~8.5, however the local protein environment can easily perturb a thiol side chain, with pKa values as low as 3.8 reported for members of the glutaredoxin family[2,4]. With the pKa of the cysteine thiol similar to physiological pH, the thiol is often deprotonated to the thiolate anion form, enhancing the reactivity of protein thiols.

Because of its unique and tunable properties, cysteine is susceptible to a variety of electrophilic and oxidative post-translational modifications (PTMs) that serve to regulate protein activity and localization in vivo[5]. These PTMs include oxidation, *S*-nitrosation, glutathionylation, prenylation, and palmitoylation, and michael adducts with lipid derived electrophiles (LDEs)[6–11] (Fig 1-1). Oxidative PTMs are dependent on physiologically relevant reactive oxygen species (ROS) and reactive nitrogen species (RNS). These oxidative modifications, in particular, oxidation and *S*-nitrosation, of regulatory cysteine residues provide the cell a key mechanism for sensing and transducing cellular signals.

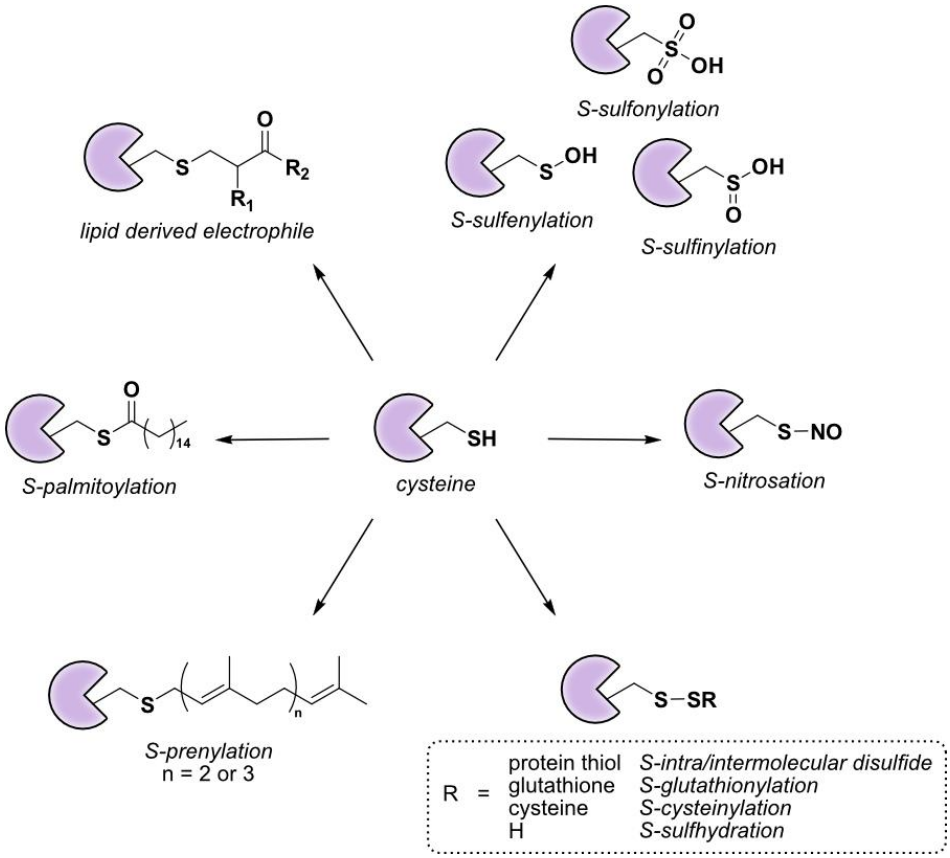

Figure 1-1 Common post-translational modifications of cysteine. Figure adapted from Couvertier *et al* (6).

1.2 CYSTEINE *S*-NITROSATION

S-nitrosation is a nitric oxide dependent, reversible, redox-based post-translational modification in which a cysteine thiol is converted to a nitrosothiol, regulating protein structure and function. This protein modification has been identified in all classes of proteins and is conserved across species including bacteria, plants, and mammals. To date, over 4,000 sites of *S*-nitrosation have been identified. *S*-nitrosation is a fundamental mechanism for cellular signaling that

accounts for a large part of NO bioactivity, important for biological processes in the nervous system, cardiovascular system, and immune system[12].

1.2.1 Terminology: *S*-nitrosation vs *S*-nitrosylation

In the literature, the terms "*S*-nitrosation" and "*S*-nitrosylation" are used somewhat interchangeably to refer to the post translational modification in which a cysteine thiol is converted to a nitrosothiol. As of 2022, the term "nitrosylation" appeared as a key term more than 24 times more often than "nitrosation" in a PubMed search[13]. Although, "nitrosylation" was coined to keep consistent with other biological post-translational modifications, such as phosphorylation (the transfer of a phosphoryl group), this terminology is chemically unfitting[14]. "Nitrosation" can be defined as the addition of a nitrosonium ion (NO^+) to a nucleophilic center (e.g. a thiol or amine) either directly or by transfer from an NO^+ donor (N_2O_3 or Fe^{II}-NO^+)[13]. Whereas, "nitrosylation" describes the coordination of the nitrosyl group, a NO radical, with a transition metal forming a nitrosyl species (X-NO, where X represents a metal center or radical species) via a direct reaction with NO[15]. Since the nitroso group (not the nitrosyl group) is transferred during this cysteine modification, the appropriate terminology is "nitrosation", which is what we will use from here on out.

1.2.2 Nitric oxide and *S*-nitrosothiol formation

There are three nitric oxide synthase isoforms in mammals responsible for the production of the reactive nitrogen species (RNS), nitric oxide ·NO: neuronal NOS (nNOS or NOS1), inducible NOS (iNOS or NOS2), and endothelial NOS (eNOS or NOS3). eNOS and nNOS are constitutively expressed, while activation occurs upon binding of calcium-calmodulin to produce lower levels of NO for paracrine signaling. iNOS is employed by the innate immune response where expression of this constitutively active isoform is induced by cytokines in order to produce cytotoxic levels of NO.

Each of these NOS isoforms utilize L-arginine and molecular oxygen (O_2) as substrates to produce one equivalent of nitric oxide (·NO) and L-citrulline and require the following cofactors: reduced nicotinamide-adenine-dinucleotide phosphate (NADPH), flavin adenine dinucleotide (FAD), flavin mononucleotide (FMN), and (6R-)5,6,7,8-tetrahydrobiopterin (BH_4), heme, and calmodulin[16]. Functional NOS exists as a homodimer, with monomers tethered by tetrahedral coordination of a zinc ion at two Cys-XXXX-Cys motifs, each contributed by a monomer[17]. Each NOS monomer is composed of two distinct domains: the carboxy-terminal reductase region and the amino-terminal oxygenase domain, connected by a calmodulin binding linker region[16,18]. In the reductase domain, electrons are transferred from NADPH via the flavins, FAD and FMN, to the BH_4 coupled heme, in the oxygenase domain. The ferric (Fe^{3+}) center of the heme is reduced to a ferrous (Fe^{2+}) center, which reacts with molecular oxygen, forming an Fe^{2+}-O_2 complex[17,19].

This BH_4 stabilized ferrous dioxygen complex subsequently oxidizes the guanidine moiety of the substrate L-arginine, bound in the oxygenase domain, producing L-citrulline and NO[16–20]. Interestingly, NOS enzymatic activity is controlled in part by NO levels, as *S*-nitrosation at the Zn^{2+} tetrathiolate cysteines of all three NOS isoforms occurs and results in dissociation of the iNOS active dimer to the inactive monomer[21–25].

The role of NO in signaling processes was first discovered when the molecule was identified as the endothelium-derived relaxing factor[26,27]. NO binds the heme center of soluble guanylate cyclase, leading to the production of cyclic guanosine monophosphate (cGMP) and the activation of cGMP dependent kinases, resulting in the transduction of numerous signaling events, most notably involved in smooth muscle relaxation[24]. It was originally thought that biological signaling by nitric oxide (NO) was primarily mediated by cGMP, however, further research suggests that the bulk of nitric oxide signaling actually occurs through a redox based protein post-translational modification on cysteines, termed *S*-nitrosation[8,28,29].

S-nitrosation is not just the addition of NO to a thiol, as NO itself is not an oxidant and does not strongly react with protein thiols[17]. Once nitric oxide is produced, a one electron oxidation is required to form a nitrosothiol, which can occur through at least three relevant pathways. These pathways include NO autooxidation to N_2O_3, radical recombination between NO and a thiyl radical, and transition metal catalyzed addition of NO to a thiol[14,30] (Fig 1-2).

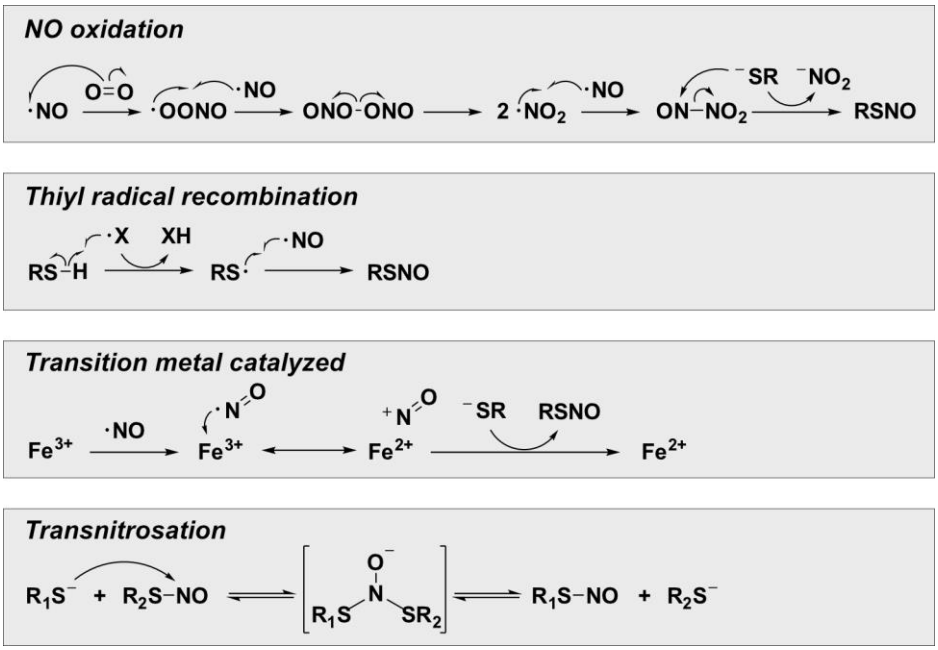

Figure 1-2 Pathways for *S*-nitrosothiol formation include (1) NO oxidation, (2) thiyl radical recombination, (3) transition metal catalyzed, and (4) transnitrosation. Figure adapted from Smith *et al*. (14)

In aerobic nitrosothiol formation, NO first reacts with oxygen to form a peroxynitrite radical (·ONOO), which can react with another equivalence of NO to form dinitrogen trioxide (N_2O_3). N_2O_3 can react with a small molecule or protein thiolate ($R\text{-}S^-$), to form an *S*-nitrosothiol (RSNO) and nitrite (NO_2^-). The reaction between N_2O_3 and glutathione occurs at a rate of 6.6×10^7 $M^{-1}S^{-1}$, to form *S*-nitrosoglutathione[31]. Because the rate is slower than diffusion and the second-order dependence on NO concentrations, it is likely N_2O_3 dependent nitrosothiol formation is favored in close proximity to the NOS isoforms[14].

In the thiyl radical recombination pathway, hydrogen abstraction by another radical (X·), results in the formation of the thiyl radical (R-S·). A nitrosothiol is subsequently produced upon radical recombination of NO and the thiyl radical. Thiyl radical recombination has a reaction rate of $1\text{-}3 \times 10^9$ $M^{-1}S^{-1}$ and is fast enough

to compete with NO binding to heme (>1.4 x 10^9 $M^{-1}S^{-1}$ for sGC)[32,33]. Since the formation of thiyl radicals can occur through NO-independent mechanisms, this reaction is first order in NO concentration and is likely favored at low O_2 concentrations[14].

There are several transition metal catalyzed pathways that are possible, which include the direct addition of NO to a thiol to form a thionitroxyl radical (RSNOH·) followed by a one electron oxidation to form a nitrosothiol. One example is the cytochrome *c* (Cyt *c*) mediated production of GSNO. Here, GSH weakly binds to the ferric Cyt *c*, and the bound GSH attacks NO, forming GSNOH·. The ferric heme then accepts an electron from the GSNOH radical to form ferrous heme and GSNO[34,35]. This reaction was found to be favorable at nanomolar NO concentrations and likely occurs during NO signaling. A similar mechanism involves NO binding to ferric heme, forming Fe^{3+}-NO. This species has significant Fe^{2+}-NO^+ character and can react with a thiol resulting in nitrosothiol formation and heme reduction[36].

Once formed, *S*-nitrosothiols can be transferred to a free thiol in a transnitrosation reaction. In this second-order S_N2 like reaction, the thiolate nucleophilically attacks the nitrogen of the *S*-nitrosothiol, forming a nitroxyl disulfide intermediate or transition state, and ultimately a new SNO[37–39]. Abundant thiol containing small molecules and proteins, such as glutathione (GSH), cysteine (Cys), and thioredoxin (Trx), are the primary mediators of transnitrosation, with *S*-nitrosoglutathione (GSNO), *S*-nitroso-cysteine (Cys-SNO), and *S*-nitroso-thioredoxin (Trx-SNO) as the corresponding *S*-nitrosated species[14,40]. Recently, a role for Coenzyme A (CoA) in *S*-nitrosation has emerged, with *S*-nitroso-coenzyme A (CoA-

SNO) adding to the list of small molecule mediators of transnitrosation[41]. It is thought that these low molecular weight *S*-nitrosothiols and protein *S*-nitrosothiols may act as "NO carriers", maintaining stability and prolong the half-life of NO for biological activity[38]. The transfer of NO between different thiols via transnitrosation is largely responsible for the activity of RSNO in vivo, and has been suggested to be a signaling mechanism for the control of cellular processes by NO.

There are many factors to consider that may impact protein transnitrosation targets and rates. Solvent accessibility and pKa of the attacking thiolate and the nitrosothiol are considered to play a role[42]. A low pKa on the attacking thiolate is thought to increase the transnitrosation rate, however there must be a delicate balance because a low pKa thiol provides a better nucleophile for initial transnitrosation but also a better leaving group for subsequent transnitrosation. Alternatively, these low pKa thiols may serve as intermediate sites of *S*-nitrosation, passing on it's NO to other target proteins in a signal transduction fashion. Other characteristics have emerged that render SNO site selectivity, such as the presence of acid/base or tyrosine groups ~8Å from the target cysteine, or a highly hydrophobic local environment[43–46]. Interestingly, these acidic and basic groups are oriented away from the nitrosated cysteine, having little effect on the pKa of that cysteine thiol. This trend suggests that these charged residues may help to confer transnitrosation selectivity via complementary charge interactions with the given transnitrosation donor[30]. Localization or compartmentalization at the site of NO generation could allow for selective *S*-nitrosation, either due to high local NO concentrations or via direct interaction and transnitrosation by NOS. For example, a

direct interaction with iNOS is required for *S*-nitrosation of cyclooxygenase-2 (COX2), enhancing COX2 catalytic activity[47]. A potential consensus sequence, [I/L]-XC-X2-[D/E], has been identified to direct site selective *S*-nitrosation for the iNOS/S100A8/S100A9 protein scaffolding transnitrosation complex[48], however there is no known sequence or structural motif associated with the majority of protein *S*-nitrosation targets.

1.2.3 Regulation of *S*-nitrosothiols

Just as SNO can be transferred, and ultimately removed from a transnitrosation donor, levels of SNOs are also controlled enzymatically by denitrosation enzymes. GSNO levels are regulated *in vivo* by two enzymes: GSNO reductase (GSNOR/ADH5) and carbonyl reductase 1 (CBR1)[49,50] (Fig 1-3A). GSNOR (aka alcohol dehydrogenase class III or glutathione-dependent formaldehyde dehydrogenase) and CBR1 degrade GSNO to glutathione sulfinamide (GSNHOH)[51]. GSNOR accounts for the majority of GSNO reductase activity under physiological conditions, with its k_{cat} value 5-fold greater than that of CBR1, despite GSNOR and CBR1 possessing similar K_M values for GSNO (~30μM)[51,52]. Since GSNOR is dependent on NADH, while CBR1 is dependent on NADPH, it is suggested that the NADH/NAD and NADPH/NADP+ ratios my influence the relative GSNO reduction rates[14]. This regulation of GSNO levels indirectly serves to regulate the level of protein-SNO, with GSNOR knockout mice displaying increased levels of both GSNO and *S*-nitrosated proteins[53]. Similar to the reduction of GSNO, CoA-SNO reduction in

humans has also been found to occur through the aldo-keto reductase 1A1 (AKR1A1). CoA-SNO is reduced in a NADPH dependent manner, resulting in CoA sulfinamide (CoASNHOH) formation[54], to indirectly regulate SNO-protein levels (Fig 1-3B).

The thioredoxin (Trx) system, comprised of Trx, Trx reductase (TrxR), and NADPH is a major protein disulfide reductase system that catalyzes denitrosation of protein-SNOs (RSNO) (Fig 1-3C). Trx denitrosates protein SNOs by forming a disulfide bond at the redox active cysteines (C32 and C35) in its active site, resulting in the production of a reduced protein thiol (RSH), nitroxyl (HNO) and oxidized Trx[52,55]. TrxR then works in an NADPH-dependent manner to re-reduce the oxidized Trx, completing the catalytic cycle. Trx1 has been shown to denitrosate over 100 protein substrates including eNOS, Casp3, and GAPDH[56–58]. It has been suggested that Trx1 denitrosation specificity may be determined by compartmentalization or protein-protein interactions[14,59,60]. Other proteins with denitrosation activity have been shown in vitro, including protein disulfide isomerase (PDI), xanthine dehydrogenase/oxidase (XDH), superoxide dismutase (SOD), and glutathione peroxidase (GPX), although their physiological relevance remains to be determined[53].

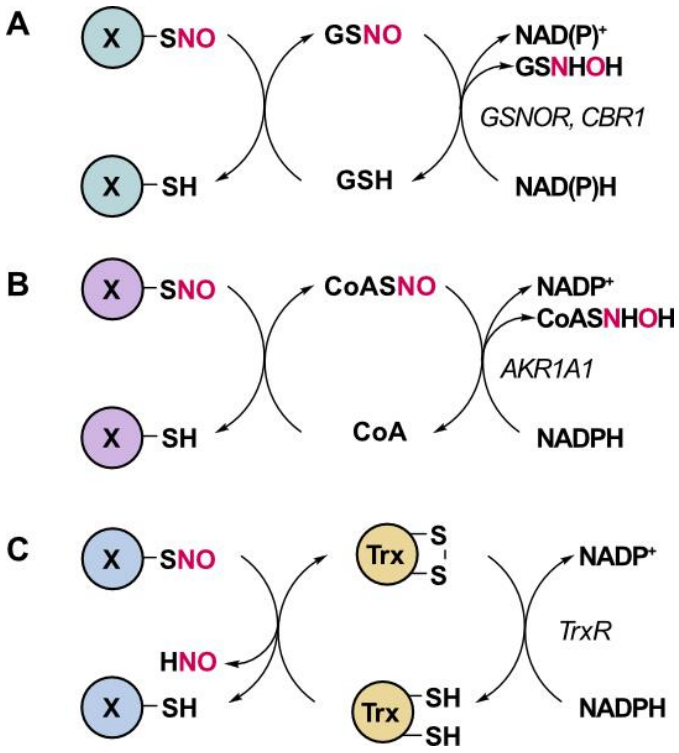

Figure 1-3 Regulation of *S*-nitrosothiols. **(A)** GSNOR and CBR1 catalyze the reduction of GSNO, **(B)** AKR1A1 catalyzes the reduction of CoA-SNO, and **(C)** The Trx/TrxR system catalyzes the reduction of numerous protein-SNOs.

1.2.4 *S*-nitrosation in health and disease

S-nitrosation is a key mechanism used by the cell to propagate NO signaling. This protein post-translational modification can exist as a transient modification, passing on the NO signal to other proteins via a transnitrosation reaction, or it can act as an end effector modification in which the formation of a protein-SNO modulates protein function. *S*-nitrosation has been shown to occur at functional cysteine residues modulating protein activity, protein-biomolecule interactions, protein structure, and protein localization[13].

Some well characterized *S*-nitrosation events that impart functional effects include *S*-nitrosation on caspase 3 (CASP3) and glyceraldehyde-3-phosphate dehydrogenase (GAPDH) [61]. CASP3 is constitutively *S*-nitrosated at its active site cysteine, inhibiting protease activity, and suppressing the apoptotic pathway[62]. On the other hand, stress or elevated levels of NO result in *S*-nitrosation of GAPDH at Cys152, initiating nuclear translocation and apoptotic cell death[63,64]. Importantly, dysregulation of *S*-nitrosation is implicated in a variety of diseases including asthma, cancer, neurodegeneration, and autoimmune disorders[30].

S-nitrosation is known to be elevated during early stages of neurodegeneration, preceding cognitive decline. One such example is *S*-nitrosation of the phosphatase and tensin homologue (PTEN), which is significantly increased in the brain during early Alzheimer's disease. PTEN regulates arguably the most important pro-survival pathway in neurons: the phosphoinositide 3-kinase (PI3K)/Akt signaling pathway. Increased *S*-nitrosation at Cys 83 of PTEN modulates enzymatic activity and protein degradation. Since the functionally relevant site of nitrosation is located within the phosphatase domain, PTEN's phosphatase activity is impaired, resulting in increased activation of Akt, promoting cell survival and neuroprotection. Additionally *S*-nitrosation also increases ubiquitination and ultimately protein degradation, although this process occurs over a longer timescale[65]. The redox active protein deglycase 1 (DJ-1) was found to mediate *S*-nitrosation of PTEN through a transnitrosation reaction, where Cys 106 on DJ-1 acts as the SNO donor[66]. This phenomenon was consistent with previous findings that Cys 106 was essential for DJ-1's neuroprotective activity and that loss of function

mutations in the DJ-1 gene are associated with early onset autosomal-recessive Parkinson's disease[67].

Abnormal *S*-nitrosation is also implicated in cancer development and progression, with NOS activity found in various tumors including brain, breast, lung, prostate, bladder, and pancreatic[68]. Furthermore, NOS activity has been associated with tumor grade, proliferation rate, and the expression of signaling components in cancer development[69]. NO can impart effects on tumor biology through various mechanisms and although these are not fully understood, there are some extensively studied *S*-nitrosation events that play a role in cancer related pathways including apoptosis, angiogenesis, cell cycle arrest, tissue invasion, metastasis, and chemoresistance.

The Src tyrosine kinase family of proteins are important in the regulation of growth and differentiation in eukaryotic cells. Specifically, c-Src is known to have a role in promoting cancer cell invasion and metastasis, with increased Src activity resulting in cells with increased growth rates, reduced adhesion, and increased metastatic potential[70]. *S*-nitrosation at cysteine 498 in the c-terminal domain of c-Src was shown to stimulate its kinase activity[71]. Additionally, β-estradiol in MCF7 breast cancer cells induces eNOS expression, resulting in increasing *S*-nitrosation and kinase activity of c-Src, and ultimately cancer cell progression[71]. NO-mediated c-Src activation was critical for the suppression of E-cadherin expression and disruption of cell-cell contacts after β-estradiol stimulation. Loss of E-cadherin not only disrupts cell-cell adhesion but also activates multiple transcriptional pathways to induce cell invasion.

Another example of *S*-nitrosation in cancer involves the B-cell lymphoma-2 protein (Bcl-2). Bcl-2 regulates apoptosis by forming heterodimers with pro-apoptotic proteins such as Bax, inhibiting cytochrome c release, and regulation of mitochondrial transmembrane potential. Overexpression of Bcl-2 occurs in many cancers, including ~70% of breast cancer, 30-60% of prostate cancer, and 90% of colorectal cancer, rendering malignant cells more resistant to apoptotic cell death[72]. *S*-nitrosation of Bcl-2 at Cys 158 and Cys 229 has been reported in human lung epithelial cancer cells, stabilizing the protein and preventing ubiquitination and subsequent proteasomal degradation[73]. Additionally, *S*-nitrosation protects Bcl-2 from degradation by the chemotherapeutic agent cis-diamminedichloroplatinum(II) (Cisplatin), conferring chemoresistance in these cancer cells[74]. A mutation of these cysteine *S*-nitrosation sites renders the protein more susceptible to apoptosis, conferring the therapeutic relevance of these cysteine nitrosation events. Impairment of Bcl-2 *S*-nitrosation has great therapeutic potential to attenuate cancer cells survival advantage and decrease Cisplatin resistance to improve outcomes with this form of chemotherapy.

1.3 CYSTEINE OXIDATION

Oxidative post translational modifications on cysteine discussed in this section are dependent on cellular reactive oxygen species (ROS). ROS give rise to multiple modifications including cysteine sulfenic acid, sulfinic acid, sulfonic acid,

disulfides, and persulfides. Oxidative stress is known to damage vital biomolecules and result in cell death, however lower levels of ROS play a critical role in cellular signaling and regulating protein function. Cysteine oxidative modifications occur on proteins from diverse functional classes and can affect protein activity, structure, localization, aggregation, and degradation, regulate key signaling pathways in pathophysiology[75].

1.3.1 ROS production and cysteine oxidative modifications

Reactive oxygen species (ROS) are produced endogenously as a byproduct of numerous cellular processes in all organisms which undergo respiration. The most prominent ROS species include the radical species superoxide ($O_2^{\cdot-}$) and hydroxyl radical (·OH)., and non-radical hydrogen peroxide (H_2O_2)[76]. $O_2^{\cdot-}$ is produced by a single electron reduction of molecular oxygen with reductants such as NADPH and $FADH_2$ acting as the electron donors. This species is found at relatively low concentration in cells, at picomolar levels[77]. H_2O_2 is poorly reactive in comparison to $O_2^{\cdot-}$, however it is highly lipophilic, and easily crosses cell membranes (~0.5 um diffusion distance), lending to inter-organelle and inter-cellular redox signaling. Direct production of H_2O_2 is mediated by dismutation of superoxide as well as xanthine and monoamine oxidases[78]. Due to its stability in aqueous environments, H_2O_2 is the most abundant ROS in eukaryotes with steady-state concentrations between 1-10 nM in cells[79]. Small perturbations in H_2O_2 levels are associated with cellular signaling and larger changes triggering stress response. ·OH is extremely

reactive, with the ability to react with almost every molecule in living cells including DNA, membrane lipids, and carbohydrates. It can be formed from $O_2^{\cdot-}$ and H_2O_2 in the presence of trace metals through the Fenton/Haber-Weiss reaction, and is found at femtomolar levels in cells[77].

Mitochondrial respiration accounts for the majority of ROS production in eukaryotes. During this process, components of the electron transport chain (ETC) reduce oxygen (O_2) to water during the synthesis of adenosine triphosphate (ATP)[80]. Partial reduction of O_2 to $O_2^{\cdot-}$ occurs when electrons passing through the ETC leak into the intermembrane region (Complex I) or the matrix of the mitochondria (Complex I and Complex III), with estimated levels of 10-200 pM of superoxide in the mitochondrial matrix. Superoxide generation in the mitochondria can also occur at α-ketoglutarate and pyruvate dehydrogenase complexes, where a reduced flavin molecule uses oxygen to produce superoxide[81].

The NADPH oxidase (NOX) is responsible for the enzyme catalyzed reduction of O_2 to $O_2^{\cdot-}$ at the plasma membrane. NOX transfers electrons across biological membranes with NADPH acting as the 2-electron donor[82]. Electrons are transferred through FAD and heme cofactors to generate two equivalents of $O_2^{\cdot-}$. H_2O_2 is produced from superoxide via dismutation. NOX is highly regulated and activation upon exposure to microorganisms and inflammatory stimuli requires the recruitment of various cytosolic regulatory elements, including NCF1, NCF2, and NCF4 in the case of the NOX2 transmembrane complex. Various NOX isoforms exist in different cell types and can localize to different biological membranes (ER,

nucleus, and mitochondria), for example NOX4 is known to localize to the nucleus in human vascular epithelial cells[83].

Following ROS production, protein cysteine thiols can be oxidized by one or two electron oxidation mechanisms, resulting in thiyl radical or sulfenic acid formation, respectively, as the initial oxidized product. ·OH generated by the Fenton reaction reacts at a diffusion-controlled rate with cysteine thiols to produce thiyl radicals. A thiyl radical can undergo radical recombination with another molecule of ·OH, resulting in sulfenic acid formation, or *S*-sulfenylation. In the case of the H_2O_2 thiol reaction, a free thiol nucleophilically attacks peroxide to form a sulfenic acid and water[84.] Displacement of the sulfenic acid by another cysteine can occur, to form an intra- or inter-molecular disulfide bond. When sulfenic acid is not readily reduced and ROS production persists in the environment, these thiols can undergo further oxidation to sulfinic acid, *S*-sulfinylation, or sulfonic acid, *S*-sulfonylation (Fig 1-4)[85]. These further oxidation steps are much slower than that of sulfenic acid or disulfide bond formation.

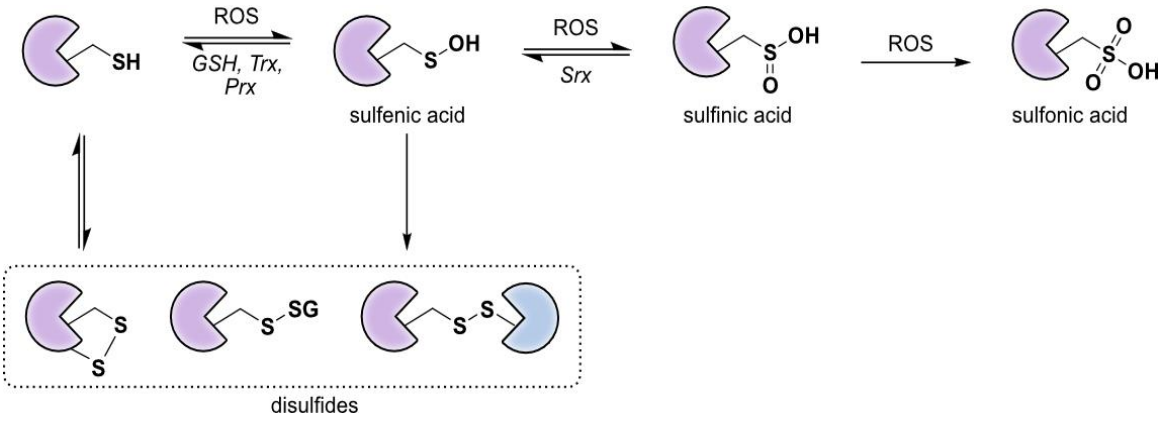

Figure 1-4 Reversible and irreversible cysteine oxidative post-translational modifications. Figure adapted from Abo *et al.* (85)

Predicting sites of cysteine oxidation can be very difficult since ROS are so reactive, and there are multiple species that can directly react with cysteine residues. However, there are a few criteria that may render a particular protein thiol more sensitive to oxidation[76]. These criteria include increased cysteine reactivity, which is often dictated by the microenvironment, which effects the pKa of the thiol as was discussed in section 1.2.1. In addition, proximity of ROS and target protein, where a protein closer to the site of ROS generation is more likely to be modified due to the short half-lives and high reactivity of these species. Oxidation prone cysteines were also found in regions containing a flanking positive or negative charge, similar to selectivity observed for *S*-nitrosation in section 1.2.1.

1.3.2 Regulation of ROS and cysteine oxidation

ROS are regulated by small molecule or protein antioxidants. Superoxide can rapidly dismutate to H_2O_2 and oxygen either spontaneously or enzymatically. The spontaneous dismutation of $O_2^{\cdot-}$ has a rate constant of $\sim 10^5$ $M^{-1}S^{-1}$ at neutral pH in aqueous solution. However, the superoxide dismutase (SOD) family of enzymes significantly increase the rate of dismutation, $\sim 10^9$ $M^{-1}S^{-1}$ [85]. SODs are highly abundant and isoforms exist in the mitochondrial matrix and intermembrane space, the cytosol, and extracellular matrix to maintain low levels of superoxide.

Catalase enzymes (CAT) have the ability to remove H_2O_2 and produce oxygen and two molecules of water. Peroxidases can also reduce H_2O_2 to two molecules of water using reductants such as glutathione, ascorbate, and thioredoxin[6]. The

peroxidases, glutathione peroxidase (Gpx) and peroxiredoxin (Prx) are widely distributed throughout the cell, while catalase enzymes are primarily found at the peroxisome. Furthermore, peroxiredoxins are much more abundant than Gpx, accounting for up to 0.8% of total soluble protein, highlighting the role of the Prx family in regulating H_2O_2 levels and ultimately redox signaling[47].

Cysteine oxidation to sulfenic acid or a disulfide is readily reversible under cytosolic conditions by small molecule antioxidants, glutathione (GSH), and redox buffering enzymes, Trx and Prx[87]. The target thiol is reduced through the transfer of the redox signal or a disulfide exchange resulting in oxidized Trx, or Prx. Oxidized Prx is reduced by Trx, and subsequent Trx reduction is mediated by thioredoxin reductase (TrxR) and NADPH. Reversibility of sulfinic acid is very context dependent as there are only a few enzymes that can achieve this reduction. The sulfiredoxin (Srx) family of enzymes reduces *S*-sulfinylation on some proteins to a reversible oxidation state by consuming ATP[88]. Cysteine sulfonylation is an irreversible modification with no known cellular reduction mechanisms. The permanence of this modification makes the effects more apparent, with sulfonic acid modifications often resulting in protein damage and degradation.

1.3.3 Cysteine oxidation in health and disease

Redox switches exist endogenously to sense and respond to elevated ROS levels in the cell. Keap1 (Kelch-like ECH-associated protein 1), a negative regulator of the transcription factor Nrf2 (nuclear factor E2-related factor 2), uses cysteine

oxidation to sense increased ROS, as the master regulator of antioxidant defense. Human Keap1 contains 27 cysteines many of which are evolutionary conserved and reactive, as they have low pKa values. Upon increased ROS, oxidation or alkylation of specific thiol residues (C151, 273, 288 and likely others) on Keap1 result in conformational changes, allowing detachment of Nrf2, escape from proteasomal degradation, and Nrf2 translocation to the nucleus, where binding to the antioxidant response element induces transcription of antioxidant enzymes[89]. Modulation of this signaling pathway is relevant to numerous therapeutic areas such as cancer, autoimmune, respiratory, endocrine, and cardiovascular diseases, with numerous clinical studies using Keap1 alkylating agents as therapeutics[90].

ROS act as signaling molecules to propagate physiological and oncogenic growth signals. For example, increasing levels of H_2O_2 correlates with cellular proliferation mediated by epidermal growth factor receptor (EGFR)[91]. Upon stimulation with the epidermal growth factor (EGF), EGFR dimerizes and is auto phosphorylated on the cytoplasmic domain, providing a scaffold for downstream kinases. Subsequent pathways including Ras/ mitogen activated kinase (MAPK) and phosphoinositide 3-kinase (PI3K) / protein kinase B (AKT) are activated which promote cellular proliferation, migration, and survival. EGFR activation also triggers the assembly of the Nox complex, whereby resulting H_2O_2 inactivates protein tyrosine phosphatases, such as PTP1B and PTEN through direct oxidation and disulfide formation at their active site cysteine residues, amplifying growth factor signaling[92–94]. EGFR is commonly upregulated or mutated in cancers including

human lung and breast cancers, making this pathway an attractive target for the development of therapeutics[91].

1.4 CHEMICAL PROTEOMIC METHODS TO INTERROGATE CYSTEINE *S*-NITROSATION AND OXIDATION

Determining the site and type of oxidative modification of cysteine is required for understanding the biological role. With this information, we can better understand the signaling mechanisms, the role in regulatory processes in cells, and how these pathways may be associated with diseases linked to oxidative stress. The similarities between several cysteine oxidation states, the low abundance, and short lifetime of these modifications provide challenges in studying cysteine oxidative modifications. Therefore, we need tools that provide high selectivity and accuracy, a means of enrichment, and quantitative analysis at the proteomic level. Here, we discuss both direct and indirect profiling of cysteine oxidative PTMs.

1.4.1 Direct chemical targeting of cysteine oxidative PTMs

Direct detection of specific cysteine PTMs provide advantages by minimizing the generation of false-positives and better reflecting endogenously relevant oxidative PTMs. However, the low abundance and labile property of endogenous cysteine PTM adducts have challenged the direct detection and enrichment of these modified species.

1.4.1.1 Chemical probes targeting *S*-nitrosothiols

Triarylphosphine probes have been successful in the direct detection of *S*-nitrosothiols (Fig 1-5). In a reaction analogous to the Staudinger ligation, triarylphosphines react with *S*-nitrosothiols to form thiol-aza-ylides. A series of phosphine probes resulted in the generation of phosphine esters that undergo rearrangement of the aza-ylide intermediate to form a more stable sulfenamide[95]. Further development of phosphine ester and thioester derivatives afforded a 'traceless' SNO ligation, that upon reaction with RSNO result in formation of a bis-ligation disulfide product where the S-N bond is maintained, and the lack of a bulky phosphine adduct is more suitable for downstream applications[96]. An alkyne version of the traceless disulfide probe, o-phosphino-benzoyl alkyne (PBZyn), has been used to click on various fluorophores or biotin for detection or enrichment purposes[97]. A major limitation of the phosphine probes is poor water solubility and biocompatibility. To this end, the water soluble, tris (4,6-dimethyl-3-sulfonatophenyl) phosphine trisodium salt hydrate (TXPTS) was developed to modify nitrosothiols forming an aza-ylide. TXPTS was shown to react with *S*-nitrosated alkyl hydroperoxide reductase C (Ahp-C SNO) and the resulting adduct *S*-alkylphosphonium was detectable by ESI-TOF MS[98]. Furthermore, derivatization of triphenylphosphines with sulfonate esters and tertiary amines improved aqueous compatibility, providing the first successful application of phosphine probes for detection of nitrosothiols within a biological sample, although only low molecular weight thiols were analyzed[99]. Despite these numerous advances, phosphine-based probes have yet to be applied within a complex proteome to identify *S*-nitrosothiols.

In addition to phosphine based probes, Doulias et al found that organomercury probes can be used to label and enrich *S*-nitrosothiols[42]. SNO reacts with phenylmercury forming a thiol-mercury conjugate. Phenylmercury that is coupled to either agarose (organomercury-conjugated resin, MRC) or biotin (phenylmercury-polyethyleneglycol-biotin, mPEGb), allows for the enrichment of *S*-nitrosation protein targets. This selective organomercury-conjugated resin has been applied for site specific proteomic analysis according to the following steps (1) free cysteine thiols are blocked with cysteine reactive electrophile, (2) *S*-nitrosated proteins are selectively captured and enriched on MRC resin or with mPEGb, (3) SNO proteins are released using performic acid or β-mercaptoethanol, which oxidizes newly reduced cysteines to sulfonic acids (+48 Da), a modification which can be detected by MS. This method allows for enrichment of SNO proteins and identification of the modified cysteine residue, with over 300 SNO peptides identified from 192 proteins in mouse liver in the pioneering study, and >1000 SNO sites from 647 proteins across mouse liver, heart, kidney, and lung[42,100]. A combination of the BST and MRC methods have been combined, where sequentially performance of these methods allowed for the identification of 113 novel SNO cysteine sites[101].

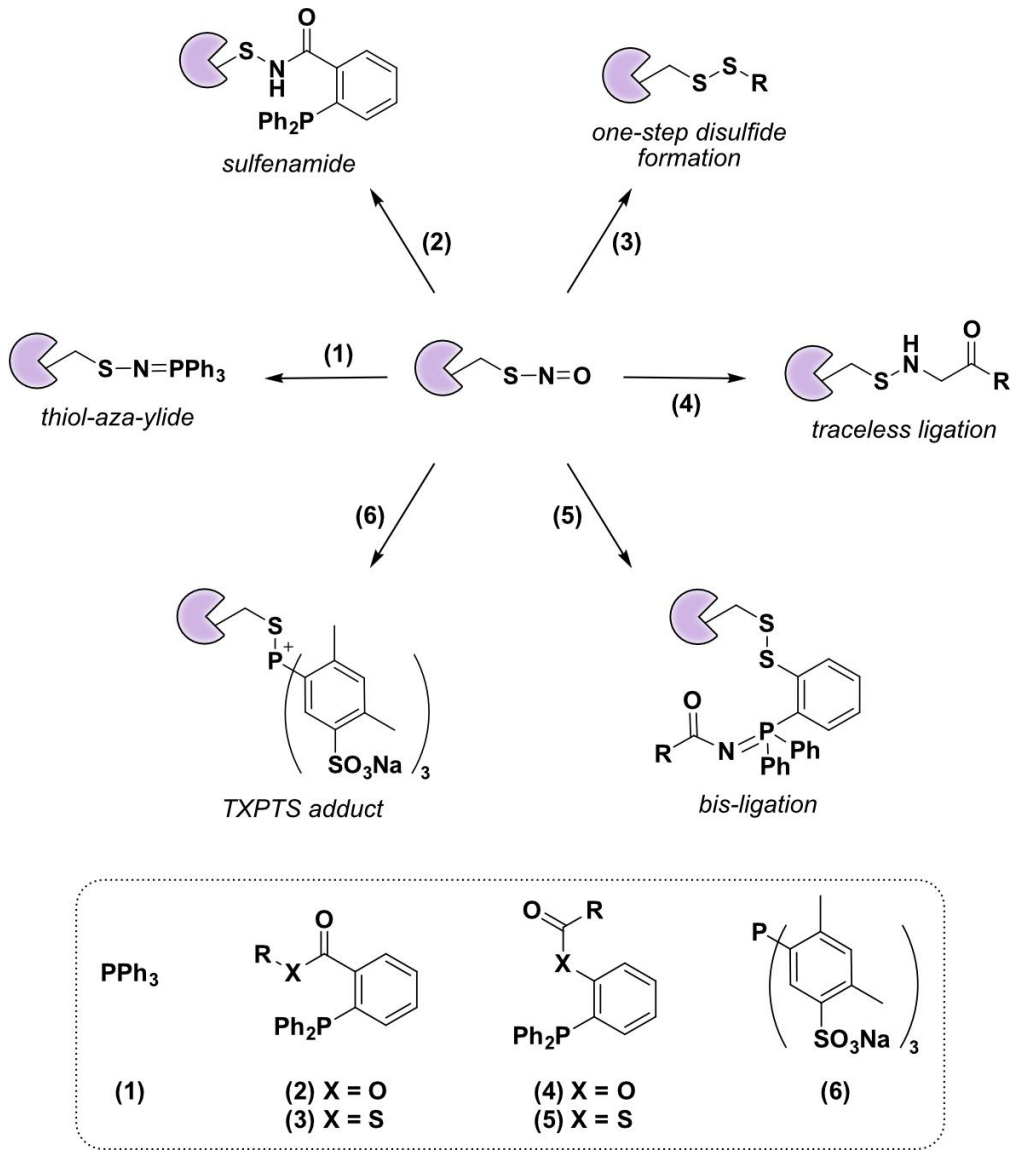

Figure 1-5 Direct chemical tagging of *S*-nitrosothiols by phosphine derivatives to form (1) thio-aza-ylides, (2) sulfenamides, (3) traceless disulfides, (4) traceless sulfenamides, (5) bis-ligation products, and (6) TXPTS adducts. Figure adapted from Couvertier *et al*. (5)

1.4.1.2 Chemical probes targeting sulfenic and sulfinic acids

To selectively profile sites of sulfenylation, dimedone based probes have been used, where the enolate form of dimedone nucleophilically attacks the sulfur of SOH, forming a covalent adduct (Fig 1-6A). Azide functionalized dimedone probes have been used to assess sulfenylation in live cells and for proteomic application, identifying 175 candidate sites of sulfenylation[102]. Quantifying the extent of sulfenic acid modification on a peptide has been achieved using a D_6-dimedone and 2-iodo dimedone probe, which selectively labels free cysteine thiol. Another method, termed isotopic tagging of oxidized and reduced cysteines (iTOCR), utilizes benzathione dioxide (BTD) and iodo-BTD probes to quantify relative levels of cysteine sulfenic acids, reversible cysteine oxidative modification, and free thiols, identifying ~600 sites of sulfenylation (Fig 1-6B)[75]. Sulfenylation in the mitochondria has been assessed using triphenylphosphonium ylide probes with enrichment handles to quantify the percent of ~2000 sites in the mitochondria[103].

Probes specific to sulfinic acid modifications have also been developed to identify protein targets that undergo *S*-sulfinylation. Similar to the mechanism by which Srx reduce sulfinic acids, 2-nitroso benzoic acid derivates (NO-Bio) undergo a chemoselective ligation with sulfinic acids (Fig 1-6C), however sites of sulfinylation are difficult to detect by MS due to complex fragmentation patterns[104]. Clickable diazene probes (DiaAlk) (Fig 1-6D) were found to circumvent this limitation, identifying ~55 protein substrates of the sulfinic acid reductase, Srx, and the site and extent of the sulfenic acid modification[99].

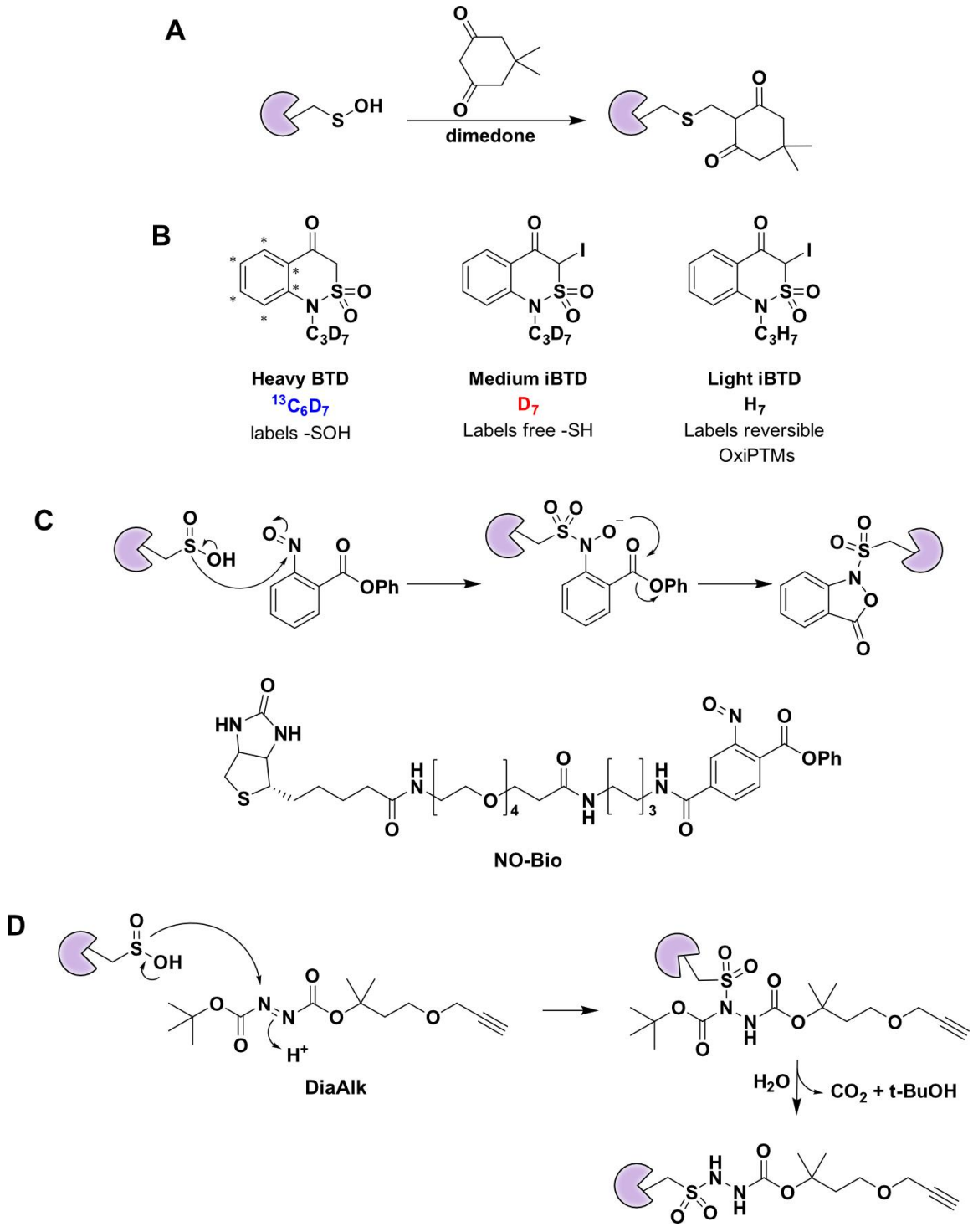

Figure 1-6 Direct chemical tagging of *S*-sulfenylation and *S*-sulfinylation. (**A**) Dimedone reaction with sulfenic acids. (**B**) Structures of benzothiazine dioxide (BTD) and iodo BTD (iBTD) probes for iTOCR. (**C**) Diazine probe (DiaAlk) reaction with sulfinic acid (**D**) Reaction of 2-nitroso benzoic acid probes with sulfinic acid and structure of NO-Bio. Figure adapted from Abo *et al*. (85).

1.4.2 Indirect profiling of cysteine oxidation

Quantitative proteomic methods to indirectly profile cysteine oxidation allow for site specific and quantitative analysis of cysteine PTMs. These methods have improved biocompatibility and mass-spec compatibility compared to the direct chemical targeting approaches. However, loss of probe labeling at the site of oxidation or a reduction of the modification is necessary, which can make it challenging to differentiate between specific modification, such as sulfenic acids, sulfinic acids, disulfides, or *S*-nitrosation. Validation should be performed when using these proteomic data for further research pursuits.

1.4.2.1 Switch technique

Reversibly oxidized cysteine modifications can be indirectly detected via a "switch" type method, requiring thiol blocking, reduction of the oxidized species, followed by labeling of nascent thiols. The original switch method, the biotin switch technique (BST), was reported by Jaffrey et al. in 2001 and has been the most widely used method to identify *S*-nitrosated proteins within a proteome. It has since been used to identify *S*-nitrosation events in a range of biological sample types including cultured cells, tissues, organelles, and plasma[105,106]. The original method followed 3 steps (1) blocking of free thiols with a thiol specific alkylating reagent (methyl methanethiosulfonate (MMTS)); (2) selective reduction of *S*-nitrosothiols with ascorbate; (3) labeling of newly reduced cysteines with a biotinylated thiol reactive agent (N- N-[6-(biotinamido)hexyl]-3'-(2'-pyridyldithio)propionamide (biotin-

HPDP)) for gel-based or mass spec-based detection (Figure 1-4). Challenges have arisen due to the indirect nature of this method. Incomplete blocking of free thiols will result in lower specificity and sensitivity. Furthermore, the selectivity and kinetics of ascorbate dependent SNO reduction has been brought into question.

Improvements to the BST have been made to address some of these drawbacks. During thiol blocking, alkylating reagents such as N-ethylmaleimide (NEM) and iodoacetamide (IA) have become more routinely used as covalent modification of cysteine results in a more stable thioether bond as opposed to the disulfide bond with MMTS. In order to increase the rate and specificity of the ascorbate reduction step, the addition of copper ions and the absence of metal chelators has provided fruitful[107]. However, there are still concerns that ascorbate can reduce other thiol modified species. In particular, ascorbate has been shown to reduce glutathione disulfide, cystine disulfide, cystinylglycine disulfide, and protein mixed disulfides[108]. Some of these limitations are circumvented by including additional positive and negative controls, such as comparing samples with and without ascorbate reduction, as well as comparing ascorbate with DTT reduction to differentiate between disulfides and *S*-nitrosothiols. Alternative reductants, including triphenylphosphine ester derivatives as well as methylhydrazine have displayed selective reduction of *S*-nitrosothiols in complex biological samples, and are unreactive with disulfides and other H_2O_2 dependent oxidized cysteine species[109,110].

Other modifications of the BST platform include SNO-RAC (SNO resin assisted capture), which utilizes a thiol reactive resin and to enrich for *S*-nitrosated

proteins following ascorbate reduction[111], as well as SNO-DIGE (fluorescence difference gel electrophoresis), where reduced SNO-proteins are labeled with fluorescent thiol reactive tags and identified by 2D-gel electrophoresis[112]. The BST has also provided inspiration for the selective profiling of *S*-sulfenylation events in cardiac tissue. In this method, arsenite is used to selectively reduce sulfenic acid modifications, followed by subsequent labeling with biotin maleimide probe for enrichment or detection[113]. The use of DTT or TCEP as a reductant can be used in a more non-specific approach to identify sites of reversible cysteine modifications, including disulfides, sulfenylation, and nitrosation.

1.4.2.2 Quantitative proteomic methods

The oxidative isotope-coded affinity tags (OxICAT) method is based on the traditional isotope-coded affinity tagging (ICAT) method to quantitatively monitor cysteine oxidation within a single sample[114]. The probes contain a cysteine reactive group (iodoacetamide, IA), a biotin enrichment handle, and a linker with 8 hydrogen or deuterium atoms, allowing for differentiation between heavy and light labeled species by mass-spectrometry (MS). These isotopically differentiated probes are used to sequentially label a sample with the following steps: (1) labeling of reactive cysteines with ICAT light probe, (2) reduction of oxidative modifications with DTT or TCEP, (3) labeling of nascent thiols with ICAT heavy probe. Labeled proteins are enriched, trypsin digested, recovered, and analyzed by LC-MS/MS. This method has been adapted for various applications including the identification of redox regulated

proteins in *E. coli* as well as interrogating cysteine oxidation in the endoplasmic reticulum[114,115].

Recently Chouchani et al, developed an OxICAT method specific to *S*-nitrosothiols, termed SNOxICAT[116]. Using ascorbate as a *S*-nitrosothiol specific reductant, they identified and quantified the extent of *S*-nitrosation on more than 1400 cysteines in response to NO^{2-} treatment in mouse cardiomyocytes. The levels of *S*-nitrosation were significantly enhanced under ischemic conditions, and many of these cysteines were found on proteins localized to the mitochondria, especially within the OXPHOS pathway.

Isotopic tandem orthogonal proteolysis – activity-based protein profiling (isoTOP-ABPP) developed by Cravatt et al. combines activity-based protein probes with quantitative mass spectrometry within complex biological systems. This method allows for direct comparison of cysteine reactivity or site occupancy across two separate samples. Chemical probes are needed with various functionalities including (1) a reactive warhead for covalently labeling target proteins, (2) a reporter tag for affinity purification or fluorescent detection, and (3) an isotopically tagged cleavable linker to minimize steric hindrance and enable the relative quantitation of probe labeling between two samples. Warheads can target specific enzyme families, such as serine hydrolases, or can be more promiscuous, reacting with a particular amino acid, such as an iodoacetamide-alkyne (IAA) probe for reactive cysteines. The use of this probe enables selective enrichment, release, and relative quantification of labeled peptides by MS. This method has been used to

predict functionally relevant cysteines within a proteome by ranking cysteine reactivity[117].

Recent work in our lab was done to develop an isoTOP-ABPP derived mass spectrometry proteomic platform using cysteine labeling to concurrently and quantitatively monitor the sensitivity to GSNO mediated transnitrosation of hundreds of cysteines within the human proteome. This platform harnesses the loss in cysteine reactivity upon nitrosation, and was used to uncover and characterize functionally relevant sites of *S*-nitrosation on Cathepsin D (CTSD) and 3-hydroxyacyl-CoA dehydrogenase type 2 (HADH2)[118].

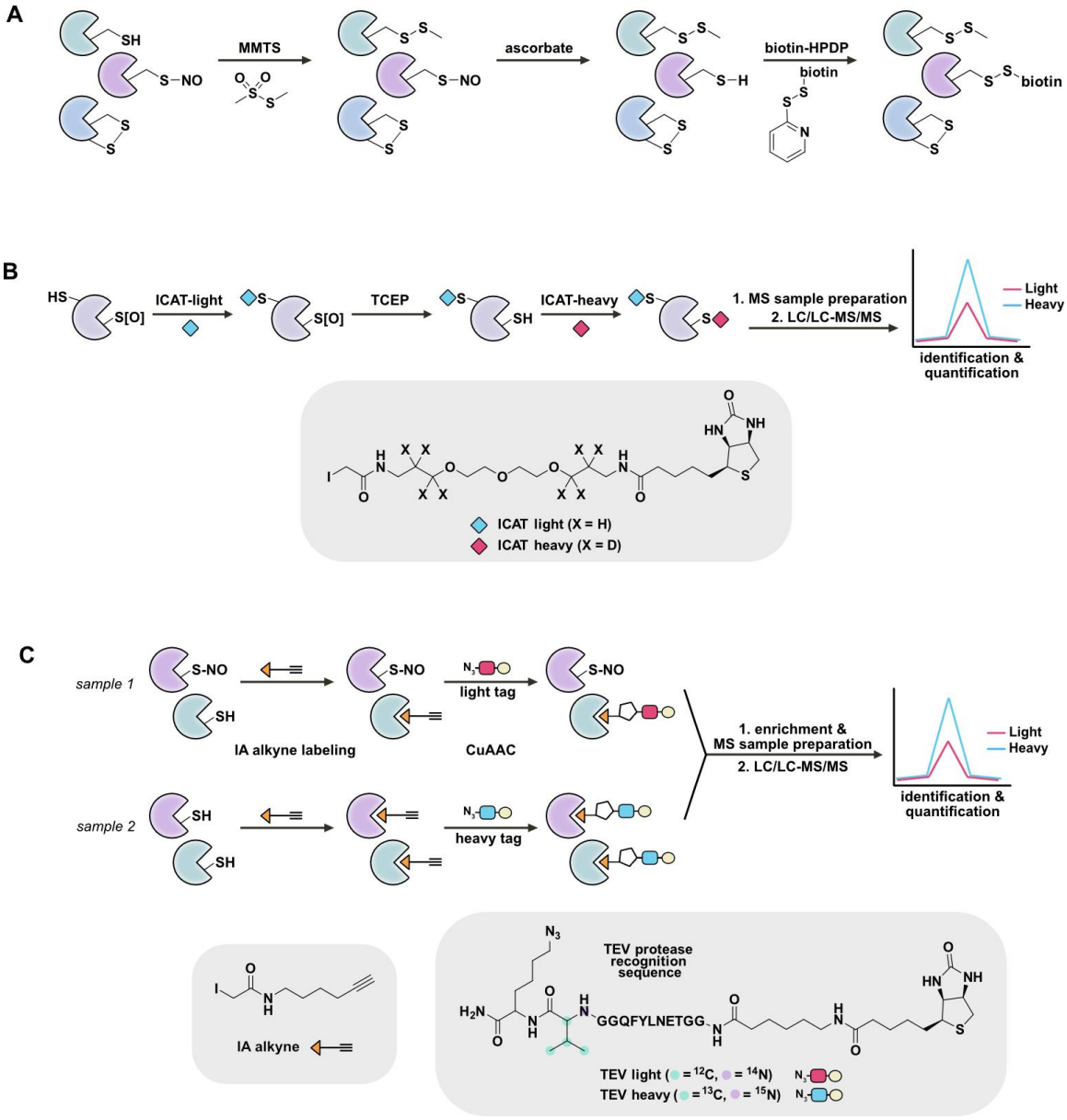

Figure 1-7 Indirect methods of identifying cysteine oxidative PTMs: (**A**) The biotin switch technique, (**B**) OxICAT, and (**C**) isoTOP-ABPP.

1.5 CONCLUSION

Although cysteine is one of the least abundant amino acids, its conservation as a functional site lends to its importance. The unique characteristics of cysteine as well as its propensity to undergo various post-translational modifications give rise to various functionalities and involvement in numerous cellular processes. There have been numerous techniques developed to study cysteine PTMs including probes for direct detection as well as the development of indirect quantitative proteomic methods to identify and quantify the extent of a modification at a particular cysteine residue.

This work is particularly focused on interrogating cysteine oxidative events mediated by RNS and ROS. The next chapter will focus on a MS based method to identify protein targets of CoA-SNO mediated *S*-nitrosation and a parallel comparison of CoA-SNO targets to other SNO donors (Chapter 2), followed by the characterization of *S*-nitrosation events on specific protein targets (Chapter 3). We also interrogate the regulatory role of cysteine oxidation in the ribonuclease inhibitor protein (RI) (Chapter 4), and cysteine reactivity to predict functionally relevant sites in the eukaryotic pathogen *Toxoplasma Gondii* (Chapter 5).

REFERENCES

(1) Pace, N. J.; Weerapana, E. Diverse Functional Roles of Reactive Cysteines. *ACS Chem. Biol* **2013**, *8* (12), 283-296

(2) Cannan, R. K.; Knight, B. C. J. G. Dissociation Constants of Cystine, Cysteine, Thioglycollic Acid and α-Thiolactic Acid. *Biochem. J.* **1927**, *21* (6), 1384–1390.

(3) Go, Y. M.; Chandler, J. D.; Jones, D. P. The Cysteine Proteome. *Free Radic. Biol. Med.* **2015**, *84*, 227–245.

(4) Yang, Y.; Wells, W. W. Identification and Characterization of the Functional Amino Acids at the Active Center of Pig Liver Thioltransferase by Site-Directed Mutagenesis. *J. Biol. Chem.* **1991**, *266* (19), 12759–12765.

(5) Couvertier, S. M.; Zhou, Y.; Weerapana, E. Chemical-Proteomic Strategies to Investigate Cysteine Posttranslational Modifications. *Biochim. Biophys. Acta - Proteins Proteomics* **2014**, *1844* (12), 2315–2330.

(6) Paulsen, C. E.; Carroll, K. S. Orchestrating Redox Signaling Networks through Regulatory Cysteine Switches. *ACS Chem. Biol.* **2010**, *5* (1), 47–62.

(7) Klomsiri, C.; Karplus, P. A.; Poole, L. B. Cysteine-Based Redox Switches in Enzymes. *Antiox. and Redox Signal*. **2011**, 1065–1077.

(8) Hess, D. T.; Matsumoto, A.; Kim, S. O.; Marshall, H. E.; Stamler, J. S. Protein S-Nitrosylation: Purview and Parameters. *Nat. Rev. Mol. Cell Biol.*. **2005**, 150–166.

(9) Lindler, M. E.; Deschenes, R. J. Palmitoylation: Policing Protein Stability and Traffic. *Nat. Rev. Mol. Cell Biol.* **2007**, *8*, 74–84.

(10) Zhang, F. L.; Casey, P. J. PROTEIN PRENYLATION: Molecular Mechanisms and Functional Consequences. **2003**, *65*, 241–269.

(11) Higdon, A.; Diers, A. R.; Oh, J. Y.; Landar, A.; Darley-Usmar, V. M. Cell Signalling by Reactive Lipid Species: New Concepts and Molecular Mechanisms. *Biochem. J* **2012**, *442*, 453–464.

(12) Anand, P.; Stamler, J. S. Enzymatic Mechanisms Regulating Protein S-Nitrosylation: Implications in Health and Disease. *J. Mol. Med.* **2012**, *90* (3), 233–244.

(13) Ye, H.; Wu, J.; Liang, Z.; Zhang, Y.; Huang, Z. Protein S-Nitrosation: Biochemistry, Identification, Molecular Mechanisms, and Therapeutic

Applications. *J. Med. Chem.* **2022**, *65* (8), 5902–5925.

(14) Smith, B. C.; Marletta, M. A. Mechanisms of S-Nitrosothiol Formation and Selectivity in Nitric Oxide Signaling. *Curr. Opin. Chem. Biol.* **2012**, *16* (5–6), 498–506.

(15) Carlström, M. Nitric Oxide Signalling in Kidney Regulation and Cardiometabolic Health. *Nat. Rev. | Nephrol.* **2021**, *17*, 575.

(16) Förstermann, U.; Sessa, W. C. Nitric Oxide Synthases: Regulation and Function. *Eur. Heart J.* **2012**, *33*, 829–837.

(17) Fernando, V.; Zheng, X.; Walia, Y.; Sharma, V.; Letson, J.; Furuta, S. S-Nitrosylation: An Emerging Paradigm of Redox Signaling. **2019**, *8*, 404.

(18) Garcin, E. D.; Bruns, C. M.; Lloyd, S. J.; Hosfield, D. J.; Tiso, M.; Gachhui, R.; Stuehr, D. J.; Tainer, J. A.; Getzoff, E. D. Structural Basis for Isozyme-Specific Regulation of Electron Transfer in Nitric-Oxide Synthase. *J. Biol. Chem.* **2004**, *279* (36), 37918–37927.

(19) Rubio-Guerra, A. F.; Vargas-Robles, H.; Ramos-Brizuela, L. M.; Escalante-Acosta, B. A.; Francisco, A.; Motozintla, R.-G. Is Tetrahydrobiopterin a Therapeutic Option in Diabetic Hypertensive Patients? *Integr. Blood Press. Control* **2010**, 3, 125-132.

(20) Moens, A. L.; Kass, D. A. Tetrahydrobiopterin and Cardiovascular Disease. **2006**.

(21) Qu, Z.-W.; Miao, W.-C.; Hu, S.-Q.; Li, C.; Zhuo, X.-L.; Zong, Y.-Y.; Wu, Y.-P.; Zhang, G.-Y. N-Methyl-D-Aspartate Receptor-Dependent Denitrosylation of Neuronal Nitric Oxide Synthase Increase the Enzyme Activity. *PLoS One* **2012**, *7* (12), 52788.

(22) Ravi, K.; Brennan, L. A.; Levic, S.; Ross, P. A.; Black, S. M. S-Nitrosylation of Endothelial Nitric Oxide Synthase Is Associated with Monomerization and Decreased Enzyme Activity. *Proc. Natl. Acad. Sci.* **2004**, *101* (8), 2619–2624.

(23) Mitchell, D. A.; Erwin, P. A.; Michel, T.; Marletta, M. A. S-Nitrosation and Regulation of Inducible Nitric Oxide Synthase. *Biochem.* **2005**. *44*, 4636-4647.

(24) Mitchell, D. A.; Michel, T.; Marletta, M. A. Effects of S-Nitrosation of Nitric Oxide Synthase. *Adv. Exp. Biol.* **2007**, *1*, 151–456.

(25) Tummala, M.; Ryzhov, V.; Ravi, K.; Black, S. M. Identification of the Cysteine Nitrosylation Sites in Human Endothelial Nitric Oxide Synthase. **2008**, *27* (1), 25–33.

(26) Palmer, R. M. J.; Ferrige, A. G.; Moncada, S. Nitric Oxide Release Accounts for the Biological Activity of Endothelium-Derived Relaxing Factor. *Nature* **1987**, *327* (6122), 524–526.

(27) Ignarro, L. J.; Buga, G. M.; Wood, K. S.; Byrns, R. E.; Chaudhuri, G. Endothelium-Derived Relaxing Factor Produced and Released from Artery and Vein Is Nitric Oxide. *Proc. Natl. Acad. Sci.* **1987**, *84* (24), 9265–9269.

(28) Stamler, J. S.; Simon, D. I.; Osborne, J. A.; Mullins, M. E.; Jaraki, O.; Michel, T.; Singel, D. J.; Loscalzo, J. S-Nitrosylation of Proteins with Nitric Oxide: Synthesis and Characterization of Biologically Active Compounds. *Proc. Natl. Acad. Sci.* **1992**, *89* (1), 444–448.

(29) Stamler, J. S.; Lamas, S.; Fang, F. C. Nitrosylation: The Prototypic Redox-Based Signaling Mechanism. *Cell*. **2001**, *106*, 675–683.

(30) Wynia-Smith, S. L.; Smith, B. C. Nitrosothiol Formation and S-Nitrosation Signaling through Nitric Oxide Synthases. *Nitric Oxide* **2017**, *63*, 52–60.

(31) Lim, C. H.; Dedon, P. C.; Deen, W. M. Kinetic Analysis of Intracellular Concentrations of Reactive Nitrogen Species. *Chem. Res. Toxicol.* **2008,** *21,* 2134-2147.

(32) Madej, E.; Folkes, L. K.; Wardman, P.; Czapski, G.; Goldstein, S. Thiyl Radicals React with Nitric Oxide to Form S-Nitrosothiols with Rate Constants near the Diffusion-Controlled Limit. *Free Radic. Biol. Med.* **2008**, *44* (12), 2013–2018.

(33) Zhao, Y.; Brandish, P. E.; Ballou, D. P.; Marletta, M. A. A Molecular Basis for Nitric Oxide Sensing by Soluble Guanylate Cyclase. *Proc. Natl. Acad. Sci.* **1999**, *96* (26), 14753–14758.

(34) Basu, S.; Keszler, A.; Azarova, N. A.; Nwanze, N.; Perlegas, A.; Shiva, S.; Broniowska, K. A.; Hogg, N.; Kim-Shapiro, D. B. A Novel Role for Cytochrome c: Efficient Catalysis of S-Nitrosothiol Formation. *Free Radic. Biol. Med.* **2010**, *48* (2), 255–263.

(35) Broniowska, K. A.; Keszler, A.; Basu, S.; Kim-Shapiro, D. B.; Hogg, N. Cytochrome C-Mediated Formation of S-Nitrosothiol in Cells. *Biochem. J.* **2012**, *442* (1), 191–197.

(36) Koppenol, W. H. Nitrosation, Thiols, and Hemoglobin: Energetics and Kinetics. *Inorg. Chem* **2012**, *51*, 41.

(37) Houk, K. N.; Hietbrink, B. N.; Bartberger, M. D.; McCarren, P. R.; Choi, B. Y.; Voyksner, R. D.; Stamler, J. S.; Toone, E. J. Nitroxyl Disulfides, Novel Intermediates in Transnitrosation Reactions. *J. Am. Chem. Soc.* **2003**, *125* (23),

6972–6976.

(38) Perissinotti, L. L.; Turjanski, A. G.; Estrin, D. A.; Doctorovich, F. Transnitrosation of Nitrosothiols: Characterization of an Elusive Intermediate. *J. Am. Chem. Soc.* **2005**, *127* (2), 486–487.

(39) Lai, C. H.; Chou, P. T. The Theoretical Comparison between Two Model NO Carriers, MeSNO and MeSeNO. *J. Mol. Model.* **2008**, *14* (1), 1–9.

(40) Broniowska, K. A.; Hogg, N. The Chemical Biology of S-Nitrosothiols. *Antioxid. Redox Signal.* **2012**, *17* (7), 969–980.

(41) Anand, P.; Hausladen, A.; Wang, Y.-J.; Zhang, G.-F.; Stomberski, C.; Brunengraber, H.; Hess, D. T.; Stamler, J. S. Identification of S-Nitroso-CoA Reductases That Regulate Protein S-Nitrosylation. *Proc. Natl. Acad. Sci.* **2014**, *111* (52), 18572–18577.

(42) Doulias, P.-T.; Greene, J. L.; Greco, T. M.; Tenopoulou, M.; Seeholzer, S. H.; Dunbrack, R. L.; Ischiropoulos, H. Structural Profiling of Endogenous S-Nitrosocysteine Residues Reveals Unique Features That Accommodate Diverse Mechanisms for Protein S-Nitrosylation. *Proc. Natl. Acad. Sci.* **2010**, *107* (39), 16958–16963.

(43) Morris, G.; Walder, K.; Carvalho, A. F.; Tye, S. J.; Lucas, K.; Berk, M.; Maes, M. The Role of Hypernitrosylation in the Pathogenesis and Pathophysiology of Neuroprogressive Diseases. *Neuroscience and Biobehavioral Reviews*. **2018**, 453–469.

(44) Nakamura, T.; Lipton, S. A. Emerging Role of Protein-Protein Transnitrosylation in Cell Signaling Pathways. *Antioxidants and Redox Signaling*. **2013**, 18 (3) 239–249.

(45) Greco, T. M.; Hodara, R.; Parastatidis, I.; Heijnen, H. F. G.; Dennehy, M. K.; Liebler, D. C.; Ischiropoulos, H. Identification of S-Nitrosylation Motifs by Site-Specific Mapping of the S-Nitrosocysteine Proteome in Human Vascular Smooth Muscle Cells. **2006**, *103* (19), 7420-7425.

(46) Marino, S. M.; Gladyshev, V. N. Structural Analysis of Cysteine S-Nitrosylation: A Modified Acid-Based Motif and the Emerging Role of Trans-Nitrosylation. *J. Mol. Biol.* **2010**, *395* (4), 844–859.

(47) Kim, S. F.; Huri, D. A.; Snyder, S. H. Inducible Nitric Oxide Synthase Binds, S-Nitrosylates, and Activates Cyclooxygenase-2. *Science.* **2005**, *310* (5756), 1966–1970.

(48) Jia, J.; Arif, A.; Terenzi, F.; Willard, B.; Plow, E. F.; Hazen, S. L.; Fox, P. L. Target-

Selective Protein S-Nitrosylation by Sequence Motif Recognition. *Cell.* **2014**, *159* (3), 623–634.

(49) Barnett, S. D.; Buxton, I. L. O. The Role of S-Nitrosoglutathione Reductase (GSNOR) in Human Disease and Therapy. *Crit. Rev. Biochem. Mol. Biol.* **2017**, 52 (3), 340–354.

(50) Bateman, R. L.; Rauh, D.; Tavshanjian, B.; Shokat, K. M. Human Carbonyl Reductase 1 Is an S-Nitrosoglutathione Reductase. *J. Biol. Chem.* **2008**, *283* (51), 35756–35762.

(51) Hedberg, J. J.; Griffiths, W. J.; Nilsson, S. J. F.; Hö, J.-O. Reduction of S-Nitrosoglutathione by Human Alcohol Dehydrogenase 3 Is an Irreversible Reaction as Analysed by Electrospray Mass Spectrometry. *Eur. J. Biochem.* **2003**, *270*, 1249–1256.

(52) Staab, C. A.; Ålander, J.; Brandt, M.; Lengqvist, J.; Morgenstern, R.; Grafström, R. C.; Höög, J. O. Reduction of S-Nitrosoglutathione by Alcohol Dehydrogenase 3 Is Facilitated by Substrate Alcohols via Direct Cofactor Recycling and Leads to GSH-Controlled Formation of Glutathione Transferase Inhibitors. *Biochem. J.* **2008**, *413* (3), 493–504.

(53) Benhar, M.; Forrester, M. T.; Stamler, J. S. Protein Denitrosylation: Enzymatic Mechanisms and Cellular Functions. *Nat. Rev. Mol. Cell Biol.* **2009**, 10 (10), 721–732.

(54) Stomberski, C. T.; Zhou, H.-L.; Wang, L.; van den Akker, F.; Stamler, J. S. Molecular Recognition of S-Nitrosothiol Substrate by Its Cognate Protein Denitrosylase. *J. Biol. Chem.* **2019**, *294* (5), 1568–1578.

(55) Sengupta, R.; Ryter, S. W.; Zuckerbraun, B. S.; Tzeng, E.; Billiar, T. R.; Stoyanovsky, D. A. Thioredoxin Catalyzes the Denitrosation of Low-Molecular Mass and Protein S-Nitrosothiols. *Biochemistry* **2007**, *46*, 10.

(56) Mitchell, D. A.; Michel, T.; Marletta, M. A. Effects of S-Nitrosation of Nitric Oxide Synthase. *Adv. Exp. Biol.* **2007**, *1*, 151–456.

(57) Benhar, M.; Forrester, M. T.; Stamler, J. S. Protein Denitrosylation: Enzymatic Mechanisms and Cellular Functions. *Nat. Rev. Mol. Cell Biol.* **2009**, *10* (10), 721-732.

(58) Sengupta, R.; Billiar, T. R.; Atkins, J. L.; Kagan, V. E.; Stoyanovsky, D. A. Nitric Oxide and Dihydrolipoic Acid Modulate the Activity of Caspase 3 in HepG2 Cells. **2009**.

(59) Benhar, M.; Forrester, M. T.; Hess, D. T.; Stamler, J. S. Regulated Protein

Denitrosylation by Cytosolic and Mitochondrial Thioredoxins. *Science.* **2008**, *320* (5879), 1050–1054.

(60) Stomberski, C. T.; Hess, D. T.; Stamler, J. S. Protein S-Nitrosylation: Determinants of Specificity and Enzymatic Regulation of S-Nitrosothiol-Based Signaling. *Antioxid. Redox Signal.* **2019**, *30* (10), 1331-1351

(61) Chen, Y.-J.; Lu, C.-T.; Su, M.-G.; Huang, K.-Y.; Ching, W.-C.; Yang, H.-H.; Liao, Y.-C.; Chen, Y.-J.; Lee, T.-Y. DbSNO 2.0: A Resource for Exploring Structural Environment, Functional and Disease Association and Regulatory Network of Protein S-Nitrosylation. *Nucleic Acids Res.* **2015**, *43* (1), 503–511.

(62) Mitchell, D. A.; Morton, S. U.; Fernhoff, N. B.; Marletta, M. A. Thioredoxin Is Required for S-Nitrosation of Procaspase-3 and the Inhibition of Apoptosis in Jurkat Cells. *Proc. Natl. Acad. Sci.* **2007**, *104* (28), 11609–11614.

(63) Hara, M. R.; Agrawal, N.; Kim, S. F.; Cascio, M. B.; Fujimuro, M.; Ozeki, Y.; Takahashi, M.; Cheah, J. H.; Tankou, S. K.; Hester, L. D.; et al. S-Nitrosylated GAPDH Initiates Apoptotic Cell Death by Nuclear Translocation Following Siah1 Binding. *Nat. Cell Biol.* **2005**, *7* (7), 665–674.

(64) Kornberg, M. D.; Sen, N.; Hara, M. R.; Juluri, K. R.; Nguyen, J. V. K.; Snowman, A. M.; Law, L.; Hester, L. D.; Snyder, S. H. GAPDH Mediates Nitrosylation of Nuclear Proteins. *Nat. Cell Biol.* **2010**, *12* (11), 1094–1100.

(65) Kwak, Y. D.; Ma, T.; Diao, S.; Zhang, X.; Chen, Y.; Hsu, J.; Lipton, S. A.; Masliah, E.; Xu, H.; Liao, F. F. NO Signaling and S-Nitrosylation Regulate PTEN Inhibition in Neurodegeneration. *Mol. Neurodegener.* **2010**, *5* (1), 1–12.

(66) Choi, M. S.; Nakamura, T.; Cho, S. J.; Han, X.; Holland, E. A.; Qu, J.; Petsko, G. A.; Yates, J. R.; Liddington, R. C.; Lipton, S. A. Transnitrosylation from DJ-1 to PTEN Attenuates Neuronal Cell Death in Parkinson's Disease Models. *J. Neurosci.* **2014**, *34* (45), 15123–15131.

(67) Bonifati, V.; Rizzu, P.; Van Baren, M. J.; Schaap, O.; Breedveld, G. J.; Krieger, E.; Dekker, M. C. J.; Squitieri, F.; Ibanez, P.; Joosse, M.; et al. Mutations in the DJ-1 Gene Associated with Autosomal Recessive Early-Onset Parkinsonism. *Science.* **2003**, *299* (5604), 256–259.

(68) Wang, Z. Protein S-Nitrosylation and Cancer. *Cancer Lett.* **2012**, *320* (2), 123–129.

(69) Fukumura, D.; Kashiwagi, S.; Jain, R. K. The Role of Nitric Oxide in Tumour Progression. *Nat. Rev. Cancer.* **2006**, *6* (7), 521–534.

(70) Irby, R. B.; Yeatman, T. J. Role of Src Expression and Activation in Human

Cancer. *Oncogene.* **2000**, *19* (49), 5636–5642.

(71) Rahman, M. A.; Senga, T.; Ito, S.; Hyodo, T.; Hasegawa, H.; Hamaguchi, M. S-Nitrosylation at Cysteine 498 of c-Src Tyrosine Kinase Regulates Nitric Oxide-Mediated Cell Invasion. *J. Biol. Chem.* **2010**, *285* (6), 3806–3814.

(72) Buolamwini, J. K. Novel Anticancer Drug Discovery. *Curr. Opin. Chem. Biol.* **1999**, *3* (4), 500–509.

(73) Azad, N.; Vallyathan, V.; Wang, L.; Tantishaiyakul, V.; Stehlik, C.; Leonard, S. S.; Rojanasakul, Y. S-Nitrosylation of Bcl-2 Inhibits Its Ubiquitin-Proteasomal Degradation. *J. Biol. Chem.* **2006,** *281* (45), 34124–34134.

(74) Chanvorachote, P.; Nimmannit, U.; Stehlik, C.; Wang, L.; Jiang, B. H.; Ongpipatanakul, B.; Rojanasakul, Y. Nitric Oxide Regulates Cell Sensitivity to Cisplatin-Induced Apoptosis through S-Nitrosylation and Inhibition of Bcl-2 Ubiquitination. *Cancer Res.* **2006**, *66* (12), 6353–6360.

(75) Lo Conte, M.; Carroll, K. S. The Redox Biochemistry of Protein Sulfenylation and Sulfinylation. *J. Biol. Chem.* **2013**, *288* (37), 26480–26488.

(76) Parvez, S.; Long, M. J. C.; Poganik, J. R.; Aye, Y. Redox Signaling by Reactive Electrophiles and Oxidants. *Chem. Rev.* **2018**, *118* (18), 8798–8888.

(77) Giorgio, M.; Trinei, M.; Migliaccio, E.; Pelicci, P. G. Hydrogen Peroxide: A Metabolic by-Product or a Common Mediator of Ageing Signals? *Nat. Rev. Mol. Cell Biol.* **2007**, *8* (9), 722–728.

(78) Kelley, E. E.; Khoo, N. K. H.; Hundley, N. J.; Malik, U. Z.; Freeman, B. A.; Tarpey, M. M. Hydrogen Peroxide Is the Major Oxidant Product of Xanthine Oxidase. *Free Radic. Biol. Med.* **2009**, *48* (4), 493–498.

(79) Sies, H. Hydrogen Peroxide as a Central Redox Signaling Molecule in Physiological Oxidative Stress: Oxidative Eustress. *Redox Biol.* **2017**, *11*, 613–619.

(80) Raha, S.; Robinson, B. H. Mitochondria, Oxygen Free Radicals, Disease and Ageing. *Trends Biochem. Sci.* **2000**, *25* (10), 502–508.

(81) Starkov, A. A.; Fiskum, G.; Chinopoulos, C.; Lorenzo, B. J.; Browne, S. E.; Patel, M. S.; Beal, M. F. Mitochondrial α-Ketoglutarate Dehydrogenase Complex Generates Reactive Oxygen Species. *J. Neurosci.* **2004**, *24* (36), 7779–7788.

(82) Lambeth, J. D. NOX Enzymes and the Biology of Reactive Oxygen. *Nat. Rev. Immunol.* **2004**, *4* (3), 181–189.

(83) Brown, D. I.; Griendling, K. K. Nox Proteins in Signal Transduction. *Free Radic. Biol. Med.* **2009**, *47* (9), 1239–1253.

(84) Poole, L. B.; Karplus, P. A.; Claiborne, A. Protein Sulfenic Acids in Redox Signaling. *Annu. Rev. Pharmacol. Toxicol.* **2004**, *44*, 325–347.

(85) Abo, M.; Weerapana, E. Chemical Probes for Redox Signaling and Oxidative Stress. *Antioxidants Redox Signal.* **2019**, *30* (10), 1369–1386.

(86) Hsu, J. L.; Hsieh, Y.; Tu, C.; O'Connor, D.; Nick, H. S.; Silverman, D. N. Catalytic Properties of Human Manganese Superoxide Dismutase. *J. Biol. Chem.* **1996**, *271* (30), 17687–17691.

(87) Veal, E. A.; Day, A. M.; Morgan, B. A. Hydrogen Peroxide Sensing and Signaling. *Mol. Cell* **2007**, *26* (1), 1–14.

(88) Biteau, B.; Labarre, J.; Toledano, M. B. ATP-Dependent Reduction of Cysteine–Sulphinic Acid by S. Cerevisiae Sulphiredoxin. *Nat.* **2003**, *425* (6961), 980–984.

(89) Taguchi, K.; Motohashi, H.; Yamamoto, M. Molecular Mechanisms of the Keap1–Nrf2 Pathway in Stress Response and Cancer Evolution. *Genes to Cells* **2011**, *16* (2), 123–140.

(90) Sihvola, V.; Levonen, A. L. Keap1 as the Redox Sensor of the Antioxidant Response. *Arch. Biochem. Biophys.* **2017**, *617*, 94–100.

(91) Truong, T. H.; Carroll, K. S. Redox Regulation of Epidermal Growth Factor Receptor Signaling through Cysteine Oxidation. *Biochem.* **2012,** 51, 9954-9965.

(92) Woo, H. A.; Yim, S. H.; Shin, D. H.; Kang, D.; Yu, D. Y.; Rhee, S. G. Inactivation of Peroxiredoxin I by Phosphorylation Allows Localized H2O2 Accumulation for Cell Signaling. *Cell.* **2010**, *140* (4), 517–528.

(93) Lee, S. R.; Yang, K. S.; Kwon, J.; Lee, C.; Jeong, W.; Rhee, S. G. Reversible Inactivation of the Tumor Suppressor PTEN by H2O2. *J. Biol. Chem.* **2002**, *277* (23), 20336–20342.

(94) Park, H. S.; Lee, S. H.; Park, D.; Lee, J. S.; Ryu, S. H.; Lee, W. J.; Rhee, S. G.; Bae, Y. S. Sequential Activation of Phosphatidylinositol 3-Kinase, BPix, Rac1, and Nox1 in Growth Factor-Induced Production of H 2 O 2 . *Mol. Cell. Biol.* **2004**, *24* (10), 4384–4394.

(95) Wang, H.; Xian, M. Fast Reductive Ligation of S-Nitrosothiols. *Angew. Chemie Int. Ed.* **2008**, *47* (35), 6598–6601.

(96) Zhang, J.; Wang, H.; Xian, M. Exploration of the "Traceless" Reductive Ligation of S-Nitrosothiols. *Org. Lett.* **2009**, *11* (2), 477–480.

(97) Clements, J. L.; Pohl, F.; Muthupandi, P.; Rogers, S. C.; Mao, J.; Doctor, A.; Birman, V. B.; Held, J. M. A Clickable Probe for Versatile Characterization of S-Nitrosothiols. *Redox Biol.* **2020**, *37*, 101707.

(98) Bechtold, E.; Reisz, J. A.; Klomsiri, C.; Tsang, A. W.; Wright, M. W.; Poole, L. B.; Furdui, C. M.; King, S. B. Water-Soluble Triarylphosphines as Biomarkers for Protein *S* -Nitrosation. *ACS Chem. Biol.* **2010**, *5* (4), 405–414.

(99) Seneviratne, U.; Godoy, L. C.; Wishnok, J. S.; Wogan, G. N.; Tannenbaum, S. R. Mechanism-Based Triarylphosphine-Ester Probes for Capture of Endogenous RSNOs. *J. Am. Chem. Soc.* **2013**, *135* (20), 7693–7704.

(100) Doulias, P. T.; Tenopoulou, M.; Greene, J. L.; Raju, K.; Ischiropoulos, H. Nitric Oxide Regulates Mitochondrial Fatty Acid Metabolism through Reversible Protein S-Nitrosylation. *Sci. Signal.* **2013**, *6* (256).

(101) Lee, Y. Il; Giovinazzo, D.; Kang, H. C.; Lee, Y.; Jeong, J. S.; Doulias, P. T.; Xie, Z.; Hu, J.; Ghasemi, M.; Ischiropoulos, H.; et al. Protein Microarray Characterization of the S-Nitrosoproteome. *Mol. Cell. Proteomics* **2014**, *13* (1), 63–72.

(102) Leonard, S. E.; Reddie, K. G.; Carroll, K. S. Mining the Thiol Proteome for Sulfenic Acid Modifications Reveals New Targets for Oxidation in Cells. *ACS Chem. Biol.* **2009**, *4* (9), 783–799.

(103) Shi, Y.; Fu, L.; Yang, J.; Carroll, K. S. Wittig Reagents for Chemoselective Sulfenic Acid Ligation Enables Global Site Stoichiometry Analysis and Redox-Controlled Mitochondrial Targeting. *Nat. Chem.* **2021**, *13* (11), 1140–1150.

(104) Lo Conte, M.; Carroll, K. S. Chemoselective Ligation of Sulfinic Acids with Aryl-Nitroso Compounds. *Angew. Chemie Int. Ed.* **2012**, *51* (26), 6502–6505.

(105) Jaffrey, S. R.; Snyder, S. H. The Biotin Switch Method for the Detection of S-Nitrosylated Proteins. *Sci. STKE* **2001**, *2001*(86), 1.

(106) Diers, A. R.; Keszler, A.; Hogg, N. Detection of S-Nitrosothiols. *Biochim. Biophys. Acta - Gen. Subj.* **2014**, *1840* (2), 892–900.

(107) Wang, X.; Kettenhofen, N. J.; Shiva, S.; Hogg, N.; Gladwin, M. T. Copper Dependence of the Biotin Switch Assay: Modified Assay for Measuring Cellular and Blood Nitrosated Proteins. *Free Radic. Biol. Med.* **2008**, *44* (7), 1362–1372.

(108) Giustarini, D.; Dalle-Donne, I.; Colombo, R.; Milzani, A.; Rossi, R. Is Ascorbate Able to Reduce Disulfide Bridges? A Cautionary Note. *Nitric Oxide* **2008**, *19* (3), 252–258.

(109) Li, S.; Wang, H.; Xian, M.; Whorton, A. R. Identification of Protein Nitrosothiols Using Phosphine-Mediated Selective Reduction. *Nitric Oxide* **2012**, *26* (1), 20–26.

(110) Wiesweg, M.; Berchner-Pfannschmidt, U.; Fandrey, J.; Petrat, F.; de Groot, H.; Kirsch, M. Rocket Fuel for the Quantification of S-Nitrosothiols. Highly Specific Reduction of S-Nitrosothiols to Thiols by Methylhydrazine. *Free Radic. Res.* **2012**, *47* (2), 104–115.

(111) Forrester, M. T.; Thompson, J. W.; Foster, M. W.; Nogueira, L.; Moseley, M. A.; Stamler, J. S. Proteomic Analysis of S-Nitrosylation and Denitrosylation by Resin-Assisted Capture. *Nat. Biotechnol.* **2009**, *27* (6), 557–559.

(112) Chouchani, E. T.; Hurd, T. R.; Nadtochiy, S. M.; Brookes, P. S.; Fearnley, I. M.; Lilley, K. S.; Smith, R. A. J.; Murphy, M. P. Identification of S-Nitrosated Mitochondrial Proteins by S-Nitrosothiol Difference in Gel Electrophoresis (SNO-DIGE): Implications for the Regulation of Mitochondrial Function by Reversible S-Nitrosation. *Biochem. J.* **2010**, *430* (1), 49–59.

(113) Saurin, A. T.; Neubert, H.; Brennan, J. P.; Eaton, P. Widespread Sulfenic Acid Formation in Tissues in Response to Hydrogen Peroxide. *Proc. Natl. Acad. Sci.* **2004**, *101* (52), 17982–17987.

(114) Leichert, L. I.; Gehrke, F.; Gudiseva, H. V.; Blackwell, T.; Ilbert, M.; Walker, A. K.; Strahler, J. R.; Andrews, P. C.; Jakob, U. Quantifying Changes in the Thiol Redox Proteome upon Oxidative Stress in Vivo. *Proc. Natl. Acad. Sci.* **2008**, *105* (24), 8197–8202.

(115) Bechtel, T. J.; Li, C.; Kisty, E. A.; Maurais, A. J.; Weerapana, E. Profiling Cysteine Reactivity and Oxidation in the Endoplasmic Reticulum. *ACS Chem. Biol.* **2020**, *15* (2), 543–553.

(116) Chouchani, E. T.; James, A. M.; Methner, C.; Pell, V. R.; Prime, T. A.; Erickson, B. K.; Forkink, M.; Lau, G. Y.; Bright, T. P.; Menger, K. E.; et al. Identification and Quantification of Protein S-Nitrosation by Nitrite in the Mouse Heart during Ischemia. *J. Biol. Chem.* **2017**, *292* (35), 14486–14495.

(117) Weerapana, E.; Wang, C.; Simon, G. M.; Richter, F.; Khare, S.; Dillon, M. B. D.; Bachovchin, D. A.; Mowen, K.; Baker, D.; Cravatt, B. F. Quantitative Reactivity Profiling Predicts Functional Cysteines in Proteomes. *Nature* **2010**, *468* (7325), 790–795.

(118) Zhou, Y.; Wynia-Smith, S. L.; Couvertier, S. M.; Kalous, K. S.; Marletta, M. A.; Smith, B. C.; Weerapana, E. Chemoproteomic Strategy to Quantitatively Monitor Transnitrosation Uncovers Functionally Relevant S-Nitrosation Sites on Cathepsin D and HADH2. *Cell Chem. Biol.* **2016**, *23* (6), 727–737.

2.0 A CHEMICAL PROTEOMIC APPROACH TO IDENTIFY PROTEIN TARGETS OF COA-SNO MEDIATED *S*-NITROSATION

2.1 INTRODUCTION

S-nitrosation is a reversible oxidative post-translational modification (PTM) in which a cysteine thiol is converted to a nitrosothiol. *S*-nitrosation is critical for NO mediated cellular signaling and regulating protein function in numerous biological processes in the nervous system, cardiovascular system, and immune system[1]. This process is controlled by cellular nitrosating agents and denitrosation enzymes. The NOS enzymes operate as SNO synthase machinery which can lead to protein or low molecular weight (LMW) *S*-nitrosothiols (protein-SNO, LMW-SNO) through two distinct pathways: (1) modification of a free thiol upon NOS dependent generation of reactive nitrogen species (RNS) such as N_2O_3, or (2) through a transnitrosation reaction, in which the auto-nitrosated NOS transfers it's NO group to a free thiol on an interacting protein or small molecule[2–5]. It is thought that the majority of *S*-nitrosothiols (SNOs) are formed and propagated through a transnitrosation reaction, with the primary mediators of cellular transnitrosation including the nitrosated version of the abundant thiol containing small molecule antioxidant glutathione (*S*-nitrosoglutathione, GSNO) and the oxidoreductase protein thioredoxin (*S*-nitrosothioredoxin, Trx-SNO)[6,7].

The levels of GSNO are enzymatically regulated by the GSNO reductase (GSNOR), and carbonyl reductase 1 (CBR1), which reduce endogenous GSNO, thereby indirectly regulating the GSNO dependent nitrosoproteome[8,9]. The thioredoxin/ thioredoxin reductase (Trx/TrxR) system acts directly on protein-SNO, akin to a transnitrosation reaction resulting in protein-SH and Trx-SNO, followed by

subsequent disulfide formation at the Trx active side and release of nitroxyl (HNO)[10,11]. TrxR then works in an NADPH-dependent manner to re-reduce the oxidized Trx, completing the catalytic cycle.

Coenzyme A (CoA) is a low molecular weight thiol that all living organisms use as a substrate or cofactor. CoA exists intracellularly at μM levels with ~4% of cellular enzymes utilizing CoA for involvement in over 100 different reactions in intermediary metabolism[12,13]. Its most notable roles include carbonyl activation in TCA cycle reactions and the transport of an acyl group (acetyl-CoA) for synthesis and oxidation of fatty acids. CoA is likely *S*-nitrosated in a similar fashion as glutathione, dependent on NO and RNS production or via transnitrosation from another nitrosothiol to form CoA-SNO. Since CoA is involved in many central metabolic reactions, CoA-SNO mediated nitrosation may provide a mechanism for metabolic regulation by NO[14].

The discovery of an enzyme in yeast (alcohol dehydrogenase 6, ADH6) with *S*-nitroso-coenzyme A (CoA-SNO) reductase activity (aldo-keto reductase 1A1 (AKR1A1) in humans) has recently highlighted the role of coenzyme A as an endogenous transnitrosating agent[14]. Similar to other reductases (GSNOR, TrxR), AKR1A1 reduces CoA-SNO to CoA-sulfinamide using NADPH, thereby indirectly regulating protein-SNO levels[15].

Lysine 127 of AKR1A1 was found essential for CoA-SNO reductase activity, and overexpression of this inactive mutant allowed for the first identification a CoA-SNO dependent nitrosoproteome in mammals using the SNO-RAC method to enrich *S*-nitrosated proteins coupled with iTRAQ MS analysis[16]. 123 proteins were

identified as CoA-SNO dependent protein-SNOs including ubiquitin-like modifier-activating enzyme 1 (Ube1a/b), a-enolase (ENO1), lactate dehydrogenase A chain (LDHA), fatty acid synthase (FASN), and ATP citrate synthase (ACLY)[16]. Many of the target proteins are involved in metabolic processes and CoA-SNO mediated *S*-nitrosation resulted in increased mitochondrial respiration and slightly increased glycolysis. Further studies found that deletion of AKR1A1 in mice protects against acute kidney injury by inhibitory *S*-nitrosation at Cys 423 and 424 of pyruvate kinase M2 (PKM2), resulting in the diversion of metabolic intermediates through the pentose phosphate pathway to alleviate oxidative stress[17]. Furthermore, AKR1A1 deletion in mice protects against cardiovascular disease by inhibitory *S*-nitrosation at Cys 301 of the cholesterol regulating protein PCSK9, resulting in lower serum cholesterol levels. *S*-nitrosation of PCSK9 inhibits secretion, which is dependent on a transnitrosation cascade involving ER cargo-selection proteins SAR1 and SURF4[18]. However, the SNO-RAC/iTRAQ method used in all of these studies is limited by its inability to identify the site of nitrosation on protein targets, as well as its inability to quantify the extent of the modification at individual cysteine residues, leaving room for further investigation of the role of individual protein-SNO events.

While a subset of target CoA-SNO proteins has been generated, the functional role of *S*-nitrosation on individual CoA-SNO target proteins has only been characterized for PKM2, and the SAR1/SURF4/PCSK9 transnitrosation cascade. Here, we aim to expand the current knowledge of CoA-SNO mediated transnitrosation. Using an isoTOP-ABPP derived chemoproteomic platform previously developed in our lab to identify targets of GSNO mediated

transnitrosation[19], we can identify and quantify the extent of CoA-SNO mediated *S*-nitrosation on 789 cysteine residues, with the proteins most sensitive to CoA-SNO involved in numerous metabolic processes. CoA-SNO treatment is done in parallel with other nitrosating agents: GSNO and PAPA-NONOate, facilitating the identification of targets with unique, as well as generic sensitivity to CoA-SNO mediated transnitrosation.

2.2 RESULTS AND DISCUSSION

2.2.1 Proteomic analysis of CoA-SNO mediated *S*-nitrosation

Our lab previously developed an isoTOP-ABPP derived mass spectrometry-based platform monitoring the susceptibility of >600 cysteine residues to transnitrosation mediated by *S*-nitrosoglutathione (GSNO). This platform allowed for the identification of numerous previously unannotated *S*-nitrosation events, including cysteines on 3-hydroxyacyl-CoA dehydrogenase type 2 (HADH2) and the lysosomal aspartyl protease cathepsin D (CTSD)[19]. Functional characterization revealed that *S*-nitrosation of Cys 58 distal to the HADH2 active site impaired catalytic activity. Similarly, *S*-nitrosation of a non-catalytic Cys 329 on CTSD inhibited proteolytic activation. By implementing a competitive cysteine-labeling strategy, this method overcomes the inability of previous methods to quantitatively determine the extent of *S*-nitrosation for each individual cysteine residues within the human proteome. Therefore, we can evaluate the sensitivity of a particular

cysteine to a given nitrosating agent, affording substrate specificity and revealing previously uncharacterized cysteine residues that regulate protein function.

With the recent uncovering of CoA-SNO as a transnitrosation donor, we wanted to adapt this proteomic platform to identify novel cysteine nitrosation events mediated by CoA-SNO. This study provides the first dataset of proteins sensitive to CoA-SNO mediated nitrosation with both the site and extent of modification on a particular cysteine residue. In order to successfully identify cysteines susceptible to CoA-SNO, we first needed to obtain the transnitrosation donor, CoA-SNO, which was produced according to Anand *et al*. by reacting the free thiol, CoA, with sodium nitrate under acidic conditions to afford the *S*-nitrosothiol[14] (Fig 2-1).

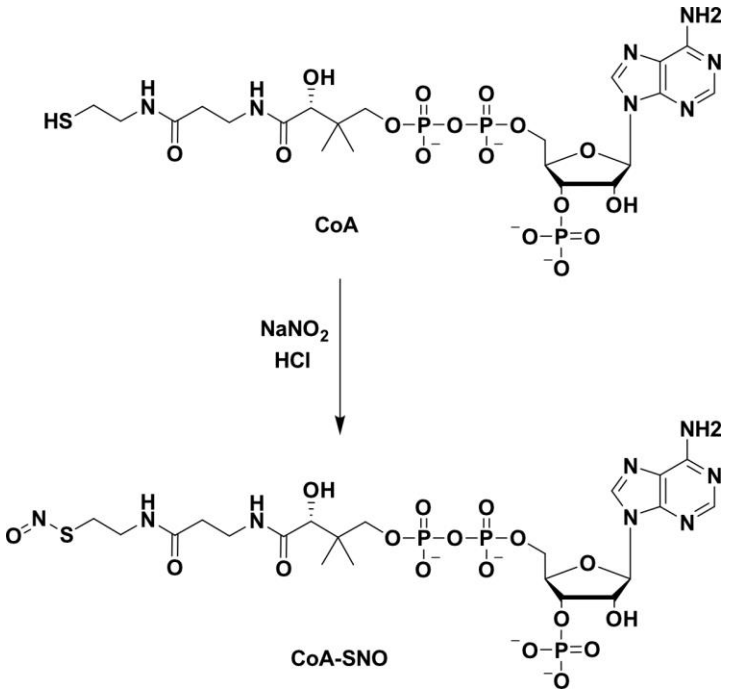

Figure 2-1 Production of *S*-nitroso-coenzyme A (CoA-SNO) is achieved via reaction of equimolar coenzyme A (CoA) and sodium nitrate ($NaNO_2$) under acidic conditions.

With CoA-SNO in hand, we moved on to identifying cysteine nitrosation events mediated by CoA-SNO, using the isoTOP-ABPP derived proteomic method (Fig 2-2). In this approach, MCF7 breast cancer cell lysate is treated with 200 μM CoA-SNO or a buffer control (0.5 M HCl). A cysteine that is converted to a *S*-nitrosothiol in response to CoA-SNO treatment, results in a loss in nucleophilicity compared to a free cysteine thiol. So, when both proteomes are then treated with a cysteine reactive iodoacetamide-alkyne probe (IA), the *S*-nitrosated cysteine displays decreased reactivity. Following alkylation by the IA probe, the alkyne is further functionalized with an isotopically encoded biotin-azide tag (Azo-Light and Azo-Heavy) through biorthogonal copper(I)-catalyzed azide-alkyne cycloaddition (CuAAC)[20,21]. This reaction affords heavy (CoA-SNO treated sample) or light (buffer control sample) labeled cysteines containing and azobenzene cleavable linker for reductive cleavage by sodium dithionite[22]. The heavy and light samples are combined and further subjected to streptavidin enrichment, on bead trypsin digestion, and sodium dithionite cleavage to afford heavy and light labeled peptides for MS analysis. MS/MS (MS2) fragmentation spectra are used to identify cysteine-labeled peptides, while the intensity of the parent ion (MS1) spectra from both the CoA-SNO treated and control samples is used to determine the a heavy:light ratio (*R*) indicative of the relative intensity of these species. A *R* value ~1 indicates that there was no change in cysteine reactivity, and therefore that cysteine is unaffected by CoA-SNO treatment, while $R > 1$ indicates there is reduced cysteine reactivity, signifying modification by CoA-SNO. The larger the *R* value, the greater percentage of cysteine modification.

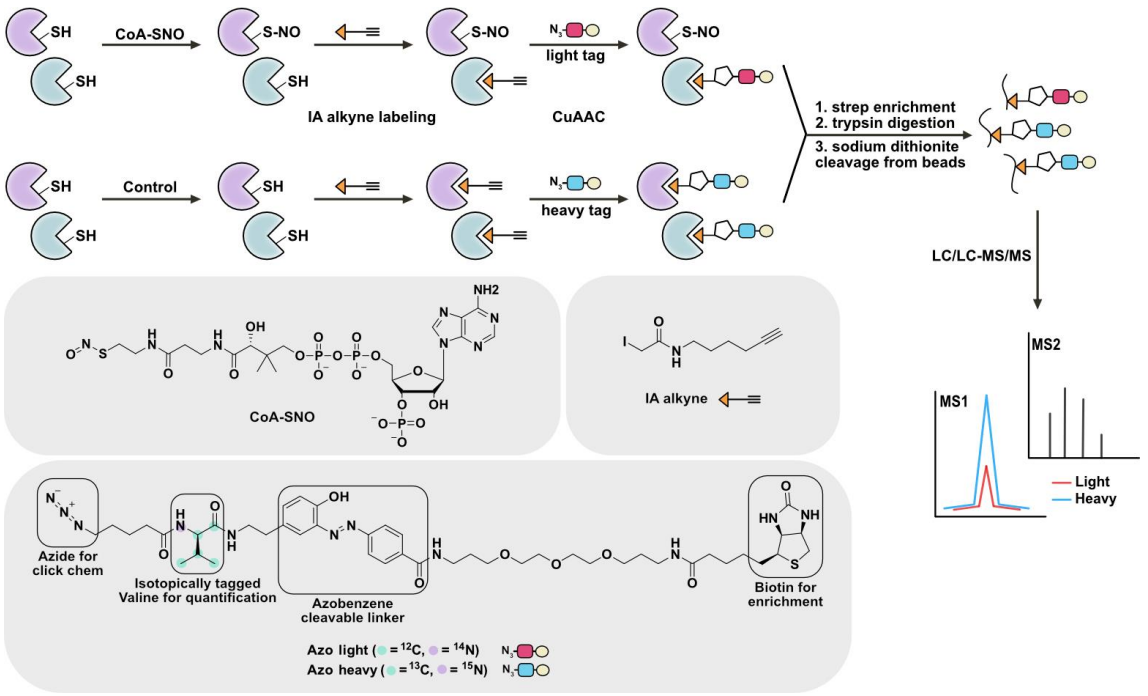

Figure 2-2 Competitive cysteine-profiling strategy to quantify sensitivity to transnitrosation. MCF7 cell lysates are treated with transnitrosation donor (CoA-SNO) or the control buffer (0.5 M HCl), followed by cysteine alkylation with iodoacetamide-alkyne, copper catalyzed click chemistry (CuAAC) with a light (CoA-SNO treated) or heavy (control) Azo tag, combination of samples, streptavidin enrichment, trypsin digestion, sodium dithionite cleavage from beads, and subsequent LC/LC-MS/MS analysis to identify and quantify the IA-probe reactive cysteine residues in each sample. A loss in cysteine reactivity is reflected in an increasing heavy:light ratio (*R*), and is indicative of transnitrosation donor mediated *S*-nitrosation or other resulting cysteine modification.

Using this platform, we were able to identify and rank 789 cysteine residues according to their sensitivity to CoA-SNO using the MS generated *R* value (Fig 2-3A, Appendix I table A2-1). The majority of cysteines were insensitive to CoA-SNO treatment with an *R* value ~1, while a smaller subset of 18 cysteines with an *R* value > 3, was considered highly sensitive to CoA-SNO (Table 2-1). This range in CoA-SNO sensitivity is reflected in the MS1 traces for individual cysteines in which the relative peak intensities of the light (blue) or heavy (red) labeled peptides correspond to the *R* value (Fig 2-3B). For example, the CoA-SNO insensitive Cys 297

on glycerol-3-phophate phosphatase (PGP) displays equal light and heavy peak intensity (R = 1.1), the moderately sensitive Cys 212 on malate dehydrogenase (MDH2) displays slightly lower heavy peak intensity (R = 1.83), and the highly sensitive Cys 845 on ATP citrate synthase (ACLY) shows very low heavy peak intensity. Some of the cysteines displaying high sensitivity to CoA-SNO have been previously reported as sites of *S*-nitrosation or are found on proteins identified as targets of *S*-nitrosation, including Cys 58 of HADH2 (R = 3.02) and Cys 329 on CTSD (R = 4.48), which were previously reported by our lab as targets of GSNO-mediated transnitrosation (Fig 2-3A, inset). We also observed the well-characterized nitrosation sensitive Cys 152 of glyceraldehyde-3-phosphate dehydrogenase (GAPDH) displaying high sensitivity to CoA-SNO (R = 4.9). *S*-nitrosation at this site is known to result in GAPDH translocation from the cytosol to the nucleus[23–25], and propagate nitric oxide signaling by GAPDH-SNO mediated transnitrosation of the nuclear proteins sirtuin-1 (SIRT1)[26], histone deacetylase 2 (HDAC2)[26], DNA dependent protein kinase (DNA-PK)[26], and nucleophosmin[27]. Identification of previously annotated nitrosation events validates our method to identify functionally relevant SNO events. Additionally, there are numerous cysteines highly susceptible to CoA-SNO mediated nitrosation that are not previously annotated and would be considered novel protein nitrosation targets, including enzymes involved in various metabolic processes, such as ornithine aminotransferase (OAT), an enzyme involved in amino acid biosynthesis.

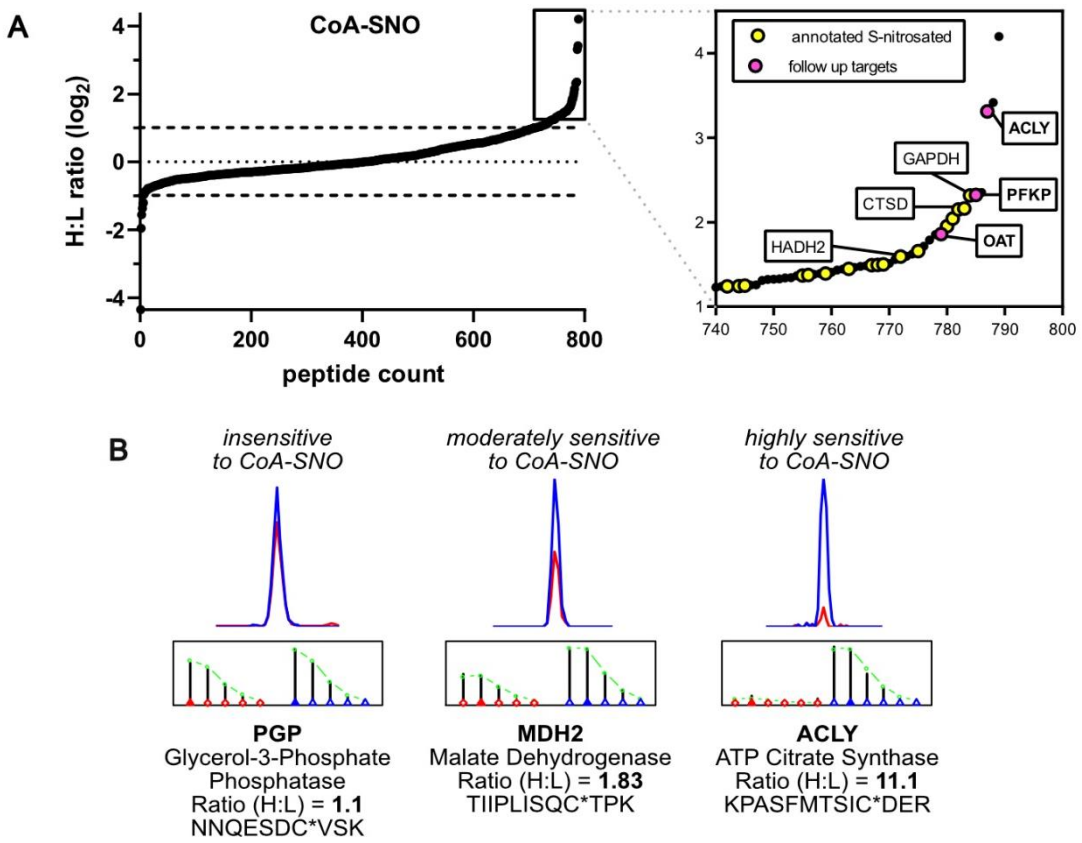

Figure 2-3 Identifying cysteines sensitive to CoA-SNO mediated transnitrosation. **(A)** Heavy:light ratios (*R*) are shown for 789 cysteine residues identified in response to CoA-SNO treatment (n=2). **(B)** representative extracted ion chromatograms and isotopic envelopes (light = red; heavy = blue) are shown for three cysteine residues with low, moderate, and high sensitivity to CoA-SNO. Ratio values are averaged across the different charge states identified, but displayed chromatograms are for a single representative charge state.

index	Uniprot ID	description	symbol	sequence	cysteine position	*R* value
772	Q99714	3-hydroxyacyl-CoA dehydrogenase type-2	HSD17B10	LGNNCVFAPADVTSEK	C58	3.02
773	Q9BQE3	Tubulin alpha-1C chain	TUBA1C	AYHEQLTVAEITNACFE PANQMVK	C295	3.02
774	P04350	Tubulin beta-4A chain	TUBB4A	LTTPTYGDLNHLVSATM SGVTTCLR	C239	3.08
775	P68363	Tubulin alpha-1B chain	TUBA1B	AYHEQLSVAEITNACFE PANQMVK	C295	3.16
776	Q92947	Glutaryl-CoA dehydrogenase, mitochondrial	GCDH	GYGCAGVSSVAYGLLAR	C115	3.29
777	Q15005	Signal peptidase complex	SPCS2	SGGSGGCSGAGGASNC	C17	3.45

		subunit 2		GTGSGR		
777	Q15005	Signal peptidase complex subunit 2	SPCS2	SGGSGGCSGAGGASNC GTGSGR	C26	3.45
778	Q9BSD7	Cancer-related nucleoside-triphosphatase	NTPCR	NADCSSGPGQR	C101	3.62
779	P04181	Ornithine aminotransferase, mitochondrial	OAT	VLPMNTGVEAGETACK	C150	3.63
780	P62888	60S ribosomal protein L30	RPL30	VCTLAIIDPGDSDIIR	C92	3.87
781	P07858	Cathepsin B	CTSB	ICEPGYSPTYK	C211	4.12
782	P31749	RAC-alpha serine/threonine-protein kinase	AKT1	TFCGTPEYLAPEVLEDN DYGR	C310	4.44
783	P07339	Cathepsin D	CTSD	AIGAVPLIQGEYMIPCEK	C329	4.48
784	P04406	Glyceraldehyde-3-phosphate dehydrogenase	GAPDH	IISNASCTTNCLAPLAK	C152	4.98
785	Q01813	ATP-dependent 6-phosphofructokinase, platelet type	PFKP	LPLMECVQMTQDVQK	C360	5.01
786	P25398	40S ribosomal protein S12	RPS12	LGEWVGLCK	C92	5.10
787	P53396	ATP-citrate synthase	ACLY	PASFMTSICDER	C845	9.92
788	P14314	Glucosidase 2 subunit beta	PRKCSH	YEQGTGCWQGPNR	C471	10.68
789	Q8NFG4	Folliculin	FLCN	VFEAEQFGCPQR	C215	18.35

Table 2-2 Cysteines highly sensitive to CoA-SNO mediated nitrosation with R >3.

A control experiment comparing both light and heavy samples left untreated by CoA-SNO displayed 509 cysteines, all with R values < 2, confirming that our MS approach works to accurately identify cysteines highly sensitive to CoA-SNO treatment (Fig 2-4, Appendix I Table A2-2).

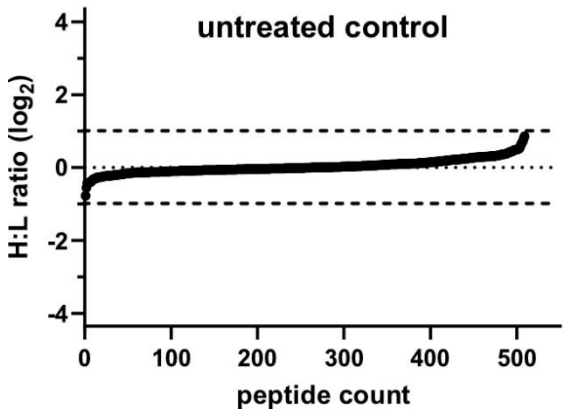

Figure 2-4 Heavy:light ratios (*R*) are shown for 509 cysteine residues identified in an untreated vs untreated control

2.2.2 Assessing the selectivity of CoA-SNO mediated *S*-nitrosation

Because transnitrosation reactions occur through small molecule-protein and protein-protein interactions, we hypothesized that a specific NO donor may target a unique subset of protein cysteine thiols. To address the question of selectivity, we compared cysteine targets of CoA-SNO to targets of other nitrosation donors. We used the transnitrosation donor, GSNO, and the nitric oxide NO donor, propylamine propylamine (PAPA) NONOate, a diazenium diolate that spontaneously dissociates ($t_{1/2}$ = 15 min) to produce two equivalents of NO. By incorporating the treatment of MCF7 lysates with 200 μM GSNO or PAPA NONOate (rather than CoA-SNO) for 1 hour at 37 °C into our chemoproteomic workflow (Fig 2-2), we were able to monitor 1038 cysteines with a heavy:light ratio in response to GSNO (Fig 2-5A, Appendix I Table A2-3), and 985 cysteines in response to PAPA NONOate (Fig 2-5B, Appendix I Table A2-4). Similar to CoA-SNO, both GSNO and PAPA NONOate display a subset of cysteine targets highly sensitive to *S*-nitrosation, with 24 cysteines

displaying *R* >3 in response to GSNO and 30 cysteines with *R* >3 in response to PAPA NONOate. Many of the cysteines highly sensitive to GSNO or PAPA NONOate were found on proteins that were previously annotated as targets of *S*-nitrosation including CTSD and GAPDH. (Fig 2-4A inset, 2-4B inset).

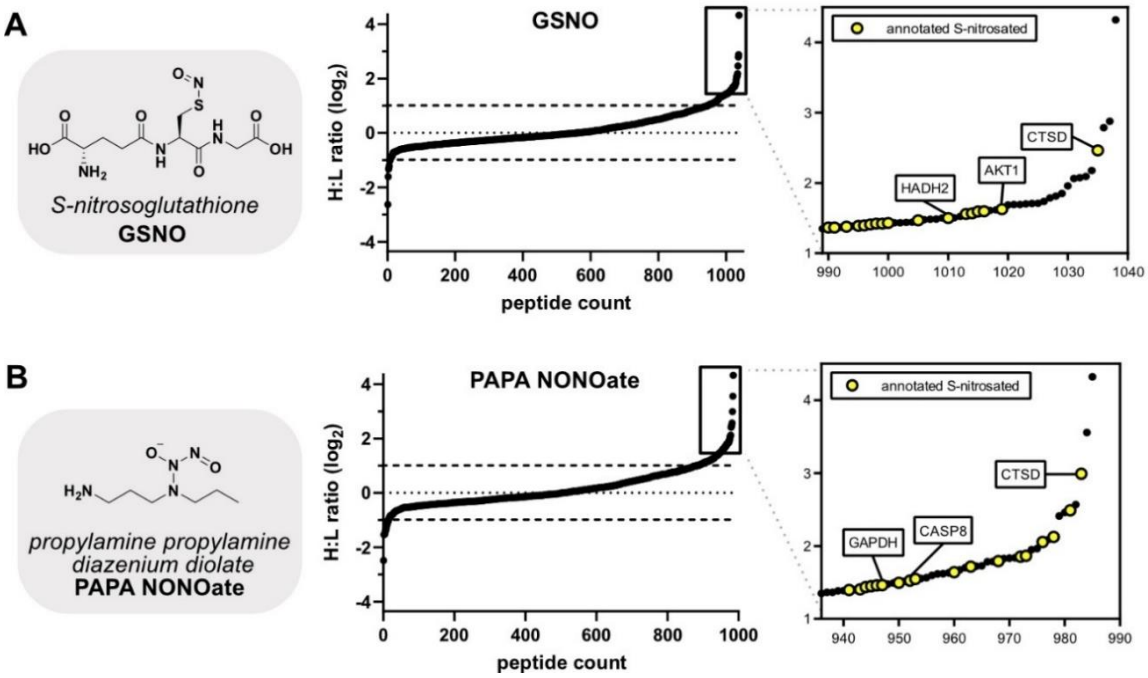

Figure 2-5 Structures of NO donors and heavy:light ratios (*R*) shown for **(A)** 1038 cysteine residues identified in GSNO treated MS analysis (n=2). Inset displays 50 most sensitive cysteines to GSNO treatment **(B)** 985 cysteine residues identified in PAPA NONOate treated MS sample (n=2). Inset displays 50 most sensitive cysteines to PAPA NONOate treatment. Previously annotated sites of nitrosation shown in yellow.

We observed 429 cysteines present with a calculated *R* value across all three datasets and directly compared individual cysteine sensitivity to the each nitrosation donor (Fig 2-6A, Appendix I Table A2-5). There are many cysteines sensitive to *S*-nitrosation by all 3 donors, however there are some cysteines uniquely sensitive to CoA-SNO mediated transnitrosation. Cys 329 on CTSD is an example of a cysteine sensitive to all 3 nitrosation donors, displaying *R* >3 in

response to CoA-SNO, GSNO, and PAPA NONOate. Alternatively, Cys 845 on ACLY displays a *R* value of 9.9 in response to CoA-SNO treatment, while both GSNO and PAPA NONOate treatment resulted in a *R* value ~1, indicating Cys 845 of ACLY is uniquely sensitive to CoA-SNO mediated *S*-nitrosation, but not GSNO or PAPA NONOate mediated nitrosation (Fig 2-6B).

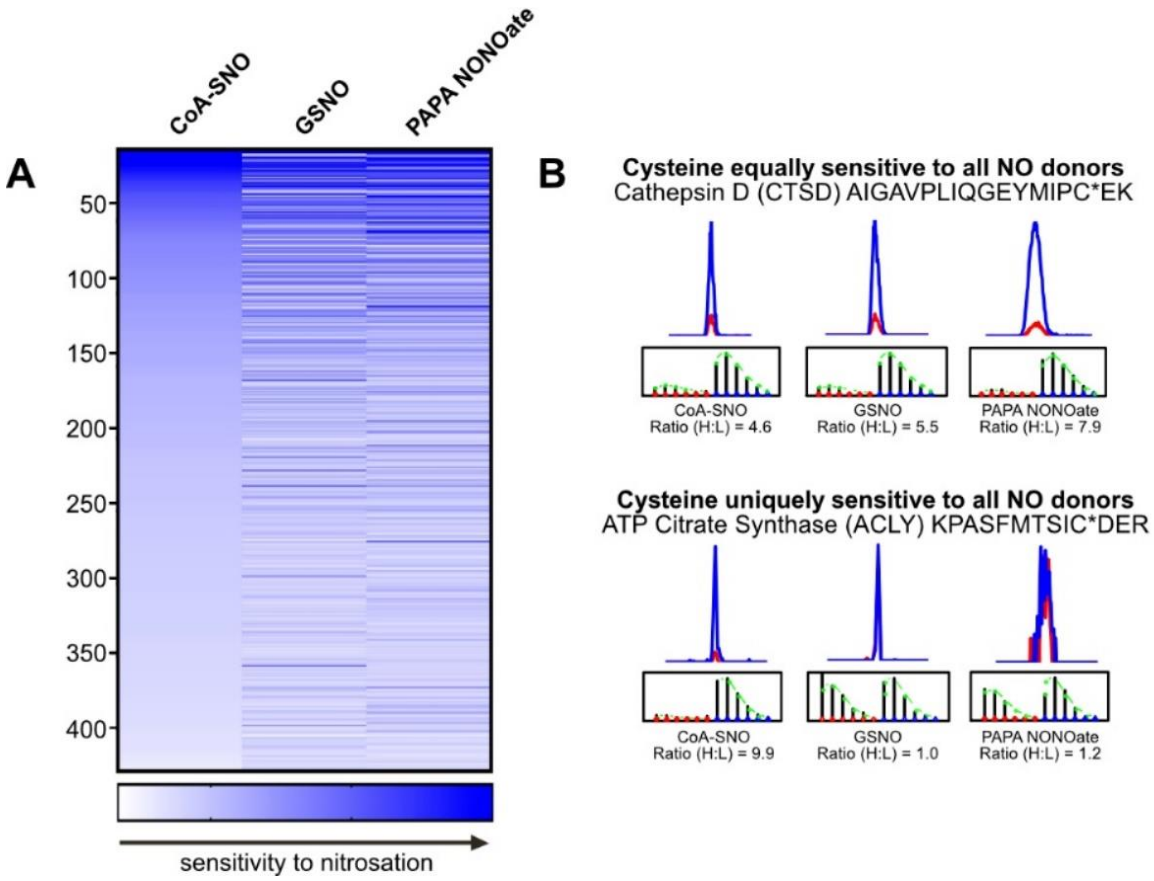

Figure 2-6 Assessing target selectivity of CoA-SNO. **(A)** Heatmap comparing the sensitivity of 489 individual cysteine residues to each of the NO donors: CoA-SNO, GSNO, and PAPA NONOate. Darker blue indicates higher sensitivity to the corresponding NO donor. **(B)** Extracted ion chromatograms display cysteines with differential sensitivity to the various NO donors, with Cys 329 CTSD being highly sensitive to CoA-SNO, GSNO, and PAPA NONOate and Cys 845 ACLY being highly sensitive to CoA-SNO, but insensitive to GSNO or PAPA NONOate.

Focusing in on the top 50 cysteine containing peptides identified as highly sensitive to CoA-SNO, GSNO, and PAPA NONOate, there was some overlap as cysteines within 10 different proteins identified as highly sensitive to all 3 NO donors, including known protein-SNO events on cathepsin B (CTSB), receptor for activated C kinase 1 (RACK1), alpha serine/threonine protein kinase 1(AKT1) (Fig 2-7). However, there were at least 20 unique cysteine containing proteins sensitive to each NO donor, many of which are uncharacterized as targets of nitrosation including the cancer-related nucleoside-triphosphatase (NTPCR) as a target of CoA-SNO, the mitochondrial matrix processing protease (MBBP) as a target of GSNO, and amidophosphoribosyltransferase (PPAT) as a target of PAPA NONOate. To understand the biological processes of the proteins most sensitive to each NO donor, we performed a gene ontology (GO) PANTHER overrepresentation test, with some biological processes overlapping and some unique to each NO donor (Table 2-2). Enrichment for glycolytic process and/or tricarboxylic acid cycle was observed in response to all 3 NO donors, which is consistent with previous reports of regulatory role *S*-nitrosation in metabolic processes[17,28]. Interestingly, Acyl-CoA dehydrogenase fatty acid beta-oxidation, a process in which CoA is added to a fatty acid, displayed over 100-fold enrichment in the subset of proteins most sensitive to CoA-SNO, but this process was not enriched in response to either GSNO or PAPA NONOate, suggesting target differentiation for the different NO donors.

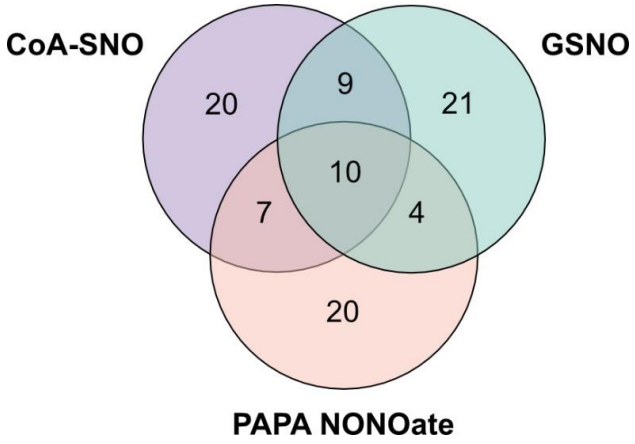

Figure 2-7 Overlap of cysteine containing proteins highly sensitive to CoA-SNO, GSNO, and PAPA NONOate. Out of the top 50 cysteine containing peptides, proteins were only counted once if more than cysteine containing peptide on the same protein was highly sensitive to a particular NO donor.

NO Donor	GO biological process	fold enrichment	raw P-value
CoA-SNO	fatty acid beta-oxidation using acyl-CoA dehydrogenase	> 100	3.71E-06
	branched-chain amino acid catabolic process	63.94	2.03E-05
	NADH metabolic process	39.49	7.64E-05
	glycolytic process	31.97	1.38E-04
	positive regulation of protein localization to nucleus	25.15	2.08E-06
	glucose metabolic process	19.63	6.65E-06
	alpha-amino acid catabolic process	19.46	6.18E-05
	cytoplasmic translation	14.44	1.88E-04
	regulation of intrinsic apoptotic signaling pathway	13.4	3.95E-05
	protein stabilization	10.27	1.35E-04
	regulation of establishment of protein localization	5.95	1.67E-04
	response to organic substance	2.65	1.57E-04
GSNO	tricarboxylic acid cycle	45.28	5.17E-05
	cytoplasmic translation	26.42	1.12E-08
	carbohydrate metabolic process	6.9	6.59E-05
	carboxylic acid metabolic process	5.12	5.32E-05
PAPA NONOate	NADH metabolic process	44.31	5.40E-05
	hexose catabolic process	38.63	7.93E-05
	glycolytic process	35.87	9.76E-05
	glucose metabolic process	26.43	1.30E-07
	cytoplasmic translation	24.3	2.09E-07
	fatty acid catabolic process	23.63	2.90E-05
	regulation of peptidase activity	7.78	3.01E-05

Table 2-2 Gene Ontology PANTHER biological process overrepresentation test for the top 50 cysteine containing proteins sensitive to CoA-SNO, GSNO, and PAPA NONOate

Certain factors have been identified to impart selectivity for target *S*-nitrosothiol formation (see section 1.2.2), including the presence of acid/base or tyrosine groups ~8Å from the target cysteine, or a highly hydrophobic local environment[29–32]. A potential consensus sequence, [I/L]-XC-X2-[D/E], has been identified to direct site selective *S*-nitrosation for the iNOS/S100A8/S100A9 protein scaffolding transnitrosation complex[33]. Similarly, we wondered if particular nitrosation donors selectively modify cysteines with a specific sequence motif surrounding the target residue. We searched the 50 cysteine containing peptides most sensitive to CoA-SNO, GSNO, and PAPA NONOate for an emerging sequence motif and compared to the median 50 peptides that were insensitive to each NO donor. There was no emergence of a sequence motif in the cysteine containing peptides highly sensitive or insensitive to each NO donor, indicating the surrounding primary sequence does not impart selectivity (Fig 2-8A). Furthermore, we hypothesized that a NO donor could target specific cysteine containing protein though a binding event. We interrogated the 50 cysteine containing peptides most sensitive to CoA-SNO, GSNO, and PAPA NONOate for binding of cofactors, and observed that there was a significant increase in binding of cofactors with CoA structural similarity ATP, GTP, FAD, and NAD, however this trend occurred in response to all 3 NO donors (Fig 2-8B).

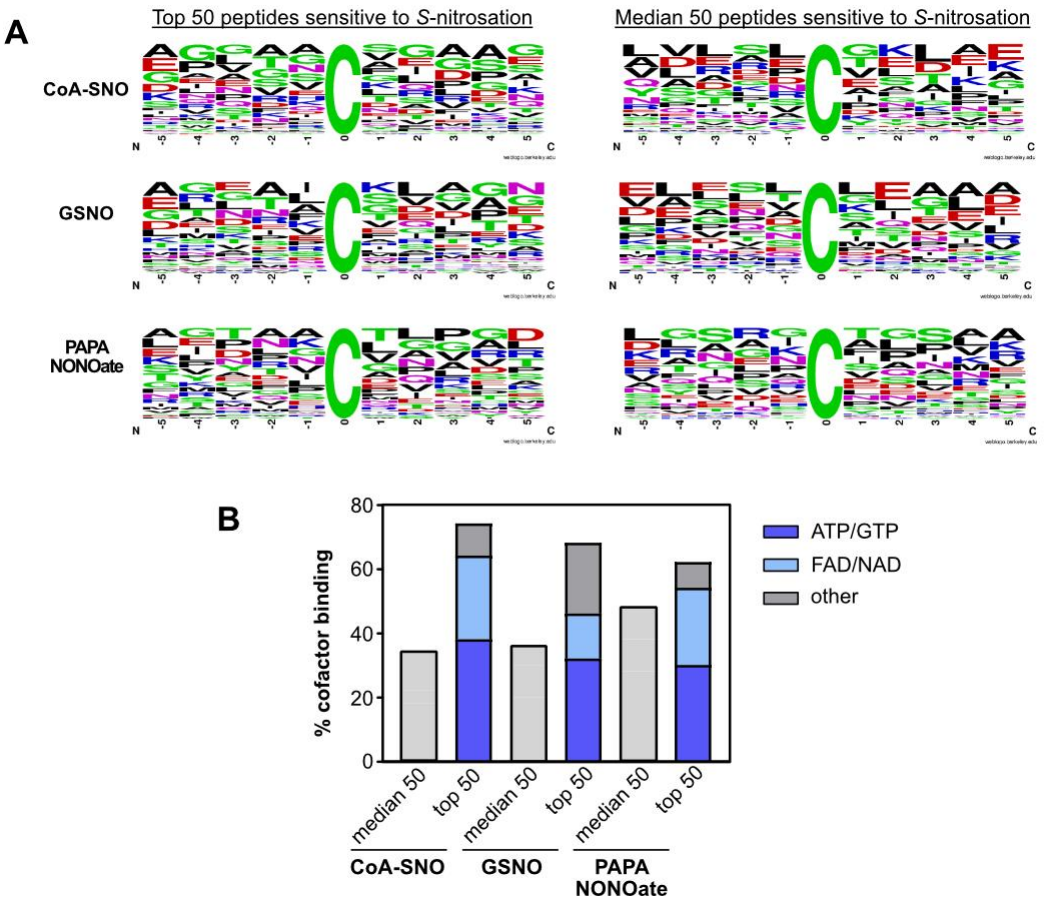

Figure 2-8 Interrogating factors that determine selectivity to NO donors. **(A)** Distribution of 5 amino acids on either side of the 50 cysteines most sensitive and 50 cysteines with median sensitivity to CoA-SNO, GSNO, and PAPA NONOate **(B)** cofactor binding of the top 50 and median 50 cysteine containing proteins sensitive to CoA-SNO, GSNO, and PAPA NONOate. Cofactors with CoA-similar structures (ATP, GTP, FAD, NAD).

2.3 CONCLUSIONS

S-nitrosation is a cysteine post-translational modification (PTM) fundamental to cellular signaling, propagating its signal via transnitrosation reactions in which a small molecule or protein nitrosothiol transfers it's NO group to a free thiol. The recent identification of AKR1A1 as a protein with selective *S*-nitroso-coenzyme A (CoA-SNO) reductase activity provided the first evidence of coenzyme A

involvement in *S*-nitrosation. The protein targets of specific transnitrosation donors, especially CoA-SNO have not been thoroughly characterized and up until this study there had been no proteomic dataset of CoA-SNO protein targets that identified the site and extent of modification at individual cysteines. Using a competitive chemical proteomic approach, we were able to quantify the extent of *S*-nitrosation on almost 800 cysteine residues in response to CoA-SNO, with a subset of cysteines highly susceptible to *S*-nitrosation, some of which are previously uncharacterized sites of *S*-nitrosation. Furthermore, we profiled the GSNO dependent nitrosoproteome and PAPA NONOate dependent nitrosoproteome, respectively ranking 1038 and 985 individual cysteine residues by their sensitivity to each NO donor. Identification of cysteines sensitive to the transnitrosating agent, GSNO, and the NO donor and PAPA-NONOate, facilitate the identification of targets with unique and generic sensitivity to CoA-SNO mediated transnitrosation. Despite attempts to understand the selectivity of the various NO donors, there was no emerging sequence motif surrounding cysteines most sensitive to nitrosation, and enrichment of cofactor binding was observed in response to all three NO donors. With these data, we can further interrogate the functional role of CoA-SNO mediated *S*-nitrosation on target proteins that remain poorly characterized.

The cysteine-profiling platform described in this work affords several advantages over the biotin switch technique and other methods to detect nitrosothiols, primarily due to the ability to quantify the extent of modification of individual cysteine residues. However, limitations currently exist that may be improved in subsequent iterations of this platform. The platform is optimized for

analysis of cell lysates treated with exogenous NO donors at supraphysiological concentrations. The data obtained provide important insight into the sensitivity of hundreds of cysteines to CoA-SNO, GSNO, and PAPA NONOate treatment, although it is possible targets may not be *S*-nitrosated to the extent predicted in vitro due to either lower cellular levels of CoA-SNO, GNSO, or NO/RNS or instability in different subcellular reducing environments. A genetic knockdown of denitrosation enzymes could serve as a way to identify and quantify more endogenously relevant SNO events. Additionally, because this method reports on a loss in cysteine reactivity with the iodoacetamide-alkyne probe, it is not guaranteed that this change in reactivity is due to nitrosation, and could be a result of another oxidative modification (sulfenic acid or disulfide bond formation). Therefore, proteins identified as targets of nitrosation should be validated using another method, such as the BST. Furthermore, the sensitivity of the current platform does not allow accurate quantification when the stoichiometry of modification is less than 5%.

2.4 METHODS

Synthesis of S-nitroso-Coenzyme A (CoA-SNO)

CoA-SNO was generated according to methods reported by Anand *et al*[34]. Briefly equal volumes of 0.3 M Coenzyme A (CoA) trihydrate, free acid (prepared in 1 M HCl) and 0.3 M sodium nitrate (NaNO2, prepared in a solution containing 100 μM diethylenetriaminepentaacetic acid (DTPA), 100 μM ethylenediaminetetraacetic

acid (EDTA)) were combined and incubating on ice for 30 min under low light conditions. The CoA-SNO concentration was determined by measuring the UV absorbance at 336 nm based on the extinction coefficient, $\varepsilon = 0.92\ mM^{-1}\ cm^{-1}$. CoA-SNO was diluted as needed in 0.5 M HCl.

Synthesis of *S*-nitrosoglutathione (GSNO)

S-nitrosoglutathione (GSNO) according to methods reported by Hart *et al*[35]. Briefly, ice cold 5 mM glutathione (GSH) dissolved in 2N HCl was combined with 5 mM $NaNO_2$ and incubated with stirring at 4°C for 40 min under low light conditions. GSNO was precipitated upon the addition of ice-cold acetone for 10 min at 4°C. The resulting pink solid was filtered and washed with H_2O, acetone, and ether and dried under house vac to afford *S*-nitrosoglutathione. *S*-nitrosoglutathione (GSNO) was dissolved in freshly made HEN buffer (125 mM 4-(2-hydroxyethyl)-1-piperazineethanesulfonic acid (HEPES) pH 7.7, 1 mM EDTA, 0.1 mM neocuproine). The GSNO concentration was determined by measuring the UV absorbance at 336 nm based on the extinction coefficient), $\varepsilon = 0.92\ mM^{-1}\ cm^{-1}$. GSNO was diluted as needed in HEN buffer.

Cell culture and lysate preparation

MCF7 cells were cultured at 37 °C under an atmosphere of 5% CO2 in RPMI 1640 medium (Corning) supplemented with 10% FBS (Atlanta Biologicals) and 1% Anti-Anti (25 µg/mL Amphotecerin B, 10,000 units/mL penicillin, 10,000 µg/mL streptomycin, Gibco). Upon reaching 100% confluency, cells were harvested by

scraping, washed three times with PBS, resuspended in an appropriate volume of PBS. Cell suspensions were sonicated using an ultrasonic tip sonicator (Cole Parmer) to obtain whole cell lysates. Lysates were centrifuged at 45,000 rpm or 45 min at 4 °C to separate soluble and insoluble lysate fractions. The insoluble fraction was discarded and the soluble fractions protein concentration was determined using the DC Protein Assay kit (Bio-Rad).

Cell lysate treatment with NO donors

Proteome samples were diluted to a 4 mg/mL solution in PBS and divided into 2 x 0.5 mL aliquots. Each aliquot was treated with either the appropriate NO donor (CoA-SNO, GSNO, or PAPA NONOate) to a final concentration of 200 μM or an equal volume of the respective control buffer (0.5 M HCl control for CoA-SNO, HEN buffer for GSNO, or 0.01 M NaOH/PBS for PAPA NONOate) for 1 hour at 37 °C. Excess NO donor was removed by filtration using a Nap-5 column (Cytiva) and proteins were eluted off the column using 1mL PBS, and aliquoted into two 500uL samples.

Chemoproteomic labeling and enrichment of cysteine residues

Each 500uL sample was treated with 100 μM IA-alkyne probe using 5μL of a 10 mM stock in DMSO[21]. The labeling reactions were incubated at room temperature for 1 hour. Click chemistry was performed by the addition of either the Light-Azo-Tag (NO donor treated sample) or Heavy-Azo-Tag (control sample) (100 μM, 5 mM stock in DMSO), 1 mM TCEP (fresh 50X stock in water), 100 μM TBTA

ligand (17X stock in DMSO:t-Butanol 1:4), and 1 mM $CuSO_4$ (50X stock in water). Samples were allowed to react at room temperature for 1 hour. The Azo-L and Azo-H samples were then mixed together and precipitated proteins were pelleted by centrifugation at 6500 x g (10 min, 4°C). Protein pellets were washed three times with cold methanol, after which pellets were solubilized in PBS containing 1.2% w/v SDS via sonication and heating (10 min, 80 °C).

The SDS-solubilized, probe-labeled proteome samples were diluted with PBS to a final SDS concentration of 0.2% w/v. The solutions were then incubated with 100 µL of streptavidin-agarose beads overnight at 4 °C, followed by incubation at room temperature for 2 hours. The beads were washed sequentially with one 0.2% SDS/PBS wash, three PBS washes, and three water washes with centrifugation (1,400 x *g,* 3 min) between washes to pellet the beads.

On-bead trypsin and Azo digestion

The washed beads were suspended in 500 µL of 6 M urea/PBS and 10 mM dithiothreitol (DTT, from 20X stock in water). Samples were incubated at 65 °C for 15 minutes. 20 mM iodoacetamide (from 50X stock in water) was then added and incubated at 37 °C with rotating for 30 minutes. Following reduction and alkylation, the sample was diluted 3-fold with PBS and centrifuged at 1,400 x *g* for 2 minutes to pellet the beads. The beads were resuspended in a mixture of 200 µL of 2 M urea/PBS, 1 mM $CaCl_2$ (100X stock in water), and trypsin (2 µg). The digestion was allowed to proceed overnight at 37 °C. The digest was separated from the beads using a mini centrifuge (Chemglass Life Sciences) and the beads were washed three

times with PBS, and three times with H_2O. Azo-labeled peptides were cleaved from the beads using 50 µL of 50 mM sodium hydrosulfite ($Na_2S_2O_4$) rotating at room temperature for 1 hour, and the supernatant was collected. 50 mM Sodium hydrosulfite (2 x 75 µL) was added to beads 2 more times with 1-hour incubations to cleave any remaining peptides from the beads. The beads were washed with 2 x 75 µL of H_2O and the washes were combined with the cleaved peptide fractions from above. Formic acid (17.5 µL) was added to the sample, which was stored at -20 °C until mass spectrometry analysis.

LC/LC-MS/MS and data analysis for isoTOP-ABPP

LC/LC-MS/MS analysis was performed on an LTQ-Orbitrap Discovery mass spectrometer (Thermo Scientific) coupled to an Agilent 1200 series HPLC. Azo digests were pressure loaded onto a 250 µm fused silica desalting column packed with 4 cm of Aqua C18 reverse phase resin (Phenomenex). The peptides were then eluted onto a biphasic column (100 µm fused silica with a 5 µm tip, packed with 10 cm C18 and 4 cm Partisphere strong cation exchange resin (SCX, Whatman) using a five-step multidimensional LC/LC-MS/MS protocol (MudPIT)[36]. Each of the five steps used a salt push (0%, 50%, 80%, 100%, 100%), followed by a gradient of 5-100% Buffer B in Buffer A (Buffer A: 95% water, 5% acetonitrile, 0.1% formic acid; Buffer B: 20% water, 80% acetonitrile, 0.1% formic acid). The flow rate through the column was set to ~0.25 µL/min and the spray voltage was set to 2.75 kV. One full MS1 scan (400-1800 MW or m/z) was followed by 8 data dependent scans of the n^{th} most intense ions with dynamic exclusion enabled.

The generated tandem MS data were searched using the SEQUEST algorithm against the *Homo Sapiens* UniProtKB database. A static modification of +57.02146 on cysteine was specified to account for iodoacetamide alkylation and differential modifications of +456.2849 (Azo-L modification) and +462.2987 (Azo-H modification) were specified on cysteine to account for probe modifications. SEQUEST output files were filtered using DTASelect 2.0. Quantification of heavy:light ratios (*R*) was performed using the CIMAGE quantification package as previously described and ratios were normalized to the median ratio of the corresponding dataset[21]. Considered cysteine containing peptides were required to be identified in two replicate datasets and have a heavy:light ratio within a 2-fold increase or decrease compared to the replicate value.

Statistical analysis of overrepresented gene ontology (GO) process using PANTHER

Panther overrepresentation gene ontology tests (http://pantherdb.org)[37] were performed on the top 50 cysteine containing proteins sensitive to each NO donor. Enriched processes were determined by GOrilla using a ranked gene ontology (GO) analysis and FDR corrected for multiple testing using Benjamini and Hochberg and Fisher methods. Enrichment (E) was defined in terms of the number of intersecting genes (b) over the number of top genes in the target set (n) divided by the total number of genes correlated to a unique GO term (B) over the total number of genes analyzed (N) (E = (b/n) / (B/N).

REFERENCES

(1) Anand, P.; Stamler, J. S. Enzymatic Mechanisms Regulating Protein S-Nitrosylation: Implications in Health and Disease. *J. Mol. Med.* **2012**, *90* (3), 233–244.

(2) Wynia-Smith, S. L.; Smith, B. C. Nitrosothiol Formation and S-Nitrosation Signaling through Nitric Oxide Synthases. *Nitric Oxide* **2017**, *63*, 52–60.

(3) Houk, K. N.; Hietbrink, B. N.; Bartberger, M. D.; McCarren, P. R.; Choi, B. Y.; Voyksner, R. D.; Stamler, J. S.; Toone, E. J. Nitroxyl Disulfides, Novel Intermediates in Transnitrosation Reactions. *J. Am. Chem. Soc.* **2003**, *125* (23), 6972–6976.

(4) Perissinotti, L. L.; Turjanski, A. G.; Estrin, D. A.; Doctorovich, F. Transnitrosation of Nitrosothiols: Characterization of an Elusive Intermediate. *J. Am. Chem. Soc.* **2005**, *127* (2), 486–487.

(5) Lai, C. H.; Chou, P. T. The Theoretical Comparison between Two Model NO Carriers, MeSNO and MeSeNO. *J. Mol. Model.* **2008**, *14* (1), 1–9.

(6) Broniowska, K. A.; Hogg, N. The Chemical Biology of S-Nitrosothiols. *Antioxid. Redox Signal.* **2012**, *17* (7), 969–980.

(7) Smith, B. C.; Marletta, M. A. Mechanisms of S-Nitrosothiol Formation and Selectivity in Nitric Oxide Signaling. *Curr. Opin. Chem. Biol.* **2012**, *16* (5–6), 498–506.

(8) Barnett, S. D.; Buxton, I. L. O. The Role of S-Nitrosoglutathione Reductase (GSNOR) in Human Disease and Therapy. *Crit. Rev. Biochem. Mol. Biol*. **2017**, 340–354.

(9) Bateman, R. L.; Rauh, D.; Tavshanjian, B.; Shokat, K. M. Human Carbonyl Reductase 1 Is an S-Nitrosoglutathione Reductase. **2008**. *283* (51). 35756-35762.

(10) Sengupta, R.; Ryter, S. W.; Zuckerbraun, B. S.; Tzeng, E.; Billiar, T. R.; Stoyanovsky, D. A. Thioredoxin Catalyzes the Denitrosation of Low-Molecular Mass and Protein S-Nitrosothiols. *Biochemistry* **2007**, *46*, 10.

(11) Staab, C. A.; Ålander, J.; Brandt, M.; Lengqvist, J.; Morgenstern, R.; Grafström, R. C.; Höög, J. O. Reduction of S-Nitrosoglutathione by Alcohol Dehydrogenase 3 Is Facilitated by Substrate Alcohols via Direct Cofactor Recycling and Leads to GSH-Controlled Formation of Glutathione Transferase Inhibitors. *Biochem. J.* **2008**, *413* (3), 493–504.

(12) Leonardi, R.; Zhang, Y. M.; Rock, C. O.; Jackowski, S. Coenzyme A: Back in Action. *Prog. Lipid Res.* **2005**, *44* (2–3), 125–153.

(13) Begley, T. P.; Kinsland, C.; Strauss, E. The Biosynthesis of Coenzyme a in Bacteria. *Vitam. Horm.* **2001**, *61*, 157–171.

(14) Anand, P.; Hausladen, A.; Wang, Y.-J.; Zhang, G.-F.; Stomberski, C.; Brunengraber, H.; Hess, D. T.; Stamler, J. S. Identification of S-Nitroso-CoA Reductases That Regulate Protein S-Nitrosylation. *Proc. Natl. Acad. Sci.* **2014**, *111* (52), 18572–18577.

(15) Stomberski, C. T.; Anand, P.; Venetos, N. M.; Hausladen, A.; Zhou, H. L.; Premont, R. T.; Stamler, J. S. AKR1A1 Is a Novel Mammalian S-Nitroso-Glutathione Reductase. *J. Biol. Chem.* **2019**, *294* (48), 18285–18293.

(16) Stomberski, C. T.; Zhou, H.-L.; Wang, L.; van den Akker, F.; Stamler, J. S. Molecular Recognition of S-Nitrosothiol Substrate by Its Cognate Protein Denitrosylase. *J. Biol. Chem.* **2019**, *294* (5), 1568–1578.

(17) Zhou, H.-L.; Zhang, R.; Anand, P.; Stomberski, C. T.; Qian, Z.; Hausladen, A.; Wang, L.; Rhee, E. P.; Parikh, S. M.; Karumanchi, S. A.; et al. Metabolic Reprogramming by the S-Nitroso-CoA Reductase System Protects against Kidney Injury. *Nature* **2019**, *565* (7737), 96–100.

(18) Stomberski, C. T.; Venetos, N. M.; Zhou, H. L.; Qian, Z.; Collison, B. R.; Field, S. J.; Premont, R. T.; Stamler, J. S. A Multienzyme S-Nitrosylation Cascade Regulates Cholesterol Homeostasis. *Cell Rep.* **2022**, *41* (4), 111538.

(19) Zhou, Y.; Wynia-Smith, S. L.; Couvertier, S. M.; Kalous, K. S.; Marletta, M. A.; Smith, B. C.; Weerapana, E. Chemoproteomic Strategy to Quantitatively Monitor Transnitrosation Uncovers Functionally Relevant S-Nitrosation Sites on Cathepsin D and HADH2. *Cell Chem. Biol.* **2016**, *23* (6), 727–737.

(20) Rostovtsev, V. V; Green, L. G.; Fokin, V. V; Sharpless, K. B. A Stepwise Huisgen Cycloaddition Process: Copper(I)-Catalyzed Regioselective "Ligation" of Azides and Terminal Alkynes. *Angew. Chem. Int. Ed* **2002**, *41* (14), 2596–2599.

(21) Weerapana, E.; Wang, C.; Simon, G. M.; Richter, F.; Khare, S.; Dillon, M. B. D.; Bachovchin, D. A.; Mowen, K.; Baker, D.; Cravatt, B. F. Quantitative Reactivity Profiling Predicts Functional Cysteines in Proteomes. *Nature* **2010**, *468* (7325), 790–795.

(22) Qian, Y.; Martell, J.; Pace, N. J.; Eric Ballard, T.; Johnson, D. S.; Weerapana, E. An Isotopically Tagged Azobenzene-Based Cleavable Linker for Quantitative Proteomics. *ChemBioChem* **2013**, *14* (12), 1410–1414.

(23) Tristan, C.; Shahani, N.; Sedlak, T. W.; Sawa, A. The Diverse Functions of GAPDH: Views from Different Subcellular Compartments. *Cell. Signal.* **2011**, *23* (2), 317–323.

(24) Li, C.; Feng, J. J.; Wu, Y. P.; Zhang, G. Y. Cerebral Ischemia-Reperfusion Induces GAPDH S-Nitrosylation and Nuclear Translocation. *Biochem.* **2012**, *77* (6), 671–678.

(25) Inadomi, C.; Murata, H.; Ihara, Y.; Goto, S.; Urata, Y.; Yodoi, J.; Kondo, T.; Sumikawa, K. Overexpression of Glutaredoxin Protects Cardiomyocytes against Nitric Oxide-Induced Apoptosis with Suppressing the S-Nitrosylation of Proteins and Nuclear Translocation of GAPDH. *Biochem. Biophys. Res. Commun.* **2012**, *425* (3), 656–661.

(26) Kornberg, M. D.; Sen, N.; Hara, M. R.; Juluri, K. R.; Nguyen, J. V. K.; Snowman, A. M.; Law, L.; Hester, L. D.; Snyder, S. H. GAPDH Mediates Nitrosylation of Nuclear Proteins. *Nat. Cell Biol.* **2010**, *12* (11), 1094–1100.

(27) Lee, S. B.; Kim, C. K.; Lee, K. H.; Ahn, J. Y. S-Nitrosylation of B23/Nucleophosmin by GAPDH Protects Cells from the SIAH1–GAPDH Death Cascade. *J. Cell Biol.* **2012**, *199* (1), 65–76.

(28) Bruegger, J. J.; Smith, B. C.; Wynia-Smith, S. L.; Marletta, M. A. Comparative and Integrative Metabolomics Reveal That S-Nitrosation Inhibits Physiologically Relevant Metabolic Enzymes. *J. Biol. Chem.* **2018**, *293*, 6282–6296.

(29) Morris, G.; Walder, K.; Carvalho, A. F.; Tye, S. J.; Lucas, K.; Berk, M.; Maes, M. The Role of Hypernitrosylation in the Pathogenesis and Pathophysiology of Neuroprogressive Diseases. *Neuroscience and Biobehavioral Reviews*. **2018**, 453–469.

(30) Nakamura, T.; Lipton, S. A. Emerging Role of Protein-Protein Transnitrosylation in Cell Signaling Pathways. *Antioxidants and Redox Signaling*. **2013**, 239–249.

(31) Greco, T. M.; Hodara, R.; Parastatidis, I.; Heijnen, H. F. G.; Dennehy, M. K.; Liebler, D. C.; Ischiropoulos, H. Identification of S-Nitrosylation Motifs by Site-Specific Mapping of the S-Nitrosocysteine Proteome in Human Vascular Smooth Muscle Cells. **2006**, *103* (19).

(32) Marino, S. M.; Gladyshev, V. N. Structural Analysis of Cysteine S-Nitrosylation: A Modified Acid-Based Motif and the Emerging Role of Trans-Nitrosylation. *J. Mol. Biol.* **2010**, *395* (4), 844–859.

(33) Jia, J.; Arif, A.; Terenzi, F.; Willard, B.; Plow, E. F.; Hazen, S. L.; Fox, P. L. Target-Selective Protein S-Nitrosylation by Sequence Motif Recognition. *Cell* **2014**,

159 (3), 623–634.

(34) Anand, P.; Hausladen, A.; Wang, Y.-J.; Zhang, G.-F.; Stomberski, C.; Brunengraber, H.; Hess, D. T.; Stamler, J. S. Identification of S-Nitroso-CoA Reductases That Regulate Protein S-Nitrosylation. *Proc. Natl. Acad. Sci.* **2014**, *111* (52), 18572–18577.

(35) Hart, T. W. Some Observations Concerning S-Nitroso-and S-Phenylsulfonyl-Derivatives of L-Cysteine and Glutathione. *Tetrahedron Lett.* **1985**, *26* (16), 2013–2016.

(36) Weerapana, E.; Speers, A. E.; Cravatt, B. F. Tandem Orthogonal Proteolysis-Activity-Based Protein Profiling (TOP-ABPP)—a General Method for Mapping Sites of Probe Modification in Proteomes. *Nat. Protoc.* **2007**, *2* (6), 1414–1425.

(37) Mi, H.; Muruganujan, A.; Casagrande, J. T.; Thomas, P. D. Large-Scale Gene Function Analysis with the PANTHER Classification System. *Nat. Protoc.* **2013**, *8* (8), 1551–1566.

3.0 FUNCTIONAL CHARACTERIZATION OF PROTEINS MODIFIED BY COA-SNO MEDIATED S-NITROSATION

This work was done in collaboration with Sarah Wynia-Smith and Brian C. Smith at Medical College of Wisconsin

3.1 INTRODUCTION

S-nitrosation is a widespread cysteine PTM that is found across all forms of life from bacteria to yeast to humans. Over 4,000 *S*-nitrosation events have been identified (dbSNO 2.0 database), with more recent predictions suggesting up to 10,000 SNO sites (pCysMod) and up to 70% of the human proteome subject to nitrostion[1–4]. *S*-nitrosation is known to impart various effects on proteins that undergo this modification such as modulating protein activity, protein-biomolecule interactions, protein structure, and protein localization[5]. The variety of effects of *S*-nitrosation are exemplified by SNO events on caspase 3 (Casp3), 3-hydroxyacyl-CoA dehydrogenase type 2 (HADH2), and heat shock protein 90 (Hsp90). Constitutive *S*-nitrosation of the active site Cys 163 on Casp3, prevents cleavage of the procaspase to its active form, inhibiting protease activity and suppressing the apoptotic pathway[6]. Cys 58 of HADH2 located distal to the active site plays a functional role as *S*-nitrosation impairs activity, likely though disruption of substrate binding. Cys 521 on the molecular chaperone Hsp90 serves as a conformational switch, where *S*-nitrosation disrupts Hsp90/activator of Hsp90 ATPase activity 1 (AHA1) interaction, inhibiting ATPase activity, and promoting interaction with the cell division cycle 37 protein (CDC37) and subsequent NF-κB signaling[7,8]. Because of the diverse effects nitrosation can have on a protein, it is important to characterize the function of individual cysteine SNO events in order to fully understand the role of *S*-nitrosation in biological processes.

While a subset of target proteins that undergo nitrosation in response to the cellular transnitrosating agent *S*-nitroso-coenzyme A (CoA-SNO) has been identified, the functional role of *S*-nitrosation on individual CoA-SNO target proteins has only been characterized for PKM2, and the SAR1/SURF4/PCSK9 transnitrosation cascade (see chapter 2). Based on the CoA-SNO dependent proteomic dataset we generated in chapter 2 (Fig 3-1) 18 cysteines were identified as highly sensitive to CoA-SNO mediated *S*-nitrosation (Table 2-1) and we looked to further understand the role of these individual SNO events. To choose relevant protein-SNO targets for further characterization, we mined for cysteines that met the following criteria: (1) demonstrated high sensitivity to CoA-SNO mediated transnitrosation (R > 3); (2) the function of the SNO event was not well understood; (3) were found on enzymes involved in metabolic pathways and implicated in human disease; and (4) were able to be recombinantly expressed for in vitro assays. We settled on three proteins to functionally characterize the role of *S*-nitrosation: phosphofructokinase, platelet type (PFKP), ATP citrate synthase (ACLY), and ornithine aminotransferase (OAT), with the goal of demonstrating the functional effects of *S*-nitrosation on these protein targets.

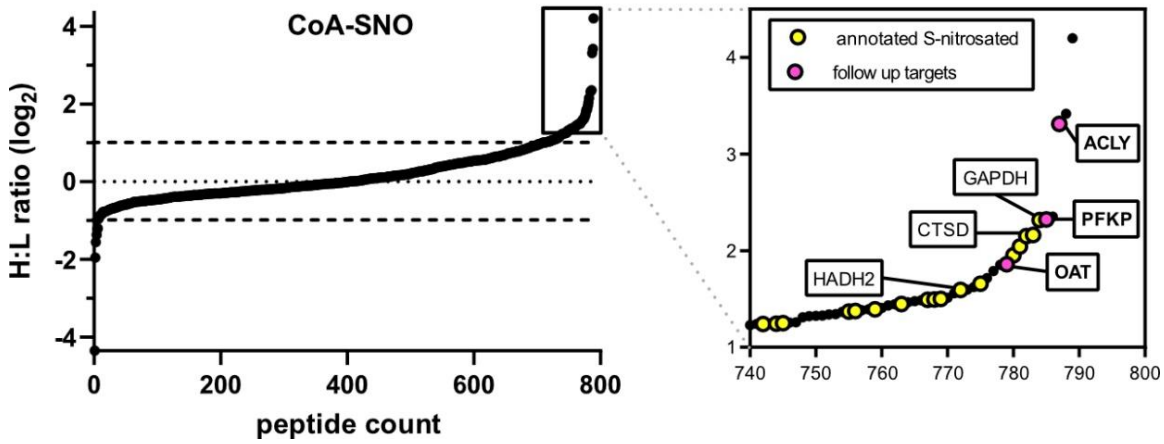

Figure 3-1 Quantitative ranking of cysteine targets sensitive to CoA-SNO mediated S-nitrosation (data from chapter 2). PFKP, ACLY, and OAT fall within a subset of targets highly sensitive CoA-SNO (inset).

Phosphofructokinase, platelet type (PFKP) is an 86 kD protein with Cys 360 identified as highly sensitive to CoA-SNO mediated *S*-nitrosation (*R* = 5.01). PFK is known as the gatekeeper of glycolysis as it regulates the first committed step of glycolysis, converting fructose-6-phospate (F-6-P) to fructose-1,6-phosphate (F-1,6-P) in an ATP dependent manner (Fig 3-2A). There are 3 PFK isoforms in mammalian cells which can make up a PFK tetramer: liver (PFKL), muscle (PFKM), and platelet (PFKP). PFKL is most abundant in liver and kidney, whereas PFKM and PFKP are the only forms present in adult muscle and platelets, respectively. In contrast, all 3 isoforms are present in brain and other tissues. Tetramer formation is required for PFK functional activity, and the equilibrium between dimer and tetramer is allosterically regulated through many metabolites. ATP, phosphoenolpyruvate, and citrate inhibit tetramer formation, providing negative feedback for glycolysis, while ADP and F-2,6-BP act as an allosteric activators[9–11]. Interestingly, Cys 360, is located

near the ATP binding pocket of PFKP[12] (Fig 3-2B), so we hypothesized that S-nitrosation could have an effect on PFKP activity.

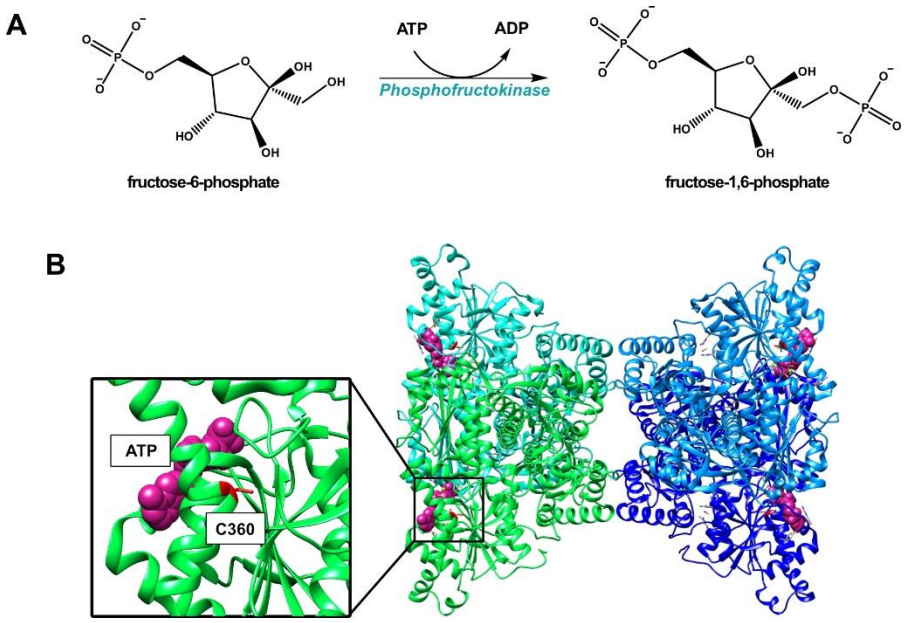

Figure 3-2 (A) PFKP catalyzes the conversion of fructose-6-phosphate (F-6-P) to fructose-1,6-phosphate (F-1,6-P) using ATP. **(B)** Functional PFKP exists as a tetramer with Cys 360 located near the ATP binding site (inset) (PDB ID: 4RH3).

Most cancer cells demonstrate increased glucose uptake and lactate production in the presence of sufficient oxygen in order to meet the high energy and biosynthetic demands of tumor cells and to facilitate their growth. This altered metabolism is known as the Warburg effect[13,14]. With PFK regulating glycolytic flux, it is not surprising that increased levels and activation of PFK has been observed in cancers. PFKP is the most prominent isoform in breast carcinoma, ascites tumor, and B and T cell leukemias, in which total PFK1 expression or activity is upregulated[15–17]. Additionally, increased EGFR signaling in cancers results in AKT1-

mediated phosphorylation of phosphofructokinase 2 (PFK2), leading to increasing F-2,6-BP production, overcoming the negative glycolytic feedback of PFK[10].

PFKM was recently identified as a target of NOS1 (neuronal NOS) mediated nitrosation, where the PDZ binding domain of PFKM facilitates interaction with NOS1[18–20]. PFKM was shown to be nitrosated at Cys 351 in a NOS1 dependent manner in ovarian cancer cells, promoting PFKM tetramer formation and enhanced enzymatic activity, resisting negative feedback. Seeing as we identified the analogous cysteine, Cys 360, of the platelet isoform, PFKP, as highly sensitive to CoA-SNO (R = 5.01) we were curious if the effects of *S*-nitrosation on PFKP were consistent with the observed effect of nitrosation of PFKM.

ATP citrate synthase (a.k.a. ATP citrate lyase (ACLY)) is a 121 kD protein with Cys 845 identified as highly sensitive to CoA-SNO mediated *S*-nitrosation (R = 9.92 (CoA-SNO)). This cytosolic enzyme links glucose metabolism with *de novo* lipid synthesis, catalyzing the conversion of ATP and citrate, produced from the TCA cycle, to oxaloacetate and acetyl-CoA (Fig 3-3A). Acetyl-CoA is a vital precursor for biosynthesis of fatty acids and cholesterol and is involved in isoprenoid-based protein modifications[21]. Acetyl CoA is also required for acetylation reactions that modify proteins, such as histone acetylation in the nucleus, regulating global chromatin architecture and gene transcription[22]. ACLY exists as a homotetramer with Cys 845 positioned within the CoA binding region at the dimer interface (Fig 3-3B)[23,24].

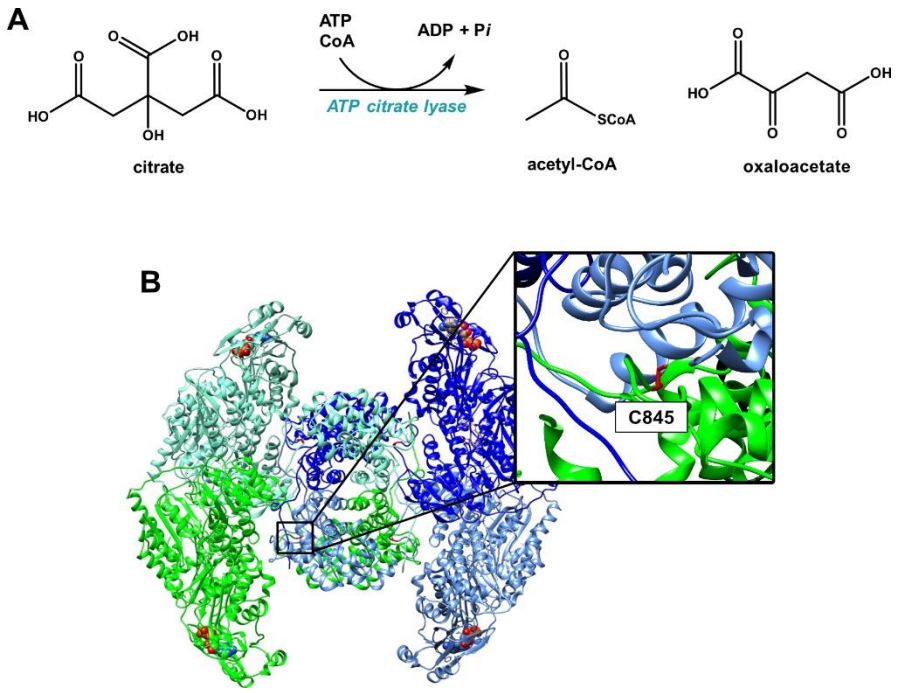

Figure 3-3 (A) ACLY catalyzes the reaction of citrate and CoA to oxaloacetate and acetyl-CoA, using ATP. **(B)** Homotetrameric structure of ACLY (PDB ID: 6O0H). Cys 845 is located within the citrate binding domain at the dimer interface.

Dysregulation of fatty acid metabolism is recognized as a component of malignant transformation in many different cancers, with increased ACLY expression and activity reported in lung, prostate, bladder, breast, liver, stomach, and colon tumors[21,25–29]. Increased levels of phosphorylated ACLY were correlated with stage, differentiation grade, and poorer prognosis in human lung adenocarcinoma[26]. It has been found that AKT1 directly phosphorylates and activates ACLY by contributing to protein stabilization[30]. Inhibition or silencing of ACLY attenuates tumor growth and suppression by downregulating the PI3K–AKT pathway and subsequent activation of the antitumor factors AMPK and p53, making ACLY a promising therapeutic target in the treatment of cancers[31,32].

Interestingly, ACLY uses CoA as a substrate, meaning that ACLY may have an increased affinity for binding CoA-SNO, rendering it a selective target of CoA-SNO mediated *S*-nitrosation. ACLY was recently reported as a target of nitrosation upon inactivation of the CoA-SNO reductase, AKR1A1 by Stomberski *et al*. however, the site of modification was not identified nor was the role of nitrosation characterized[33]. With this previous evidence validating our proteomic data, we looked to further investigate the role Cys 845 on ACLY and characterize the effects of *S*-nitrosation.

Ornithine aminotransferase (OAT) is a 48 kD mitochondrial protein with Cys 150 identified as highly sensitive to CoA-SNO mediated *S*-nitrosation (R = 3.63). OAT plays a role in amino acid biosynthesis, converting α-ketoglutarate (α-KG) and L-ornithine (L-Orn) to glutamate (Glu) and glutamate-5-semialdehyde (GSA), which spontaneously rearranges to form pyroline-5-carboxylate (P5C), a precursor for proline production (Fig 3-4A). This reaction is reversible but favors the degradation of ornithine and requires a pyridoxal-5-phosphate (PLP) cofactor covalently bound to lysine 292 through formation of a Schiff base, generating the enzymatic active site[34]. Interestingly, Cys 150 is located near the PLP cofactor and the dimer interface[35] (Fig 3-4B), and we hypothesize that nitrosation at this site could impact OAT activity.

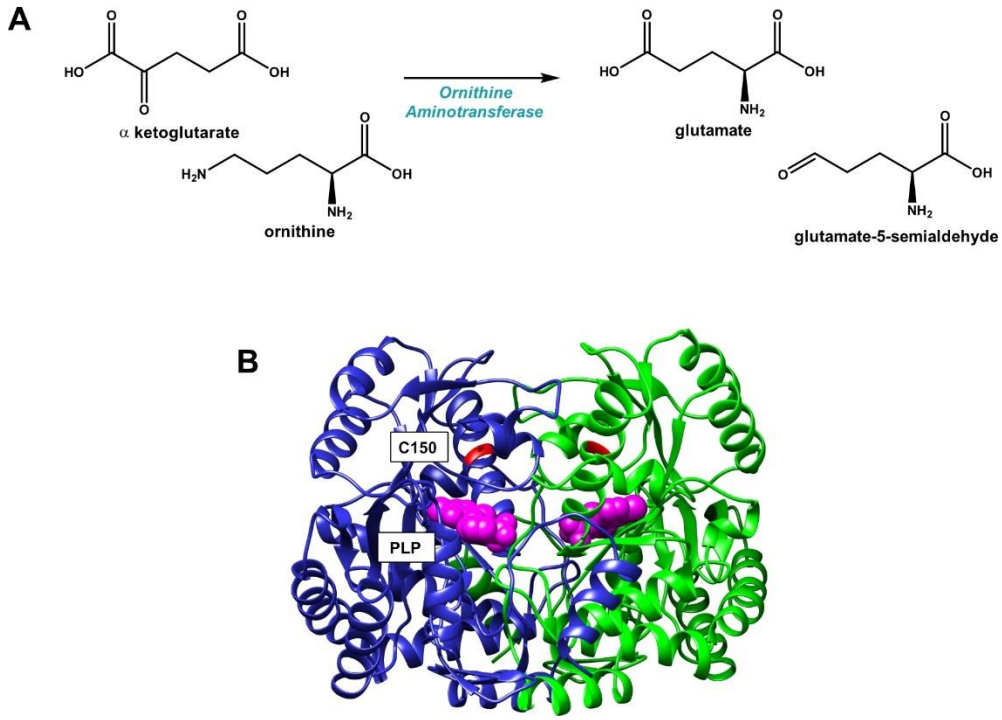

Figure 3-4 (A) OAT catalyzes the transformation of a-ketoglutarate and ornithine to glutamate and glutamate-5-semialdehyde. **(B)** OAT exists as a homodimer with Cys 150 located near the PLP cofactor biding site (PDB ID: 1OAT).

Mutations in the OAT gene causes gyrate atrophy, a rare but serious inherited disease associated with progressive retinal deterioration and blindness. Genetic mutations of OAT can lead to reduced expression levels or reduced activity of the protein with the majority of missense mutations located within the active site (K292R, R180T, G142E, and Y55H) or the at the dimer interface (P300L, T181M, R154L, G121D, C93F, N54K, and G51D)[36]. Additionally, aberrant Wnt/β-catenin signaling results in high expression levels of OAT in some cancers, where the enzyme can make tumor cells independent of the glutamine supply. Since OAT plays a critical role in the progression of hepatocellular carcinoma, investigation of highly potent and selective inhibitors of the enzyme are of great clinical interest[37].

Interestingly, OAT is connected to arginine metabolism. Nitric oxide synthase (NOS) and arginase (ARG) compete for arginine as a substrate to produce either NO and citrulline or urea and ornithine, respectively. Here, activation of iNOS can produce cytotoxic amounts of NO and/or modulate cellular pathways through *S*-nitrosation, while activation of ARG results in polyamine synthesis and cellular proliferation. Just downstream of ARG is ornithine decarboxylase 1 (ODC1) and OAT which both utilize ornithine as a substrate. ODC1 is known to undergo *S*-nitrosation at its active site Cys 360, inhibiting protein activity and polyamine synthesis, directing arginine though the NOS pathway as opposed to the ARG pathway[38,39]. Because of its role in the arginine metabolic pathway, and the regulatory role of *S*-nitrosation on ODC1, we hypothesized that *S*-nitrosation of OAT may provide some sort of feedback signal in NO production.

3.2 RESULTS AND DISCUSSION

3.2.1 Functional characterization of PFKP *S*-nitrosation at Cys 360

The first step was to confirm nitrosation of PFKP in response to CoA-SNO treatment. Recombinant PFKP was expressed and purified using the Bac-2-Bac™ baculovirus-insect cell protein expression system (Invitrogen™). Here, Sf9 cells from the fall armyworm, *Spodoptera frugiperda*, were transfected with recombinant bacmid DNA encoding PFKP with an N-terminal His-tag to produce recombinant baculovirus particles. This recombinant baculovirus was then amplified and used to

infect Sf9 cells for recombinant PFKP protein expression and the purified protein was obtained through immobilized metal affinity chromatography (IMAC).

To confirm nitrosation of PFKP, we subjected purified PFKP to treatment with 0 – 30 μM CoA-SNO followed by the biotin switch technique. Following the nitrosation reaction, remaining free thiols were capped with iodoacetamide. *S*-nitrosothiols were then selectively reduced with ascorbate and further reacted with a biotin-linked iodoacetamide for detection by biotin blot analysis. We observe that PFKP is nitrosated in response to CoA-SNO treatment, with increased nitrosation observed upon increasing CoA-SNO levels (Fig 3-5A). Since the signal is ascorbate dependent, this suggests that PFKP is nitrosated and not undergoing an alternative modification. Out of the 16 total cysteine residues on PFKP, Cys 360 was the only cysteine highly sensitive to CoA-SNO treatment in our proteomic data. A cysteine to serine mutation at position 360 (PFKP C360S) resulted in a loss of signal upon CoA-SNO treatment, indicating that nitrosation is dependent on Cys 360 (Fig 3-5B). Furthermore, *S*-nitrosation of WT PFKP occurs in response to the various NO donors: CoA-SNO, GSNO, and methylamine hexamethylene methylamine (MAHMA) NONOate (a diazenium diolate with a $t_{1/2}$ = 2.7 min at 22°C pH 7.4) (Fig 3-5C). These data are consistent with our proteomic data, where Cys 360 of PFKP was highly sensitive to all 3 donors with R >3 (R = 3.89 (GSNO), R = 5.01 (CoA-SNO), R = 5.92 (PAPA NONOate)).

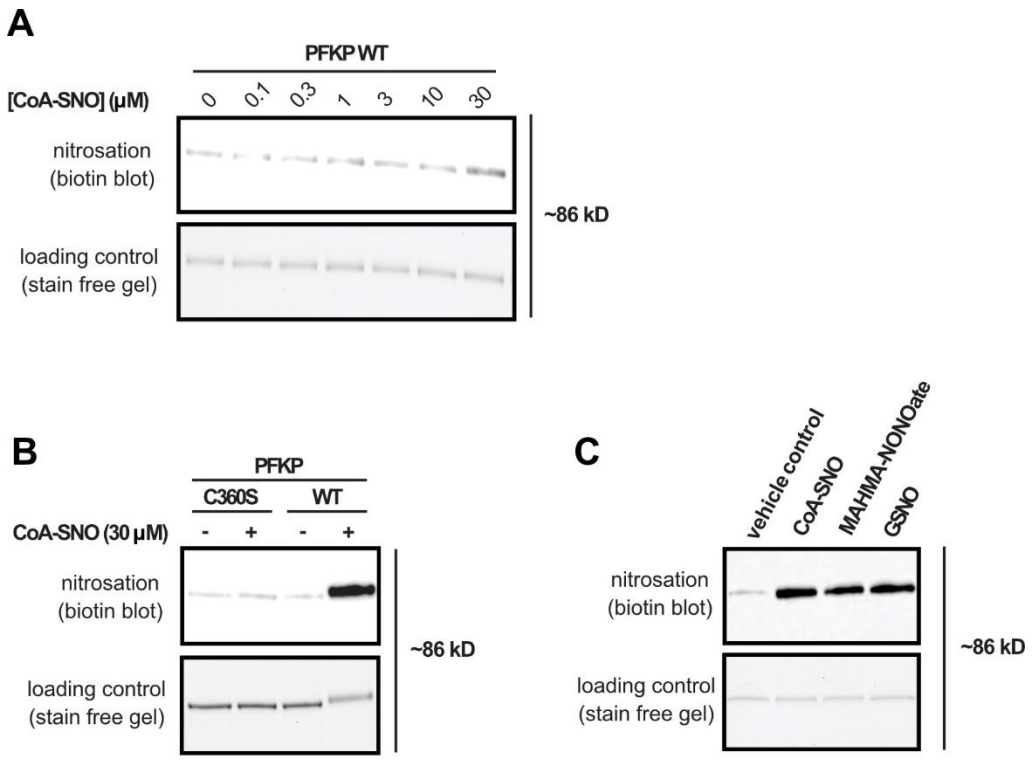

Figure 3-5 (A) Treatment of PFKP WT with increasing concentrations of CoA-SNO (0-30 μM) shows increased levels of PFKP-SNO monitored by the biotin switch assay. **(B)** Nitrosation of PFKP by 30 μM CoA-SNO is dependent on Cys 360 with undetectable nitrosation in the PFKP cysteine 360 to serine mutant (C360S) monitored by the biotin switch assay. **(C)** Treatment of PFKP with 30 μM CoA-SNO, GSNO, and PAPA NONOate results in PFKP-SNO formation as monitored by the biotin switch assay.

Upon confirming nitrosation of PFKP at Cys 360, we wanted to interrogate the effects of Cys 360 nitrostion on PFKP activity. Seeing as Cys 360 is located proximal to the ATP binding pocket of PFKP, we hypothesized that nitrosation at this site may disrupt activity. In order to monitor changes in PFKP enzymatic activity in response to *S*-nitrosation, we used the PFK colorimetric activity assay (Sigma-Aldrich). In this coupled assay, PFKP converts fructose-6-phosphase and ATP to fructose-1,6-bisphosphate and ADP. The resulting ADP is converted by the provided enzyme mixture to AMP and NADH. NADH then reduces a colorless probe resulting in a colorimetric (450 nm) product proportional to the PFK activity. To our

surprise, upon *S*-nitrosation of PFKP, enzyme activity is decreased to 38.7% compared to the non-nitrosated PFKP. However, the activity of the *S*-nitrosated vs non-nitrosated PFKP mutant, C360S, is unchanged, suggesting that this change in enzymatic activity upon nitrosation is dependent on Cys 360. This data suggests that *S*-nitrosation at Cys 360, results in a loss of enzymatic activity, which contrasts with the activation observed for PFKM in a previous study. It is possible that the different PFK isoforms are differentially regulated by nitrosation. Unlike PFKM, PFKP does not harbor a PDZ binding domain and is not known to interact with NOS, suggesting that a different means of nitrosation could alter the effects of this modification on protein activity.

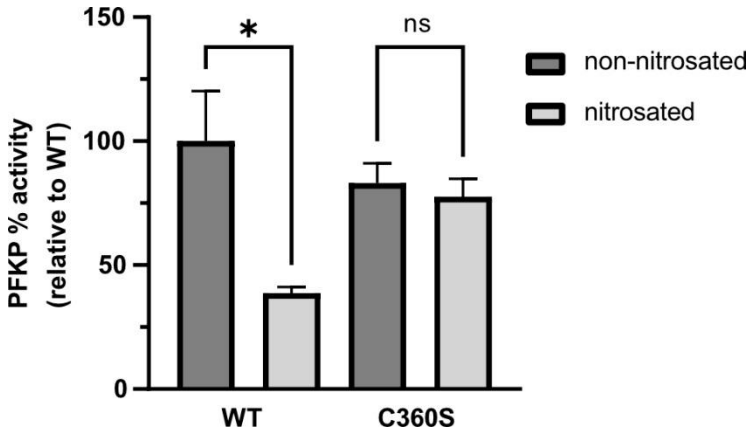

Figure 3-6 Nitrosation of PFKP inhibits enzymatic activity in the WT protein while the mutant C360S is resistant to activity changes (* = significant, $P < 0.05$; ns = not significant).

3.2.2 Functional characterization of ACLY *S*-nitrosation at Cys 845

The first step in characterizing ACLY *S*-nitrosation was to confirm ACLY-SNO formation in response to CoA-SNO treatment. ACLY was recombinantly expressed and purified from *E. coli* and subjected to treatment with CoA-SNO. Using the biotin switch technique, we were able to see that ACLY is nitrosated in response to CoA-SNO treatment, with increased nitrosation corresponding with increasing CoA-SNO levels (Fig 3-7A), with the ascorbate dependent signal verifying nitrosation as opposed to an alternative cysteine modification. Out of the 16 cysteine residues on ACLY, nitrosation of ACLY by CoA-SNO was dependent on Cys 845, as a cysteine to serine mutation (C845S) at this site results in a loss of signal, consistent with the site of modification identified in our proteomic data (Fig 3-7B). Next, we wanted to investigate nitrosation in response to other NO donors. Our proteomic data suggests selective nitrosation of ACLY by CoA-SNO, but not by GSNO or PAPA NONOate (R = 0.95 (GSNO), R = 9.92 (CoA-SNO), R = 1.18 (PAPA NONOate)). Upon treatment of ACLY with 30 μM CoA-SNO, GSNO, and MAHMA NONOate, *S*-nitrosation occurs selectively with CoA-SNO (Fig 3-7C). Background signal in the control, MAHMA NONOate, and GSNO treated samples is likely due to incomplete blocking of free thiols, a known limitation of the biotin switch assay.

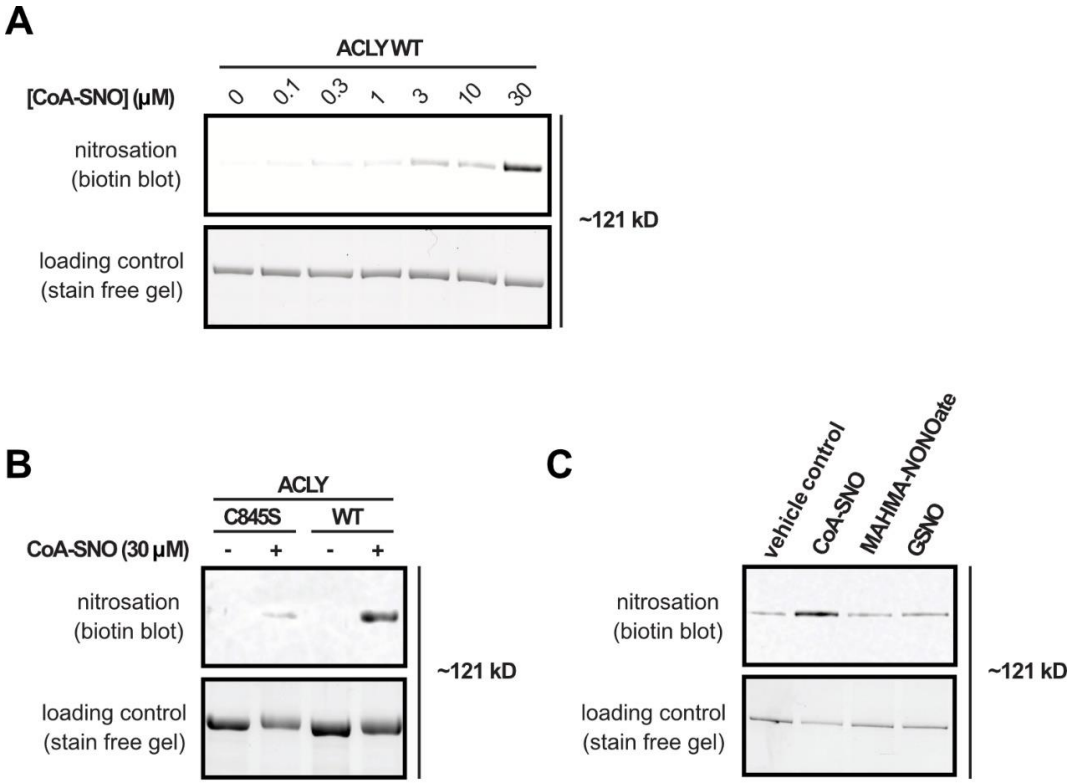

Figure 3-7 (A) Treatment of ACLY WT with increasing concentrations of CoA-SNO (0-30 μM) shows increased levels of ACLY-SNO monitored by the biotin switch assay. **(B)** Nitrosation of ACLY by 30 μM CoA-SNO is dependent on Cys 845 with undetectable nitrosation in the ACLY cysteine 845 to serine mutant (C845S) monitored by the biotin switch assay. **(C)** Treatment of ACLY with 30 μM CoA-SNO, GSNO, and PAPA NONOate results in ACLY-SNO formation as monitored by the biotin switch assay.

We hypothesize that *S*-nitrosation at Cys 845 positioned near the ACLY dimer interface could alter ACLY enzymatic activity. To monitor changes in protein activity upon nitrosation of ACLY, we utilized the ADP-glo assay (Promega). Here, ADP produced during the ACLY catalytic reaction is converted to ATP, which is then used to generate light in a luciferase reaction. The luminescence generated correlates with the production of ADP and ultimately ACLY activity. We observed a stark decrease in ACLY activity, with the nitrosated ACLY displaying 12.5% activity compared to that of the non-nitrosated control (Fig 3-8A). Additionally, we do see

ACLY C845S activity decreased upon nitrosation to 55.7% compared to the non-nitrosated control, however these changes are not significant ($p > 0.05$). Mutation of Cys 845 was found to lower the inhibition by GSNO ~5-fold (C845S GSNO IC_{50} = 77.09 µM) compared to the WT ACLY (GSNO IC_{50} = 15.70 µM) (Fig 3-8B). Taken together this data indicates that nitrosation of ACLY decreases enzymatic activity and Cys 845 is essential for regulating activity.

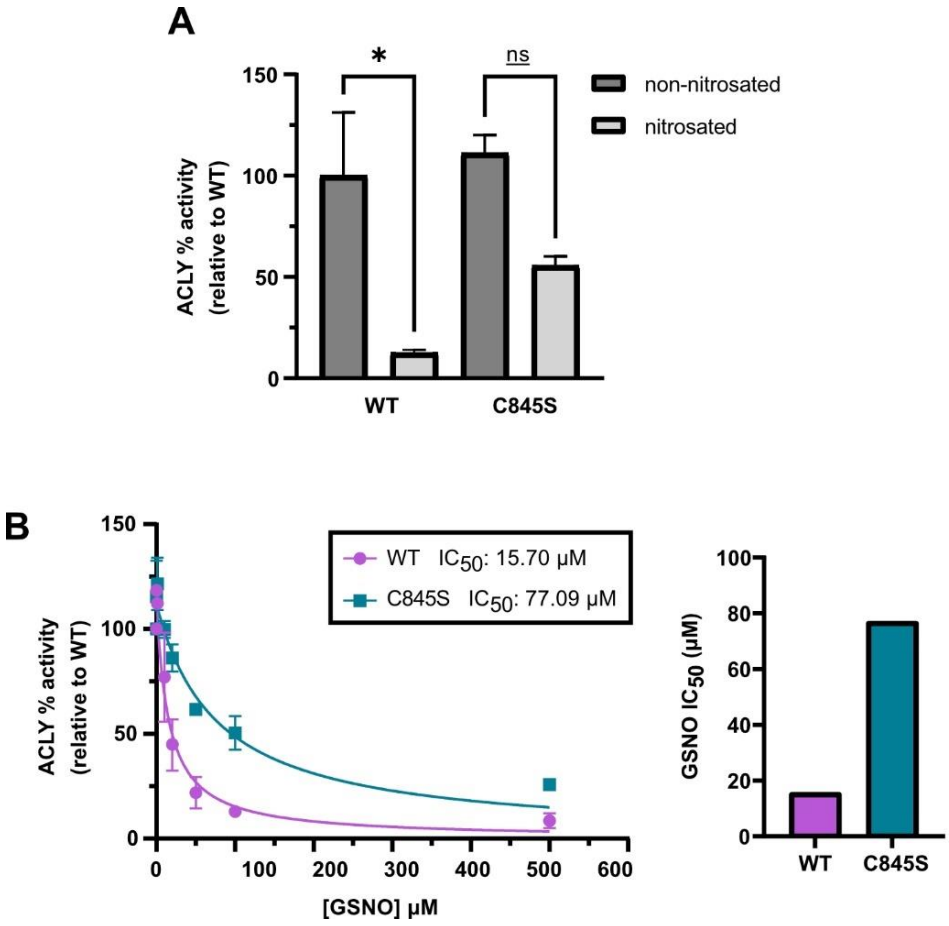

Figure 3-8 (A) Nitrosation of ACLY inhibits enzymatic activity in the WT protein while the mutant C845A is more resistant to activity changes (* = significant, $p < 0.05$; ns = not significant). **(B)** Inhibition of ACLY WT and C845S by increasing levels of GSNO (0-500 µM).

We wondered if nitrosation could have an effect on protein stability, potentially through a resulting protein conformational change. We monitored the stability of nitrosated and non-nitrosated WT and C845S ACLY, using a derivative of the cellular thermal stability assay (CETSA)[40]. Instead of cellular lysate, we subject both nitrosated and non-nitrosated WT and C845S recombinant ACLY to heating over a temperature range of 35 – 75 °C and quantified protein in the soluble fraction to calculate a melting temperature (Tm). The Tm of WT and mutant ACLY was reported as 51.95 °C and 52.28 °C, respectively and upon nitrosation, WT and C845S Tm increased to 53.32 °C and 53.90 °C, respectively (Fig 3-9). However, due to high error, all changes in Tm were within the range of error, leaving us with inconclusive results. An alternative technique is currently being employed to more sensitively monitor changes in protein stability.

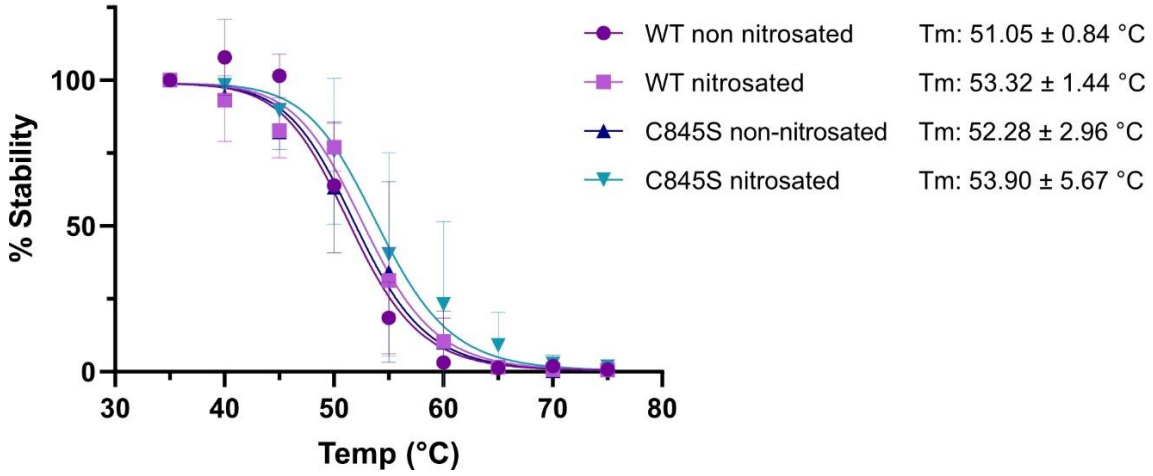

Figure 3-9 Thermal stability of non-nitrosated and nitrosated ACLY WT and C845S (n = 2).

3.2.3 Functional characterization of OAT *S*-nitrosation at Cys 150

The first step in characterizing OAT *S*-nitrosation was to confirm OAT-SNO formation in response to CoA-SNO treatment. The hepatic form of OAT (amino acid 26-439, removal of the mitochondrial targeting sequence) was recombinantly expressed and purified from *E. coli* and subjected to treatment with CoA-SNO. Using the biotin switch technique, we were able to see that OAT is nitrosated in response to CoA-SNO treatment, with a strong signal observed upon treatment with 30 μM CoA-SNO (Fig 3-10A). The ascorbate dependent signal suggests *S*-nitrosation of OAT as opposed to an alternative modification. The loss of signal when cysteine 150 is mutated to serine (C150S), validates that OAT nitrosation occurs at Cys 150 (Fig 3-10B). While proteomic data suggests OAT is sensitive to CoA-SNO and GSNO, we did not identify the peptide containing Cys 150 in the PAPA NONOate dataset (R = 3.45 (GSNO), R = 3.63 (CoA-SNO)). When treating purified OAT with various nitrosation donors, we see that OAT is the most sensitive to CoA-SNO, while a lower signal is observed upon treatment with GSNO and MAHMA NONOate (Fig 3-10C).

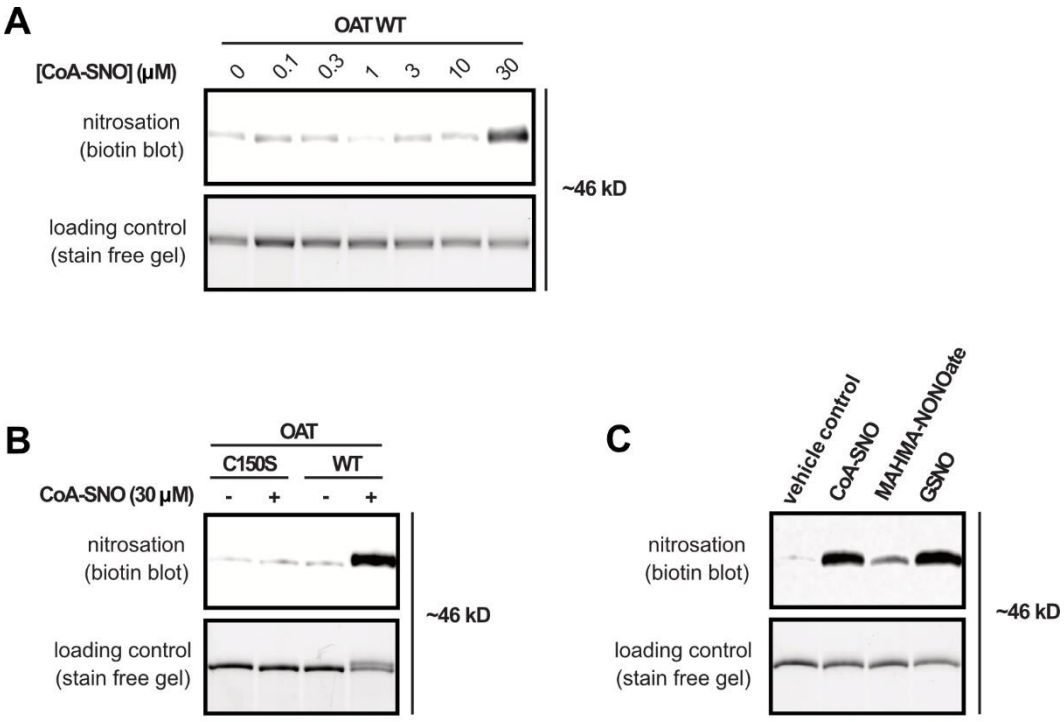

Figure 3-10 (A) Treatment of OAT WT with increasing concentrations of CoA-SNO (0-30 μM) shows increased levels of OAT-SNO monitored by the biotin switch assay. **(B)** Nitrosation of OAT by 30 μM CoA-SNO is dependent on Cys 150 with undetectable nitrosation in the OAT cysteine 150 to serine mutant (C150S) monitored by the biotin switch assay. **(C)** Treatment of OAT with 30 μM CoA-SNO, GSNO, and PAPA NONOate results in OAT-SNO formation as monitored by the biotin switch assay.

We hypothesized that *S*-nitrosation of Cys 150 may have an effect on OAT activity, as Cys 150 is located proximal to the essential PLP cofactor. To determine the effects of nitrosation on OAT function, we performed a colorimetric activity assay monitoring the production of P5C. P5C is a spontaneously rearranged product of glutamate-5-semialdehyde, that forms a colored product upon reaction with ninhydrin. Formation of this product is monitored by absorbance at 512 nm, reporting on OAT activity[41,42]. The activity of the nitrosated WT OAT was slightly lower, 64.5%, compared to the non-nitrosated control, although the changes were not significant ($p > 0.05$) (Fig 3-11E). This same trend was also observed with the

C150A mutant, where nitrosation slightly lowered the activity of OAT C150A to 75% compared to the non-nitrosated OAT C150A, however the change in activity was not significant ($p > 0.05$).

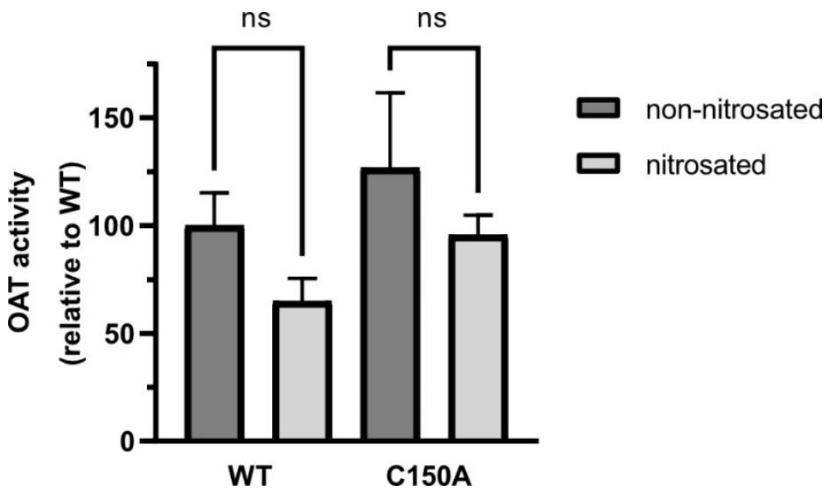

Figure 3-11 Nitrosation of OAT inhibits enzymatic activity in the WT and C150A protein (ns = not significant, $p < 0.05$).

Since nitrosation did not have a significant change on OAT activity, we thought alternative functional effects could be observed upon nitrosation. We looked at the effects of nitrosation on OAT thermal stability, and protein-protein interactions (PPIs) via immunoprecipitation (IP). There were no changes in the thermal stability of WT and mutant OAT, and no change upon nitrosation (Fig 3-12A). Furthermore, we expressed OAT WT and C150S in HEK 293T cells, followed by IP. We expected that if Cys 150 is important for PPIs, we would observe a decrease in PPIs with the expression of a C150S mutant. The results obtained show an opposite trend where PPIs decrease with the expression of the WT OAT, although many proteins are mitochondrial and/or known OAT interactors, such as pyroline-5-carboxylase reductase 1 and 2 (PYCR1 and PYCR2) validating that we did enrich

for OAT interacting proteins (Fig 3-12B). Although we do not see changes in OAT activity, or stability, it is possible that *S*-nitrosation of OAT has an alternative role that we did not investigate. *S*-nitrosation of OAT could alter its localization or could play a role in a transnitrosation cascade, passing on its SNO to another target protein. Further studies are required to interrogate these possibilities.

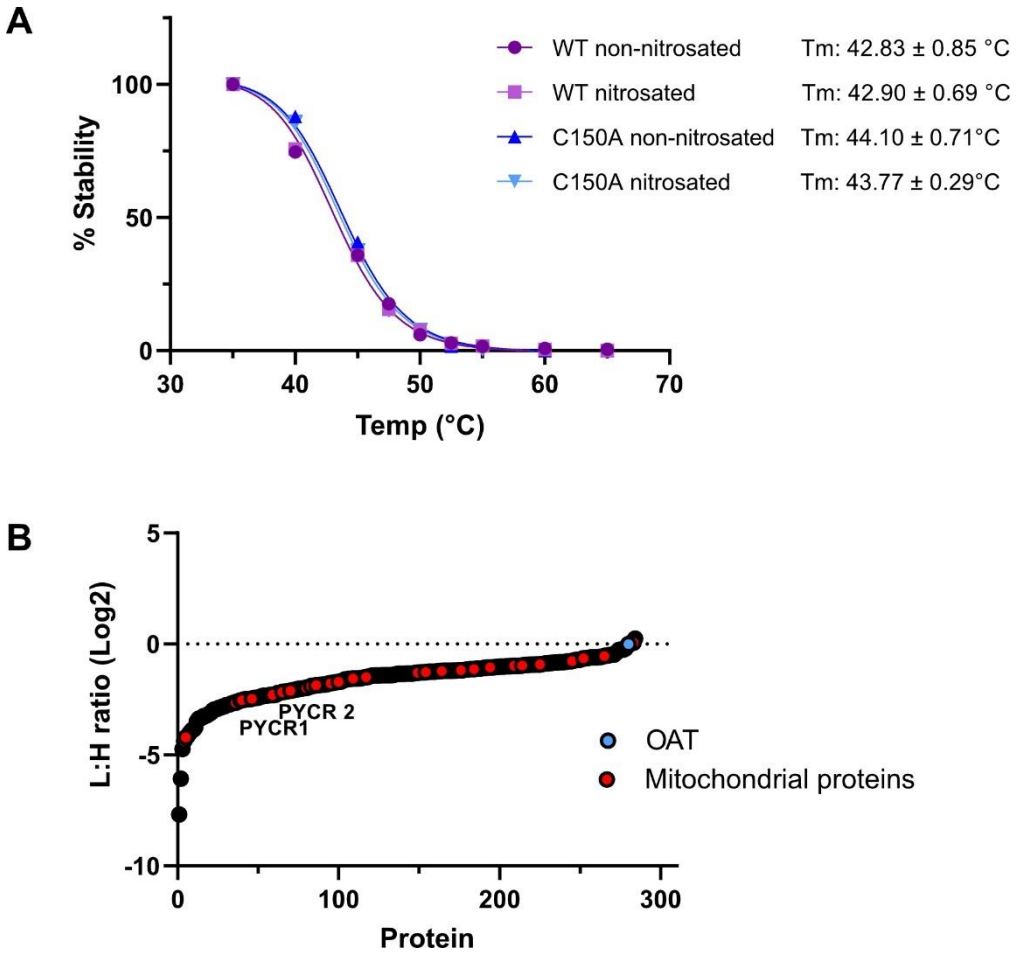

Figure 3-12 (A) Thermal stability of non-nitrosated and nitrosated WT and C150A OAT. **(B)** L:H ratios quantifying relative changes in protein levels upon immunoprecipitation with OAT WT (light labeled) or OAT C150S (heavy labeled) (n = 3).

3.3 CONCLUSION

Many of the protein targets identified in our proteomic studies as highly susceptible to nitrosation by CoA-SNO, GSNO, and PAPA NONOate are involved in metabolic processes, with some known targets of nitrosation. Furthermore, many of these protein targets play a role in various diseases. As there are only a few CoA-SNO dependent protein targets in which the functional effects of nitrosation are understood, we wanted to interrogate the role of nitrosation on proteins highly sensitive to CoA-SNO mediated nitrosation. PFKP, ACLY, and OAT are all proteins involved in metabolic processes (glycolysis, fatty acid metabolism, and amino acid biosynthesis, respectively) with disease relevance, and high susceptibility to nitrosation by CoA-SNO. We were able to confirm nitrosation on each of these protein targets and show that nitrosation was dependent on a specific cysteine residue (Cys 360 on PFKP, Cys 845 on ACLY, and Cys 150 on OAT). Further interrogation showed that nitrosation of PFKP resulted in decreased enzymatic activity, which was rescued by mutation at the site of nitrosation. A similar effect on activity was observed upon nitrosation of ACLY, with the mutation at the modified cysteine more resistant to activity changes upon nitrosation. OAT appeared to undergo slightly altered activity upon nitrosation, although these changes were not significant. Further work is currently underway to use more sensitive methods to determine the effects of nitrosation on PFKP, ACLY, and OAT protein stability.

With this data we show that nitrosation regulates protein activity in diverse metabolic processes. However, there are known SNO events on related proteins

within these processes. Both PFKP and ACLY activity are indirectly regulated by AKT1, whose activity is inhibited by nitrosation. Related to ACLY, *S*-nitrosation of fatty acid synthase (FASN) is a mechanism to regulate fatty acid metabolism. In relation to OAT *S*-nitrosation, ODC1 is regulated by *S*-nitrosation in the arginine/citrulline metabolic pathway. The interplay of these *S*-nitrosation events is of interest as they could co-occur to regulate metabolic pathways in different physiological contexts. Further work to characterize the effect of these individual SNO events on metabolic function should be done to tease out the role of a single SNO event versus induction of nonspecific *S*-nitrosation in cells.

3.4 METHODS

PFKP subcloning

Recombinant PFKP was prepared by baculovirus expression as described previously[43]. Briefly, complementary DNA (cDNA) encoding the 784 amino acid isoform 1 of *Homo sapiens* PFKP (NM_002627.4) was cloned into pFastBac HTa vector. Site-directed mutagenesis was performed to obtain cysteine to serine mutant, PFKP C360S, using the QuickChange Lightening Mutagenesis Kit (Agilent) with the appropriate primers (Table 3-1). All constructs were verified by DNA sequencing (Genewiz).

PFKP expression and purification

Baculovirus was generated using the Bac-to-Bac Expression system (Invitrogen) according to the manufacturer's protocols. The viral stock was then used to infect *Spodoptera frugiperda* Sf9 cells at a density of 2 x 10^6 cells/mL at a multiplicity of infection of 2 for 48 hr with shaking at 27 °C. Cell pellets were harvested by centrifugation 5,000 rpm for 10 min, resuspended in in 20 mM HEPES pH 7.5, 100 mM KCl, 1 mM ATP, 1 mM MgCl2, 1 mM TCEP, 5% (v/v) glycerol, and lysed using an ultrasonic tip sonicator. The lysate was centrifuged at 15,000 rpm for 10 min and the supernatant was collected as the soluble fraction. The expressed protein was purified using a Ni-NTA packed chromatography column. The soluble lysate was loaded onto the column, followed by 4 washes with 25 mM imidazole pH 7.4. Protein was eluted from the column with 4 aliquots of 250 mM imidazole pH 7.4, buffer exchanged into 20 mM HEPES pH 7.5, 100 mM KCl, 1 mM ATP, 1 mM MgCl2, 1 mM TCEP, 5% (v/v) glycerol using Zeba Spin Desalting column, concentrated with an Amicon Ultracel-10K Centrifugal Filter Unit, and stored at -80 °C until further use.

PFKP activity assay

The purified PFKP enzyme activity was monitored using the PFK colorimetric assay (Sigma, catalog # MAK093), which utilizes an enzyme mix to convert the PFKP dependent product ADP to AMP and NADH. The resulting NADH reduces a colorless probe resulting in a colorimetric (450 nm) product proportional to the PFK activity present. PFKP WT and C360S (100 µL of 0.8 µM in PFK assay buffer) were pre-treated with 0 to 500 µM GSNO (in HEN) and incubated for one hour at 37 °C. PFKP

reactions were initiated upon addition of PFKP (25 µL, 0.4 µM final concentration) to a clear flat bottom 96-well plate containing 50 µL master mix (per well - 42 µL assay buffer, 2 µL enzyme mix, 2 µL developer, 2 µL ATP, 2 µL substrate). Reactions were incubated at 37 °C for 5 min then absorbance at 450 nm was monitored over 50 min with 5 min integrals at 37 °C using the Synergy Neo2 plate reader (BioTek).

ACLY subcloning

The cDNA ORF clone (OHu14076) encoding the 1101 amino acid isoform 1 of *Homo sapiens* ACLY (NM_001096.2) was purchased in a pET-24b (+) bacterial expression vector (GenScript). Site-directed mutagenesis was performed to obtain cysteine to serine mutant, ACLY C845S, using the QuickChange Lightening Mutagenesis Kit (Agilent) with the appropriate primers (Table 3-1). All constructs were verified by DNA sequencing (Genewiz).

ACLY expression and purification

ACLY (WT, C845S) was expressed in *Escherichia coli* BL21 (DE3) cells. Cells were inoculated in 5 mL LB medium containing 50 µg/mL kanamycin at 37 °C overnight. 2 mL from the overnight culture was added to 500 mL LB medium containing 50 µg/mL kanamycin and the culture was grown at 37 °C until reaching an OD_{600} of ~0.6. Protein expression was then induced by the addition of 0.5 mM IPTG and grown at 25 °C overnight. Cells were harvested by centrifugation at 5,000 rpm for 10 min, resuspended in DPBS, and lysed using an ultrasonic tip sonicator. The lysate was centrifuged at 15,000 rpm for 10 min and the supernatant was

collected as the soluble fraction. The expressed protein was purified using a Ni-NTA packed chromatography column. The soluble lysate was loaded onto the column, followed by 4 washes with 25 mM imidazole pH 7.4. Protein was eluted from the column with 4 aliquots of 250 mM imidazole pH 7.4 and buffer exchanged into 20 mM Tris pH 7.4, 300 mM NaCl, and 2 mM DTT using a Zeba Spin Desalting column and stored at -80 °C until further use.

ACLY activity assay

The purified ACLY enzyme activity was monitored by ADP production using the ADP-glo assay kit (Promega). In brief, ACLY WT and C845S (100 µL of 132 nM) in 1x kinase buffer (40 mM Tris pH 7.4, 20 mM $MgCl_2$, 0.1 mg/mL BSA) was incubated with 0 to 500 µM GSNO (in HEN) for one hour at 37 °C. Excess GSNO was removed using a P-6 column to buffer exchange into fresh 1x kinase buffer. To monitor ACLY activity, reactions were initiated upon addition of ACLY (7.5 µL, 40 nM final concentration) to white opaque 96-well plate containing 17.5 µL master mix (100 µM ATP, 200 µM CoA, 200 µM citrate in 1x kinase buffer, final concentrations) and incubated for up to 20 min. Reactions were quenched upon the addition of 25 µL of ADP-glo reagent and incubated for 45 min at room temperature. Subsequently, 50 µL of kinase detection reagent was added followed by another 45 min incubation at room temperature. Luminescence was measured using a Synergy Neo2 BioTek plate reader with a 0.2 second integration time, gain of 135, and a 1mM read height.

OAT subcloning

The cDNA ORF clone (OHu26094) encoding the 439 amino acid isoform 1 of *Homo sapiens* OAT (NM_000274.3) was purchased in a pET-24b (+) bacterial expression vector (GenScript). The hepatic and renal forms (amino acid 26-439 and 36-439, respectively) of OAT were generated by removing the mitochondrial targeting sequence using Gibson assembly to with the primers in Table 3-1. Site-directed mutagenesis was performed to obtain cysteine to serine mutant (OAT C150S) and the cysteine to serine mutant (OAT C150A) using the QuickChange Lightening Mutagenesis Kit (Agilent) with the appropriate primers (Table 3-1).

For the immunoprecipitation studies, full length OAT WT and C150S with a Kozak initiation sequence and a C-terminal FLAG tag was cloned into the pcDNA3.1 (+) mammalian expression vector using Gibson assembly. The primers used for this cloning are listed in table 3-1 as OAT pcDNA3.1 (+) Gibson forward and reverse. All constructs were verified by DNA sequencing (Genewiz).

OAT expression and purification

OAT (WT, C150S, C150A) was expressed in *Escherichia coli* BL21 (DE3) cells. Cells were inoculated in 5 mL LB medium containing 50 μg/mL kanamycin at 37 °C overnight. 1 mL from the overnight culture was added to 500 mL LB medium containing 50 μg/mL kanamycin and the culture was grown at 37 °C until reaching an OD_{600} of ~0.6. Protein expression was then induced by the addition of 0.1 mM IPTG and grown at 25 °C overnight. Cells were harvested by centrifugation at 5,000 rpm for 10 min, resuspended in PBS, and lysed using an ultrasonic tip sonicator. The

lysate was centrifuged at 15,000 rpm for 10 min and the supernatant was collected as the soluble fraction. The expressed protein was purified using a Ni-NTA packed chromatography column. The soluble lysate was loaded onto the column, followed by 4 washes with 25 mM imidazole pH 7.4. Protein was eluted from the column with 4 aliquots of 250 mM imidazole pH 7.4 and buffer exchanged into 50 mM HEPES pH 7.4, 500 mM KCl, 10% (v/v) glycerol, and 1% (v/v) triton X-100 using a Zeba Spin Desalting Column and stored at -80 °C until further use.

OAT activity assay

OAT activity was assayed by monitoring the production of glutamate-5-semialdehyde via absorbance at 512 nm as previously described[41,42]. OAT WT, C150S, and C150A (100 µL of 0.25 µg/mL in HEN buffer (or 5.6 µM)) was pre-incubated with 1 mM GSNO (in HEN) for 1 hour at 37 °C, followed by a buffer exchange into 100 mM phosphate buffer, pH 7.4, using a P-6 column (Bio-Rad). To monitor OAT activity, a 500 µL reaction mixture was set up containing 50 µM pyridoxal-5-phosphate (PLP), 0.3 mM α-ketoglutarate, and 12 mM ornithine in 100 mM phosphate buffer, pH 7.4. OAT was added to the mixture at a final concentration of 0.1 µM to initiate the reaction, and incubated at 37 °C with shaking for up to 7.5 min. Ninhydrin (0.16% final concentration) and HCl (0.4 M, final concentration) were added to the reaction mixture and incubated at 100 °C for 5 min. Following incubation, 250 µL ethanol was added to the reaction mixture and absorbance levels were monitored at 512 nm.

Biotin Switch Assay

All cysteine residues in purified ACLY, OAT, and PFKP were first fully pre-reduced by incubation with 1 mM TCEP for 15 min at room temperature, followed by desalting with a Micro BioSpin-6 column (Bio-Rad). Desalted protein was incubated with either (A) 0-30 μM CoA-SNO or (B) 30 μM CoA-SNO, GSNO, and MAHMA NONOate for 60 min at 37 °C in PBS in a 50-μL total volume under low ambient light conditions. Free thiols were next alkylated by incubation with an equal volume of 2× HDNSU-IA blocking buffer (200 mM HEPES, pH 7.7, 2 mM DPTA, 0.2 mM neocuproine, 2% (w/v) SDS, 6 M urea, 200 mM iodoacetamide) for 1 h at 37 °C. The proteins were precipitated with 1 mL of pre-chilled high purity acetone overnight at −20 °C. Precipitated protein was pelleted via centrifugation at 12,000 × *g* at 4 °C for 10 minutes, and the supernatant was discarded. Pellets were washed once with 1 mL of cold (−20 °C) acetone and pelleted via centrifugation at 12,000 × *g*, and the supernatant was removed. The pellets were air-dried for 15 min at room temperature, resuspended into label buffer (PBS with 1% (w/v) SDS, 30 mM ascorbate, 100 μM EZ-link biotin iodoacetamide), and incubated for 1 h at 37 °C. Reactions were quenched with 5× Laemmli sample buffer containing 50 mM dithiothreitol (DTT). Each sample was loaded onto a Bio-Rad Any kDa TGX stain-free gel; protein loading was verified by stain-free gel imaging under UV light using a ChemiDoc MP imager (Bio-Rad). Proteins were transferred to a nitrocellulose membrane using a TransBlot Turbo semi-dry transfer system (Bio-Rad), and the membrane was blocked for 1 h at room temperature in PBS containing 0.1% (v/v) Tween 20 (PBST) and 2.5% (w/v) dry milk. Vectastain biotin staining solution was

made up according to the Vectastain ABC kit (Vector Laboratories, Burlingame, CA, USA), where reagents A and B were diluted into PBST and incubated for 20 min at room temperature prior to use. The membrane was then washed three times for 5 min with PBST and rocked for 40 min at room temperature with Vectastain solution. Following incubation, the membrane was again washed three times for 5 min in PBST and imaged after a 2 min incubation in chemiluminescence buffer (50 mM Na_2HPO_4, 50 mM $NaHCO_3$, 150 mM NaCl, 10 mM $NaBO_3$, 225 µM *p*-coumaric acid, 1.5 mM luminol, and 0.6% (v/v) H_2O_2).

Thermal Stability Assay

Purified protein samples were buffer exchanged into HEN buffer and treated with 500 µM GSNO or HEN buffer (control) for 1 hour at 37 °C. Each sample was then split into 9 x 50 µL aliquots and heated for 15 minutes at varying temperatures: 35 – 75 °C for ACLY and 35 – 65 °C for OAT. Following heating, samples were incubated on ice for 10 min and subsequently centrifuged at 10,000 rpm for 10 min. The soluble protein fraction was collected and analyzed by SDS-PAGE. Gel bands were quantified using the ImageJ software and plotted in the GraphPad Prism 9 software. Tm values were calculated using the nonlinear regression dose-response EC50 shift analysis, where X is concentration, and the confidence interval set to 95%.

OAT immunoprecipitation and ReDiMe analysis

OAT WT and C150S pcDNA3.1(+) constructs were used for transient transfection in HEK 293T, which was achieved using polyethylenimine (PEI). After 48 hours, cells were washed with PBS, harvested and lysed in the Thermo Pierce IP Lysis Buffer in the presence of Pierce Universal Nuclease. Lysate was clarified upon centrifugation (16,000 x g, 20 min). Overexpression of OAT WT and OAT C150S was confirmed via western blotting using the anti-FLAG antibody (Cell Signaling Technologies). Soluble lysate was incubated with Anti-DYKDDDK Magnetic Agarose Resin (Thermo Pierce) pre-equilibrated with IP Lysis Buffer (25 °C, 1 hr) to enrich for OAT protein interactors. The resin was washed with PBS and H_2O, and proteins were eluted by boiling the sample with 30 µL 8 M urea in 100 mM TEAB (95 °C, 10 min). Reductive alkylation was performed by the sequential addition of 100 mM TEAB (70 µL), 1.5 µL of 1 M DTT (65 ºC, 15 min), and 2.5 µL of 400 mM iodoacetamide (25 ºC, 30 min). Reactions were diluted with additional 100 mM TEAB (120 µL) and tryptic digestion performed by the addition of 2 µg of sequencing-grade trypsin (4 µL of 20 µg diluted in TEAB) and 2.5 µL of 100 mM CaCl2 (37 ºC, overnight). After tryptic digest, reductive dimethylation was performed by the addition of 4 µL of 20% light (OAT WT) or heavy (OAT C150S) formaldehyde and 20 µL of 0.6 M sodium cyanoborohydride (25 ºC, 2 hours). The reaction was quenched by the addition of 4 µL ammonium hydroxide (25 ºC, 15 min). The light (Fe- S deficient) and heavy (control) tryptic peptide samples were then combined, desalted on a Sep-Pak, dried by speed-vac, and resuspended in 100% H_2O, 0.1 % formic acid.

MS proteomic analysis of OAT IP samples

Peptide analysis was then achieved by LC/LC-MS/MS using an Orbitrap Exploris 240 mass spectrometer (Thermo Scientific) coupled to a Dionex Ultimate 3000 RSLC nano system (Thermo Scientific). 5µL of peptide sample was injected directly onto an Acclaim PepMap 100 loading column. Peptides were eluted onto an Acclaim PepMap RSLC and separated with a 160 min gradient of 5% - 99% Buffer B in Buffer A (Buffer A: 100% H_2O, 0.1% formic acid; Buffer B: 80% acetonitrile, 20% H_2O, 0.1% formic acid). Instrumentation operated at a flow rate of 0.3 µL/min buffer through the column and spray voltage of 2.1 kV. One full MS scan (350-1800 m/z, 120,000 resolution, RF lens 65%, AGC target 300%, automatic maximum injection time, profile mode) was obtained every 2 seconds with dynamic exclusion (repeat count 2, duration 10 s), isotopic exclusion (assigned), and apex detection (30% desired apex window) enabled. A variable number of MS2 scans (15,000 resolution, AGC 75%, maximum injection time 100 ms, centroid mode) were obtained between each MS1 scan based on the highest precursor masses, filtered for monoisotopic peak determination, theoretical precursor isotopic envelope fit, intensity (5E4), and charge state (2-6). MS2 analysis consisted of the isolation of precursor ions (isolation window 2 m/z) followed by high-energy collision dissociation (HCD) (collision energy 30%).

Proteome Discoverer analysis and data processing

MS data analysis was performed using Thermo Proteome Discoverer software (PD; version 2.4.1.15). Protein identification was achieved using the

SequestHT and Percolator algorithms against a *Homo sapiens* proteome UniprotKB database. The protease enzyme was set as trypsin with a maximum of 2 missed cleavages allowed. The peptide precursor mass tolerance was set to 10ppm with a fragment mass tolerance of 0.02 Da. MS datasets were independently searched for light and heavy ReDiMe labeled peptides; for these searches, static modifications on lysine and the peptide N-terminus of +28.0313 (light) or +34.0632 (heavy) were used[44]. Dynamic modifications included methionine oxidation (+ 15.995), N-terminal acetylation (+42.011) and/or methionine loss (-89.030 / -131.040). The false discovery rate (FDR) for peptide identification was set at 1% for highly confident peptide hits. All considered peptides were present in at least 3 replicates with at least 2 unique peptides. All L:H ratio values were normalized to the OAT average ratio, then the average L:H ratio was calculated for each protein and proteins with a standard error of the mean (SEM) > 0.3 were removed from the final protein dataset.

Primers for mutagenesis and cloning

PFKP C360S Forward	CTGAGTCATCTGCACGCTCTCCATCAGCGGCAGG
PFKP C360S Reverse	CCTGCCGCTGATGGAGAGCGTGCAGATGACTCAG
ACLY C845S Forward	CCTGTCCTCGCTCATCGCTGATGCTGGTCATGAACGAGG
ACLY C845S Reverse	CCTCGTTCATGACCAGCATCAGCGATGAGCGAGGACAGG
OAT C150S Forward	CACTTACGAGCTAGTTTACTGGCAGTCTCTCCAGCCTC
OAT C150S Reverse	GAGGCTGGAGAGACTGCCAGTAAACTAGCTCGTAAGTG
OAT C150A Forward	CACTTACGAGCTAGTTTAGCGGCAGTCTCTCCAGCCTC
OAT C150A Reverse	GAGGCTGGAGAGACTGCCGCTAAACTAGCTCGTAAGTG
OAT 25-419 Gibson Forward	AACTTTAAGAAGGAGATATACATATGACATCTGTTGCAA CTAAAAAAACA
OAT 35-419 Gibson	AACTTTAAGAAGGAGATATACATATGGGCCCTCCAACCT

Forward	CT
OAT Gibson Reverse	ATCTCAGTGGTGGTGGTGGTGCTCGAGGAAAGACAA GATGGTCTTGTT
OAT pcDNA-3.1 (+) Gibson forward	GAGACCCAAGCTGGCTAGCGTTTAAACTTAGCCACCATGT TTTCCAAACTAGCAC
OAT pcDNA-3.1 (+) Gibson reverse	CCACTGTGCTGGATATCTGCAGTCACTTATCGTCGTCATC CTTGTAATCGAAAGACAAGATGGTC

Table 3-1 Primers used for PFKP, ACLY, and OAT mutagenesis and cloning. All primers listed 5' to 3'.

REFERENCES

(1) Chen, Y.-J.; Lu, C.-T.; Su, M.-G.; Huang, K.-Y.; Ching, W.-C.; Yang, H.-H.; Liao, Y.-C.; Chen, Y.-J.; Lee, T.-Y. DbSNO 2.0: A Resource for Exploring Structural Environment, Functional and Disease Association and Regulatory Network of Protein S-Nitrosylation. *Nucleic Acids Res.* **2015**, *43* (1), 503–511.

(2) Li, S.; Yu, K.; Wu, G.; Zhang, Q.; Wang, P.; Zheng, J.; Liu, Z. X.; Wang, J.; Gao, X.; Cheng, H. PCysMod: Prediction of Multiple Cysteine Modifications Based on Deep Learning Framework. *Front. Cell Dev. Biol.* **2021**, *9*, 117.

(3) Abunimer, A.; Smith, K.; Wu, T. J.; Lam, P.; Simonyan, V.; Mazumder, R. Single-Nucleotide Variations in Cardiac Arrhythmias: Prospects for Genomics and Proteomics Based Biomarker Discovery and Diagnostics. *Genes.* **2014**, *5* (2), 254–269.

(4) Stomberski, C. T.; Hess, D. T.; Stamler, J. S. Protein S-Nitrosylation: Determinants of Specificity and Enzymatic Regulation of S-Nitrosothiol-Based Signaling. *Antioxid. Redox Signal.* **2019**, *30* (10), 1331-1351.

(5) Ye, H.; Wu, J.; Liang, Z.; Zhang, Y.; Huang, Z. Protein S-Nitrosation: Biochemistry, Identification, Molecular Mechanisms, and Therapeutic Applications. *J. Med. Chem.* **2022**, *65* (8), 5902–5925.

(6) Mitchell, D. A.; Morton, S. U.; Fernhoff, N. B.; Marletta, M. A. Thioredoxin Is Required for S-Nitrosation of Procaspase-3 and the Inhibition of Apoptosis in Jurkat Cells. *Proc. Natl. Acad. Sci.* **2007**, *104* (28), 11609–11614.

(7) Martínez-Ruiz, A.; Villanueva, L.; De Orduña, C. G.; López-Ferrer, D.; Ángeles Higueras, M.; Tarín, C.; Rodríguez-Crespo, I.; Vázquez, J.; Lamas, S. S-Nitrosylation of Hsp90 Promotes the Inhibition of Its ATPase and Endothelial Nitric Oxide Synthase Regulatory Activities. *Proc. Natl. Acad. Sci.* **2005**, *102* (24), 8525–8530.

(8) Zhao, S.; Tang, X.; Miao, Z.; Chen, Y.; Cao, J.; Song, T.; You, D.; Zhong, Y.; Lin, Z.; Wang, D.; et al. Hsp90 S-Nitrosylation at Cys521, as a Conformational Switch, Modulates Cycling of Hsp90-AHA1-CDC37 Chaperone Machine to Aggravate Atherosclerosis. *Redox Biol.* **2022**, *52*, 102290.

(9) Marin-Hernandez, A.; Gallardo-Perez, J. C.; Ralph, S. J.; Rodriguez-Enriquez, S.; Moreno-Sanchez, R. HIF-1α Modulates Energy Metabolism in Cancer Cells by Inducing Over-Expression of Specific Glycolytic Isoforms. *Mini-Reviews Med. Chem.* **2009**, *9* (9), 1084–1101.

(10) Lee, J. H.; Liu, R.; Li, J.; Wang, Y.; Tan, L.; Li, X. J.; Qian, X.; Zhang, C.; Xia, Y.; Xu, D.; et al. EGFR-Phosphorylated Platelet Isoform of Phosphofructokinase 1 Promotes PI3K Activation. *Mol. Cell* **2018**, *70* (2), 197-210.

(11) Marsin, A. S.; Bertrand, L.; Rider, M. H.; Deprez, J.; Beauloye, C.; Vincent, M. F.; Van den Berghe, G.; Carling, D.; Hue, L. Phosphorylation and Activation of Heart PFK-2 by AMPK Has a Role in the Stimulation of Glycolysis during Ischaemia. *Curr. Biol.* **2000**, *10* (20), 1247–1255.

(12) Kloos, M.; Brüser, A.; Kirchberger, J.; Schöneberg, T.; Sträter, N. Crystal Structure of Human Platelet Phosphofructokinase-1 Locked in an Activated Conformation. *Biochem. J.* **2015**, *469* (3), 421–432.

(13) Warburg, O. On the Origin of Cancer Cells. *Science.* **1956**, *123* (3191), 309–314.

(14) Heiden, M. G. V.; Cantley, L. C.; Thompson, C. B. Understanding the Warburg Effect: The Metabolic Requirements of Cell Proliferation. *Science.* **2009**, *324* (5930), 1029–1033.

(15) Moon, J. S.; Kim, H. E.; Koh, E.; Park, S. H.; Jin, W. J.; Park, B. W.; Park, S. W.; Kim, K. S. Krüppel-like Factor 4 (KLF4) Activates the Transcription of the Gene for the Platelet Isoform of Phosphofructokinase (PFKP) in Breast Cancer. *J. Biol. Chem.* **2011**, *286* (27), 23808–23816.

(16) Sánchez-Martínez, C.; Aragón, J. Analysis of Phosphofructokinase Subunits and Isozymes in Ascites Tumor Cells and Its Original Tissue, Murine Mammary Gland. *FEBS Lett.* **1997**, *409* (1), 86–90.

(17) Shobhana Vora; James P. Halper; Daniel M. Knowles. Alterations in the Activity and Isozymic Profile of Human Phosphofructokinase during Malignant Transformation in Vivo and in Vitro: Transformation- and Progression-Linked Discriminants of Malignancy. *Cancer Res.* **1985**, *45* (7), 2993–3001.

(18) Gao, W.; Huang, M.; Chen, X.; Chen, J.; Zou, Z.; Li, L.; Ji, K.; Nie, Z.; Yang, B.; Wei, Z.; et al. The Role of S-Nitrosylation of PFKM in Regulation of Glycolysis in Ovarian Cancer Cells. *Cell Death Dis.* **2021**, *12* (4).

(19) Strieker, N. L.; Christopherson, K. S.; Yi, B. A.; Schatz, P. J.; Raab, R. W.; Dawes, G.; Bassett, D. E.; Bredt, D. S.; Li, M. PDZ Domain of Neuronal Nitric Oxide Synthase Recognizes Novel C-Terminal Peptide Sequences. *Nat. Biotechnol.* **1997**, *15* (4), 336–342.

(20) Marcondes, M. C.; Sola-Penna, M.; Torres, R. D. S. G.; Zancan, P. Muscle-Type 6-Phosphofructo-1-Kinase and Aldolase Associate Conferring Catalytic

Advantages for Both Enzymes. *IUBMB Life* **2011**, *63* (6), 435–445.

(21) Zaidi, N.; Swinnen, J. V.; Smans, K. ATP-Citrate Lyase: A Key Player in Cancer Metabolism. *Cancer Res.* **2012**, *72* (15), 3709–3714.

(22) Wellen, K. E.; Hatzivassiliou, G.; Sachdeva, U. M.; Bui, T. V.; Cross, J. R.; Thompson, C. B. ATP-Citrate Lyase Links Cellular Metabolism to Histone Acetylation. *Science.* **2009**, *324* (5930), 1076–1080.

.

(23) Verschueren, K. H. G.; Blanchet, C.; Felix, J.; Dansercoer, A.; De Vos, D.; Bloch, Y.; Van Beeumen, J.; Svergun, D.; Gutsche, I.; Savvides, S. N.; et al. Structure of ATP Citrate Lyase and the Origin of Citrate Synthase in the Krebs Cycle. *Nature.* **2019**, *568* (7753), 571–575.

(24) Wei, J.; Leit, S.; Kuai, J.; Therrien, E.; Rafi, S.; Harwood, H. J.; DeLaBarre, B.; Tong, L. An Allosteric Mechanism for Potent Inhibition of Human ATP-Citrate Lyase. *Nature*. **2019**, 566–570.

(25) Monaco, M. E.; Monaco; E., M. Fatty Acid Metabolism in Breast Cancer Subtypes. *Oncotarget* **2017**, *8* (17), 29487–29500.

(26) Migita, T.; Narita, T.; Nomura, K.; Miyagi, E.; Inazuka, F.; Matsuura, M.; Ushijima, M.; Mashima, T.; Seimiya, H.; Satoh, Y.; et al. ATP Citrate Lyase: Activation and Therapeutic Implications in Non–Small Cell Lung Cancer. *Cancer Res.* **2008**, *68* (20), 8547–8554.

(27) Yancy, H. F.; Mason, J. A.; Peters, S.; Thompson, C. E.; Littleton, G. K.; Jett, M.; Day, A. A. Metastatic Progression and Gene Expression between Breast Cancer Cell Lines from African American and Caucasian Women. *J. Carcinog.* **2007**, *6*, 8.

(28) Turyn, J.; Schlichtholz, B.; Dettlaff-Pokora, A.; Presler, M.; Goyke, E.; Matuszewski, M.; Kmieć, Z.; Krajka, K.; Swierczynski, J. Increased Activity of Glycerol 3-Phosphate Dehydrogenase and Other Lipogenic Enzymes in Human Bladder Cancer. *Horm. Metab. Res.* **2003**, *35* (10), 565–569.

(29) Halliday, K. R.; Fenoglio-Preiser, C.; Sillerud, L. O. Differentiation of Human Tumors from Nonmalignant Tissue by Natural-Abundance 13C NMR Spectroscopy. *Magn. Reson. Med.* **1988**, *7* (4), 384–411.

(30) Berwick, D. C.; Hers, I.; Heesom, K. J.; Kelly Moule, S.; Tavaré, J. M. The Identification of ATP-Citrate Lyase as a Protein Kinase B (Akt) Substrate in Primary Adipocytes. *J. Biol. Chem.* **2002**, *277* (37), 33895–33900.

(31) Hatzivassiliou, G.; Zhao, F.; Bauer, D. E.; Andreadis, C.; Shaw, A. N.; Dhanak, D.; Hingorani, S. R.; Tuveson, D. A.; Thompson, C. B. ATP Citrate Lyase Inhibition

Can Suppress Tumor Cell Growth. *Cancer Cell* **2005**, *8* (4), 311–321.

(32) Wei, X.; Shi, J.; Lin, Q.; Ma, X.; Pang, Y.; Mao, H.; Li, R.; Lu, W.; Wang, Y.; Liu, P. Targeting ACLY Attenuates Tumor Growth and Acquired Cisplatin Resistance in Ovarian Cancer by Inhibiting the PI3K–AKT Pathway and Activating the AMPK–ROS Pathway. *Front. Oncol.* **2021**, *11*, 749.

(33) Stomberski, C. T.; Zhou, H.-L.; Wang, L.; van den Akker, F.; Stamler, J. S. Molecular Recognition of S-Nitrosothiol Substrate by Its Cognate Protein Denitrosylase. *J. Biol. Chem.* **2019**, *294* (5), 1568–1578.

(34) Ginguay, A.; Cynober, L.; Curis, E.; Nicolis, I. Ornithine Aminotransferase, an Important Glutamate-Metabolizing Enzyme at the Crossroads of Multiple Metabolic Pathways. *Biology.* **2017**, *6* (4), 18.

(35) Shen, B. W.; Hennig, M.; Hohenester, E.; Jansonius, J. N.; Schirmer, T. Crystal Structure of Human Recombinant Ornithine Aminotransferase. *J. Mol. Biol.* **1998**, *277* (1), 81–102.

(36) Montioli, R.; Bellezza, I.; Desbats, M. A.; Borri Voltattorni, C.; Salviati, L.; Cellini, B. Deficit of Human Ornithine Aminotransferase in Gyrate Atrophy: Molecular, Cellular, and Clinical Aspects. *Biochim. Biophys. Acta - Proteins Proteomics* **2021**, *1869* (1), 140555.

(37) Zigmond, E.; Ya'acov, A. Ben; Lee, H.; Lichtenstein, Y.; Shalev, Z.; Smith, Y.; Zolotarov, L.; Ziv, E.; Kalman, R.; Le, H. V.; et al. Suppression of Hepatocellular Carcinoma by Inhibition of Overexpressed Ornithine Aminotransferase. *ACS Med. Chem. Lett.* **2015**, *6* (8), 840–844.

(38) Wei, Z.; Oh, J.; Flavell, R. A.; Crawford, J. M. LACC1 Bridges NOS2 and Polyamine Metabolism in Inflammatory Macrophages. *Nat.* **2022**, *609* (7926), 348–353.

(39) Bauer, P. M.; Buga, G. M.; Fukuto, J. M.; Pegg, A. E.; Ignarro, L. J. Nitric Oxide Inhibits Ornithine Decarboxylase ViaS-Nitrosylation of Cysteine 360 in the Active Site of the Enzyme. *J. Biol. Chem.* **2001**, *276* (37), 34458–34464.

(40) Molina, D. M.; Jafari, R.; Ignatushchenko, M.; Seki, T.; Larsson, E. A.; Dan, C.; Sreekumar, L.; Cao, Y.; Nordlund, P. Monitoring Drug Target Engagement in Cells and Tissues Using the Cellular Thermal Shift Assay. *Science.* **2013**, *341* (6141), 84–87.

(41) Kim, H. R.; Rho, H. W.; Park, J. W.; Park, B. H.; Kim, J. S.; Lee, M. W. Assay of Ornithine Aminotransferase with Ninhydrin. *Anal. Biochem.* **1994**, *223* (2), 205–207.

(42) Jortzik, E.; Fritz-Wolf, K.; Sturm, N.; Hipp, M.; Rahlfs, S.; Becker, K. Redox

Regulation of Plasmodium Falciparum Ornithine δ-Aminotransferase. *J. Mol. Biol.* **2010**, *402* (2), 445–459.

(43) Webb, B. A.; Forouhar, F.; Szu, F. E.; Seetharaman, J.; Tong, L.; Barber, D. L. Structures of Human Phosphofructokinase-1 and Atomic Basis of Cancer-Associated Mutations. *Nature* **2015**, *523* (7558), 111–114.

(44) Boersema, P. J.; Raijmakers, R.; Lemeer, S.; Mohammed, S.; Heck, A. J. R. Multiplex Peptide Stable Isotope Dimethyl Labeling for Quantitative Proteomics. *Nat. Protoc.* **2009**, *4* (4), 484–494.

4.0 INVESTIGATING THE ROLE OF CYSTEINE OXIDATION ON THE HUMAN RIBONUCLEASE INHIBITOR PROTEIN

This work was done in collaboration with Evans C. Wralsted and Ronald T. Raines at Massachusetts Institute of Technology

4.1 INTRODUCTION

The human ribonuclease inhibitor (RI) is a 50 kD cytosolic protein that protects cells against invading secretory pancreatic type ribonucleases (ptRNases: human RNase 1, bovine RNase A, and other pancreatic type RNases) by preventing RNA cleavage and ultimately cell death[1]. This protein was discovered and characterized over 50 years ago and has been found in every mammalian cell studied, suggesting its evolutionary importance[2–4]. RI mRNA is ubiquitously expressed, coupled with relatively high protein levels in the cytosol (4 mmol/L or 4 μM)[5]. With its sub-femtomolar affinity for pancreatic type RNases, Kd = 2.9 x 10^{-16}, the tightest interaction known between biomolecules[2,5,6], RI has been able to capture RNases, which have invaded all cell types within the human body.

Secretory ribonucleases play an important role in the body, clearing out both mRNA and non-coding RNA that is no longer needed. Upon endocytosis into cells, ribonucleases pose a threat to cellular viability which is kept in check by RI. However, this toxicity can be harnessed as an interesting therapeutic. Previous work has shown that RNase A was toxic to tumor cells both in vitro and in vivo, however efficacy required large quantities of the enzyme into a tumor[7–9]. More recently, homologs of RNase A, such as Onconase derived from *Rana pipiens* (Ranpirnase; Strativa Pharmaceuticals) have overcome this need for high dosing with their ability to evade RI and degrade cellular RNA[10]. Onconase is the first RNase that has been clinically applied in cancer therapy and it was even granted orphan drug status for unresectable malignant mesothelioma in the USA, Europe, and Australia[11–13]. In

addition, overexpression of RI has been shown to protect against the epithelial-to-mesenchymal transition of EJ cells[14] and oxidation of RI has been linked to the effectiveness of certain cancer treatments[15].

In addition to controlling the activity of RNases, it has been suggested that RI could play a role in maintaining intracellular redox homeostasis[2,16,17]. Human ribonuclease inhibitor contains 15 homologous leucine-rich repeats and 32 cysteine residues, many of which are found at a constant position within the repeating unit. All of the cysteine residues are in the reduced form, and 27 of these cysteines are conserved in pig and rat, suggesting an important structural or functional role[18]. It has been suggested that oxidation of RI occurs in an "all-or-none", highly cooperative fashion, where oxidation of a single cysteine leads to a cascade of disulfide bond formation and the complete inactivation of RI[18]. This mechanism was proposed by Fominaya and Hofsteenge, who used the oxidizing agent, DTNB (5,5' -dithiobis(2-nitrobenzoic acid), to interrogate the effect of modification by thiol-disulfide interchange, with the products of RI and DTNB consisting of either fully modified inactive (disulfide containing) and unmodified active (thiol containing) RI molecules, with no mixed intermediates detected[18]. The oxidized RI exists in an open conformation which disrupts RI-RNase complexes, releasing functional, active ribonuclease[2,5]. However, the mechanism of RI oxidation in a more biologically relevant setting remains to be characterized.

Furthermore, pig kidney epithelial cells (LLC-PK_1) treated with the oxidant H_2O_2, show a decrease in RI levels[19]. Blázquez *et al.* attribute oxidation of RI as a marker for proteolytic degradation, a commonly observed phenomenon for

oxidatively damaged proteins[20]. The inactivating effects of H_2O_2 oxidation in cells was enhanced upon inhibition of glutathione synthesis, suggesting that RI is inactivated depending on the redox state of the cell. We hypothesize that RI acts as a sensor to oxidative stress, where upon RI oxidation, active RNase is released into the cell, triggering cell death.

Remaining questions concerning RI oxidation and inactivation include the order of cysteine oxidation events that result in RI conformational change. Here, we aim to provide a residue-level analysis of cysteine oxidation on RI. Using a mass spectrometry-based cysteine profiling platform[21], we rank RI cysteines by reactivity and further quantify the extent of oxidation at individual cysteine residues. RI oxidation *in vitro* by hydrogen peroxide highlights slightly preferential oxidation of particular cysteines on RI, indicating that the "all-or-none" oxidation mechanism may be reliant on specific initial cysteine oxidation events.

4.2 RESULTS AND DISCUSSION

4.2.1 Identification of RI cysteine residues by mass spectrometry analysis

In order to monitor cysteine reactivity and oxidation on RI by quantitative mass spectrometry-based methods, first we had to ensure that the peptides identified contained a majority of the 32 cysteine residues on RI. To do this, we performed a tryptic digest of RI recombinantly expressed and purified from *E. coli* to obtain a peptide mixture. We identified 29 cysteine residues out of the 32 cysteine

on RI, providing 90.6% coverage of cysteines on RI (Fig 4-1, Table 4-1). The only cysteines that were not identified were Cys 134 and 142, which fall on the same tryptic peptide, and cysteine 427. Out of the RI cysteines, 34% (11 out of 32) were found on a peptide which contained only a single cysteine, whereas 56% (18 out of 32) were found on a peptide with at least one other cysteine residue. This finding was not very surprising, as many of the cysteines on RI are located in very close proximity. Although this was something of note because multiple cysteines on a single peptide can complicate quantitative analysis of mass spec data.

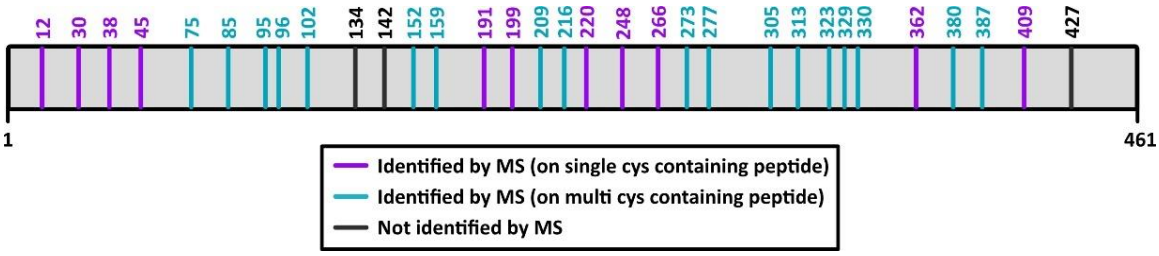

Figure 4-1 Position of cysteine residues on Ribonuclease Inhibitor protein (RI). Upon MS analysis of the purified RI tryptic digest, cysteines were either identified on a peptide with only one cysteine (purple), identified on a cysteine with multiple (2-4) cysteines (teal), or not identified by MS (black).

Cysteine Position	Total # Spectral Counts	Peptide Sequence	Spectral Counts
12	92	SLDIQSLDIQCEELSDAR DIQSLDIQCEELSDAR	91 1
30	36	WAELLPLLQQCQVVR	36
38	104	LDDCGLTEAR	104
45	31	CKDISSALR	31
75	7	SNELGDVGVHC SNELGDVGVHCVLQGL SNELGDVGVHCVLQGLQTPS	2 1 4
75/85	111	SNELGDVGVHCVLQGLQTPSCK SNELGDVGVHCVLQGLQTPSCKIQK ELGDVGVHCVLQGLQTPSCK GDVGVHCVLQGLQTPSCK VGVHCVLQGLQTPSCK HCVLQGLQTPSCK CVLQGLQTPSCK	98 1 1 4 1 3 3
95/96	137	LSLQNCCLTGAG	1
95/96/102	136	IQKLSLQNCCLTGAGCGVLSSTLR	1

		LSLQNCCLTGAGCGVLSSTLR	102
		SLQNCCLTGAGCGVLSSTLR	31
		CCLTGAGCGVLSSTLR	2
96/102	11	CLTGAGCGVLSSTLR	11
102	8	LTGAGCGVLSSTLR	7
		GAGCGVLSSTLR	1
152/159	55	LEKLQLEYCSLSAASCEPLASVLR	1
		LQLEYCSLSAASCEPLASVLR	37
		CSLSAASCEPLASVLR	17
159	16	SLSAASCEPLASVLR	4
		SAASCEPLASVLR	11
		AASCEPLASVLR	1
191	75	VLCQGLK	71
191/199	3	VLCQGLKDSPCQLEALK	3
191/199/209/216	1	VLCQGLKDSPCQLEALKLESCGVTSDNCR	1
199	58	DSPCQLEALK	53
		SPCQLEALK	1
		PCQLEALK	4
199/209	1	DSPCQLEALKLESC	1
199/209/216	50	DSPCQLEALKLESCGVTSDNCR	50
209/216	38	LKLESCGVTSDNCR	1
		LESCGVTSDNCR	37
220	56	DLCGIVASK	56
248	117	LGDVGMAELCPGLLHPSSR	104
		LGDVGMAELCPGLLHPS	9
		GDVGMAELCPGLLHPSSR	1
		DVGMAELCPGLLHPSSR	1
		MAELCPGLLHPSSR	1
		AELCPGLLHPSSR	1
266	30	TLWIWECGITAK	29
		IWECGITAK	1
273/277	7	GCGDLCR	7
305/313	1	LLCETLLEPGCQLESLWVK	1
323/329/330	138	SCSFTAACCSHFSSVLAQNR	129
		SCSFTAACCSH	1
		SCSFTAACCSHF	8
329/330	24	SFTAACCSHFSSVLAQNR	1
		TAACCSHFSSVLAQNR	16
		ACCSHFSSVLAQNR	3
		CCSHFSSVLAQNR	4
330	11	CSHFSSVLAQNR	11
362	65	ELCQGLGQPGSVLR	65
380/387	40	RVLWLADCDVSDSSCSSLAATLLANHSLR	1
		VLWLADCDVSDSSCSSLAATLLANH	1
		VLWLADCDVSDSSCSSLAATLLANHSLR	38
409	2	NCLGDAGILQLVESVR	1
		CLGDAGILQLVESVR	1

Table 4-1 Cysteine containing peptides identified upon MS analysis of RI tryptic digest and the corresponding peptides spectral counts. Cysteine residues are highlighted in red and multiple cysteine containing peptides highlighted in green.

4.2.2 Profiling cysteine reactivity in RI

To better understand how cysteines regulate RI function, we wanted to rank cysteines by their reactivity. Cysteine reactivity has been shown to be a predictor of functional cysteine residues[22]. We hypothesized that highly reactive cysteines may have higher propensity to undergo oxidation before the remainder of cysteines on RI, and subsequent RI inactivation. We use a derivative of the isoTOP-ABPP platform established by Weerapana *et al.* to enable quantitative analysis of native cysteine reactivity (Fig 4-2)[22]. Here, we took recombinant RI, split the sample into two fractions, and treated either fraction with 10 μM iodoacetamide-alkyne light (IA-light) or 100 μM iodoacetamide-alkyne heavy (IA-heavy) probes that were developed in house by Abo *et al.*[23]. Subsequent cysteine capping with iodoacetamide (non-alkyne version), tryptic digest, and LC-MS/MS analysis of the RI peptide mixture was performed. We were able to forgo an enrichment step, as our sample was a purified protein as opposed to a complex proteome. The MS analysis of IA-light and IA-heavy labeled peptides affords a heavy:light ratio, *R*, for each identified cysteine that reflects the difference in signal intensity between light and heavy tag-conjugated RI cysteines. If the *R* value is close to 1, this indicates saturation of cysteine labeling at lower concentrations of IA-light, thus representing a reactive cysteine. Whereas, $R > 1$ indicates that a cysteine was predominantly labeled by IA-heavy, suggesting that high concentrations of the cysteine reactive probe are needed, representing an unreactive cysteine.

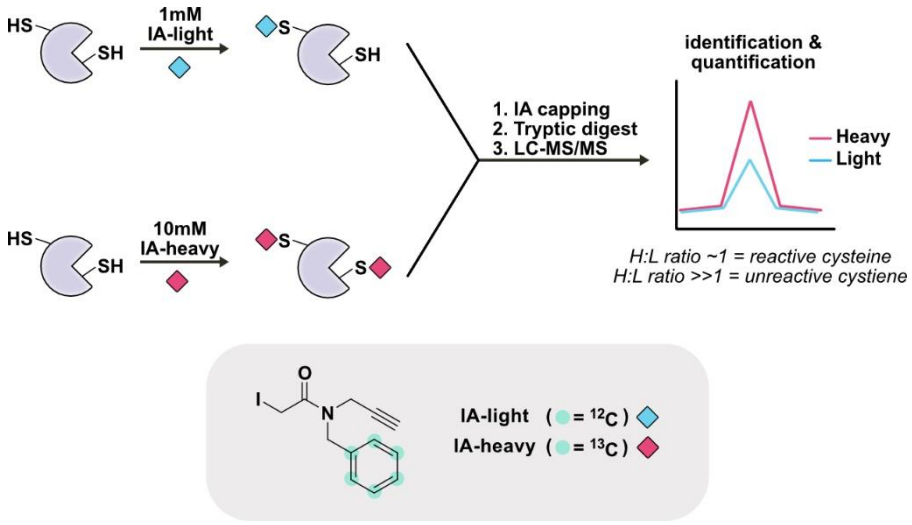

Figure 4-2 IsoTOP-ABPP derived MS workflow to identify and quantify cysteine reactivity on RI. An *R* value ~1 indicates a reactive cysteine residue while *R* >> 1 indicates an unreactive cysteine.

By subjecting RI to cysteine reactivity profiling, we obtained an *R* value for 21 cysteines on RI which was used to rank these cysteine residues by reactivity (Fig 4-3, Table 4-2). Cysteines were grouped by reactivity into the following categories: (1) high reactivity (R < 2); (2) moderate reactivity (2 < R < 3); and (3) low reactivity (R > 3). 9 cysteines were identified as highly reactive (Cys 95, 96, 102, 191, 209, 216, 305, 313, 362), 6 were identified with moderate reactivity (Cys 199, 248, 273, 277, 380, 387), and 6 were identified with low reactivity (Cys 30, 45, 75, 85, 220, 409). 5 more cysteines were identified on MS observed peptides, however without quantitative data. Looking at the position of cysteines on the RI crystal structure, the cysteines with low reactivity are located closer to the N and C terminus of the

protein, nearby the RNase binding region, whereas highly reactive cysteines are found throughout the midsection of this horseshoe-like structure (Fig 4-2)[6]. Whether a cysteine is found on an alpha-helix or a loop does not seem to correlate with reactivity.

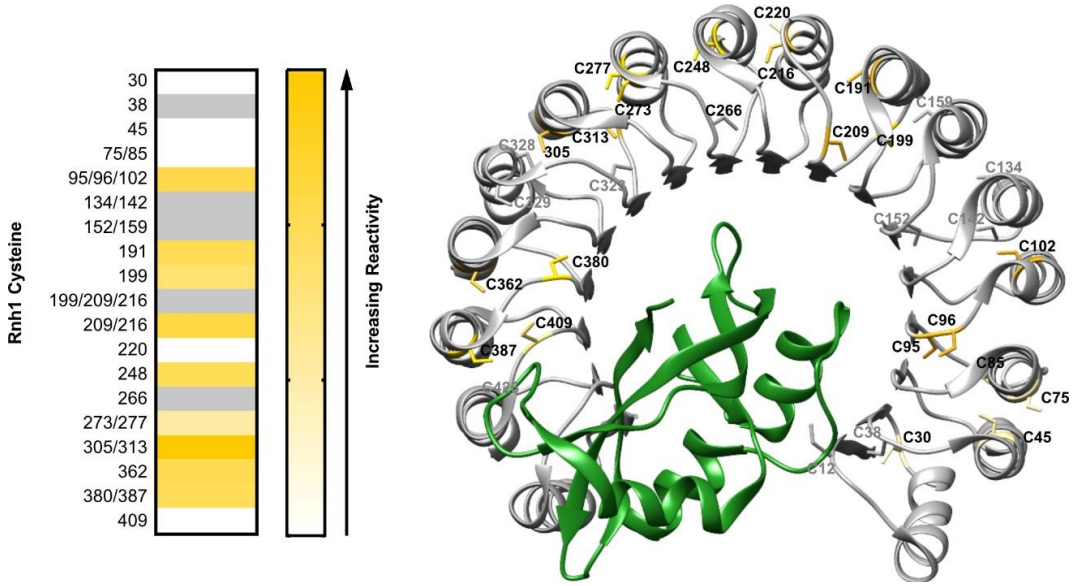

Figure 4-3 Ranking RI cysteines by reactivity. Heatmap shows reactive cysteines in dark yellow (grey = cysteine containing peptide that was identified with no reported *R* value). Cysteine position within the RI monomer is highlighted with the corresponding color from the heatmap. Bound RNase1 is shown in green.

Cysteine Position	Peptide Sequence	R value
30	WAELLPLLQQCQVVR	5.33
38	LDDCGLTEAR	-
45	CKDISSALR	4.88
75, 85	SNELGDVGVHCVLQGLQTPSCK	4.44
95, 96, 102	LSLQNCCLTGAGCGVLSSTLR	1.88
134, 142	TLPTLQELHLSDNLLGDAGLQLLCEGLLDPQCR	-
152, 159	LQLEYCSLSAASCEPLASVLR	-
191	VLCQGLK	1.98
199	DSPCQLEALK	2.33
199, 209, 216	DSPC*QLEALKLESC*GVTSDNCR	-
209, 216	LESCGVTSDNCR	1.82
220	DLCGIVASK	4.68
248	LGDVGMAELCPGLLHPSSR	2.02
273, 277	GCGDLCR	2.92
305, 313	LLCETLLEPGCQLESLWVK	1.00

362	ELCQGLGQPGSVLR	1.96
380, 387	VLWLADCDVSDSSCSSLAATLLANHSLR	2.07
409	ELDLSNNCLGDAGILQLVESVR	4.19

Table 4-2 RI cysteine containing peptides identified by MS and their reported cysteine reactivity *R* values.

4.2.3 Profiling cysteine oxidation in RI

With the observed variability in cysteine reactivity, we wondered if highly reactive cysteines are more prone to oxidation, resulting in preferential cysteine oxidation before the "all-or-none" RI oxidation switch and inactivation occurs. We hypothesized that an initial oxidation event at one or more specific cysteine residues may initiate a protein conformation change, thus allowing for the remainder of cysteines to become oxidized, likely though disulfide bond formation. To understand the role of individual cysteine residues in the transition from fully reduced (active) to fully oxidized (inactive) RI, we needed to monitor oxidation at individual cysteines within RI. The oxidative isotope coded affinity tagging (OxICAT) method adapts thiol-trapping techniques with isotopically encoded alkylating reagents to interrogate the cysteine oxidation state and has been used to report on cysteine oxidation within a single sample[21,24].

Here, we subjected purified RI to treatment with a range of oxidants (H_2O_2, GSSG, H_2O_2/Fe^{2+}). All reduced cysteine thiols were capped with isotopically encoded N-ethylmaleimide-light tag (NEM-light) (Fig 4-4). Reversibly oxidized cysteine thiols were then reduced using tris(2-carboxyethyl)phosphine (TCEP) and subsequently reacted with isotopically encoded N-ethylmaleimide-heavy tag (NEM-heavy). Trypsin digestion and LC-MS/MS analysis of the RI peptide mixture was performed.

The abundance of the of NEM-light and NEM-heavy labeled peptides affords a light: heavy (L/H) ratio. A L/H ratio >> 1, indicates a cysteine residue is predominantly in the reduced form, a L/H ratio = 1 indicates a cysteine is 50% reduced/50% oxidized, while a L/H ratio << 1 indicates a cysteine is predominantly oxidized. These light:heavy ratio values were used to determine the percentage of oxidation for each identified cysteine residue within the sample.

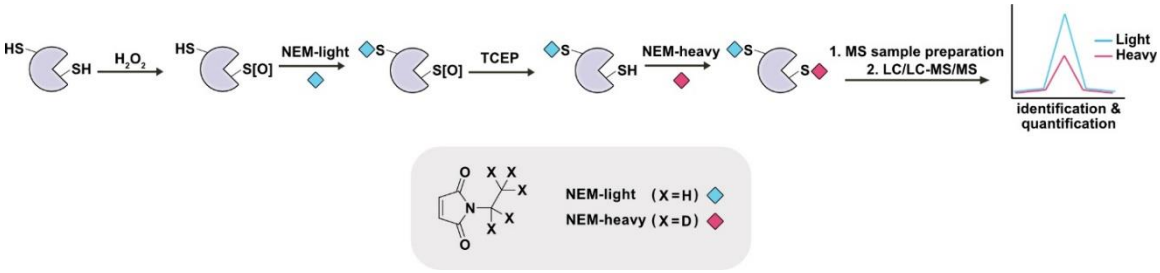

Figure 4-4 OxICAT workflow to quantitatively monitor cysteine oxidation on RI. *R* >> 1, indicates a cysteine residue is predominantly reduced, while *R* = 1 indicates a cysteine is 50% reduced and 50% oxidized, and *R* << 1 indicates a cysteine is predominantly oxidized.

We first treated RI with a range of oxidants or redox environments including H_2O_2, varied GSH/GSSG mixtures, or GSSG alone, which did not allow for observation of RI in a transitionary oxidation state. However H_2O_2 alone is a poor oxidant in biological systems compared to ·OH (H_2O_2 rate constant (reaction with protein thiol) = 2.9 $L \cdot mol^{-1} \cdot sec^{-1}$; ·OH rate constant (reaction with protein thiol) = 10^{10} $L \cdot mol^{-1} \cdot sec^{-1}$) and H_2O_2 toxicity is exerted indirectly via transition metal catalyzed oxidation (Fenton/Haber Weiss chemistry) that produces ·OH[25]. With this in mind, we switched to treating RI with H_2O_2 in the presence of Fe^{2+}.

Using the OxICAT method, were able to monitor oxidation on 27 of the 32 cysteines on RI in response to treatment with 0, 1, 5, 10, and 20 mM H_2O_2 in the 2presence of Fe^{2+}. In the untreated control sample (0 mM H_2O_2) most cysteines are

predominantly reduced with an average percent oxidation of 8.43%. We observed increasing oxidation upon treatment with higher concentrations of H_2O_2, with the average cysteine percent oxidation reaching 87% upon treatment with 20 mM H_2O_2 (Fig 4-5A), indicating almost complete oxidation. Intermediate levels of H_2O_2 (5 and 10 mM) afforded cysteines with an average percent oxidation of 42.8 and 56.3%, respectively, suggesting at these concentrations we may be able to identify preferentially oxidized cysteines. To interrogate preferential oxidation, we plotted the percent oxidation of each cysteine containing peptide at each of the H_2O_2 concentrations. As anticipated, at higher H_2O_2 levels, we see almost complete cysteine oxidation for each peptide (Fig 4-5B, Table 4-3). However, at lower and intermediate H_2O_2 levels we can see certain cysteine containing peptides are oxidized at higher levels than others. In particular, Cys 38 and 45 appear to be slightly more sensitive to oxidation than other cysteine containing peptides, a trend which is observed in the 1 mM, 5 mM and 10 mM H_2O_2 treatment conditions. Other cysteine containing peptides do show slight preferential oxidation within certain treatment conditions, such as cysteine 409 upon 5 mM and 10 mM H_2O_2 treatment, however this trend seems to appear with higher H_2O_2 levels, indicating that there may be an order to cysteine oxidation in the RI oxidation mechanism.

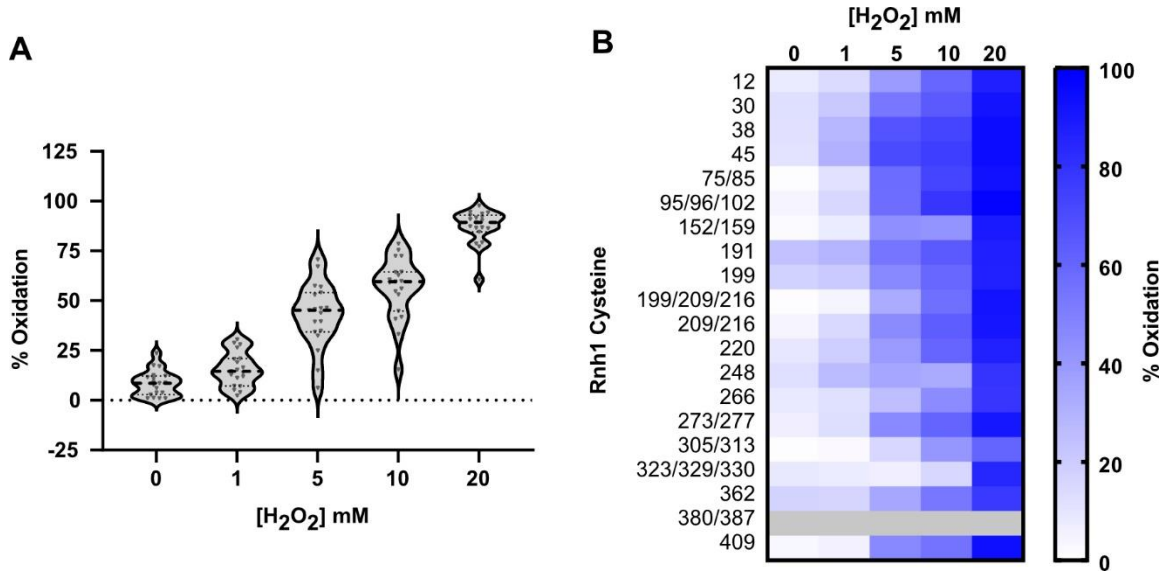

Figure 4-5 (A) Levels of RI cysteine oxidation upon treatment with 0, 1, 5, 10, or 20 mM H_2O_2. **(B)** Extent of RI cysteine oxidation at individual cysteine containing peptides identified within each treatment condition.

Cysteine Position	Peptide Sequence	% Oxidation				
		0 mM	1 mM	5 mM	10 mM	20 mM
12	MSLDIQSLDIQCEELSDAR	7.63	13.87	39.42	59.51	86.75
30	WAELLPLLQQCQVVR	12.19	20.88	52.97	64.47	91.66
38	LDDCGLTEAR	11.62	28.12	67.18	72.41	94.52
45	CKDISSALR	10.77	30.50	70.67	75.41	94.16
75, 85	SNELGDVGVHCVLQGLQTPSCK	0.99	11.23	57.41	72.41	92.89
95, 96, 102	LSLQNCCLTGAGCGVLSSTLR	3.87	15.36	56.90	78.62	97.66
152, 159	LQLEYCSLSAASCEPLASVLR	1.20	7.06	43.84	41.75	89.37
191	VLCQGLK	23.54	28.77	54.00	64.33	87.37
199	DSPCQLEALK	17.62	20.71	46.23	59.08	86.28
199, 209, 216	DSPCQLEALKLESCGVTSDNCR	0.99	4.10	32.41	56.01	92.08
209, 216	LESCGVTSDNCR	3.79	14.51	45.21	62.86	90.95
220	DLCGIVASK	9.23	19.02	39.52	59.87	86.54
248	ELALGSNKLGDVGMAELCPGLLHPSSR	12.51	26.47	34.76	33.20	79.15
266	TLWIWECGITAK	8.51	11.98	24.91	44.86	78.68
273, 277	GCGDLCR	6.10	12.77	45.66	60.53	90.29
305, 313	LLCETLLEPGCQLESLWVK	0.99	2.27	14.95	40.80	60.57
323, 329, 330	SCSFTAACCSHFSSVLAQNR	8.84	7.15	6.24	15.44	84.57
362	ELCQGLGQPGSVLR	17.02	16.41	34.31	53.02	77.19
409	ELDLSNNCLGDAGILQLVESVR	2.77	5.16	46.43	54.63	93.68

Table 4-3 Percent oxidation on RI cysteines upon treatment with 0 - 20 mM H_2O_2.

There are many cysteines found on peptides with more than one cysteine residue. Since the generated *R* value and corresponding percent oxidation value do not differentiate between different cysteines on the same peptide, we looked to the MS traces to ensure that we can assign a *R* value to the whole peptide and not just one of the cysteines on that peptide. We confirmed that multi-cysteine containing peptides exist as dually labeled with the same NEM tag, and the mixed species (one cysteine modified with NEM-light and one NEM-heavy) does not predominate or effect the reported *R* value. Here, we show the MS1 traces of the peptide containing cysteines 209 and 216 from the 0 mM and 20 mM H_2O_2 treatments (Fig 4-6). In the 0 mM sample, this peptide predominantly exists as the dually NEM-light labeled species (reduced), while in the 20 mM sample, the peptide predominantly exists as dually NEM-heavy labeled (oxidized), corresponding with the reported percent oxidation values (3.79 % (0 mM) and 90.95% (20 mM)).

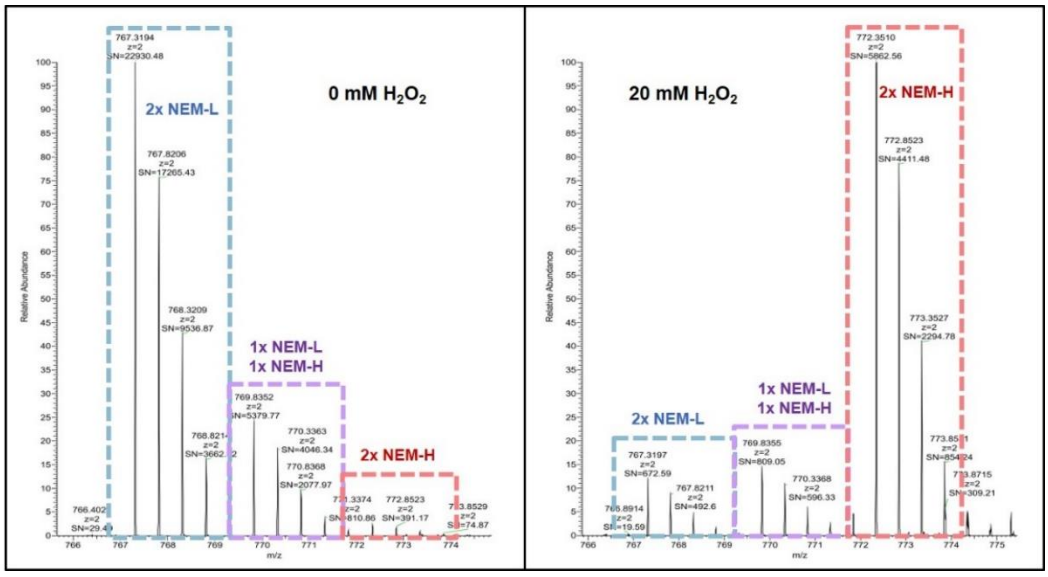

Figure 4-6 MS1 traces for the RI peptide AA 209-217: LESCGVTSDNCR. Cysteines 209 and 216 are predominantly labeled with 2x NEM-light in the 0mM H_2O_2 sample or 2x NEM-heavy in the 20 mM H_2O_2 sample.

To our surprise, we observed no correlation between cysteine oxidation and reactivity. There was a wide range in percent oxidation for the cysteines that fell into the subgroups of low, moderate, or high reactivity (Fig 4-7) and we saw no significant changes in the median percent cysteine oxidation for cysteines across different reactivity subgroups. Interestingly, potential sites of preferential oxidation (Cys 45 and Cys 409) were identified within the low reactivity subgroup, while a ratio value for Cys 38 was not obtained within the cysteine reactivity dataset.

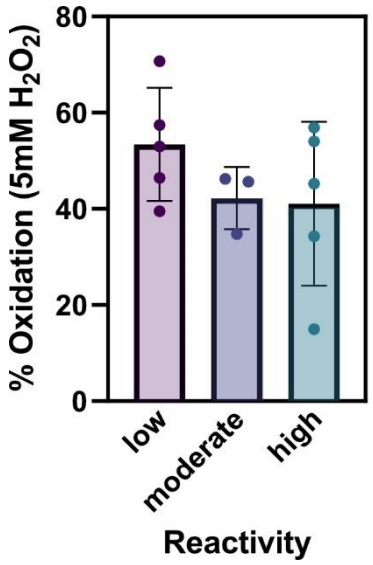

Figure 4-7 Median percent oxidation values broken up by cysteine reactivity subgroups (low, moderate, and high reactivity).

4.3 CONCLUSIONS AND FUTURE DIRECTIONS

The cytosolic ribonuclease inhibitor (RI) protein is found throughout the human body, working to protect our cells from the toxic activity of invading pancreatic type RNases. It is established that the fully reduced RI is active and binds

RNases, whereas fully oxidized RI undergoes a conformational change and loses the ability to bind RNase[18]. Here, we investigated the role of individual cysteine residues in the transition from an active to inactive RI. We found that RI cysteines can be monitored by LC-MS/MS and cysteine residues differ in reactivity, with the least reactive cysteines neat the N- or C-terminus of the protein, proximal to the RNase binding region. Interrogation of cysteine oxidation, shows that RI does primarily exist in fully reduced or fully oxidized states, as the previously described of RI "all-or-none" oxidation suggests. However, during the transition from fully reduced (active) to fully oxidized (inactive) certain cysteines (Cys 38, 45, and 409) are oxidized to a greater extent than others, suggesting preferential oxidation at these sites. Interestingly, all of these sites of preferential oxidation were shown to have low reactivity and are located near the RNase binding region.

Further investigation is required for understanding the potential role of sites of preferential oxidation. Assessing oxidation of RI with mutations of the preferentially oxidized sites, Cys 38 and Cys 45, would help to determine if these sites are required for an initial RI oxidation event., and subsequent oxidation of the remainder of RI cysteines. Determining the effects of RI oxidation *in Cellulo* in response to endogenously produced ROS would help to gain a better understanding of RI as a redox switch and understand conditions in which RI becomes inactive and induces cell death. In order to study RI oxidation *in Cellulo* we would treat cells -/+ EGF to activate NOX and the subsequent production of reactive oxygen species (ROS)[26], then quantify levels of RI oxidation on individual cysteines.

Furthermore, RI has also been shown to undergo phosphorylation by ERK-pathway kinases, and kinase inhibitors prevent RI phosphorylation[1]. Future studies will explore the interplay between phosphorylation and cysteine oxidation, hypothesizing that kinase inhibitors will affect the susceptibility of RI to oxidation i*n Cellulo*. Lastly, upon establishing RI oxidation under physiologically relevant increases in ROS, we can work to correlate RI oxidation with RNase-driven toxicity and cell death.

4.4 METHODS

MS sample preparation: trypsin digestion of purified RI

Recombinant RI (100 μg) was purified from E coli and provided to us from the Raines lab. RI (100 μg) was buffer exchanged into PBS using a micro bio-spin p6 column pre equilibrated with PBS) and subsequently precipitated with 10% trichloroacetic acid (TCA) in PBS (-80 °C, 1 hr or overnight). After briefly thawing, precipitated proteins were pelleted (15,000 rpm, 10 min). Supernatants were discarded and the protein pellets were washed with 500uL ice cold acetone, followed by centrifugation (5,000 rpm, 10 min). The washed pellets were resuspended in 30 μL of 8 M urea in PBS and underwent sonication to resolubilize. 70 μL of 100 mM ammonium bicarbonate was added to bring sample volumes to 100 μL. Reductive alkylation was performed by treated samples with 15 mM DTT (65 °C, 15 min), followed by 12.5 mM iodoacetamide (25 °C, 30 min). Samples were

diluted upon addition of 120 µL of PBS and in-solution trypsin digestion was performed by adding trypsin (2.0 µg) and 1.0 mM calcium chloride (37 °C, overnight). 10 µL of MS-grade formic acid was added, and samples were centrifuged at 15,000 rpm for 20 min. The supernatant was collected and stored at -20 °C until MS analysis.

MS sample preparation: evaluating RI cysteine reactivity

Methods for studying cysteine reactivity were adapted from Weerapana, E. *et al.* and Abo, M. *et al.*[22,23]. The purified RI samples (100 µg) were buffer exchanged into PBS, split into two equal fractions, and treated with 10 µM isotopically encoded 'light' IA-alkyne or 100 µM isotopically encoded 'heavy' IA-alkyne (from 1 mM and 10 mM stocks in DMSO, respectively) (25 °C, 1 hr). Light and heavy IA-alkyne labeled proteins were precipitated with 10% TCA in PBS (-80 °C, 1hr or overnight). After briefly thawing, precipitated proteins were pelleted (15,000 rpm, 10 min). The resulting protein pellets were washed with 500uL ice cold acetone, and samples were combined, followed by centrifugation (5,000 rpm, 10 min). Samples then followed the remainder of the tryptic digest protocol: including denaturation in urea, reductive alkylation with DTT and IA, and in solution trypsin digestion.

LC–MS/MS analysis for RI trypsin digestion and cysteine reactivity studies

Liquid chromatography with tandem mass spectrometry (LC-MS/MS) analysis was performed on an LTQ-Orbitrap Discovery mass spectrometer (Thermo Scientific) coupled to an Agilent 1200 Series HPLC. RI peptide samples were split in

half and pressure loaded onto 250 μm fused silica desalting columns (Agilent) packed with 4 cm Aqua C18 reverse phase resin (Phenomenex). Peptides were then eluted onto a column consisting of 100 μm fused silica packed with 10 cm C18, followed by a gradient of 5–100% Buffer B in Buffer A (Buffer A: 95% H_2O, 5% acetonitrile, and 0.1% formic acid; Buffer B: 20% H_2O, 80% acetonitrile, and 0.1% formic acid) at a flow rate of 250 nl min^{-1}. Eluted peptides were injected into the mass spectrometer by electrospray ionization (spray voltage set at 2.75 kV). For every MS1 survey scan (400–1800 m/z), eight data-dependent scans were run for the *n*th most intense ions with dynamic exclusion enabled.

MS data analysis: RI trypsin digestion and cysteine reactivity studies

The generated tandem MS data were searched using the SEQUEST algorithm[27] against the *E. coli* K12 proteome UniprotKB database with the full-length human RI amino acid sequence added. A static modification of +57.02146 on cysteine was specified to account for alkylation with IA. For cysteine reactivity studies, the additional variable modifications were assigned on cysteine to account for IA-alkyne light or heavy probe modification: +128.0626 (light) and +134.0827 (heavy). Output files from SEQUEST were filtered using DTASelect 2.0 to afford a list of tryptic peptides. For cysteine reactivity studies, quantification of isotopic heavy:light ratios was performed using the CIMAGE quantification package as previously described[22]. Overlapping tryptic peptides containing the same labeled cysteine (but different charge states or tryptic termini) were grouped and the

median reported as the final heavy:light ratio (*R*). *R* values were averaged across two replicates.

MS sample preparation: evaluating RI cysteine oxidation with OxICAT

Methods for using OxICAT to study cysteine oxidation in purified RI were adapted from Bechtel, T. *et al.*[21]. Purified RI protein (50ug) underwent buffer exchange into PBS and was subsequently treated with a mixture of H_2O_2, $FeSO_4$, and EDTA in a ratio of 100:1:3 (H_2O_2:$FeSO_4$:EDTA) as described by Kocha *et al.*[28] with final concentrations of 0, 1, 5, 10, or 20 mM H_2O_2 (25 °C, 2 hr). Following oxidation, RI protein was precipitated with 10% TCA) in PBS (-80 °C, 1 hr or overnight). After briefly thawing, precipitated proteins were pelleted (15,000 rpm, 10 min). Supernatants were discarded and the protein pellets were washed with 500uL ice cold acetone, followed by centrifugation (5,000 rpm, 10 min). The precipitated protein pellets were resuspended in 100 µL denaturing alkylation buffer (DAB: 6 M urea, 200 mM Tris-Cl, pH 8.5, 10 mM EDTA, 0.5% SDS). Samples were labeled with 10 mM light IA-alkyne (2 µL of 500 mM stock in DMSO) (37 °C, 2 hr) with constant agitation. Any cell debris was pelleted by centrifugation (16,000 x g, 1 min) and the supernatant was diluted 3-fold with H_2O (300 µL total volume). Protein was precipitated upon the addition of 5 volumes (1.5 mL) cold acetone (-20 °C, 2hr), then pelleted at 4 °C (4,500 x g, 30 min). Pellet was washed with 500 µL ice-cold acetone, centrifuged at 4 °C (4,500 x g, 10 min), then allowed to air dry. After drying, pellet was resuspended in 80 µL of DAB. Reversibly oxidized cysteines were reduced by incubating sample with 2.5 mM TCEP (37 °C, 5 min). Reduced samples were

diluted with 120 µL DAB (200 µL final volume), and cysteines were capped with 10 mM heavy IA-alkyne (4 µL of 500 mM stock in DMSO) and incubated at 37 °C for 2 hr. Samples were diluted 3-fold with H_2O (600 µL total). Protein was precipitated with 5 volumes (3 mL) of ice-cold acetone (-20 °C ,2 hr or overnight), then pelleted at 4°C (4,500 x g, 30 min). Pellet was washed with 500 µL cold acetone, centrifuged (4,500 x g, 10 min), then allowed to air dry. After drying, pellet was resuspended in 2 M urea followed by in solution trypsin digest.

LC-MS/MS analysis: RI cysteine oxidation with OxICAT

RI OxICAT peptide samples were dried down by speed vac and resuspended in 250 µL 100% H_2O, 0.1 % formic acid. Samples were analyzed by liquid chromatography with tandem mass spectrometry (LC-MS/MS) using an Orbitrap Exploris 240 mass spectrometer (Thermo Scientific) coupled to a Dionex Ultimate 3000 RSLC nano system (Thermo Scientific). 5µL of peptide sample was injected directly onto an Acclaim PepMap 100 loading column. Peptides were eluted onto an Acclaim PepMap RSLC and separated with a 60 min gradient of 5% - 99% Buffer B in Buffer A (Buffer A: 100% H_2O, 0.1% formic acid; Buffer B: 80% acetonitrile, 20% H_2O, 0.1% formic acid). Instrumentation operated at a flow rate of 0.3 µL/min buffer through the column and spray voltage of 2.1 kV. One full MS scan (350-1800 m/z, 120,000 resolution, RF lens 65%, AGC target 300%, automatic maximum injection time, profile mode) was obtained every 2 seconds with dynamic exclusion (repeat count 2, duration 10 s), isotopic exclusion (assigned), and apex detection (30% desired apex window) enabled. A variable number of MS2 scans (15,000 resolution,

AGC 75%, maximum injection time 100 ms, centroid mode) were obtained between each MS1 scan based on the highest precursor masses, filtered for monoisotopic peak determination, theoretical precursor isotopic envelope fit, intensity (5E4), and charge state (2-6). MS2 analysis consisted of the isolation of precursor ions (isolation window 2 m/z) followed by high-energy collision dissociation (HCD) (collision energy 30%).

MS data analysis: RI cysteine oxidation with OxICAT

RI OxICAT MS data was analyzed using the Thermo Proteome Discoverer software (PD; version 2.4.1.15). Protein identification was achieved using the SequestHT algorithm searching against an *E. coli* K12 proteome UniprotKB database with the full-length human RI amino acid sequence added. Fixed value PSM validator with a maximum delta Cn of 0.5. The protease enzyme was set as trypsin with a maximum of 2 missed cleavages allowed. The peptide precursor mass tolerance was set to 10 ppm with a fragment mass tolerance of 0.02 Da. Dynamic modifications included methionine oxidation (+ 15.995), N-terminal acetylation (+42.011) and/or methionine loss (-131.040), and cysteine alkylation by either light-NEM (+125.048) and heavy-NEM (+130.079). The false discovery rate (FDR) for peptide identification was set at 1% for highly confident peptide hits and peptides were required to have at least 5 peptide spectral matches (PSMs). Overlapping tryptic peptides containing the same labeled cysteine (but different charge states or tryptic termini) were grouped and the median reported as the final light:heavy ratio (*R*). Singleton ratio values (R = 0.1 or R = 100) were only considered if there was not

another non-singleton replicate value. Average L:H ratios were calculated from two replicates and converted to percent oxidation values by the following equation: (1-(L:H/(L:H+1))*100).

REFERENCES

(1) Hoang, T. T.; Caglar Tanrikulu, I.; Vatland, Q. A.; Hoang, T. M.; Raines, R. T. A Human Ribonuclease Variant and ERK-Pathway Inhibitors Exhibit Highly Synergistic Toxicity for Cancer Cells. *Mol. Cancer Ther.* **2018**, *17* (12), 2622–2632.

(2) Lomax, J. E.; Bianchetti, C. M.; Chang, A.; Phillips, G. N.; Fox, B. G.; Raines, R. T. Functional Evolution of Ribonuclease Inhibitor: Insights from Birds and Reptiles. *J. Mol. Biol.* **2014**, *426* (17), 3041–3056.

(3) Girija, N. S.; Sreenivasan, A. A. Characterization of Ribonucleases and Ribonuclease Inhibitor in Subcellular Fractions from Rat Adrenals. *Biochem J.* **1966**. *98,* 562-566.

(4) Roth, J. S. Ribonuclease IX. Further Studies on Ribonuclease Inhibitor. *BBA Spec. Sect. Nucleic Acids Relat. Subj.* **1962**, *61* (6), 903–915.

(5) Dickson, K. A.; Haigis, M. C.; Raines, R. T. Ribonuclease Inhibitor: Structure and Function. *Progress in Nucleic Acid Research and Molecular Biology*. **2005**, 349–374.

(6) Johnson, R. J.; McCoy, J. G.; Bingman, C. A.; Phillips, G. N.; Raines, R. T. Inhibition of Human Pancreatic Ribonuclease by the Human Ribonuclease Inhibitor Protein. *J. Mol. Biol.* **2007**, *368* (2), 434–449.

(7) Ledoux, L.; Baltus, E. Action de La Ribonucléase Sur Les Cellules Du Carcinome d'Ehrlich. *Experientia* **1954**, *10* (12), 500–501.

(8) Ledoux, L. Action of Ribonuclease on Two Solid Tumours in Vivo. *Nature* **1955**, *176* (4470), 36–37.

(9) Haigis, M. C.; Kurten, E. L.; Raines, R. T. Ribonuclease Inhibitor as an Intracellular Sentry. *Nucleic Acids Res.* **2003**, *31* (3), 1024–1032.

(10) Haigis, M. C.; Kurten, E. L.; Raines, R. T. Ribonuclease Inhibitor as an Intracellular Sentry. *Nucleic Acids Res.* **2003**, *31* (3), 1024–1032.

(11) Altomare, D. A.; Rybak, S. M.; Pei, J.; Maizel, J. V.; Cheung, M.; Testa, J. R.; Shogen, K. Onconase Responsive Genes in Human Mesothelioma Cells: Implications for an RNA Damaging Therapeutic Agent. *BMC Cancer* **2010**, *10* (1), 1–12.

(12) Mikulski, S. M.; Costanzi, J. J.; Vogelzang, N. J.; McCachren, S.; Taub, R. N.; Chun, H.; Mittelman, A.; Panella, T.; Puccio, C.; Fine, R.; et al. Phase II Trial of a Single Weekly Intravenous Dose of Ranpirnase in Patients With Unresectable

Malignant Mesothelioma. *J. Clin. Oncol.* **2002**, *20* (1), 274–281.

(13) Shen, R.; Li, J.; Ye, D.; Wang, Q.; Fei, J. Combination of Onconase and Dihydroartemisinin Synergistically Suppresses Growth and Angiogenesis of Non–Small-Cell Lung Carcinoma and Malignant Mesothelioma. *Acta Biochim. Biophys..* **2016**, *48* (10), 894–901.

(14) Zhuang, X.; Lv, M.; Zhong, Z.; Zhang, L.; Jiang, R.; Chen, J. Interplay between Intergrin-Linked Kinase and Ribonuclease Inhibitor Affects Growth and Metastasis of Bladder Cancer through Signaling ILK Pathways. **2016**.

(15) Leland, P. A.; Staniszewski, K. E.; Kim, B. M.; Raines, R. T. Endowing Human Pancreatic Ribonuclease with Toxicity for Cancer Cells. *J. Biol. Chem.* **2001**, *276* (46), 43095–43102.

(16) Cui, X. Y.; Fu, P. F.; Pan, D. N.; Zhao, Y.; Zhao, J.; Zhao, B. C. The Antioxidant Effects of Ribonuclease Inhibitor. *Free Radic. Res.* **2003**, *37* (10), 1079–1085.

(17) Monti, D. M.; Montesano Gesualdi, N.; Matoušek, J.; Esposito, F.; D'Alessio, G. The Cytosolic Ribonuclease Inhibitor Contributes to Intracellular Redox Homeostasis. *FEBS Lett.* **2007**, *581* (5), 930–934.

(18) Fominaya, J. M.; Hofsteenges, J. Inactivation of Ribonuclease Inhibitor by Thiol-Disulfide Exchange. *J. Biol. Chem.* **1992**, *267* (34), 24655–24660.

(19) Blázquez, M.; Fominaya, J. M.; Hofsteenge, J. Oxidation of Sulfhydryl Groups of Ribonuclease Inhibitor in Epithelial Cells Is Sufficient for Its Intracellular Degradation *J. Biol. Chem.* **1996**; Vol. 271.

(20) Pacifici, R. E.; Davies, K. J. A. Protein Degradation as an Index of Oxidative Stress. *Methods Enzymol.* **1990**, *186* (C), 485–502.

(21) Bechtel, T. J.; Li, C.; Kisty, E. A.; Maurais, A. J.; Weerapana, E. Profiling Cysteine Reactivity and Oxidation in the Endoplasmic Reticulum. *ACS Chem. Biol.* **2020**, *15* (2), 543–553.

(22) Weerapana, E.; Wang, C.; Simon, G. M.; Richter, F.; Khare, S.; Dillon, M. B. D.; Bachovchin, D. A.; Mowen, K.; Baker, D.; Cravatt, B. F. Quantitative Reactivity Profiling Predicts Functional Cysteines in Proteomes. *Nature* **2010**, *468* (7325), 790–795.

(23) Abo, M.; Li, C.; Weerapana, E. Isotopically-Labeled Iodoacetamide-Alkyne Probes for Quantitative Cysteine-Reactivity Profiling. *Mol. Pharm.* **2018**, *15* (3), 743–749.

(24) Leichert, L. I.; Gehrke, F.; Gudiseva, H. V.; Blackwell, T.; Ilbert, M.; Walker, A. K.;

Strahler, J. R.; Andrews, P. C.; Jakob, U. Quantifying Changes in the Thiol Redox Proteome upon Oxidative Stress in Vivo. *Proc. Natl. Acad. Sci.* **2008**, *105* (24), 8197–8202.

(25) Collin, F. Chemical Basis of Reactive Oxygen Species Reactivity and Involvement in Neurodegenerative Diseases. *Int. J. Mol. Sci. 2019, Vol. 20, Page 2407* **2019**, *20* (10), 2407.

(26) Van Heerebeek, L.; Meischl, C.; Stooker, W.; Meijer, C. J. L. M.; Niessen, H. W. M.; Roos, D. NADPH Oxidase(s): New Source(s) of Reactive Oxygen Species in the Vascular System? *Journal of Clinical Pathology*. **2002**, 561–568.

(27) Eng, J. K.; McCormack, A. L.; Yates, J. R. An Approach to Correlate Tandem Mass Spectral Data of Peptides with Amino Acid Sequences in a Protein Database. *J. Am. Soc. Mass Spectrom.* **1994**, *5* (11), 976–989.

(28) Kocha, T.; Yamaguchi, M.; Ohtaki, H.; Fukuda, T.; Aoyagi, T. Hydrogen Peroxide-Mediated Degradation of Protein: Different Oxidation Modes of Copper- and Iron-Dependent Hydroxyl Radicals on the Degradation of Albumin. *Biochim. Biophys. Acta - Protein Struct. Mol. Enzymol.* **1997**, *1337* (2), 319–326.

5.0 CHEMICAL PROTEOMIC METHODS TO IDENTIFY REACTIVE CYSTIENES IN TOXOPLASMA GONDII

A significant portion of the work described in this chapter has been published in:

Benns, H.J., Storch, M., Falco, J.A., Fisher, F.R. Tamaki, F., Alves, E., Wincott, J.C., Milne, R., Wiedemar, N., Craven, G., Baragana, B., Wyllie, S., Baum, J. Baldwin, G.S., Weerapana, E., Tate, E.W., Child, M.A. CRISPR-based oligo recombineering prioritizes apicomplexan cysteines for drug discovery. *Nature Microbiology* **7**, 1891-1905 (2022).

5.1 INTRODUCTION

Only a small percentage of human gene products are druggable using traditional modes of non-covalent ligand design[1]. Covalent ligands offer advantages over non-covalent ligands including an increased target residency time, resulting in more durable pharmacological action. Additionally, covalent ligands have the potential to achieve improved potency for shallow binding pockets over non-covalent ligands, affording potential 'druggability' of previously 'undruggable' protein targets[2]. A resurgence of targeted covalent inhibitors has occurred in recent years[3,4], with covalent chemical probes and drugs for hydrolases, kinases, and oncogenic GTPases[5–9]. This resurgence is likely attributed to chemical proteomic strategies, such as activity-based protein profiling (ABPP), that profile ligands for proteins within complex biological systems. Specifically, cysteine reactivity profiling aids in covalent-inhibitor development through identification of functional cysteines that lead to modulation of protein activity through covalent modification[10].

In order to globally characterize cysteine functionality in proteomes, Weerapana *et al.* developed an isotopic tandem-orthogonal activity-based protein profiling (isoTOP-ABPP) method[11]. Here, the cysteine reactive electrophile, iodoacetamide, is used to quantitatively profile intrinsic cysteine reactivity. This method allows for identification of hyper-reactive cysteines that predict functional sites within the proteome, including sites of nucleophilic and reductive catalysis and sites of oxidative modification.

Our goal is to apply the iso-TOP ABPP platform to an understudied organism with relevance in human health, *Toxoplasma Gondii. T. gondii* is an intracellular parasitic protozoan (apicomplexan) that causes toxoplasmosis, and is evolutionarily related to the malaria parasite *Plasmodium falciparum*[12]. It is suggested that 30-50% of the worlds human population carry the Toxoplasma parasite, but most do not show symptoms of infection because the immune system prevents illness[13]. However, a Toxoplasma infection can be severe and sometimes fatal in people with compromised immune systems or when passed from a pregnant woman to a developing infant in the womb. Current frontline therapeutics are ineffective against the chronic bradyzoite lifecycle stage and limited by toxicity[14], highlighting the need for rapid identification and prioritization of new therapeutic targets. The identification of highly reactive cysteines in *T. gondii* will afford insight into functionally relevant sites, providing a handle for the development of covalent inhibitors as therapeutics.

5.2 RESULTS AND DISCUSSION

To prioritize functional sites for drug discovery in *T. gondii*, we applied a variation of the isoTOP-ABPP platform (Fig 5-1). Here, we treat extracellular *T. gondii* tachyzoites with either 10 μM or 100 μM iodoacetamide-alkyne (IA-alkyne)[15]. Following alkylation by the IA probe, the alkyne is further functionalized with an isotopically encoded biotin-azide tag: Azo-Light (100 μM IA-alkyne sample) or Azo-

Heavy (10 μM IA-alkyne sample) through biorthogonal copper(I)-catalyzed azide-alkyne cycloaddition (CuAAC)[11,16]. This reaction affords heavy or light labeled cysteines containing and azobenzene cleavable linker for reductive cleavage by sodium dithionite[17]. The heavy and light samples are combined and further subjected to streptavidin enrichment, on bead trypsin digestion, and sodium dithionite cleavage to afford heavy and light labeled peptides for MS analysis. MS/MS (MS2) fragmentation spectra are used to identify cysteine-labeled peptides, while the intensity of the parent ion (MS1) spectra from both the light and heavy labeled samples is used to determine a light:heavy ratio (*R*) indicative of the relative intensity of the light and heavy tag-conjugated cysteines. If the *R* value is close to 1, this indicates saturation of cysteine labeling at lower concentrations of IA in the heavy labeled sample, thus representing a reactive cysteine. Whereas, $R > 1$ indicates that a cysteine was predominantly labeled by IA in the light labeled sample, suggesting that high concentrations of the cysteine reactive probe are needed, representing an unreactive cysteine.

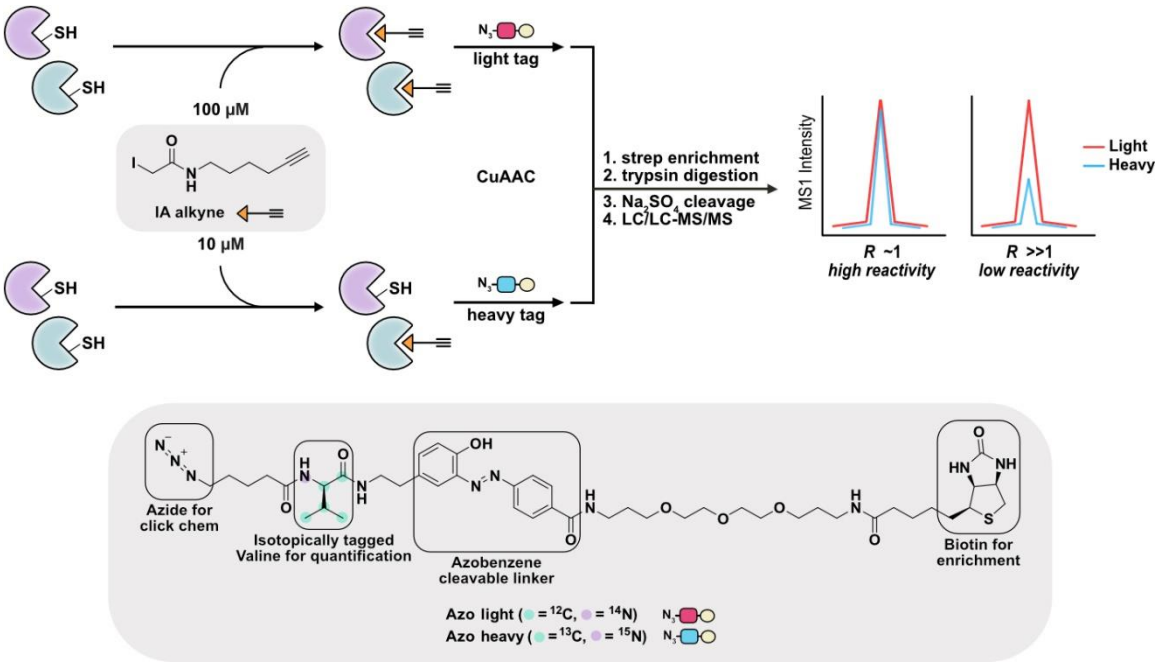

Figure 5-1 Iso-TOP ABPP workflow to profile cysteine reactivity in *T gondii* parasites. *T gondii* soluble lysates were independently labeled with high (100 µM) and low (10 µM) concentrations of the IA-alkyne probe. Labelled samples were then click-conjugated to isotopically differentiated, reductant-cleavable biotin tags (heavy (blue) and light (red) for 10 µM and 100 µM treatment groups, respectively), combined and enriched on streptavidin-immobilized beads. Immobilized proteins were then subject to tandem on-bead trypsin digestion and sodium hydrosulfite treatment, eluting probe-modified peptides for LC/LC–MS/MS analysis. *R* values represent the differences in MS1 peak intensities between the light- and heavy-conjugated proteomes, reporting on cysteine reactivity.

Using this platform, we were able to quantify reactivity on 1,097 cysteines from 691 proteins in *T. gondii* tachyzoites (Fig 5-2, Appendix I Table A5-1). Cysteines displayed a range in reactivity, and were partitioned into subgroups according to their reported *R* value: (1) high reactivity ($R < 3$); (2) moderate reactivity ($R = 3\text{-}5$); and (3) low reactivity ($R > 5$). As 'hyperreactivity' was previously found to be a predictor of functionality in cells, we were further interested in the subgroup of cysteines with high reactivity. There were 130 cysteines identified with high reactivity from 97 proteins (Appendix I Table A5-2).

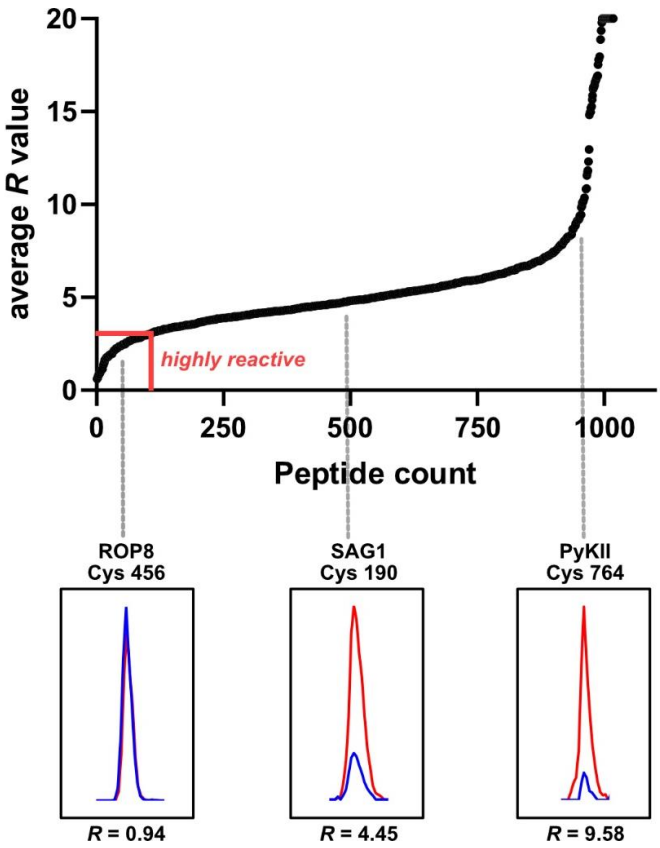

Figure 5-2 Ranked average *R* values for probe-labelled peptides from two independent experiments (n = 2). Representative MS1 chromatograms of cysteines within three groups of reactivity (high, *R* < 3; medium, R = 3–5; low, *R* > 5) are annotated. Red = light labeled peptide signal intensity; blue = heavy labeled peptide signal intensity. Figure adapted from Benns *et al.*

Proteins with known functional cysteines were identified within the highly reactive subgroup including thioredoxin family proteins, which utilize catalytic cysteines to maintain redox homeostasis and protect the parasite against ROS produced by the host immune system. In addition, we observe highly reactive cysteines within well-characterized parasite proteins for which no functional role has previously been attributed to the identified cysteines. For example, myosin F (MyoF) is a known essential motor protein[18], however the role of cysteines on this protein has not been investigated. The presence of previously unannotated functional sites, highlights the potential for identifying novel modalities for drug

discovery. A Gene Ontology analysis revealed that cysteines with high reactivity were found encoded in genes with diverse molecular functions, biological processes and subcellular localizations (Fig 5-3A). Interestingly, we observed enrichment in translation and ribosome associated proteins, prioritizing translation as a biological process to target for parasitic drug development with numerous ligandable cysteine-protein targets.

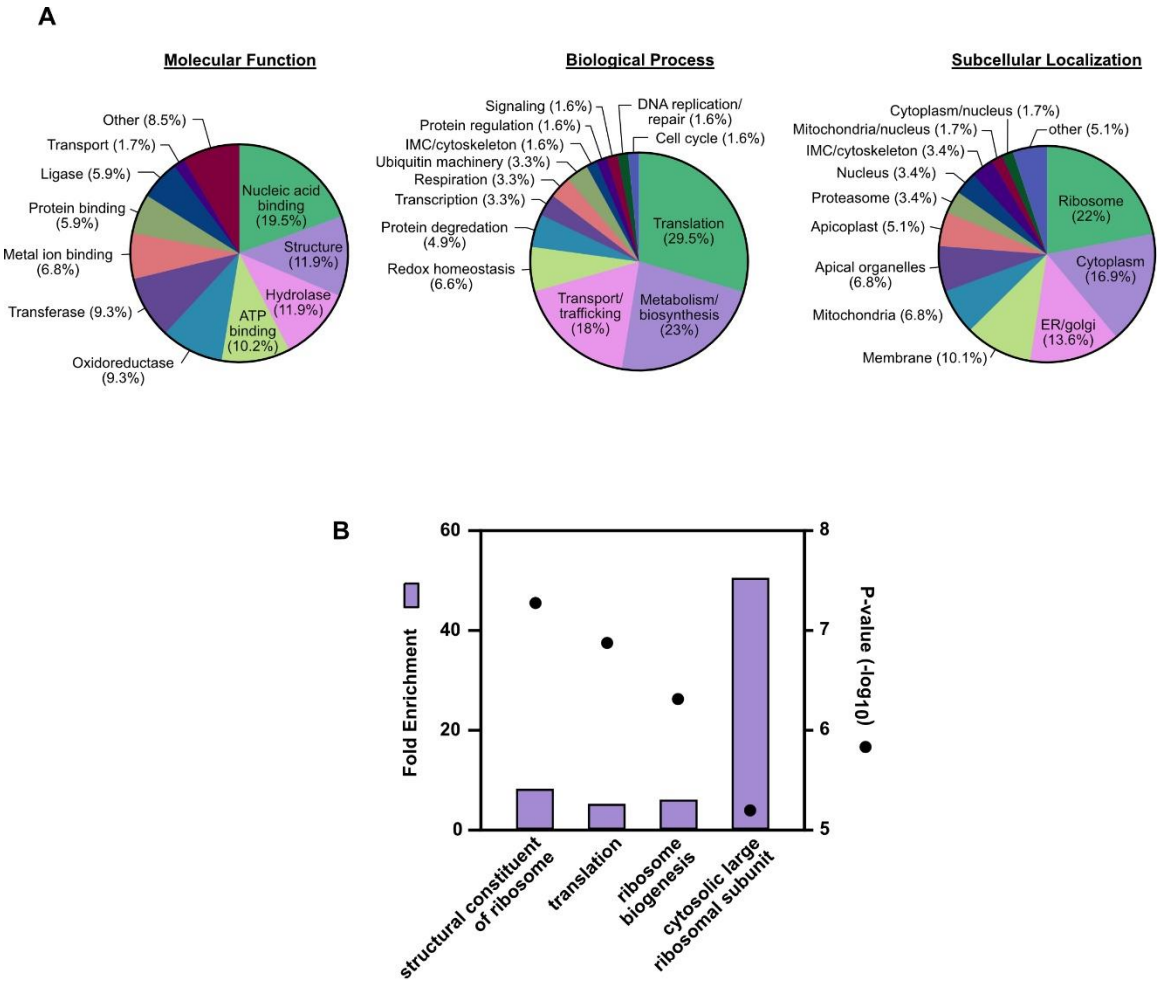

Figure 5-3 (A) Highly reactive cysteine-containing genes with functional annotations for three gene ontology categories; molecular function, biological process and subcellular localization. **(B)** Enrichment analysis of functional annotations in annotated genes containing highly electrophile-sensitive cysteines relative to the T. gondii genome. Fold change is plotted (purple bar) against statistical significance (black dot) determined from a two-tailed Fisher's exact test. Figure adapted from Benns *et al*.

Using the subset of highly reactive cysteine residues identified by iso-TOP ABPP, our collaborators further interrogated cysteine contribution to protein function. They developed a novel methodology termed CRISPR-based oligo recombineering (CORe), in which mutations at highly reactive cysteine sites are scanned for effects on cellular fitness. Mutations that perturb protein function will similarly impact cellular fitness and comparison of wild type and cysteine mutants affords unbiased prioritization of chemically reactive sites for drug discovery. Using this methodology, a subset of the highly reactive cysteines (~17%) were shown to be fitness conferring. Translation associated genes were further enriched in the fitness conferring cysteines, many of which are conserved in the malaria parasite *P. falciparum*, but not in humans. A focused cysteine reactive fragment library identified a lead parasite-selective molecule, 11H07, which inhibited parasite translation. Further studies are needed to optimize and deconvolute the target of this small molecule fragment. Cysteine-targeted inhibition of protein translation in the malaria parasite is a new potential therapeutic modality, highlighting the utility and importance of this platform in drug discovery.

5.3 CONCLUSIONS

The iso-TOP ABPP derived MS platform allowed for identification and quantification of reactivity of over 1,000 ligandable cysteines within the *T. gondii* proteome. Within the subset of highly reactive cysteines, we observed significant

enrichment in ribosome and translation related proteins. Highly reactive cysteines are likely to predict functional sites, however prioritization of these sites as targets for drug discovery has remained biased up until this point. Previously, target selection has been based on the availability of existing functional information or assays for the associated protein class, resulting in targets being overlooked with untapped therapeutic value. Combining isoTOP-ABPP with the CORe platform, allowed for further refining of functional cysteines in *T. gondii*. This focusing of drug discovery pipelines on functional sites on identified targets will aid in accelerating the discovery of targets and next-generation small-molecule therapeutics. In particular, application of this methodology allowed for prioritization of parasitic translation for drug development. The translation of our findings to the related malaria parasite *P. falciparum* provides the first evidence for this potential, with covalent inhibition of apicomplexan parasite translation being a possible new modality for novel broad-spectrum anti-microbials. Further application of this methodology to various amino acids and organisms has potential to expand our understanding of protein sequence–function relationships in complex biological systems.

5.4 METHODS

Cysteine labelling and click chemistry

Cell pellets of *T. gondii* RHΔ*ku80*Δ*hxgprt* parasites were lysed by sonication in PBS (pH 7.4) and soluble fractions separated by centrifugation at 3,500 x *g* for 5 min. Protein concentrations were determined using the DC Protein Assay Kit (Bio-Rad) and a NanoDrop 2000c Spectrophotometer (Thermo Scientific). Proteome samples diluted to 2 mg/ml were treated with 10 or 100 µM IA-alkyne (from 1 mM and 10 mM stocks in DMSO, respectively) and incubated for 1 hr at room temperature with rotation. The labelled proteins were then subject to click chemistry by addition of 100 µM Azo-L or Azo-H, 1 mM TCEP, 100 µM TBTA and 1 mM $CuSO_4$ (final concentrations). Click reactions were incubated for 1 hr at room temperature with shaking. The Azo-L/H-labelled protein samples were then precipitated by adding trichloroacetic acid to 10% (v/v) concentration. After overnight storage at −80 °C, precipitated proteins were pelleted by centrifugation (17,000 x *g*, 10 min), washed three times with chilled MeOH and resolubilized in 1.2% SDS in PBS by gentle sonication and heating (80 °C, 10 min).

Enrichment and on-bead digestion

Labeled proteome samples were diluted to 0.2% SDS with PBS. The resulting samples were then added to 100 µl of Pierce streptavidin beaded agarose resin (Thermo Scientific) and incubated overnight at 4 °C followed by a further 2 hr at room temperature. Protein-bound beads were washed with 1 x 0.2% SDS in PBS, 3 x PBS and 3 x H_2O before resuspending in 6 M urea in PBS plus 10 mM DTT and incubating at 65 °C for 15 min. Reduced samples were then alkylated by adding IAA to a final concentration of 20 mM and incubating for 30 min at 37 °C with rotation.

Samples were diluted three-fold with PBS and centrifuged (1,400 x *g*, 2 min) to pellet the beads. The beads were resuspended in a mixture of 200 µl of 2 M urea in PBS, 1 mM $CaCl_2$ and 2 µg trypsin (Promega) and incubated overnight at 37 °C. The beads were separated from the digest by centrifugation and washed three times with PBS and three times with H_2O. Azo-labelled peptides were then cleaved by adding 50 mM sodium hydrosulfite ($Na_2S_2O_4$) and rotating at room temperature for 1 hr. Eluted peptides were then collected from the supernatant, and $Na_2S_2O_4$ cleavage was repeated twice more to fractionate the sample. Between each cleavage, the beads were washed with 2 x H_2O and combined with the previous elution. Formic acid was added to the sample to 20% (v/v) concentration before storing at −20 °C until MS analysis.

LC/LC–MS/MS analysis, peptide identification and quantification

Liquid chromatography with tandem mass spectrometry (LC/LC-MS/MS) analysis was performed on an LTQ-Orbitrap Discovery mass spectrometer (Thermo Scientific) coupled to an Agilent 1200 Series HPLC. Azo digests were pressure loaded onto 250 µm fused silica desalting columns (Agilent) packed with 4 cm Aqua C18 reverse phase resin (Phenomenex). Peptides were then eluted onto a biphasic column consisting of 100 µm fused silica packed with 10 cm C18 and 4 cm PartiSphere SCX resin (Whatman) following a five-step multi-dimensional LC/LC–MS/MS protocol (MudPIT). Each step used a salt push (0%, 50%, 80%, 100% and 100%) followed by an elution gradient of 5–100% Buffer B in Buffer A (Buffer A: 95% H_2O, 5% MeCN and 0.1% formic acid; Buffer B: 20% H_2O, 80% MeCN and 0.1%

formic acid) at a flow rate of 250 nl min^{-1}. Eluted peptides were injected into the mass spectrometer by electrospray ionization (spray voltage set at 2.75 kV). For every MS1 survey scan (400–1800 m/z), eight data-dependent scans were run for the nth most intense ions with dynamic exclusion enabled.

The generated tandem MS data were searched using the SEQUEST algorithm[19] against the *T. gondii* database (GT1 proteome), *Toxo*DB (www.toxodb.org). A static modification of +57.02146 on cysteine was specified to account for alkylation with IAA. Variable modifications of +456.2849 and +462.2987 were further assigned on cysteine to account for the probe modification with the isotopically light (Azo-L) and heavy (Azo-H) variant of the IA-alkyne-Azo adduct, respectively. Output files from SEQUEST were filtered using DTASelect 2.0. Quantification of isotopic light:heavy ratios was performed using the CIMAGE quantification package as previously described[11]. Overlapping tryptic peptides containing the same labeled cysteine (but different charge states or tryptic termini) were grouped and the median reported as the final light:heavy ratio (R). R values were averaged across biological replicates, and peptides with relative standard deviation (SD) of the ≥ 50% R value were removed.

Gene Ontology enrichment analysis

Functional annotation of highly reactive cysteine containing proteins was performed using BLASTP, Gene Ontology and InterPro searches within Blast2GO 5 PRO software[20]. Consensus protein sequences were BLASTP searched against the non-redundant (nr) NCBI protein database using an E-value cut-off of 10^{-6}. Gene

Ontology terms were then mapped from the top 20 hits and merged with annotations derived from the InterPro database (www.ebi.ac.uk/interpro). Assignments were further optimized using Annex augmentation. Enrichment of annotations was assessed using Fisher's exact test against the *T. gondii* proteome (strain GT1; UniProt Taxonomy ID 507601) at <0.05 false discovery rate. All hypothetical proteins with no functional annotations were removed from data before performing enrichment analyses.

REFERENCES

(1) Moellering, R. E.; Cravatt, B. F. How Chemoproteomics Can Enable Drug Discovery and Development. *Chem. Biol.* **2012**, *19* (1), 11–22.

(2) Mah, R.; Thomas, J. R.; Shafer, C. M. Drug Discovery Considerations in the Development of Covalent Inhibitors. *Bioorg. Med. Chem. Lett.* **2014**, *24* (1), 33–39.

(3) Singh, J.; Petter, R. C.; Baillie, T. A.; Whitty, A. The Resurgence of Covalent Drugs. *Nat. Rev. Drug Discov.* **2011**, *10* (4), 307–317.

(4) Nakayama, S.; Atsumi, R.; Takakusa, H.; Kobayashi, Y.; Kurihara, A.; Nagai, Y.; Nakai, D.; Okazaki, O. A Zone Classification System for Risk Assessment of Idiosyncratic Drug Toxicity Using Daily Dose and Covalent Binding. *Drug Metab. Dispos.* **2009**, *37* (9), 1970–1977.

(5) Pan, Z.; Scheerens, H.; Li, S. J.; Schultz, B. E.; Sprengeler, P. A.; Burrill, L. C.; Mendonca, R. V.; Sweeney, M. D.; Scott, K. C. K.; Grothaus, P. G.; et al. Discovery of Selective Irreversible Inhibitors for Bruton's Tyrosine Kinase. *ChemMedChem* **2007**, *2* (1), 58–61.

(6) Patricelli, M. P.; Szardenings, A. K.; Liyanage, M.; Nomanbhoy, T. K.; Wu, M.; Weissig, H.; Aban, A.; Chun, D.; Tanner, S.; Kozarich, J. W. Functional Interrogation of the Kinome Using Nucleotide Acyl Phosphates. *Biochemistry* **2007**, *46* (2), 350–358.

(7) Ogasawara, D.; Ichu, T. A.; Jing, H.; Hulce, J. J.; Reed, A.; Ulanovskaya, O. A.; Cravatt, B. F. Discovery and Optimization of Selective and in Vivo Active Inhibitors of the Lysophosphatidylserine Lipase α/β-Hydrolase Domain-Containing 12 (ABHD12). *J. Med. Chem.* **2019**, *62* (3), 1643–1656.

(8) Bachovchin, D. A.; Ji, T.; Li, W.; Simon, G. M.; Blankman, J. L.; Adibekian, A.; Hoover, H.; Niessen, S.; Cravatt, B. F. Superfamily-Wide Portrait of Serine Hydrolase Inhibition Achieved by Library-versus-Library Screening. *Proc. Natl. Acad. Sci.* **2010**, *107* (49), 20941–20946.

(9) Ostrem, J. M.; Peters, U.; Sos, M. L.; Wells, J. A.; Shokat, K. M. K-Ras(G12C) Inhibitors Allosterically Control GTP Affinity and Effector Interactions. *Nature.* **2013**, *503* (7477), 548–551.

(10) Maurais, A. J.; Weerapana, E. Reactive-Cysteine Profiling for Drug Discovery. *Curr. Opin. Chem. Biol.* **2019**, *50*, 29–36.

(11) Weerapana, E.; Wang, C.; Simon, G. M.; Richter, F.; Khare, S.; Dillon, M. B. D.; Bachovchin, D. A.; Mowen, K.; Baker, D.; Cravatt, B. F. Quantitative Reactivity

Profiling Predicts Functional Cysteines in Proteomes. *Nature* **2010**, *468* (7325), 790–795.

(12) Kim, K.; Weiss, L. M. Toxoplasma Gondii: The Model Apicomplexan. *Int. J. Parasitol.* **2004**, *34* (3), 423–432.

(13) Flegr, J.; Prandota, J.; Sovičková, M.; Israili, Z. H. Toxoplasmosis – A Global Threat. Correlation of Latent Toxoplasmosis with Specific Disease Burden in a Set of 88 Countries. *PLoS One* **2014**, *9* (3).

(14) Ben-Harari, R. R.; Goodwin, E.; Casoy, J. Adverse Event Profile of Pyrimethamine-Based Therapy in Toxoplasmosis: A Systematic Review. *Drugs R D* **2017**, *17* (4), 523–544.

(15) Abo, M.; Li, C.; Weerapana, E. Isotopically-Labeled Iodoacetamide-Alkyne Probes for Quantitative Cysteine-Reactivity Profiling. *Mol. Pharm.* **2018**, *15* (3), 743–749.

(16) Rostovtsev, V. V; Green, L. G.; Fokin, V. V; Sharpless, K. B. A Stepwise Huisgen Cycloaddition Process: Copper(I)-Catalyzed Regioselective "Ligation" of Azides and Terminal Alkynes. *Angew. Chem. Int. Ed* **2002**, *41* (14), 2596–2599.

(17) Qian, Y.; Martell, J.; Pace, N. J.; Eric Ballard, T.; Johnson, D. S.; Weerapana, E. An Isotopically Tagged Azobenzene-Based Cleavable Linker for Quantitative Proteomics. *ChemBioChem* **2013**, *14* (12), 1410–1414.

(18) Jacot, D.; Daher, W.; Soldati-Favre, D. Toxoplasma Gondii Myosin F, an Essential Motor for Centrosomes Positioning and Apicoplast Inheritance. *EMBO J.* **2013**, *32* (12), 1702–1716.

(19) Eng, J. K.; McCormack, A. L.; Yates, J. R. An Approach to Correlate Tandem Mass Spectral Data of Peptides with Amino Acid Sequences in a Protein Database. *J. Am. Soc. Mass Spectrom.* **1994**, *5* (11), 976–989.

(20) Conesa, A.; Götz, S.; García-Gómez, J. M.; Terol, J.; Talón, M.; Robles, M. Blast2GO: A Universal Tool for Annotation, Visualization and Analysis in Functional Genomics Research. *Bioinformatics* **2005**, *21* (18), 3674–3676.

APPENDIX I

Mass spectrometry tables

Table A2-1 Ranking cysteines by sensitivity to CoA-SNO. 789 cysteine containing peptides from MCF7 cell lysate were ranked by R values. R value is the average heavy:light ratio from two individual datasets with replicate values required to fall within two-fold of each other.

index	Uniprot ID	description	symbol	sequence	*R* value	*R* (log2)
1	Q15149	PLEC Plectin	PLEC	CDNFTSSWR	0.05	-4.35
2	P34896	SHMT1 Serine hydroxymethyltransferase, cytosolic	SHMT1	AVLEALGSCLNNK	0.26	-1.96
3	P30044	PRDX5 Peroxiredoxin-5, mitochondrial	PRDX5	ALNVEPDGTGLTCSLAPNIISQL	0.34	-1.55
4	Q9BQ69	MACROD1 O-acetyl-ADP-ribose deacetylase MACROD1	MACROD1	AAGPLLTDECR	0.39	-1.37
5	P61981	YWHAG 14-3-3 protein gamma	YWHAG	NCSETQYESK	0.43	-1.22
6	O75828	CBR3 Carbonyl reductase [NADPH] 3	CBR3	ILVNACCPGPVK	0.44	-1.20
7	P31948	STIP1 Stress-induced-phosphoprotein 1	STIP1	ALSVGNIDDALQCYSEAIK	0.51	-0.96
8	P50990	CCT8 T-complex protein 1 subunit theta	CCT8	IAVYSCPFDGMITETK	0.53	-0.92
9	P49591	SARS Serine--tRNA ligase, cytoplasmic	SARS	TICAILENYQTEK	0.55	-0.87
10	P55212	CASP6 Caspase-6	CASP6	GTCADR	0.55	-0.87
11	O43175	PHGDH D-3-phosphoglycerate dehydrogenase	PHGDH	VLISDSLDPCCR	0.55	-0.85
12	Q04917	YWHAH 14-3-3 protein eta	YWHAH	NCNDFQYESK	0.56	-0.84
13	O43707	ACTN4 Alpha-actinin-4	ACTN4	ELPPDQAEYCIAR	0.57	-0.82
14	P53041	PPP5C Serine/threonine-protein phosphatase 5	PPP5C	TECYGYALGDATR	0.58	-0.78
15	P19367	HK1 Hexokinase-1	HK1	AAQLCGAGMAAVVDK	0.59	-0.77
16	Q9UGI8	TES Testin	TES	TQYSCYCCK	0.59	-0.77
17	P04632	CAPNS1 Calpain small subunit 1	CAPNS1	TDGFGIDTCR	0.59	-0.77
18	P61981	YWHAG 14-3-3 protein gamma	YWHAG	ELEAVCQDVLSLLDNYLIK	0.59	-0.77
19	O00399	DCTN6 Dynactin subunit 6	DCTN6	IAPGAVVCVESEIR	0.59	-0.76
20	P04632	CAPNS1 Calpain small subunit 1	CAPNS1	YSDESGNMDFDNFISCLVR	0.60	-0.75
21	P52788	SMS Spermine synthase	SMS	LYCPVEFSK	0.60	-0.74
22	P61158	ACTR3 Actin-related protein 3	ACTR3	LPACVVDCGTGYTK	0.60	-0.74
23	P23434	GCSH Glycine cleavage system H protein,	GCSH	SCYEDGWLIK	0.61	-0.72

		mitochondrial				
24	P30041	PRDX6 Peroxiredoxin-6	PRDX6	DFTPVCTTELGR	0.61	-0.72
25	P22314	UBA1 Ubiquitin-like modifier-activating enzyme 1	UBA1	DNPGVVTCLDEAR	0.61	-0.72
26	Q9Y696	CLIC4 Chloride intracellular channel protein 4	CLIC4	DEFTNTCPSDK	0.61	-0.71
27	Q15633	TARBP2 RISC-loading complex subunit TARBP2	TARBP2	SCSLGSLGALGPACCR	0.61	-0.70
28	P0DMV8	HSPA1A Heat shock 70 kDa protein 1A	HSPA1A	ELEQVCNPIISGLYQGAGGPGPGGFGAQGPK	0.62	-0.70
29	P28838	LAP3 Cytosol aminopeptidase	LAP3	QVVDCQLADVNNIGK	0.62	-0.69
30	Q15185	PTGES3 Prostaglandin E synthase 3	PTGES3	LTFSCLGGSDNFK	0.62	-0.69
31	P26641	EEF1G Elongation factor 1-gamma	EEF1G	VPAFEGDDGFCVFESNAIAYYVSNEELR	0.63	-0.68
32	P13693	TPT1 Translationally-controlled tumor protein	TPT1	EIADGLCLEVEGK	0.63	-0.68
33	P07237	P4HB Protein disulfide-isomerase	P4HB	EECPAVR	0.63	-0.67
34	Q96FJ2	DYNLL2 Dynein light chain 2, cytoplasmic	DYNLL2	NADMSEDMQQDAVDCATQAMEK	0.63	-0.66
35	P61970	NUTF2 Nuclear transport factor 2	NUTF2	NINDAWVCTNDMFR	0.63	-0.66
36	P12004	PCNA Proliferating cell nuclear antigen	PCNA	DLSHIGDAVVISCAK	0.63	-0.66
37	P21266	GSTM3 Glutathione S-transferase Mu 3	GSTM3	LCYSSDHEK	0.64	-0.65
38	Q08211	DHX9 ATP-dependent RNA helicase A	DHX9	NFLYAWCGK	0.64	-0.65
39	P62258	YWHAE 14-3-3 protein epsilon	YWHAE	LICCDILDVLDK	0.64	-0.64
40	Q86SX6	GLRX5 Glutaredoxin-related protein 5, mitochondrial	GLRX5	GTPEQPQCGFSNAVVQILR	0.65	-0.63
41	P78417	GSTO1 Glutathione S-transferase omega-1	GSTO1	LNECVDHTPK	0.65	-0.63
42	O00299	CLIC1 Chloride intracellular channel protein 1	CLIC1	EEFASTCPDDEEIELAYEQVAK	0.65	-0.63
43	Q99460	PSMD1 26S proteasome non-ATPase regulatory subunit 1	PSMD1	VLTMPETCR	0.65	-0.62
44	Q99873	PRMT1 Protein arginine N-methyltransferase 1	PRMT1	GQLCELSCSTDYR	0.65	-0.61

45	P55072	VCP Transitional endoplasmic reticulum ATPase	VCP	AIANECQANFISIK	0.65	-0.61
46	O75874	IDH1 Isocitrate dehydrogenase [NADP] cytoplasmic	IDH1	SEGGFIWACK	0.66	-0.61
47	P04155	TFF1 Trefoil factor 1	TFF1	GVPWCFYPNTIDVPPEEECEF	0.66	-0.60
48	Q04917	YWHAH 14-3-3 protein eta	YWHAH	ELETVCNDVLSLLDK	0.66	-0.59
49	Q9Y2Q5	LAMTOR2 Ragulator complex protein LAMTOR2	LAMTOR2	FILMDCMEGR	0.66	-0.59
50	Q9BY32	ITPA Inosine triphosphate pyrophosphatase	ITPA	GCQDFGWDPCFQPDGYEQTYAEMPK	0.66	-0.59
51	Q7L2H7	EIF3M Eukaryotic translation initiation factor 3 subunit	EIF3M	VAASCGAIQYIPTELDQVR	0.66	-0.59
52	P23528	CFL1 Cofilin-1	CFL1	HELQANCYEEVK	0.67	-0.57
53	Q9BSH4	TACO1 Translational activator of cytochrome c oxidase 1	TACO1	LDSLGLCSVSCALEFIPNSK	0.68	-0.57
54	P63279	UBE2I SUMO-conjugating enzyme UBC9	UBE2I	QILLGIQELLNEPNIQDPAQAEAYTIYCQNR	0.68	-0.57
55	Q14697	GANAB Neutral alpha-glucosidase AB	GANAB	DGSDYEGWCWPGSAGYPDFTNPTMR	0.68	-0.57
56	Q9UNH7	SNX6 Sorting nexin-6	SNX6	IGSSLYALGTQDSTDICK	0.68	-0.56
57	O95628	CNOT4 CCR4-NOT transcription complex subunit 4	CNOT4	AIQCVNNVVVDGR	0.68	-0.56
58	Q96C86	DCPS m7GpppX diphosphatase	DCPS	EAGVGNGTCAPVR	0.68	-0.56
59	P23528	CFL1 Cofilin-1	CFL1	AVLFCLSEDK	0.68	-0.55
60	P29401	TKT Transketolase	TKT	MAAISESNINLCGSHCGVSIGEDGPSQMALEDLAMFR	0.69	-0.54
61	Q13404	UBE2V1 Ubiquitin-conjugating enzyme E2 variant 1	UBE2V1	LPQPPEGQCYSN	0.69	-0.53
62	Q9H6S3	EPS8L2 Epidermal growth factor receptor kinase substrate	EPS8L2	SGQAGYVPCNILGEAR	0.69	-0.53
63	Q15691	MAPRE1 Microtubule-associated protein RP/EB family member	MAPRE1	NIELICQENEGENDPVLQR	0.69	-0.53

64	Q7Z4V5	HDGFL2 Hepatoma-derived growth factor-related protein 2	HDGFL2	CGSSEDLHDSVR	0.70	-0.52
65	Q14653	IRF3 Interferon regulatory factor 3	IRF3	QVFQQTISCPEGLR	0.70	-0.52
66	P62826	RAN GTP-binding nuclear protein Ran	RAN	VCENIPIVLCGNK	0.70	-0.52
67	Q99873	PRMT1 Protein arginine N-methyltransferase 1	PRMT1	VIGIECSSISDYAVK	0.70	-0.52
68	P14625	HSP90B1 Endoplasmin	HSP90B1	LTESPCALVASQYGWS GNMER	0.70	-0.52
69	P39687	ANP32A Acidic leucine-rich nuclear phosphoprotein 32	ANP32A	SLDLFNCEVTNLNDYR	0.70	-0.51
70	Q9Y696	CLIC4 Chloride intracellular channel protein 4	CLIC4	AGSDGESIGNCPFSQR	0.70	-0.51
71	P37802	TAGLN2 Transgelin-2	TAGLN2	DGTVLCELINALYPEGQ APVK	0.70	-0.51
72	Q86VP6	CAND1 Cullin-associated NEDD8-dissociated protein 1	CAND1	HCECAEEGTR	0.70	-0.51
73	P14678	SNRPB Small nuclear ribonucleoprotein-associated protein	SNRPB	CILQDGR	0.71	-0.50
74	O00299	CLIC1 Chloride intracellular channel protein 1	CLIC1	IGNCPFSQR	0.71	-0.50
75	P00558	PGK1 Phosphoglycerate kinase 1	PGK1	GCITIIGGGDTATCCAK	0.71	-0.50
76	Q04724	TLE1 Transducin-like enhancer protein 1	TLE1	SPVSQLDCLNR	0.71	-0.50
77	P49773	HINT1 Histidine triad nucleotide-binding protein 1	HINT1	CAADLGLNK	0.71	-0.50
78	P80404	ABAT 4-aminobutyrate aminotransferase, mitochondrial	ABAT	GVVLGGCGDK	0.71	-0.50
79	P62937	PPIA Peptidyl-prolyl cis-trans isomerase A	PPIA	ITIADCGQLE	0.71	-0.50
80	P31947	SFN 14-3-3 protein sigma	SFN	GEELSCEER	0.71	-0.50
81	Q7Z4G1	COMMD6 COMM domain-containing protein 6	COMMD6	LGMAVSSDTCR	0.71	-0.49
82	P31150	GDI1 Rab GDP dissociation inhibitor alpha	GDI1	NTNDANSCQIIIPQNQV NR	0.71	-0.49
83	Q76NI1	KNDC1 Protein very KIND	KNDC1	TACPSLQEATR	0.71	-0.49
84	P60174	TPI1 Triosephosphate isomerase	TPI1	IAVAAQNCYK	0.71	-0.49

85	Q99798	ACO2 Aconitate hydratase, mitochondrial	ACO2	DLGGIVLANACGPCIGQWDR	0.71	-0.49
86	P26599	PTBP1 Polypyrimidine tract-binding protein 1	PTBP1	LSLDGQNIYNACCTLR	0.72	-0.48
87	Q15181	PPA1 Inorganic pyrophosphatase	PPA1	HTGCCGDNDPIDVCEIGSK	0.72	-0.48
88	Q9UPM8	AP4E1 AP-4 complex subunit epsilon-1	AP4E1	SSCSTLPDYLLYQCQK	0.72	-0.48
89	Q9NXG2	THUMPD1 THUMP domain-containing protein 1	THUMPD1	CDAGGPR	0.72	-0.48
90	P30043	BLVRB Flavin reductase (NADPH)	BLVRB	CLTTDEYDGHSTYPSHQYQ	0.72	-0.48
91	Q8NBS9	TXNDC5 Thioredoxin domain-containing protein 5	TXNDC5	VDCTAHSDVCSAQGVR	0.72	-0.48
92	Q8N3X1	FNBP4 Formin-binding protein 4	FNBP4	ATGGLCLLGAYADSDDDDNDVSEK	0.72	-0.47
93	Q12765	SCRN1 Secernin-1	SCRN1	TQSPCFGDDDPAK	0.72	-0.47
94	P61081	UBE2M NEDD8-conjugating enzyme Ubc12	UBE2M	LVICPDEGFYK	0.72	-0.47
95	P21266	GSTM3 Glutathione S-transferase Mu 3	GSTM3	CLDEFPNLK	0.72	-0.47
96	P55735	SEC13 Protein SEC13 homolog	SEC13	FASGGCDNLIK	0.72	-0.47
97	Q14790	CASP8 Caspase-8	CASP8	VFFIQACQGDNYQK	0.72	-0.47
98	Q52LJ0	FAM98B Protein FAM98B	FAM98B	SLCNLEESITSAGR	0.72	-0.47
99	Q86VP6	CAND1 Cullin-associated NEDD8-dissociated protein 1	CAND1	CLGPLVSK	0.73	-0.46
100	P30086	PEBP1 Phosphatidylethanolamine-binding protein 1	PEBP1	APVAGTCYQAEWDDYVPK	0.73	-0.46
101	P49419	ALDH7A1 Alpha-aminoadipic semialdehyde dehydrogenase	ALDH7A1	STCTINYSK	0.73	-0.46
102	Q9Y676	MRPS18B 28S ribosomal protein S18b, mitochondrial	MRPS18B	VVGNPCPICR	0.73	-0.46
103	P22626	HNRNPA2B1 Heterogeneous nuclear ribonucleoproteins A2/B1	HNRNPA2B1	LTDCVVMR	0.73	-0.45
104	P49915	GMPS GMP synthase [glutamine-hydrolyzing]	GMPS	ACTTEEDQEK	0.73	-0.45

105	P22061	PCMT1 Protein-L-isoaspartate(D-aspartate) O-methyltransferase	PCMT1	ALDVGSGSGILTACFAR	0.73	-0.45
106	O95292	VAPB Vesicle-associated membrane protein-associated pro	VAPB	CVFELPAENDK	0.73	-0.45
107	Q9BXV9	GON7 EKC/KEOPS complex subunit GON7	GON7	VSCEAPGDGDPFQGLLSGVAQMK	0.74	-0.44
108	P21964	COMT Catechol O-methyltransferase	COMT	YLPDTLLLEECGLLR	0.74	-0.44
109	P25789	PSMA4 Proteasome subunit alpha type-4	PSMA4	YLLQYQEPIPCEQLVTALCDIK	0.74	-0.44
110	P63104	YWHAZ 14-3-3 protein zeta/delta	YWHAZ	DICNDVLSLLEK	0.74	-0.43
111	P62937	PPIA Peptidyl-prolyl cis-trans isomerase A	PPIA	IIPGFMCQGGDFTR	0.74	-0.43
112	P05198	EIF2S1 Eukaryotic translation initiation factor 2 subunit	EIF2S1	AGLNCSTENMPIK	0.74	-0.43
113	P47756	CAPZB F-actin-capping protein subunit beta	CAPZB	DETVSDCSPHIANIGR	0.74	-0.43
114	O14662	STX16 Syntaxin-16	STX16	ACSEQEGR	0.75	-0.42
115	P22234	PAICS Multifunctional protein ADE2	PAICS	CGETAFIAPQCEMIPIEWVCR	0.75	-0.42
116	O14561	NDUFAB1 Acyl carrier protein, mitochondrial	NDUFAB1	LMCPQEIVDYIADK	0.75	-0.42
117	P62304	SNRPE Small nuclear ribonucleoprotein E	SNRPE	IEGCIIGFDEYMNLVLDDAEEIHSK	0.75	-0.42
118	Q8WVJ2	NUDCD2 NudC domain-containing protein 2	NUDCD2	AQDIQCGLQSR	0.75	-0.41
119	P55209	NAP1L1 Nucleosome assembly protein 1-like 1	NAP1L1	DQNPAECK	0.75	-0.41
120	P30153	PPP2R1A Serine/threonine-protein phosphatase 2A 65 kDa reg	PPP2R1A	LNIISNLDCVNEVIGIR	0.75	-0.41
121	Q15813	TBCE Tubulin-specific chaperone E	TBCE	NCAVSCAGEK	0.76	-0.40
122	Q9NVG8	TBC1D13 TBC1 domain family member 13	TBC1D13	ELSFSGIPCEGGLR	0.76	-0.40
123	P17029	ZKSCAN1 Zinc finger protein with KRAB and SCAN domains 1	ZKSCAN1	FCYQNTFGPR	0.76	-0.40
124	Q6IA69	NADSYN1 Glutamine-dependent NAD(+) synthetase	NADSYN1	NSSQETCTR	0.76	-0.40
125	P11940	PABPC1 Polyadenylate-binding protein 1	PABPC1	GFGFVCFSSPEEATK	0.76	-0.40

126	P60174	TPI1 Triosephosphate isomerase	TPI1	VPADTEVVCAPPTAYIDFAR	0.76	-0.39
127	Q9NQR4	NIT2 Omega-amidase NIT2	NIT2	VGLGICYDMR	0.76	-0.39
128	Q9P1F3	ABRACL Costars family protein ABRACL	ABRACL	CANLFEALVGTLK	0.76	-0.39
129	P08238	HSP90AB1 Heat shock protein HSP 90-beta	HSP90AB1	VFIMDSCDELIPEYLNFIR	0.76	-0.39
130	Q01518	CAP1 Adenylyl cyclase-associated protein 1	CAP1	ALLVTASQCQQPAENK	0.76	-0.39
131	Q5TFE4	NT5DC1 5-nucleotidase domain-containing protein 1	NT5DC1	ENCGIYFPEIK	0.76	-0.39
132	Q12931	TRAP1 Heat shock protein 75 kDa, mitochondrial	TRAP1	SPAAECLSEK	0.76	-0.39
133	P38646	HSPA9 Stress-70 protein, mitochondrial	HSPA9	CELSSSVQTDINLPYLTMDSSGPK	0.76	-0.39
134	Q99497	PARK7 Protein/nucleic acid deglycase DJ-1	PARK7	DVVICPDASLEDAK	0.77	-0.39
135	Q9BXB4	OSBPL11 Oxysterol-binding protein-related protein 11	OSBPL11	NSSCGGGISSSSSSR	0.77	-0.38
136	P00813	ADA Adenosine deaminase	ADA	FDYYMPAIAGCR	0.77	-0.38
137	P13797	PLS3 Plastin-3	PLS3	EGICALGGTSELSSEGTQHSYSEEEK	0.77	-0.38
138	P46940	IQGAP1 Ras GTPase-activating-like protein IQGAP1	IQGAP1	TCLDNLASK	0.77	-0.37
139	P47897	QARS Glutamine--tRNA ligase	QARS	GPSGCVESLEVTCR	0.77	-0.37
140	P27348	YWHAQ 14-3-3 protein theta	YWHAQ	DNLTLWTSDSAGEECDAAEGAEN	0.77	-0.37
141	P31949	S100A11 Protein S100-A11	S100A11	CIESLIAVFQK	0.77	-0.37
142	Q15369	ELOC Elongin-C	ELOC	TYGGCEGPDAMYVK	0.77	-0.37
143	Q15149	PLEC Plectin	PLEC	LLEAQACTGGIIDPSTGER	0.78	-0.37
144	P0DMV8	HSPA1A Heat shock 70 kDa protein 1A	HSPA1A	FEELCSDLFR	0.78	-0.37
145	Q9UK39	NOCT Nocturnin	NOCT	TDCPSTHPPIR	0.78	-0.37
146	Q9H910	JPT2 Jupiter microtubule associated homolog 2	JPT2	DHVFLCEGEEPK	0.78	-0.37
147	Q9UKV3	ACIN1 Apoptotic chromatin condensation inducer in the nu	ACIN1	DPSSGQEVATPPVPQLQVCEPK	0.78	-0.36

148	Q09666	AHNAK Neuroblast differentiation-associated protein AHNA	AHNAK	LEGDLTGPSVDVEVPDVELECPDAK	0.78	-0.36
149	P07737	PFN1 Profilin-1	PFN1	CYEMASHLR	0.78	-0.36
150	Q53FT3	HIKESHI Protein Hikeshi	HIKESHI	MFGCLVAGR	0.78	-0.36
151	P21291	CSRP1 Cysteine and glycine-rich protein 1	CSRP1	CSQAVYAAEK	0.78	-0.36
152	P54577	YARS Tyrosine--tRNA ligase, cytoplasmic	YARS	AFCEPGNVENNGVLSFIK	0.78	-0.36
153	P27348	YWHAQ 14-3-3 protein theta	YWHAQ	YLAEVACGDDR	0.78	-0.35
154	Q7L8W6	DPH6 Diphthine--ammonia ligase	DPH6	CEGDEVEDLYELLK	0.78	-0.35
155	O14950	MYL12B Myosin regulatory light chain 12B	MYL12B	NAFACFDEEATGTIQEDYLR	0.78	-0.35
156	Q5VV42	CDKAL1 Threonylcarbamoyladenosine tRNA methylthiotransfer	CDKAL1	IVLAGCVPQAQPR	0.78	-0.35
157	P35237	SERPINB6 Serpin B6	SERPINB6	SCDFLSSFR	0.79	-0.35
158	Q5TFE4	NT5DC1 5-nucleotidase domain-containing protein 1	NT5DC1	HFLSDTGMACR	0.79	-0.35
159	Q9BXJ9	NAA15 N-alpha-acetyltransferase 15, NatA auxiliary subun	NAA15	LFNTAVCESK	0.79	-0.35
160	P49915	GMPS GMP synthase [glutamine-hydrolyzing]	GMPS	VICAEEPYICK	0.79	-0.35
161	P49588	AARS Alanine--tRNA ligase, cytoplasmic	AARS	CLSVMEAK	0.79	-0.34
162	P49458	SRP9 Signal recognition particle 9 kDa protein	SRP9	VTDDLVCLVYK	0.79	-0.34
163	Q8N1F7	NUP93 Nuclear pore complex protein Nup93	NUP93	SSGQSAQLLSHEPGDPPCLR	0.79	-0.34
164	P14866	HNRNPL Heterogeneous nuclear ribonucleoprotein L	HNRNPL	ASLNGADIYSGCCTLK	0.79	-0.34
165	O75874	IDH1 Isocitrate dehydrogenase [NADP] cytoplasmic	IDH1	DLAACIK	0.79	-0.34
166	P62993	GRB2 Growth factor receptor-bound protein 2	GRB2	VLNEECDQNWYK	0.79	-0.34
167	Q8N6M0	OTUD6B OTU domain-containing protein 6B	OTUD6B	DCALTVVALR	0.79	-0.34
168	Q96HE7	ERO1A ERO1-like protein alpha	ERO1A	HDDSSDNFCEADDIQSPEAEYVDLLLNPER	0.79	-0.34

169	P15153	RAC2 Ras-related C3 botulinum toxin substrate 2	RAC2	YLECSALTQR	0.79	-0.33
170	Q06203	PPAT Amidophosphoribosyltransferase	PPAT	SGHCTACLTGK	0.80	-0.33
171	P53041	PPP5C Serine/threonine-protein phosphatase 5	PPP5C	TECAEPPR	0.80	-0.33
172	Q14980	NUMA1 Nuclear mitotic apparatus protein 1	NUMA1	VEELQACVETAR	0.80	-0.33
173	P60174	TPI1 Triosephosphate isomerase	TPI1	IIYGGSVTGATCK	0.80	-0.32
174	Q7Z6Z7	HUWE1 E3 ubiquitin-protein ligase HUWE1	HUWE1	AQCETLSPDGLPEEQPQTTK	0.80	-0.32
175	Q9H993	ARMT1 Protein-glutamate O-methyltransferase	ARMT1	CGADWEEYIK	0.80	-0.32
176	P21266	GSTM3 Glutathione S-transferase Mu 3	GSTM3	YTCGEAPDYDR	0.80	-0.32
177	Q9NYL2	MAP3K20 Mitogen-activated protein kinase 20	MAP3K20	FDDLQFFENCGGGSFGSVYR	0.80	-0.31
178	P26641	EEF1G Elongation factor 1-gamma	EEF1G	AAAPAPEEEMDECEQALAAEPK	0.80	-0.31
179	Q9BU89	DOHH Deoxyhypusine hydroxylase	DOHH	PACLAALQAHADDPER	0.80	-0.31
180	P04075	ALDOA Fructose-bisphosphate aldolase A	ALDOA	YASICQQNGIVPIVEPEILPDGDHDLK	0.81	-0.31
181	P63010	AP2B1 AP-2 complex subunit beta	AP2B1	ECHLNADTVSSK	0.81	-0.31
182	P58107	EPPK1 Epiplakin	EPPK1	YLEGTSCIAGVLVPAK	0.81	-0.31
183	Q13057	COASY Bifunctional coenzyme A synthase	COASY	YATSCYSCCPR	0.81	-0.31
184	P14868	DARS Aspartate--tRNA ligase, cytoplasmic	DARS	LEYCEALAMLR	0.81	-0.31
185	P31939	ATIC Bifunctional purine biosynthesis protein PURH	ATIC	VCMVYDLYK	0.81	-0.31
186	P36507	MAP2K2 Dual specificity mitogen-activated protein kinase	MAP2K2	LCDFGVSGQLIDSMANSFVGTR	0.81	-0.31
187	Q16854	DGUOK Deoxyguanosine kinase, mitochondrial	DGUOK	ACTAQSLGNLLDMMYR	0.81	-0.31
188	Q9NNX1	TUFT1 Tuftelin	TUFT1	SNNADCQAER	0.81	-0.31
189	P63208	SKP1 S-phase kinase-associated protein 1	SKP1	GLLDVTCK	0.81	-0.31

190	Q96FW1	OTUB1 Ubiquitin thioesterase OTUB1	OTUB1	PDGNCFYR	0.81	-0.30
191	Q99873	PRMT1 Protein arginine N-methyltransferase 1	PRMT1	VEDLTFTSPFCLQVK	0.81	-0.30
192	Q9BV86	NTMT1 N-terminal Xaa-Pro-Lys N-methyltransferase 1	NTMT1	TGTSCALDCGAGIGR	0.81	-0.30
193	P51610	HCFC1 Host cell factor 1	HCFC1	LVIYGGMSGCR	0.81	-0.30
194	Q06323	PSME1 Proteasome activator complex subunit 1	PSME1	GPPCGPVNCNEK	0.81	-0.30
195	Q1KMD3	HNRNPUL2 Heterogeneous nuclear ribonucleoprotein U-like pro	HNRNPUL2	LQEALDAEMLEDEAGGGGAGPGGACK	0.81	-0.30
196	Q96EI5	TCEAL4 Transcription elongation factor A protein-like 4	TCEAL4	PEVTCTLEDK	0.81	-0.30
197	P49189	ALDH9A1 4-trimethylaminobutyraldehyde dehydrogenase	ALDH9A1	TVCVEMGDVESAF	0.81	-0.30
198	Q9Y490	TLN1 Talin-1	TLN1	AVTDSINQLITMCTQQAPGQK	0.81	-0.30
199	Q9P0L0	VAPA Vesicle-associated membrane protein-associated pro	VAPA	CVFEMPNENDK	0.81	-0.30
200	P49721	PSMB2 Proteasome subunit beta type-2	PSMB2	NLADCLR	0.81	-0.30
201	P14866	HNRNPL Heterogeneous nuclear ribonucleoprotein L	HNRNPL	QPAIMPGQSYGLEDGSCSYK	0.81	-0.30
202	Q99614	TTC1 Tetratricopeptide repeat protein 1	TTC1	ALEMCPSCFQK	0.81	-0.30
203	P00505	GOT2 Aspartate aminotransferase, mitochondrial	GOT2	EYLPIGGLAEFCK	0.82	-0.29
204	Q9BQ61	C19orf43 Uncharacterized protein C19orf43	C19orf43	AHQCGDDDK	0.82	-0.29
205	P49023	PXN Paxillin	PXN	TSSVSNPQDSVGSPCSR	0.82	-0.29
206	Q16644	MAPKAPK3 MAP kinase-activated protein kinase 3	MAPKAPK3	ETTQNALQTPCYTPYYVAPEVLGPEK	0.82	-0.29
207	Q8N806	UBR7 Putative E3 ubiquitin-protein ligase UBR7	UBR7	VEQNSEPCAGSSSESDLQTVFK	0.82	-0.29
208	P28074	PSMB5 Proteasome subunit beta type-5	PSMB5	VIEINPYLLGTMAGGAADCSFWER	0.82	-0.29
209	P63167	DYNLL1 Dynein light chain 1, cytoplasmic	DYNLL1	NADMSEEMQQDSVECATQALEK	0.82	-0.29

210	Q09666	AHNAK Neuroblast differentiation-associated protein AHNA	AHNAK	VDVECPDVNIEGPEGK	0.82	-0.29
211	Q9HCC0	MCCC2 Methylcrotonoyl-CoA carboxylase beta chain	MCCC2	LPCIYLVDSGGAYLPR	0.82	-0.29
212	Q04206	RELA Transcription factor p65	RELA	DGFYEAELCPDR	0.82	-0.29
213	Q96EY8	MMAB Cob(I)yrinic acid a,c-diamide adenosyltransferase	MMAB	IQCTLQDVGSALATPCSSAR	0.82	-0.28
214	Q9NTK5	OLA1 Obg-like ATPase 1	OLA1	STFFNVLTNSQASAENFPFCTIDPNESR	0.82	-0.28
215	Q9NUQ9	FAM49B Protein FAM49B	FAM49B	VLTCTDLEQGPNFFLDFENAQPTESEK	0.82	-0.28
216	Q9NZZ3	CHMP5 Charged multivesicular body protein 5	CHMP5	APPPSLTDCIGTVDSR	0.83	-0.27
217	P19367	HK1 Hexokinase-1	HK1	AILQQLGLNSTCDDSILVK	0.83	-0.27
218	Q99471	PFDN5 Prefoldin subunit 5	PFDN5	DCLNVLNK	0.83	-0.27
219	P61158	ACTR3 Actin-related protein 3	ACTR3	YSYVCPDLVK	0.83	-0.27
220	A6NDU8	C5orf51 UPF0600 protein C5orf51	C5orf51	CPIQLNEGVSFQDLDTAK	0.83	-0.27
221	P68036	UBE2L3 Ubiquitin-conjugating enzyme E2 L3	UBE2L3	GQVCLPVISAENWK	0.83	-0.27
222	P49321	NASP Nuclear autoantigenic sperm protein	NASP	SVSGTDVQEECR	0.83	-0.27
223	P07741	APRT Adenine phosphoribosyltransferase	APRT	VVVVDDLLATGGTMNAACELLGR	0.83	-0.27
224	O94979	SEC31A Protein transport protein Sec31A	SEC31A	CLSSATDPQTK	0.83	-0.27
225	Q9NQ88	TIGAR Fructose-2,6-bisphosphatase TIGAR	TIGAR	EQFSQGSPSNCLETSLAEIFPLGK	0.83	-0.27
226	P49588	AARS Alanine--tRNA ligase, cytoplasmic	AARS	AVYTQDCPLAAAK	0.83	-0.26
227	Q15019	SEPT2 Septin-2	2-Sep	LTVVDTPGYGDAINCR	0.83	-0.26
228	P14649	MYL6B Myosin light chain 6B	MYL6B	ILYSQCGDVMR	0.83	-0.26
229	Q00536	CDK16 Cyclin-dependent kinase 16	CDK16	LEHEEGAPCTAIR	0.84	-0.26
230	Q9BYG5	PARD6B Partitioning defective 6 homolog beta	PARD6B	HGAGSGCLGTMEVK	0.84	-0.26

231	P49327	FASN Fatty acid synthase	FASN	AINCATSGVVGLVNCLR	0.84	-0.25
232	Q14151	SAFB2 Scaffold attachment factor B2	SAFB2	ILDILGETCK	0.84	-0.25
233	P61978	HNRNPK Heterogeneous nuclear ribonucleoprotein K	HNRNPK	GSDFDCELR	0.84	-0.25
234	Q16644	MAPKAPK3 MAP kinase-activated protein kinase 3	MAPKAPK 3	QAGSSSASQGCNNQ	0.84	-0.25
235	Q15020	SART3 Squamous cell carcinoma antigen recognized by T-ce	SART3	CAAVDVEPPSK	0.84	-0.25
236	O60701	UGDH UDP-glucose 6-dehydrogenase	UGDH	ASVGFGGSCFQK	0.84	-0.24
237	Q9Y490	TLN1 Talin-1	TLN1	AGALQCSPSDAYTK	0.84	-0.24
238	P00519	ABL1 Tyrosine-protein kinase ABL1	ABL1	ELQICPATAGSGPAATQ DFSK	0.84	-0.24
239	Q9H773	DCTPP1 dCTP pyrophosphatase 1	DCTPP1	YTELPHGAISEDQAVGP ADIPCDSTGQTST	0.84	-0.24
240	P00492	HPRT1 Hypoxanthine-guanine phosphoribosyltransferase	HPRT1	SYCNDQSTGDIK	0.84	-0.24
241	O75348	ATP6V1G1 V-type proton ATPase subunit G 1	ATP6V1G1	GSCSTEVEK	0.85	-0.24
242	O14980	XPO1 Exportin-1	XPO1	LDINLLDNVVNCLYHGE GAQQR	0.85	-0.24
243	P21291	CSRP1 Cysteine and glycine-rich protein 1	CSRP1	DGEIYCK	0.85	-0.24
244	Q9Y296	TRAPPC4 Trafficking protein particle complex subunit 4	TRAPPC4	CELFDQNLK	0.85	-0.24
245	P14618	PKM Pyruvate kinase PKM	PKM	GIFPVLCK	0.85	-0.23
246	Q14566	MCM6 DNA replication licensing factor MCM6	MCM6	LGFSEYCR	0.85	-0.23
247	Q96FW 1	OTUB1 Ubiquitin thioesterase OTUB1	OTUB1	QEPLGSDSEGVNCLAYD EAIMAQQDR	0.85	-0.23
248	Q9HCY8	S100A14 Protein S100-A14	S100A14	IANLGSCNDSK	0.85	-0.23
249	P49327	FASN Fatty acid synthase	FASN	TGGAYGEDLGADYNLS QVCDGK	0.85	-0.23
250	P61978	HNRNPK Heterogeneous nuclear ribonucleoprotein K	HNRNPK	IIPTLEEGLQLPSPTATSQ LPLESDAVECLNYQHYK	0.85	-0.23

251	Q9BVL2	NUP58 Nucleoporin p58/p45	NUP58	DENLPPVICQDVENLQK	0.85	-0.23
252	Q15181	PPA1 Inorganic pyrophosphatase	PPA1	GISCMNTTLSESPFK	0.86	-0.23
253	P33316	DUT Deoxyuridine 5-triphosphate nucleotidohydrolase,	DUT	TDIQIALPSGCYGR	0.86	-0.23
254	Q8TEX9	IPO4 Importin-4	IPO4	DNICGALAR	0.86	-0.22
255	P13639	EEF2 Elongation factor 2	EEF2	YVEPIEDVPCGNIVGLV GVDQFLVK	0.86	-0.22
256	Q9NVU 0	POLR3E DNA-directed RNA polymerase III subunit RPC5	POLR3E	AAGTDSFNGHPPQGCA STPVAR	0.86	-0.22
257	P15924	DSP Desmoplakin	DSP	ACGSEIMQK	0.86	-0.22
258	P60981	DSTN Destrin	DSTN	LGGSLIVAFEGCPV	0.86	-0.22
259	P15924	DSP Desmoplakin	DSP	TASEDSCK	0.86	-0.21
260	Q9Y446	PKP3 Plakophilin-3	PKP3	DLAGAPPGEVVGCFTP QSR	0.86	-0.21
261	Q9NVG 8	TBC1D13 TBC1 domain family member 13	TBC1D13	LLQDYPITDVCQILQK	0.86	-0.21
262	Q96A49	SYAP1 Synapse-associated protein 1	SYAP1	TQEDEEEISTSPGVSEFV SDAFDACNLNQEDLR	0.86	-0.21
263	O60664	PLIN3 Perilipin-3	PLIN3	DIAQQLQATCTSLGSSI QGLPTNVK	0.86	-0.21
264	Q9BV86	NTMT1 N-terminal Xaa-Pro-Lys N-methyltransferase 1	NTMT1	IICSAGLSLLAEER	0.87	-0.21
265	Q9ULW 0	TPX2 Targeting protein for Xklp2	TPX2	TVEICPFSFDSR	0.87	-0.21
266	O60361	NME2P1 Putative nucleoside diphosphate kinase	NME2P1	SCAHDWVYE	0.87	-0.21
267	P37235	HPCAL1 Hippocalcin-like protein 1	HPCAL1	LLQCDPSSASQF	0.87	-0.21
268	P50395	GDI2 Rab GDP dissociation inhibitor beta	GDI2	TDDYLDQPCYETINR	0.87	-0.21
269	P38606	ATP6V1A V-type proton ATPase catalytic subunit A	ATP6V1A	WDFTPCK	0.87	-0.21
270	Q9BRP1	PDCD2L Programmed cell death protein 2-like	PDCD2L	SQCLQVPER	0.87	-0.21
271	P04406	GAPDH Glyceraldehyde-3-phosphate dehydrogenase	GAPDH	VPTANVSVVDLTCR	0.87	-0.20
272	Q9BRP1	PDCD2L Programmed cell death protein 2-like	PDCD2L	YSWSGEPLFLTCPTSEVT ELPACSQCGGQR	0.87	-0.20

273	P30084	ECHS1 Enoyl-CoA hydratase, mitochondrial	ECHS1	ICPVETLVEEAIQCAEK	0.87	-0.20
274	P41227	NAA10 N-alpha-acetyltransferase 10	NAA10	GNSPPSSGEACR	0.87	-0.20
275	P53582	METAP1 Methionine aminopeptidase 1	METAP1	VCETDGCSSEAK	0.87	-0.20
276	P21266	GSTM3 Glutathione S-transferase Mu 3	GSTM3	IAAYLQSDQFCK	0.87	-0.20
277	P17676	CEBPB CCAAT/enhancer-binding protein beta	CEBPB	APPTACYAGAAPAPSQVK	0.87	-0.20
278	Q16630	CPSF6 Cleavage and polyadenylation specificity factor su	CPSF6	ELHGQNPVVTPCNK	0.88	-0.19
279	P51858	HDGF Hepatoma-derived growth factor	HDGF	CGDLVFAK	0.88	-0.19
280	P38646	HSPA9 Stress-70 protein, mitochondrial	HSPA9	GAVVGIDLGTTNSCVAVMEGK	0.88	-0.19
281	P61758	VBP1 Prefoldin subunit 3	VBP1	DSCGK	0.88	-0.19
282	Q9HCC0	MCCC2 Methylcrotonoyl-CoA carboxylase beta chain	MCCC2	NIAQIAVVMGSCTAGGAYVPAMADENIIVR	0.88	-0.19
283	P33240	CSTF2 Cleavage stimulation factor subunit 2	CSTF2	LCVQNSPQEAR	0.88	-0.19
284	P49419	ALDH7A1 Alpha-aminoadipic semialdehyde dehydrogenase	ALDH7A1	GSDCGIVNVNIPTSGAEIGGAFGGEK	0.88	-0.19
285	P18669	PGAM1 Phosphoglycerate mutase 1	PGAM1	YADLTEDQLPSCESLK	0.88	-0.19
286	P21333	FLNA Filamin-A	FLNA	AHVVPCFDASK	0.88	-0.19
287	P49589	CARS Cysteine--tRNA ligase, cytoplasmic	CARS	VQPQWSPPAGTQPCR	0.88	-0.18
288	P60981	DSTN Destrin	DSTN	CSTPEEIK	0.88	-0.18
289	P00966	ASS1 Argininosuccinate synthase	ASS1	FELSCYSLAPQIK	0.88	-0.18
290	P60900	PSMA6 Proteasome subunit alpha type-6	PSMA6	CDPAGYYCGFK	0.88	-0.18
291	Q9NSY1	BMP2K BMP-2-inducible protein kinase	BMP2K	SEGGSGGGAAGGGAGGAGAGAGCGSGGSSVGVR	0.88	-0.18
292	Q9P2T1	GMPR2 GMP reductase 2	GMPR2	VGIGPGSVCTTR	0.88	-0.18
293	Q9UNE7	STUB1 E3 ubiquitin-protein ligase CHIP	STUB1	AQQACIEAK	0.88	-0.18
294	Q14103	HNRNPD Heterogeneous nuclear ribonucleoprotein D0	HNRNPD	FGEVVDCTLK	0.89	-0.17
295	P00338	LDHA L-lactate dehydrogenase A chain	LDHA	VIGSGCNLDSAR	0.89	-0.17

296	P40926	MDH2 Malate dehydrogenase, mitochondrial	MDH2	EGVVECSFVK	0.89	-0.17
297	Q96RS6	NUDCD1 NudC domain-containing protein 1	NUDCD1	DSAQCAAIAER	0.89	-0.17
298	Q09666	AHNAK Neuroblast differentiation-associated protein AHNA	AHNAK	GPFVEAEVPDVDLECPDAK	0.89	-0.17
299	Q9UQ35	SRRM2 Serine/arginine repetitive matrix protein 2	SRRM2	SVSPCSNVESR	0.89	-0.17
300	P58107	EPPK1 Epiplakin	EPPK1	CGYFDEEMNR	0.89	-0.17
301	P21964	COMT Catechol O-methyltransferase	COMT	IVDAVIQEHQPSVLLELGAYCGYSAVR	0.89	-0.17
302	P38117	ETFB Electron transfer flavoprotein subunit beta	ETFB	EVIAVSCGPAQCQETIR	0.89	-0.16
303	Q9NQX3	GPHN Gephyrin	GPHN	VTTGAPIPCGADAVVQVEDTELIR	0.90	-0.16
304	O00233	PSMD9 26S proteasome non-ATPase regulatory subunit 9	PSMD9	GIGMNEPLVDCEGYPR	0.90	-0.16
305	P52272	HNRNPM Heterogeneous nuclear ribonucleoprotein M	HNRNPM	GCAVVEFK	0.90	-0.16
306	Q9UGI8	TES Testin	TES	LPCEMDAQGPK	0.90	-0.15
307	Q9H1B7	IRF2BPL Interferon regulatory factor 2-binding protein	IRF2BPL	AHGCFQDGR	0.90	-0.15
308	Q08379	GOLGA2 Golgin subfamily A member 2	GOLGA2	CEAPDANQQLQQAMEER	0.90	-0.14
309	Q9BX63	BRIP1 Fanconi anemia group J protein	BRIP1	LANNSDCILAK	0.91	-0.14
310	Q92879	CELF1 CUGBP Elav-like family member 1	CELF1	AMHQAQTMEGCSSPMVVK	0.91	-0.14
311	P12270	TPR Nucleoprotein TPR	TPR	DCQEQAK	0.91	-0.14
312	Q06323	PSME1 Proteasome activator complex subunit 1	PSME1	EDLCTK	0.91	-0.14
313	P60709	ACTB Actin, cytoplasmic 1	ACTB	CPEALFQPSFLGMESCGIHETTFNSIMK	0.91	-0.14
314	O43765	SGTA Small glutamine-rich tetratricopeptide repeat-cont	SGTA	AICIDPAYSK	0.91	-0.13
315	Q13796	SHROOM2 Protein Shroom2	SHROOM2	CLLDSLQPER	0.91	-0.13
316	P13639	EEF2 Elongation factor 2	EEF2	IWCFGPDGTGPNILTDITK	0.91	-0.13

317	P49915	GMPS GMP synthase [glutamine-hydrolyzing]	GMPS	TVGVQGDCR	0.91	-0.13
318	P30041	PRDX6 Peroxiredoxin-6	PRDX6	DINAYNCEEPTEK	0.92	-0.13
319	Q13572	ITPK1 Inositol-tetrakisphosphate 1-kinase	ITPK1	ICSPPFMELTSLCGDDTMR	0.92	-0.12
320	P35568	IRS1 Insulin receptor substrate 1	IRS1	CTPGTGLGTSPALAGDEAASAADLDNR	0.92	-0.12
321	Q09666	AHNAK Neuroblast differentiation-associated protein AHNA	AHNAK	LEGDLTGPSVGVEVPDVELECPDAK	0.92	-0.12
322	Q8WW01	TSEN15 tRNA-splicing endonuclease subunit Sen15	TSEN15	GDSEPTPGCSGLGPGGVR	0.92	-0.12
323	Q5U5X0	LYRM7 Complex III assembly factor LYRM7	LYRM7	DLLVENVPYCDAPTQK	0.92	-0.12
324	P0C5J1	FAM86B2 Putative protein N-methyltransferase FAM86B2	FAM86B2	NPETCQLFTTELGR	0.92	-0.12
325	P31943	HNRNPH1 Heterogeneous nuclear ribonucleoprotein H	HNRNPH1	GLPWSCSADEVQR	0.92	-0.12
326	Q86VP6	CAND1 Cullin-associated NEDD8-dissociated protein 1	CAND1	TVIGELPPASSGSALAANVCK	0.92	-0.12
327	O75663	TIPRL TIP41-like protein	TIPRL	VACAEEWQESR	0.92	-0.12
328	Q9UJW0	DCTN4 Dynactin subunit 4	DCTN4	LLQPDFQPVCASQLYPR	0.92	-0.11
329	Q96HE7	ERO1A ERO1-like protein alpha	ERO1A	CFCQVSGYLDDCTCDVETIDR	0.93	-0.11
330	Q15365	PCBP1 Poly(rC)-binding protein 1	PCBP1	QICLVMLETLSQSPQGR	0.93	-0.11
331	Q9Y508	RNF114 E3 ubiquitin-protein ligase RNF114	RNF114	DCGGAAQLAGPAAEADPLGR	0.93	-0.11
332	Q96QK1	VPS35 Vacuolar protein sorting-associated protein 35	VPS35	TQCALAASK	0.93	-0.11
333	P20700	LMNB1 Lamin-B1	LMNB1	CQSLTEDLEFR	0.93	-0.11
334	O43865	AHCYL1 S-adenosylhomocysteine hydrolase-like protein 1	AHCYL1	LCVPAMNVNDSVTK	0.93	-0.11
335	P57721	PCBP3 Poly(rC)-binding protein 3	PCBP3	INISEGNCPER	0.93	-0.11
336	Q9HCC0	MCCC2 Methylcrotonoyl-CoA carboxylase beta chain, mitoch	MCCC2	MVAAVACAQVPK	0.93	-0.11
337	O15371	EIF3D Eukaryotic translation initiation	EIF3D	FMTPVIQDNPSGWGPCAVPEQFR	0.93	-0.11

		factor 3 subunit				
338	Q7L1Q6	BZW1 Basic leucine zipper and W2 domain-containing protein	BZW1	FDPTQFQDCIIQGLTETGTDLEAVAK	0.93	-0.10
339	P27361	MAPK3 Mitogen-activated protein kinase 3	MAPK3	ISPFEHQTYCQR	0.93	-0.10
340	O43684	BUB3 Mitotic checkpoint protein BUB3	BUB3	TPCNAGTFSQPEK	0.93	-0.10
341	O76003	GLRX3 Glutaredoxin-3	GLRX3	ELEASEELDTICPK	0.93	-0.10
342	Q9Y4L1	HYOU1 Hypoxia up-regulated protein 1	HYOU1	VEFEELCADLFER	0.93	-0.10
343	P41091	EIF2S3 Eukaryotic translation initiation factor 2 subunit	EIF2S3	IVLTNPVCTEVGEK	0.94	-0.10
344	Q9BQ69	MACROD1 O-acetyl-ADP-ribose deacetylase MACROD1	MACROD1	LEVDAIVNAANSSLLGGGGVDGCIHR	0.94	-0.10
345	O95295	SNAPIN SNARE-associated protein Snapin	SNAPIN	EQIDNLATELCR	0.94	-0.10
346	P51659	HSD17B4 Peroxisomal multifunctional enzyme type 2	HSD17B4	ICDFENASK	0.94	-0.09
347	Q13526	PIN1 Peptidyl-prolyl cis-trans isomerase NIMA-interacting	PIN1	SGEEDFESLASQFSDCSSAK	0.94	-0.09
348	Q7Z6Z7	HUWE1 E3 ubiquitin-protein ligase HUWE1	HUWE1	NPDIFTEVANCCIR	0.94	-0.09
349	Q96I15	SCLY Selenocysteine lyase	SCLY	DAPAPAASQPSGCGK	0.94	-0.08
350	Q9BRJ7	NUDT16L1 Tudor-interacting repair regulator protein	NUDT16L1	CQLLFALK	0.94	-0.08
351	Q9BSH5	HDHD3 Haloacid dehalogenase-like hydrolase domain-containing	HDHD3	DFSHPCTWQVLDGAEDTLR	0.95	-0.08
352	Q9ULV4	CORO1C Coronin-1C	CORO1C	DTICNQDER	0.95	-0.08
353	Q6Y7W6	GIGYF2 GRB10-interacting GYF protein 2	GIGYF2	ACDESFQPLGDIMK	0.95	-0.08
354	P78371	CCT2 T-complex protein 1 subunit beta	CCT2	TVYGGGCSEMLMAHAVTQLANR	0.95	-0.08
355	O95671	ASMTL N-acetylserotonin O-methyltransferase-like protein	ASMTL	VDASACGMER	0.95	-0.08
356	P49327	FASN Fatty acid synthase	FASN	LTPGCEAEAETEAICFFVQQFTDMEHNR	0.95	-0.07

357	Q9NY27	PPP4R2 Serine/threonine-protein phosphatase 4 regulatory	PPP4R2	NVMVVSCVYPSSEK	0.95	-0.07
358	Q15365	PCBP1 Poly(rC)-binding protein 1	PCBP1	AITIAGVPQSVTECVK	0.95	-0.07
359	P43686	PSMC4 26S proteasome regulatory subunit 6B	PSMC4	ISGADINSICQESGMLAVR	0.95	-0.07
360	P51858	HDGF Hepatoma-derived growth factor	HDGF	SCVEEPEPEPEAAEGDGDK	0.95	-0.07
361	Q01433	AMPD2 AMP deaminase 2	AMPD2	CGVPFTDLLDAAK	0.96	-0.07
362	O15446	CD3EAP DNA-directed RNA polymerase I subunit RPA34	CD3EAP	VLSSCPQAGEATLLAPSTEAGGGLTCASAPQGTLR	0.96	-0.07
363	O60701	UGDH UDP-glucose 6-dehydrogenase	UGDH	ISSINSISALCEATGADVEEVATAIGMDQR	0.96	-0.06
364	Q14694	USP10 Ubiquitin carboxyl-terminal hydrolase 10	USP10	SSVELPPYSGTVLCGTQAVDK	0.96	-0.06
365	Q9NRL3	STRN4 Striatin-4	STRN4	CTVDGSPHELESR	0.96	-0.06
366	Q69YQ0	SPECC1L Cytospin-A	SPECC1L	STCPSAAPSASAPAMTTVENK	0.96	-0.06
367	Q15370	ELOB Elongin-B	ELOB	ADDTFEALCIEPFSSPPELPDVMK	0.96	-0.06
368	P08134	RHOC Rho-related GTP-binding protein RhoC	RHOC	LVIVGDGACGK	0.96	-0.05
369	Q09666	AHNAK Neuroblast differentiation-associated protein AHNA	AHNAK	SSGCDVNLPGVNVK	0.96	-0.05
370	Q3LXA3	TKFC Triokinase/FMN cyclase	TKFC	AAGDGDCGTTHSR	0.96	-0.05
371	Q9HBM1	SPC25 Kinetochore protein Spc25	SPC25	STDTSCQMAGLR	0.96	-0.05
372	Q9BZE9	ASPSCR1 Tether containing UBX domain for GLUT4	ASPSCR1	CYDPVGK	0.97	-0.05
373	P33316	DUT Deoxyuridine 5-triphosphate nucleotidohydrolase,	DUT	IAQLICER	0.97	-0.05
374	P52895	AKR1C2 Aldo-keto reductase family 1 member C2	AKR1C2	EEPWVDPNSPVLLEDPVLCALAK	0.97	-0.05
375	Q8IWX8	CHERP Calcium homeostasis endoplasmic reticulum protein	CHERP	LALEQQQLICK	0.97	-0.05
376	Q86YH6	PDSS2 Decaprenyl-diphosphate synthase subunit 2	PDSS2	CLLSDELSNIAMQVR	0.97	-0.05

377	O95671	ASMTL N-acetylserotonin O-methyltransferase-like protein	ASMTL	FSSACDVGGCTGALAR	0.97	-0.05
378	P40222	TXLNA Alpha-taxilin	TXLNA	VTEAPCYPGAPSTEASG QTGPQEPTSAR	0.97	-0.05
379	O43790	KRT86 Keratin, type II cuticular Hb6	KRT86	DLNMDCIIAEIK	0.97	-0.05
380	P49720	PSMB3 Proteasome subunit beta type-3	PSMB3	NCVAIAADR	0.97	-0.04
381	Q7Z2Z2	EFL1 Elongation factor-like GTPase 1	EFL1	ICDGCIIVVDAVEGVCP QTQAVLR	0.97	-0.04
382	P38606	ATP6V1A V-type proton ATPase catalytic subunit A	ATP6V1A	VLDALFPCVQGGTTAIP GAFGCGK	0.97	-0.04
383	O15144	ARPC2 Actin-related protein 2/3 complex subunit 2	ARPC2	NCFASVFEK	0.97	-0.04
384	P20810	CAST Calpastatin	CAST	SECK	0.98	-0.04
385	Q9BTE3	MCMBP Mini-chromosome maintenance complex-binding protei	MCMBP	DASALLDPMECTDTAEE QR	0.98	-0.03
386	Q9P258	RCC2 Protein RCC2	RCC2	AVQDLCGWR	0.98	-0.03
387	P21333	FLNA Filamin-A	FLNA	TPCEEILVK	0.98	-0.03
388	P13639	EEF2 Elongation factor 2	EEF2	VTDGALVVVDCVSGVC VQTETVLR	0.98	-0.03
389	Q15366	PCBP2 Poly(rC)-binding protein 2	PCBP2	AITIAGIPQSIIECVK	0.98	-0.03
390	Q9C0C9	UBE2O (E3-independent) E2 ubiquitin-conjugating enzyme	UBE2O	CYNEMALIR	0.98	-0.02
391	Q9Y3F4	STRAP Serine-threonine kinase receptor-associated protein	STRAP	CVLPEEDSGELAK	0.98	-0.02
392	O14818	PSMA7 Proteasome subunit alpha type-7	PSMA7	ICALDDNVCMAFAGLT ADAR	0.98	-0.02
393	Q9UL25	RAB21 Ras-related protein Rab-21	RAB21	YCENK	0.98	-0.02
394	P49327	FASN Fatty acid synthase	FASN	ADEASELACPTPK	0.99	-0.02
395	A6NDG 6	PGP Glycerol-3-phosphate phosphatase	PGP	NNQESDCVSK	0.99	-0.01
396	P52597	HNRNPF Heterogeneous nuclear ribonucleoprotein F	HNRNPF	DLSYCLSGMYDHR	0.99	-0.01
397	Q13185	CBX3 Chromobox protein homolog 3	CBX3	LTWHSCPEDEAQ	0.99	-0.01
398	P53990	IST1 homolog	IST1	IVADQLCAK	0.99	-0.01
399	Q04637	EIF4G1 Eukaryotic translation initiation	EIF4G1	LQGINCGPDFTPSFANL GR	0.99	-0.01

		factor 4 gamma 1				
400	P43897	TSFM Elongation factor Ts, mitochondrial	TSFM	TGYSFVNCK	0.99	-0.01
401	O15355	PPM1G Protein phosphatase 1G	PPM1G	GTEAGQVGEPGIPTGEAGPSCSSASDK	1.00	-0.01
402	O60701	UGDH UDP-glucose 6-dehydrogenase	UGDH	DVLNLVYLCEALNLPEVAR	1.00	-0.01
403	Q14558	PRPSAP1 Phosphoribosyl pyrophosphate synthase-associated p	PRPSAP1	VFSANSTAACTELAK	1.00	0.00
404	P46109	CRKL Crk-like protein	CRKL	VPCAYDK	1.00	0.00
405	Q13045	FLII Protein flightless-1 homolog	FLII	TGLCYLPEELAALQK	1.00	0.00
406	Q07866	KLC1 Kinesin light chain 1	KLC1	YEVAVPLCK	1.01	0.01
407	Q8IV50	LYSMD2 LysM and putative peptidoglycan-binding domain-con	LYSMD2	LFTNDCIFLK	1.01	0.01
408	O15541	RNF113A RING finger protein 113A	RNF113A	AVDQVCTFLFK	1.01	0.01
409	P57721	PCBP3 Poly(rC)-binding protein 3	PCBP3	LVVPASQCGSLIGK	1.01	0.01
410	P37837	TALDO1 Transaldolase	TALDO1	ALAGCDFLTISPK	1.01	0.01
411	P13639	EEF2 Elongation factor 2	EEF2	CELLYEGPPDDEAAMGIK	1.01	0.01
412	P36954	POLR2I DNA-directed RNA polymerase II subunit RPB9	POLR2I	NCDYQQEADNSCIYVNK	1.01	0.02
413	P82932	MRPS6 28S ribosomal protein S6, mitochondrial	MRPS6	ECEGIVPVPLAEK	1.01	0.02
414	Q16643	DBN1 Drebrin	DBN1	EGTQASEGYFSQSQEEEFAQSEELCAK	1.01	0.02
415	P17844	DDX5 Probable ATP-dependent RNA helicase DDX5	DDX5	LIDFLECGK	1.01	0.02
416	P34897	SHMT2 Serine hydroxymethyltransferase, mitochondrial	SHMT2	EVCDEVK	1.01	0.02
417	Q9ULA0	DNPEP Aspartyl aminopeptidase	DNPEP	NDTPCGTTIGPILASR	1.01	0.02
418	P30050	RPL12 60S ribosomal protein L12	RPL12	CTGGEVGATSALAPK	1.02	0.02
419	P58107	EPPK1 Epiplakin	EPPK1	CVPDPDTGLYMLQLAGR	1.02	0.02
420	Q9Y285	FARSA Phenylalanine--tRNA ligase alpha subunit	FARSA	VNLQMVYDSPLCR	1.02	0.02

421	Q99832	CCT7 T-complex protein 1 subunit eta	CCT7	EGTDSSQGIPQLVSNISACQVIAEAVR	1.02	0.03
422	P14618	PKM Pyruvate kinase PKM	PKM	CDENILWLDYK	1.02	0.03
423	P14618	PKM Pyruvate kinase PKM	PKM	AEGSDVANAVLDGADCIMLSGETAK	1.02	0.03
424	P35998	PSMC2 26S proteasome regulatory subunit 7	PSMC2	LCPNSTGAEIR	1.03	0.04
425	Q8NFF5	FLAD1 FAD synthase	FLAD1	LHYGTDPCTGQPFR	1.03	0.04
426	P50991	CCT4 T-complex protein 1 subunit delta	CCT4	AQDIEAGDGTTSVVIIAGSLLDSCTK	1.03	0.05
427	Q15365	PCBP1 Poly(rC)-binding protein 1	PCBP1	LVVPATQCGSLIGK	1.04	0.05
428	Q8IX01	SUGP2 SURP and G-patch domain-containing protein 2	SUGP2	PTSADCAVR	1.04	0.05
429	O43175	PHGDH D-3-phosphoglycerate dehydrogenase	PHGDH	NAGNCLSPAVIVGLLK	1.04	0.06
430	P42575	CASP2 Caspase-2	CASP2	MFFIQACR	1.04	0.06
431	P35579	MYH9 Myosin-9	MYH9	MEDSVGCLETAEEVK	1.04	0.06
432	Q8NDH3	NPEPL1 Probable aminopeptidase NPEPL1	NPEPL1	IVDTPCNEMNTDTFLEEINK	1.05	0.06
433	Q32MZ4	LRRFIP1 Leucine-rich repeat flightless-interacting protein	LRRFIP1	IAAESSENVDCPENPK	1.05	0.07
434	O15075	DCLK1 Serine/threonine-protein kinase DCLK1	DCLK1	VCSSMDENDGPGEEVSEEGFQIPATITER	1.05	0.08
435	P55795	HNRNPH2 Heterogeneous nuclear ribonucleoprotein H2	HNRNPH2	GLPWSCSADEVMR	1.05	0.08
436	P08238	HSP90AB1 Heat shock protein HSP 90-beta	HSP90AB1	GFEVVYMTEPIDEYCVQQLK	1.05	0.08
437	P10809	HSPD1 60 kDa heat shock protein, mitochondrial	HSPD1	CEFQDAYVLLSEK	1.06	0.08
438	Q8TDH9	BLOC1S5 Biogenesis of lysosome-related organelles complex	BLOC1S5	LQAANDSVCR	1.06	0.08
439	Q8TD30	GPT2 Alanine aminotransferase 2	GPT2	GYMGECGYR	1.06	0.08
440	Q9HCH5	SYTL2 Synaptotagmin-like protein 2	SYTL2	SPADELSHCVEPEPSQVPGGSSR	1.06	0.08
441	P10599	TXN Thioredoxin	TXN	CMPTFQFFK	1.06	0.08

442	P49327	FASN Fatty acid synthase	FASN	DPETLVGYSMVGCQR	1.06	0.09
443	O14929	HAT1 Histone acetyltransferase type B catalytic subunit	HAT1	VDENFDCVEADDVEGK	1.06	0.09
444	Q9Y5P6	GMPPB Mannose-1-phosphate guanyltransferase beta	GMPPB	LCSGPGIVGNVLVDPSAR	1.07	0.09
445	P60842	EIF4A1 Eukaryotic initiation factor 4A-I	EIF4A1	VVMALGDYMGASCHACIGGTNVR	1.07	0.09
446	Q9Y3F4	STRAP Serine-threonine kinase receptor-associated protei	STRAP	IGFPETTEEELEEIASENSDCIFPSAPDVK	1.07	0.09
447	O95671	ASMTL N-acetylserotonin O-methyltransferase-like protein	ASMTL	AEAGEAGQATAEAECHR	1.07	0.10
448	O75369	FLNB Filamin-B	FLNB	VAVTEGCQPSR	1.07	0.10
449	Q86UP2	KTN1 Kinectin	KTN1	ECMAGTSGSEEVK	1.07	0.10
450	P42566	EPS15 Epidermal growth factor receptor substrate 15	EPS15	GSDPFASDCFFR	1.07	0.10
451	P46782	RPS5 40S ribosomal protein S5	RPS5	AQCPIVER	1.08	0.10
452	P10599	TXN Thioredoxin	TXN	LVVVDFSATWCGPCK	1.08	0.11
453	Q00765	REEP5 Receptor expression-enhancing protein 5	REEP5	NCMTDLLAK	1.08	0.11
454	P80404	ABAT 4-aminobutyrate aminotransferase, mitochondrial	ABAT	TMGCLATTHSK	1.08	0.11
455	Q14980	NUMA1 Nuclear mitotic apparatus protein 1	NUMA1	LDFVCSFLQK	1.08	0.11
456	Q6PI48	DARS2 Aspartate--tRNA ligase, mitochondrial	DARS2	LICLVTGSPSIR	1.08	0.11
457	Q8WYP5	AHCTF1 Protein ELYS	AHCTF1	LVCSGENDNHGQIANLPSAVTSDQK	1.08	0.11
458	P02795	MT2A Metallothionein-2	MT2A	SCCSCCPVGCAK	1.08	0.11
459	P62191	PSMC1 26S proteasome regulatory subunit 4	PSMC1	AICTEAGLMALR	1.08	0.11
460	Q9Y2Q3	GSTK1 Glutathione S-transferase kappa 1	GSTK1	ETTEAACR	1.08	0.12
461	Q9NQT5	EXOSC3 Exosome complex component RRP40	EXOSC3	LLAPDCEIIQEVGK	1.08	0.12
462	Q9Y4E1	WASHC2C WASH complex subunit 2C	WASHC2C	GCDPDAHPK	1.08	0.12
463	Q13330	MTA1 Metastasis-associated protein MTA1	MTA1	ALDCSSSVR	1.09	0.12

464	Q86UY8	NT5DC3 5-nucleotidase domain-containing protein 3	NT5DC3	YICYAEQTR	1.09	0.12
465	Q07065	CKAP4 Cytoskeleton-associated protein 4	CKAP4	SSSSSSASAAAAAAAASSSASCSR	1.09	0.13
466	P62851	RPS25 40S ribosomal protein S25	RPS25	LCK	1.10	0.13
467	Q96HP0	DOCK6 Dedicator of cytokinesis protein 6	DOCK6	AGCALSAESSR	1.10	0.13
468	Q9HCC0	MCCC2 Methylcrotonoyl-CoA carboxylase beta chain, mitoch	MCCC2	AATGEEVSAEDLGGADLHCR	1.10	0.13
469	Q16576	RBBP7 Histone-binding protein RBBP7	RBBP7	VHIPNDDAQFDASHCDSDK	1.10	0.14
470	Q92945	KHSRP Far upstream element-binding protein 2	KHSRP	VQQACEMVMDILR	1.10	0.14
471	Q10567	AP1B1 AP-1 complex subunit beta-1	AP1B1	DCEDPNPLIR	1.11	0.15
472	P30519	HMOX2 Heme oxygenase 2	HMOX2	GALEGSSCPFR	1.11	0.15
473	Q14C86	GAPVD1 GTPase-activating protein and VPS9 domain-containing	GAPVD1	FSLCSDNLEGISEGPSNR	1.11	0.15
474	P07384	CAPN1 Calpain-1 catalytic subunit	CAPN1	LEICNLTPDALK	1.11	0.15
475	P12004	PCNA Proliferating cell nuclear antigen	PCNA	CAGNEDIITLR	1.11	0.15
476	P62745	RHOB Rho-related GTP-binding protein RhoB	RHOB	LVVVGDGACGK	1.11	0.16
477	P14618	PKM Pyruvate kinase PKM	PKM	NTGIICTIGPASR	1.12	0.16
478	O43815	STRN Striatin	STRN	CYIASAGADALAK	1.12	0.16
479	P25398	RPS12 40S ribosomal protein S12	RPS12	QAHLCVLASNCDEPMYVK	1.12	0.16
480	P67936	TPM4 Tropomyosin alpha-4 chain	TPM4	EENVGLHQTLDQTLNELNCI	1.12	0.16
481	O60610	DIAPH1 Protein diaphanous homolog 1	DIAPH1	AGCAVTSLLASELTK	1.12	0.16
482	P08134	RHOC Rho-related GTP-binding protein RhoC	RHOC	ISAFGYLECSAK	1.12	0.16
483	O95817	BAG3 BAG family molecular chaperone regulator 3	BAG3	SQSPAASDCSSSSSSASLPSSGR	1.12	0.17
484	O95671	ASMTL N-acetylserotonin O-methyltransferase-like protein	ASMTL	LTACQVATAFNLSR	1.12	0.17
485	P40926	MDH2 Malate dehydrogenase, mitochondrial	MDH2	SQETECTYFSTPLLLGK	1.12	0.17

486	Q86VY4	TSPYL5 Testis-specific Y-encoded-like protein 5	TSPYL5	APETCSTAGR	1.13	0.17
487	Q06330	RBPJ Recombining binding protein suppressor of hairless	RBPJ	IIQFQATPCPK	1.13	0.17
488	P15924	DSP Desmoplakin	DSP	ETQTECEWTVDTSK	1.13	0.17
489	Q9NXW9	ALKBH4 Alpha-ketoglutarate-dependent dioxygenase alkB	ALKBH4	EAPGSLLLCSAPSAAPEALVDSVIAPSR	1.13	0.18
490	O76039	CDKL5 Cyclin-dependent kinase-like 5	CDKL5	LCDFGFAR	1.13	0.18
491	Q9P2R7	SUCLA2 Succinate--CoA ligase [ADP-forming] subunit beta,	SUCLA2	ICNQVLVCER	1.13	0.18
492	Q8TCU6	PREX1 Phosphatidylinositol 3,4,5-trisphosphate-dependent	PREX1	CLPAAEGDPQGQGLHDGSFGPASGTLGQEDR	1.14	0.18
493	Q15004	PCLAF PCNA-associated factor	PCLAF	ACPLQPDHTNDEK	1.14	0.19
494	Q9BV86	NTMT1 N-terminal Xaa-Pro-Lys N-methyltransferase 1	NTMT1	DNMAQEGVILDDVDSSVCR	1.14	0.19
495	P60763	RAC3 Ras-related C3 botulinum toxin substrate 3	RAC3	AVLCPPPVK	1.14	0.19
496	P13639	EEF2 Elongation factor 2	EEF2	STLTDSLVCK	1.14	0.19
497	P25205	MCM3 DNA replication licensing factor MCM3	MCM3	SVHYCPATK	1.15	0.20
498	Q9UHD8	SEPT9 Septin-9	9-Sep	SQEATEAAPSCVGDMADTPR	1.15	0.20
499	O75822	EIF3J Eukaryotic translation initiation factor 3 subunit	EIF3J	ITNSLTVLCSEK	1.15	0.20
500	Q9UJX4	ANAPC5 Anaphase-promoting complex subunit 5	ANAPC5	LIEESCPQLANSVQIR	1.15	0.20
501	O60361	NME2P1 Putative nucleoside diphosphate kinase	NME2P1	GDFCIQVGR	1.15	0.20
502	P38117	ETFB Electron transfer flavoprotein subunit beta	ETFB	EVIAVSC*GPAQC*QETIR	1.16	0.22
503	Q58A45	PAN3 PAN2-PAN3 deadenylation complex subunit PAN3	PAN3	SSNFGYITSCYK	1.17	0.22
504	Q96CP2	FLYWCH2 FLYWCH family member 2	FLYWCH2	TEDSGLAAGPPEAAGENFAPCSVAPGK	1.17	0.23
505	Q15631	TSN Translin	TSN	ETAAACVEK	1.18	0.24

506	Q00610	CLTC Clathrin heavy chain 1	CLTC	VIQCFAETGQVQK	1.18	0.24
507	P42704	LRPPRC Leucine-rich PPR motif-containing protein	LRPPRC	SCGSLLPELK	1.18	0.24
508	Q86XN7	PROSER1 Proline and serine-rich protein 1	PROSER1	CYAPSAIPTPQR	1.18	0.24
509	P30042	C21orf33 ES1 protein homolog, mitochondrial	C21orf33	DCK	1.18	0.24
510	P60981	DSTN Destrin	DSTN	HECQANGPEDLNR	1.18	0.24
511	Q9ULV4	CORO1C Coronin-1C	CORO1C	CDLISIPK	1.19	0.25
512	P31943	HNRNPH1 Heterogeneous nuclear ribonucleoprotein H	HNRNPH1	DLNYCFSGMSDHR	1.20	0.26
513	P18085	ARF4 ADP-ribosylation factor 4	ARF4	NICFTVWDVGGQDR	1.20	0.26
514	Q9BRA2	TXNDC17 Thioredoxin domain-containing protein 17	TXNDC17	SWCPDCVQAEPVVR	1.20	0.26
515	Q8TEX9	IPO4 Importin-4	IPO4	APAALPALCDLLASAADPQIR	1.20	0.26
516	P21333	FLNA Filamin-A	FLNA	THEAEIVEGENHTYCIR	1.20	0.26
517	P34932	HSPA4 Heat shock 70 kDa protein 4	HSPA4	CTPACISFGPK	1.20	0.26
518	P38117	ETFB Electron transfer flavoprotein subunit beta	ETFB	QAIDDDCNQTGQMTAGFLDWPQGTFASQVTLEGDK	1.20	0.27
519	O60502	MGEA5 Protein O-GlcNAcase	MGEA5	ANSSVVSVNCK	1.20	0.27
520	Q7Z2W4	ZC3HAV1 Zinc finger CCCH-type antiviral protein 1	ZC3HAV1	NSNVDSSYLESLYQSCPR	1.21	0.28
521	Q7Z6Z7	HUWE1 E3 ubiquitin-protein ligase HUWE1	HUWE1	DQSAQCTASK	1.21	0.28
522	P46776	RPL27A 60S ribosomal protein L27a	RPL27A	NQSFCPTVNLDK	1.22	0.29
523	P46013	MKI67 Proliferation marker protein Ki-67	MKI67	ADVEGELLACR	1.23	0.29
524	Q9NQ88	TIGAR Fructose-2,6-bisphosphatase TIGAR	TIGAR	EECPVFTPPGGETLDQVK	1.23	0.30
525	Q9UN37	VPS4A Vacuolar protein sorting-associated protein 4A	VPS4A	LLEPVVCMSDMLR	1.23	0.30
526	P40227	CCT6A T-complex protein 1 subunit zeta	CCT6A	NAIDDGCVVPGAGAVEVAMAEALIK	1.23	0.30

527	P21953	BCKDHB 2-oxoisovalerate dehydrogenase subunit beta	BCKDHB	SGDLFNCGSLTIR	1.23	0.30
528	O00148	DDX39A ATP-dependent RNA helicase DDX39A	DDX39A	AIVDCGFEHPSEVQHECIPQAILGMDVLCQAK	1.23	0.30
529	P08708	RPS17 40S ribosomal protein S17	RPS17	VCEEIAIIPSK	1.24	0.31
530	Q13636	RAB31 Ras-related protein Rab-31	RAB31	VCLLGDTGVGK	1.24	0.31
531	Q9HA64	FN3KRP Ketosamine-3-kinase	FN3KRP	ATGHSGGGCISQGR	1.25	0.32
532	P48643	CCT5 T-complex protein 1 subunit epsilon	CCT5	ETGANLAICQWGFDDEANHLLLQNNLPAVR	1.25	0.32
533	O15355	PPM1G Protein phosphatase 1G	PPM1G	CSGDGVGAPR	1.25	0.33
534	P30084	ECHS1 Enoyl-CoA hydratase, mitochondrial	ECHS1	ALNALCDGLIDELNQALK	1.25	0.33
535	Q13155	AIMP2 Aminoacyl tRNA synthase complex-interacting	AIMP2	SCENLAPFNTALK	1.26	0.33
536	P07814	EPRS Bifunctional glutamate/proline--tRNA ligase	EPRS	LGVENCYFPMFVSQSALEK	1.26	0.33
537	Q9NZT2	OGFR Opioid growth factor receptor	OGFR	DCNGDTPNLSFYR	1.26	0.34
538	Q96QR8	PURB Transcriptional activator protein Pur-beta	PURB	GGGGGPCGFQPASR	1.27	0.34
539	Q92879	CELF1 CUGBP Elav-like family member 1	CELF1	GCAFVTFTTR	1.28	0.36
540	P34897	SHMT2 Serine hydroxymethyltransferase, mitochondrial	SHMT2	YYGGAEVVDEIELLCQR	1.28	0.36
541	P62195	PSMC5 26S proteasome regulatory subunit 8	PSMC5	NIDINDVTPNCR	1.29	0.36
542	P48735	IDH2 Isocitrate dehydrogenase [NADP], mitochondrial	IDH2	SSGGFVWACK	1.29	0.37
543	P48735	IDH2 Isocitrate dehydrogenase [NADP], mitochondrial	IDH2	VCVETVESGAMTK	1.30	0.38
544	P20810	CAST Calpastatin	CAST	AAAPAPVSEAVCR	1.30	0.38
545	P24752	ACAT1 Acetyl-CoA acetyltransferase, mitochondrial	ACAT1	QGEYGLASICNGGGGASAMLIQK	1.30	0.38
546	P48047	ATP5O ATP synthase subunit O, mitochondrial	ATP5O	GEVPCTVTSASPLEEATLSELK	1.30	0.38

547	Q04760	GLO1 Lactoylglutathione lyase	GLO1	CDFPIMK	1.30	0.38
548	P50991	CCT4 T-complex protein 1 subunit delta	CCT4	TLSGMESYCVR	1.30	0.38
549	P34897	SHMT2 Serine hydroxymethyltransferase, mitochondrial	SHMT2	AALEALGSCLNNK	1.31	0.39
550	O15075	DCLK1 Serine/threonine-protein kinase DCLK1	DCLK1	YQDDFLLDESECR	1.31	0.39
551	P46782	RPS5 40S ribosomal protein S5	RPS5	TIAECLADELINAAK	1.31	0.39
552	P56192	MARS Methionine--tRNA ligase, cytoplasmic	MARS	LFVSDGVPGCLPVLAAAGR	1.32	0.40
553	Q9NSD9	FARSB Phenylalanine--tRNA ligase beta subunit	FARSB	CAEIFAR	1.32	0.40
554	P54886	ALDH18A1 Delta-1-pyrroline-5-carboxylate synthase	ALDH18A1	GDECGLALGR	1.32	0.41
555	Q8NDH3	NPEPL1 Probable aminopeptidase NPEPL1	NPEPL1	DCGGAAAVLGAFR	1.33	0.41
556	P06730	EIF4E Eukaryotic translation initiation factor 4E	EIF4E	IAIWTTECENR	1.33	0.41
557	P53597	SUCLG1 Succinate--CoA ligase [ADP/GDP-forming] subunit al	SUCLG1	LIGPNCPGVINPGECK	1.33	0.41
558	P04899	GNAI2 Guanine nucleotide-binding protein G(i) subunit al	GNAI2	EIYTHFTCATDTK	1.33	0.41
559	P09622	DLD Dihydrolipoyl dehydrogenase, mitochondrial	DLD	NETLGGTCLNVGCIPSK	1.34	0.42
560	Q9NWZ3	IRAK4 Interleukin-1 receptor-associated kinase 4	IRAK4	CLNVGLIR	1.34	0.43
561	Q99836	MYD88 Myeloid differentiation primary response protein M	MYD88	FITVCDYTNPCTK	1.34	0.43
562	Q9NR46	SH3GLB2 Endophilin-B2	SH3GLB2	SQTTYYAQCYR	1.35	0.43
563	P61962	DCAF7 DDB1- and CUL4-associated factor 7	DCAF7	VPCTPVAR	1.35	0.44
564	P58107	EPPK1 Epiplakin	EPPK1	ELVALCR	1.35	0.44
565	P50991	CCT4 T-complex protein 1 subunit delta	CCT4	LGGTIDDCELVEGLVLTQK	1.35	0.44
566	P43897	TSFM Elongation factor Ts, mitochondrial	TSFM	FECGEGEEAAETE	1.35	0.44
567	Q7L3B6	CDC37L1 Hsp90 co-chaperone Cdc37-like 1	CDC37L1	MCLWSTDAISK	1.36	0.45

568	O94979	SEC31A Protein transport protein Sec31A	SEC31A	SCATFSSSHR	1.36	0.45
569	P49207	RPL34 60S ribosomal protein L34	RPL34	AYGGSMCAK	1.37	0.45
570	P55769	SNU13 NHP2-like protein 1	SNU13	LLDLVQQSCNYK	1.37	0.45
571	P62195	PSMC5 26S proteasome regulatory subunit 8	PSMC5	GVCTEAGMYALR	1.37	0.46
572	Q99590	SCAF11 Protein SCAF11	SCAF11	VYQPVSCPLSDLSENVESVVNEEK	1.38	0.46
573	Q9NP73	ALG13 Putative bifunctional UDP-N-acetylglucosamine	ALG13	ADLVISHAGAGSCLETLEK	1.38	0.46
574	P10809	HSPD1 60 kDa heat shock protein, mitochondrial	HSPD1	CIPALDSLTPANEDQK	1.39	0.47
575	Q27J81	INF2 Inverted formin-2	INF2	LGPQDSDPTEANLESADPELCIR	1.39	0.47
576	Q9UJX3	ANAPC7 Anaphase-promoting complex subunit 7	ANAPC7	PSTGNSASTPQSQCLPSEIEVK	1.39	0.47
577	P63220	RPS21 40S ribosomal protein S21	RPS21	TYAICGAIR	1.39	0.47
578	P52943	CRIP2 Cysteine-rich protein 2	CRIP2	ASSVTTFTGEPNTCPR	1.39	0.48
579	Q13155	AIMP2 Aminoacyl tRNA synthase complex-interacting	AIMP2	FSIQTMCPIEGEGNIAR	1.39	0.48
580	P62330	ARF6 ADP-ribosylation factor 6	ARF6	NWYVQPSCATSGDGLYEGLTWLTSNYK	1.40	0.48
581	Q32MZ4	LRRFIP1 Leucine-rich repeat flightless-interacting protein	LRRFIP1	CEMSEHPSQTVR	1.40	0.48
582	P35125	USP6 Ubiquitin carboxyl-terminal hydrolase 6	USP6	SGTSCPSSK	1.40	0.49
583	Q16555	DPYSL2 Dihydropyrimidinase-related protein 2	DPYSL2	GLYDGPVCEVSVTPK	1.40	0.49
584	P09110	ACAA1 3-ketoacyl-CoA thiolase, peroxisomal	ACAA1	DCLIPMGITSENVAER	1.40	0.49
585	Q53H96	PYCR3 Pyrroline-5-carboxylate reductase 3	PYCR3	AATMSAVEAATCR	1.41	0.49
586	Q14694	USP10 Ubiquitin carboxyl-terminal hydrolase 10	USP10	TPSYSISSTLNPQAPEFILGCTASK	1.42	0.50
587	Q99832	CCT7 T-complex protein 1 subunit eta	CCT7	QLCDNAGFDATNILNK	1.42	0.50
588	P29401	TKT Transketolase	TKT	QAFTDVATGSLGQGLGAACGMAYTGK	1.42	0.51

589	P46782	RPS5 40S ribosomal protein S5	RPS5	VNQAIWLLCTGAR	1.43	0.51
590	P12532	CKMT1A Creatine kinase U-type, mitochondrial	CKMT1A	LGYILTCPSNLGTGLR	1.43	0.51
591	O14579	COPE Coatomer subunit epsilon	COPE	NAFYIGSYQQCINEAQR	1.43	0.52
592	P08243	ASNS Asparagine synthetase [glutamine-hydrolyzing]	ASNS	FENVNGYTNCCFGFHR	1.43	0.52
593	Q08211	DHX9 ATP-dependent RNA helicase A	DHX9	SSVNCPFSSQDMK	1.43	0.52
594	P68104	EEF1A1 Elongation factor 1-alpha 1	EEF1A1	PMCVESFSDYPPLGR	1.43	0.52
595	O75934	BCAS2 Pre-mRNA-splicing factor SPF27	BCAS2	NDITAWQECVNNSMAQLEHQAVR	1.44	0.52
596	P36873	PPP1CC Serine/threonine-protein phosphatase PP1-gamma cat	PPP1CC	TFTDCFNCLPIAAIVDEK	1.44	0.53
597	P31689	DNAJA1 DnaJ homolog subfamily A member 1	DNAJA1	GAVECCPNCR	1.45	0.54
598	Q9C0C9	UBE2O (E3-independent) E2 ubiquitin-conjugating enzyme	UBE2O	NCAQGEGSMAK	1.45	0.54
599	O60568	PLOD3 Procollagen-lysine,2-oxoglutarate 5-dioxygenase 3	PLOD3	GLDYEGGGCR	1.45	0.54
600	Q16822	PCK2 Phosphoenolpyruvate carboxykinase [GTP], mitochondrial	PCK2	QCPIMDPAWEAPEGVPIDAIIFGGR	1.45	0.54
601	Q05086	UBE3A Ubiquitin-protein ligase E3A	UBE3A	GAPNNSCSEIK	1.45	0.54
602	P08865	RPSA 40S ribosomal protein SA	RPSA	YVDIAIPCNNK	1.46	0.54
603	Q86W50	METTL16 U6 small nuclear RNA (adenine-(43)-N(6))-methyltrans	METTL16	VTYTEFCQGR	1.46	0.54
604	O95757	HSPA4L Heat shock 70 kDa protein 4L	HSPA4L	GCALQCAILSPAFK	1.46	0.55
605	P49368	CCT3 T-complex protein 1 subunit gamma	CCT3	NLQDAMQVCR	1.46	0.55
606	Q9H1K1	ISCU Iron-sulfur cluster assembly enzyme ISCU, mitochondria	ISCU	NVGTGLVGAPACGDVMK	1.47	0.55
607	P35998	PSMC2 26S proteasome regulatory subunit 7	PSMC2	PDVTYSDVGGCK	1.47	0.55
608	Q96I99	SUCLG2 Succinate--CoA ligase [GDP-forming] subunit beta,	SUCLG2	SCNGPVLVGSPQGGVDIEEVAASNPELIFK	1.47	0.55

609	Q5T0W9	FAM83B Protein FAM83B	FAM83B	SCVPSSFAQEESAR	1.47	0.55
610	P61289	PSME3 Proteasome activator complex subunit 3	PSME3	LDECEEAFQGTK	1.47	0.55
611	P62280	RPS11 40S ribosomal protein S11	RPS11	CPFTGNVSIR	1.47	0.56
612	Q13371	PDCL Phosducin-like protein	PDCL	CAPASSSVPAEAELAGEGISVNTGPK	1.47	0.56
613	Q27J81	INF2 Inverted formin-2	INF2	CPASEPGLDATTASESR	1.48	0.56
614	Q9H0C8	ILKAP Integrin-linked kinase-associated serine/threonine	ILKAP	CGVTSVPDIR	1.48	0.56
615	Q86XN7	PROSER1 Proline and serine-rich protein 1	PROSER1	DGEECTNEGK	1.48	0.56
616	Q9Y5Q8	GTF3C5 General transcription factor 3C polypeptide 5	GTF3C5	VCTNPVDR	1.48	0.56
617	Q92989	CLP1 Polyribonucleotide 5-hydroxyl-kinase Clp1	CLP1	VGAPTIPDSCLPLGMSQEDNQLK	1.48	0.57
618	Q1KMD3	HNRNPUL2 Heterogeneous nuclear ribonucleoprotein U-like pro	HNRNPUL2	NFILDQCNVYNSGQR	1.48	0.57
619	P85037	FOXK1 Forkhead box protein K1	FOXK1	SGGLQTPECLSR	1.49	0.57
620	P60866	RPS20 40S ribosomal protein S20	RPS20	VCADLIR	1.49	0.58
621	Q8TAQ2	SMARCC2 SWI/SNF complex subunit SMARCC2	SMARCC2	NLAGDVCAIMR	1.50	0.58
622	Q9P2R7	SUCLA2 Succinate--CoA ligase [ADP-forming] subunit beta,	SUCLA2	ILACDDLDEAAR	1.50	0.58
623	Q9HAV4	XPO5 Exportin-5	XPO5	DSLDQFDCK	1.51	0.59
624	P05388	RPLP0 60S acidic ribosomal protein P0	RPLP0	CFIVGADNVGSK	1.51	0.59
625	O14744	PRMT5 Protein arginine N-methyltransferase 5	PRMT5	DLNCVPEIADTLGAVAK	1.51	0.60
626	Q96T51	RUFY1 RUN and FYVE domain-containing protein 1	RUFY1	ICSLQEEQQQLR	1.52	0.60
627	P05388	RPLP0 60S acidic ribosomal protein P0	RPLP0	AGAIAPCEVTVPAQNTGLGPEK	1.52	0.61
628	Q86VY4	TSPYL5 Testis-specific Y-encoded-like protein 5	TSPYL5	EYGCGPSGQVVSR	1.53	0.61
629	P62857	RPS28 40S ribosomal protein S28	RPS28	TGSQGQCTQVR	1.54	0.62

630	Q9UL25	RAB21 Ras-related protein Rab-21	RAB21	VVLLGEGCVGK	1.54	0.62
631	P62879	GNB2 Guanine nucleotide-binding protein G(I)/G(S)/G(T)	GNB2	ELPGHTGYLSCCR	1.54	0.63
632	P62701	RPS4X 40S ribosomal protein S4, X isoform	RPS4X	FDTGNLCMVTGGANLGR	1.55	0.63
633	Q04721	NOTCH2 Neurogenic locus notch homolog protein 2	NOTCH2	NIDDCPNHR	1.56	0.64
634	Q6PKG0	LARP1 La-related protein 1	LARP1	TASISSSPSEGTPTVGSYGCTPQSLPK	1.56	0.65
635	P08559	PDHA1 Pyruvate dehydrogenase E1 component subunit alpha,	PDHA1	VDGMDILCVR	1.56	0.65
636	P10809	HSPD1 60 kDa heat shock protein, mitochondrial	HSPD1	AAVEEGIVLGGGCALLR	1.57	0.65
637	P27797	CALR Calreticulin	CALR	HEQNIDCGGGYVK	1.57	0.65
638	P55809	OXCT1 Succinyl-CoA:3-ketoacid coenzyme A transferase 1,	OXCT1	STGCDFAVSPK	1.57	0.65
639	Q9NP81	SARS2 Serine--tRNA ligase, mitochondrial	SARS2	GAVFEGCGMTPNANPSQIYNIDPAR	1.57	0.65
640	P02795	MT2A Metallothionein-2	MT2A	CAQGCICK	1.57	0.65
641	P60709	ACTB Actin, cytoplasmic 1	ACTB	LCYVALDFEQEMATAASSSSLEK	1.58	0.66
642	Q16822	PCK2 Phosphoenolpyruvate carboxykinase [GTP], mitochond	PCK2	VLDWICR	1.58	0.66
643	P63241	EIF5A Eukaryotic translation initiation factor 5A-1	EIF5A	YEDICPSTHNMDVPNIK	1.59	0.67
644	P40926	MDH2 Malate dehydrogenase, mitochondrial	MDH2	TIIPLISQCTPK	1.59	0.67
645	Q06587	RING1 E3 ubiquitin-protein ligase RING1	RING1	FCSDCIVTALR	1.60	0.68
646	P35998	PSMC2 26S proteasome regulatory subunit 7	PSMC2	SVCTEAGMFAIR	1.60	0.68
647	Q00613	HSF1 Heat shock factor protein 1	HSF1	QECMDSK	1.60	0.68
648	P62333	PSMC6 26S proteasome regulatory subunit 10B	PSMC6	AVASQLDCNFLK	1.61	0.68
649	P27448	MARK3 MAP/microtubule affinity-regulating kinase 3	MARK3	LDTFCGSPPYAAPELFQGK	1.62	0.69

650	P27635	RPL10 60S ribosomal protein L10	RPL10	MLSCAGADR	1.62	0.69
651	P49327	FASN Fatty acid synthase	FASN	AFDTAGNGYCR	1.62	0.70
652	Q92598	HSPH1 Heat shock protein 105 kDa	HSPH1	LMSSNSTDLPLNIECFMNDK	1.63	0.70
653	Q16186	ADRM1 Proteasomal ubiquitin receptor ADRM1	ADRM1	TDQDEEHCR	1.64	0.71
654	Q05639	EEF1A2 Elongation factor 1-alpha 2	EEF1A2	PMCVESFSQYPPLGR	1.66	0.73
655	O60504	SORBS3 Vinexin	SORBS3	LCDDGPQLPTSPR	1.66	0.73
656	O75083	WDR1 WD repeat-containing protein 1	WDR1	CFSIDNPGYEPEVVAVHPGGDTVAIGGVDGNVR	1.66	0.73
657	P22102	GART Trifunctional purine biosynthetic protein adenosin	GART	LLEGDGGPNTGGMGAYCPAPQVSNDLLLK	1.66	0.73
658	Q7L0Y3	TRMT10C Mitochondrial ribonuclease P protein 1	TRMT10C	LNLATECLPLDK	1.67	0.74
659	P11802	CDK4 Cyclin-dependent kinase 4	CDK4	LMDVCATSR	1.67	0.74
660	O15355	PPM1G Protein phosphatase 1G	PPM1G	CVVSEAGK	1.67	0.74
661	P62333	PSMC6 26S proteasome regulatory subunit 10B	PSMC6	NVCTEAGMFAIR	1.67	0.74
662	P78527	PRKDC DNA-dependent protein kinase catalytic subunit	PRKDC	CLMDQATDPNILGR	1.69	0.76
663	P31153	MAT2A S-adenosylmethionine synthase isoform type-2	MAT2A	VACETVAK	1.69	0.76
664	O00244	ATOX1 Copper transport protein ATOX1	ATOX1	VCIESEHSMDTLLATLK	1.69	0.76
665	P50914	RPL14 60S ribosomal protein L14	RPL14	ALVDGPCTQVR	1.69	0.76
666	Q8IYQ7	THNSL1 Threonine synthase-like 1	THNSL1	TCPVIISSTAHYSK	1.70	0.77
667	P49327	FASN Fatty acid synthase	FASN	DGLLENQTPEFFQDVCK	1.71	0.77
668	O95833	CLIC3 Chloride intracellular channel protein 3	CLIC3	ASEDGESVGHCPSCQR	1.72	0.78
669	Q86W42	THOC6 THO complex subunit 6 homolog	THOC6	AQVPGSSPGLLSLSLNQQPAAPECK	1.72	0.78
670	P45954	ACADSB Short/branched chain specific acyl-CoA dehydrogenase	ACADSB	ASSTCPLTFENVK	1.72	0.79
671	P62333	PSMC6 26S proteasome regulatory subunit 10B	PSMC6	GCLLYGPPGTGK	1.73	0.79
672	P35579	MYH9 Myosin-9	MYH9	CNGVLEGIR	1.73	0.79

673	P30084	ECHS1 Enoyl-CoA hydratase, mitochondrial	ECHS1	EMQNLSFQDCYSSK	1.73	0.79
674	Q15386	UBE3C Ubiquitin-protein ligase E3C	UBE3C	LPTASTCMNLLK	1.75	0.81
675	P46940	IQGAP1 Ras GTPase-activating-like protein IQGAP1	IQGAP1	QIPAITCIQSQWR	1.75	0.81
676	P15924	DSP Desmoplakin	DSP	DANSENCNK	1.77	0.82
677	Q92616	GCN1 eIF-2-alpha kinase activator GCN1	GCN1	CLQTLLDTK	1.77	0.82
678	P15924	DSP Desmoplakin	DSP	YQAECSQFK	1.77	0.82
679	P04899	GNAI2 Guanine nucleotide-binding protein G(i) subunit al	GNAI2	QLFALSCTAEEQGVLPDDLSGVIR	1.78	0.83
680	P16455	MGMT Methylated-DNA--protein-cysteine methyltransferase	MGMT	VVCSSGAVGNYSGGLAVK	1.78	0.84
681	O60716	CTNND1 Catenin delta-1	CTNND1	YQEAAPNVANNTGPHAASCFGAK	1.79	0.84
682	O95067	CCNB2 G2/mitotic-specific cyclin-B2	CCNB2	VAAAASCLSQK	1.79	0.84
683	P54646	PRKAA2 5-AMP-activated protein kinase catalytic subunit	PRKAA2	TSCGSPNYAAPEVISGR	1.80	0.85
684	P62266	RPS23 40S ribosomal protein S23	RPS23	ITAFVPNDGCLNFIEENDEVLVAGFGR	1.81	0.86
685	P42025	ACTR1B Beta-centractin	ACTR1B	ACYLSINPQK	1.81	0.86
686	Q9H0U6	MRPL18 39S ribosomal protein L18, mitochondrial	MRPL18	NVVACESIGR	1.83	0.87
687	P35579	MYH9 Myosin-9	MYH9	VEDMAELTCLNEASVLHNLK	1.83	0.87
688	Q96PK6	RBM14 RNA-binding protein 14	RBM14	IFVGNVSAACTSQELR	1.84	0.88
689	P31153	MAT2A S-adenosylmethionine synthase isoform type-2	MAT2A	ICDQISDAVLDAHLQQDPDAK	1.85	0.89
690	P23396	RPS3 40S ribosomal protein S3	RPS3	GCEVVVSGK	1.86	0.89
691	Q99436	PSMB7 Proteasome subunit beta type-7	PSMB7	NCSK	1.87	0.91
692	P58107	EPPK1 Epiplakin	EPPK1	YLQGTGCIAGLLLPGSQER	1.88	0.91
693	P42356	PI4KA Phosphatidylinositol 4-kinase alpha	PI4KA	GGGGGGGGGGGCSGSGSSASR	1.88	0.91
694	P68363	TUBA1B Tubulin alpha-1B chain	TUBA1B	YMACCLLYR	1.89	0.92

695	P24298	GPT Alanine aminotransferase 1	GPT	LLEETGICVVPGSGFGQR	1.89	0.92
696	Q8N8R5	C2orf69 UPF0565 protein C2orf69	C2orf69	CSLSAEVR	1.89	0.92
697	O75369	FLNB Filamin-B	FLNB	SGCIVNNLAEFTVDPK	1.90	0.92
698	Q12906	ILF3 Interleukin enhancer-binding factor 3	ILF3	CLAALASLR	1.91	0.93
699	P49411	TUFM Elongation factor Tu, mitochondrial	TUFM	GEETPVIVGSALCALEGR	1.91	0.93
700	O00567	NOP56 Nucleolar protein 56	NOP56	IINDNATYCR	1.91	0.94
701	Q9Y399	MRPS2 28S ribosomal protein S2, mitochondrial	MRPS2	DCGEYAHTR	1.95	0.96
702	Q13748	TUBA3C Tubulin alpha-3C/D chain	TUBA3C	TIQFVDWCPTGFK	1.95	0.96
703	P27707	DCK Deoxycytidine kinase	DCK	SCPSFSASSEGTR	1.95	0.96
704	P40926	MDH2 Malate dehydrogenase, mitochondrial	MDH2	GCDVVVIPAGVPR	1.96	0.97
705	Q9BZQ6	EDEM3 ER degradation-enhancing alpha-mannosidase-like pr	EDEM3	VPCGFAAMK	1.97	0.98
706	P40926	MDH2 Malate dehydrogenase, mitochondrial	MDH2	GYLGPEQLPDCLK	1.98	0.99
707	P50213	IDH3A Isocitrate dehydrogenase [NAD] subunit alpha, mito	IDH3A	IEAACFATIK	1.99	0.99
708	P78527	PRKDC DNA-dependent protein kinase catalytic subunit	PRKDC	VEQLFQVMNGILAQDSACSQR	2.00	1.00
709	P15924	DSP Desmoplakin	DSP	GVITDQNSDGYCQTGTMSR	2.00	1.00
710	Q96P16	RPRD1A Regulation of nuclear pre-mRNA domain-containing p	RPRD1A	HVSSETDESCK	2.00	1.00
711	Q9UPN9	TRIM33 E3 ubiquitin-protein ligase TRIM33	TRIM33	QEPGTEDEICSFSGGVK	2.00	1.00
712	P13804	ETFA Electron transfer flavoprotein subunit alpha, mito	ETFA	CDK	2.01	1.00
713	Q8IU81	IRF2BP1 Interferon regulatory factor 2-binding protein 1	IRF2BP1	EPAPAEALPQQYPEPAPAALCGPPPR	2.01	1.01
714	P23919	DTYMK Thymidylate kinase	DTYMK	LVEALCAAGHR	2.01	1.01
715	P51553	IDH3G Isocitrate dehydrogenase [NAD] subunit gamma, mito	IDH3G	HACVPVDFEEVHVSSNADEEDIR	2.02	1.02

716	P62280	RPS11 40S ribosomal protein S11	RPS11	DVQIGDIVTVGECR	2.04	1.03
717	P42677	RPS27 40S ribosomal protein S27	RPS27	LTEGCSFR	2.05	1.03
718	Q8NE71	ABCF1 ATP-binding cassette sub-family F member 1	ABCF1	ICIVGPNGVGK	2.05	1.03
719	P68363	TUBA1B Tubulin alpha-1B chain	TUBA1B	SIQFVDWCPTGFK	2.05	1.04
720	Q8TCU6	PREX1 Phosphatidylinositol 3,4,5-trisphosphate-dependent	PREX1	LCVLNEILGTER	2.06	1.04
721	P34932	HSPA4 Heat shock 70 kDa protein 4	HSPA4	SVMDATQIAGLNCLR	2.07	1.05
722	A6NNZ2	cimageipi-sp	A6NNZ2	TAVCDIPPR	2.08	1.06
723	P04350	TUBB4A Tubulin beta-4A chain	TUBB4A	VSDTVVEPYNATLSVHQLVENTDETYCIDNEALYDICFR	2.09	1.07
724	Q96SI9	STRBP Spermatid perinuclear RNA-binding protein	STRBP	CLNALASLR	2.09	1.07
725	Q06203	PPAT Amidophosphoribosyltransferase	PPAT	CELENCQPFVVETLHGK	2.10	1.07
726	Q06210	GFPT1 Glutamine--fructose-6-phosphate aminotransferase [	GFPT1	VDSTTCLFPVEEK	2.11	1.08
727	Q15365	PCBP1 Poly(rC)-binding protein 1	PCBP1	VMTIPYQPMPASSPVICAGGQDR	2.11	1.08
728	Q9BQE3	TUBA1C Tubulin alpha-1C chain	TUBA1C	AVCMLSNTTAVAEAWAR	2.13	1.09
729	P55060	CSE1L Exportin-2	CSE1L	NLFEDQNTLTSICEK	2.14	1.10
730	P48735	IDH2 Isocitrate dehydrogenase [NADP], mitochondrial	IDH2	NYDGDVQSDILAQGFGSLGLMTSVLVCPDGK	2.14	1.10
731	P13639	EEF2 Elongation factor 2	EEF2	DLEEDHACIPIK	2.15	1.10
732	P13804	ETFA Electron transfer flavoprotein subunit alpha, mito	ETFA	TIYAGNALCTVK	2.17	1.12
733	P30876	POLR2B DNA-directed RNA polymerase II subunit RPB2	POLR2B	DCQIAHGAAQFLR	2.19	1.13
734	P35270	SPR Sepiapterin reductase	SPR	TVVNISSLCALQPFK	2.20	1.14
735	A6NNZ2	cimageipi-sp	A6NNZ2	NMMAACDPR	2.26	1.17

736	P32322	PYCR1 Pyrroline-5-carboxylate reductase 1, mitochondrial	PYCR1	SLLINAVEASCIR	2.27	1.18
737	Q9Y5Y2	NUBP2 Cytosolic Fe-S cluster assembly factor NUBP2	NUBP2	VGILDVDLCGPSIPR	2.27	1.18
738	P68363	TUBA1B Tubulin alpha-1B chain	TUBA1B	AVCMLSNTTAIAEAWAR	2.32	1.22
739	O00244	ATOX1 Copper transport protein ATOX1	ATOX1	HEFSVDMTCGGCAEAVSR	2.33	1.22
740	P42166	TMPO Lamina-associated polypeptide 2, isoform alpha	TMPO	GGTLFGGEVCK	2.34	1.23
741	Q02252	ALDH6A1 Methylmalonate-semialdehyde dehydrogenase	ALDH6A1	VCNLIDSGTK	2.36	1.24
742	P50213	IDH3A Isocitrate dehydrogenase [NAD] subunit alpha, mito	IDH3A	CSDFTEEICR	2.36	1.24
743	Q02252	ALDH6A1 Methylmalonate-semialdehyde dehydrogenase	ALDH6A1	AEMDAAIASCK	2.37	1.24
744	P21333	FLNA Filamin-A	FLNA	LQVEPAVDTSGVQCYGPGIEGQGVFR	2.37	1.24
745	Q99832	CCT7 T-complex protein 1 subunit eta	CCT7	CQVFEETQIGGER	2.38	1.25
746	P22570	FDXR NADPH:adrenodoxin oxidoreductase, mitochondrial	FDXR	ALEIPGEELPGVCSAR	2.39	1.26
747	Q92598	HSPH1 Heat shock protein 105 kDa	HSPH1	PVTDCVISVPSFFTDAER	2.39	1.26
748	Q9Y4R8	TELO2 Telomere length regulation protein TEL2 homolog	TELO2	TPQPGSPSPNTPCLPEAAVSQPGSAVASDWR	2.48	1.31
749	P63244	RACK1 Receptor of activated protein C kinase 1	RACK1	AEPPQCTSLAWSADGQTLFAGYTDNLVR	2.50	1.32
750	Q96JK2	DCAF5 DDB1- and CUL4-associated factor 5	DCAF5	ASGSTLNSGSGNCPR	2.51	1.33
751	Q96JB5	CDK5RAP3 CDK5 regulatory subunit-associated protein 3	CDK5RAP3	CQQLQQEYSR	2.51	1.33
752	Q8NBJ7	SUMF2 Sulfatase-modifying factor 2	SUMF2	CAADAGR	2.53	1.34
753	Q9Y6Y0	IVNS1ABP Influenza virus NS1A-binding protein	IVNS1ABP	NFASCMGDSR	2.53	1.34

754	Q13501	SQSTM1 Sequestosome-1	SQSTM1	SSSQPSSCCSDPSK	2.58	1.37
755	P17987	TCP1 T-complex protein 1 subunit alpha	TCP1	GANDFMCDEMER	2.58	1.37
756	P49411	TUFM Elongation factor Tu, mitochondrial	TUFM	NMITGTAPLDGCILVVAANDGPMPQTR	2.60	1.38
757	P54136	RARS Arginine--tRNA ligase, cytoplasmic	RARS	NCGCLGASPNLEQLQEENLK	2.61	1.38
758	Q96I99	SUCLG2 Succinate--CoA ligase [GDP-forming] subunit beta,	SUCLG2	IDATQVEVNPFGETPEGQVVCFDAK	2.62	1.39
759	P40939	HADHA Trifunctional enzyme subunit alpha, mitochondrial	HADHA	EVEAVIPDHCIFASNTSALPISEIAAVSK	2.63	1.39
760	P26440	IVD Isovaleryl-CoA dehydrogenase, mitochondrial	IVD	ACDEGHCTAK	2.65	1.41
761	Q16822	PCK2 Phosphoenolpyruvate carboxykinase [GTP], mitochond	PCK2	VECVGDDIAWMR	2.70	1.43
762	P53384	NUBP1 Cytosolic Fe-S cluster assembly factor NUBP1	NUBP1	LCASGAGATPDTAIEEIK	2.72	1.44
763	P13804	ETFA Electron transfer flavoprotein subunit alpha, mito	ETFA	LGGEVSCLVAGTK	2.73	1.45
764	P04183	TK1 Thymidine kinase, cytosolic	TK1	NTMEALPACLLR	2.76	1.47
765	Q02543	RPL18A 60S ribosomal protein L18a	RPL18A	DLTTAGAVTQCYR	2.78	1.48
766	P17858	PFKL ATP-dependent 6-phosphofructokinase, liver type	PFKL	VFANAPDSACVIGLK	2.80	1.49
767	P07858	CTSB Cathepsin B	CTSB	GQDHCGIESEVVAGIPR	2.81	1.49
768	Q08211	DHX9 ATP-dependent RNA helicase A	DHX9	AAECNIVVTQPR	2.82	1.49
769	Q99714	HSD17B10 3-hydroxyacyl-CoA dehydrogenase type-2	HSD17B10	VDVAVNCAGIAVASK	2.83	1.50
770	Q92947	GCDH Glutaryl-CoA dehydrogenase, mitochondrial	GCDH	GELLGCFGLTEPNSGSDPSSMETR	2.85	1.51
771	Q9NRZ9	HELLS Lymphoid-specific helicase	HELLS	CNGQPVPFQQPK	2.95	1.56
772	Q99714	HSD17B10 3-hydroxyacyl-CoA dehydrogenase type-2	HSD17B10	LGNNCVFAPADVTSEK	3.02	1.59

773	Q9BQE3	TUBA1C Tubulin alpha-1C chain	TUBA1C	AYHEQLTVAEITNACFE PANQMVK	3.02	1.60
774	P04350	TUBB4A Tubulin beta-4A chain	TUBB4A	LTTPTYGDLNHLVSATM SGVTTCLR	3.08	1.62
775	P68363	TUBA1B Tubulin alpha-1B chain	TUBA1B	AYHEQLSVAEITNACFE PANQMVK	3.16	1.66
776	Q92947	GCDH Glutaryl-CoA dehydrogenase, mitochondrial	GCDH	GYGCAGVSSVAYGLLAR	3.29	1.72
777	Q15005	SPCS2 Signal peptidase complex subunit 2	SPCS2	SGGSGGCSGAGGASNC GTGSGR	3.45	1.79
778	Q9BSD7	NTPCR Cancer-related nucleoside-triphosphatase	NTPCR	NADCSSGPGQR	3.62	1.85
779	P04181	OAT Ornithine aminotransferase, mitochondrial	OAT	VLPMNTGVEAGETACK	3.63	1.86
780	P62888	RPL30 60S ribosomal protein L30	RPL30	VCTLAIIDPGDSDIIR	3.87	1.95
781	P07858	CTSB Cathepsin B	CTSB	ICEPGYSPTYK	4.12	2.04
782	P31749	AKT1 RAC-alpha serine/threonine-protein kinase	AKT1	TFCGTPEYLAPEVLEDN DYGR	4.44	2.15
783	P07339	CTSD Cathepsin D	CTSD	AIGAVPLIQGEYMIPCEK	4.48	2.16
784	P04406	GAPDH Glyceraldehyde-3-phosphate dehydrogenase	GAPDH	IISNASCTTNCLAPLAK	4.98	2.32
785	Q01813	PFKP ATP-dependent 6-phosphofructokinase, platelet type	PFKP	LPLMECVQMTQDVQK	5.01	2.32
786	P25398	RPS12 40S ribosomal protein S12	RPS12	LGEWVGLCK	5.10	2.35
787	P53396	ACLY ATP-citrate synthase	ACLY	PASFMTSICDER	9.92	3.31
788	P14314	PRKCSH Glucosidase 2 subunit beta	PRKCSH	YEQGTGCWQGPNR	10.68	3.42
789	Q8NFG 4	FLCN Folliculin	FLCN	VFEAEQFGCPQR	18.35	4.20

Table A2-2 Ranking cysteines by sensitivity to untreated control. 509 cysteine containing peptides from MCF7 cell lysate were reported with R values. R value is the average heavy:light ratio from two individual datasets.

index	Uniprot ID	description	symbol	sequence	*R* value	*R* (log2)
1	P35998	PSMC2 26S proteasome regulatory subunit 7	PSMC2	LCPNSTGAEIR	0.59	-0.77
2	Q12849	GRSF1 G-rich sequence factor 1	GRSF1	YIELFLNSCPK	0.68	-0.55
3	P30042	C21orf33 ES1 protein homolog, mitochondrial	C21orf33	DCK	0.74	-0.43
4	O95671	ASMTL N-acetylserotonin O-methyltransferase-like protein	ASMTL	VDASACGMER	0.74	-0.43
5	Q96KC8	DNAJC1 DnaJ homolog subfamily C member 1	DNAJC1	DSVTCSPGMVR	0.75	-0.41
6	Q00536	CDK16 Cyclin-dependent kinase 16	CDK16	LEHEEGAPCTAIR	0.75	-0.41
7	Q6P996	PDXDC1 Pyridoxal-dependent decarboxylase domain-containing	PDXDC1	HSCDALNR	0.76	-0.39
8	Q9P2X3	IMPACT Protein IMPACT	IMPACT	IYCEDK	0.77	-0.37
9	P36578	RPL4 60S ribosomal protein L4	RPL4	SGQGAFGNMCR	0.79	-0.33
10	Q9NYL2	MAP3K20 Mitogen-activated protein kinase 20	MAP3K20	ICDFGASR	0.80	-0.32
11	Q7Z4W1	DCXR L-xylulose reductase	DCXR	GVPGAIVNVSSQCSQR	0.81	-0.31
12	Q09666	AHNAK Neuroblast differentiation-associated protein AHNA	AHNAK	VDVECPDVNIEGPEGK	0.81	-0.30
13	Q9NX24	NHP2 H/ACA ribonucleoprotein complex subunit 2	NHP2	ADPDGPEAQAEACSGER	0.81	-0.30
14	P53582	METAP1 Methionine aminopeptidase 1	METAP1	VCETDGCSSEAK	0.83	-0.28
15	P30041	PRDX6 Peroxiredoxin-6	PRDX6	DINAYNCEEPTEK	0.83	-0.27
16	P09496	CLTA Clathrin light chain A	CLTA	LCDFNPK	0.83	-0.27
17	Q96RS6	NUDCD1 NudC domain-containing protein 1	NUDCD1	DSAQCAAIAER	0.83	-0.26
18	P49247	RPIA Ribose-5-phosphate isomerase	RPIA	GGAGNTSTSCGDSNSICPAPSTMSK	0.83	-0.26
19	Q8IYQ7	THNSL1 Threonine synthase-like 1	THNSL1	LGEMIETAYGENFACSK	0.84	-0.26
20	O14733	MAP2K7 Dual specificity mitogen-activated protein kinase	MAP2K7	SAGCAAYMAPER	0.84	-0.25
21	O00567	NOP56 Nucleolar protein 56	NOP56	IINDNATYCR	0.84	-0.25
22	Q15631	TSN Translin	TSN	ETAAACVEK	0.84	-0.24
23	P62888	RPL30 60S ribosomal protein L30	RPL30	VCTLAIIDPGDSDIIR	0.85	-0.24

24	Q9NQT5	EXOSC3 Exosome complex component RRP40	EXOSC3	LLAPDCEIIQEVGK	0.85	-0.24
25	Q13155	AIMP2 Aminoacyl tRNA synthase complex-interacting	AIMP2	SCENLAPFNTALK	0.85	-0.23
26	Q6XZF7	DNMBP Dynamin-binding protein	DNMBP	SLDQTSPCPLVLVR	0.85	-0.23
27	P63208	SKP1 S-phase kinase-associated protein 1	SKP1	GLLDVTCK	0.86	-0.23
28	Q9UPN9	TRIM33 E3 ubiquitin-protein ligase TRIM33	TRIM33	CDPVPAANGAIR	0.86	-0.22
29	Q04726	TLE3 Transducin-like enhancer protein 3	TLE3	FTVAESCDR	0.86	-0.22
30	Q13057	COASY Bifunctional coenzyme A synthase	COASY	YATSCYSCCPR	0.86	-0.22
31	P04406	GAPDH Glyceraldehyde-3-phosphate dehydrogenase	GAPDH	IISNASCTTNCLAPLAK	0.86	-0.22
32	A6NDG6	PGP Glycerol-3-phosphate phosphatase	PGP	NNQESDCVSK	0.86	-0.21
33	Q9NUQ9	FAM49B Protein FAM49B	FAM49B	VLTCTDLEQGPNFFLDFENAQPTESEK	0.87	-0.21
34	P52943	CRIP2 Cysteine-rich protein 2	CRIP2	ASSVTTFTGEPNTCPR	0.87	-0.20
35	P49591	SARS Serine--tRNA ligase, cytoplasmic	SARS	TICAILENYQTEK	0.87	-0.20
36	P51649	ALDH5A1 Succinate-semialdehyde dehydrogenase, mitochondria	ALDH5A1	NTGQTCVCSNQFLVQR	0.87	-0.20
37	Q9BUK6	MSTO1 Protein misato homolog 1	MSTO1	EPPGELCPDVLYR	0.87	-0.20
38	Q9NPJ8	NXT2 NTF2-related export protein 2	NXT2	TYVDQACR	0.87	-0.20
39	P61289	PSME3 Proteasome activator complex subunit 3	PSME3	LDECEEAFQGTK	0.87	-0.20
40	Q07065	CKAP4 Cytoskeleton-associated protein 4	CKAP4	SSSSSSASAAAAAAAASSSASCSR	0.88	-0.19
41	Q99873	PRMT1 Protein arginine N-methyltransferase 1	PRMT1	VIGIECSSISDYAVK	0.88	-0.19
42	P49023	PXN Paxillin	PXN	TSSVSNPQDSVGSPCSR	0.88	-0.18
43	P48200	IREB2 Iron-responsive element-binding protein 2	IREB2	CAIQNAPNPGGGDLQK	0.89	-0.18
44	Q1KMD3	HNRNPUL2 Heterogeneous nuclear ribonucleoprotein U-like pro	HNRNPUL2	NFILDQCNVYNSGQR	0.89	-0.18
45	P48506	GCLC Glutamate--cysteine ligase catalytic subunit	GCLC	GGNAVVDGCGK	0.89	-0.17
46	Q9H6T0	ESRP2 Epithelial splicing regulatory protein 2	ESRP2	AEAAALSTQCR	0.89	-0.17

47	O14744	PRMT5 Protein arginine N-methyltransferase 5	PRMT5	DLNCVPEIADTLGAVAK	0.89	-0.17
48	P51812	RPS6KA3 Ribosomal protein S6 kinase alpha-3	RPS6KA3	AENGLLMTPCYTANFVAPEVLK	0.89	-0.16
49	Q96I15	SCLY Selenocysteine lyase	SCLY	DAPAPAASQPSGCGK	0.90	-0.16
50	P49591	SARS Serine--tRNA ligase, cytoplasmic	SARS	YAGLSTCFR	0.90	-0.15
51	P55060	CSE1L Exportin-2	CSE1L	SQICDNAALYAQK	0.90	-0.15
52	P24752	ACAT1 Acetyl-CoA acetyltransferase, mitochondrial	ACAT1	IHMGSCAENTAK	0.90	-0.15
53	Q9NZA1	CLIC5 Chloride intracellular channel protein 5	CLIC5	AGIDGESIGNCPFSQR	0.90	-0.15
54	P42356	PI4KA Phosphatidylinositol 4-kinase alpha	PI4KA	GGGGGGGGGGGCSGSGSSASR	0.90	-0.15
55	Q96HP0	DOCK6 Dedicator of cytokinesis protein 6	DOCK6	AGCALSAESSR	0.90	-0.15
56	P55060	CSE1L Exportin-2	CSE1L	ICAVGITK	0.91	-0.14
57	Q3SY69	ALDH1L2 Mitochondrial 10-formyltetrahydrofolate dehydrogenase	ALDH1L2	SPLIIFNDCELDK	0.91	-0.14
58	Q9BSD7	NTPCR Cancer-related nucleoside-triphosphatase	NTPCR	NADCSSGPGQR	0.91	-0.14
59	Q9H9P8	L2HGDH L-2-hydroxyglutarate dehydrogenase, mitochondrial	L2HGDH	ISELSGCTPDPR	0.91	-0.14
60	Q9UJU6	DBNL Drebrin-like protein	DBNL	AEEDVEPECIMEK	0.91	-0.14
61	O43815	STRN Striatin	STRN	CYIASAGADALAK	0.91	-0.14
62	P17655	CAPN2 Calpain-2 catalytic subunit	CAPN2	WNDNCPSWNTIDPEER	0.91	-0.14
63	Q15370	ELOB Elongin-B	ELOB	ADDTFEALCIEPFSSPPELPDVMK	0.91	-0.14
64	P49915	GMPS GMP synthase [glutamine-hydrolyzing]	GMPS	TVGVQGDCR	0.91	-0.14
65	P61158	ACTR3 Actin-related protein 3	ACTR3	LPACVVDCGTGYTK	0.91	-0.13
66	O14929	HAT1 Histone acetyltransferase type B catalytic subunit	HAT1	VDENFDCVEADDVEGK	0.91	-0.13
67	P53396	ACLY ATP-citrate synthase	ACLY	FICTTSAIQNR	0.91	-0.13
68	P45985	MAP2K4 Dual specificity mitogen-activated protein kinase	MAP2K4	LCDFGISGQLVDSIAK	0.92	-0.13
69	P10644	PRKAR1A cAMP-dependent protein kinase type I-alpha	PRKAR1A	ECELYVQK	0.92	-0.13
70	P82932	MRPS6 28S ribosomal protein S6, mitochondrial	MRPS6	ECEGIVPVPLAEK	0.92	-0.13
71	O95833	CLIC3 Chloride intracellular channel protein 3	CLIC3	ASEDGESVGHCPSCQR	0.92	-0.13

72	Q9P1Z2	CALCOCO1 Calcium-binding and coiled-coil domain-containing	CALCOCO1	VEAACVR	0.92	-0.13
73	P16455	MGMT Methylated-DNA--protein-cysteine methyltransferase	MGMT	VVCSSGAVGNYSGGLAVK	0.92	-0.13
74	Q9NNX1	TUFT1 Tuftelin	TUFT1	SNNADCQAER	0.92	-0.12
75	Q9HC84	MUC5B Mucin-5B	MUC5B	AQAACANAR	0.92	-0.12
76	P50749	RASSF2 Ras association domain-containing protein 2	RASSF2	ILQGPCEQISK	0.92	-0.12
77	Q9NX70	MED29 Mediator of RNA polymerase II transcription	MED29	LAHECLSQSCDSAK	0.92	-0.12
78	Q9UKV8	AGO2 Protein argonaute-2	AGO2	SFFTASEGCSNPLGGGR	0.92	-0.12
79	P35250	RFC2 Replication factor C subunit 2	RFC2	TTSILCLAR	0.92	-0.12
80	Q14C86	GAPVD1 GTPase-activating protein and VPS9 domain-containing	GAPVD1	FSLCSDNLEGISEGPSNR	0.92	-0.12
81	Q9UNH7	SNX6 Sorting nexin-6	SNX6	IGSSLYALGTQDSTDICK	0.92	-0.12
82	P53384	NUBP1 Cytosolic Fe-S cluster assembly factor NUBP1	NUBP1	GASCQGCPNQR	0.92	-0.12
83	P50851	LRBA Lipopolysaccharide-responsive and beige-like ancho	LRBA	CSGIGDNPGSETAAPR	0.92	-0.12
84	P31749	AKT1 RAC-alpha serine/threonine-protein kinase	AKT1	TFCGTPEYLAPEVLEDNDYGR	0.92	-0.12
85	P55212	CASP6 Caspase-6	CASP6	GTCADR	0.92	-0.12
86	Q99832	CCT7 T-complex protein 1 subunit eta	CCT7	EGTDSSQGIPQLVSNISACQVIAEAVR	0.92	-0.12
87	O15075	DCLK1 Serine/threonine-protein kinase DCLK1	DCLK1	YQDDFLLDESECR	0.92	-0.12
88	Q9UPM8	AP4E1 AP-4 complex subunit epsilon-1	AP4E1	SSCSTLPDYLLYQCQK	0.92	-0.11
89	Q13148	TARDBP TAR DNA-binding protein 43	TARDBP	VTEDENDEPIEIPSEDDGTVLLSTVTAQFPGACGLR	0.92	-0.11
90	P49411	TUFM Elongation factor Tu, mitochondrial	TUFM	GEETPVIVGSALCALEGR	0.93	-0.11
91	Q9BY32	ITPA Inosine triphosphate pyrophosphatase	ITPA	GCQDFGWDPCFQPDGYEQTYAEMPK	0.93	-0.11
92	Q9NTK5	OLA1 Obg-like ATPase 1	OLA1	STFFNVLTNSQASAENFPFCTIDPNESR	0.93	-0.11

93	Q9Y696	CLIC4 Chloride intracellular channel protein 4	CLIC4	AGSDGESIGNCPFSQR	0.93	-0.11
94	P30281	CCND3 G1/S-specific cyclin-D3	CCND3	ASYFQCVQR	0.93	-0.11
95	Q7Z4W1	DCXR L-xylulose reductase	DCXR	AVTNHSVYCSTK	0.93	-0.11
96	O43865	AHCYL1 S-adenosylhomocysteine hydrolase-like protein 1	AHCYL1	LCVPAMNVNDSVTK	0.93	-0.11
97	Q15019	SEPT2 Septin-2	43345	LTVVDTPGYGDAINCR	0.93	-0.11
98	P13804	ETFA Electron transfer flavoprotein subunit alpha, mito	ETFA	TIYAGNALCTVK	0.93	-0.11
99	P68363	TUBA1B Tubulin alpha-1B chain	TUBA1B	SIQFVDWCPTGFK	0.93	-0.10
100	Q01082	SPTBN1 Spectrin beta chain, non-erythrocytic 1	SPTBN1	PCDPQVIR	0.93	-0.10
101	Q09666	AHNAK Neuroblast differentiation-associated protein AHNA	AHNAK	LEGDLTGPSVDVEVPDVELECPDAK	0.93	-0.10
102	Q9NR33	POLE4 DNA polymerase epsilon subunit 4	POLE4	DAYCCAQQGK	0.93	-0.10
103	Q9NYL2	MAP3K20 Mitogen-activated protein kinase kinase 20	MAP3K20	FDDLQFFENCGGGSFGSVYR	0.93	-0.10
104	Q9BTE3	MCMBP Mini-chromosome maintenance complex-binding protei	MCMBP	DASALLDPMECTDTAEEQR	0.93	-0.10
105	Q99996	AKAP9 A-kinase anchor protein 9	AKAP9	LTGQQGEEPSLVSPSTSCGSLTER	0.93	-0.10
106	Q7Z2W4	ZC3HAV1 Zinc finger CCCH-type antiviral protein 1	ZC3HAV1	NSNVDSSYLESLYQSCPR	0.93	-0.10
107	Q71U36	TUBA1A Tubulin alpha-1A chain	TUBA1A	TIQFVDWCPTGFK	0.93	-0.10
108	P11586	MTHFD1 C-1-tetrahydrofolate synthase, cytoplasmic	MTHFD1	GDLNDCFIPCTPK	0.94	-0.10
109	Q9C0C9	UBE2O (E3-independent) E2 ubiquitin-conjugating enzyme	UBE2O	CYNEMALIR	0.94	-0.09
110	P67936	TPM4 Tropomyosin alpha-4 chain	TPM4	EENVGLHQTLDQTLNELNCI	0.94	-0.09
111	P02765	AHSG Alpha-2-HS-glycoprotein	AHSG	CDSSPDSAEDVR	0.94	-0.09
112	Q9BT09	CNPY3 Protein canopy homolog 3	CNPY3	DTSCLAEQWSGK	0.94	-0.09
113	Q9H3P7	ACBD3 Golgi resident protein GCP60	ACBD3	QVLMGPYNPDTCPEVGFFDVLGNDR	0.94	-0.09
114	P10809	HSPD1 60 kDa heat shock protein, mitochondrial	HSPD1	AAVEEGIVLGGGCALLR	0.94	-0.09
115	Q8WW01	TSEN15 tRNA-splicing endonuclease subunit Sen15	TSEN15	GDSEPTPGCSGLGPGGVR	0.94	-0.09

116	Q9H1K1	ISCU Iron-sulfur cluster assembly enzyme ISCU, mitochondrial	ISCU	NVGTGLVGAPACGDVMK	0.94	-0.09
117	O75369	FLNB Filamin-B	FLNB	MDGTYACSYTPVK	0.94	-0.09
118	P48735	IDH2 Isocitrate dehydrogenase [NADP], mitochondrial	IDH2	SSGGFVWACK	0.94	-0.08
119	Q9Y3F4	STRAP Serine-threonine kinase receptor-associated protei	STRAP	IGFPETTEEELEEIASENSDCIFPSAPDVK	0.94	-0.08
120	P55769	SNU13 NHP2-like protein 1	SNU13	LLDLVQQSCNYK	0.94	-0.08
121	O95671	ASMTL N-acetylserotonin O-methyltransferase-like protein	ASMTL	FSSACDVGGCTGALAR	0.94	-0.08
122	P15924	DSP Desmoplakin	DSP	NQCTQVVQER	0.94	-0.08
123	P05388	RPLP0 60S acidic ribosomal protein P0	RPLP0	CFIVGADNVGSK	0.94	-0.08
124	P23528	CFL1 Cofilin-1	CFL1	HELQANCYEEVK	0.94	-0.08
125	A6NNZ2	cimageipi-sp|A6NNZ2|TBB8L_HUMAN Tubulin beta-8 chain-like protein LOC260334	cimageipi-sp|A6NNZ2|TBB8L_HUMAN	NMMAACDPR	0.94	-0.08
126	P45973	CBX5 Chromobox protein homolog 5	CBX5	IIGATDSCGDLMFLMK	0.95	-0.08
127	P38117	ETFB Electron transfer flavoprotein subunit beta	ETFB	EVIAVSCGPAQCQETIR	0.95	-0.08
128	P62333	PSMC6 26S proteasome regulatory subunit 10B	PSMC6	AVASQLDCNFLK	0.95	-0.08
129	Q00765	REEP5 Receptor expression-enhancing protein 5	REEP5	NCMTDLLAK	0.95	-0.08
130	P07814	EPRS Bifunctional glutamate/proline--tRNA ligase	EPRS	LGVENCYFPMFVSQSALEK	0.95	-0.08
131	P09110	ACAA1 3-ketoacyl-CoA thiolase, peroxisomal	ACAA1	DCLIPMGITSENVAER	0.95	-0.08
132	O14733	MAP2K7 Dual specificity mitogen-activated protein kinase	MAP2K7	LCDFGISGR	0.95	-0.08
133	Q13526	PIN1 Peptidyl-prolyl cis-trans isomerase NIMA-interacting	PIN1	SGEEDFESLASQFSDCSSAK	0.95	-0.08
134	P14868	DARS Aspartate--tRNA ligase, cytoplasmic	DARS	LEYCEALAMLR	0.95	-0.07
135	P30084	ECHS1 Enoyl-CoA hydratase, mitochondrial	ECHS1	EMQNLSFQDCYSSK	0.95	-0.07
136	Q8TC07	TBC1D15 TBC1 domain family member 15	TBC1D15	TLLVNCQNK	0.95	-0.07
137	P24941	CDK2 Cyclin-dependent kinase 2	CDK2	APEILLGCK	0.95	-0.07

138	O75874	IDH1 Isocitrate dehydrogenase [NADP] cytoplasmic	IDH1	SEGGFIWACK	0.95	-0.07
139	Q12765	SCRN1 Secernin-1	SCRN1	TQSPCFGDDDPAK	0.95	-0.07
140	Q9H9E3	COG4 Conserved oligomeric Golgi complex subunit 4	COG4	CSEISAELIR	0.95	-0.07
141	P23396	RPS3 40S ribosomal protein S3	RPS3	GLCAIAQAESLR	0.95	-0.07
142	Q52LJ0	FAM98B Protein FAM98B	FAM98B	INDALSCEYECR	0.95	-0.07
143	Q9BRA2	TXNDC17 Thioredoxin domain-containing protein 17	TXNDC17	SWCPDCVQAEPVVR	0.95	-0.07
144	P50990	CCT8 T-complex protein 1 subunit theta	CCT8	IAVYSCPFDGMITETK	0.95	-0.07
145	P42166	TMPO Lamina-associated polypeptide 2, isoform alpha	TMPO	SGIQPLCPER	0.95	-0.07
146	Q68CP9	ARID2 AT-rich interactive domain-containing protein 2	ARID2	SCSNAAFALK	0.95	-0.07
147	P30041	PRDX6 Peroxiredoxin-6	PRDX6	DFTPVCTTELGR	0.95	-0.07
148	Q92575	UBXN4 UBX domain-containing protein 4	UBXN4	SETSVANGSQSESSVSTPSASFEPNNTCENSQSR	0.95	-0.07
149	P49327	FASN Fatty acid synthase	FASN	ADEASELACPTPK	0.95	-0.07
150	Q9P2R3	ANKFY1 Rabankyrin-5	ANKFY1	GSHTDAPDTATGNCLLQR	0.95	-0.07
151	Q9NS86	LANCL2 LanC-like protein 2	LANCL2	SVVCQESDLPDELLYGR	0.96	-0.07
152	Q15149	PLEC Plectin	PLEC	AFCGFEDPR	0.96	-0.07
153	O95336	PGLS 6-phosphogluconolactonase	PGLS	AACCLAGAR	0.96	-0.07
154	P14854	COX6B1 Cytochrome c oxidase subunit 6B1	COX6B1	GGDISVCEWYQR	0.96	-0.06
155	O14972	DSCR3 Down syndrome critical region protein 3	DSCR3	VETCGCAEGYAR	0.96	-0.06
156	Q8WU76	SCFD2 Sec1 family domain-containing protein 2	SCFD2	ALAQVFCEESGLSPLLQK	0.96	-0.06
157	P42765	ACAA2 3-ketoacyl-CoA thiolase, mitochondrial	ACAA2	EAEVVLCGGTESMSQAPYCVR	0.96	-0.06
158	P37802	TAGLN2 Transgelin-2	TAGLN2	NMACVQR	0.96	-0.06
159	P04183	TK1 Thymidine kinase, cytosolic	TK1	YSSSFCTHDR	0.96	-0.06
160	Q10567	AP1B1 AP-1 complex subunit beta-1	AP1B1	DCPLNAEAASSK	0.96	-0.06
161	P50991	CCT4 T-complex protein 1 subunit delta	CCT4	LGGTIDDCELVEGLVLTQK	0.96	-0.06
162	P46776	RPL27A 60S ribosomal protein L27a	RPL27A	NQSFCPTVNLDK	0.96	-0.06
163	Q06587	RING1 E3 ubiquitin-protein ligase RING1	RING1	FCSDCIVTALR	0.96	-0.06
164	P35998	PSMC2 26S proteasome regulatory subunit 7	PSMC2	SVCTEAGMFAIR	0.96	-0.06

165	Q9Y2S2	CRYL1 Lambda-crystallin homolog	CRYL1	VILSSSTSCLMPSK	0.96	-0.06
166	P28838	LAP3 Cytosol aminopeptidase	LAP3	QVVDCQLADVNNIGK	0.96	-0.06
167	P54886	ALDH18A1 Delta-1-pyrroline-5-carboxylate synthase	ALDH18A1	GDECGLALGR	0.96	-0.06
168	O15355	PPM1G Protein phosphatase 1G	PPM1G	CSGDGVGAPR	0.96	-0.05
169	O75348	ATP6V1G1 V-type proton ATPase subunit G 1	ATP6V1G1	GSCSTEVEK	0.96	-0.05
170	P33240	CSTF2 Cleavage stimulation factor subunit 2	CSTF2	LCVQNSPQEAR	0.96	-0.05
171	O14745	SLC9A3R1 Na(+)/H(+) exchange regulatory cofactor NHE-RF1	SLC9A3R1	IVEVNGVCMEGK	0.96	-0.05
172	P13639	EEF2 Elongation factor 2	EEF2	STLTDSLVCK	0.96	-0.05
173	Q7Z6M1	RABEPK Rab9 effector protein with kelch motifs	RABEPK	NCLQVLNPETR	0.96	-0.05
174	P62857	RPS28 40S ribosomal protein S28	RPS28	TGSQGQCTQVR	0.96	-0.05
175	P41250	GARS Glycine--tRNA ligase	GARS	SCYDLSCHAR	0.96	-0.05
176	Q16555	DPYSL2 Dihydropyrimidinase-related protein 2	DPYSL2	GLYDGPVCEVSVTPK	0.97	-0.05
177	Q15149	PLEC Plectin	PLEC	LCFEGLR	0.97	-0.05
178	P24752	ACAT1 Acetyl-CoA acetyltransferase, mitochondrial	ACAT1	QGEYGLASICNGGGGASAMLIQK	0.97	-0.05
179	P21333	FLNA Filamin-A	FLNA	VGTECGNQK	0.97	-0.05
180	P08134	RHOC Rho-related GTP-binding protein RhoC	RHOC	LVIVGDGACGK	0.97	-0.04
181	P62280	RPS11 40S ribosomal protein S11	RPS11	DVQIGDIVTVGECR	0.97	-0.04
182	A6NNZ2	cimageipi-sp|A6NNZ2|TBB8L_HUMAN Tubulin beta-8 chain-like protein LOC260334	cimageipi-sp|A6NNZ2|TBB8L_HUMAN	TAVCDIPPR	0.97	-0.04
183	Q52LJ0	FAM98B Protein FAM98B	FAM98B	SLCNLEESITSAGR	0.97	-0.04
184	P37235	HPCAL1 Hippocalcin-like protein 1	HPCAL1	LLQCDPSSASQF	0.97	-0.04
185	P51610	HCFC1 Host cell factor 1	HCFC1	VAGINACGR	0.97	-0.04
186	P07858	CTSB Cathepsin B	CTSB	ICEPGYSPTYK	0.97	-0.04
187	Q92616	GCN1 eIF-2-alpha kinase activator GCN1	GCN1	CLQTLLDTK	0.97	-0.04
188	P00519	ABL1 Tyrosine-protein kinase ABL1	ABL1	ELQICPATAGSGPAATQDFSK	0.97	-0.04
189	Q9ULA0	DNPEP Aspartyl aminopeptidase	DNPEP	NDTPCGTTIGPILASR	0.97	-0.04

190	P10809	HSPD1 60 kDa heat shock protein, mitochondrial	HSPD1	CEFQDAYVLLSEK	0.97	-0.04
191	Q96CD2	PPCDC Phosphopantothenoylcysteine decarboxylase	PPCDC	ASCPAAAPLMER	0.97	-0.04
192	A6NDU8	C5orf51 UPF0600 protein C5orf51	C5orf51	CPIQLNEGVSFQDLDTAK	0.97	-0.04
193	Q09666	AHNAK Neuroblast differentiation-associated protein AHNA	AHNAK	GPFVEAEVPDVDLECPDAK	0.97	-0.04
194	Q9BQ24	ZFYVE21 Zinc finger FYVE domain-containing protein 21	ZFYVE21	MCFVDPVR	0.97	-0.04
195	P30044	PRDX5 Peroxiredoxin-5, mitochondrial	PRDX5	ALNVEPDGTGLTCSLAPNIISQL	0.97	-0.04
196	Q9NVG8	TBC1D13 TBC1 domain family member 13	TBC1D13	LLQDYPITDVCQILQK	0.97	-0.04
197	Q9UPN9	TRIM33 E3 ubiquitin-protein ligase TRIM33	TRIM33	QEPGTEDEICSFSGGVK	0.97	-0.04
198	Q96JB5	CDK5RAP3 CDK5 regulatory subunit-associated protein 3	CDK5RAP3	CQQLQQEYSR	0.97	-0.04
199	Q7Z6Z7	HUWE1 E3 ubiquitin-protein ligase HUWE1	HUWE1	AQCETLSPDGLPEEQPQTTK	0.97	-0.04
200	P83731	RPL24 60S ribosomal protein L24	RPL24	VELCSFSGYK	0.98	-0.04
201	O95817	BAG3 BAG family molecular chaperone regulator 3	BAG3	SQSPAASDCSSSSSSASLPSSGR	0.98	-0.04
202	P13639	EEF2 Elongation factor 2	EEF2	DLEEDHACIPIK	0.98	-0.03
203	P31947	SFN 14-3-3 protein sigma	SFN	GEELSCEER	0.98	-0.03
204	Q9HCC0	MCCC2 Methylcrotonoyl-CoA carboxylase beta chain, mitoch	MCCC2	AATGEEVSAEDLGGADLHCR	0.98	-0.03
205	Q96I24	FUBP3 Far upstream element-binding protein 3	FUBP3	SSGCFPNMAAK	0.98	-0.03
206	P26641	EEF1G Elongation factor 1-gamma	EEF1G	AAAPAPEEEMDECEQALAAEPK	0.98	-0.03
207	Q09666	AHNAK Neuroblast differentiation-associated protein AHNA	AHNAK	LEGDLTGPSVGVEVPDVELECPDAK	0.98	-0.03
208	Q9UI10	EIF2B4 Translation initiation factor eIF-2B subunit delta	EIF2B4	VQTDAFVSNELDDPDDLQCK	0.98	-0.03
209	P68363	TUBA1B Tubulin alpha-1B chain	TUBA1B	AVCMLSNTTAIAEAWAR	0.98	-0.03
210	P48047	ATP5O ATP synthase subunit O, mitochondrial	ATP5O	GEVPCTVTSASPLEEATLSELK	0.98	-0.03
211	Q99590	SCAF11 Protein SCAF11	SCAF11	VYQPVSCPLSDLSENVESVVNEEK	0.98	-0.03
212	O15067	PFAS Phosphoribosylformylglycinamidine synthase	PFAS	FCDNSSAIQGK	0.98	-0.03
213	P55060	CSE1L Exportin-2	CSE1L	LLTECPPMMDTE	0.98	-0.03

				YTK		
214	P27348	YWHAQ 14-3-3 protein theta	YWHAQ	YLAEVACGDDR	0.98	-0.03
215	Q7RTV0	PHF5A PHD finger-like domain-containing protein 5A	PHF5A	ICDECNYGSYQGR	0.98	-0.03
216	Q9HBM1	SPC25 Kinetochore protein Spc25	SPC25	STDTSCQMAGLR	0.98	-0.03
217	Q9NP73	ALG13 Putative bifunctional UDP-N-acetylglucosamine tran	ALG13	ADLVISHAGAGSCLETLEK	0.98	-0.03
218	Q99614	TTC1 Tetratricopeptide repeat protein 1	TTC1	VTDTQEAECAGPPVPDPK	0.98	-0.03
219	P49411	TUFM Elongation factor Tu, mitochondrial	TUFM	GDECELLGHSK	0.98	-0.03
220	Q99798	ACO2 Aconitate hydratase, mitochondrial	ACO2	VGLIGSCTNSSYEDMGR	0.98	-0.03
221	Q96P16	RPRD1A Regulation of nuclear pre-mRNA domain-containing p	RPRD1A	HVSSETDESCK	0.98	-0.03
222	P60866	RPS20 40S ribosomal protein S20	RPS20	TPCGEGSK	0.98	-0.03
223	Q96F86	EDC3 Enhancer of mRNA-decapping protein 3	EDC3	SQDVAVSPQQQQCSK	0.98	-0.03
224	O14950	MYL12B Myosin regulatory light chain 12B	MYL12B	NAFACFDEEATGTIQEDYLR	0.98	-0.03
225	P24385	CCND1 G1/S-specific cyclin-D1	CCND1	AAEEEEEEEEEVDLACTPTDVR	0.98	-0.03
226	Q9Y5M8	SRPRB Signal recognition particle receptor subunit beta	SRPRB	AVLLVGLCDSGK	0.98	-0.03
227	P53384	NUBP1 Cytosolic Fe-S cluster assembly factor NUBP1	NUBP1	LCASGAGATPDTAIEEIK	0.98	-0.02
228	Q00839	HNRNPU Heterogeneous nuclear ribonucleoprotein U	HNRNPU	AVVVCPK	0.98	-0.02
229	O14545	TRAFD1 TRAF-type zinc finger domain-containing protein 1	TRAFD1	AVCEADQSHGGPR	0.98	-0.02
230	P15924	DSP Desmoplakin	DSP	YQAECSQFK	0.98	-0.02
231	Q14247	CTTN Src substrate cortactin	CTTN	CALGWDHQEK	0.98	-0.02
232	Q06323	PSME1 Proteasome activator complex subunit 1	PSME1	GPPCGPVNCNEK	0.99	-0.02
233	P28838	LAP3 Cytosol aminopeptidase	LAP3	SAGACTAAAFLK	0.99	-0.02
234	O15075	DCLK1 Serine/threonine-protein kinase DCLK1	DCLK1	VCSSMDENDGPGEEVSEEGFQIPATITER	0.99	-0.02
235	O60216	RAD21 Double-strand-break repair protein rad21 homolog	RAD21	TGAESISLLELCR	0.99	-0.02
236	Q01813	PFKP ATP-dependent 6-phosphofructokinase, platelet type	PFKP	LPLMECVQMTQDVQK	0.99	-0.02
237	P62993	GRB2 Growth factor receptor-bound protein 2	GRB2	VLNEECDQNWYK	0.99	-0.02

238	Q9P0W2	HMG20B SWI/SNF-related matrix-associated actin-dependent	HMG20B	GGDCDGFSTFDVPIFTEEFLDQNK	0.99	-0.02
239	Q96BF6	NACC2 Nucleus accumbens-associated protein 2	NACC2	NTLANSCGTGIR	0.99	-0.01
240	P24385	CCND1 G1/S-specific cyclin-D1	CCND1	AEETCAPSVSYFK	0.99	-0.01
241	P05388	RPLP0 60S acidic ribosomal protein P0	RPLP0	AGAIAPCEVTVPAQNTGLGPEK	0.99	-0.01
242	Q9UNE7	STUB1 E3 ubiquitin-protein ligase CHIP	STUB1	AQQACIEAK	0.99	-0.01
243	Q9BSD7	NTPCR Cancer-related nucleoside-triphosphatase	NTPCR	VCVIDEIGK	0.99	-0.01
244	P49458	SRP9 Signal recognition particle 9 kDa protein	SRP9	VTDDLVCLVYK	0.99	-0.01
245	Q49AR2	C5orf22 UPF0489 protein C5orf22	C5orf22	LCNNQEENDAVSSAK	0.99	-0.01
246	Q96EY8	MMAB Cob(I)yrinic acid a,c-diamide adenosyltransferase,	MMAB	IQCTLQDVGSALATPCSSAR	0.99	-0.01
247	Q9Y2X3	NOP58 Nucleolar protein 58	NOP58	TYDPSGDSTLPTCSK	0.99	-0.01
248	P00492	HPRT1 Hypoxanthine-guanine phosphoribosyltransferase	HPRT1	SYCNDQSTGDIK	0.99	-0.01
249	P09497	CLTB Clathrin light chain B	CLTB	VAQLCDFNPK	0.99	-0.01
250	P15924	DSP Desmoplakin	DSP	ETQTECEWTVDTSK	0.99	-0.01
251	Q6QNY0	BLOC1S3 Biogenesis of lysosome-related organelles complex	BLOC1S3	GDLCALAER	0.99	-0.01
252	P46734	MAP2K3 Dual specificity mitogen-activated protein kinase	MAP2K3	TMDAGCK	0.99	-0.01
253	O43837	IDH3B Isocitrate dehydrogenase [NAD] subunit beta, mitochondrial	IDH3B	LGDGLFLQCCEEVAELYPK	0.99	-0.01
254	Q9NUU7	DDX19A ATP-dependent RNA helicase DDX19A	DDX19A	VLVTTNVCAR	0.99	-0.01
255	P46782	RPS5 40S ribosomal protein S5	RPS5	AQCPIVER	1.00	-0.01
256	Q9BV36	MLPH Melanophilin	MLPH	DSPQSLTDESCSEK	1.00	-0.01
257	Q9UGI8	TES Testin	TES	LPCEMDAQGPK	1.00	-0.01
258	P57721	PCBP3 Poly(rC)-binding protein 3	PCBP3	INISEGNCPER	1.00	-0.01
259	Q9NVC6	MED17 Mediator of RNA polymerase II transcription subunit	MED17	MELLMSALSPCLL	1.00	0.00
260	P36873	PPP1CC Serine/threonine-protein phosphatase PP1-gamma cat	PPP1CC	GNHECASINR	1.00	0.00
261	Q13185	CBX3 Chromobox protein homolog 3	CBX3	LTWHSCPEDEAQ	1.00	0.00

262	Q86SX6	GLRX5 Glutaredoxin-related protein 5, mitochondrial	GLRX5	GTPEQPQCGFSNAVVQILR	1.00	0.00
263	Q8TAQ2	SMARCC2 SWI/SNF complex subunit SMARCC2	SMARCC2	NLAGDVCAIMR	1.00	0.00
264	Q99836	MYD88 Myeloid differentiation primary response protein M	MYD88	FITVCDYTNPCTK	1.00	0.00
265	Q68CP9	ARID2 AT-rich interactive domain-containing protein 2	ARID2	IVTISDPNNAGCSATMVAVPAGADPSTVAK	1.00	0.00
266	P49915	GMPS GMP synthase [glutamine-hydrolyzing]	GMPS	VICAEEPYICK	1.00	0.00
267	P50914	RPL14 60S ribosomal protein L14	RPL14	ALVDGPCTQVR	1.00	0.00
268	Q9NY27	PPP4R2 Serine/threonine-protein phosphatase 4 regulatory	PPP4R2	NVMVVSCVYPSSEK	1.00	0.00
269	P54646	PRKAA2 5-AMP-activated protein kinase catalytic subunit	PRKAA2	TSCGSPNYAAPEVISGR	1.00	0.00
270	Q9BQ69	MACROD1 O-acetyl-ADP-ribose deacetylase MACROD1	MACROD1	AAGPLLTDECR	1.00	0.00
271	P27348	YWHAQ 14-3-3 protein theta	YWHAQ	DNLTLWTSDSAGEECDAAEGAEN	1.00	0.00
272	P27707	DCK Deoxycytidine kinase	DCK	SCPSFSASSEGTR	1.00	0.01
273	Q9Y570	PPME1 Protein phosphatase methylesterase 1	PPME1	QCEGITSPEGSK	1.00	0.01
274	Q8N163	CCAR2 Cell cycle and apoptosis regulator protein 2	CCAR2	VVTQNICQYR	1.00	0.01
275	P48735	IDH2 Isocitrate dehydrogenase [NADP], mitochondrial	IDH2	CATITPDEAR	1.01	0.01
276	P09622	DLD Dihydrolipoyl dehydrogenase, mitochondrial	DLD	NETLGGTCLNVGCIPSK	1.01	0.01
277	P10809	HSPD1 60 kDa heat shock protein, mitochondrial	HSPD1	CIPALDSLTPANEDQK	1.01	0.01
278	P49588	AARS Alanine--tRNA ligase, cytoplasmic	AARS	CLSVMEAK	1.01	0.01
279	Q1KMD3	HNRNPUL2 Heterogeneous nuclear ribonucleoprotein U-like pro	HNRNPUL2	DLLVQQASQCLSK	1.01	0.01
280	P27635	RPL10 60S ribosomal protein L10	RPL10	MLSCAGADR	1.01	0.01
281	P21333	FLNA Filamin-A	FLNA	THEAEIVEGENHTYCIR	1.01	0.01
282	Q99933	BAG1 BAG family molecular chaperone regulator 1	BAG1	DLQAEALCK	1.01	0.01
283	Q99714	HSD17B10 3-hydroxyacyl-CoA dehydrogenase type-2	HSD17B10	LGNNCVFAPADVTSEK	1.01	0.01
284	Q9BV79	MECR Enoyl-[acyl-carrier-protein] reductase, mitochondrial	MECR	LALNCVGGK	1.01	0.01

285	P40227	CCT6A T-complex protein 1 subunit zeta	CCT6A	NAIDDGCVVPGAGAVEVAMAEALIK	1.01	0.01
286	Q08379	GOLGA2 Golgin subfamily A member 2	GOLGA2	CEAPDANQQLQQAMEER	1.01	0.01
287	O95671	ASMTL N-acetylserotonin O-methyltransferase-like protein	ASMTL	AEAGEAGQATAEAECHR	1.01	0.02
288	Q9NZZ3	CHMP5 Charged multivesicular body protein 5	CHMP5	APPPSLTDCIGTVDSR	1.01	0.02
289	P37198	NUP62 Nuclear pore glycoprotein p62	NUP62	DIIEHLNTSGAPADTSDPLQQICK	1.01	0.02
290	O95685	PPP1R3D Protein phosphatase 1 regulatory subunit 3D	PPP1R3D	SLSCLSDLDGGVALEPR	1.01	0.02
291	P63010	AP2B1 AP-2 complex subunit beta	AP2B1	DCEDPNPLIR	1.01	0.02
292	Q9ULX6	AKAP8L A-kinase anchor protein 8-like	AKAP8L	GQCMSGASR	1.01	0.02
293	Q16822	PCK2 Phosphoenolpyruvate carboxykinase [GTP], mitochond	PCK2	YVAAAFPSACGK	1.01	0.02
294	P51610	HCFC1 Host cell factor 1	HCFC1	ACAAGTPAVIR	1.01	0.02
295	P35658	NUP214 Nuclear pore complex protein Nup214	NUP214	ACFQVGTSEEMK	1.01	0.02
296	P42765	ACAA2 3-ketoacyl-CoA thiolase, mitochondrial	ACAA2	EECDK	1.02	0.02
297	Q969H6	POP5 Ribonuclease P/MRP protein subunit POP5	POP5	SCLLEEEEESGEEAAEAME	1.02	0.02
298	P28331	NDUFS1 NADH-ubiquinone oxidoreductase 75 kDa subunit, mitochondrial	NDUFS1	VVAACAMPVMK	1.02	0.02
299	Q9UMS0	NFU1 met iron-sulfur cluster scaffold homolog, mitochondrial	NFU1	LQGSCTSCPSSIITLK	1.02	0.02
300	P46527	CDKN1B Cyclin-dependent kinase inhibitor 1B	CDKN1B	TDPSDSQTGLAEQCAGIR	1.02	0.02
301	Q96FW1	OTUB1 Ubiquitin thioesterase OTUB1	OTUB1	QEPLGSDSEGVNCLAYDEAIMAQQDR	1.02	0.03
302	P50151	GNG10 Guanine nucleotide-binding protein G(I)/G(S)/G(O)	GNG10	VSQAAAELQQYCMQNACK	1.02	0.03
303	P26196	DDX6 Probable ATP-dependent RNA helicase DDX6	DDX6	GNEFEDYCLK	1.02	0.03
304	P07858	CTSB Cathepsin B	CTSB	GQDHCGIESEVVAGIPR	1.02	0.03
305	P15924	DSP Desmoplakin	DSP	DANSENCNK	1.02	0.03
306	Q9NQR4	NIT2 Omega-amidase NIT2	NIT2	VGLGICYDMR	1.02	0.03
307	Q06210	GFPT1 Glutamine--fructose-6-phosphate aminotransferase [	GFPT1	VDSTTCLFPVEEK	1.02	0.03

308	Q9UHD8	SEPT9 Septin-9	43352	SQEATEAAPSCVGDMADTPR	1.02	0.04
309	O43765	SGTA Small glutamine-rich tetratricopeptide repeat-cont	SGTA	AIELNPANAVYFCNR	1.02	0.04
310	Q16643	DBN1 Drebrin	DBN1	EGTQASEGYFSQSQEEEFAQSEELCAK	1.03	0.04
311	Q14694	USP10 Ubiquitin carboxyl-terminal hydrolase 10	USP10	SSVELPPYSGTVLCGTQAVDK	1.03	0.04
312	Q16822	PCK2 Phosphoenolpyruvate carboxykinase [GTP], mitochond	PCK2	YNNCWLAR	1.03	0.04
313	Q9BRQ0	PYGO2 Pygopus homolog 2	PYGO2	SEVNDDQDAILCEASCQK	1.03	0.04
314	P27797	CALR Calreticulin	CALR	HEQNIDCGGGYVK	1.03	0.04
315	Q16822	PCK2 Phosphoenolpyruvate carboxykinase [GTP], mitochond	PCK2	VECVGDDIAWMR	1.03	0.04
316	P31943	HNRNPH1 Heterogeneous nuclear ribonucleoprotein H	HNRNPH1	DLNYCFSGMSDHR	1.03	0.04
317	Q14657	LAGE3 EKC/KEOPS complex subunit LAGE3	LAGE3	GGHSCR	1.03	0.04
318	P49841	GSK3B Glycogen synthase kinase-3 beta	GSK3B	LCDFGSAK	1.03	0.04
319	P14866	HNRNPL Heterogeneous nuclear ribonucleoprotein L	HNRNPL	QPAIMPGQSYGLEDGSCSYK	1.03	0.04
320	O43765	SGTA Small glutamine-rich tetratricopeptide repeat-cont	SGTA	AICIDPAYSK	1.03	0.04
321	Q6AI08	HEATR6 HEAT repeat-containing protein 6	HEATR6	EDSCSGSDAGSAAGSTYEPSPMR	1.03	0.05
322	P62879	GNB2 Guanine nucleotide-binding protein G(I)/G(S)/G(T)	GNB2	TFVSGACDASIK	1.03	0.05
323	Q04760	GLO1 Lactoylglutathione lyase	GLO1	CDFPIMK	1.03	0.05
324	Q06323	PSME1 Proteasome activator complex subunit 1	PSME1	EDLCTK	1.03	0.05
325	P61158	ACTR3 Actin-related protein 3	ACTR3	YSYVCPDLVK	1.03	0.05
326	P55735	SEC13 Protein SEC13 homolog	SEC13	FASGGCDNLIK	1.03	0.05
327	Q9BX63	BRIP1 Fanconi anemia group J protein	BRIP1	LANNSDCILAK	1.03	0.05
328	Q6UWE0	LRSAM1 E3 ubiquitin-protein ligase LRSAM1	LRSAM1	DVASAMQQMLTESCK	1.04	0.05
329	P63244	RACK1 Receptor of activated protein C kinase 1	RACK1	VWNLANCK	1.04	0.05
330	Q6PKG0	LARP1 La-related protein 1	LARP1	TASISSSPSEGTPTVGSYGCTPQSLPK	1.04	0.06
331	Q9HCY8	S100A14 Protein S100-A14	S100A14	IANLGSCNDSK	1.04	0.06
332	P51553	IDH3G Isocitrate dehydrogenase [NAD] subunit	IDH3G	LGDGLFLQCCR	1.04	0.06

		gamma, mito				
333	O00233	PSMD9 26S proteasome non-ATPase regulatory subunit 9	PSMD9	GIGMNEPLVDCEGYPR	1.04	0.06
334	Q9BR61	ACBD6 Acyl-CoA-binding domain-containing protein 6	ACBD6	DQDGCLPEEVTGCK	1.04	0.06
335	Q16644	MAPKAPK3 MAP kinase-activated protein kinase 3	MAPKAPK3	QAGSSSASQGCNNQ	1.04	0.06
336	O60361	NME2P1 Putative nucleoside diphosphate kinase	NME2P1	GDFCIQVGR	1.04	0.06
337	P25205	MCM3 DNA replication licensing factor MCM3	MCM3	YVLCTAPR	1.04	0.06
338	P49368	CCT3 T-complex protein 1 subunit gamma	CCT3	TLIQNCGASTIR	1.05	0.06
339	P50416	CPT1A Carnitine O-palmitoyltransferase 1, liver isoform	CPT1A	TLETANCMSSQTK	1.05	0.07
340	Q5VZ89	DENND4C DENN domain-containing protein 4C	DENND4C	CANVNNSSTTSQR	1.05	0.07
341	Q9Y5Y2	NUBP2 Cytosolic Fe-S cluster assembly factor NUBP2	NUBP2	AVHQCDR	1.05	0.07
342	Q99714	HSD17B10 3-hydroxyacyl-CoA dehydrogenase type-2	HSD17B10	VDVAVNCAGIAVASK	1.05	0.07
343	P58107	EPPK1 Epiplakin	EPPK1	YLCGLGAVGGVR	1.05	0.07
344	O43390	HNRNPR Heterogeneous nuclear ribonucleoprotein R	HNRNPR	SAFLCGVMK	1.05	0.07
345	Q9H9P8	L2HGDH L-2-hydroxyglutarate dehydrogenase, mitochondrial	L2HGDH	ACFLGATVK	1.05	0.07
346	P14854	COX6B1 Cytochrome c oxidase subunit 6B1	COX6B1	VYQSLCPTSWVTDWDEQR	1.05	0.07
347	O00148	DDX39A ATP-dependent RNA helicase DDX39A	DDX39A	HFVLDECDK	1.05	0.08
348	Q9Y508	RNF114 E3 ubiquitin-protein ligase RNF114	RNF114	DCGGAAQLAGPAAEADPLGR	1.05	0.08
349	Q9UL40	ZNF346 Zinc finger protein 346	ZNF346	NQCLFTNTQCK	1.06	0.08
350	Q15691	MAPRE1 Microtubule-associated protein RP/EB family member	MAPRE1	NIELICQENEGENDPVLQR	1.06	0.08
351	Q9P2T1	GMPR2 GMP reductase 2	GMPR2	VTQQVNPIFSEAC	1.06	0.08
352	Q9BQE3	TUBA1C Tubulin alpha-1C chain	TUBA1C	AVCMLSNTTAVAEAWAR	1.06	0.08
353	P07339	CTSD Cathepsin D	CTSD	AIGAVPLIQGEYMIPCEK	1.06	0.08
354	Q9UL25	RAB21 Ras-related protein Rab-21	RAB21	VVLLGEGCVGK	1.06	0.09
355	P14618	PKM Pyruvate kinase PKM	PKM	CCSGAIIVLTK	1.06	0.09
356	Q9P2E9	RRBP1 Ribosome-binding protein 1	RRBP1	AMEALATAEQACK	1.06	0.09

357	P62306	SNRPF Small nuclear ribonucleoprotein F	SNRPF	CNNVLYIR	1.07	0.09
358	Q14204	DYNC1H1 Cytoplasmic dynein 1 heavy chain 1	DYNC1H1	VQYPQSQACK	1.07	0.09
359	Q96CD2	PPCDC Phosphopantothenoylcysteine decarboxylase	PPCDC	LVCGDEGLGAMAEVGTIVDK	1.07	0.09
360	P52630	STAT2 Signal transducer and activator of transcription 2	STAT2	GLSCLVSYQDDPLTK	1.07	0.09
361	O15355	PPM1G Protein phosphatase 1G	PPM1G	GTEAGQVGEPGIPTGEAGPSCSSASDK	1.07	0.09
362	Q8NDH3	NPEPL1 Probable aminopeptidase NPEPL1	NPEPL1	IVDTPCNEMNTDTFLEEINK	1.07	0.09
363	Q96HE7	ERO1A ERO1-like protein alpha	ERO1A	CFCQVSGYLDDCTCDVETIDR	1.07	0.10
364	Q9Y315	DERA Deoxyribose-phosphate aldolase	DERA	GITTAAVCVYPAR	1.07	0.10
365	P52272	HNRNPM Heterogeneous nuclear ribonucleoprotein M	HNRNPM	ACQIFVR	1.07	0.10
366	P00966	ASS1 Argininosuccinate synthase	ASS1	FELSCYSLAPQIK	1.07	0.10
367	P13639	EEF2 Elongation factor 2	EEF2	CELLYEGPPDDEAAMGIK	1.07	0.10
368	P49915	GMPS GMP synthase [glutamine-hydrolyzing]	GMPS	ACTTEEDQEK	1.07	0.10
369	Q16822	PCK2 Phosphoenolpyruvate carboxykinase [GTP], mitochond	PCK2	VLDWICR	1.07	0.10
370	Q6KC79	NIPBL Nipped-B-like protein	NIPBL	SPQPVCSPAGSEGTPK	1.07	0.10
371	P78417	GSTO1 Glutathione S-transferase omega-1	GSTO1	LNECVDHTPK	1.08	0.10
372	P15880	RPS2 40S ribosomal protein S2	RPS2	GCTATLGNFAK	1.08	0.11
373	Q7L1Q6	BZW1 Basic leucine zipper and W2 domain-containing protein	BZW1	FDPTQFQDCIIQGLTETGTDLEAVAK	1.08	0.11
374	P63244	RACK1 Receptor of activated protein C kinase 1	RACK1	FSPNSSNPIIVSCGWDK	1.08	0.11
375	Q13596	SNX1 Sorting nexin-1	SNX1	LQEVECEEQR	1.08	0.11
376	Q14694	USP10 Ubiquitin carboxyl-terminal hydrolase 10	USP10	TAGQPEGGPGADFGQSCFPAEAGR	1.08	0.11
377	Q96HE7	ERO1A ERO1-like protein alpha	ERO1A	HDDSSDNFCEADDIQSPEAEYVDLLLNPER	1.08	0.11
378	O75362	ZNF217 Zinc finger protein 217	ZNF217	QTETAADCR	1.08	0.11
379	P02795	MT2A Metallothionein-2	MT2A	CAQGCICK	1.08	0.11
380	Q14980	NUMA1 Nuclear mitotic apparatus protein 1	NUMA1	NSFYMGTCQDEPEQLDDWNR	1.08	0.11

381	P21266	GSTM3 Glutathione S-transferase Mu 3	GSTM3	YTCGEAPDYDR	1.08	0.11
382	P04155	TFF1 Trefoil factor 1	TFF1	GCCFDDTVR	1.08	0.11
383	P35568	IRS1 Insulin receptor substrate 1	IRS1	CTPGTGLGTSPALAGDEAASAADLDNR	1.08	0.11
384	P33316	DUT Deoxyuridine 5-triphosphate nucleotidohydrolase,	DUT	TDIQIALPSGCYGR	1.08	0.12
385	P02545	LMNA Prelamin-A/C	LMNA	AQNTWGCGNSLR	1.08	0.12
386	P54136	RARS Arginine--tRNA ligase, cytoplasmic	RARS	NCGCLGASPNLEQLQEENLK	1.09	0.12
387	O60701	UGDH UDP-glucose 6-dehydrogenase	UGDH	ASVGFGGSCFQK	1.09	0.12
388	P61163	ACTR1A Alpha-centractin	ACTR1A	ACYLSINPQK	1.09	0.13
389	P63220	RPS21 40S ribosomal protein S21	RPS21	TYAICGAIR	1.09	0.13
390	Q9H0C8	ILKAP Integrin-linked kinase-associated serine/threonine	ILKAP	CGVTSVPDIR	1.09	0.13
391	P49327	FASN Fatty acid synthase	FASN	DPETLVGYSMVGCQR	1.09	0.13
392	Q9NZL4	HSPBP1 Hsp70-binding protein 1	HSPBP1	DACDTVR	1.09	0.13
393	Q7Z406	MYH14 Myosin-14	MYH14	VGEEEECSR	1.09	0.13
394	P14923	JUP Junction plakoglobin	JUP	GIMEEDEACGR	1.10	0.13
395	P49591	SARS Serine--tRNA ligase, cytoplasmic	SARS	ELVSCSNCTDYQAR	1.10	0.14
396	P42166	TMPO Lamina-associated polypeptide 2, isoform alpha	TMPO	TYDAASYICEAAFDEVK	1.10	0.14
397	Q9Y2Q3	GSTK1 Glutathione S-transferase kappa 1	GSTK1	ETTEAACR	1.10	0.14
398	P62826	RAN GTP-binding nuclear protein Ran	RAN	VCENIPIVLCGNK	1.10	0.14
399	P20810	CAST Calpastatin	CAST	AAAPAPVSEAVCR	1.10	0.14
400	P15924	DSP Desmoplakin	DSP	ACGSEIMQK	1.11	0.14
401	P48556	PSMD8 26S proteasome non-ATPase regulatory subunit 8	PSMD8	CGEELGR	1.11	0.15
402	P52895	AKR1C2 Aldo-keto reductase family 1 member C2	AKR1C2	EEPWVDPNSPVLLEDPVLCALAK	1.11	0.15
403	P00367	GLUD1 Glutamate dehydrogenase 1, mitochondrial	GLUD1	CAVVDVPFGGAK	1.11	0.16
404	Q9UGI8	TES Testin	TES	TQYSCYCCK	1.11	0.16
405	Q92947	GCDH Glutaryl-CoA dehydrogenase, mitochondrial	GCDH	GELLGCFGLTEPNSGSDPSSMETR	1.11	0.16
406	Q01518	CAP1 Adenylyl cyclase-associated protein 1	CAP1	ALLVTASQCQQPAENK	1.12	0.16

407	P51858	HDGF Hepatoma-derived growth factor	HDGF	SCVEEPEPEPEAAEGDGDK	1.12	0.16
408	P21333	FLNA Filamin-A	FLNA	LQVEPAVDTSGVQCYGPGIEGQGVFR	1.12	0.17
409	Q9NRP2	CMC2 COX assembly mitochondrial protein 2 homolog	CMC2	FFGYCNDVDR	1.12	0.17
410	P49753	ACOT2 Acyl-coenzyme A thioesterase 2, mitochondrial	ACOT2	SEFYANEACK	1.12	0.17
411	Q9H773	DCTPP1 dCTP pyrophosphatase 1	DCTPP1	YTELPHGAISEDQAVGPADIPCDSTGQTST	1.13	0.17
412	Q96SW2	CRBN Protein cereblon	CRBN	VAACLPIDDVLR	1.13	0.18
413	P18031	PTPN1 Tyrosine-protein phosphatase non-receptor type 1	PTPN1	DCPIK	1.13	0.18
414	P46459	NSF Vesicle-fusing ATPase	NSF	SQLSCVVVDDIER	1.13	0.18
415	Q14160	SCRIB Protein scribble homolog	SCRIB	SEACPCQPDSGSPLPAEEEK	1.13	0.18
416	Q9BXV9	GON7 EKC/KEOPS complex subunit GON7	GON7	VSCEAPGDGDPFQGLLSGVAQMK	1.13	0.18
417	Q9P2R7	SUCLA2 Succinate--CoA ligase [ADP-forming] subunit beta,	SUCLA2	ICNQVLVCER	1.14	0.19
418	Q9HCC0	MCCC2 Methylcrotonoyl-CoA carboxylase beta chain, mitoch	MCCC2	MVAAVACAQVPK	1.14	0.19
419	P17858	PFKL ATP-dependent 6-phosphofructokinase, liver type	PFKL	VFANAPDSACVIGLK	1.15	0.20
420	Q13371	PDCL Phosducin-like protein	PDCL	CAPASSSVPAEAELAGEGISVNTGPK	1.15	0.20
421	Q13045	FLII Protein flightless-1 homolog	FLII	TGLCYLPEELAALQK	1.15	0.20
422	P21266	GSTM3 Glutathione S-transferase Mu 3	GSTM3	PVC	1.15	0.20
423	Q96EI5	TCEAL4 Transcription elongation factor A protein-like 4	TCEAL4	PEVTCTLEDK	1.15	0.21
424	P27816	MAP4 Microtubule-associated protein 4	MAP4	CSLPAEEDSVLEK	1.16	0.21
425	Q9NVN8	GNL3L Guanine nucleotide-binding protein-like 3-like pro	GNL3L	ACSVGAVPGITK	1.16	0.21
426	P23381	WARS Tryptophan--tRNA ligase, cytoplasmic	WARS	ADCPPGNPAPTSNHGPDATEAEEDFVDPWTVQTSSAK	1.16	0.21
427	Q5T0W9	FAM83B Protein FAM83B	FAM83B	SCVPSSFAQEESAR	1.16	0.21

428	P11940	PABPC1 Polyadenylate-binding protein 1	PABPC1	GFGFVCFSSPEEATK	1.16	0.22
429	P04406	GAPDH Glyceraldehyde-3-phosphate dehydrogenase	GAPDH	VPTANVSVVDLTCR	1.16	0.22
430	P51858	HDGF Hepatoma-derived growth factor	HDGF	CGDLVFAK	1.17	0.22
431	Q96CM8	ACSF2 Acyl-CoA synthetase family member 2, mitochondrial	ACSF2	MVSTPIGGLSYVQGCTK	1.17	0.22
432	P14618	PKM Pyruvate kinase PKM	PKM	AEGSDVANAVLDGADCIMLSGETAK	1.17	0.23
433	P50213	IDH3A Isocitrate dehydrogenase [NAD] subunit alpha, mito	IDH3A	IEAACFATIK	1.17	0.23
434	P27708	CAD carillon protein	CAD	VHVDCMTSQK	1.17	0.23
435	P60981	DSTN Destrin	DSTN	LGGSLIVAFEGCPV	1.17	0.23
436	P15924	DSP Desmoplakin	DSP	GVITDQNSDGYCQTGTMSR	1.18	0.24
437	Q92917	GPKOW G patch domain and KOW motifs-containing protein	GPKOW	GCTPSGEGADSEPR	1.18	0.24
438	P40926	MDH2 Malate dehydrogenase, mitochondrial	MDH2	SQETECTYFSTPLLLGK	1.18	0.24
439	P63104	YWHAZ 14-3-3 protein zeta/delta	YWHAZ	DICNDVLSLLEK	1.19	0.25
440	Q9H8W4	PLEKHF2 Pleckstrin homology domain-containing family F mem	PLEKHF2	ICDFCYDLLSAGDMATCQPAR	1.19	0.25
441	P21281	ATP6V1B2 V-type proton ATPase subunit B, brain isoform	ATP6V1B2	TSCEFTGDILR	1.19	0.25
442	P60981	DSTN Destrin	DSTN	HECQANGPEDLNR	1.19	0.25
443	P47756	CAPZB F-actin-capping protein subunit beta	CAPZB	DETVSDCSPHIANIGR	1.19	0.25
444	P07237	P4HB Protein disulfide-isomerase	P4HB	EECPAVR	1.19	0.25
445	P00338	LDHA L-lactate dehydrogenase A chain	LDHA	VIGSGCNLDSAR	1.19	0.25
446	P50135	HNMT Histamine N-methyltransferase	HNMT	VQAQYPGVCINNEVVEPSAEQIAK	1.20	0.26
447	Q1KMD3	HNRNPUL2 Heterogeneous nuclear ribonucleoprotein U-like pro	HNRNPUL2	LQEALDAEMLEDEAGGGGAGPGGACK	1.20	0.26
448	Q27J81	INF2 Inverted formin-2	INF2	CPASEPGLDATTASESR	1.20	0.27
449	P62191	PSMC1 26S proteasome regulatory subunit 4	PSMC1	AICTEAGLMALR	1.21	0.27
450	O75663	TIPRL TIP41-like protein	TIPRL	CVNNYQGMLK	1.21	0.27

451	P30876	POLR2B DNA-directed RNA polymerase II subunit RPB2	POLR2B	THTYECR	1.21	0.28
452	Q96A49	SYAP1 Synapse-associated protein 1	SYAP1	TQEDEEEISTSPG VSEFVSDAFDAC NLNQEDLR	1.21	0.28
453	Q13569	TDG G/T mismatch-specific thymine DNA glycosylase	TDG	CIYEIFSK	1.21	0.28
454	Q27J81	INF2 Inverted formin-2	INF2	AVLLASDAQECTL EEVVER	1.21	0.28
455	P48735	IDH2 Isocitrate dehydrogenase [NADP], mitochondrial	IDH2	VCVETVESGAMT K	1.22	0.29
456	P35080	PFN2 Profilin-2	PFN2	DSLYVDGDCTMD IR	1.22	0.29
457	P49327	FASN Fatty acid synthase	FASN	AFDTAGNGYCR	1.22	0.29
458	P25789	PSMA4 Proteasome subunit alpha type-4	PSMA4	ATCIGNNSAAAVS MLK	1.22	0.29
459	Q14697	GANAB Neutral alpha-glucosidase AB	GANAB	DGSDYEGWCWP GSAGYPDFTNPT MR	1.22	0.29
460	P63167	DYNLL1 Dynein light chain 1, cytoplasmic	DYNLL1	NADMSEEMQQD SVECATQALEK	1.22	0.29
461	P61981	YWHAG 14-3-3 protein gamma	YWHAG	NCSETQYESK	1.22	0.29
462	Q9UHF7	TRPS1 Zinc finger transcription factor Trps1	TRPS1	ATEETGQAQSGQ ANCQGLSPVSVA SK	1.23	0.29
463	P29401	TKT Transketolase	TKT	QAFTDVATGSLG QGLGAACGMAY TGK	1.23	0.30
464	Q7L5N1	COPS6 COP9 signalosome complex subunit 6	COPS6	TCNTMNQFVNK	1.23	0.30
465	Q8N987	NECAB1 N-terminal EF-hand calcium-binding protein 1	NECAB1	ETLNQLQSLQNSL ECAMETTEEQTR	1.23	0.30
466	P21291	CSRP1 Cysteine and glycine-rich protein 1	CSRP1	DGEIYCK	1.23	0.30
467	Q7Z2Z2	EFL1 Elongation factor-like GTPase 1	EFL1	LAAAQGQAPLEP TQDGSAIETCPK	1.23	0.30
468	P02795	MT2A Metallothionein-2	MT2A	SCCSCCPVGCAK	1.24	0.30
469	P04155	TFF1 Trefoil factor 1	TFF1	GVPWCFYPNTID VPPEEECEF	1.24	0.31
470	Q6ISB3	GRHL2 Grainyhead-like protein 2 homolog	GRHL2	NCLGTSEAQSNLS GGENR	1.24	0.31
471	P25789	PSMA4 Proteasome subunit alpha type-4	PSMA4	LNEDMACSVAGI TSDANVLTNELR	1.24	0.31
472	P19367	HK1 Hexokinase-1	HK1	AAQLCGAGMAA VVDK	1.24	0.31
473	P62937	PPIA Peptidyl-prolyl cis-trans isomerase A	PPIA	ITIADCGQLE	1.24	0.31
474	Q15365	PCBP1 Poly(rC)-binding protein 1	PCBP1	AITIAGVPQSVTE CVK	1.25	0.32

475	O43823	AKAP8 A-kinase anchor protein 8	AKAP8	ANDGGLAAGAPAMHMASYGPEPCTDNSDSLIAK	1.25	0.32
476	Q9C0C2	TNKS1BP1 182 kDa tankyrase-1-binding protein	TNKS1BP1	NMAPGAVCSPGESK	1.25	0.32
477	P04632	CAPNS1 Calpain small subunit 1	CAPNS1	YSDESGNMDFDNFISCLVR	1.26	0.33
478	P14649	MYL6B Myosin light chain 6B	MYL6B	ILYSQCGDVMR	1.26	0.33
479	Q86U28	ISCA2 Iron-sulfur cluster assembly 2 homolog, mitochondrial	ISCA2	LQVEGGGCSGFQYK	1.26	0.34
480	Q01813	PFKP ATP-dependent 6-phosphofructokinase, platelet type	PFKP	FTTDDSICVLGISK	1.26	0.34
481	P12270	TPR Nucleoprotein TPR	TPR	DCQEQAK	1.28	0.35
482	P23396	RPS3 40S ribosomal protein S3	RPS3	GCEVVVSGK	1.28	0.36
483	P04075	ALDOA Fructose-bisphosphate aldolase A	ALDOA	ALANSLACQGK	1.28	0.36
484	P61758	VBP1 Prefoldin subunit 3	VBP1	DSCGK	1.29	0.37
485	Q96FJ2	DYNLL2 Dynein light chain 2, cytoplasmic	DYNLL2	NADMSEDMQQDAVDCATQAMEK	1.29	0.37
486	P55084	HADHB Trifunctional enzyme subunit beta, mitochondrial	HADHB	EGGQYGLVAACAAGGQGHAMIVEAYPK	1.30	0.37
487	P60174	TPI1 Triosephosphate isomerase	TPI1	IAVAAQNCYK	1.30	0.37
488	P60174	TPI1 Triosephosphate isomerase	TPI1	IIYGGSVTGATCK	1.31	0.39
489	Q9HC84	MUC5B Mucin-5B	MUC5B	AAGGAVCEQPLGLECR	1.31	0.39
490	O75663	TIPRL TIP41-like protein	TIPRL	VACAEEWQESR	1.32	0.40
491	Q02790	FKBP4 Peptidyl-prolyl cis-trans isomerase FKBP4	FKBP4	TQLAVCQQR	1.34	0.42
492	P60174	TPI1 Triosephosphate isomerase	TPI1	VPADTEVVCAPPTAYIDFAR	1.35	0.43
493	Q08211	DHX9 ATP-dependent RNA helicase A	DHX9	SSVNCPFSSQDMK	1.35	0.43
494	Q8WV74	NUDT8 Nucleoside diphosphate-linked moiety X motif 8	NUDT8	LAGLTCSGAEGLAR	1.36	0.45
495	P61978	HNRNPK Heterogeneous nuclear ribonucleoprotein K	HNRNPK	LFQECCPHSTDR	1.36	0.45
496	P61970	NUTF2 Nuclear transport factor 2	NUTF2	NINDAWVCTNDMFR	1.37	0.46
497	Q92616	GCN1 eIF-2-alpha kinase activator GCN1	GCN1	CLQNPSSDIR	1.40	0.49
498	P18669	PGAM1 Phosphoglycerate mutase 1	PGAM1	YADLTEDQLPSCESLK	1.40	0.49

499	Q15185	PTGES3 Prostaglandin E synthase 3	PTGES3	LTFSCLGGSDNFK	1.40	0.49
500	Q9ULV4	CORO1C Coronin-1C	CORO1C	DTICNQDER	1.41	0.50
501	P30101	PDIA3 Protein disulfide-isomerase A3	PDIA3	VDCTANTNTCNK	1.42	0.51
502	Q9NQR4	NIT2 Omega-amidase NIT2	NIT2	TLSPGDSFSTFDTPYCR	1.43	0.52
503	Q8NBS9	TXNDC5 Thioredoxin domain-containing protein 5	TXNDC5	VDCTAHSDVCSAQGVR	1.44	0.53
504	Q6NUK1	SLC25A24 Calcium-binding mitochondrial carrier protein SCaM	SLC25A24	TGQYSGIYDCAK	1.49	0.58
505	P55795	HNRNPH2 Heterogeneous nuclear ribonucleoprotein H2	HNRNPH2	GLPWSCSADEVMR	1.56	0.64
506	P30086	PEBP1 Phosphatidylethanolamine-binding protein 1	PEBP1	APVAGTCYQAEWDDYVPK	1.59	0.67
507	O00299	CLIC1 Chloride intracellular channel protein 1	CLIC1	EEFASTCPDDEEIELAYEQVAK	1.66	0.73
508	P30626	SRI Sorcin	SRI	DTAQQGVVNFPYDDFIQCVMSV	1.75	0.80
509	Q9NR46	SH3GLB2 Endophilin-B2	SH3GLB2	SQTTYYAQCYR	1.81	0.86

Table A2-3 Ranking cysteines by sensitivity to GSNO. 1038 cysteine containing peptides from MCF7 cell lysate were reported with R values. R value is the average heavy:light ratio from two individual datasets.

index	UniProt ID	description	symbol	sequence	*R* value	*R* (log2)
1	P53618	COPB1 Coatomer subunit beta	COPB1	ECR	0.16	-2.63
2	Q8IXH7	NELFCD Negative elongation factor C/D	NELFCD	ACQALGAMLSK	0.33	-1.61
3	P04406	GAPDH Glyceraldehyde-3-phosphate dehydrogenase	GAPDH	VPTANVSVVDLTCR	0.40	-1.32
4	P30044	PRDX5 Peroxiredoxin-5, mitochondrial	PRDX5	ALNVEPDGTGLTCSLAPNIISQL	0.41	-1.30
5	Q99497	PARK7 Protein/nucleic acid deglycase DJ-1	PARK7	DPVQCSR	0.43	-1.21
6	P24534	EEF1B2 Elongation factor 1-beta	EEF1B2	LEECVR	0.44	-1.20
7	P09467	FBP1 Fructose-1,6-bisphosphatase 1	FBP1	LLYECNPMAYVMEK	0.49	-1.02
8	P41250	GARS Glycine--tRNA ligase	GARS	CSVLPLSQNQEFMPFVK	0.52	-0.95
9	P15924	DSP Desmoplakin	DSP	DFLQGSSCIAGIYNETTK	0.53	-0.91
10	Q8TD30	GPT2 Alanine aminotransferase 2	GPT2	ILQACGGNSLGSYSASQGVNCIR	0.54	-0.90
11	P18031	PTPN1 Tyrosine-protein phosphatase non-receptor type 1	PTPN1	HEASDFPCR	0.54	-0.89
12	P31350	RRM2 Ribonucleoside-diphosphate reductase subunit M2	RRM2	LIGMNCTLMK	0.55	-0.88
13	P04155	TFF1 Trefoil factor 1	TFF1	GVPWCFYPNTIDVPPEEECEF	0.55	-0.86
14	P17844	DDX5 Probable ATP-dependent RNA helicase DDX5	DDX5	GVEICIATPGR	0.57	-0.81
15	O75223	GGCT Gamma-glutamylcyclotransferase	GGCT	NPSAAFFCVAR	0.57	-0.80
16	P30043	BLVRB Flavin reductase (NADPH)	BLVRB	CLTTDEYDGHSTYPSHQYQ	0.59	-0.75
17	P29762	CRABP1 Cellular retinoic acid-binding protein 1	CRABP1	IHCTQTLLEGDGPK	0.61	-0.72
18	O75832	PSMD10 26S proteasome non-ATPase regulatory subunit 10	PSMD10	GAQVNAVNQNGCTPLHYAASK	0.61	-0.72
19	P23528	CFL1 Cofilin-1	CFL1	HELQANCYEEVK	0.61	-0.72
20	Q14696	MESDC2 LDLR chaperone MESD	MESDC2	CADVTLEGQVYPGK	0.61	-0.71

21	P00558	PGK1 Phosphoglycerate kinase 1	PGK1	GCITIIGGGDTATCCAK	0.61	-0.70
22	O43765	SGTA Small glutamine-rich tetratricopeptide repeat-cont	SGTA	LGNYAGAVQDCER	0.61	-0.70
23	O75828	CBR3 Carbonyl reductase [NADPH] 3	CBR3	ILVNACCPGPVK	0.62	-0.70
24	Q96SZ5	ADO 2-aminoethanethiol dioxygenase	ADO	EASSSACDLPR	0.62	-0.69
25	Q96Q11	TRNT1 CCA tRNA nucleotidyltransferase 1, mitochondrial	TRNT1	YQGEHCLLK	0.62	-0.68
26	O75400	PRPF40A Pre-mRNA-processing factor 40 homolog A	PRPF40A	LSGSSLCSGSWVSADGFLR	0.63	-0.68
27	P36954	POLR2I DNA-directed RNA polymerase II subunit RPB9	POLR2I	NCDYQQEADNSCIYVNK	0.63	-0.67
28	O75369	FLNB Filamin-B	FLNB	SSFLVDCSK	0.63	-0.67
29	O94979	SEC31A Protein transport protein Sec31A	SEC31A	CLSSATDPQTK	0.63	-0.67
30	A0A075B759	PPIAL4E Peptidyl-prolyl cis-trans isomerase A-like 4E	PPIAL4E	IIPGFMCQGGDFTR	0.63	-0.67
31	Q9BYG5	PARD6B Partitioning defective 6 homolog beta	PARD6B	HGAGSGCLGTMEVK	0.64	-0.65
32	P60174	TPI1 Triosephosphate isomerase	TPI1	VAHALAEGLGVIACIGEK	0.64	-0.64
33	P25398	RPS12 40S ribosomal protein S12	RPS12	QAHLCVLASNCDEPMYVK	0.64	-0.63
34	P15924	DSP Desmoplakin	DSP	LLEAQACTGGIIHPTTGQK	0.65	-0.63
35	P02795	MT2A Metallothionein-2	MT2A	CAQGCICK	0.65	-0.62
36	P61158	ACTR3 Actin-related protein 3	ACTR3	LPACVVDCGTGYTK	0.65	-0.61
37	P30626	SRI Sorcin	SRI	PFNLETCR	0.66	-0.61
38	P10768	ESD S-formylglutathione hydrolase	ESD	CPALYWLSGLTCTEQNFISK	0.66	-0.61
39	P15153	RAC2 Ras-related C3 botulinum toxin substrate 2	RAC2	CVVVGDGAVGK	0.66	-0.61
40	P23528	CFL1 Cofilin-1	CFL1	AVLFCLSEDK	0.66	-0.60
41	P55212	CASP6 Caspase-6	CASP6	GTCADR	0.66	-0.59
42	P31949	S100A11 Protein S100-A11	S100A11	CIESLIAVFQK	0.66	-0.59
43	P61981	YWHAG 14-3-3 protein gamma	YWHAG	ELEAVCQDVLSLLDNYLIK	0.66	-0.59
44	P26368	U2AF2 Splicing factor U2AF 65 kDa subunit	U2AF2	PVDGVEVPGCGK	0.67	-0.59
45	A6NMY6	ANXA2P2 Putative annexin A2-like protein	ANXA2P2	GLGTDEDSLIEIICSR	0.67	-0.58

46	P00505	GOT2 Aspartate aminotransferase, mitochondrial	GOT2	EYLPIGGLAEFCK	0.67	-0.58
47	Q9P0L0	VAPA Vesicle-associated membrane protein-associated pro	VAPA	CVFEMPNENDK	0.67	-0.58
48	Q53T59	HS1BP3 HCLS1-binding protein 3	HS1BP3	LFDDPDLGGAIPLGDSLLLPAACESGGPTPSLSHR	0.67	-0.58
49	P31946	YWHAB 14-3-3 protein beta/alpha	YWHAB	IEAELQDICNDVLELLDK	0.67	-0.58
50	P62937	PPIA Peptidyl-prolyl cis-trans isomerase A	PPIA	ITIADCGQLE	0.67	-0.58
51	P06733	ENO1 Alpha-enolase	ENO1	SGETEDTFIADLVVGLCTGQIK	0.67	-0.57
52	P00558	PGK1 Phosphoglycerate kinase 1	PGK1	FCLDNGAK	0.67	-0.57
53	P21291	CSRP1 Cysteine and glycine-rich protein 1	CSRP1	SCFLCMVCK	0.67	-0.57
54	Q9Y696	CLIC4 Chloride intracellular channel protein 4	CLIC4	IEEFLEEVLCPPK	0.67	-0.57
55	P60174	TPI1 Triosephosphate isomerase	TPI1	IAVAAQNCYK	0.68	-0.57
56	P60174	TPI1 Triosephosphate isomerase	TPI1	IIYGGSVTGATCK	0.68	-0.55
57	Q9H479	FN3K Fructosamine-3-kinase	FN3K	AFGGPGAGCISEGR	0.68	-0.55
58	O95372	LYPLA2 Acyl-protein thioesterase 2	LYPLA2	TYPGVMHSSCPQEMAAVK	0.68	-0.55
59	Q9Y2Z0	SUGT1 Protein SGT1 homolog	SUGT1	PDDAQYYCQR	0.68	-0.55
60	P60981	DSTN Destrin	DSTN	AVIFCLSADK	0.68	-0.55
61	P07237	P4HB Protein disulfide-isomerase	P4HB	EECPAVR	0.69	-0.54
62	P30086	PEBP1 Phosphatidylethanolamine-binding protein 1	PEBP1	APVAGTCYQAEWDDYVPK	0.69	-0.54
63	P61081	UBE2M NEDD8-conjugating enzyme Ubc12	UBE2M	TCDISFSDPDDLLNFK	0.69	-0.54
64	Q12931	TRAP1 Heat shock protein 75 kDa, mitochondrial	TRAP1	NIYYLCAPNR	0.69	-0.54
65	P22234	PAICS Multifunctional protein ADE2	PAICS	ACGNFGIPCELR	0.69	-0.54
66	P63104	YWHAZ 14-3-3 protein zeta/delta	YWHAZ	DICNDVLSLLEK	0.69	-0.54
67	P60174	TPI1 Triosephosphate isomerase	TPI1	VPADTEVVCAPPTAYIDFAR	0.69	-0.54
68	P50395	GDI2 Rab GDP dissociation inhibitor beta	GDI2	TDDYLDQPCYETINR	0.69	-0.53

69	P30086	PEBP1 Phosphatidylethanolamine-binding protein 1	PEBP1	CDEPILSNR	0.69	-0.53
70	Q9HC38	GLOD4 Glyoxalase domain-containing protein 4	GLOD4	ALLGYADNQCK	0.69	-0.53
71	P04632	CAPNS1 Calpain small subunit 1	CAPNS1	YSDESGNMDFDNFISCLVR	0.69	-0.53
72	Q14247	CTTN Src substrate cortactin	CTTN	HCSQVDSVR	0.69	-0.53
73	P30153	PPP2R1A Serine/threonine-protein phosphatase 2A 65 kDa reg	PPP2R1A	ENVIMSQILPCIK	0.69	-0.53
74	P21291	CSRP1 Cysteine and glycine-rich protein 1	CSRP1	CSQAVYAAEK	0.70	-0.52
75	P31939	ATIC Bifunctional purine biosynthesis protein PURH	ATIC	VCMVYDLYK	0.70	-0.52
76	P14174	MIF Macrophage migration inhibitory factor	MIF	LLCGLLAER	0.70	-0.52
77	P63104	YWHAZ 14-3-3 protein zeta/delta	YWHAZ	YDDMAACMK	0.70	-0.52
78	P13693	TPT1 Translationally-controlled tumor protein	TPT1	EIADGLCLEVEGK	0.70	-0.52
79	Q96S19	METTL26 Methyltransferase-like 26	METTL26	CTEGLFR	0.70	-0.51
80	O14776	TCERG1 Transcription elongation regulator 1	TCERG1	YLVLDCVPEER	0.70	-0.51
81	P00491	PNP Purine nucleoside phosphorylase	PNP	ACVMMQGR	0.70	-0.51
82	Q02790	FKBP4 Peptidyl-prolyl cis-trans isomerase FKBP4	FKBP4	TQLAVCQQR	0.70	-0.51
83	P00558	PGK1 Phosphoglycerate kinase 1	PGK1	TGQATVASGIPAGWMGLDCGPESSK	0.70	-0.51
84	P08238	HSP90AB1 Heat shock protein HSP 90-beta	HSP90AB1	LVSSPCCIVTSTYGWTANMER	0.70	-0.51
85	Q9NS86	LANCL2 LanC-like protein 2	LANCL2	SVVCQESDLPDELLYGR	0.70	-0.51
86	O00299	CLIC1 Chloride intracellular channel protein 1	CLIC1	FLDGNELTLADCNLLPK	0.70	-0.51
87	P22314	UBA1 Ubiquitin-like modifier-activating enzyme 1	UBA1	DNPGVVTCLDEAR	0.70	-0.51
88	P22061	PCMT1 Protein-L-isoaspartate(D-aspartate) O-methyltransferase	PCMT1	ALDVGSGSGILTACFAR	0.71	-0.50
89	P00338	LDHA L-lactate dehydrogenase A chain	LDHA	DDVFLSVPCILGQNGISDLVK	0.71	-0.50
90	O60361	NME2P1 Putative nucleoside diphosphate kinase	NME2P1	GDFCIQVGR	0.71	-0.50

91	P07900	HSP90AA1 Heat shock protein HSP 90-alpha	HSP90AA1	LVTSPCCIVTSTYGWTANMER	0.71	-0.50
92	P42765	ACAA2 3-ketoacyl-CoA thiolase, mitochondrial	ACAA2	LCGSGFQSIVNGCQEICVK	0.71	-0.50
93	Q6ISB3	GRHL2 Grainyhead-like protein 2 homolog	GRHL2	NCLGTSEAQSNLSGGENR	0.71	-0.50
94	P27348	YWHAQ 14-3-3 protein theta	YWHAQ	YDDMATCMK	0.71	-0.50
95	Q96EK6	GNPNAT1 Glucosamine 6-phosphate N-acetyltransferase	GNPNAT1	ITLECLPQNVGFYK	0.71	-0.50
96	Q9Y3D0	FAM96B Mitotic spindle-associated MMXD complex subunit MI	FAM96B	VAAALENTHLLEVVNQCLSAR	0.71	-0.50
97	Q1KMD3	HNRNPUL2 Heterogeneous nuclear ribonucleoprotein U-like pro	HNRNPUL2	LQEALDAEMLEDEAGGGGAGPGGACK	0.71	-0.50
98	Q9UHX1	PUF60 Poly(U)-binding-splicing factor PUF60	PUF60	ALAIMCR	0.71	-0.50
99	Q9NZZ3	CHMP5 Charged multivesicular body protein 5	CHMP5	APPPSLTDCIGTVDSR	0.71	-0.49
100	P0DMV8	HSPA1A Heat shock 70 kDa protein 1A	HSPA1A	ELEQVCNPIISGLYQGAGGPGPGGFGAQGPK	0.71	-0.49
101	P35237	SERPINB6 Serpin B6	SERPINB6	SCDFLSSFR	0.71	-0.49
102	P61978	HNRNPK Heterogeneous nuclear ribonucleoprotein K	HNRNPK	LFQECCPHSTDR	0.71	-0.49
103	P04075	ALDOA Fructose-bisphosphate aldolase A	ALDOA	YASICQQNGIVPIVEPEILPDGDHDLK	0.71	-0.49
104	Q16644	MAPKAPK3 MAP kinase-activated protein kinase 3	MAPKAPK3	QAGSSSASQGCNNQ	0.71	-0.49
105	P19367	HK1 Hexokinase-1	HK1	AAQLCGAGMAAVVDK	0.71	-0.49
106	Q9NYL9	TMOD3 Tropomodulin-3	TMOD3	CFSLAATR	0.71	-0.49
107	Q9UL46	PSME2 Proteasome activator complex subunit 2	PSME2	CGFLPGNEK	0.71	-0.49
108	P51649	ALDH5A1 Succinate-semialdehyde dehydrogenase, mitochondria	ALDH5A1	AAYEAFCR	0.72	-0.48
109	Q96FJ2	DYNLL2 Dynein light chain 2, cytoplasmic	DYNLL2	NADMSEDMQQDAVDCATQAMEK	0.72	-0.48
110	Q15019	SEPT2 Septin-2	2-Sep	LTVVDTPGYGDAINCR	0.72	-0.48
111	P60604	UBE2G2 Ubiquitin-conjugating enzyme E2 G2	UBE2G2	VCISILHAPGDDPMGYESSAER	0.72	-0.48

112	P07737	PFN1 Profilin-1	PFN1	CYEMASHLR	0.72	-0.48
113	Q96AE4	FUBP1 Far upstream element-binding protein 1	FUBP1	SCMLTGTPESVQSAK	0.72	-0.47
114	P52209	PGD 6-phosphogluconate dehydrogenase, decarboxylating	PGD	VGTGEPCCDWVGDEGAGHFVK	0.72	-0.47
115	Q15369	ELOC Elongin-C	ELOC	TYGGCEGPDAMYVK	0.72	-0.47
116	Q13330	MTA1 Metastasis-associated protein MTA1	MTA1	ALDCSSSVR	0.72	-0.47
117	Q13526	PIN1 Peptidyl-prolyl cis-trans isomerase NIMA-interacting	PIN1	SGEEDFESLASQFSDCSSAK	0.72	-0.47
118	Q9Y508	RNF114 E3 ubiquitin-protein ligase RNF114	RNF114	SHVATCSK	0.73	-0.46
119	P61011	SRP54 Signal recognition particle 54 kDa protein	SRP54	TCLICADTFR	0.73	-0.46
120	P39687	ANP32A Acidic leucine-rich nuclear phosphoprotein 32 fami	ANP32A	SLDLFNCEVTNLNDYR	0.73	-0.46
121	P57721	PCBP3 Poly(rC)-binding protein 3	PCBP3	QICVVMLESPPK	0.73	-0.45
122	P45974	USP5 Ubiquitin carboxyl-terminal hydrolase 5	USP5	AQVPFSSCLEAYGAPEQVDDFWSTALQAK	0.73	-0.45
123	Q9BXV9	GON7 EKC/KEOPS complex subunit GON7	GON7	VSCEAPGDGDPFQGLLSGVAQMK	0.73	-0.45
124	P30084	ECHS1 Enoyl-CoA hydratase, mitochondrial	ECHS1	ICPVETLVEEAIQCAEK	0.73	-0.45
125	P61086	UBE2K Ubiquitin-conjugating enzyme E2 K	UBE2K	IENLCAMGFDR	0.73	-0.45
126	Q01518	CAP1 Adenylyl cyclase-associated protein 1	CAP1	ALLVTASQCQQPAENK	0.73	-0.45
127	P60981	DSTN Destrin	DSTN	LGGSLIVAFEGCPV	0.73	-0.45
128	P52209	PGD 6-phosphogluconate dehydrogenase, decarboxylating	PGD	CLSSLK	0.73	-0.44
129	P30153	PPP2R1A Serine/threonine-protein phosphatase 2A 65 kDa reg	PPP2R1A	LNIISNLDCVNEVIGIR	0.74	-0.44
130	P52272	HNRNPM Heterogeneous nuclear ribonucleoprotein M	HNRNPM	FNECGHVLYADIK	0.74	-0.44
131	P27348	YWHAQ 14-3-3 protein theta	YWHAQ	SICTTVLELLDK	0.74	-0.44
132	Q9NQ88	TIGAR Fructose-2,6-bisphosphatase TIGAR	TIGAR	EQFSQGSPSNCLETSLAEIFPLGK	0.74	-0.44
133	P0DMV8	HSPA1A Heat shock 70 kDa protein 1A	HSPA1A	FEELCSDLFR	0.74	-0.44

134	Q9BS26	ERP44 Endoplasmic reticulum resident protein 44	ERP44	VDCDQHSDIAQR	0.74	-0.44
135	Q04917	YWHAH 14-3-3 protein eta	YWHAH	ELETVCNDVLSLLDK	0.74	-0.44
136	P21964	COMT Catechol O-methyltransferase	COMT	YLPDTLLLEECGLLR	0.74	-0.44
137	Q7L1Q6	BZW1 Basic leucine zipper and W2 domain-containing protein	BZW1	TDVCVFAAQEDLETMQAFAQVFNK	0.74	-0.44
138	Q3LXA3	TKFC Triokinase/FMN cyclase	TKFC	VCSTLLGLEEHLNALDR	0.74	-0.44
139	P61970	NUTF2 Nuclear transport factor 2	NUTF2	NINDAWVCTNDMFR	0.74	-0.43
140	Q96DV4	MRPL38 39S ribosomal protein L38, mitochondrial	MRPL38	VAEGQVTCPYLPPFPAR	0.74	-0.43
141	Q9NZA1	CLIC5 Chloride intracellular channel protein 5	CLIC5	AGIDGESIGNCPFSQR	0.74	-0.43
142	P40926	MDH2 Malate dehydrogenase, mitochondrial	MDH2	SQETECTYFSTPLLLGK	0.74	-0.43
143	O00299	CLIC1 Chloride intracellular channel protein 1	CLIC1	EEFASTCPDDEEIELAYEQVAK	0.74	-0.43
144	P23381	WARS Tryptophan--tRNA ligase, cytoplasmic	WARS	GIFGFTDSDCIGK	0.74	-0.43
145	Q9HBM1	SPC25 Kinetochore protein Spc25	SPC25	STDTSCQMAGLR	0.74	-0.43
146	Q15365	PCBP1 Poly(rC)-binding protein 1	PCBP1	AITIAGVPQSVTECVK	0.74	-0.43
147	Q9Y3D2	MSRB2 Methionine-R-sulfoxide reductase B2, mitochondrial	MSRB2	GQAGGGGPGTGPGLGEAGSLATCELPLAK	0.74	-0.43
148	P28074	PSMB5 Proteasome subunit beta type-5	PSMB5	VIEINPYLLGTMAGGAADCSFWER	0.74	-0.43
149	Q5TFE4	NT5DC1 5-nucleotidase domain-containing protein 1	NT5DC1	ENCGIYFPEIK	0.74	-0.43
150	O43707	ACTN4 Alpha-actinin-4	ACTN4	ELPPDQAEYCIAR	0.74	-0.42
151	Q96FW1	OTUB1 Ubiquitin thioesterase OTUB1	OTUB1	PDGNCFYR	0.75	-0.42
152	Q14181	POLA2 DNA polymerase alpha subunit B	POLA2	VLGCPEALTGSYK	0.75	-0.42
153	O43395	PRPF3 U4/U6 small nuclear ribonucleoprotein Prp3	PRPF3	VLGFSEPTVVTAALNCVGK	0.75	-0.42
154	Q09666	AHNAK Neuroblast differentiation-associated protein AHNA	AHNAK	VDVECPDVNIEGPEGK	0.75	-0.42
155	P37802	TAGLN2 Transgelin-2	TAGLN2	DGTVLCELINALYPEGQAPVK	0.75	-0.42

156	Q9H8M7	MINDY3 Ubiquitin carboxyl-terminal hydrolase MINDY-3	MINDY3	SSPGLSDTIFCR	0.75	-0.42
157	Q9Y3C6	PPIL1 Peptidyl-prolyl cis-trans isomerase-like 1	PPIL1	VCQGIGMVNR	0.75	-0.41
158	Q16643	DBN1 Drebrin	DBN1	CACASHVAK	0.75	-0.41
159	P52788	SMS Spermine synthase	SMS	LYCPVEFSK	0.75	-0.41
160	O00299	CLIC1 Chloride intracellular channel protein 1	CLIC1	IGNCPFSQR	0.75	-0.41
161	Q12931	TRAP1 Heat shock protein 75 kDa, mitochondrial	TRAP1	SPAAECLSEK	0.75	-0.41
162	P12004	PCNA Proliferating cell nuclear antigen	PCNA	CAGNEDIITLR	0.75	-0.41
163	Q15691	MAPRE1 Microtubule-associated protein RP/EB family member	MAPRE1	NIELICQENEGENDPVLQR	0.75	-0.41
164	O43707	ACTN4 Alpha-actinin-4	ACTN4	ICDQWDALGSLTHSR	0.76	-0.40
165	Q7L5D6	GET4 Golgi to ER traffic protein 4 homolog	GET4	EQNYCESR	0.76	-0.40
166	P53041	PPP5C Serine/threonine-protein phosphatase 5	PPP5C	TECYGYALGDATR	0.76	-0.40
167	P09110	ACAA1 3-ketoacyl-CoA thiolase, peroxisomal	ACAA1	DCLIPMGITSENVAER	0.76	-0.40
168	Q9UMS4	PRPF19 Pre-mRNA-processing factor 19	PRPF19	IWSVPNASCVQVVR	0.76	-0.39
169	P11142	HSPA8 Heat shock cognate 71 kDa protein	HSPA8	VCNPIITK	0.76	-0.39
170	Q7L1Q6	BZW1 Basic leucine zipper and W2 domain-containing protein	BZW1	IQEYCYDNIHFMK	0.76	-0.39
171	Q5JS54	PSMG4 Proteasome assembly chaperone 4	PSMG4	NLAVAMCSR	0.76	-0.39
172	P50990	CCT8 T-complex protein 1 subunit theta	CCT8	IAVYSCPFDGMITETK	0.76	-0.39
173	P49773	HINT1 Histidine triad nucleotide-binding protein 1	HINT1	CAADLGLNK	0.76	-0.39
174	P04075	ALDOA Fructose-bisphosphate aldolase A	ALDOA	ALANSLACQGK	0.76	-0.39
175	P24534	EEF1B2 Elongation factor 1-beta	EEF1B2	SYIEGYVPSQADVAVFEAVSSPPPADLCHALR	0.76	-0.39
176	P78417	GSTO1 Glutathione S-transferase omega-1	GSTO1	LNECVDHTPK	0.76	-0.39
177	P14618	PKM Pyruvate kinase PKM	PKM	GIFPVLCK	0.76	-0.39
178	Q86SX6	GLRX5 Glutaredoxin-related protein 5, mitochondrial	GLRX5	GTPEQPQCGFSNAVVQILR	0.76	-0.39

179	P00492	HPRT1 Hypoxanthine-guanine phosphoribosyltransferase	HPRT1	SYCNDQSTGDIK	0.76	-0.39
180	Q7L2H7	EIF3M Eukaryotic translation initiation factor 3 subunit	EIF3M	YTVYCSLIK	0.76	-0.39
181	Q96EY8	MMAB Cob(I)yrinic acid a,c-diamide adenosyltransferase,	MMAB	IQCTLQDVGSALATPCSSAR	0.77	-0.38
182	Q9H910	JPT2 Jupiter microtubule associated homolog 2	JPT2	DHVFLCEGEEPK	0.77	-0.38
183	P13639	EEF2 Elongation factor 2	EEF2	CLYASVLTAQPR	0.77	-0.38
184	Q9Y696	CLIC4 Chloride intracellular channel protein 4	CLIC4	AGSDGESIGNCPFSQR	0.77	-0.38
185	O14561	NDUFAB1 Acyl carrier protein, mitochondrial	NDUFAB1	LMCPQEIVDYIADK	0.77	-0.38
186	Q9UGI8	TES Testin	TES	TQYSCYCCK	0.77	-0.38
187	O43592	XPOT Exportin-T	XPOT	ISPDAWQVCAEALAQR	0.77	-0.38
188	P31948	STIP1 Stress-induced-phosphoprotein 1	STIP1	ALSVGNIDDALQCYSEAIK	0.77	-0.38
189	Q9NVG8	TBC1D13 TBC1 domain family member 13	TBC1D13	LLQDYPITDVCQILQK	0.77	-0.38
190	P23526	AHCY Adenosylhomocysteinase	AHCY	FDNLYGCR	0.77	-0.38
191	P21291	CSRP1 Cysteine and glycine-rich protein 1	CSRP1	DGEIYCK	0.77	-0.38
192	Q92598	HSPH1 Heat shock protein 105 kDa	HSPH1	FICEQDHQNFLR	0.77	-0.37
193	P37837	TALDO1 Transaldolase	TALDO1	ALAGCDFLTISPK	0.77	-0.37
194	O60664	PLIN3 Perilipin-3	PLIN3	DIAQQLQATCTSLGSSIQGLPTNVK	0.77	-0.37
195	Q96SW2	CRBN Protein cereblon	CRBN	VQILPECVLPSTMSAVQLESLNK	0.77	-0.37
196	Q9H2U2	PPA2 Inorganic pyrophosphatase 2, mitochondrial	PPA2	ILSCGEVIHVK	0.78	-0.37
197	Q15813	TBCE Tubulin-specific chaperone E	TBCE	NCAVSCAGEK	0.78	-0.37
198	Q8WVJ2	NUDCD2 NudC domain-containing protein 2	NUDCD2	AQDIQCGLQSR	0.78	-0.37
199	P26440	IVD Isovaleryl-CoA dehydrogenase, mitochondrial	IVD	ASGAVGLSYGAHSNLCINQLVR	0.78	-0.36
200	P55735	SEC13 Protein SEC13 homolog	SEC13	FASGGCDNLIK	0.78	-0.36

201	P23381	WARS Tryptophan--tRNA ligase, cytoplasmic	WARS	DIIACGFDINK	0.78	-0.36
202	P18669	PGAM1 Phosphoglycerate mutase 1	PGAM1	YADLTEDQLPSCESLK	0.78	-0.36
203	Q6NXG1	ESRP1 Epithelial splicing regulatory protein 1	ESRP1	FESGTCSK	0.78	-0.36
204	Q04637	EIF4G1 Eukaryotic translation initiation factor 4 gamma 1	EIF4G1	NHDEESLECLCR	0.78	-0.36
205	Q14151	SAFB2 Scaffold attachment factor B2	SAFB2	ILDILGETCK	0.78	-0.36
206	Q9BWD1	ACAT2 Acetyl-CoA acetyltransferase, cytosolic	ACAT2	ATVAPEDVSEVIFGHVLAAGCGQNPVR	0.78	-0.36
207	P25788	PSMA3 Proteasome subunit alpha type-3	PSMA3	CKDGVVFGVEK	0.78	-0.36
208	Q99873	PRMT1 Protein arginine N-methyltransferase 1	PRMT1	GQLCELSCSTDYR	0.78	-0.36
209	Q9NTK5	OLA1 Obg-like ATPase 1	OLA1	PEYDIMCK	0.78	-0.36
210	Q6QNY0	BLOC1S3 Biogenesis of lysosome-related organelles complex	BLOC1S3	GDLCALAER	0.78	-0.36
211	Q9HCY8	S100A14 Protein S100-A14	S100A14	IANLGSCNDSK	0.78	-0.35
212	Q9P0R6	GSKIP GSK3-beta interaction protein	GSKIP	YCLELTEAGLK	0.78	-0.35
213	P30153	PPP2R1A Serine/threonine-protein phosphatase 2A 65 kDa reg	PPP2R1A	NLCSDDTPMVR	0.78	-0.35
214	P62487	POLR2G DNA-directed RNA polymerase II subunit RPB7	POLR2G	LFTEVEGTCTGK	0.78	-0.35
215	P31150	GDI1 Rab GDP dissociation inhibitor alpha	GDI1	NTNDANSCQIIIPQNQVNR	0.79	-0.35
216	O14979	HNRNPDL Heterogeneous nuclear ribonucleoprotein D-like	HNRNPDL	FGEVVDCTIK	0.79	-0.35
217	P62306	SNRPF Small nuclear ribonucleoprotein F	SNRPF	CNNVLYIR	0.79	-0.35
218	O95292	VAPB Vesicle-associated membrane protein-associated pro	VAPB	CVFELPAENDK	0.79	-0.34
219	P31939	ATIC Bifunctional purine biosynthesis protein PURH	ATIC	YTQSNSVCYAK	0.79	-0.34
220	O60701	UGDH UDP-glucose 6-dehydrogenase	UGDH	ISSINSISALCEATGADVEEVATAIGMDQR	0.79	-0.34

221	P24752	ACAT1 Acetyl-CoA acetyltransferase, mitochondrial	ACAT1	QGEYGLASICNGGGGASAMLIQK	0.79	-0.34
222	P61978	HNRNPK Heterogeneous nuclear ribonucleoprotein K	HNRNPK	GSDFDCELR	0.79	-0.34
223	O75874	IDH1 Isocitrate dehydrogenase [NADP] cytoplasmic	IDH1	SEGGFIWACK	0.79	-0.34
224	O60361	NME2P1 Putative nucleoside diphosphate kinase	NME2P1	SCAHDWVYE	0.79	-0.34
225	Q7Z6Z7	HUWE1 E3 ubiquitin-protein ligase HUWE1	HUWE1	DQSAQCTASK	0.79	-0.33
226	Q96RS6	NUDCD1 NudC domain-containing protein 1	NUDCD1	LPTDLTACDNR	0.79	-0.33
227	P31947	SFN 14-3-3 protein sigma	SFN	GEELSCEER	0.79	-0.33
228	Q9UGI8	TES Testin	TES	LPCEMDAQGPK	0.79	-0.33
229	P37802	TAGLN2 Transgelin-2	TAGLN2	NMACVQR	0.80	-0.33
230	P10768	ESD S-formylglutathione hydrolase	ESD	VFEHDSVELNCK	0.80	-0.33
231	P55735	SEC13 Protein SEC13 homolog	SEC13	VFIWTCDDASSNTWSPK	0.80	-0.33
232	P02795	MT2A Metallothionein-2	MT2A	SCCSCCPVGCAK	0.80	-0.33
233	P21266	GSTM3 Glutathione S-transferase Mu 3	GSTM3	CLDEFPNLK	0.80	-0.33
234	P36969	GPX4 Phospholipid hydroperoxide glutathione peroxidase,	GPX4	ICVNGDDAHPLWK	0.80	-0.33
235	Q15366	PCBP2 Poly(rC)-binding protein 2	PCBP2	AITIAGIPQSIIECVK	0.80	-0.33
236	O43747	AP1G1 AP-1 complex subunit gamma-1	AP1G1	FTCTVNR	0.80	-0.33
237	P13639	EEF2 Elongation factor 2	EEF2	CELLYEGPPDDEAAMGIK	0.80	-0.33
238	Q52LJ0	FAM98B Protein FAM98B	FAM98B	INDALSCEYECR	0.80	-0.32
239	P17844	DDX5 Probable ATP-dependent RNA helicase DDX5	DDX5	LIDFLECGK	0.80	-0.32
240	Q9NVU0	POLR3E DNA-directed RNA polymerase III subunit RPC5	POLR3E	AAGTDSFNGHPPQGCASTPVAR	0.80	-0.32
241	P53602	MVD Diphosphomevalonate decarboxylase	MVD	DGDPLPSSLSCK	0.80	-0.32
242	Q7Z6M1	RABEPK Rab9 effector protein with kelch motifs	RABEPK	NCLQVLNPETR	0.80	-0.32
243	O75131	CPNE3 Copine-3	CPNE3	NCLNPQFSK	0.80	-0.32

244	Q9NR45	NANS Sialic acid synthase	NANS	QLLPCEMACNEK	0.80	-0.31
245	P24752	ACAT1 Acetyl-CoA acetyltransferase, mitochondrial	ACAT1	IHMGSCAENTAK	0.80	-0.31
246	P13639	EEF2 Elongation factor 2	EEF2	ETVSEESNVLCLSK	0.81	-0.31
247	P31947	SFN 14-3-3 protein sigma	SFN	VETELQGVCDTVLGLLDSHLIK	0.81	-0.31
248	P47756	CAPZB F-actin-capping protein subunit beta	CAPZB	DETVSDCSPHIANIGR	0.81	-0.31
249	Q8WUM4	PDCD6IP Programmed cell death 6-interacting protein	PDCD6IP	CSDIVFAR	0.81	-0.31
250	P14625	HSP90B1 Endoplasmin	HSP90B1	LTESPCALVASQYGWSGNMER	0.81	-0.31
251	P49327	FASN Fatty acid synthase	FASN	ACLDTAVENMPSLK	0.81	-0.31
252	Q96EI5	TCEAL4 Transcription elongation factor A protein-like 4	TCEAL4	PEVTCTLEDK	0.81	-0.31
253	P14649	MYL6B Myosin light chain 6B	MYL6B	ILYSQCGDVMR	0.81	-0.31
254	Q9NQ88	TIGAR Fructose-2,6-bisphosphatase TIGAR	TIGAR	EECPVFTPPGGETLDQVK	0.81	-0.31
255	Q14247	CTTN Src substrate cortactin	CTTN	CALGWDHQEK	0.81	-0.31
256	P60953	CDC42 Cell division control protein 42 homolog	CDC42	YVECSALTQK	0.81	-0.31
257	Q9NQ88	TIGAR Fructose-2,6-bisphosphatase TIGAR	TIGAR	CSLPATLSR	0.81	-0.30
258	P56537	EIF6 Eukaryotic translation initiation factor 6	EIF6	ASFENNCEIGCFAK	0.81	-0.30
259	Q9BQ69	MACROD1 O-acetyl-ADP-ribose deacetylase MACROD1	MACROD1	LEVDAIVNAANSSLLGGGGVDGCIHR	0.81	-0.30
260	P41250	GARS Glycine--tRNA ligase	GARS	SCYDLSCHAR	0.81	-0.30
261	Q09666	AHNAK Neuroblast differentiation-associated protein AHNA	AHNAK	LEGDLTGPSVDVEVPDVELECPDAK	0.81	-0.30
262	Q9Y365	STARD10 START domain-containing protein 10	STARD10	MECCDVPAETLYDVLHDIEYR	0.81	-0.30
263	Q92598	HSPH1 Heat shock protein 105 kDa	HSPH1	LCGPYEK	0.81	-0.30
264	Q9C0C9	UBE2O (E3-independent) E2 ubiquitin-conjugating enzyme	UBE2O	CYNEMALIR	0.81	-0.30
265	Q9H993	ARMT1 Protein-glutamate O-methyltransferase	ARMT1	CGADWEEYIK	0.81	-0.30
266	Q06124	PTPN11 Tyrosine-protein phosphatase non-receptor type 11	PTPN11	QGFWEEFETLQQQECK	0.81	-0.30

267	P33240	CSTF2 Cleavage stimulation factor subunit 2	CSTF2	LCVQNSPQEAR	0.81	-0.30
268	Q8N6T3	ARFGAP1 ADP-ribosylation factor GTPase-activating protein	ARFGAP1	EFLESQEDYDPCWSLQEK	0.81	-0.30
269	Q8N806	UBR7 Putative E3 ubiquitin-protein ligase UBR7	UBR7	VEQNSEPCAGSSSESDLQTVFK	0.82	-0.29
270	P61158	ACTR3 Actin-related protein 3	ACTR3	LGYAGNTEPQFIIPSCIAIK	0.82	-0.29
271	P07900	HSP90AA1 Heat shock protein HSP 90-alpha	HSP90AA1	VFIMDNCEELIPEYLNFIR	0.82	-0.29
272	Q5TDH0	DDI2 Protein DDI1 homolog 2	DDI2	NVLVIGTTGSQTTFLPEGELPECAR	0.82	-0.29
273	O43765	SGTA Small glutamine-rich tetratricopeptide repeat-cont	SGTA	AICIDPAYSK	0.82	-0.29
274	P49458	SRP9 Signal recognition particle 9 kDa protein	SRP9	VTDDLVCLVYK	0.82	-0.29
275	P49915	GMPS GMP synthase [glutamine-hydrolyzing]	GMPS	ACTTEEDQEK	0.82	-0.29
276	P49327	FASN Fatty acid synthase	FASN	AINCATSGVVGLVNCLR	0.82	-0.29
277	P13639	EEF2 Elongation factor 2	EEF2	IWCFGPDGTGPNILTDITK	0.82	-0.29
278	Q14103	HNRNPD Heterogeneous nuclear ribonucleoprotein D0	HNRNPD	FGEVVDCTLK	0.82	-0.29
279	Q08J23	NSUN2 tRNA (cytosine(34)-C(5))-methyltransferase	NSUN2	YEPDSANPDALQCPIVLCGWR	0.82	-0.29
280	Q7Z2Z2	EFL1 Elongation factor-like GTPase 1	EFL1	ICDGCIIVVDAVEGVCPQTQAVLR	0.82	-0.29
281	P50990	CCT8 T-complex protein 1 subunit theta	CCT8	QITSYGETCPGLEQYAIK	0.82	-0.28
282	P55072	VCP Transitional endoplasmic reticulum ATPase	VCP	QAAPCVLFFDELDSIAK	0.82	-0.28
283	Q15149	PLEC Plectin	PLEC	LLEAQACTGGIIDPSTGER	0.82	-0.28
284	P21283	ATP6V1C1 V-type proton ATPase subunit C 1	ATP6V1C1	TCQQTWEK	0.82	-0.28
285	Q16543	CDC37 Hsp90 co-chaperone Cdc37	CDC37	CIDSGLWVPNSK	0.83	-0.28
286	O14745	SLC9A3R1 Na(+)/H(+) exchange regulatory cofactor NHE-RF1	SLC9A3R1	IVEVNGVCMEGK	0.83	-0.28
287	Q9BXJ9	NAA15 N-alpha-acetyltransferase 15, NatA auxiliary subun	NAA15	LFNTAVCESK	0.83	-0.27

288	P55786	NPEPPS Puromycin-sensitive aminopeptidase	NPEPPS	DGVCVR	0.83	-0.27
289	Q96QK1	VPS35 Vacuolar protein sorting-associated protein 35	VPS35	TQCALAASK	0.83	-0.27
290	Q2TAA2	IAH1 Isoamyl acetate-hydrolyzing esterase 1 homolog	IAH1	VILITPTPLCETAWEEQCIIQGCK	0.83	-0.27
291	Q7L1Q6	BZW1 Basic leucine zipper and W2 domain-containing protein	BZW1	FDPTQFQDCIIQGLTETGTDLEAVAK	0.83	-0.27
292	Q9H773	DCTPP1 dCTP pyrophosphatase 1	DCTPP1	YTELPHGAISEDQAVGPADIPCDSTGQTST	0.83	-0.27
293	Q99460	PSMD1 26S proteasome non-ATPase regulatory subunit 1	PSMD1	VLTMPETCR	0.83	-0.27
294	Q8WVV9	HNRNPLL Heterogeneous nuclear ribonucleoprotein L-like	HNRNPLL	LCFSTSSHL	0.83	-0.27
295	P61978	HNRNPK Heterogeneous nuclear ribonucleoprotein K	HNRNPK	IIPTLEEGLQLPSPTATSQLPLESDAVECLNYQHYK	0.83	-0.27
296	Q96HE7	ERO1A ERO1-like protein alpha	ERO1A	HDDSSDNFCEADDIQSPEAEYVDLLLNPER	0.83	-0.27
297	P30084	ECHS1 Enoyl-CoA hydratase, mitochondrial	ECHS1	ALNALCDGLIDELNQALK	0.83	-0.27
298	O43488	AKR7A2 Aflatoxin B1 aldehyde reductase member 2	AKR7A2	QVETELFPCLR	0.83	-0.26
299	P17844	DDX5 Probable ATP-dependent RNA helicase DDX5	DDX5	GDGPICLVLAPTR	0.83	-0.26
300	Q6KB66	KRT80 Keratin, type II cytoskeletal 80	KRT80	CHIDLSGIVEEVK	0.83	-0.26
301	P51149	RAB7A Ras-related protein Rab-7a	RAB7A	AQAWCYSK	0.83	-0.26
302	Q7L2H7	EIF3M Eukaryotic translation initiation factor 3 subunit	EIF3M	LLYEALVDCK	0.83	-0.26
303	P62258	YWHAE 14-3-3 protein epsilon	YWHAE	LICCDILDVLDK	0.83	-0.26
304	P14866	HNRNPL Heterogeneous nuclear ribonucleoprotein L	HNRNPL	VFNVFCLYGNVEK	0.83	-0.26
305	P00338	LDHA L-lactate dehydrogenase A chain	LDHA	VIGSGCNLDSAR	0.84	-0.26
306	Q5TFE4	NT5DC1 5-nucleotidase domain-containing protein	NT5DC1	HFLSDTGMACR	0.84	-0.26

		1				
307	P40926	MDH2 Malate dehydrogenase, mitochondrial	MDH2	TIIPLISQCTPK	0.84	-0.26
308	Q14980	NUMA1 Nuclear mitotic apparatus protein 1	NUMA1	HLCQQLQAEQAAAEK	0.84	-0.26
309	Q6P587	FAHD1 Acylpyruvase FAHD1, mitochondrial	FAHD1	SFTASCPVSAFVPK	0.84	-0.25
310	Q9Y224	C14orf166 UPF0568 protein C14orf166	C14orf166	LTALDYHNPAGFNCK	0.84	-0.25
311	P04062	GBA Glucosylceramidase	GBA	VPMASCDFSIR	0.84	-0.25
312	O75348	ATP6V1G1 V-type proton ATPase subunit G 1	ATP6V1G1	GSCSTEVEK	0.84	-0.25
313	P12814	ACTN1 Alpha-actinin-1	ACTN1	ICDQWDNLGALTQK	0.84	-0.25
314	Q6P2E9	EDC4 Enhancer of mRNA-decapping protein 4	EDC4	LCTQLEGLQSTVTGHVER	0.84	-0.25
315	Q8WW01	TSEN15 tRNA-splicing endonuclease subunit Sen15	TSEN15	GDSEPTPGCSGLGPGGVR	0.84	-0.25
316	O43175	PHGDH D-3-phosphoglycerate dehydrogenase	PHGDH	VLISDSLDPCCR	0.84	-0.25
317	P42566	EPS15 Epidermal growth factor receptor substrate 15	EPS15	GSDPFASDCFFR	0.84	-0.25
318	P00966	ASS1 Argininosuccinate synthase	ASS1	FELSCYSLAPQIK	0.84	-0.24
319	P78417	GSTO1 Glutathione S-transferase omega-1	GSTO1	FCPFAER	0.84	-0.24
320	Q9NQX3	GPHN Gephyrin	GPHN	VTTGAPIPCGADAVVQVEDTELIR	0.84	-0.24
321	P13639	EEF2 Elongation factor 2	EEF2	TFCQLILDPIFK	0.84	-0.24
322	P49591	SARS Serine--tRNA ligase, cytoplasmic	SARS	TICAILENYQTEK	0.85	-0.24
323	Q9NRR5	UBQLN4 Ubiquilin-4	UBQLN4	EEIVICDR	0.85	-0.24
324	P14866	HNRNPL Heterogeneous nuclear ribonucleoprotein L	HNRNPL	LCFSTAQHAS	0.85	-0.24
325	P29401	TKT Transketolase	TKT	QAFTDVATGSLGQGLGAACGMAYTGK	0.85	-0.24
326	O95865	DDAH2 N(G),N(G)-dimethylarginine dimethylaminohydrolase	DDAH2	GLCGMGGPR	0.85	-0.24
327	P49589	CARS Cysteine--tRNA ligase, cytoplasmic	CARS	VQPQWSPPAGTQPCR	0.85	-0.24
328	Q9H3P7	ACBD3 Golgi resident protein GCP60	ACBD3	QVLMGPYNPDTCPEVGFFDVLGNDR	0.85	-0.23

329	O15327	INPP4B Type II inositol 3,4-bisphosphate 4-phosphatase	INPP4B	SLNCIIAMVDK	0.85	-0.23
330	Q13200	PSMD2 26S proteasome non-ATPase regulatory subunit 2	PSMD2	NECDPALALLSDYVLHNSNTMR	0.85	-0.23
331	P14618	PKM Pyruvate kinase PKM	PKM	NTGIICTIGPASR	0.85	-0.23
332	Q9HAV7	GRPEL1 GrpE protein homolog 1, mitochondrial	GRPEL1	ATQCVPK	0.85	-0.23
333	Q9H0W8	SMG9 Protein SMG9	SMG9	EDFCPR	0.85	-0.23
334	O14950	MYL12B Myosin regulatory light chain 12B	MYL12B	NAFACFDEEATGTIQEDYLR	0.85	-0.23
335	O14980	XPO1 Exportin-1	XPO1	LDINLLDNVVNCLYHGEGAQQR	0.85	-0.23
336	Q9UK41	VPS28 Vacuolar protein sorting-associated protein 28	VPS28	LDCPLAMER	0.86	-0.22
337	Q09666	AHNAK Neuroblast differentiation-associated protein AHNA	AHNAK	GPFVEAEVPDVDLECPDAK	0.86	-0.22
338	Q13596	SNX1 Sorting nexin-1	SNX1	LQEVECEEQR	0.86	-0.22
339	Q9NTK5	OLA1 Obg-like ATPase 1	OLA1	STFFNVLTNSQASAENFPFCTIDPNESR	0.86	-0.22
340	P54105	CLNS1A Methylosome subunit pICln	CLNS1A	SDCLGEHLYVMVNAK	0.86	-0.22
341	P14868	DARS Aspartate--tRNA ligase, cytoplasmic	DARS	LEYCEALAMLR	0.86	-0.22
342	Q01581	HMGCS1 Hydroxymethylglutaryl-CoA synthase, cytoplasmic	HMGCS1	NNLSYDCIGR	0.86	-0.22
343	Q9Y5L0	TNPO3 Transportin-3	TNPO3	IVCTPGQGLGDLR	0.86	-0.22
344	P25789	PSMA4 Proteasome subunit alpha type-4	PSMA4	ATCIGNNSAAAVSMLK	0.86	-0.22
345	P60981	DSTN Destrin	DSTN	CSTPEEIK	0.86	-0.22
346	P52907	CAPZA1 F-actin-capping protein subunit alpha-1	CAPZA1	TIDGQQTIIACIESHQFQPK	0.86	-0.22
347	P49327	FASN Fatty acid synthase	FASN	LSIPTYGLQCTR	0.86	-0.21
348	P49327	FASN Fatty acid synthase	FASN	DPETLVGYSMVGCQR	0.86	-0.21
349	P21333	FLNA Filamin-A	FLNA	MDCQECPEGYR	0.86	-0.21
350	Q04917	YWHAH 14-3-3 protein eta	YWHAH	NCNDFQYESK	0.86	-0.21
351	Q15185	PTGES3 Prostaglandin E synthase 3	PTGES3	SILCCLR	0.86	-0.21
352	Q96FW1	OTUB1 Ubiquitin thioesterase OTUB1	OTUB1	QEPLGSDSEGVNCLAYDEAIMAQQDR	0.86	-0.21
353	Q14697	GANAB Neutral alpha-glucosidase AB	GANAB	DGSDYEGWCWPGSAGYPDFTNPTMR	0.86	-0.21

354	P02533	KRT14 Keratin, type I cytoskeletal 14	KRT14	CEMEQQNQEYK	0.87	-0.21
355	Q9NY33	DPP3 Dipeptidyl peptidase 3	DPP3	FSTIASSYEECR	0.87	-0.21
356	Q9NQR4	NIT2 Omega-amidase NIT2	NIT2	VGLGICYDMR	0.87	-0.21
357	O75369	FLNB Filamin-B	FLNB	VAVTEGCQPSR	0.87	-0.21
358	P30084	ECHS1 Enoyl-CoA hydratase, mitochondrial	ECHS1	EMQNLSFQDCYSSK	0.87	-0.21
359	P12532	CKMT1A Creatine kinase U-type, mitochondrial	CKMT1A	LGYILTCPSNLGTGLR	0.87	-0.21
360	Q9NRF8	CTPS2 CTP synthase 2	CTPS2	GLGLSPDLIVCR	0.87	-0.20
361	P50135	HNMT Histamine N-methyltransferase	HNMT	VQAQYPGVCINNEVVEPSAEQIAK	0.87	-0.20
362	P22626	HNRNPA2B1 Heterogeneous nuclear ribonucleoproteins A2/B1	HNRNPA2B1	LTDCVVMR	0.87	-0.20
363	O75663	TIPRL TIP41-like protein	TIPRL	VACAEEWQESR	0.87	-0.20
364	Q99873	PRMT1 Protein arginine N-methyltransferase 1	PRMT1	VEDLTFTSPFCLQVK	0.87	-0.20
365	P14618	PKM Pyruvate kinase PKM	PKM	AEGSDVANAVLDGADCIMLSGETAK	0.87	-0.20
366	P19367	HK1 Hexokinase-1	HK1	AILQQLGLNSTCDDSILVK	0.87	-0.20
367	Q9Y4P1	ATG4B Cysteine protease ATG4B	ATG4B	NFPAIGGTGPTSDTGWGCMLR	0.87	-0.20
368	Q9NY27	PPP4R2 Serine/threonine-protein phosphatase 4 regulatory	PPP4R2	LCELLTDPR	0.87	-0.19
369	P21266	GSTM3 Glutathione S-transferase Mu 3	GSTM3	LCYSSDHEK	0.87	-0.19
370	P27348	YWHAQ 14-3-3 protein theta	YWHAQ	YLAEVACGDDR	0.87	-0.19
371	P08238	HSP90AB1 Heat shock protein HSP 90-beta	HSP90AB1	VFIMDSCDELIPEYLNFIR	0.88	-0.19
372	Q9UPM8	AP4E1 AP-4 complex subunit epsilon-1	AP4E1	SSCSTLPDYLLYQCQK	0.88	-0.19
373	P26641	EEF1G Elongation factor 1-gamma	EEF1G	AAAPAPEEEMDECEQALAAEPK	0.88	-0.19
374	Q13098	GPS1 COP9 signalosome complex subunit 1	GPS1	CAAGLAELAAR	0.88	-0.19
375	A0AVT1	UBA6 Ubiquitin-like modifier-activating enzyme 6	UBA6	PNVGCQQDSEELLK	0.88	-0.18
376	Q9H2U2	PPA2 Inorganic pyrophosphatase 2, mitochondrial	PPA2	STNCFGDNDPIDVCEIGSK	0.88	-0.18

377	Q8IWX8	CHERP Calcium homeostasis endoplasmic reticulum protein	CHERP	LALEQQQLICK	0.88	-0.18
378	P38646	HSPA9 Stress-70 protein, mitochondrial	HSPA9	CELSSSVQTDINLPYLTMDSSGPK	0.88	-0.18
379	Q9HCC0	MCCC2 Methylcrotonoyl-CoA carboxylase beta chain, mitoch	MCCC2	NIAQIAVVMGSCTAGGAYVPAMADENIIVR	0.88	-0.18
380	Q7L3B6	CDC37L1 Hsp90 co-chaperone Cdc37-like 1	CDC37L1	MCLWSTDAISK	0.88	-0.18
381	P57721	PCBP3 Poly(rC)-binding protein 3	PCBP3	INISEGNCPER	0.88	-0.18
382	Q96FX7	TRMT61A tRNA (adenine(58)-N(1))-methyltransferase	TRMT61A	FCSFSPCIEQVQR	0.88	-0.18
383	P62820	RAB1A Ras-related protein Rab-1A	RAB1A	CDLTTK	0.88	-0.18
384	Q5F1R6	DNAJC21 DnaJ homolog subfamily C member 21	DNAJC21	CHYEALGVR	0.88	-0.18
385	P15153	RAC2 Ras-related C3 botulinum toxin substrate 2	RAC2	YLECSALTQR	0.88	-0.18
386	Q09666	AHNAK Neuroblast differentiation-associated protein AHNA	AHNAK	SSGCDVNLPGVNVK	0.88	-0.18
387	P41240	CSK Tyrosine-protein kinase CSK	CSK	SVLGGDCLLK	0.89	-0.18
388	Q52LJ0	FAM98B Protein FAM98B	FAM98B	SLCNLEESITSAGR	0.89	-0.18
389	P49327	FASN Fatty acid synthase	FASN	LTPGCEAEAETEAICFFVQQFTDMEHNR	0.89	-0.17
390	P00519	ABL1 Tyrosine-protein kinase ABL1	ABL1	ELQICPATAGSGPAATQDFSK	0.89	-0.17
391	Q9Y296	TRAPPC4 Trafficking protein particle complex subunit 4	TRAPPC4	CELFDQNLK	0.89	-0.17
392	Q86VP6	CAND1 Cullin-associated NEDD8-dissociated protein 1	CAND1	NCIGDFLK	0.89	-0.17
393	P28838	LAP3 Cytosol aminopeptidase	LAP3	ADMGGAATICSAIVSAAK	0.89	-0.17
394	Q9ULA0	DNPEP Aspartyl aminopeptidase	DNPEP	ISASCQHPTAFEEAIPK	0.89	-0.17
395	Q15599	SLC9A3R2 Na(+)/H(+) exchange regulatory cofactor NHE-RF2	SLC9A3R2	VTPTEEHVEGPLPSPVTNGTSPAQLNGGSACSSR	0.89	-0.17
396	Q7Z434	MAVS Mitochondrial antiviral-signaling protein	MAVS	GCELVDLADEVASVYQSYQPR	0.89	-0.17
397	Q9Y6E0	STK24 Serine/threonine-protein kinase 24	STK24	SQACGGNLGSIEELR	0.89	-0.17

398	Q9ULA0	DNPEP Aspartyl aminopeptidase	DNPEP	NDTPCGTTIGPILASR	0.89	-0.17
399	Q9BV86	NTMT1 N-terminal Xaa-Pro-Lys N-methyltransferase 1	NTMT1	IICSAGLSLLAEER	0.89	-0.17
400	Q8N1F7	NUP93 Nuclear pore complex protein Nup93	NUP93	SSGQSAQLLSHEPGDPPCLR	0.89	-0.17
401	Q08J23	NSUN2 tRNA (cytosine(34)-C(5))-methyltransferase	NSUN2	MVYSTCSLNPIEDEAVIASLLEK	0.89	-0.17
402	P31150	GDI1 Rab GDP dissociation inhibitor alpha	GDI1	TDDYLDQPCLETVNR	0.89	-0.16
403	P08238	HSP90AB1 Heat shock protein HSP 90-beta	HSP90AB1	GFEVVYMTEPIDEYCVQQLK	0.89	-0.16
404	P14866	HNRNPL Heterogeneous nuclear ribonucleoprotein L	HNRNPL	QPAIMPGQSYGLEDGSCSYK	0.89	-0.16
405	Q92879	CELF1 CUGBP Elav-like family member 1	CELF1	GCAFVTFTTR	0.89	-0.16
406	P25398	RPS12 40S ribosomal protein S12	RPS12	VVGCSCVVVK	0.89	-0.16
407	P14866	HNRNPL Heterogeneous nuclear ribonucleoprotein L	HNRNPL	ASLNGADIYSGCCTLK	0.90	-0.16
408	P49591	SARS Serine--tRNA ligase, cytoplasmic	SARS	YAGLSTCFR	0.90	-0.16
409	Q9H074	PAIP1 Polyadenylate-binding protein-interacting protein	PAIP1	ELLNALFSNPMDDNLICAVK	0.90	-0.16
410	Q3LXA3	TKFC Triokinase/FMN cyclase	TKFC	AAGDGDCGTTHSR	0.90	-0.15
411	Q01433	AMPD2 AMP deaminase 2	AMPD2	CGVPFTDLLDAAK	0.90	-0.15
412	Q7Z4W1	DCXR L-xylulose reductase	DCXR	GVPGAIVNVSSQCSQR	0.90	-0.15
413	Q14653	IRF3 Interferon regulatory factor 3	IRF3	QVFQQTISCPEGLR	0.90	-0.15
414	P12004	PCNA Proliferating cell nuclear antigen	PCNA	LMDLDVEQLGIPEQEYSCVVK	0.90	-0.15
415	Q9HAV7	GRPEL1 GrpE protein homolog 1, mitochondrial	GRPEL1	LYGIQAFCK	0.90	-0.15
416	Q9NZL4	HSPBP1 Hsp70-binding protein 1	HSPBP1	DACDTVR	0.90	-0.15
417	P24752	ACAT1 Acetyl-CoA acetyltransferase, mitochondrial	ACAT1	QAVLGAGLPISTPCTTINK	0.90	-0.15
418	P33316	DUT Deoxyuridine 5-triphosphate nucleotidohydrolase,	DUT	TDIQIALPSGCYGR	0.90	-0.15
419	P30041	PRDX6 Peroxiredoxin-6	PRDX6	DINAYNCEEPTEK	0.90	-0.15
420	Q09666	AHNAK Neuroblast differentiation-associated protein AHNA	AHNAK	LEGDLTGPSVGVEVPDVELECPDAK	0.90	-0.15

421	P45985	MAP2K4 Dual specificity mitogen-activated protein kinase	MAP2K4	LCDFGISGQLVDSIAK	0.90	-0.14
422	P13639	EEF2 Elongation factor 2	EEF2	YVEPIEDVPCGNIVGLVGVDQFLVK	0.90	-0.14
423	Q9UK39	NOCT Nocturnin	NOCT	TDCPSTHPPIR	0.90	-0.14
424	P84085	ARF5 ADP-ribosylation factor 5	ARF5	NICFTVWDVGGQDK	0.91	-0.14
425	P53990	IST1 IST1 homolog	IST1	IVADQLCAK	0.91	-0.14
426	Q13185	CBX3 Chromobox protein homolog 3	CBX3	GFTDADNTWEPEENLDCPELIEAFLNSQK	0.91	-0.14
427	Q9UNM6	PSMD13 26S proteasome non-ATPase regulatory subunit 13	PSMD13	LEFWCTDVK	0.91	-0.14
428	P78347	GTF2I General transcription factor II-I	GTF2I	SILSPGGSCGPIK	0.91	-0.14
429	P21333	FLNA Filamin-A	FLNA	AHVVPCFDASK	0.91	-0.14
430	P21281	ATP6V1B2 V-type proton ATPase subunit B, brain isoform	ATP6V1B2	GPVVLAEDFLDIMGQPINPQCR	0.91	-0.14
431	P63208	SKP1 S-phase kinase-associated protein 1	SKP1	GLLDVTCK	0.91	-0.14
432	P35270	SPR Sepiapterin reductase	SPR	TVVNISSLCALQPFK	0.91	-0.13
433	P61158	ACTR3 Actin-related protein 3	ACTR3	YSYVCPDLVK	0.91	-0.13
434	Q9NR46	SH3GLB2 Endophilin-B2	SH3GLB2	SQTTYYAQCYR	0.91	-0.13
435	P22234	PAICS Multifunctional protein ADE2	PAICS	CGETAFIAPQCEMIPIEWVCR	0.91	-0.13
436	Q9UNH7	SNX6 Sorting nexin-6	SNX6	IGSSLYALGTQDSTDICK	0.91	-0.13
437	P30281	CCND3 G1/S-specific cyclin-D3	CCND3	ASYFQCVQR	0.91	-0.13
438	P58107	EPPK1 Epiplakin	EPPK1	CGYFDEEMNR	0.91	-0.13
439	P35080	PFN2 Profilin-2	PFN2	DSLYVDGDCTMDIR	0.92	-0.13
440	P07741	APRT Adenine phosphoribosyltransferase	APRT	VVVVDDLLATGGTMNAACELLGR	0.92	-0.13
441	O43684	BUB3 Mitotic checkpoint protein BUB3	BUB3	TPCNAGTFSQPEK	0.92	-0.12
442	P53611	RABGGTB Geranylgeranyl transferase type-2 subunit beta	RABGGTB	DDYEYCMSEYLR	0.92	-0.12
443	P11940	PABPC1 Polyadenylate-binding protein 1	PABPC1	GFGFVCFSSPEEATK	0.92	-0.12
444	P27348	YWHAQ 14-3-3 protein theta	YWHAQ	DNLTLWTSDSAGEECDAAEGAEN	0.92	-0.12

445	P48739	PITPNB Phosphatidylinositol transfer protein beta isoform	PITPNB	VVLPCSVQEYQVGQLYSVAEASK	0.92	-0.12
446	P51659	HSD17B4 Peroxisomal multifunctional enzyme type 2	HSD17B4	ICDFENASK	0.92	-0.12
447	O43865	AHCYL1 S-adenosylhomocysteine hydrolase-like protein 1	AHCYL1	LCVPAMNVNDSVTK	0.92	-0.12
448	P47756	CAPZB F-actin-capping protein subunit beta	CAPZB	GCWDSIHVVEVQEK	0.92	-0.12
449	O14980	XPO1 Exportin-1	XPO1	TSESLCQNNMVILK	0.92	-0.12
450	Q15365	PCBP1 Poly(rC)-binding protein 1	PCBP1	LVVPATQCGSLIGK	0.92	-0.12
451	Q5VWZ2	LYPLAL1 Lysophospholipase-like protein 1	LYPLAL1	CIVSPAGR	0.92	-0.12
452	P10599	TXN Thioredoxin	TXN	CMPTFQFFK	0.92	-0.11
453	Q9H8W4	PLEKHF2 Pleckstrin homology domain-containing family F mem	PLEKHF2	ICDFCYDLLSAGDMATCQPAR	0.92	-0.11
454	P13797	PLS3 Plastin-3	PLS3	VDLNSNGFICDYELHELFK	0.93	-0.11
455	Q96RS6	NUDCD1 NudC domain-containing protein 1	NUDCD1	DSAQCAAIAER	0.93	-0.11
456	O14545	TRAFD1 TRAF-type zinc finger domain-containing protein 1	TRAFD1	AVCEADQSHGGPR	0.93	-0.11
457	O75822	EIF3J Eukaryotic translation initiation factor 3 subunit	EIF3J	ITNSLTVLCSEK	0.93	-0.11
458	P51858	HDGF Hepatoma-derived growth factor	HDGF	CGDLVFAK	0.93	-0.11
459	P50991	CCT4 T-complex protein 1 subunit delta	CCT4	AQDIEAGDGTTSVVIIAGSLLDSCTK	0.93	-0.11
460	P15924	DSP Desmoplakin	DSP	ACGSEIMQK	0.93	-0.11
461	P36507	MAP2K2 Dual specificity mitogen-activated protein kinase	MAP2K2	LCDFGVSGQLIDSMANSFVGTR	0.93	-0.11
462	Q8WVJ2	NUDCD2 NudC domain-containing protein 2	NUDCD2	DAANCWTSLLESEYAADPWVQDQMQR	0.93	-0.11
463	Q06323	PSME1 Proteasome activator complex subunit 1	PSME1	GPPCGPVNCNEK	0.93	-0.11
464	P49368	CCT3 T-complex protein 1 subunit gamma	CCT3	NLQDAMQVCR	0.93	-0.10
465	Q7L2H7	EIF3M Eukaryotic translation initiation factor 3 subunit	EIF3M	VAASCGAIQYIPTELDQVR	0.93	-0.10

466	P41227	NAA10 N-alpha-acetyltransferase 10	NAA10	GNSPPSSGEACR	0.93	-0.10
467	P58107	EPPK1 Epiplakin	EPPK1	YLEGTSCIAGVLVPAK	0.93	-0.10
468	Q6P2E9	EDC4 Enhancer of mRNA-decapping protein 4	EDC4	SCQAMFQQINDSFR	0.93	-0.10
469	P35579	MYH9 Myosin-9	MYH9	LEEEQIILEDQNCK	0.93	-0.10
470	Q15181	PPA1 Inorganic pyrophosphatase	PPA1	HTGCCGDNDPIDVCEIGSK	0.93	-0.10
471	B4DXR9	ZNF732 Zinc finger protein 732	ZNF732	CLDPAQQNLYR	0.93	-0.10
472	Q13155	AIMP2 Aminoacyl tRNA synthase complex-interacting	AIMP2	FSIQTMCPIEGEGNIAR	0.93	-0.10
473	Q15008	PSMD6 26S proteasome non-ATPase regulatory subunit 6	PSMD6	DNNMAPYYEALCK	0.93	-0.10
474	P10599	TXN Thioredoxin	TXN	LVVVDFSATWCGPCK	0.93	-0.10
475	Q9Y3D2	MSRB2 Methionine-R-sulfoxide reductase B2, mitochondrial	MSRB2	YCSGTGWPSFSEAHGTSGSDESHTGILR	0.93	-0.10
476	P13489	RNH1 Ribonuclease inhibitor	RNH1	DLCGIVASK	0.93	-0.10
477	O75153	CLUH Clustered mitochondria protein homolog	CLUH	CLTQQAVALQR	0.94	-0.10
478	P46527	CDKN1B Cyclin-dependent kinase inhibitor 1B	CDKN1B	TDPSDSQTGLAEQCAGIR	0.94	-0.10
479	P38117	ETFB Electron transfer flavoprotein subunit beta	ETFB	EVIAVSCGPAQCQETIR	0.94	-0.09
480	P14618	PKM Pyruvate kinase PKM	PKM	CDENILWLDYK	0.94	-0.09
481	P18085	ARF4 ADP-ribosylation factor 4	ARF4	NICFTVWDVGGQDR	0.94	-0.09
482	Q15796	SMAD2 Mothers against decapentaplegic homolog 2	SMAD2	AITTQNCNTK	0.94	-0.09
483	P34897	SHMT2 Serine hydroxymethyltransferase, mitochondrial	SHMT2	GLELIASENFCSR	0.94	-0.09
484	Q9Y5P6	GMPPB Mannose-1-phosphate guanyltransferase beta	GMPPB	LCSGPGIVGNVLVDPSAR	0.94	-0.09
485	Q9Y3A3	MOB4 MOB-like protein phocein	MOB4	HTLDGAACLLNSNK	0.94	-0.09
486	P26196	DDX6 Probable ATP-dependent RNA helicase DDX6	DDX6	GNEFEDYCLK	0.94	-0.08

487	O15382	BCAT2 Branched-chain-amino-acid aminotransferase, mitoch	BCAT2	EVFGSGTACQVCPVHR	0.94	-0.08
488	Q9Y508	RNF114 E3 ubiquitin-protein ligase RNF114	RNF114	DCGGAAQLAGPAAEADPLGR	0.94	-0.08
489	Q9UI30	TRMT112 Multifunctional methyltransferase subunit TRM112-l	TRMT112	ICPVEFNPNFVAR	0.94	-0.08
490	Q8N335	GPD1L Glycerol-3-phosphate dehydrogenase 1-like protein	GPD1L	ICDEITGR	0.95	-0.08
491	Q9UPN9	TRIM33 E3 ubiquitin-protein ligase TRIM33	TRIM33	CDPVPAANGAIR	0.95	-0.08
492	Q9NYL2	MAP3K20 Mitogen-activated protein kinase 20	MAP3K20	FDDLQFFENCGGGSFGSVYR	0.95	-0.08
493	Q9P1F3	ABRACL Costars family protein ABRACL	ABRACL	CANLFEALVGTLK	0.95	-0.08
494	Q9NQR4	NIT2 Omega-amidase NIT2	NIT2	TLSPGDSFSTFDTPYCR	0.95	-0.07
495	Q9HCC0	MCCC2 Methylcrotonoyl-CoA carboxylase beta chain, mitoch	MCCC2	LPCIYLVDSGGAYLPR	0.95	-0.07
496	P53396	ACLY ATP-citrate synthase	ACLY	FICTTSAIQNR	0.95	-0.07
497	P12004	PCNA Proliferating cell nuclear antigen	PCNA	DLSHIGDAVVISCAK	0.96	-0.07
498	P49327	FASN Fatty acid synthase	FASN	ADEASELACPTPK	0.96	-0.07
499	O00233	PSMD9 26S proteasome non-ATPase regulatory subunit 9	PSMD9	GIGMNEPLVDCEGYPR	0.96	-0.06
500	P57081	WDR4 tRNA (guanine-N(7)-)-methyltransferase non-catalytic	WDR4	SGDVYSFSVLEPHGCGR	0.96	-0.06
501	P31943	HNRNPH1 Heterogeneous nuclear ribonucleoprotein H	HNRNPH1	GLPFGCSK	0.96	-0.06
502	O95336	PGLS 6-phosphogluconolactonase	PGLS	LCWFLDEAAAR	0.96	-0.06
503	O43765	SGTA Small glutamine-rich tetratricopeptide repeat-cont	SGTA	AIELNPANAVYFCNR	0.96	-0.06
504	P49419	ALDH7A1 Alpha-aminoadipic semialdehyde dehydrogenase	ALDH7A1	GEVITTYCPANNEPIAR	0.96	-0.06
505	Q5VZ89	DENND4C DENN domain-containing protein 4C	DENND4C	CANVNNSSTTSQR	0.96	-0.06
506	Q92905	COPS5 COP9 signalosome complex subunit 5	COPS5	IEDFGVHCK	0.96	-0.06
507	P05198	EIF2S1 Eukaryotic translation initiation factor 2 subunit	EIF2S1	AGLNCSTENMPIK	0.96	-0.06

508	Q9BWJ5	SF3B5 Splicing factor 3B subunit 5	SF3B5	MLQPCGPPADK	0.96	-0.06
509	P26599	PTBP1 Polypyrimidine tract-binding protein 1	PTBP1	LSLDGQNIYNACCTLR	0.96	-0.06
510	P63010	AP2B1 AP-2 complex subunit beta	AP2B1	DCEDPNPLIR	0.96	-0.05
511	P18031	PTPN1 Tyrosine-protein phosphatase non-receptor type 1	PTPN1	CAQYWPQK	0.96	-0.05
512	Q7Z6Z7	HUWE1 E3 ubiquitin-protein ligase HUWE1	HUWE1	AQCETLSPDGLPEEQPQTTK	0.97	-0.05
513	Q9NX24	NHP2 H/ACA ribonucleoprotein complex subunit 2	NHP2	ADPDGPEAQAEACSGER	0.97	-0.05
514	P11413	G6PD Glucose-6-phosphate 1-dehydrogenase	G6PD	CISEVQANNVVLGQYVGNPDGEGEATK	0.97	-0.05
515	Q7Z4W1	DCXR L-xylulose reductase	DCXR	AVTNHSVYCSTK	0.97	-0.05
516	Q9ULC4	MCTS1 Malignant T-cell-amplified sequence 1	MCTS1	ENVSNCIQLK	0.97	-0.05
517	Q9P289	STK26 Serine/threonine-protein kinase 26	STK26	SIAVAEAACPGITDK	0.97	-0.05
518	Q8TEX9	IPO4 Importin-4	IPO4	APAALPALCDLLASAADPQIR	0.97	-0.05
519	Q9Y265	RUVBL1 RuvB-like 1	RUVBL1	VPFCPMVGSEVYSTEIK	0.97	-0.05
520	P51812	RPS6KA3 Ribosomal protein S6 kinase alpha-3	RPS6KA3	AENGLLMTPCYTANFVAPEVLK	0.97	-0.04
521	P57721	PCBP3 Poly(rC)-binding protein 3	PCBP3	LVVPASQCGSLIGK	0.97	-0.04
522	Q15020	SART3 Squamous cell carcinoma antigen recognized by T-ce	SART3	CAAVDVEPPSK	0.97	-0.04
523	P60900	PSMA6 Proteasome subunit alpha type-6	PSMA6	ITENIGCVMTGMTADSR	0.97	-0.04
524	Q9H3U1	UNC45A Protein unc-45 homolog A	UNC45A	TESPVLTSSCR	0.97	-0.04
525	Q06323	PSME1 Proteasome activator complex subunit 1	PSME1	EDLCTK	0.98	-0.04
526	Q9UJU6	DBNL Drebrin-like protein	DBNL	AEEDVEPECIMEK	0.98	-0.03
527	Q13045	FLII Protein flightless-1 homolog	FLII	TGLCYLPEELAALQK	0.98	-0.03
528	P51858	HDGF Hepatoma-derived growth factor	HDGF	SCVEEPEPEPEAAEGDGDK	0.98	-0.03
529	P60842	EIF4A1 Eukaryotic initiation factor 4A-I	EIF4A1	VVMALGDYMGASCHACIGGTNVR	0.98	-0.03

530	P15924	DSP Desmoplakin	DSP	ELDECFAQANDQMEILDSLIR	0.98	-0.03
531	P23381	WARS Tryptophan--tRNA ligase, cytoplasmic	WARS	ADCPPGNPAPTSNHGPDATEAEEDFVDPWTVQTSSAK	0.98	-0.03
532	P49591	SARS Serine--tRNA ligase, cytoplasmic	SARS	ELVSCSNCTDYQAR	0.98	-0.03
533	O00231	PSMD11 26S proteasome non-ATPase regulatory subunit 11	PSMD11	TTANAIYCPPK	0.98	-0.03
534	P07947	YES1 Tyrosine-protein kinase Yes	YES1	AANILVGENLVCK	0.98	-0.02
535	P14618	PKM Pyruvate kinase PKM	PKM	CCSGAIIVLTK	0.98	-0.02
536	P55795	HNRNPH2 Heterogeneous nuclear ribonucleoprotein H2	HNRNPH2	GLPWSCSADEVMR	0.98	-0.02
537	P62993	GRB2 Growth factor receptor-bound protein 2	GRB2	VLNEECDQNWYK	0.98	-0.02
538	O43390	HNRNPR Heterogeneous nuclear ribonucleoprotein R	HNRNPR	SAFLCGVMK	0.98	-0.02
539	Q14C86	GAPVD1 GTPase-activating protein and VPS9 domain-containing	GAPVD1	FSLCSDNLEGISEGPSNR	0.98	-0.02
540	P49588	AARS Alanine--tRNA ligase, cytoplasmic	AARS	AVYTQDCPLAAAK	0.99	-0.02
541	Q96AE4	FUBP1 Far upstream element-binding protein 1	FUBP1	IQQESGCK	0.99	-0.02
542	P12532	CKMT1A Creatine kinase U-type, mitochondrial	CKMT1A	GLSLPPACTR	0.99	-0.02
543	P35270	SPR Sepiapterin reductase	SPR	AVCLLTGASR	0.99	-0.02
544	P49915	GMPS GMP synthase [glutamine-hydrolyzing]	GMPS	VICAEEPYICK	0.99	-0.02
545	P13489	RNH1 Ribonuclease inhibitor	RNH1	ELDLSNNCLGDAGILQLVESVR	0.99	-0.02
546	Q9UQ80	PA2G4 Proliferation-associated protein 2G4	PA2G4	AAHLCAEAALR	0.99	-0.02
547	Q99873	PRMT1 Protein arginine N-methyltransferase 1	PRMT1	VIGIECSSISDYAVK	0.99	-0.02
548	Q99536	VAT1 Synaptic vesicle membrane protein VAT-1 homolog	VAT1	CLVLTGFGGYDK	0.99	-0.02
549	O43175	PHGDH D-3-phosphoglycerate dehydrogenase	PHGDH	CGEEIAVQFVDMVK	0.99	-0.02
550	Q7Z2Z2	EFL1 Elongation factor-like GTPase 1	EFL1	LAAAQGQAPLEPTQDGSAIETCPK	0.99	-0.01
551	P15924	DSP Desmoplakin	DSP	NQCTQVVQER	0.99	-0.01
552	P35579	MYH9 Myosin-9	MYH9	MEDSVGCLETAEEVK	0.99	-0.01

553	O75821	EIF3G Eukaryotic translation initiation factor 3 subunit	EIF3G	EDLNCQEEEDPMNK	0.99	-0.01
554	P25789	PSMA4 Proteasome subunit alpha type-4	PSMA4	LNEDMACSVAGITSDANVLTNELR	0.99	-0.01
555	Q08211	DHX9 ATP-dependent RNA helicase A	DHX9	LAAQSCALSLVR	0.99	-0.01
556	Q14980	NUMA1 Nuclear mitotic apparatus protein 1	NUMA1	VEELQACVETAR	1.00	-0.01
557	Q1KMD3	HNRNPUL2 Heterogeneous nuclear ribonucleoprotein U-like pro	HNRNPUL2	EGCTEVSLLR	1.00	0.00
558	P30041	PRDX6 Peroxiredoxin-6	PRDX6	DFTPVCTTELGR	1.00	0.00
559	Q9UBB4	ATXN10 Ataxin-10	ATXN10	HAELIASTFVDQCK	1.00	0.00
560	Q9BYT8	NLN Neurolysin, mitochondrial	NLN	IVHLQETCDLGK	1.00	0.00
561	P20700	LMNB1 Lamin-B1	LMNB1	CQSLTEDLEFR	1.00	0.00
562	P53004	BLVRA Biliverdin reductase A	BLVRA	MTVCLETEK	1.00	0.00
563	Q15185	PTGES3 Prostaglandin E synthase 3	PTGES3	HLNEIDLFHCIDPNDSK	1.00	0.00
564	P62826	RAN GTP-binding nuclear protein Ran	RAN	VCENIPIVLCGNK	1.00	0.00
565	O14744	PRMT5 Protein arginine N-methyltransferase 5	PRMT5	DLNCVPEIADTLGAVAK	1.00	0.01
566	Q07866	KLC1 Kinesin light chain 1	KLC1	YEVAVPLCK	1.01	0.01
567	Q13155	AIMP2 Aminoacyl tRNA synthase complex-interacting	AIMP2	VELPTCMYR	1.01	0.01
568	Q8N6M0	OTUD6B OTU domain-containing protein 6B	OTUD6B	DCALTVVALR	1.01	0.01
569	P51610	HCFC1 Host cell factor 1	HCFC1	LVIYGGMSGCR	1.01	0.01
570	P49419	ALDH7A1 Alpha-aminoadipic semialdehyde dehydrogenase	ALDH7A1	GSDCGIVNVNIPTSGAEIGGAFGGEK	1.01	0.01
571	P04632	CAPNS1 Calpain small subunit 1	CAPNS1	TDGFGIDTCR	1.01	0.01
572	P27707	DCK Deoxycytidine kinase	DCK	WCNVQSTQDEFEELTMSQK	1.01	0.02
573	Q9Y2S2	CRYL1 Lambda-crystallin homolog	CRYL1	VILSSSTSCLMPSK	1.01	0.02
574	Q15370	ELOB Elongin-B	ELOB	ADDTFEALCIEPFSSPPELPDVMK	1.01	0.02
575	P63167	DYNLL1 Dynein light chain 1, cytoplasmic	DYNLL1	NADMSEEMQQDSVECATQALEK	1.01	0.02
576	P17676	CEBPB CCAAT/enhancer-binding protein beta	CEBPB	APPTACYAGAAPAPSQVK	1.01	0.02
577	Q13148	TARDBP TAR DNA-binding protein 43	TARDBP	NPVSQCMR	1.01	0.02

578	Q9Y676	MRPS18B 28S ribosomal protein S18b, mitochondrial	MRPS18B	VVGNPCPICR	1.02	0.02
579	Q00765	REEP5 Receptor expression-enhancing protein 5	REEP5	NCMTDLLAK	1.02	0.02
580	P21266	GSTM3 Glutathione S-transferase Mu 3	GSTM3	YTCGEAPDYDR	1.02	0.03
581	O60610	DIAPH1 Protein diaphanous homolog 1	DIAPH1	DMPLLSCLESLR	1.02	0.03
582	O43790	KRT86 Keratin, type II cuticular Hb6	KRT86	DLNMDCIIAEIK	1.02	0.03
583	Q9H2U2	PPA2 Inorganic pyrophosphatase 2, mitochondrial	PPA2	GQPCSQNYR	1.02	0.03
584	O15067	PFAS Phosphoribosylformylglycinamidine synthase	PFAS	FCDNSSAIQGK	1.02	0.03
585	P49321	NASP Nuclear autoantigenic sperm protein	NASP	PTDGASSSNCVTDISHLVR	1.02	0.03
586	P35568	IRS1 Insulin receptor substrate 1	IRS1	CTPGTGLGTSPALAGDEAASAADLDNR	1.02	0.03
587	Q9P258	RCC2 Protein RCC2	RCC2	AVQDLCGWR	1.02	0.03
588	Q2VPK5	CTU2 Cytoplasmic tRNA 2-thiolation protein 2	CTU2	VMTGDSCTR	1.02	0.03
589	Q6P1X6	C8orf82 UPF0598 protein C8orf82	C8orf82	YEAAFPFLSPCGR	1.03	0.04
590	Q9BV79	MECR Enoyl-[acyl-carrier-protein] reductase, mitochondrial	MECR	LALNCVGGK	1.03	0.04
591	P21964	COMT Catechol O-methyltransferase	COMT	LITIEINPDCAAITQR	1.03	0.04
592	Q9NP72	RAB18 Ras-related protein Rab-18	RAB18	LDNWLNELETYCTR	1.03	0.04
593	Q6PI48	DARS2 Aspartate--tRNA ligase, mitochondrial	DARS2	LICLVTGSPSIR	1.03	0.04
594	Q7RTV0	PHF5A PHD finger-like domain-containing protein 5A	PHF5A	PCTLVR	1.03	0.04
595	Q9H1B7	IRF2BPL Interferon regulatory factor 2-binding protein-lik	IRF2BPL	AHGCFQDGR	1.03	0.04
596	P58107	EPPK1 Epiplakin	EPPK1	CVPDPDTGLYMLQLAGR	1.03	0.05
597	P13639	EEF2 Elongation factor 2	EEF2	VTDGALVVVDCVSGVCVQTETVLR	1.03	0.05
598	Q9HA64	FN3KRP Ketosamine-3-kinase	FN3KRP	ATGHSGGGCISQGR	1.04	0.05
599	A6NDU8	C5orf51 UPF0600 protein C5orf51	C5orf51	CPIQLNEGVSFQDLDTAK	1.04	0.05

600	Q93052	LPP Lipoma-preferred partner	LPP	TYITDPVSAPCAPPLQPK	1.04	0.05
601	Q04637	EIF4G1 Eukaryotic translation initiation factor 4 gamma 1	EIF4G1	LQGINCGPDFTPSFANLGR	1.04	0.05
602	Q92879	CELF1 CUGBP Elav-like family member 1	CELF1	AMHQAQTMEGCSSPMVVK	1.04	0.05
603	O00571	DDX3X ATP-dependent RNA helicase DDX3X	DDX3X	WCDK	1.04	0.06
604	P49915	GMPS GMP synthase [glutamine-hydrolyzing]	GMPS	TVGVQGDCR	1.04	0.06
605	P53396	ACLY ATP-citrate synthase	ACLY	PASFMTSICDER	1.04	0.06
606	Q99832	CCT7 T-complex protein 1 subunit eta	CCT7	EGTDSSQGIPQLVSNISACQVIAEAVR	1.04	0.06
607	Q9BTE3	MCMBP Mini-chromosome maintenance complex-binding protei	MCMBP	DASALLDPMECTDTAEEQR	1.04	0.06
608	O43865	AHCYL1 S-adenosylhomocysteine hydrolase-like protein 1	AHCYL1	FDNLYCCR	1.05	0.07
609	P40222	TXLNA Alpha-taxilin	TXLNA	VTEAPCYPGAPSTEASGQTGPQEPTSAR	1.05	0.07
610	Q06323	PSME1 Proteasome activator complex subunit 1	PSME1	GPPC*GPVNC*NEK	1.05	0.07
611	Q14694	USP10 Ubiquitin carboxyl-terminal hydrolase 10	USP10	SSVELPPYSGTVLCGTQAVDK	1.06	0.08
612	Q15233	NONO Non-POU domain-containing octamer-binding protein	NONO	FACHSASLTVR	1.06	0.08
613	Q15003	NCAPH Condensin complex subunit 2	NCAPH	CEIDPMFQK	1.06	0.08
614	A8MT19	RHPN2P1 Putative rhophilin-2-like protein RHPN2P1	RHPN2P1	VLCAAQER	1.06	0.08
615	P52943	CRIP2 Cysteine-rich protein 2	CRIP2	ASSVTTFTGEPNTCPR	1.06	0.08
616	Q9Y2Q3	GSTK1 Glutathione S-transferase kappa 1	GSTK1	ETTEAACR	1.06	0.08
617	P82932	MRPS6 28S ribosomal protein S6, mitochondrial	MRPS6	ECEGIVPVPLAEK	1.06	0.09
618	P42704	LRPPRC Leucine-rich PPR motif-containing protein, mitochondrial	LRPPRC	SCGSLLPELK	1.06	0.09
619	Q9UNE7	STUB1 E3 ubiquitin-protein ligase CHIP	STUB1	YPEAAACYGR	1.06	0.09
620	Q9UNE7	STUB1 E3 ubiquitin-protein ligase CHIP	STUB1	AQQACIEAK	1.07	0.09

621	P53618	COPB1 Coatomer subunit beta	COPB1	VCHANPSER	1.07	0.10
622	Q9H8W4	PLEKHF2 Pleckstrin homology domain-containing family F mem	PLEKHF2	ISIVENCFGAAGQPLTIPGR	1.07	0.10
623	Q9BRA2	TXNDC17 Thioredoxin domain-containing protein 17	TXNDC17	SWCPDCVQAEPVVR	1.07	0.10
624	P78406	RAE1 mRNA export factor	RAE1	APNYSCVMTGSWDK	1.07	0.10
625	Q9BRA2	TXNDC17 Thioredoxin domain-containing protein 17	TXNDC17	SWC*PDC*VQAEPVVR	1.07	0.10
626	Q676U5	ATG16L1 Autophagy-related protein 16-1	ATG16L1	IAECLQTISDLETECLDLR	1.07	0.10
627	Q06203	PPAT Amidophosphoribosyltransferase	PPAT	CELENCQPFVVETLHGK	1.07	0.10
628	O94979	SEC31A Protein transport protein Sec31A	SEC31A	SDQLQQAVQSQGFINYCQK	1.07	0.10
629	P38117	ETFB Electron transfer flavoprotein subunit beta	ETFB	HSMNPFCEIAVEEAVR	1.08	0.11
630	P49841	GSK3B Glycogen synthase kinase-3 beta	GSK3B	TTSFAESCK	1.08	0.11
631	O00148	DDX39A ATP-dependent RNA helicase DDX39A	DDX39A	AIVDCGFEHPSEVQHECIPQAILGMDVLCQAK	1.08	0.11
632	P40926	MDH2 Malate dehydrogenase, mitochondrial	MDH2	GYLGPEQLPDCLK	1.08	0.11
633	O00232	PSMD12 26S proteasome non-ATPase regulatory subunit 12	PSMD12	AIYDTPCIQAESEK	1.09	0.12
634	P30050	RPL12 60S ribosomal protein L12	RPL12	CTGGEVGATSALAPK	1.09	0.12
635	P60763	RAC3 Ras-related C3 botulinum toxin substrate 3	RAC3	AVLCPPPVK	1.09	0.13
636	Q7L2J0	MEPCE 7SK snRNA methylphosphate capping enzyme	MEPCE	CAPSAGSPAAAVGR	1.09	0.13
637	Q13263	TRIM28 Transcription intermediary factor 1-beta	TRIM28	HEPLVLFCESCDTLTCR	1.09	0.13
638	P32322	PYCR1 Pyrroline-5-carboxylate reductase 1, mitochondrial	PYCR1	SLLINAVEASCIR	1.09	0.13
639	P58107	EPPK1 Epiplakin	EPPK1	LLDAQLATGGLVCPAR	1.09	0.13
640	Q9BX63	BRIP1 Fanconi anemia group J protein	BRIP1	LANNSDCILAK	1.10	0.13

641	P34932	HSPA4 Heat shock 70 kDa protein 4	HSPA4	LMSANASDLPLSIECFMNDVDVSGTMNR	1.10	0.13
642	P21266	GSTM3 Glutathione S-transferase Mu 3	GSTM3	IAAYLQSDQFCK	1.10	0.14
643	A6NDG6	PGP Glycerol-3-phosphate phosphatase	PGP	NNQESDCVSK	1.10	0.14
644	P60709	ACTB Actin, cytoplasmic 1	ACTB	CPEALFQPSFLGMESCGIHETTFNSIMK	1.10	0.14
645	P48643	CCT5 T-complex protein 1 subunit epsilon	CCT5	EMNPALGIDCLHK	1.10	0.14
646	Q9HCC0	MCCC2 Methylcrotonoyl-CoA carboxylase beta chain, mitoch	MCCC2	MVAAVACAQVPK	1.11	0.15
647	O14929	HAT1 Histone acetyltransferase type B catalytic subunit	HAT1	VDENFDCVEADDVEGK	1.11	0.15
648	P49327	FASN Fatty acid synthase	FASN	CVLLSNLSSTSHVPEVDPGSAELQK	1.11	0.15
649	Q9UHD8	SEPT9 Septin-9	9-Sep	SQEATEAAPSCVGDMADTPR	1.11	0.16
650	Q13148	TARDBP TAR DNA-binding protein 43	TARDBP	VTEDENDEPIEIPSEDDGTVLLSTVTAQFPGACGLR	1.11	0.16
651	Q9Y4L1	HYOU1 Hypoxia up-regulated protein 1	HYOU1	VEFEELCADLFER	1.12	0.16
652	Q7Z4V5	HDGFL2 Hepatoma-derived growth factor-related protein 2	HDGFL2	CGSSEDLHDSVR	1.12	0.16
653	Q5RKV6	EXOSC6 Exosome complex component MTR3	EXOSC6	APPGGCEER	1.12	0.17
654	Q14566	MCM6 DNA replication licensing factor MCM6	MCM6	LGFSEYCR	1.12	0.17
655	P07384	CAPN1 Calpain-1 catalytic subunit	CAPN1	LEICNLTPDALK	1.12	0.17
656	P61247	RPS3A 40S ribosomal protein S3a	RPS3A	ACQSIYPLHDVFVR	1.13	0.17
657	Q8NDH3	NPEPL1 Probable aminopeptidase NPEPL1	NPEPL1	IVDTPCNEMNTDTFLEEINK	1.13	0.18
658	Q9UBF2	COPG2 Coatomer subunit gamma-2	COPG2	VVVVQAISALCQK	1.13	0.18
659	Q9NS86	LANCL2 LanC-like protein 2	LANCL2	VTCDQTYLLR	1.14	0.18
660	P49327	FASN Fatty acid synthase	FASN	AFDTAGNGYCR	1.14	0.18
661	P38117	ETFB Electron transfer flavoprotein subunit beta	ETFB	EVIAVSC*GPAQC*QETIR	1.14	0.18
662	Q9BRP1	PDCD2L Programmed cell death protein 2-like	PDCD2L	YSWSGEPLFLTCPTSEVTELPACSQCGGQR	1.14	0.19

663	P35658	NUP214 Nuclear pore complex protein Nup214	NUP214	ACFQVGTSEEMK	1.14	0.19
664	P62714	PPP2CB Serine/threonine-protein phosphatase 2A catalytic	PPP2CB	CGNQAAIMELDDTLK	1.14	0.19
665	O95671	ASMTL N-acetylserotonin O-methyltransferase-like protein	ASMTL	AEAGEAGQATAEAECHR	1.14	0.19
666	Q9BUH6	C9orf142 Protein PAXX	C9orf142	CPGESLINPGFK	1.15	0.20
667	P49327	FASN Fatty acid synthase	FASN	DGLLENQTPEFFQDVCK	1.15	0.20
668	Q9Y295	DRG1 Developmentally-regulated GTP-binding protein 1	DRG1	GGINLTATCPQSELDAETVK	1.15	0.20
669	P60866	RPS20 40S ribosomal protein S20	RPS20	TPCGEGSK	1.15	0.20
670	P21964	COMT Catechol O-methyltransferase	COMT	GSSCFECTHYQSFLEYR	1.15	0.20
671	O95433	AHSA1 Activator of 90 kDa heat shock protein ATPase homo	AHSA1	NGETELCMEGR	1.15	0.21
672	Q96PK6	RBM14 RNA-binding protein 14	RBM14	IFVGNVDGADTTPEELAALFAPYGTVMSCAVMK	1.15	0.21
673	Q9Y3F4	STRAP Serine-threonine kinase receptor-associated protei	STRAP	IGFPETTEEELEEIASENSDCIFPSAPDVK	1.16	0.21
674	Q96T51	RUFY1 RUN and FYVE domain-containing protein 1	RUFY1	LCPEASDIATSVR	1.16	0.21
675	Q9UBF6	RNF7 RING-box protein 2	RNF7	VQVMDACLR	1.16	0.22
676	Q12959	DLG1 Disks large homolog 1	DLG1	LLAVNNVCLEEVTHEEAVTALK	1.16	0.22
677	P10809	HSPD1 60 kDa heat shock protein, mitochondrial	HSPD1	CEFQDAYVLLSEK	1.16	0.22
678	Q15149	PLEC Plectin	PLEC	VLSSSGSEAAVPSVCFLVPPPNQEAQEAVTR	1.16	0.22
679	O43175	PHGDH D-3-phosphoglycerate dehydrogenase	PHGDH	NAGNCLSPAVIVGLLK	1.17	0.22
680	O95336	PGLS 6-phosphogluconolactonase	PGLS	AACCLAGAR	1.17	0.22
681	P78406	RAE1 mRNA export factor	RAE1	VFTASCDK	1.17	0.22
682	Q6KB66	KRT80 Keratin, type II cytoskeletal 80	KRT80	DLDAECLHR	1.17	0.23

683	P62195	PSMC5 26S proteasome regulatory subunit 8	PSMC5	NIDINDVTPNCR	1.17	0.23
684	O75940	SMNDC1 Survival of motor neuron-related-splicing factor 3	SMNDC1	VGVGTCGIADK	1.17	0.23
685	P17987	TCP1 T-complex protein 1 subunit alpha	TCP1	SLHDALCVVK	1.17	0.23
686	P31943	HNRNPH1 Heterogeneous nuclear ribonucleoprotein H	HNRNPH1	GLPWSCSADEVQR	1.17	0.23
687	P42704	LRPPRC Leucine-rich PPR motif-containing protein, mitochondrial	LRPPRC	AILQENGCLSDSDMFSQAGLR	1.18	0.23
688	Q9UHB9	SRP68 Signal recognition particle subunit SRP68	SRP68	FETFCLDPSLVTK	1.18	0.23
689	P07814	EPRS Bifunctional glutamate/proline--tRNA ligase	EPRS	PTPSLNNNCTTSEDSLVLYNR	1.18	0.24
690	P13639	EEF2 Elongation factor 2	EEF2	STLTDSLVCK	1.18	0.24
691	Q96HP0	DOCK6 Dedicator of cytokinesis protein 6	DOCK6	AGCALSAESSR	1.18	0.24
692	O43252	PAPSS1 Bifunctional 3-phosphoadenosine 5-phosphosulfate	PAPSS1	GCTVWLTGLSGAGK	1.18	0.24
693	Q9UBT2	UBA2 SUMO-activating enzyme subunit 2	UBA2	VLVVGAGGIGCELLK	1.18	0.24
694	Q8TEX9	IPO4 Importin-4	IPO4	ACQSCPSEPNTAALQAALAR	1.19	0.25
695	P62241	RPS8 40S ribosomal protein S8	RPS8	LDVGNFSWGSECCTR	1.19	0.25
696	Q9P2T1	GMPR2 GMP reductase 2	GMPR2	VGIGPGSVCTTR	1.19	0.25
697	Q8TCU6	PREX1 Phosphatidylinositol 3,4,5-trisphosphate-dependent	PREX1	LGACQMVMCGTGMQR	1.19	0.25
698	P56545	CTBP2 C-terminal-binding protein 2	CTBP2	DCTVEMPILK	1.19	0.26
699	Q96AT9	RPE Ribulose-phosphate 3-epimerase	RPE	IGPSILNSDLANLGAECLR	1.20	0.26
700	P33316	DUT Deoxyuridine 5-triphosphate nucleotidohydrolase,	DUT	IAQLICER	1.20	0.26
701	O43175	PHGDH D-3-phosphoglycerate dehydrogenase	PHGDH	ALQSGQCAGAALDVFTEEPPR	1.20	0.26
702	P09110	ACAA1 3-ketoacyl-CoA thiolase, peroxisomal	ACAA1	PEQLGDICVGNVLQPGAGAIMAR	1.20	0.26
703	O76003	GLRX3 Glutaredoxin-3	GLRX3	ELEASEELDTICPK	1.20	0.27
704	P67936	TPM4 Tropomyosin alpha-4 chain	TPM4	EENVGLHQTLDQTLNELNCI	1.21	0.27

705	P25205	MCM3 DNA replication licensing factor MCM3	MCM3	SVHYCPATK	1.21	0.27
706	P38606	ATP6V1A V-type proton ATPase catalytic subunit A	ATP6V1A	VLDALFPCVQGGTTAIPGAFGCGK	1.21	0.27
707	O75934	BCAS2 Pre-mRNA-splicing factor SPF27	BCAS2	IENLELMSQHGCNAWK	1.21	0.27
708	Q14980	NUMA1 Nuclear mitotic apparatus protein 1	NUMA1	QFCSTQAALQAMER	1.21	0.28
709	Q16822	PCK2 Phosphoenolpyruvate carboxykinase [GTP], mitochond	PCK2	YVAAAFPSACGK	1.21	0.28
710	Q9NQR4	NIT2 Omega-amidase NIT2	NIT2	IVSLPECFNSPYGAK	1.21	0.28
711	Q13185	CBX3 Chromobox protein homolog 3	CBX3	LTWHSCPEDEAQ	1.22	0.28
712	Q8N163	CCAR2 Cell cycle and apoptosis regulator protein 2	CCAR2	VVTQNICQYR	1.22	0.28
713	P62714	PPP2CB Serine/threonine-protein phosphatase 2A catalytic	PPP2CB	NVVTIFSAPNYCYR	1.22	0.29
714	Q8TCU6	PREX1 Phosphatidylinositol 3,4,5-trisphosphate-dependent	PREX1	CLPAAEGDPQGQGLHDGSFGPASGTLGQEDR	1.22	0.29
715	Q9UJX3	ANAPC7 Anaphase-promoting complex subunit 7	ANAPC7	PSTGNSASTPQSQCLPSEIEVK	1.22	0.29
716	O15355	PPM1G Protein phosphatase 1G	PPM1G	GTEAGQVGEPGIPTGEAGPSCSSASDK	1.22	0.29
717	Q16576	RBBP7 Histone-binding protein RBBP7	RBBP7	VHIPNDDAQFDASHCDSDK	1.22	0.29
718	Q00535	CDK5 Cyclin-dependent-like kinase 5	CDK5	ISAEEALQHPYFSDFCPP	1.23	0.30
719	P00367	GLUD1 Glutamate dehydrogenase 1, mitochondrial	GLUD1	CAVVDVPFGGAK	1.23	0.30
720	O75390	CS Citrate synthase, mitochondrial	CS	LPCVAAK	1.23	0.30
721	Q15181	PPA1 Inorganic pyrophosphatase	PPA1	CDPDAAR	1.23	0.30
722	Q7Z2W4	ZC3HAV1 Zinc finger CCCH-type antiviral protein 1	ZC3HAV1	NSNVDSSYLESLYQSCPR	1.23	0.30
723	Q16186	ADRM1 Proteasomal ubiquitin receptor ADRM1	ADRM1	VPQCPSGR	1.24	0.31
724	Q14166	TTLL12 Tubulin--tyrosine ligase-like protein 12	TTLL12	VMQPQILEVNFNPDCER	1.24	0.31
725	P08708	RPS17 40S ribosomal protein S17	RPS17	VCEEIAIIPSK	1.24	0.31

726	P16455	MGMT Methylated-DNA--protein-cysteine methyltransferase	MGMT	VVCSSGAVGNYSGGLAVK	1.24	0.31
727	O75369	FLNB Filamin-B	FLNB	MDGTYACSYTPVK	1.24	0.31
728	O60502	MGEA5 Protein O-GlcNAcase	MGEA5	ANSSVVSVNCK	1.25	0.32
729	Q9H0C8	ILKAP Integrin-linked kinase-associated serine/threonine	ILKAP	CGVTSVPDIR	1.25	0.32
730	P49458	SRP9 Signal recognition particle 9 kDa protein	SRP9	HSDGNLCVK	1.25	0.32
731	Q5VYK3	ECM29 Proteasome-associated protein ECM29 homolog	ECM29	ESSCLALNDLLR	1.25	0.32
732	Q27J81	INF2 Inverted formin-2	INF2	AVLLASDAQECTLEEVVER	1.25	0.32
733	Q15181	PPA1 Inorganic pyrophosphatase	PPA1	GISCMNTTLSESPFK	1.25	0.32
734	P49327	FASN Fatty acid synthase	FASN	LGMLSPEGTCK	1.26	0.33
735	Q9C0C2	TNKS1BP1 182 kDa tankyrase-1-binding protein	TNKS1BP1	NMAPGAVCSPGESK	1.26	0.33
736	P45984	MAPK9 Mitogen-activated protein kinase 9	MAPK9	TACTNFMMTPYVVTR	1.26	0.34
737	Q7L5Y1	ENOSF1 Mitochondrial enolase superfamily member 1	ENOSF1	ALQFLQIDSCR	1.27	0.34
738	P55060	CSE1L Exportin-2	CSE1L	LLTECPPMMDTEYTK	1.27	0.34
739	P31943	HNRNPH1 Heterogeneous nuclear ribonucleoprotein H	HNRNPH1	DLNYCFSGMSDHR	1.27	0.34
740	P55769	SNU13 NHP2-like protein 1	SNU13	LLDLVQQSCNYK	1.27	0.34
741	P0DMM9	SULT1A3 Sulfotransferase 1A3	SULT1A3	MAGCSLSFR	1.27	0.34
742	P62191	PSMC1 26S proteasome regulatory subunit 4	PSMC1	AICTEAGLMALR	1.27	0.35
743	P38646	HSPA9 Stress-70 protein, mitochondrial	HSPA9	GAVVGIDLGTTNSCVAVMEGK	1.28	0.36
744	P13489	RNH1 Ribonuclease inhibitor	RNH1	LDDCGLTEAR	1.28	0.36
745	P48643	CCT5 T-complex protein 1 subunit epsilon	CCT5	MLVIEQCK	1.29	0.36
746	Q9Y2R9	MRPS7 28S ribosomal protein S7, mitochondrial	MRPS7	NCEPMIGLVPILK	1.29	0.36
747	Q9HCC0	MCCC2 Methylcrotonoyl-CoA carboxylase beta chain, mitoch	MCCC2	AATGEEVSAEDLGGADLHCR	1.29	0.36
748	P46782	RPS5 40S ribosomal protein S5	RPS5	VNQAIWLLCTGAR	1.29	0.36

749	O94979	SEC31A Protein transport protein Sec31A	SEC31A	SCATFSSSHR	1.29	0.37
750	P55060	CSE1L Exportin-2	CSE1L	SQICDNAALYAQK	1.29	0.37
751	P37198	NUP62 Nuclear pore glycoprotein p62	NUP62	DIIEHLNTSGAPADTSDPLQQICK	1.29	0.37
752	Q13155	AIMP2 Aminoacyl tRNA synthase complex-interacting	AIMP2	SCENLAPFNTALK	1.29	0.37
753	Q6YN16	HSDL2 Hydroxysteroid dehydrogenase-like protein 2	HSDL2	TAIHTAAMDMLGGPGIESQCR	1.30	0.37
754	P34897	SHMT2 Serine hydroxymethyltransferase, mitochondrial	SHMT2	NTCPGDR	1.30	0.38
755	P61247	RPS3A 40S ribosomal protein S3a	RPS3A	LFCVGFTK	1.31	0.39
756	P13489	RNH1 Ribonuclease inhibitor	RNH1	WAELLPLLQQCQVVR	1.31	0.39
757	P58107	EPPK1 Epiplakin	EPPK1	YLCGLGAVGGVR	1.31	0.39
758	P48735	IDH2 Isocitrate dehydrogenase [NADP], mitochondrial	IDH2	SSGGFVWACK	1.32	0.40
759	P38117	ETFB Electron transfer flavoprotein subunit beta	ETFB	QAIDDDCNQTGQMTAGFLDWPQGTFASQVTLEGDK	1.32	0.40
760	P54577	YARS Tyrosine--tRNA ligase, cytoplasmic	YARS	AFCEPGNVENNGVLSFIK	1.32	0.40
761	Q9UMS0	NFU1 iron-sulfur cluster scaffold homolog, mitochondrial	NFU1	LQGSCTSCPSSIITLK	1.32	0.40
762	P43686	PSMC4 26S proteasome regulatory subunit 6B	PSMC4	ISGADINSICQESGMLAVR	1.32	0.41
763	P25398	RPS12 40S ribosomal protein S12	RPS12	LVEALCAEHQINLIK	1.33	0.41
764	Q08211	DHX9 ATP-dependent RNA helicase A	DHX9	SSVNCPFSSQDMK	1.33	0.42
765	O60701	UGDH UDP-glucose 6-dehydrogenase	UGDH	ASVGFGGSCFQK	1.34	0.42
766	Q5T0W9	FAM83B Protein FAM83B	FAM83B	SCVPSSFAQEESAR	1.34	0.42
767	P22314	UBA1 Ubiquitin-like modifier-activating enzyme 1	UBA1	VLGPYTFSICDTSNFSDYIR	1.34	0.42
768	P68104	EEF1A1 Elongation factor 1-alpha 1	EEF1A1	NMITGTSQADCAVLIVAAGVGEFEAGISK	1.34	0.42
769	P28838	LAP3 Cytosol aminopeptidase	LAP3	SAGACTAAAFLK	1.34	0.43

770	P15924	DSP Desmoplakin	DSP	LENINGVTDGYLNSLCTVR	1.35	0.43
771	Q15185	PTGES3 Prostaglandin E synthase 3	PTGES3	LTFSCLGGSDNFK	1.35	0.43
772	P62888	RPL30 60S ribosomal protein L30	RPL30	VCTLAIIDPGDSDIIR	1.35	0.43
773	Q9Y6K5	OAS3 2-5-oligoadenylate synthase 3	OAS3	QDCFNMAQGFR	1.35	0.43
774	P54886	ALDH18A1 Delta-1-pyrroline-5-carboxylate synthase	ALDH18A1	GDECGLALGR	1.35	0.44
775	Q9P2R7	SUCLA2 Succinate--CoA ligase [ADP-forming] subunit beta,	SUCLA2	ICNQVLVCER	1.36	0.44
776	P07814	EPRS Bifunctional glutamate/proline--tRNA ligase	EPRS	LGVENCYFPMFVSQSALEK	1.36	0.44
777	A6NCN2	KRT87P Putative keratin-87 protein	KRT87P	QDMACLIR	1.36	0.44
778	Q9NUU7	DDX19A ATP-dependent RNA helicase DDX19A	DDX19A	VLVTTNVCAR	1.36	0.44
779	P34932	HSPA4 Heat shock 70 kDa protein 4	HSPA4	CTPACISFGPK	1.36	0.44
780	O75150	RNF40 E3 ubiquitin-protein ligase BRE1B	RNF40	EIQPCLAESR	1.36	0.45
781	Q9NQC3	RTN4 Reticulon-4	RTN4	YSNSALGHVNCTIK	1.36	0.45
782	O94885	SASH1 SAM and SH3 domain-containing protein 1	SASH1	CGIPEALVQR	1.37	0.45
783	P80404	ABAT 4-aminobutyrate aminotransferase, mitochondrial	ABAT	TMGCLATTHSK	1.37	0.46
784	P08559	PDHA1 Pyruvate dehydrogenase E1 component subunit alpha,	PDHA1	VDGMDILCVR	1.38	0.46
785	P17987	TCP1 T-complex protein 1 subunit alpha	TCP1	GANDFMCDEMER	1.38	0.47
786	Q16822	PCK2 Phosphoenolpyruvate carboxykinase [GTP], mitochond	PCK2	QCPIMDPAWEAPEGVPIDAIIFGGR	1.39	0.47
787	Q27J81	INF2 Inverted formin-2	INF2	CPASEPGLDATTASESR	1.39	0.48
788	Q16555	DPYSL2 Dihydropyrimidinase-related protein 2	DPYSL2	AITIANQTNCPLYITK	1.39	0.48
789	Q9NQT5	EXOSC3 Exosome complex component RRP40	EXOSC3	LLAPDCEIIQEVGK	1.39	0.48

790	Q9UL25	RAB21 Ras-related protein Rab-21	RAB21	VVLLGEGCVGK	1.39	0.48
791	P82933	MRPS9 28S ribosomal protein S9, mitochondrial	MRPS9	LLTSQCGAAEEEFVQR	1.40	0.48
792	Q6P474	PDXDC2P Putative pyridoxal-dependent decarboxylase domain-	PDXDC2P	QLVPASGLTVMDLEAEGTCLR	1.40	0.48
793	P10809	HSPD1 60 kDa heat shock protein, mitochondrial	HSPD1	CIPALDSLTPANEDQK	1.40	0.48
794	Q9BU89	DOHH Deoxyhypusine hydroxylase	DOHH	PACLAALQAHADDPER	1.40	0.49
795	Q00610	CLTC Clathrin heavy chain 1	CLTC	IHEGCEEPATHNALAK	1.41	0.49
796	P62316	SNRPD2 Small nuclear ribonucleoprotein Sm D2	SNRPD2	HCNMVLENVK	1.41	0.49
797	Q86VY4	TSPYL5 Testis-specific Y-encoded-like protein 5	TSPYL5	APETCSTAGR	1.41	0.49
798	Q16555	DPYSL2 Dihydropyrimidinase-related protein 2	DPYSL2	GLYDGPVCEVSVTPK	1.41	0.50
799	Q5T4S7	UBR4 E3 ubiquitin-protein ligase UBR4	UBR4	HTACNEQQR	1.41	0.50
800	P46782	RPS5 40S ribosomal protein S5	RPS5	TIAECLADELINAAK	1.42	0.50
801	P49902	NT5C2 Cytosolic purine 5-nucleotidase	NT5C2	YTSCETGFK	1.42	0.50
802	P30626	SRI Sorcin	SRI	DTAQQGVVNFPYDDFIQCVMSV	1.42	0.50
803	Q9Y285	FARSA Phenylalanine--tRNA ligase alpha subunit	FARSA	VNLQMVYDSPLCR	1.42	0.51
804	P21333	FLNA Filamin-A	FLNA	THEAEIVEGENHTYCIR	1.42	0.51
805	Q6AI08	HEATR6 HEAT repeat-containing protein 6	HEATR6	SSDMDDITFCMLLQNALK	1.42	0.51
806	P62714	PPP2CB Serine/threonine-protein phosphatase 2A catalytic	PPP2CB	LQEVPHEGPMCDLLWSDPDDR	1.43	0.51
807	P48556	PSMD8 26S proteasome non-ATPase regulatory subunit 8	PSMD8	CGEELGR	1.43	0.51
808	P34897	SHMT2 Serine hydroxymethyltransferase, mitochondrial	SHMT2	AALEALGSCLNNK	1.43	0.52
809	P23396	RPS3 40S ribosomal protein S3	RPS3	GLCAIAQAESLR	1.43	0.52
810	P50991	CCT4 T-complex protein 1 subunit delta	CCT4	TLSGMESYCVR	1.44	0.53
811	Q99832	CCT7 T-complex protein 1 subunit eta	CCT7	CAMTALSSK	1.44	0.53

812	P60981	DSTN Destrin	DSTN	HECQANGPEDLNR	1.44	0.53
813	P22102	GART Trifunctional purine biosynthetic protein adenosin	GART	QVLVAPGNAGTACSEK	1.45	0.53
814	P07814	EPRS Bifunctional glutamate/proline--tRNA ligase	EPRS	INEAVECLLSLK	1.46	0.54
815	Q92616	GCN1 eIF-2-alpha kinase activator GCN1	GCN1	CLQNPSSDIR	1.46	0.54
816	Q15631	TSN Translin	TSN	ETAAACVEK	1.46	0.55
817	P19367	HK1 Hexokinase-1	HK1	TVCGVVSR	1.47	0.55
818	Q9NP73	ALG13 Putative bifunctional UDP-N-acetylglucosamine tran	ALG13	ADLVISHAGAGSCLETLEK	1.47	0.56
819	Q9UHD8	SEPT9 Septin-9	9-Sep	LTVIDTPGFGDHINNENCWQPIMK	1.47	0.56
820	Q9H6T0	ESRP2 Epithelial splicing regulatory protein 2	ESRP2	AEAAALSTQCR	1.48	0.56
821	P22102	GART Trifunctional purine biosynthetic protein adenosin	GART	LLEGDGGPNTGGMGAYCPAPQVSNDLLLK	1.48	0.57
822	O15027	SEC16A Protein transport protein Sec16A	SEC16A	TEAYEYAQSLGAETCPLPSFQVFK	1.48	0.57
823	P06865	HEXA Beta-hexosaminidase subunit alpha	HEXA	GVQAQPLNVGFCEQEFEQT	1.48	0.57
824	P83881	RPL36A 60S ribosomal protein L36a	RPL36A	LECVEPNCR	1.49	0.57
825	Q14152	EIF3A Eukaryotic translation initiation factor 3 subunit	EIF3A	NICQQVNIK	1.49	0.57
826	P55060	CSE1L Exportin-2	CSE1L	ICAVGITK	1.49	0.58
827	P62333	PSMC6 26S proteasome regulatory subunit 10B	PSMC6	GCLLYGPPGTGK	1.50	0.58
828	P36578	RPL4 60S ribosomal protein L4	RPL4	SGQGAFGNMCR	1.50	0.59
829	Q9Y3L5	RAP2C Ras-related protein Rap-2c	RAP2C	ALAQEWGCPFMETSAK	1.51	0.59
830	P78406	RAE1 mRNA export factor	RAE1	CWEVQDSGQTIPK	1.51	0.60
831	Q92598	HSPH1 Heat shock protein 105 kDa	HSPH1	SVLDAAQIVGLNCLR	1.51	0.60
832	P15880	RPS2 40S ribosomal protein S2	RPS2	GCTATLGNFAK	1.51	0.60
833	Q96QR8	PURB Transcriptional activator protein Pur-beta	PURB	GGGGGPCGFQPASR	1.52	0.60
834	P30519	HMOX2 Heme oxygenase 2	HMOX2	GALEGSSCPFR	1.52	0.60
835	P31153	MAT2A S-adenosylmethionine synthase isoform type-2	MAT2A	TCNVLVALEQQSPDIAQGVHLDR	1.52	0.61
836	Q9UN37	VPS4A Vacuolar protein sorting-associated protein	VPS4A	LLEPVVCMSDMLR	1.52	0.61

		4A				
837	P62316	SNRPD2 Small nuclear ribonucleoprotein Sm D2	SNRPD2	NNTQVLINCR	1.53	0.61
838	Q96CM8	ACSF2 Acyl-CoA synthetase family member 2, mitochondrial	ACSF2	MVSTPIGGLSYVQGCTK	1.54	0.63
839	Q6P996	PDXDC1 Pyridoxal-dependent decarboxylase domain-containing	PDXDC1	HSCDALNR	1.55	0.63
840	P26641	EEF1G Elongation factor 1-gamma	EEF1G	FPEELTQTFMSCNLITGMFQR	1.56	0.64
841	Q8TCU6	PREX1 Phosphatidylinositol 3,4,5-trisphosphate-dependent	PREX1	LCVLNEILGTER	1.56	0.64
842	B5ME19	EIF3CL Eukaryotic translation initiation factor 3 subunit	EIF3CL	GCILTLVER	1.57	0.65
843	P15924	DSP Desmoplakin	DSP	ETQTECEWTVDTSK	1.57	0.65
844	P68363	TUBA1B Tubulin alpha-1B chain	TUBA1B	YMACCLLYR	1.57	0.65
845	Q86U28	ISCA2 Iron-sulfur cluster assembly 2 homolog, mitochondrial	ISCA2	SSFQVLNNPQAQQGCSCGSSFSIK	1.57	0.65
846	Q96I99	SUCLG2 Succinate--CoA ligase [GDP-forming] subunit beta,	SUCLG2	SCNGPVLVGSPQGGVDIEEVAASNPELIFK	1.57	0.65
847	Q1KMD3	HNRNPUL2 Heterogeneous nuclear ribonucleoprotein U-like pro	HNRNPUL2	CDYMDEVTYGELEK	1.57	0.65
848	P56192	MARS Methionine--tRNA ligase, cytoplasmic	MARS	LFVSDGVPGCLPVLAAAGR	1.58	0.66
849	Q86UU0	BCL9L B-cell CLL/lymphoma 9-like protein	BCL9L	TGNGGAQSQHQNVNQGPTCNVGSK	1.58	0.66
850	P51610	HCFC1 Host cell factor 1	HCFC1	ACAAGTPAVIR	1.58	0.66
851	O95833	CLIC3 Chloride intracellular channel protein 3	CLIC3	ASEDGESVGHCPSCQR	1.58	0.66
852	P62333	PSMC6 26S proteasome regulatory subunit 10B	PSMC6	AVASQLDCNFLK	1.59	0.67
853	Q1KMD3	HNRNPUL2 Heterogeneous nuclear ribonucleoprotein U-like pro	HNRNPUL2	NFILDQCNVYNSGQR	1.59	0.67
854	Q27J81	INF2 Inverted formin-2	INF2	QEEVCVIDALLADIR	1.60	0.67
855	Q86VY4	TSPYL5 Testis-specific Y-encoded-like protein 5	TSPYL5	EYGCGPSGQVVSR	1.60	0.67
856	P60709	ACTB Actin, cytoplasmic 1	ACTB	LCYVALDFEQEMATAASSSSLEK	1.60	0.68

857	P05388	RPLP0 60S acidic ribosomal protein P0	RPLP0	AGAIAPCEVTVPAQNT GLGPEK	1.60	0.68
858	P62195	PSMC5 26S proteasome regulatory subunit 8	PSMC5	GVCTEAGMYALR	1.60	0.68
859	P32322	PYCR1 Pyrroline-5-carboxylate reductase 1, mitochondrial	PYCR1	CMTNTPVVVR	1.60	0.68
860	O15355	PPM1G Protein phosphatase 1G	PPM1G	CSGDGVGAPR	1.61	0.69
861	Q99832	CCT7 T-complex protein 1 subunit eta	CCT7	QLCDNAGFDATNILNK	1.61	0.69
862	Q8TAQ 2	SMARCC2 SWI/SNF complex subunit SMARCC2	SMARC C2	NLAGDVCAIMR	1.61	0.69
863	P05388	RPLP0 60S acidic ribosomal protein P0	RPLP0	CFIVGADNVGSK	1.61	0.69
864	P62333	PSMC6 26S proteasome regulatory subunit 10B	PSMC6	NVCTEAGMFAIR	1.62	0.69
865	P50213	IDH3A Isocitrate dehydrogenase [NAD] subunit alpha, mito	IDH3A	IEAACFATIK	1.62	0.69
866	P06730	EIF4E Eukaryotic translation initiation factor 4E	EIF4E	IAIWTTECENR	1.62	0.70
867	P10809	HSPD1 60 kDa heat shock protein, mitochondrial	HSPD1	AAVEEGIVLGGGCALLR	1.62	0.70
868	O15020	SPTBN2 Spectrin beta chain, non-erythrocytic 2	SPTBN2	IHCLENVDK	1.63	0.70
869	Q9BV86	NTMT1 N-terminal Xaa-Pro-Lys N-methyltransferase 1	NTMT1	DNMAQEGVILDDVDSS VCR	1.63	0.70
870	P35998	PSMC2 26S proteasome regulatory subunit 7	PSMC2	PDVTYSDVGGCK	1.63	0.71
871	P62140	PPP1CB Serine/threonine-protein phosphatase PP1-beta	PPP1CB	ICGDIHGQYTDLLR	1.63	0.71
872	Q9P2E9	RRBP1 Ribosome-binding protein 1	RRBP1	HMAAASAECQNYAK	1.64	0.71
873	P0CG22	DHRS4L1 Putative dehydrogenase/reductase SDR family member	DHRS4L 1	VNCLAPGLIK	1.64	0.72
874	P61106	RAB14 Ras-related protein Rab-14	RAB14	SCLLHQFTEK	1.64	0.72
875	O75934	BCAS2 Pre-mRNA-splicing factor SPF27	BCAS2	NDITAWQECVNNSMA QLEHQAVR	1.65	0.72
876	P62333	PSMC6 26S proteasome regulatory subunit 10B	PSMC6	DHQPCIIFMDEIDAIGG R	1.65	0.72
877	P35914	HMGCL Hydroxymethylglutaryl-CoA lyase, mitochondrial	HMGCL	LLEAGNFICQALNR	1.65	0.73

878	O43837	IDH3B Isocitrate dehydrogenase [NAD] subunit beta, mitochondrial	IDH3B	LGDGLFLQCCEEVAELY PK	1.66	0.73
879	P27635	RPL10 60S ribosomal protein L10	RPL10	MLSCAGADR	1.67	0.74
880	Q9NP81	SARS2 Serine--tRNA ligase, mitochondrial	SARS2	GAVFEGCGMTPNANPS QIYNIDPAR	1.67	0.74
881	P62879	GNB2 Guanine nucleotide-binding protein G(I)/G(S)/G(T)	GNB2	ELPGHTGYLSCCR	1.67	0.74
882	Q9BUK6	MSTO1 Protein misato homolog 1	MSTO1	EPPGELCPDVLYR	1.69	0.76
883	Q9BV86	NTMT1 N-terminal Xaa-Pro-Lys N-methyltransferase 1	NTMT1	TGTSCALDCGAGIGR	1.69	0.76
884	P62857	RPS28 40S ribosomal protein S28	RPS28	TGSQGQCTQVR	1.70	0.76
885	P54646	PRKAA2 5-AMP-activated protein kinase catalytic subunit	PRKAA2	TSCGSPNYAAPEVISGR	1.72	0.78
886	P15924	DSP Desmoplakin	DSP	YQAECSQFK	1.72	0.78
887	O15143	ARPC1B Actin-related protein 2/3 complex subunit 1B	ARPC1B	IVTCGTDR	1.72	0.79
888	P31689	DNAJA1 DnaJ homolog subfamily A member 1	DNAJA1	GAVECCPNCR	1.73	0.79
889	Q14204	DYNC1H1 Cytoplasmic dynein 1 heavy chain 1	DYNC1H 1	LQGATCNNNK	1.73	0.79
890	P46776	RPL27A 60S ribosomal protein L27a	RPL27A	NQSFCPTVNLDK	1.73	0.79
891	P46782	RPS5 40S ribosomal protein S5	RPS5	AQCPIVER	1.73	0.79
892	Q14318	FKBP8 Peptidyl-prolyl cis-trans isomerase FKBP8	FKBP8	CLNNLAASQLK	1.74	0.80
893	O95747	OXSR1 Serine/threonine-protein kinase OSR1	OXSR1	CQTSMDELLK	1.74	0.80
894	P53597	SUCLG1 Succinate--CoA ligase [ADP/GDP-forming] subunit al	SUCLG1	LIGPNCPGVINPGECK	1.74	0.80
895	O15075	DCLK1 Serine/threonine-protein kinase DCLK1	DCLK1	YQDDFLLDESECR	1.76	0.81
896	Q1KMD 3	HNRNPUL2 Heterogeneous nuclear ribonucleoprotein U-like pro	HNRNP UL2	DLLVQQASQCLSK	1.76	0.82
897	P36873	PPP1CC Serine/threonine-protein phosphatase PP1-gamma cat	PPP1CC	GNHECASINR	1.76	0.82
898	Q07020	RPL18 60S ribosomal protein L18	RPL18	GCGTVLLSGPR	1.77	0.82

899	Q9P2R7	SUCLA2 Succinate--CoA ligase [ADP-forming] subunit beta,	SUCLA2	ILACDDLDEAAR	1.77	0.83
900	P35579	MYH9 Myosin-9	MYH9	VEDMAELTCLNEASVLHNLK	1.78	0.83
901	Q9H1K1	ISCU Iron-sulfur cluster assembly enzyme ISCU, mitochondrial	ISCU	NVGTGLVGAPACGDVMK	1.79	0.84
902	P21333	FLNA Filamin-A	FLNA	LQVEPAVDTSGVQCYGPGIEGQGVFR	1.79	0.84
903	P48735	IDH2 Isocitrate dehydrogenase [NADP], mitochondrial	IDH2	VCVETVESGAMTK	1.80	0.84
904	P61160	ACTR2 Actin-related protein 2	ACTR2	VVVCDNGTGFVK	1.80	0.85
905	Q7L0Y3	TRMT10C Mitochondrial ribonuclease P protein 1	TRMT10C	LNLATECLPLDK	1.81	0.85
906	Q15233	NONO Non-POU domain-containing octamer-binding protein	NONO	CSEGSFLLTTFPR	1.81	0.86
907	Q02252	ALDH6A1 Methylmalonate-semialdehyde dehydrogenase	ALDH6A1	AEMDAAIASCK	1.82	0.86
908	P27797	CALR Calreticulin	CALR	HEQNIDCGGGYVK	1.82	0.86
909	P62318	SNRPD3 Small nuclear ribonucleoprotein Sm D3	SNRPD3	VLHEAEGHIVTCETNTGEVYR	1.82	0.86
910	Q16637	SMN1 Survival motor neuron protein	SMN1	NGDICETSGK	1.82	0.86
911	Q02218	OGDH 2-oxoglutarate dehydrogenase, mitochondrial	OGDH	AEQFYCGDTEGK	1.82	0.87
912	Q6PKG0	LARP1 La-related protein 1	LARP1	TASISSSPSEGTPTVGSYGCTPQSLPK	1.82	0.87
913	Q05639	EEF1A2 Elongation factor 1-alpha 2	EEF1A2	PMCVESFSQYPPLGR	1.84	0.88
914	P51570	GALK1 Galactokinase	GALK1	QCEEVAR	1.86	0.89
915	P35914	HMGCL Hydroxymethylglutaryl-CoA lyase, mitochondrial	HMGCL	NINCSIEESFQR	1.86	0.89
916	P68363	TUBA1B Tubulin alpha-1B chain	TUBA1B	SIQFVDWCPTGFK	1.86	0.89
917	O00244	ATOX1 Copper transport protein ATOX1	ATOX1	VCIESEHSMDTLLATLK	1.86	0.89
918	Q8TCU6	PREX1 Phosphatidylinositol 3,4,5-trisphosphate-dependent	PREX1	PINALDELCR	1.86	0.90
919	P08865	RPSA 40S ribosomal protein SA	RPSA	YVDIAIPCNNK	1.86	0.90

920	Q27J81	INF2 Inverted formin-2	INF2	LGPQDSDPTEANLESADPELCIR	1.87	0.90
921	P35998	PSMC2 26S proteasome regulatory subunit 7	PSMC2	LCPNSTGAEIR	1.88	0.91
922	P49411	TUFM Elongation factor Tu, mitochondrial	TUFM	GDECELLGHSK	1.89	0.92
923	Q6NUK1	SLC25A24 Calcium-binding mitochondrial carrier protein SCaM	SLC25A24	TGQYSGIYDCAK	1.89	0.92
924	Q99714	HSD17B10 3-hydroxyacyl-CoA dehydrogenase type-2	HSD17B10	VDVAVNCAGIAVASK	1.89	0.92
925	P36873	PPP1CC Serine/threonine-protein phosphatase PP1-gamma cat	PPP1CC	TFTDCFNCLPIAAIVDEK	1.89	0.92
926	P63241	EIF5A Eukaryotic translation initiation factor 5A-1	EIF5A	YEDICPSTHNMDVPNIK	1.90	0.93
927	P43897	TSFM Elongation factor Ts, mitochondrial	TSFM	FECGEGEEAAETE	1.90	0.93
928	P62753	RPS6 40S ribosomal protein S6	RPS6	LNISFPATGCQK	1.90	0.93
929	Q71U36	TUBA1A Tubulin alpha-1A chain	TUBA1A	TIQFVDWCPTGFK	1.91	0.93
930	P63244	RACK1 Receptor of activated protein C kinase 1	RACK1	FSPNSSNPIIVSCGWDK	1.92	0.94
931	Q08211	DHX9 ATP-dependent RNA helicase A	DHX9	AAECNIVVTQPR	1.92	0.94
932	P51553	IDH3G Isocitrate dehydrogenase [NAD] subunit gamma, mito	IDH3G	LGDGLFLQCCR	1.92	0.94
933	Q6AI08	HEATR6 HEAT repeat-containing protein 6	HEATR6	LCALR	1.93	0.95
934	P62829	RPL23 60S ribosomal protein L23	RPL23	ISLGLPVGAVINCADNTGAK	1.94	0.95
935	P68104	EEF1A1 Elongation factor 1-alpha 1	EEF1A1	PMCVESFSDYPPLGR	1.94	0.96
936	P51553	IDH3G Isocitrate dehydrogenase [NAD] subunit gamma, mito	IDH3G	HACVPVDFEEVHVSSNADEEDIR	1.95	0.96
937	O60506	SYNCRIP Heterogeneous nuclear ribonucleoprotein Q	SYNCRIP	GYAFVTFCTK	1.95	0.97
938	P22102	GART Trifunctional purine biosynthetic protein adenosin	GART	SAGVQCFGPTAEAAQLESSK	1.97	0.97
939	Q9GZT4	SRR Serine racemase	SRR	CATQLVWER	1.97	0.98
940	O75439	PMPCB Mitochondrial-processing peptidase subunit beta	PMPCB	LCTSVTESEVAR	1.97	0.98

941	P04350	TUBB4A Tubulin beta-4A chain	TUBB4A	LTTPTYGDLNHLVSATMSGVTTCLR	1.98	0.98
942	P50991	CCT4 T-complex protein 1 subunit delta	CCT4	LGGTIDDCELVEGLVLTQK	1.98	0.98
943	P27707	DCK Deoxycytidine kinase	DCK	SCPSFSASSEGTR	1.98	0.98
944	P35998	PSMC2 26S proteasome regulatory subunit 7	PSMC2	SVCTEAGMFAIR	1.98	0.99
945	Q8TC07	TBC1D15 TBC1 domain family member 15	TBC1D15	TLLVNCQNK	1.99	0.99
946	P48735	IDH2 Isocitrate dehydrogenase [NADP], mitochondrial	IDH2	CATITPDEAR	2.02	1.01
947	P48735	IDH2 Isocitrate dehydrogenase [NADP], mitochondrial	IDH2	NYDGDVQSDILAQGFGSLGLMTSVLVCPDGK	2.03	1.02
948	Q92598	HSPH1 Heat shock protein 105 kDa	HSPH1	CTPSVISFGSK	2.04	1.03
949	P82912	MRPS11 28S ribosomal protein S11, mitochondrial	MRPS11	ASHNNTQIQVVSASNEPLAFASCGTEGFR	2.04	1.03
950	P08865	RPSA 40S ribosomal protein SA	RPSA	ADHQPLTEASYVNLPTIALCNTDSPLR	2.05	1.04
951	O00743	PPP6C Serine/threonine-protein phosphatase 6 catalytic s	PPP6C	CGNIASIMVFK	2.06	1.04
952	P50914	RPL14 60S ribosomal protein L14	RPL14	ALVDGPCTQVR	2.06	1.04
953	P68363	TUBA1B Tubulin alpha-1B chain	TUBA1B	AVCMLSNTTAIAEAWAR	2.07	1.05
954	Q16822	PCK2 Phosphoenolpyruvate carboxykinase [GTP], mitochond	PCK2	VECVGDDIAWMR	2.09	1.06
955	Q9BYV8	CEP41 Centrosomal protein of 41 kDa	CEP41	LASQAATTMCER	2.09	1.07
956	P11586	MTHFD1 C-1-tetrahydrofolate synthase, cytoplasmic	MTHFD1	GDLNDCFIPCTPK	2.10	1.07
957	P04350	TUBB4A Tubulin beta-4A chain	TUBB4A	NMMAACDPR	2.10	1.07
958	P08134	RHOC Rho-related GTP-binding protein RhoC	RHOC	ISAFGYLECSAK	2.10	1.07
959	P04350	TUBB4A Tubulin beta-4A chain	TUBB4A	TAVCDIPPR	2.11	1.07
960	Q96GW9	MARS2 Methionine--tRNA ligase, mitochondrial	MARS2	INPSETYPAFCTTCFPSEPGLVGPSVR	2.13	1.09
961	Q96HY7	DHTKD1 Probable 2-oxoglutarate dehydrogenase E1 component	DHTKD1	VEELCPFPLDSLQQEMSK	2.14	1.10

962	P08134	RHOC Rho-related GTP-binding protein RhoC	RHOC	LVIVGDGACGK	2.14	1.10
963	P13639	EEF2 Elongation factor 2	EEF2	DLEEDHACIPIK	2.15	1.10
964	P07384	CAPN1 Calpain-1 catalytic subunit	CAPN1	CLQSGTLFR	2.15	1.10
965	P23919	DTYMK Thymidylate kinase	DTYMK	LVEALCAAGHR	2.16	1.11
966	Q96CD2	PPCDC Phosphopantothenoylcysteine decarboxylase	PPCDC	ASCPAAAPLMER	2.17	1.11
967	O15355	PPM1G Protein phosphatase 1G	PPM1G	CVVSEAGK	2.17	1.12
968	Q9Y5Y2	NUBP2 Cytosolic Fe-S cluster assembly factor NUBP2	NUBP2	VGILDVDLCGPSIPR	2.22	1.15
969	Q9BQE3	TUBA1C Tubulin alpha-1C chain	TUBA1C	AVCMLSNTTAVAEAWAR	2.22	1.15
970	P62280	RPS11 40S ribosomal protein S11	RPS11	CPFTGNVSIR	2.23	1.16
971	Q99832	CCT7 T-complex protein 1 subunit eta	CCT7	TMMACGGSIQTSVNALSADVLGR	2.24	1.16
972	P48735	IDH2 Isocitrate dehydrogenase [NADP], mitochondrial	IDH2	DLAGCIHGLSNVK	2.26	1.17
973	Q99832	CCT7 T-complex protein 1 subunit eta	CCT7	DMFCAGR	2.27	1.18
974	P54136	RARS Arginine--tRNA ligase, cytoplasmic	RARS	NCGCLGASPNLEQLQEENLK	2.28	1.19
975	P40939	HADHA Trifunctional enzyme subunit alpha, mitochondrial	HADHA	CLAPMMSEVIR	2.28	1.19
976	Q9Y399	MRPS2 28S ribosomal protein S2, mitochondrial	MRPS2	DCGEYAHTR	2.33	1.22
977	P33993	MCM7 DNA replication licensing factor MCM7	MCM7	CSILAAANPAYGR	2.37	1.24
978	P58107	EPPK1 Epiplakin	EPPK1	TSYAQLLEECPR	2.38	1.25
979	Q15365	PCBP1 Poly(rC)-binding protein 1	PCBP1	VMTIPYQPMPASSPVICAGGQDR	2.44	1.28
980	Q6AI08	HEATR6 HEAT repeat-containing protein 6	HEATR6	CLANLVSNAPYDR	2.44	1.29
981	P49411	TUFM Elongation factor Tu, mitochondrial	TUFM	NMITGTAPLDGCILVVAANDGPMPQTR	2.47	1.30
982	P62280	RPS11 40S ribosomal protein S11	RPS11	DVQIGDIVTVGECR	2.50	1.32
983	P58107	EPPK1 Epiplakin	EPPK1	YLQGTGCIAGLLLPGSQER	2.51	1.33
984	Q9P2R3	ANKFY1 Rabankyrin-5	ANKFY1	GSHTDAPDTATGNCLLQR	2.52	1.33

985	Q99832	CCT7 T-complex protein 1 subunit eta	CCT7	YNFFTGCPK	2.52	1.34
986	Q9Y5Y2	NUBP2 Cytosolic Fe-S cluster assembly factor NUBP2	NUBP2	AVHQCDR	2.53	1.34
987	P62249	RPS16 40S ribosomal protein S16	RPS16	TATAVAHCK	2.54	1.35
988	P45954	ACADSB Short/branched chain specific acyl-CoA dehydrogenase	ACADSB	ASSTCPLTFENVK	2.54	1.35
989	P13804	ETFA Electron transfer flavoprotein subunit alpha, mito	ETFA	TIYAGNALCTVK	2.55	1.35
990	P50914	RPL14 60S ribosomal protein L14	RPL14	CMQLTDFILK	2.58	1.37
991	Q9Y305	ACOT9 Acyl-coenzyme A thioesterase 9, mitochondrial	ACOT9	SLEICHPQER	2.58	1.37
992	P33992	MCM5 DNA replication licensing factor MCM5	MCM5	CSVLAAANSVFGR	2.58	1.37
993	P63244	RACK1 Receptor of activated protein C kinase 1	RACK1	VWNLANCK	2.60	1.38
994	P13804	ETFA Electron transfer flavoprotein subunit alpha, mito	ETFA	LGGEVSCLVAGTK	2.61	1.39
995	P62701	RPS4X 40S ribosomal protein S4, X isoform	RPS4X	FDTGNLCMVTGGANLGR	2.62	1.39
996	P62979	RPS27A Ubiquitin-40S ribosomal protein S27a	RPS27A	CCLTYCFNK	2.63	1.40
997	P62879	GNB2 Guanine nucleotide-binding protein G(I)/G(S)/G(T)	GNB2	ACGDSTLTQITAGLDPVGR	2.66	1.41
998	P68363	TUBA1B Tubulin alpha-1B chain	TUBA1B	AYHEQLSVAEITNACFEPANQMVK	2.68	1.42
999	P49411	TUFM Elongation factor Tu, mitochondrial	TUFM	GEETPVIVGSALCALEGR	2.68	1.42
1000	O00743	PPP6C Serine/threonine-protein phosphatase 6 catalytic s	PPP6C	GAFCDLVWSDPEDVDTWAISPR	2.70	1.43
1001	P51553	IDH3G Isocitrate dehydrogenase [NAD] subunit gamma, mito	IDH3G	TSLDLYANVIHCK	2.70	1.43
1002	Q9Y6K9	IKBKG NF-kappa-B essential modulator	IKBKG	CQQQMAEDK	2.70	1.43
1003	P62136	PPP1CA Serine/threonine-protein phosphatase PP1-alpha cat	PPP1CA	IYGFYDECK	2.71	1.44
1004	Q9BQE3	TUBA1C Tubulin alpha-1C chain	TUBA1C	AYHEQLTVAEITNACFEPANQMVK	2.72	1.44

1005	Q6NXE6	ARMC6 Armadillo repeat-containing protein 6	ARMC6	DCEDVAK	2.76	1.47
1006	Q02543	RPL18A 60S ribosomal protein L18a	RPL18A	DLTTAGAVTQCYR	2.78	1.48
1007	Q9BW83	IFT27 Intraflagellar transport protein 27 homolog	IFT27	CILAGDPAVGK	2.79	1.48
1008	Q8TCU6	PREX1 Phosphatidylinositol 3,4,5-trisphosphate-dependent	PREX1	TVCSNINETK	2.80	1.49
1009	Q01813	PFKP ATP-dependent 6-phosphofructokinase, platelet type	PFKP	NESCSENYTTDFIYQLYSEEGK	2.83	1.50
1010	Q99714	HSD17B10 3-hydroxyacyl-CoA dehydrogenase type-2	HSD17B10	LGNNCVFAPADVTSEK	2.83	1.50
1011	Q8NE71	ABCF1 ATP-binding cassette sub-family F member 1	ABCF1	ICIVGPNGVGK	2.83	1.50
1012	P53597	SUCLG1 Succinate--CoA ligase [ADP/GDP-forming] subunit al	SUCLG1	IICQGFTGK	2.88	1.52
1013	P50991	CCT4 T-complex protein 1 subunit delta	CCT4	EDIEFICK	2.95	1.56
1014	O60716	CTNND1 Catenin delta-1	CTNND1	YQEAAPNVANNTGPHAASCFGAK	2.97	1.57
1015	P27635	RPL10 60S ribosomal protein L10	RPL10	VDEFPLCGHMVSDEYEQLSSEALEAAR	3.02	1.59
1016	Q13162	PRDX4 Peroxiredoxin-4	PRDX4	EEECHFYAGGQVYPGEASR	3.02	1.60
1017	P36873	PPP1CC Serine/threonine-protein phosphatase PP1-gamma cat	PPP1CC	HDLDLICR	3.05	1.61
1018	Q9Y6K9	IKBKG NF-kappa-B essential modulator	IKBKG	CLEENQELR	3.07	1.62
1019	P31749	AKT1 RAC-alpha serine/threonine-protein kinase	AKT1	TFCGTPEYLAPEVLEDNDYGR	3.08	1.63
1020	P22570	FDXR NADPH:adrenodoxin oxidoreductase, mitochondrial	FDXR	AVPTGDMEDLPCGLVLSSIGYK	3.22	1.69
1021	O95747	OXSR1 Serine/threonine-protein kinase OSR1	OXSR1	TFVGTPCWMAPEVMEQVR	3.23	1.69
1022	P04183	TK1 Thymidine kinase, cytosolic	TK1	YSSSFCTHDR	3.23	1.69
1023	Q02252	ALDH6A1 Methylmalonate-semialdehyde dehydrogenase	ALDH6A1	VCNLIDSGTK	3.25	1.70
1024	P50213	IDH3A Isocitrate dehydrogenase [NAD] subunit alpha, mito	IDH3A	CSDFTEEICR	3.27	1.71

1025	P63244	RACK1 Receptor of activated protein C kinase 1	RACK1	AEPPQCTSLAWSADGQ TLFAGYTDNLVR	3.27	1.71
1026	P17858	PFKL ATP-dependent 6-phosphofructokinase, liver type	PFKL	VFANAPDSACVIGLK	3.33	1.74
1027	P04181	OAT Ornithine aminotransferase, mitochondrial	OAT	VLPMNTGVEAGETACK	3.45	1.79
1028	Q53H96	PYCR3 Pyrroline-5-carboxylate reductase 3	PYCR3	SDVCTPGGTTIYGLHAL EQGGLR	3.51	1.81
1029	O00244	ATOX1 Copper transport protein ATOX1	ATOX1	HEFSVDMTCGGCAEAV SR	3.61	1.85
1030	Q01813	PFKP ATP-dependent 6-phosphofructokinase, platelet type	PFKP	LPLMECVQMTQDVQK	3.89	1.96
1031	Q9BSD7	NTPCR Cancer-related nucleoside-triphosphatase	NTPCR	NADCSSGPGQR	4.18	2.06
1032	O75439	PMPCB Mitochondrial-processing peptidase subunit beta	PMPCB	TNMLLQLDGSTPICEDI GR	4.21	2.08
1033	P25398	RPS12 40S ribosomal protein S12	RPS12	LGEWVGLCK	4.27	2.09
1034	Q9BSD7	NTPCR Cancer-related nucleoside-triphosphatase	NTPCR	VCVIDEIGK	4.52	2.18
1035	P07339	CTSD Cathepsin D	CTSD	AIGAVPLIQGEYMIPCEK	5.51	2.46
1036	P14314	PRKCSH Glucosidase 2 subunit beta	PRKCSH	YEQGTGCWQGPNR	6.89	2.79
1037	P63244	RACK1 Receptor of activated protein C kinase 1	RACK1	YWLCAATGPSIK	7.34	2.88
1038	Q9BSJ8	ESYT1 Extended synaptotagmin-1	ESYT1	LGTQTFCSR	20.00	4.32

Table A2-4 Ranking cysteines by sensitivity to PAPA NONOate. 985 cysteine containing peptides from MCF7 cell lysate were reported with R values. R value is the average heavy:light ratio from two individual datasets.

index	UniProt ID	description	symbol	sequence	*R* value	*R* (log2)
1	P18031	PTPN1 Tyrosine-protein phosphatase non-receptor type 1	PTPN1	HEASDFPCR	0.18	-2.48
2	P04406	GAPDH Glyceraldehyde-3-phosphate dehydrogenase	GAPDH	VPTANVSVVDLTCR	0.35	-1.53
3	P10768	ESD S-formylglutathione hydrolase	ESD	SVSAFAPICNPVLCP WGK	0.35	-1.52
4	P30044	PRDX5 Peroxiredoxin-5, mitochondrial	PRDX5	ALNVEPDGTGLTCSL APNIISQL	0.35	-1.52
5	P30044	PRDX5 Peroxiredoxin-5, mitochondrial	PRDX5	GVLFGVPGAFTPGCS K	0.35	-1.52
6	Q99497	PARK7 Protein/nucleic acid deglycase DJ-1	PARK7	DPVQCSR	0.38	-1.40
7	O43583	DENR Density-regulated protein	DENR	VLYCGVCSLPTEYCEY MPDVAK	0.39	-1.36
8	Q96HE7	ERO1A ERO1-like protein alpha	ERO1A	IWNVIYEENCFK	0.41	-1.30
9	P14923	JUP Junction plakoglobin	JUP	EAMCPGVSGEDSSLL LATQVEGQATNLQR	0.43	-1.21
10	Q9BWD 1	ACAT2 Acetyl-CoA acetyltransferase, cytosolic	ACAT2	ATVAPEDVSEVIFGH VLAAGCGQNPVR	0.45	-1.17
11	P61981	YWHAG 14-3-3 protein gamma	YWHAG	NCSETQYESK	0.46	-1.13
12	O95159	ZFPL1 Zinc finger protein-like 1	ZFPL1	LCNIPLASR	0.48	-1.07
13	P13489	RNH1 Ribonuclease inhibitor	RNH1	WAELLPLLQQCQVV R	0.49	-1.04
14	P13489	RNH1 Ribonuclease inhibitor	RNH1	SNELGDVGVHCVLQ GLQTPSCK	0.49	-1.03
15	Q9Y3D0	FAM96B Mitotic spindle-associated MMXD complex subunit MI	FAM96B	VAAALENTHLLEVVN QCLSAR	0.51	-0.96
16	P32119	PRDX2 Peroxiredoxin-2	PRDX2	LVQAFQYTDEHGEVC PAGWK	0.52	-0.96
17	P21266	GSTM3 Glutathione S-transferase Mu 3	GSTM3	IAAYLQSDQFCK	0.53	-0.91
18	Q13263	TRIM28 Transcription intermediary factor 1-beta	TRIM28	AATDAQDANQCCTS CEDNAPATSYCVECS EPLCETCVEAHQR	0.54	-0.90
19	P49591	SARS Serine--tRNA ligase, cytoplasmic	SARS	TICAILENYQTEK	0.55	-0.86

20	O43681	ASNA1 ATPase ASNA1	ASNA1	PCK	0.56	-0.83
21	P23528	CFL1 Cofilin-1	CFL1	CTLAEK	0.56	-0.83
22	P30041	PRDX6 Peroxiredoxin-6	PRDX6	DFTPVCTTELGR	0.56	-0.83
23	O43175	PHGDH D-3-phosphoglycerate dehydrogenase	PHGDH	ALVDHENVISCPHLGASTK	0.56	-0.83
24	P02795	MT2A Metallothionein-2	MT2A	CAQGCICK	0.57	-0.81
25	Q9Y3P9	RABGAP1 Rab GTPase-activating protein 1	RABGAP1	LTYLGCASVNAPR	0.58	-0.79
26	P49327	FASN Fatty acid synthase	FASN	AAPLDSIHSLAAYYIDCIR	0.58	-0.79
27	P19367	HK1 Hexokinase-1	HK1	TVCGVVSR	0.58	-0.78
28	P02795	MT2A Metallothionein-2	MT2A	SCCSCCPVGCAK	0.59	-0.77
29	Q9UL46	PSME2 Proteasome activator complex subunit 2	PSME2	CGFLPGNEK	0.60	-0.73
30	P30101	PDIA3 Protein disulfide-isomerase A3	PDIA3	FIQENIFGICPHMTEDNK	0.61	-0.72
31	P25398	RPS12 40S ribosomal protein S12	RPS12	QAHLCVLASNCDEPMYVK	0.61	-0.72
32	P04155	TFF1 Trefoil factor 1	TFF1	GVPWCFYPNTIDVPPEEECEF	0.61	-0.70
33	P13489	RNH1 Ribonuclease inhibitor	RNH1	ELCQGLGQPGSVLR	0.62	-0.69
34	Q9ULC4	MCTS1 Malignant T-cell-amplified sequence 1	MCTS1	FVLSGANIMCPGLTSPGAK	0.62	-0.68
35	P09382	LGALS1 Galectin-1	LGALS1	FNAHGDANTIVCNSK	0.62	-0.68
36	Q9BT78	COPS4 COP9 signalosome complex subunit 4	COPS4	CQQLAAYGILEK	0.63	-0.67
37	P25398	RPS12 40S ribosomal protein S12	RPS12	VVGCSCVVVK	0.63	-0.66
38	P13639	EEF2 Elongation factor 2	EEF2	ETVSEESNVLCLSK	0.63	-0.66
39	P15924	DSP Desmoplakin	DSP	LLEAQACTGGIIHPTTGQK	0.64	-0.65
40	P14625	HSP90B1 Endoplasmin	HSP90B1	LTESPCALVASQYGWSGNMER	0.64	-0.64
41	P45974	USP5 Ubiquitin carboxyl-terminal hydrolase 5	USP5	VCASEK	0.64	-0.64
42	P33316	DUT Deoxyuridine 5-triphosphate nucleotidohydrolase,	DUT	TDIQIALPSGCYGR	0.64	-0.64
43	O60216	RAD21 Double-strand-break repair protein rad21 homolog	RAD21	CLTPLVPEDLR	0.64	-0.63
44	P41250	GARS Glycine--tRNA ligase	GARS	CSVLPLSQNQEFMPFVK	0.65	-0.62

45	P49588	AARS Alanine--tRNA ligase, cytoplasmic	AARS	NVGCLQEALQLATSFAQLR	0.65	-0.61
46	O43175	PHGDH D-3-phosphoglycerate dehydrogenase	PHGDH	GILVMNTPNGNSLSAAELTCGMIMCLAR	0.65	-0.61
47	Q16762	TST Thiosulfate sulfurtransferase	TST	VDLSQPLIATCR	0.66	-0.60
48	Q9H1B7	IRF2BPL Interferon regulatory factor 2-binding protein-lik	IRF2BPL	EGVPGADMLPQPYLDASCPMLPTALVSLSR	0.67	-0.59
49	P51659	HSD17B4 Peroxisomal multifunctional enzyme type 2	HSD17B4	FIYEGSSDFSCLPTFGVIIGQK	0.67	-0.58
50	Q9Y570	PPME1 Protein phosphatase methylesterase 1	PPME1	GLSNLFLSCPIPK	0.67	-0.58
51	P52788	SMS Spermine synthase	SMS	LYCPVEFSK	0.67	-0.57
52	P13693	TPT1 Translationally-controlled tumor protein	TPT1	EIADGLCLEVEGK	0.67	-0.57
53	P11940	PABPC1 Polyadenylate-binding protein 1	PABPC1	ALYDTFSAFGNILSCK	0.68	-0.56
54	P40925	MDH1 Malate dehydrogenase, cytoplasmic	MDH1	VIVVGNPANTNCLTASK	0.68	-0.56
55	P30084	ECHS1 Enoyl-CoA hydratase, mitochondrial	ECHS1	EMQNLSFQDCYSSK	0.68	-0.55
56	Q9UNE7	STUB1 E3 ubiquitin-protein ligase CHIP	STUB1	YPEAAACYGR	0.69	-0.54
57	P30086	PEBP1 Phosphatidylethanolamine-binding protein 1	PEBP1	CDEPILSNR	0.69	-0.54
58	P30084	ECHS1 Enoyl-CoA hydratase, mitochondrial	ECHS1	ICPVETLVEEAIQCAEK	0.69	-0.54
59	P31948	STIP1 Stress-induced-phosphoprotein 1	STIP1	CMMAQYNR	0.69	-0.54
60	Q9H2U2	PPA2 Inorganic pyrophosphatase 2, mitochondrial	PPA2	STNCFGDNDPIDVCEIGSK	0.69	-0.53
61	P06733	ENO1 Alpha-enolase	ENO1	SGETEDTFIADLVVGLCTGQIK	0.69	-0.53
62	Q9H2C0	GAN Gigaxonin	GAN	ECSNIPLSQPQQGEAMLANFK	0.69	-0.53
63	Q9BXV9	GON7 EKC/KEOPS complex subunit GON7	GON7	VSCEAPGDGDPFQGLLSGVAQMK	0.69	-0.53
64	Q9BSH4	TACO1 Translational activator of cytochrome c oxidase 1	TACO1	LDSLGLCSVSCALEFIPNSK	0.69	-0.53
65	B4DXR9	ZNF732 Zinc finger protein 732	ZNF732	CLDPAQQNLYR	0.69	-0.53

66	P23526	AHCY Adenosylhomocysteinase	AHCY	FDNLYGCR	0.69	-0.53
67	P62633	CNBP Cellular nucleic acid-binding protein	CNBP	DCDHADEQK	0.69	-0.53
68	P80404	ABAT 4-aminobutyrate aminotransferase, mitochondrial	ABAT	TMGCLATTHSK	0.69	-0.53
69	P30086	PEBP1 Phosphatidylethanolamine-binding protein 1	PEBP1	APVAGTCYQAEWDDYVPK	0.70	-0.52
70	O43707	ACTN4 Alpha-actinin-4	ACTN4	ELPPDQAEYCIAR	0.70	-0.52
71	P60953	CDC42 Cell division control protein 42 homolog	CDC42	YVECSALTQK	0.70	-0.52
72	P00558	PGK1 Phosphoglycerate kinase 1	PGK1	TGQATVASGIPAGWMGLDCGPESSK	0.70	-0.52
73	Q9HBH1	PDF Peptide deformylase, mitochondrial	PDF	CVGLSAPQLGVPR	0.70	-0.52
74	P00558	PGK1 Phosphoglycerate kinase 1	PGK1	GCITIIGGGDTATC*C*AK	0.70	-0.52
75	P30084	ECHS1 Enoyl-CoA hydratase, mitochondrial	ECHS1	IC*PVETLVEEAIQC*AEK	0.70	-0.52
76	Q15185	PTGES3 Prostaglandin E synthase 3	PTGES3	LTFSCLGGSDNFK	0.70	-0.52
77	Q15369	ELOC Elongin-C	ELOC	VCMYFTYK	0.70	-0.51
78	A6NHG4	DDTL D-dopachrome decarboxylase-like protein	DDTL	LCAAAASILGK	0.70	-0.51
79	P21291	CSRP1 Cysteine and glycine-rich protein 1	CSRP1	SCFLCMVCK	0.70	-0.51
80	P40925	MDH1 Malate dehydrogenase, cytoplasmic	MDH1	AICDHVR	0.70	-0.51
81	P50552	VASP Vasodilator-stimulated phosphoprotein	VASP	MQPDQQVVINCAIVR	0.70	-0.51
82	Q9H2U2	PPA2 Inorganic pyrophosphatase 2, mitochondrial	PPA2	ILSCGEVIHVK	0.70	-0.51
83	P52788	SMS Spermine synthase	SMS	YFTQGNCVNLTEALSLYEEQLGR	0.70	-0.51
84	Q9Y696	CLIC4 Chloride intracellular channel protein 4	CLIC4	DEFTNTCPSDK	0.71	-0.50
85	P57721	PCBP3 Poly(rC)-binding protein 3	PCBP3	QICVVMLESPPK	0.71	-0.50
86	P07900	HSP90AA1 Heat shock protein HSP 90-alpha	HSP90AA1	LVTSPCCIVTSTYGWTANMER	0.71	-0.50
87	P28838	LAP3 Cytosol	LAP3	QVVDCQLADVNNIG	0.71	-0.50

		aminopeptidase		K		
88	P52594	AGFG1 Arf-GAP domain and FG repeat-containing protein 1	AGFG1	HGNEVCK	0.71	-0.50
89	Q6UWE0	LRSAM1 E3 ubiquitin-protein ligase LRSAM1	LRSAM1	SCSLLSLATIK	0.71	-0.50
90	Q9BWJ5	SF3B5 Splicing factor 3B subunit 5	SF3B5	MLQPCGPPADK	0.71	-0.50
91	O14545	TRAFD1 TRAF-type zinc finger domain-containing protein 1	TRAFD1	AVCEADQSHGGPR	0.71	-0.49
92	Q09666	AHNAK Neuroblast differentiation-associated protein AHNA	AHNAK	VDVECPDVNIEGPEGK	0.72	-0.48
93	Q12931	TRAP1 Heat shock protein 75 kDa, mitochondrial	TRAP1	SPAAECLSEK	0.72	-0.48
94	P25788	PSMA3 Proteasome subunit alpha type-3	PSMA3	CKDGVVFGVEK	0.72	-0.48
95	O60701	UGDH UDP-glucose 6-dehydrogenase	UGDH	DVLNLVYLCEALNLPEVAR	0.72	-0.48
96	O75874	IDH1 Isocitrate dehydrogenase [NADP] cytoplasmic	IDH1	CATITPDEK	0.72	-0.48
97	P50395	GDI2 Rab GDP dissociation inhibitor beta	GDI2	TYDATTHFETTCDDIK	0.72	-0.47
98	O75608	LYPLA1 Acyl-protein thioesterase 1	LYPLA1	LAGVTALSCWLPLR	0.72	-0.47
99	P27348	YWHAQ 14-3-3 protein theta	YWHAQ	YDDMATCMK	0.72	-0.47
100	O60701	UGDH UDP-glucose 6-dehydrogenase	UGDH	ISSINSISALCEATGADVEEVATAIGMDQR	0.72	-0.47
101	O95372	LYPLA2 Acyl-protein thioesterase 2	LYPLA2	TYPGVMHSSCPQEMAAVK	0.72	-0.47
102	P30040	ERP29 Endoplasmic reticulum resident protein 29	ERP29	GQGVYLGMPGCLPVYDALAGEFIR	0.72	-0.47
103	Q9BQ69	MACROD1 O-acetyl-ADP-ribose deacetylase MACROD1	MACROD1	SCYLSSLDLLLEHR	0.72	-0.47
104	Q3LXA3	TKFC Triokinase/FMN cyclase	TKFC	AAGDGDCGTTHSR	0.72	-0.47
105	P04632	CAPNS1 Calpain small subunit 1	CAPNS1	TDGFGIDTCR	0.72	-0.47
106	P21266	GSTM3 Glutathione S-transferase Mu 3	GSTM3	YTCGEAPDYDR	0.72	-0.47
107	P0DMV8	HSPA1A Heat shock 70 kDa protein 1A	HSPA1A	AAAIGIDLGTTYSCVGVFQHGK	0.72	-0.46
108	Q12849	GRSF1 G-rich sequence factor 1	GRSF1	YIELFLNSCPK	0.72	-0.46

109	P18669	PGAM1 Phosphoglycerate mutase 1	PGAM1	YADLTEDQLPSCESLK	0.73	-0.46
110	O60701	UGDH UDP-glucose 6-dehydrogenase	UGDH	ASVGFGGSCFQK	0.73	-0.46
111	P23528	CFL1 Cofilin-1	CFL1	AVLFCLSEDK	0.73	-0.46
112	P14174	MIF Macrophage migration inhibitory factor	MIF	LLCGLLAER	0.73	-0.46
113	P63104	YWHAZ 14-3-3 protein zeta/delta	YWHAZ	YDDMAACMK	0.73	-0.46
114	P21333	FLNA Filamin-A	FLNA	ATCAPQHGAPGPGP ADASK	0.73	-0.46
115	P22314	UBA1 Ubiquitin-like modifier-activating enzyme 1	UBA1	DNPGVVTCLDEAR	0.73	-0.46
116	P02545	LMNA Prelamin-A/C	LMNA	AQNTWGCGNSLR	0.73	-0.46
117	A0A075 B759	PPIAL4E Peptidyl-prolyl cis-trans isomerase A-like 4E	PPIAL4E	IIPGFMCQGGDFTR	0.73	-0.46
118	P12004	PCNA Proliferating cell nuclear antigen	PCNA	CAGNEDIITLR	0.73	-0.45
119	Q04917	YWHAH 14-3-3 protein eta	YWHAH	NCNDFQYESK	0.73	-0.45
120	Q9NRF9	POLE3 DNA polymerase epsilon subunit 3	POLE3	AASVFVLYATSCANN FAMK	0.73	-0.45
121	P60981	DSTN Destrin	DSTN	AVIFCLSADK	0.73	-0.45
122	Q7LG56	RRM2B Ribonucleoside-diphosphate reductase subunit M2 B	RRM2B	IEQEFLTEALPVGLIG MNCILMK	0.73	-0.45
123	Q9H2U 2	PPA2 Inorganic pyrophosphatase 2, mitochondrial	PPA2	GQPCSQNYR	0.73	-0.45
124	Q96Q11	TRNT1 CCA tRNA nucleotidyltransferase 1, mitochondrial	TRNT1	YQGEHCLLK	0.73	-0.44
125	Q96AT9	RPE Ribulose-phosphate 3-epimerase	RPE	IGPSILNSDLANLGAE CLR	0.74	-0.44
126	Q04724	TLE1 Transducin-like enhancer protein 1	TLE1	SPVSQLDCLNR	0.74	-0.44
127	P31949	S100A11 Protein S100-A11	S100A11	CIESLIAVFQK	0.74	-0.44
128	P11413	G6PD Glucose-6-phosphate 1-dehydrogenase	G6PD	NIHESCMSQIGWNR	0.74	-0.43
129	P60174	TPI1 Triosephosphate isomerase	TPI1	VAHALAEGLGVIACIG EK	0.74	-0.43
130	P55072	VCP Transitional endoplasmic reticulum ATPase	VCP	GVLFYGPPGCGK	0.74	-0.43
131	P62937	PPIA Peptidyl-prolyl cis-	PPIA	ITIADCGQLE	0.74	-0.43

		trans isomerase A				
132	P22626	HNRNPA2B1 Heterogeneous nuclear ribonucleoproteins A2/B1	HNRNPA2B1	LTDCVVMR	0.74	-0.43
133	P09467	FBP1 Fructose-1,6-bisphosphatase 1	FBP1	GTGELTQLLNSLCTAVK	0.74	-0.43
134	P22061	PCMT1 Protein-L-isoaspartate(D-aspartate) O-methyltransferase	PCMT1	ALDVGSGSGILTACFAR	0.74	-0.43
135	O14662	STX16 Syntaxin-16	STX16	ACSEQEGR	0.74	-0.43
136	Q14847	LASP1 LIM and SH3 domain protein 1	LASP1	ACFHCETCK	0.74	-0.43
137	Q9UHX1	PUF60 Poly(U)-binding-splicing factor PUF60	PUF60	ALAIMCR	0.74	-0.42
138	P13489	RNH1 Ribonuclease inhibitor	RNH1	ELDLSNNCLGDAGILQLVESVR	0.74	-0.42
139	O43765	SGTA Small glutamine-rich tetratricopeptide repeat-cont	SGTA	AIELNPANAVYFCNR	0.75	-0.42
140	O75223	GGCT Gamma-glutamylcyclotransferase	GGCT	NPSAAFFCVAR	0.75	-0.42
141	P30041	PRDX6 Peroxiredoxin-6	PRDX6	DINAYNCEEPTEK	0.75	-0.42
142	P21964	COMT Catechol O-methyltransferase	COMT	LITIEINPDCAAITQR	0.75	-0.42
143	P50135	HNMT Histamine N-methyltransferase	HNMT	VQAQYPGVCINNEVVEPSAEQIAK	0.75	-0.42
144	P61981	YWHAG 14-3-3 protein gamma	YWHAG	ELEAVCQDVLSLLDNYLIK	0.75	-0.42
145	O00299	CLIC1 Chloride intracellular channel protein 1	CLIC1	FLDGNELTLADCNLLPK	0.75	-0.42
146	Q9UBE0	SAE1 SUMO-activating enzyme subunit 1	SAE1	YCFSEMAPVCAVVGGILAQEIVK	0.75	-0.41
147	Q96E11	MRRF Ribosome-recycling factor, mitochondrial	MRRF	SPQLILVNMASFPECTAAAIK	0.75	-0.41
148	P22234	PAICS Multifunctional protein ADE2	PAICS	SNGLGPVMSGNTAYPVISCPPLTPDWGVQDVWSSLR	0.75	-0.41
149	P60174	TPI1 Triosephosphate isomerase	TPI1	IAVAAQNCYK	0.75	-0.41
150	P60174	TPI1 Triosephosphate isomerase	TPI1	VPADTEVVCAPPTAYIDFAR	0.75	-0.41
151	P37802	TAGLN2 Transgelin-2	TAGLN2	QYDADLEQILIQWITTQCR	0.75	-0.41
152	P25789	PSMA4 Proteasome subunit alpha type-4	PSMA4	YLLQYQEPIPCEQLVTALCDIK	0.75	-0.41
153	Q9Y490	TLN1 Talin-1	TLN1	AGALQCSPSDAYTK	0.75	-0.41
154	Q96GA7	SDSL Serine	SDSL	MLVEPACGAALAAIY	0.76	-0.40

		dehydratase-like		SGLLR		
155	Q969T9	WBP2 WW domain-binding protein 2	WBP2	DCEIK	0.76	-0.40
156	Q08211	DHX9 ATP-dependent RNA helicase A	DHX9	LAAQSCALSLVR	0.76	-0.40
157	P37837	TALDO1 Transaldolase	TALDO1	ALAGCDFLTISPK	0.76	-0.40
158	P06733	ENO1 Alpha-enolase	ENO1	FGANAILGVSLAVCK	0.76	-0.40
159	P52272	HNRNPM Heterogeneous nuclear ribonucleoprotein M	HNRNPM	FNECGHVLYADIK	0.76	-0.40
160	P62258	YWHAE 14-3-3 protein epsilon	YWHAE	LICCDILDVLDK	0.76	-0.40
161	P07737	PFN1 Profilin-1	PFN1	CYEMASHLR	0.76	-0.40
162	P61970	NUTF2 Nuclear transport factor 2	NUTF2	NINDAWVCTNDMFR	0.76	-0.40
163	Q92598	HSPH1 Heat shock protein 105 kDa	HSPH1	FICEQDHQNFLR	0.76	-0.40
164	O60701	UGDH UDP-glucose 6-dehydrogenase	UGDH	AVQALCAVYEHWVPR	0.76	-0.40
165	P50991	CCT4 T-complex protein 1 subunit delta	CCT4	IGLIQFCLSAPK	0.76	-0.39
166	P08238	HSP90AB1 Heat shock protein HSP 90-beta	HSP90AB1	LVSSPCCIVTSTYGWTANMER	0.76	-0.39
167	P49419	ALDH7A1 Alpha-aminoadipic semialdehyde dehydrogenase	ALDH7A1	STCTINYSK	0.76	-0.39
168	P0DMV8	HSPA1A Heat shock 70 kDa protein 1A	HSPA1A	ELEQVCNPIISGLYQGAGGPGPGGFGAQGPK	0.76	-0.39
169	P04075	ALDOA Fructose-bisphosphate aldolase A	ALDOA	ALANSLACQGK	0.76	-0.39
170	O75369	FLNB Filamin-B	FLNB	CLATGPGIASTVK	0.76	-0.39
171	P50990	CCT8 T-complex protein 1 subunit theta	CCT8	AHEILPNLVCCSAK	0.76	-0.39
172	O95292	VAPB Vesicle-associated membrane protein-associated pro	VAPB	NVCFK	0.76	-0.39
173	P55212	CASP6 Caspase-6	CASP6	GTCADR	0.76	-0.39
174	Q9Y3C6	PPIL1 Peptidyl-prolyl cis-trans isomerase-like 1	PPIL1	VCQGIGMVNR	0.76	-0.39
175	P60174	TPI1 Triosephosphate isomerase	TPI1	IIYGGSVTGATCK	0.77	-0.39
176	P52209	PGD 6-phosphogluconate dehydrogenase, decarboxylating	PGD	CLSSLK	0.77	-0.38
177	Q96FJ2	DYNLL2 Dynein light chain 2, cytoplasmic	DYNLL2	NADMSEDMQQDAVDCATQAMEK	0.77	-0.38
178	P63104	YWHAZ 14-3-3 protein	YWHAZ	DICNDVLSLLEK	0.77	-0.38

		zeta/delta				
179	Q9C0C2	TNKS1BP1 182 kDa tankyrase-1-binding protein	TNKS1BP1	EHGVGGVSQCPEPGLR	0.77	-0.38
180	P04075	ALDOA Fructose-bisphosphate aldolase A	ALDOA	YASICQQNGIVPIVEPEILPDGDHDLK	0.77	-0.38
181	P62306	SNRPF Small nuclear ribonucleoprotein F	SNRPF	CNNVLYIR	0.77	-0.38
182	Q16644	MAPKAPK3 MAP kinase-activated protein kinase 3	MAPKAPK3	QAGSSSASQGCNNQ	0.77	-0.38
183	P19404	NDUFV2 NADH dehydrogenase [ubiquinone] flavoprotein 2, mi	NDUFV2	FSCEPAGGLTSLTEPPK	0.77	-0.38
184	P11142	HSPA8 Heat shock cognate 71 kDa protein	HSPA8	GPAVGIDLGTTYSCVGVFQHGK	0.77	-0.38
185	P04632	CAPNS1 Calpain small subunit 1	CAPNS1	YSDESGNMDFDNFISCLVR	0.77	-0.38
186	O14561	NDUFAB1 Acyl carrier protein, mitochondrial	NDUFAB1	LMCPQEIVDYIADK	0.77	-0.38
187	P23528	CFL1 Cofilin-1	CFL1	HELQANCYEEVK	0.77	-0.37
188	P60842	EIF4A1 Eukaryotic initiation factor 4A-I	EIF4A1	VVMALGDYMGASCHACIGGTNVR	0.77	-0.37
189	Q8IXM2	BAP18 Chromatin complexes subunit BAP18	BAP18	FGDDLNHISCVIK	0.77	-0.37
190	Q02790	FKBP4 Peptidyl-prolyl cis-trans isomerase FKBP4	FKBP4	TQLAVCQQR	0.77	-0.37
191	Q1KMD3	HNRNPUL2 Heterogeneous nuclear ribonucleoprotein U-like pro	HNRNPUL2	LQEALDAEMLEDEAGGGGAGPGGACK	0.78	-0.36
192	P01111	NRAS GTPase NRas	NRAS	TGEGFLCVFAINNSK	0.78	-0.36
193	P00505	GOT2 Aspartate aminotransferase, mitochondrial	GOT2	EYLPIGGLAEFCK	0.78	-0.36
194	P36776	LONP1 Lon protease homolog, mitochondrial	LONP1	VLFICTANVTDTIPEPLR	0.78	-0.36
195	P55735	SEC13 Protein SEC13 homolog	SEC13	FASGGCDNLIK	0.78	-0.36
196	P07237	P4HB Protein disulfide-isomerase	P4HB	EECPAVR	0.78	-0.36
197	O43707	ACTN4 Alpha-actinin-4	ACTN4	CQLEINFNTLQTK	0.78	-0.36
198	Q9ULC4	MCTS1 Malignant T-cell-amplified sequence 1	MCTS1	ENVSNCIQLK	0.78	-0.36
199	P29373	CRABP2 Cellular retinoic acid-binding	CRABP2	ELTNDGELILTMTADDVVCTR	0.78	-0.36

		protein 2				
200	P0DMV8	HSPA1A Heat shock 70 kDa protein 1A	HSPA1A	FEELCSDLFR	0.78	-0.35
201	P31948	STIP1 Stress-induced-phosphoprotein 1	STIP1	ALSVGNIDDALQCYSEAIK	0.78	-0.35
202	P10768	ESD S-formylglutathione hydrolase	ESD	CPALYWLSGLTCTEQNFISK	0.78	-0.35
203	P46459	NSF Vesicle-fusing ATPase	NSF	GILLYGPPGCGK	0.78	-0.35
204	Q9H773	DCTPP1 dCTP pyrophosphatase 1	DCTPP1	YTELPHGAISEDQAVGPADIPCDSTGQTST	0.78	-0.35
205	O95292	VAPB Vesicle-associated membrane protein-associated pro	VAPB	CVFELPAENDK	0.78	-0.35
206	Q15365	PCBP1 Poly(rC)-binding protein 1	PCBP1	AITIAGVPQSVTECVK	0.78	-0.35
207	O15382	BCAT2 Branched-chain-amino-acid aminotransferase, mitoch	BCAT2	EVFGSGTACQVCPVHR	0.79	-0.35
208	Q02750	MAP2K1 Dual specificity mitogen-activated protein kinase	MAP2K1	ELELMFGCQVEGDAAETPPR	0.79	-0.35
209	P13984	GTF2F2 General transcription factor IIF subunit 2	GTF2F2	AECR	0.79	-0.34
210	Q9HAV7	GRPEL1 GrpE protein homolog 1, mitochondrial	GRPEL1	ATQCVPK	0.79	-0.34
211	P15927	RPA2 Replication protein A 32 kDa subunit	RPA2	ACPR	0.79	-0.34
212	P21333	FLNA Filamin-A	FLNA	VHSPSGALEECYVTEIDQDK	0.79	-0.34
213	P58107	EPPK1 Epiplakin	EPPK1	CVPDPDTGLYMLQLAGR	0.79	-0.34
214	Q14697	GANAB Neutral alpha-glucosidase AB	GANAB	DGSDYEGWCWPGSAGYPDFTNPTMR	0.79	-0.34
215	P78417	GSTO1 Glutathione S-transferase omega-1	GSTO1	FCPFAER	0.79	-0.34
216	P21266	GSTM3 Glutathione S-transferase Mu 3	GSTM3	HNMCGETEEEK	0.79	-0.34
217	Q7L2H7	EIF3M Eukaryotic translation initiation factor 3 subunit	EIF3M	VAASCGAIQYIPTELDQVR	0.79	-0.34
218	P52272	HNRNPM Heterogeneous nuclear ribonucleoprotein M	HNRNPM	ACQIFVR	0.79	-0.34
219	P49773	HINT1 Histidine triad nucleotide-binding	HINT1	CAADLGLNK	0.79	-0.34

		protein 1				
220	O75348	ATP6V1G1 V-type proton ATPase subunit G 1	ATP6V1G1	GSCSTEVEK	0.79	-0.34
221	P28074	PSMB5 Proteasome subunit beta type-5	PSMB5	VIEINPYLLGTMAGG AADCSFWER	0.79	-0.34
222	P14618	PKM Pyruvate kinase PKM	PKM	CCSGAIIVLTK	0.80	-0.33
223	P33240	CSTF2 Cleavage stimulation factor subunit 2	CSTF2	LCVQNSPQEAR	0.80	-0.33
224	Q86VP6	CAND1 Cullin-associated NEDD8-dissociated protein 1	CAND1	HCECAEEGTR	0.80	-0.33
225	Q04726	TLE3 Transducin-like enhancer protein 3	TLE3	SPISQLDCLNR	0.80	-0.33
226	P37802	TAGLN2 Transgelin-2	TAGLN2	DGTVLCELINALYPEG QAPVK	0.80	-0.33
227	P13639	EEF2 Elongation factor 2	EEF2	IWCFGPDGTGPNILT DITK	0.80	-0.33
228	P07900	HSP90AA1 Heat shock protein HSP 90-alpha	HSP90AA1	VFIMDNCEELIPEYLN FIR	0.80	-0.33
229	P36405	ARL3 ADP-ribosylation factor-like protein 3	ARL3	LSCVPVLIFANK	0.80	-0.33
230	P61077	UBE2D3 Ubiquitin-conjugating enzyme E2 D3	UBE2D3	VLLSICSLLCDPNPDD PLVPEIAR	0.80	-0.33
231	Q9HAV 7	GRPEL1 GrpE protein homolog 1, mitochondrial	GRPEL1	LYGIQAFCK	0.80	-0.33
232	P15311	EZR Ezrin	EZR	EGILSDEIYCPPETAVL LGSYAVQAK	0.80	-0.32
233	Q09666	AHNAK Neuroblast differentiation-associated protein AHNA	AHNAK	LEGDLTGPSVDVEVP DVELECPDAK	0.80	-0.32
234	Q92879	CELF1 CUGBP Elav-like family member 1	CELF1	GCAFVTFTTR	0.80	-0.32
235	P50395	GDI2 Rab GDP dissociation inhibitor beta	GDI2	TDDYLDQPCYETINR	0.80	-0.32
236	Q9Y490	TLN1 Talin-1	TLN1	VVAPTISSPVCQEQLV EAGR	0.80	-0.32
237	Q15366	PCBP2 Poly(rC)-binding protein 2	PCBP2	AITIAGIPQSIIECVK	0.80	-0.32
238	Q99460	PSMD1 26S proteasome non-ATPase regulatory subunit 1	PSMD1	VLTMPETCR	0.80	-0.32
239	Q14657	LAGE3 EKC/KEOPS complex subunit LAGE3	LAGE3	GGHSCR	0.80	-0.32
240	P61970	NUTF2 Nuclear	NUTF2	TQLGAIYIDASCLTWE	0.80	-0.32

		transport factor 2		GQQFQGK		
241	P15153	RAC2 Ras-related C3 botulinum toxin substrate 2	RAC2	YLECSALTQR	0.80	-0.32
242	P61978	HNRNPK Heterogeneous nuclear ribonucleoprotein K	HNRNPK	LFQECCPHSTDR	0.80	-0.32
243	P13639	EEF2 Elongation factor 2	EEF2	LMEPIYLVEIQCPEQV VGGIYGVLNR	0.80	-0.32
244	P13639	EEF2 Elongation factor 2	EEF2	CLYASVLTAQPR	0.80	-0.31
245	P57721	PCBP3 Poly(rC)-binding protein 3	PCBP3	INISEGNCPER	0.80	-0.31
246	Q06323	PSME1 Proteasome activator complex subunit 1	PSME1	GPPC*GPVNC*NEK	0.80	-0.31
247	P52209	PGD 6-phosphogluconate dehydrogenase, decarboxylating	PGD	AVSTGVQAGIPMPCF TTALSFYDGYR	0.81	-0.31
248	P78417	GSTO1 Glutathione S-transferase omega-1	GSTO1	LNECVDHTPK	0.81	-0.31
249	P00558	PGK1 Phosphoglycerate kinase 1	PGK1	GCITIIGGGDTATCCA K	0.81	-0.31
250	P21291	CSRP1 Cysteine and glycine-rich protein 1	CSRP1	DGEIYCK	0.81	-0.31
251	P13798	APEH Acylamino-acid-releasing enzyme	APEH	QPALSAACLGPEVTT QYGGQYR	0.81	-0.31
252	P53582	METAP1 Methionine aminopeptidase 1	METAP1	VCETDGCSSEAK	0.81	-0.31
253	O60701	UGDH UDP-glucose 6-dehydrogenase	UGDH	EVVESCR	0.81	-0.31
254	P14618	PKM Pyruvate kinase PKM	PKM	NTGIICTIGPASR	0.81	-0.31
255	Q16643	DBN1 Drebrin	DBN1	CACASHVAK	0.81	-0.31
256	P21964	COMT Catechol O-methyltransferase	COMT	IVDAVIQEHQPSVLLE LGAYCGYSAVR	0.81	-0.30
257	Q9H6S3	EPS8L2 Epidermal growth factor receptor kinase substrate	EPS8L2	SGQAGYVPCNILGEA R	0.81	-0.30
258	P36954	POLR2I DNA-directed RNA polymerase II subunit RPB9	POLR2I	NCDYQQEADNSCIYV NK	0.81	-0.30
259	P14618	PKM Pyruvate kinase PKM	PKM	AEGSDVANAVLDGA DCIMLSGETAK	0.81	-0.30
260	Q7Z434	MAVS Mitochondrial antiviral-signaling protein	MAVS	NFSNFCNVDVVEILPY LPCLTAR	0.81	-0.30
261	P14866	HNRNPL Heterogeneous nuclear ribonucleoprotein L	HNRNPL	LCFSTAQHAS	0.81	-0.30
262	P22234	PAICS Multifunctional	PAICS	ITSCIFQLLQEAGIK	0.81	-0.30

		protein ADE2				
263	P57721	PCBP3 Poly(rC)-binding protein 3	PCBP3	LVVPASQCGSLIGK	0.81	-0.30
264	Q01433	AMPD2 AMP deaminase 2	AMPD2	CGVPFTDLLDAAK	0.81	-0.30
265	P26641	EEF1G Elongation factor 1-gamma	EEF1G	VPAFEGDDGFCVFES NAIAYYVSNEELR	0.81	-0.30
266	Q16851	UGP2 UTP--glucose-1-phosphate uridylyltransferase	UGP2	LNGGLGTSMGCK	0.81	-0.30
267	Q14694	USP10 Ubiquitin carboxyl-terminal hydrolase 10	USP10	SSVELPPYSGTVLCGT QAVDK	0.82	-0.29
268	P10620	MGST1 Microsomal glutathione S-transferase 1	MGST1	VFANPEDCVAFGK	0.82	-0.29
269	P51946	CCNH Cyclin-H	CCNH	TCLSQLLDIMK	0.82	-0.29
270	Q00796	SORD Sorbitol dehydrogenase	SORD	YCNTWPVAISMLASK	0.82	-0.29
271	P00338	LDHA L-lactate dehydrogenase A chain	LDHA	VIGSGCNLDSAR	0.82	-0.29
272	P09110	ACAA1 3-ketoacyl-CoA thiolase, peroxisomal	ACAA1	DCLIPMGITSENVAER	0.82	-0.29
273	P25789	PSMA4 Proteasome subunit alpha type-4	PSMA4	ATCIGNNSAAAVSML K	0.82	-0.29
274	P62820	RAB1A Ras-related protein Rab-1A	RAB1A	CDLTTK	0.82	-0.28
275	P63279	UBE2I SUMO-conjugating enzyme UBC9	UBE2I	QILLGIQELLNEPNIQ DPAQAEAYTIYCQNR	0.82	-0.28
276	P15924	DSP Desmoplakin	DSP	HQNQNTIQELLQNCS DCLMR	0.82	-0.28
277	P49753	ACOT2 Acyl-coenzyme A thioesterase 2, mitochondrial	ACOT2	SEFYANEACK	0.82	-0.28
278	P11940	PABPC1 Polyadenylate-binding protein 1	PABPC1	GFGFVCFSSPEEATK	0.82	-0.28
279	O14950	MYL12B Myosin regulatory light chain 12B	MYL12B	NAFACFDEEATGTIQ EDYLR	0.82	-0.28
280	Q15365	PCBP1 Poly(rC)-binding protein 1	PCBP1	LVVPATQCGSLIGK	0.82	-0.28
281	P42704	LRPPRC Leucine-rich PPR motif-containing protein, mitochondrial	LRPPRC	IHDVLCK	0.83	-0.28
282	P31943	HNRNPH1 Heterogeneous nuclear ribonucleoprotein H	HNRNPH1	GLPWSCSADEVQR	0.83	-0.28
283	Q13200	PSMD2 26S proteasome non-ATPase regulatory subunit 2	PSMD2	GTLTLCPYHSDR	0.83	-0.27

284	Q7L1Q6	BZW1 Basic leucine zipper and W2 domain-containing prot	BZW1	IQEYCYDNIHFMK	0.83	-0.27
285	Q9Y696	CLIC4 Chloride intracellular channel protein 4	CLIC4	FLDGNEMTLADCNLLPK	0.83	-0.27
286	Q7RTV0	PHF5A PHD finger-like domain-containing protein 5A	PHF5A	ICDECNYGSYQGR	0.83	-0.27
287	P26641	EEF1G Elongation factor 1-gamma	EEF1G	AAAPAPEEEMDECEQALAAEPK	0.83	-0.26
288	P30153	PPP2R1A Serine/threonine-protein phosphatase 2A 65 kDa reg	PPP2R1A	LNIISNLDCVNEVIGIR	0.83	-0.26
289	O60664	PLIN3 Perilipin-3	PLIN3	DIAQQLQATCTSLGSSIQGLPTNVK	0.84	-0.26
290	Q14980	NUMA1 Nuclear mitotic apparatus protein 1	NUMA1	PQLDLSIDSLDLSCEEGTPLSITSK	0.84	-0.26
291	Q9NS86	LANCL2 LanC-like protein 2	LANCL2	AFVNPFPDYEAAAGALLASGAAEETGCVR	0.84	-0.26
292	Q86YH6	PDSS2 Decaprenyl-diphosphate synthase subunit 2	PDSS2	CLLSDELSNIAMQVR	0.84	-0.26
293	Q9BRA2	TXNDC17 Thioredoxin domain-containing protein 17	TXNDC17	SWC*PDC*VQAEPVVR	0.84	-0.26
294	Q9BY32	ITPA Inosine triphosphate pyrophosphatase	ITPA	GCQDFGWDPCFQPDGYEQTYAEMPK	0.84	-0.25
295	Q96KB5	PBK Lymphokine-activated killer T-cell-originated prot	PBK	SVLCSTPTINIPASPFMQK	0.84	-0.25
296	Q9H5N1	RABEP2 Rab GTPase-binding effector protein 2	RABEP2	EETEVLEASLCSLR	0.84	-0.25
297	O00299	CLIC1 Chloride intracellular channel protein 1	CLIC1	EEFASTCPDDEEIELAYEQVAK	0.84	-0.25
298	Q9Y3D5	MRPS18C 28S ribosomal protein S18c, mitochondrial	MRPS18C	HITGLCGK	0.84	-0.25
299	Q9NXG2	THUMPD1 THUMP domain-containing protein 1	THUMPD1	CDAGGPR	0.84	-0.25
300	P37802	TAGLN2 Transgelin-2	TAGLN2	NMACVQR	0.84	-0.25
301	P49458	SRP9 Signal recognition particle 9 kDa protein	SRP9	VTDDLVCLVYK	0.84	-0.25
302	P22314	UBA1 Ubiquitin-like modifier-activating enzyme 1	UBA1	VLGPYTFSICDTSNFSDYIR	0.84	-0.24
303	P14618	PKM Pyruvate kinase	PKM	GIFPVLCK	0.85	-0.24

		PKM				
304	O95817	BAG3 BAG family molecular chaperone regulator 3	BAG3	SQSPAASDCSSSSSSASLPSSGR	0.85	-0.24
305	Q96FW1	OTUB1 Ubiquitin thioesterase OTUB1	OTUB1	PDGNCFYR	0.85	-0.24
306	P55263	ADK Adenosine kinase	ADK	TGCTFPEK	0.85	-0.24
307	Q15262	PTPRK Receptor-type tyrosine-protein phosphatase kappa	PTPRK	YLCEGTESPYQTGQLHPAIR	0.85	-0.24
308	P31943	HNRNPH1 Heterogeneous nuclear ribonucleoprotein H	HNRNPH1	GLPFGCSK	0.85	-0.24
309	P20810	CAST Calpastatin	CAST	SECK	0.85	-0.24
310	Q99460	PSMD1 26S proteasome non-ATPase regulatory subunit 1	PSMD1	SNCK	0.85	-0.24
311	Q7L1Q6	BZW1 Basic leucine zipper and W2 domain-containing prot	BZW1	FDPTQFQDCIIQGLTETGTDLEAVAK	0.85	-0.23
312	Q5RKV6	EXOSC6 Exosome complex component MTR3	EXOSC6	APPGGCEER	0.85	-0.23
313	P14868	DARS Aspartate--tRNA ligase, cytoplasmic	DARS	LEYCEALAMLR	0.85	-0.23
314	Q13185	CBX3 Chromobox protein homolog 3	CBX3	CPQIVIAFYEER	0.85	-0.23
315	A6NDG6	PGP Glycerol-3-phosphate phosphatase	PGP	FIAGTGCLVR	0.85	-0.23
316	P27348	YWHAQ 14-3-3 protein theta	YWHAQ	DNLTLWTSDSAGEECDAAEGAEN	0.85	-0.23
317	Q12765	SCRN1 Secernin-1	SCRN1	TQSPCFGDDDPAK	0.85	-0.23
318	Q6ISB3	GRHL2 Grainyhead-like protein 2 homolog	GRHL2	NCLGTSEAQSNLSGGENR	0.86	-0.22
319	Q09666	AHNAK Neuroblast differentiation-associated protein AHNA	AHNAK	GPFVEAEVPDVDLECPDAK	0.86	-0.22
320	O60361	NME2P1 Putative nucleoside diphosphate kinase	NME2P1	GDFCIQVGR	0.86	-0.22
321	P30084	ECHS1 Enoyl-CoA hydratase, mitochondrial	ECHS1	ALNALCDGLIDELNQALK	0.86	-0.22
322	Q15691	MAPRE1 Microtubule-associated protein RP/EB family member	MAPRE1	NIELICQENEGENDPVLQR	0.86	-0.22
323	P21281	ATP6V1B2 V-type proton ATPase subunit B, brain isoform	ATP6V1B2	TSCEFTGDILR	0.86	-0.22

324	P25789	PSMA4 Proteasome subunit alpha type-4	PSMA4	LNEDMACSVAGITSDANVLTNELR	0.86	-0.21
325	O43390	HNRNPR Heterogeneous nuclear ribonucleoprotein R	HNRNPR	SAFLCGVMK	0.86	-0.21
326	Q09666	AHNAK Neuroblast differentiation-associated protein AHNA	AHNAK	LEGDLTGPSVGVEVPDVELECPDAK	0.86	-0.21
327	Q15369	ELOC Elongin-C	ELOC	TYGGCEGPDAMYVK	0.86	-0.21
328	Q9H0C8	ILKAP Integrin-linked kinase-associated serine/threonine	ILKAP	CGVTSVPDIR	0.86	-0.21
329	Q9H3P7	ACBD3 Golgi resident protein GCP60	ACBD3	QVLMGPYNPDTCPEVGFFDVLGNDR	0.87	-0.21
330	Q92530	PSMF1 Proteasome inhibitor PI31 subunit	PSMF1	QPPWCDPLGPFVVGGEDLDPFGPR	0.87	-0.21
331	P10599	TXN Thioredoxin	TXN	CMPTFQFFK	0.87	-0.21
332	P15924	DSP Desmoplakin	DSP	ACGSEIMQK	0.87	-0.20
333	P07814	EPRS Bifunctional glutamate/proline--tRNA ligase	EPRS	LSSCDSFTSTINELNHCLSLR	0.87	-0.20
334	P49591	SARS Serine--tRNA ligase, cytoplasmic	SARS	YAGLSTCFR	0.87	-0.20
335	P12004	PCNA Proliferating cell nuclear antigen	PCNA	LMDLDVEQLGIPEQEYSCVVK	0.87	-0.20
336	P61978	HNRNPK Heterogeneous nuclear ribonucleoprotein K	HNRNPK	IIPTLEEGLQLPSPTATSQLPLESDAVECLNYQHYK	0.87	-0.20
337	P14866	HNRNPL Heterogeneous nuclear ribonucleoprotein L	HNRNPL	VFNVFCLYGNVEK	0.87	-0.20
338	P13639	EEF2 Elongation factor 2	EEF2	YVEPIEDVPCGNIVGLVGVDQFLVK	0.87	-0.20
339	P12532	CKMT1A Creatine kinase U-type, mitochondrial	CKMT1A	TTPTGWTLDQCIQTGVDNPGHPFIK	0.87	-0.20
340	Q6P2E9	EDC4 Enhancer of mRNA-decapping protein 4	EDC4	SCQAMFQQINDSFR	0.87	-0.19
341	P10599	TXN Thioredoxin	TXN	LVVVDFSATWCGPCK	0.87	-0.19
342	Q15149	PLEC Plectin	PLEC	LLEAQACTGGIIDPSTGER	0.87	-0.19
343	P08238	HSP90AB1 Heat shock protein HSP 90-beta	HSP90AB1	VFIMDSCDELIPEYLNFIR	0.87	-0.19
344	P27348	YWHAQ 14-3-3 protein theta	YWHAQ	YLAEVACGDDR	0.87	-0.19
345	P21333	FLNA Filamin-A	FLNA	AHVVPCFDASK	0.88	-0.19
346	Q96EY8	MMAB Cob(I)yrinic acid a,c-diamide adenosyltransferase,	MMAB	IQCTLQDVGSALATPCSSAR	0.88	-0.19
347	O15371	EIF3D Eukaryotic	EIF3D	FMTPVIQDNPSGWG	0.88	-0.19

		translation initiation factor 3 subunit		PCAVPEQFR		
348	P22234	PAICS Multifunctional protein ADE2	PAICS	ACGNFGIPCELR	0.88	-0.19
349	Q8NCW5	NAXE NAD(P)H-hydrate epimerase	NAXE	SPPTVLVICGPGNNGGDGLVCAR	0.88	-0.19
350	Q9Y3B4	SF3B6 Splicing factor 3B subunit 6	SF3B6	NACDHLSGFNVCNR	0.88	-0.19
351	Q96EI5	TCEAL4 Transcription elongation factor A protein-like 4	TCEAL4	PEVTCTLEDK	0.88	-0.19
352	P47756	CAPZB F-actin-capping protein subunit beta	CAPZB	GCWDSIHVVEVQEK	0.88	-0.19
353	A1X283	SH3PXD2B SH3 and PX domain-containing protein 2B	SH3PXD2B	GPQCEGHESR	0.88	-0.18
354	P51149	RAB7A Ras-related protein Rab-7a	RAB7A	AQAWCYSK	0.88	-0.18
355	P49321	NASP Nuclear autoantigenic sperm protein	NASP	PTDGASSSNCVTDISHLVR	0.88	-0.18
356	Q9NTK5	OLA1 Obg-like ATPase 1	OLA1	STFFNVLTNSQASAENFPFCTIDPNESR	0.88	-0.18
357	Q9HCC0	MCCC2 Methylcrotonoyl-CoA carboxylase beta chain, mitoch	MCCC2	LPCIYLVDSGGAYLPR	0.88	-0.18
358	P20618	PSMB1 Proteasome subunit beta type-1	PSMB1	TVIGCSGFHGDCLTLTK	0.88	-0.18
359	Q8WVJ2	NUDCD2 NudC domain-containing protein 2	NUDCD2	DAANCWTSLLESEYAADPWVQDQMQR	0.88	-0.18
360	P49419	ALDH7A1 Alpha-aminoadipic semialdehyde dehydrogenase	ALDH7A1	GSDCGIVNVNIPTSGAEIGGAFGGEK	0.89	-0.18
361	Q9NZZ3	CHMP5 Charged multivesicular body protein 5	CHMP5	APPPSLTDCIGTVDSR	0.89	-0.17
362	Q96HE7	ERO1A ERO1-like protein alpha	ERO1A	HDDSSDNFCEADDIQSPEAEYVDLLLNPER	0.89	-0.17
363	P63167	DYNLL1 Dynein light chain 1, cytoplasmic	DYNLL1	NADMSEEMQQDSVECATQALEK	0.89	-0.17
364	P78371	CCT2 T-complex protein 1 subunit beta	CCT2	SLHDALCVLAQTVK	0.89	-0.17
365	P58107	EPPK1 Epiplakin	EPPK1	YLEGTSCIAGVLVPAK	0.89	-0.17
366	Q15370	ELOB Elongin-B	ELOB	ADDTFEALCIEPFSSPPELPDVMK	0.89	-0.17
367	Q9NPF4	OSGEP Probable tRNA N6-adenosine threonylcarbamoyltransferase	OSGEP	AMAHCGSQEALIVGGVGCNVR	0.89	-0.17
368	Q7Z6Z7	HUWE1 E3 ubiquitin-	HUWE1	AQCETLSPDGLPEEQ	0.89	-0.17

		protein ligase HUWE1		PQTTK		
369	Q14247	CTTN Src substrate cortactin	CTTN	HCSQVDSVR	0.89	-0.17
370	O75362	ZNF217 Zinc finger protein 217	ZNF217	CIPQLDPFTTFQAWQLATK	0.89	-0.17
371	Q9BW61	DDA1 DET1- and DDB1-associated protein 1	DDA1	FHADSVCK	0.89	-0.17
372	Q14980	NUMA1 Nuclear mitotic apparatus protein 1	NUMA1	APVPSTCSSTFPEELSPPSHQAK	0.89	-0.16
373	P00966	ASS1 Argininosuccinate synthase	ASS1	FELSCYSLAPQIK	0.89	-0.16
374	P60981	DSTN Destrin	DSTN	LGGSLIVAFEGCPV	0.89	-0.16
375	O94903	PROSC Pyridoxal phosphate homeostasis protein	PROSC	ILSLCPEIK	0.89	-0.16
376	Q7Z5L9	IRF2BP2 Interferon regulatory factor 2-binding protein 2	IRF2BP2	AHGCFPEGR	0.89	-0.16
377	P60981	DSTN Destrin	DSTN	HECQANGPEDLNR	0.89	-0.16
378	P78347	GTF2I General transcription factor II-I	GTF2I	SILSPGGSCGPIK	0.89	-0.16
379	P49915	GMPS GMP synthase [glutamine-hydrolyzing]	GMPS	ACTTEEDQEK	0.89	-0.16
380	P21964	COMT Catechol O-methyltransferase	COMT	GTVLLADNVICPGAPDFLAHVR	0.89	-0.16
381	Q9Y5P6	GMPPB Mannose-1-phosphate guanyltransferase beta	GMPPB	LCSGPGIVGNVLVDPSAR	0.89	-0.16
382	Q09666	AHNAK Neuroblast differentiation-associated protein AHNA	AHNAK	SSGCDVNLPGVNVK	0.89	-0.16
383	Q96RS6	NUDCD1 NudC domain-containing protein 1	NUDCD1	DSAQCAAIAER	0.89	-0.16
384	P41250	GARS Glycine--tRNA ligase	GARS	SCYDLSCHAR	0.90	-0.16
385	P50570	DNM2 Dynamin-2	DNM2	LQDAFSSIGQSCHLDLPQIAVVGGQSAGK	0.90	-0.16
386	P60981	DSTN Destrin	DSTN	CSTPEEIK	0.90	-0.16
387	P00558	PGK1 Phosphoglycerate kinase 1	PGK1	ACANPAAGSVILLENLR	0.90	-0.15
388	Q9BQ24	ZFYVE21 Zinc finger FYVE domain-containing protein 21	ZFYVE21	MCFVDPVR	0.90	-0.15
389	Q14914	PTGR1 Prostaglandin reductase 1	PTGR1	IAICGAISTYNR	0.90	-0.15
390	P49589	CARS Cysteine--tRNA ligase, cytoplasmic	CARS	VQPQWSPPAGTQPCR	0.90	-0.15
391	Q96FW1	OTUB1 Ubiquitin thioesterase OTUB1	OTUB1	QEPLGSDSEGVNCLAYDEAIMAQQDR	0.90	-0.15
392	O14980	XPO1 Exportin-1	XPO1	LDINLLDNVVNCLYHGEGAQQR	0.90	-0.15

393	Q86SX6	GLRX5 Glutaredoxin-related protein 5, mitochondrial	GLRX5	GTPEQPQCGFSNAVVQILR	0.90	-0.14
394	P51659	HSD17B4 Peroxisomal multifunctional enzyme type 2	HSD17B4	ICDFENASK	0.90	-0.14
395	P60763	RAC3 Ras-related C3 botulinum toxin substrate 3	RAC3	AVLCPPPVK	0.90	-0.14
396	Q9Y365	STARD10 START domain-containing protein 10	STARD10	MECCDVPAETLYDVLHDIEYR	0.90	-0.14
397	P30101	PDIA3 Protein disulfide-isomerase A3	PDIA3	VDCTANTNTCNK	0.91	-0.14
398	Q9Y2Q3	GSTK1 Glutathione S-transferase kappa 1	GSTK1	ETTEAACR	0.91	-0.14
399	Q14247	CTTN Src substrate cortactin	CTTN	CALGWDHQEK	0.91	-0.14
400	P33316	DUT Deoxyuridine 5-triphosphate nucleotidohydrolase,	DUT	IAQLICER	0.91	-0.14
401	Q9Y3D2	MSRB2 Methionine-R-sulfoxide reductase B2, mitochondrial	MSRB2	GQAGGGGPGTGPGLGEAGSLATCELPLAK	0.91	-0.14
402	O75569	PRKRA Interferon-inducible double-stranded RNA-dependent	PRKRA	ANASICFAVPDPLMPDPSK	0.91	-0.14
403	Q9NRG0	CHRAC1 Chromatin accessibility complex protein 1	CHRAC1	ATELFVQCLATYSYR	0.91	-0.13
404	Q13526	PIN1 Peptidyl-prolyl cis-trans isomerase NIMA-interacting	PIN1	SGEEDFESLASQFSDCSSAK	0.91	-0.13
405	Q92598	HSPH1 Heat shock protein 105 kDa	HSPH1	LCGPYEK	0.92	-0.13
406	Q04637	EIF4G1 Eukaryotic translation initiation factor 4 gamma 1	EIF4G1	LQGINCGPDFTPSFANLGR	0.92	-0.13
407	P47756	CAPZB F-actin-capping protein subunit beta	CAPZB	DETVSDCSPHIANIGR	0.92	-0.12
408	Q93052	LPP Lipoma-preferred partner	LPP	TYITDPVSAPCAPPLQPK	0.92	-0.12
409	Q9UMS4	PRPF19 Pre-mRNA-processing factor 19	PRPF19	QELSHALYQHDAACR	0.92	-0.12
410	P21333	FLNA Filamin-A	FLNA	THEAEIVEGENHTYCIR	0.92	-0.12
411	Q6IA69	NADSYN1 Glutamine-dependent NAD(+) synthetase	NADSYN1	NSSQETCTR	0.92	-0.12
412	Q9NZL4	HSPBP1 Hsp70-binding protein 1	HSPBP1	ALFAISCLVR	0.92	-0.12

413	Q9Y696	CLIC4 Chloride intracellular channel protein 4	CLIC4	AGSDGESIGNCPFSQR	0.92	-0.12
414	Q96EK6	GNPNAT1 Glucosamine 6-phosphate N-acetyltransferase	GNPNAT1	ITLECLPQNVGFYK	0.92	-0.12
415	Q9NVU0	POLR3E DNA-directed RNA polymerase III subunit RPC5	POLR3E	AAGTDSFNGHPPQGCASTPVAR	0.92	-0.12
416	Q9H2U2	PPA2 Inorganic pyrophosphatase 2, mitochondrial	PPA2	CNGGAINCTNVQISDSPFR	0.92	-0.11
417	P53041	PPP5C Serine/threonine-protein phosphatase 5	PPP5C	TECAEPPR	0.92	-0.11
418	P35270	SPR Sepiapterin reductase	SPR	TVVNISSLCALQPFK	0.92	-0.11
419	P62826	RAN GTP-binding nuclear protein Ran	RAN	VCENIPIVLCGNK	0.93	-0.11
420	Q9UL25	RAB21 Ras-related protein Rab-21	RAB21	YCENK	0.93	-0.11
421	P61158	ACTR3 Actin-related protein 3	ACTR3	LGYAGNTEPQFIIPSCIAIK	0.93	-0.11
422	O14980	XPO1 Exportin-1	XPO1	DLLGLCEQK	0.93	-0.11
423	Q13573	SNW1 SNW domain-containing protein 1	SNW1	IPPCISNWK	0.93	-0.11
424	Q9Y3A3	MOB4 MOB-like protein phocein	MOB4	HTLDGAACLLNSNK	0.93	-0.11
425	Q9NX24	NHP2 H/ACA ribonucleoprotein complex subunit 2	NHP2	ADPDGPEAQAEACSGER	0.93	-0.11
426	P30048	PRDX3 Thioredoxin-dependent peroxide reductase, mitochondria	PRDX3	AFQYVETHGEVCPANWTPDSPTIK	0.93	-0.11
427	Q9Y2S7	POLDIP2 Polymerase delta-interacting protein 2	POLDIP2	DCPHISQR	0.93	-0.10
428	Q9Y3F4	STRAP Serine-threonine kinase receptor-associated protei	STRAP	IGFPETTEEELEEIASENSDCIFPSAPDVK	0.93	-0.10
429	O75663	TIPRL TIP41-like protein	TIPRL	VACAEEWQESR	0.93	-0.10
430	Q6PI48	DARS2 Aspartate--tRNA ligase, mitochondrial	DARS2	LICLVTGSPSIR	0.93	-0.10
431	Q8NEU8	APPL2 DCC-interacting protein 13-beta	APPL2	QESSCPSQNLK	0.93	-0.10
432	P52272	HNRNPM Heterogeneous nuclear ribonucleoprotein M	HNRNPM	GCGVVK	0.93	-0.10
433	Q86U28	ISCA2 Iron-sulfur cluster assembly 2 homolog,	ISCA2	SSFQVLNNPQAQQGCSCGSSFSIK	0.93	-0.10

		mitochondrial				
434	P11413	G6PD Glucose-6-phosphate 1-dehydrogenase	G6PD	TQVCGILR	0.93	-0.10
435	Q15149	PLEC Plectin	PLEC	AFCGFEDPR	0.93	-0.10
436	P31947	SFN 14-3-3 protein sigma	SFN	GEELSCEER	0.93	-0.10
437	Q99536	VAT1 Synaptic vesicle membrane protein VAT-1 homolog	VAT1	ACGLNFADLMAR	0.94	-0.10
438	Q15067	ACOX1 Peroxisomal acyl-coenzyme A oxidase 1	ACOX1	LVCGMVSYLNDLPSQR	0.94	-0.10
439	P42126	ECI1 Enoyl-CoA delta isomerase 1, mitochondrial	ECI1	LYQSNLVLVSAINGACPAGGCLVALTCDYR	0.94	-0.10
440	P51610	HCFC1 Host cell factor 1	HCFC1	TCLPGFPGAPCAIK	0.94	-0.10
441	Q13131	PRKAA1 5-AMP-activated protein kinase catalytic subunit	PRKAA1	ICDGIFYTPQYLNPSVISLLK	0.94	-0.09
442	P21333	FLNA Filamin-A	FLNA	CSGPGLSPGMVR	0.94	-0.09
443	Q9UNE7	STUB1 E3 ubiquitin-protein ligase CHIP	STUB1	AQQACIEAK	0.94	-0.09
444	Q9Y508	RNF114 E3 ubiquitin-protein ligase RNF114	RNF114	DCGGAAQLAGPAAEADPLGR	0.94	-0.09
445	P17676	CEBPB CCAAT/enhancer-binding protein beta	CEBPB	APPTACYAGAAPAPSQVK	0.94	-0.09
446	Q9Y6E2	BZW2 Basic leucine zipper and W2 domain-containing prot	BZW2	VQEYCYDNIHFMK	0.94	-0.09
447	P53602	MVD Diphosphomevalonate decarboxylase	MVD	DGDPLPSSLSCK	0.94	-0.09
448	Q9NQR4	NIT2 Omega-amidase NIT2	NIT2	TLSPGDSFSTFDTPYCR	0.94	-0.09
449	Q9BRA2	TXNDC17 Thioredoxin domain-containing protein 17	TXNDC17	SWCPDCVQAEPVVR	0.94	-0.09
450	P08708	RPS17 40S ribosomal protein S17	RPS17	VCEEIAIIPSK	0.94	-0.09
451	Q9UI30	TRMT112 Multifunctional methyltransferase subunit TRM112-l	TRMT112	ICPVEFNPNFVAR	0.94	-0.09
452	P40926	MDH2 Malate dehydrogenase, mitochondrial	MDH2	SQETECTYFSTPLLLGK	0.95	-0.08
453	Q8IY81	FTSJ3 pre-rRNA processing protein FTSJ3	FTSJ3	QQLPQTPPSCLK	0.95	-0.08

454	Q96EV8	DTNBP1 Dysbindin	DTNBP1	PPSSSSTCTDSATR	0.95	-0.08
455	Q9H0C8	ILKAP Integrin-linked kinase-associated serine/threonine	ILKAP	FILLACDGLFK	0.95	-0.08
456	Q99459	CDC5L Cell division cycle 5-like protein	CDC5L	LECLK	0.95	-0.07
457	P51610	HCFC1 Host cell factor 1	HCFC1	LVIYGGMSGCR	0.95	-0.07
458	Q9Y4P1	ATG4B Cysteine protease ATG4B	ATG4B	NFPAIGGTGPTSDTGWGCMLR	0.95	-0.07
459	Q14566	MCM6 DNA replication licensing factor MCM6	MCM6	LVFLACCVAPTNPR	0.95	-0.07
460	O95352	ATG7 Ubiquitin-like modifier-activating enzyme ATG7	ATG7	CLLLGAGTLGCNVAR	0.96	-0.06
461	Q96SW2	CRBN Protein cereblon	CRBN	VQILPECVLPSTMSAVQLESLNK	0.96	-0.06
462	Q5TFE4	NT5DC1 5-nucleotidase domain-containing protein 1	NT5DC1	HFLSDTGMACR	0.96	-0.06
463	P63208	SKP1 S-phase kinase-associated protein 1	SKP1	ENQWCEEK	0.96	-0.06
464	Q06210	GFPT1 Glutamine--fructose-6-phosphate aminotransferase [	GFPT1	DWEANACK	0.96	-0.06
465	P48163	ME1 NADP-dependent malic enzyme	ME1	SQMYSTDYDQILPDCYSWPEEVQK	0.96	-0.06
466	Q9Y5R8	TRAPPC1 Trafficking protein particle complex subunit 1	TRAPPC1	NPLCPLGQTVQSELFR	0.96	-0.06
467	P09110	ACAA1 3-ketoacyl-CoA thiolase, peroxisomal	ACAA1	PEQLGDICVGNVLQPGAGAIMAR	0.96	-0.06
468	Q9Y3C4	TPRKB EKC/KEOPS complex subunit TPRKB	TPRKB	LSSQEESIGTLLDAIICR	0.96	-0.06
469	P36507	MAP2K2 Dual specificity mitogen-activated protein kinase	MAP2K2	LCDFGVSGQLIDSMANSFVGTR	0.96	-0.06
470	O43684	BUB3 Mitotic checkpoint protein BUB3	BUB3	TPCNAGTFSQPEK	0.96	-0.06
471	P36969	GPX4 Phospholipid hydroperoxide glutathione peroxidase,	GPX4	ICVNGDDAHPLWK	0.96	-0.06
472	P10809	HSPD1 60 kDa heat shock protein, mitochondrial	HSPD1	CEFQDAYVLLSEK	0.96	-0.05
473	P61586	RHOA Transforming protein RhoA	RHOA	IGAFGYMECSAK	0.96	-0.05
474	Q8NBF2	NHLRC2 NHL repeat-containing protein 2	NHLRC2	AILFSQPLQITDTQQGCIAPVELR	0.96	-0.05
475	Q8TB45	DEPTOR DEP domain-	DEPTOR	SPSSQETHDSPFCLR	0.96	-0.05

		containing mTOR-interacting protein				
476	Q5T0W9	FAM83B Protein FAM83B	FAM83B	LCSSSDTLVSEGEENQK	0.97	-0.05
477	O95336	PGLS 6-phosphogluconolactonase	PGLS	LCWFLDEAAAR	0.97	-0.05
478	P50990	CCT8 T-complex protein 1 subunit theta	CCT8	NIQACK	0.97	-0.05
479	O75521	ECI2 Enoyl-CoA delta isomerase 2, mitochondrial	ECI2	WLSDECTNAVVNFLSR	0.97	-0.05
480	P16152	CBR1 Carbonyl reductase [NADPH] 1	CBR1	ILLNACCPGWVR	0.97	-0.04
481	P10809	HSPD1 60 kDa heat shock protein, mitochondrial	HSPD1	CIPALDSLTPANEDQK	0.97	-0.04
482	Q9UPY8	MAPRE3 Microtubule-associated protein RP/EB family member	MAPRE3	LSNVAPPCILR	0.97	-0.04
483	Q9Y3E2	BOLA1 BolA-like protein 1	BOLA1	ENSQLDTSPPCLGGNK	0.97	-0.04
484	O00233	PSMD9 26S proteasome non-ATPase regulatory subunit 9	PSMD9	GIGMNEPLVDCEGYPR	0.97	-0.04
485	O14976	GAK Cyclin-G-associated kinase	GAK	LCDFGSATTISHYPDYSWSAQR	0.97	-0.04
486	P38646	HSPA9 Stress-70 protein, mitochondrial	HSPA9	CELSSSVQTDINLPYLTMDSSGPK	0.98	-0.04
487	P62857	RPS28 40S ribosomal protein S28	RPS28	TGSQGQCTQVR	0.98	-0.04
488	P56381	ATP5E ATP synthase subunit epsilon, mitochondrial	ATP5E	YSQICAK	0.98	-0.04
489	P62993	GRB2 Growth factor receptor-bound protein 2	GRB2	VLNEECDQNWYK	0.98	-0.03
490	Q92879	CELF1 CUGBP Elav-like family member 1	CELF1	AMHQAQTMEGCSSPMVVK	0.98	-0.03
491	Q7Z6Z7	HUWE1 E3 ubiquitin-protein ligase HUWE1	HUWE1	DQSAQCTASK	0.98	-0.03
492	P42126	ECI1 Enoyl-CoA delta isomerase 1, mitochondrial	ECI1	YCIGLNETQLGIIAPFWLK	0.98	-0.03
493	P35270	SPR Sepiapterin reductase	SPR	AVCLLTGASR	0.98	-0.03
494	P22234	PAICS Multifunctional protein ADE2	PAICS	CGETAFIAPQCEMIPIEWVCR	0.98	-0.02
495	Q99829	CPNE1 Copine-1	CPNE1	NCSSPEFSK	0.98	-0.02
496	Q06323	PSME1 Proteasome activator complex	PSME1	GPPCGPVNCNEK	0.98	-0.02

		subunit 1				
497	Q9UNH7	SNX6 Sorting nexin-6	SNX6	IGSSLYALGTQDSTDICK	0.99	-0.02
498	P67936	TPM4 Tropomyosin alpha-4 chain	TPM4	EENVGLHQTLDQTLNELNCI	0.99	-0.01
499	Q9UHD8	SEPT9 Septin-9	9-Sep	SQEATEAAPSCVGDMADTPR	0.99	-0.01
500	Q00765	REEP5 Receptor expression-enhancing protein 5	REEP5	NCMTDLLAK	1.00	-0.01
501	Q7L2J0	MEPCE 7SK snRNA methylphosphate capping enzyme	MEPCE	CAPSAGSPAAAVGR	1.00	-0.01
502	Q9NQR4	NIT2 Omega-amidase NIT2	NIT2	VGLGICYDMR	1.00	-0.01
503	Q9GZZ9	UBA5 Ubiquitin-like modifier-activating enzyme 5	UBA5	EGVCAASLPTTMGVVAGILVQNVLK	1.00	0.00
504	Q96I24	FUBP3 Far upstream element-binding protein 3	FUBP3	SSGCFPNMAAK	1.00	0.00
505	Q9C0C9	UBE2O (E3-independent) E2 ubiquitin-conjugating enzyme	UBE2O	CYNEMALIR	1.00	0.00
506	Q15257	PTPA Serine/threonine-protein phosphatase 2A activator	PTPA	AGHCAPSEAIEK	1.00	0.00
507	Q96KB5	PBK Lymphokine-activated killer T-cell-originated prot	PBK	INPICNDHYR	1.00	0.00
508	Q9UHI6	DDX20 Probable ATP-dependent RNA helicase DDX20	DDX20	EALPVSLPQIPCLSSFK	1.00	0.01
509	P00492	HPRT1 Hypoxanthine-guanine phosphoribosyltransferase	HPRT1	SPGVVISDDEPGYDLDLFCIPNHYAEDLER	1.00	0.01
510	Q14139	UBE4A Ubiquitin conjugation factor E4 A	UBE4A	SQQEICEQLNINHMIQR	1.01	0.01
511	Q7RTV0	PHF5A PHD finger-like domain-containing protein 5A	PHF5A	PCTLVR	1.01	0.01
512	P01111	NRAS GTPase NRas	NRAS	CDLPTR	1.01	0.01
513	Q00610	CLTC Clathrin heavy chain 1	CLTC	VIQCFAETGQVQK	1.01	0.01
514	Q9BV79	MECR Enoyl-[acyl-carrier-protein] reductase, mitochondrial	MECR	LALNCVGGK	1.01	0.01
515	P51659	HSD17B4 Peroxisomal multifunctional enzyme	HSD17B4	SNIHCNTIAPNAGSR	1.01	0.01

		type 2				
516	Q9HCC0	MCCC2 Methylcrotonoyl-CoA carboxylase beta chain, mitoch	MCCC2	MVAAVACAQVPK	1.01	0.01
517	Q10567	AP1B1 AP-1 complex subunit beta-1	AP1B1	DCPLNAEAASSK	1.01	0.02
518	Q9NQC3	RTN4 Reticulon-4	RTN4	YSNSALGHVNCTIK	1.01	0.02
519	P51649	ALDH5A1 Succinate-semialdehyde dehydrogenase, mitochondria	ALDH5A1	NTGQTCVCSNQFLVQR	1.01	0.02
520	Q99832	CCT7 T-complex protein 1 subunit eta	CCT7	EGTDSSQGIPQLVSNISACQVIAEAVR	1.02	0.02
521	P21964	COMT Catechol O-methyltransferase	COMT	GSSCFECTHYQSFLEYR	1.02	0.03
522	P61158	ACTR3 Actin-related protein 3	ACTR3	YSYVCPDLVK	1.02	0.03
523	Q9UKV8	AGO2 Protein argonaute-2	AGO2	SFFTASEGCSNPLGGGR	1.02	0.03
524	Q9NXH9	TRMT1 tRNA (guanine(26)-N(2))-dimethyltransferase	TRMT1	FSAACGPPVTPECEHCGQR	1.02	0.03
525	Q14694	USP10 Ubiquitin carboxyl-terminal hydrolase 10	USP10	TPSYSISSTLNPQAPEFILGCTASK	1.02	0.03
526	P07737	PFN1 Profilin-1	PFN1	CSVIR	1.03	0.04
527	O75083	WDR1 WD repeat-containing protein 1	WDR1	CFSIDNPGYEPEVVAVHPGGDTVAIGGVDGNVR	1.03	0.04
528	P40227	CCT6A T-complex protein 1 subunit zeta	CCT6A	NAIDDGCVVPGAGAVEVAMAEALIK	1.03	0.04
529	Q9BV86	NTMT1 N-terminal Xaa-Pro-Lys N-methyltransferase 1	NTMT1	IICSAGLSLLAEER	1.03	0.05
530	Q9P2R7	SUCLA2 Succinate--CoA ligase [ADP-forming] subunit beta,	SUCLA2	ICNQVLVCER	1.03	0.05
531	Q15631	TSN Translin	TSN	ETAAACVEK	1.04	0.05
532	Q9Y3D5	MRPS18C 28S ribosomal protein S18c, mitochondrial	MRPS18C	NVQLLSQFVSPFTGCIYGR	1.04	0.06
533	Q14980	NUMA1 Nuclear mitotic apparatus protein 1	NUMA1	HPSSPECLVSAQK	1.04	0.06
534	Q6P1X6	C8orf82 UPF0598 protein C8orf82	C8orf82	YEAAFPFLSPCGR	1.04	0.06
535	P13639	EEF2 Elongation factor 2	EEF2	STLTDSLVCK	1.04	0.06
536	P28838	LAP3 Cytosol aminopeptidase	LAP3	SAGACTAAAFLK	1.04	0.06
537	Q15019	SEPT2 Septin-2	2-Sep	LTVVDTPGYGDAINC	1.04	0.06

				R		
538	Q86VP6	CAND1 Cullin-associated NEDD8-dissociated protein 1	CAND1	LSTLCPSAVLQR	1.04	0.06
539	Q9UL25	RAB21 Ras-related protein Rab-21	RAB21	VVLLGEGCVGK	1.05	0.06
540	P10809	HSPD1 60 kDa heat shock protein, mitochondrial	HSPD1	AAVEEGIVLGGGCAL LR	1.05	0.07
541	Q9ULV4	CORO1C Coronin-1C	CORO1C	DTICNQDER	1.05	0.07
542	Q9UL40	ZNF346 Zinc finger protein 346	ZNF346	NQCLFTNTQCK	1.05	0.07
543	O75363	BCAS1 Breast carcinoma-amplified sequence 1	BCAS1	GCNPSGHTQSVTTPE PAK	1.05	0.07
544	P13639	EEF2 Elongation factor 2	EEF2	TFCQLILDPIFK	1.05	0.07
545	O75153	CLUH Clustered mitochondria protein homolog	CLUH	CLTQQAVALQR	1.05	0.07
546	O15355	PPM1G Protein phosphatase 1G	PPM1G	GTEAGQVGEPGIPTG EAGPSCSSASDK	1.05	0.07
547	Q7L5N1	COPS6 COP9 signalosome complex subunit 6	COPS6	TCNTMNQFVNK	1.05	0.07
548	P29401	TKT Transketolase	TKT	QAFTDVATGSLGQGL GAACGMAYTGK	1.05	0.08
549	O00148	DDX39A ATP-dependent RNA helicase DDX39A	DDX39A	AIVDCGFEHPSEVQH ECIPQAILGMDVLCQ AK	1.05	0.08
550	Q8TCU6	PREX1 Phosphatidylinositol 3,4,5-trisphosphate-dependent	PREX1	PINALDELCR	1.05	0.08
551	Q9Y678	COPG1 Coatomer subunit gamma-1	COPG1	CSFDVVK	1.06	0.08
552	P61106	RAB14 Ras-related protein Rab-14	RAB14	SCLLHQFTEK	1.06	0.08
553	Q07960	ARHGAP1 Rho GTPase-activating protein 1	ARHGAP1	IIVFSACR	1.06	0.08
554	Q15020	SART3 Squamous cell carcinoma antigen recognized by T-ce	SART3	CAAVDVEPPSK	1.06	0.09
555	P42575	CASP2 Caspase-2	CASP2	MFFIQACR	1.06	0.09
556	O60232	SSSCA1 Sjoegren syndrome/scleroderma autoantigen 1	SSSCA1	AAQGPPAPAVPPNT DVMACTQTALLQK	1.07	0.09
557	O95817	BAG3 BAG family molecular chaperone regulator 3	BAG3	QCGQVAAAAAAQPP ASHGPER	1.07	0.10
558	Q13546	RIPK1 Receptor-interacting	RIPK1	GPNCIEHNEALLEEAK	1.07	0.10

		serine/threonine-protein kina				
559	P49327	FASN Fatty acid synthase	FASN	ADEASELACPTPK	1.07	0.10
560	Q5T160	RARS2 Probable arginine--tRNA ligase, mitochondrial	RARS2	LLGITPVCR	1.07	0.10
561	P61289	PSME3 Proteasome activator complex subunit 3	PSME3	LDECEEAFQGTK	1.07	0.10
562	P00367	GLUD1 Glutamate dehydrogenase 1, mitochondrial	GLUD1	CAVVDVPFGGAK	1.07	0.10
563	Q15185	PTGES3 Prostaglandin E synthase 3	PTGES3	HLNEIDLFHCIDPNDSK	1.08	0.11
564	P51610	HCFC1 Host cell factor 1	HCFC1	ACAAGTPAVIR	1.08	0.11
565	Q13425	SNTB2 Beta-2-syntrophin	SNTB2	LVHSGSGCR	1.08	0.11
566	P42704	LRPPRC Leucine-rich PPR motif-containing protein, mitochodrial	LRPPRC	SCGSLLPELK	1.08	0.11
567	Q9HCC0	MCCC2 Methylcrotonoyl-CoA carboxylase beta chain, mitoch	MCCC2	NIAQIAVVMGSCTAGGAYVPAMADENIIVR	1.08	0.11
568	Q9HC38	GLOD4 Glyoxalase domain-containing protein 4	GLOD4	SLNYWCNLLGMK	1.08	0.12
569	P49327	FASN Fatty acid synthase	FASN	LSIPTYGLQCTR	1.08	0.12
570	Q27J81	INF2 Inverted formin-2	INF2	LGPQDSDPTEANLESADPELCIR	1.09	0.12
571	Q8WUM4	PDCD6IP Programmed cell death 6-interacting protein	PDCD6IP	DTIVLLCK	1.09	0.12
572	Q86UU0	BCL9L B-cell CLL/lymphoma 9-like protein	BCL9L	TGNGGAQSQHQNVNQGPTCNVGSK	1.09	0.12
573	Q9P0L0	VAPA Vesicle-associated membrane protein-associated pro	VAPA	YCVR	1.09	0.12
574	P49327	FASN Fatty acid synthase	FASN	DPETLVGYSMVGCQR	1.09	0.12
575	P61106	RAB14 Ras-related protein Rab-14	RAB14	FMADCPHTIGVEFGTR	1.09	0.12
576	P14678	SNRPB Small nuclear ribonucleoprotein-associated protein	SNRPB	CILQDGR	1.09	0.13
577	Q13185	CBX3 Chromobox protein homolog 3	CBX3	LTWHSCPEDEAQ	1.10	0.13
578	P07814	EPRS Bifunctional	EPRS	PTPSLNNNCTTSEDSL	1.10	0.13

		glutamate/proline--tRNA ligase		VLYNR		
579	Q9ULZ3	PYCARD Apoptosis-associated speck-like protein containing	PYCARD	LFSFTPAWNWTCK	1.10	0.14
580	O95340	PAPSS2 Bifunctional 3-phosphoadenosine 5-phosphosulfate	PAPSS2	GCTVWLTGLSGAGK	1.10	0.14
581	P25205	MCM3 DNA replication licensing factor MCM3	MCM3	YVLCTAPR	1.10	0.14
582	O43865	AHCYL1 S-adenosylhomocysteine hydrolase-like protein 1	AHCYL1	LCVPAMNVNDSVTK	1.10	0.14
583	P49327	FASN Fatty acid synthase	FASN	AINCATSGVVGLVNCLR	1.11	0.14
584	Q9HCC0	MCCC2 Methylcrotonoyl-CoA carboxylase beta chain, mitoch	MCCC2	ITLIIGGSYGAGNYGMCGR	1.11	0.14
585	O95295	SNAPIN SNARE-associated protein Snapin	SNAPIN	EQIDNLATELCR	1.11	0.15
586	Q9BYG5	PARD6B Partitioning defective 6 homolog beta	PARD6B	HGAGSGCLGTMEVK	1.11	0.15
587	P48643	CCT5 T-complex protein 1 subunit epsilon	CCT5	VVNSCHR	1.11	0.15
588	P60604	UBE2G2 Ubiquitin-conjugating enzyme E2 G2	UBE2G2	VCISILHAPGDDPMGYESSAER	1.11	0.15
589	O95716	RAB3D Ras-related protein Rab-3D	RAB3D	LVDVICEK	1.11	0.15
590	P37198	NUP62 Nuclear pore glycoprotein p62	NUP62	DIIEHLNTSGAPADTSDPLQQICK	1.12	0.16
591	Q99714	HSD17B10 3-hydroxyacyl-CoA dehydrogenase type-2	HSD17B10	VCNFLASQVPFPSR	1.12	0.16
592	Q15233	NONO Non-POU domain-containing octamer-binding protein	NONO	FACHSASLTVR	1.12	0.16
593	O00231	PSMD11 26S proteasome non-ATPase regulatory subunit 11	PSMD11	TTANAIYCPPK	1.12	0.16
594	A6NCN2	KRT87P Putative keratin-87 protein	KRT87P	QDMACLIR	1.12	0.16
595	Q8NDH3	NPEPL1 Probable aminopeptidase NPEPL1	NPEPL1	IVDTPCNEMNTDTFLEEINK	1.12	0.17
596	P78371	CCT2 T-complex	CCT2	TVYGGGCSEMLMAH	1.12	0.17

		protein 1 subunit beta		AVTQLANR		
597	Q07866	KLC1 Kinesin light chain 1	KLC1	ACK	1.12	0.17
598	Q96CD2	PPCDC Phosphopantothenoylcysteine decarboxylase	PPCDC	ASCPAAAPLMER	1.13	0.17
599	Q1KMD3	HNRNPUL2 Heterogeneous nuclear ribonucleoprotein U-like pro	HNRNPUL2	EGCTEVSLLR	1.13	0.17
600	P53396	ACLY ATP-citrate synthase	ACLY	FICTTSAIQNR	1.13	0.18
601	Q9Y266	NUDC Nuclear migration protein nudC	NUDC	WTQTLSELDLAVPFCVNFR	1.13	0.18
602	P38117	ETFB Electron transfer flavoprotein subunit beta	ETFB	EVIAVSC*GPAQC*QETIR	1.13	0.18
603	P59998	ARPC4 Actin-related protein 2/3 complex subunit 4	ARPC4	ATLQAALCLENFSSQVVER	1.14	0.19
604	Q14980	NUMA1 Nuclear mitotic apparatus protein 1	NUMA1	QFCSTQAALQAMER	1.14	0.19
605	Q5MNZ6	WDR45B WD repeat domain phosphoinositide-interacting prot	WDR45B	CNYLALVGGGK	1.14	0.19
606	P38646	HSPA9 Stress-70 protein, mitochondrial	HSPA9	GAVVGIDLGTTNSCVAVMEGK	1.14	0.19
607	O15355	PPM1G Protein phosphatase 1G	PPM1G	CSGDGVGAPR	1.14	0.19
608	O14929	HAT1 Histone acetyltransferase type B catalytic subunit	HAT1	VDENFDCVEADDVEGK	1.14	0.19
609	Q9NR46	SH3GLB2 Endophilin-B2	SH3GLB2	SQTTYYAQCYR	1.15	0.20
610	P68036	UBE2L3 Ubiquitin-conjugating enzyme E2 L3	UBE2L3	GQVCLPVISAENWK	1.15	0.20
611	P00492	HPRT1 Hypoxanthine-guanine phosphoribosyltransferase	HPRT1	SYCNDQSTGDIK	1.15	0.20
612	P37235	HPCAL1 Hippocalcin-like protein 1	HPCAL1	LLQCDPSSASQF	1.15	0.20
613	Q8N163	CCAR2 Cell cycle and apoptosis regulator protein 2	CCAR2	VHLTPYTVDSPICDFLELQR	1.15	0.20
614	Q6ISB3	GRHL2 Grainyhead-like protein 2 homolog	GRHL2	GQASQTQCNSSSDGK	1.15	0.20
615	P51812	RPS6KA3 Ribosomal protein S6 kinase alpha-3	RPS6KA3	AENGLLMTPCYTANFVAPEVLK	1.15	0.20
616	Q9BRJ7	NUDT16L1 Tudor-	NUDT16L	VLGLGLGCLR	1.15	0.20

		interacting repair regulator protein	1			
617	Q14980	NUMA1 Nuclear mitotic apparatus protein 1	NUMA1	HLCQQLQAEQAAAEK	1.15	0.20
618	Q8TEX9	IPO4 Importin-4	IPO4	APAALPALCDLLASAADPQIR	1.15	0.21
619	P62714	PPP2CB Serine/threonine-protein phosphatase 2A catalytic	PPP2CB	NVVTIFSAPNYCYR	1.15	0.21
620	Q8N987	NECAB1 N-terminal EF-hand calcium-binding protein 1	NECAB1	ETLNQLQSLQNSLECAMETTEEQTR	1.16	0.21
621	Q6PKG0	LARP1 La-related protein 1	LARP1	TASISSSPSEGTPTVGSYGCTPQSLPK	1.16	0.21
622	Q9HA64	FN3KRP Ketosamine-3-kinase	FN3KRP	ATGHSGGGCISQGR	1.16	0.21
623	O00571	DDX3X ATP-dependent RNA helicase DDX3X	DDX3X	WCDK	1.16	0.21
624	P38117	ETFB Electron transfer flavoprotein subunit beta	ETFB	EVIAVSCGPAQCQETIR	1.16	0.22
625	Q9UPN9	TRIM33 E3 ubiquitin-protein ligase TRIM33	TRIM33	QEPGTEDEICSFSGGVK	1.16	0.22
626	Q16822	PCK2 Phosphoenolpyruvate carboxykinase [GTP], mitochond	PCK2	QCPIMDPAWEAPEGVPIDAIIFGGR	1.16	0.22
627	Q15233	NONO Non-POU domain-containing octamer-binding protein	NONO	CSEGSFLLTTFPR	1.16	0.22
628	Q9NQ88	TIGAR Fructose-2,6-bisphosphatase TIGAR	TIGAR	EECPVFTPPGGETLDQVK	1.17	0.22
629	O75934	BCAS2 Pre-mRNA-splicing factor SPF27	BCAS2	NDITAWQECVNNSMAQLEHQAVR	1.17	0.22
630	Q8TAQ2	SMARCC2 SWI/SNF complex subunit SMARCC2	SMARCC2	NLAGDVCAIMR	1.17	0.23
631	Q7L5Y1	ENOSF1 Mitochondrial enolase superfamily member 1	ENOSF1	ALQFLQIDSCR	1.17	0.23
632	P53618	COPB1 Coatomer subunit beta	COPB1	ISLCLK	1.17	0.23
633	Q7Z6Z7	HUWE1 E3 ubiquitin-protein ligase HUWE1	HUWE1	HIIEDPCTLR	1.18	0.23
634	Q9BUH6	C9orf142 Protein PAXX	C9orf142	CPGESLINPGFK	1.18	0.24
635	P53396	ACLY ATP-citrate synthase	ACLY	PASFMTSICDER	1.18	0.24
636	P07741	APRT Adenine phosphoribosyltransfer	APRT	VVVVDDLLATGGTMNAACELLGR	1.18	0.24

		ase				
637	P46782	RPS5 40S ribosomal protein S5	RPS5	VNQAIWLLCTGAR	1.18	0.24
638	Q14258	TRIM25 E3 ubiquitin/ISG15 ligase TRIM25	TRIM25	NTVLCNVVEQFLQADLAR	1.18	0.24
639	Q9P2T1	GMPR2 GMP reductase 2	GMPR2	VTQQVNPIFSEAC	1.18	0.24
640	Q9HCC0	MCCC2 Methylcrotonoyl-CoA carboxylase beta chain, mitoch	MCCC2	AATGEEVSAEDLGGADLHCR	1.18	0.24
641	Q9Y2H0	DLGAP4 Disks large-associated protein 4	DLGAP4	DTDSDTQDANDSSCK	1.18	0.24
642	Q96IJ6	GMPPA Mannose-1-phosphate guanyltransferase alpha	GMPPA	LLPAITILGCR	1.19	0.25
643	P63220	RPS21 40S ribosomal protein S21	RPS21	TYAICGAIR	1.19	0.25
644	P38117	ETFB Electron transfer flavoprotein subunit beta	ETFB	HSMNPFCEIAVEEAVR	1.19	0.25
645	Q9UHD8	SEPT9 Septin-9	9-Sep	LTVIDTPGFGDHINNENCWQPIMK	1.20	0.26
646	P48200	IREB2 Iron-responsive element-binding protein 2	IREB2	CAIQNAPNPGGGDLQK	1.20	0.26
647	Q96IF1	AJUBA LIM domain-containing protein ajuba	AJUBA	PCSNR	1.20	0.26
648	P56192	MARS Methionine--tRNA ligase, cytoplasmic	MARS	LFVSDGVPGCLPVLAAAGR	1.21	0.27
649	Q00610	CLTC Clathrin heavy chain 1	CLTC	IHEGCEEPATHNALAK	1.21	0.27
650	O95336	PGLS 6-phosphogluconolactonase	PGLS	AACCLAGAR	1.21	0.27
651	Q9BQ69	MACROD1 O-acetyl-ADP-ribose deacetylase MACROD1	MACROD1	LEVDAIVNAANSSLLGGGGVDGCIHR	1.21	0.28
652	Q14839	CHD4 Chromodomain-helicase-DNA-binding protein 4	CHD4	HLCEPGADGAETFADGVPR	1.21	0.28
653	P26599	PTBP1 Polypyrimidine tract-binding protein 1	PTBP1	LSLDGQNIYNACCTLR	1.21	0.28
654	Q08211	DHX9 ATP-dependent RNA helicase A	DHX9	LQISHEAAACITGLR	1.21	0.28
655	Q16576	RBBP7 Histone-binding protein RBBP7	RBBP7	VHIPNDDAQFDASHCDSDK	1.22	0.28
656	P09497	CLTB Clathrin light	CLTB	VAQLCDFNPK	1.22	0.29

		chain B				
657	Q14C86	GAPVD1 GTPase-activating protein and VPS9 domain-containing	GAPVD1	FSLCSDNLEGISEGPSNR	1.22	0.29
658	P55769	SNU13 NHP2-like protein 1	SNU13	LLDLVQQSCNYK	1.23	0.30
659	P40926	MDH2 Malate dehydrogenase, mitochondrial	MDH2	TIIPLISQCTPK	1.23	0.30
660	Q7Z4W1	DCXR L-xylulose reductase	DCXR	GVPGAIVNVSSQCSQR	1.23	0.30
661	Q99873	PRMT1 Protein arginine N-methyltransferase 1	PRMT1	VIGIECSSISDYAVK	1.24	0.31
662	O43175	PHGDH D-3-phosphoglycerate dehydrogenase	PHGDH	NAGNCLSPAVIVGLLK	1.24	0.31
663	Q7Z2W4	ZC3HAV1 Zinc finger CCCH-type antiviral protein 1	ZC3HAV1	NSNVDSSYLESLYQSCPR	1.24	0.31
664	P14678	SNRPB Small nuclear ribonucleoprotein-associated protein	SNRPB	HMNLILCDCDEFR	1.24	0.31
665	P68104	EEF1A1 Elongation factor 1-alpha 1	EEF1A1	DGNASGTTLLEALDCILPPTR	1.24	0.32
666	O00299	CLIC1 Chloride intracellular channel protein 1	CLIC1	IGNCPFSQR	1.25	0.32
667	Q7Z4W1	DCXR L-xylulose reductase	DCXR	AVTNHSVYCSTK	1.25	0.32
668	Q99832	CCT7 T-complex protein 1 subunit eta	CCT7	CAMTALSSK	1.26	0.33
669	Q8WVV9	HNRNPLL Heterogeneous nuclear ribonucleoprotein L-like	HNRNPLL	LCFSTSSHL	1.27	0.34
670	P22830	FECH Ferrochelatase, mitochondrial	FECH	AIAFTQYPQYSCSTTGSSLNAIYR	1.27	0.34
671	Q9P258	RCC2 Protein RCC2	RCC2	AVQDLCGWR	1.27	0.35
672	P27708	CAD Ferro chelatase protein	CAD	VHVDCMTSQK	1.28	0.35
673	P54646	PRKAA2 5-AMP-activated protein kinase catalytic subunit	PRKAA2	TSCGSPNYAAPEVISGR	1.28	0.35
674	Q16186	ADRM1 Proteasomal ubiquitin receptor ADRM1	ADRM1	TDQDEEHCR	1.28	0.36
675	P62191	PSMC1 26S proteasome regulatory subunit 4	PSMC1	AICTEAGLMALR	1.28	0.36
676	P60709	ACTB Actin, cytoplasmic 1	ACTB	CPEALFQPSFLGMESCGIHETTFNSIMK	1.28	0.36
677	P58107	EPPK1 Epiplakin	EPPK1	YLCGLGAVGGVR	1.28	0.36

678	P53384	NUBP1 Cytosolic Fe-S cluster assembly factor NUBP1	NUBP1	GASCQGCPNQR	1.28	0.36
679	P42166	TMPO Lamina-associated polypeptide 2, isoform alpha	TMPO	SGIQPLCPER	1.29	0.36
680	P30281	CCND3 G1/S-specific cyclin-D3	CCND3	ASYFQCVQR	1.29	0.37
681	P12268	IMPDH2 Inosine-5-monophosphate dehydrogenase 2	IMPDH2	VGMGSGSICITQEVLACGR	1.29	0.37
682	P43686	PSMC4 26S proteasome regulatory subunit 6B	PSMC4	GVLMYGPPGCGK	1.30	0.38
683	Q8NDH3	NPEPL1 Probable aminopeptidase NPEPL1	NPEPL1	VTEELWQAALSTLNPNPTDSCPLYLNYATVAALPCR	1.30	0.38
684	P27361	MAPK3 Mitogen-activated protein kinase 3	MAPK3	ISPFEHQTYCQR	1.30	0.38
685	P38117	ETFB Electron transfer flavoprotein subunit beta	ETFB	QAIDDDCNQTGQMTAGFLDWPQGTFASQVTLEGDK	1.30	0.38
686	P46782	RPS5 40S ribosomal protein S5	RPS5	TIAECLADELINAAK	1.31	0.39
687	Q2TAA2	IAH1 Isoamyl acetate-hydrolyzing esterase 1 homolog	IAH1	VILITPTPLCETAWEEQCIIQGCK	1.31	0.39
688	P62879	GNB2 Guanine nucleotide-binding protein G(I)/G(S)/G(T)	GNB2	TFVSGACDASIK	1.32	0.40
689	Q96P16	RPRD1A Regulation of nuclear pre-mRNA domain-containing p	RPRD1A	HVSSETDESCK	1.32	0.40
690	P23443	RPS6KB1 Ribosomal protein S6 kinase beta-1	RPS6KB1	PECFELLR	1.32	0.40
691	O60547	GMDS GDP-mannose 4,6 dehydratase	GMDS	LHYGDLTDSTCLVK	1.32	0.40
692	P12532	CKMT1A Creatine kinase U-type, mitochondrial	CKMT1A	LGYILTCPSNLGTGLR	1.33	0.41
693	Q13057	COASY Bifunctional coenzyme A synthase	COASY	YATSCYSCCPR	1.33	0.41
694	P13639	EEF2 Elongation factor 2	EEF2	VTDGALVVVDCVSGVCVQTETVLR	1.33	0.41
695	O94903	PROSC Pyridoxal phosphate homeostasis protein	PROSC	CAADVK	1.33	0.41
696	P55060	CSE1L Exportin-2	CSE1L	LSTACPGR	1.33	0.41
697	P49189	ALDH9A1 4-trimethylaminobutyral	ALDH9A1	GALMANFLTQGQVCCNGTR	1.33	0.42

		dehyde dehydrogenase				
698	Q15019	SEPT2 Septin-2	2-Sep	LTVVDTPGYGDAINC*RDC*FK	1.34	0.42
699	P45984	MAPK9 Mitogen-activated protein kinase 9	MAPK9	TACTNFMMTPYVVTR	1.34	0.42
700	P49327	FASN Fatty acid synthase	FASN	AFDTAGNGYCR	1.34	0.42
701	P62195	PSMC5 26S proteasome regulatory subunit 8	PSMC5	NIDINDVTPNCR	1.34	0.43
702	P46777	RPL5 60S ribosomal protein L5	RPL5	VGLTNYAAAYCTGLLLAR	1.34	0.43
703	P31943	HNRNPH1 Heterogeneous nuclear ribonucleoprotein H	HNRNPH1	DLNYCFSGMSDHR	1.34	0.43
704	Q96AB3	ISOC2 Isochorismatase domain-containing protein 2	ISOC2	VLPGSSVLFLCDMQEK	1.36	0.44
705	Q9UBT2	UBA2 SUMO-activating enzyme subunit 2	UBA2	VLVVGAGGIGCELLK	1.36	0.44
706	P68363	TUBA1B Tubulin alpha-1B chain	TUBA1B	ECISIHVGQAGVQIGNACWELYCLEHGIQPDGQMPSDK	1.36	0.44
707	Q27J81	INF2 Inverted formin-2	INF2	CPASEPGLDATTASESR	1.36	0.45
708	Q8N163	CCAR2 Cell cycle and apoptosis regulator protein 2	CCAR2	VVTQNICQYR	1.36	0.45
709	Q8IWB7	WDFY1 WD repeat and FYVE domain-containing protein 1	WDFY1	IWDMTPVVGCSLATGFSPH	1.36	0.45
710	Q9NQR4	NIT2 Omega-amidase NIT2	NIT2	IVSLPECFNSPYGAK	1.37	0.45
711	P13639	EEF2 Elongation factor 2	EEF2	DLEEDHACIPIK	1.37	0.45
712	P54886	ALDH18A1 Delta-1-pyrroline-5-carboxylate synthase	ALDH18A1	GDECGLALGR	1.38	0.46
713	P13995	MTHFD2 Bifunctional methylenetetrahydrofolate dehydrogenase	MTHFD2	MCLDQYSMLPATPWGVWEIIK	1.38	0.46
714	O95671	ASMTL N-acetylserotonin O-methyltransferase-like protein	ASMTL	LTACQVATAFNLSR	1.38	0.47
715	Q13362	PPP2R5C Serine/threonine-protein phosphatase 2A 56 kDa reg	PPP2R5C	CVSSPHFQVAER	1.39	0.47
716	P60866	RPS20 40S ribosomal protein S20	RPS20	TPCGEGSK	1.39	0.47

717	Q9GZT4	SRR Serine racemase	SRR	CATQLVWER	1.39	0.47
718	P24468	NR2F2 COUP transcription factor 2	NR2F2	FGSQCMQPNNIMGI ENICELAAR	1.39	0.48
719	P19838	NFKB1 Nuclear factor NF-kappa-B p105 subunit	NFKB1	YVCEGPSHGGLPGAS SEK	1.39	0.48
720	Q13268	DHRS2 Dehydrogenase/reduct ase SDR family member 2, mitochondrial	DHRS2	VNCVVPGIIK	1.39	0.48
721	P11172	UMPS Uridine 5-monophosphate synthase	UMPS	LHSVCTLSK	1.40	0.48
722	Q02252	ALDH6A1 Methylmalonate-semialdehyde dehydrogenase	ALDH6A1	CMALSTAVLVGEAK	1.40	0.48
723	P60981	DSTN Destrin	DSTN	ACIAEK	1.40	0.49
724	P61026	RAB10 Ras-related protein Rab-10	RAB10	CDMDDK	1.40	0.49
725	P07814	EPRS Bifunctional glutamate/proline--tRNA ligase	EPRS	LGVENCYFPMFVSQS ALEK	1.41	0.50
726	P34897	SHMT2 Serine hydroxymethyltransfer ase, mitochondrial	SHMT2	YYGGAEVVDEIELLCQ R	1.41	0.50
727	P49327	FASN Fatty acid synthase	FASN	LTPGCEAEAETEAICF FVQQFTDMEHNR	1.41	0.50
728	O00244	ATOX1 Copper transport protein ATOX1	ATOX1	VCIESEHSMDTLLATL K	1.41	0.50
729	P68104	EEF1A1 Elongation factor 1-alpha 1	EEF1A1	PMCVESFSDYPPLGR	1.41	0.50
730	P08134	RHOC Rho-related GTP-binding protein RhoC	RHOC	ISAFGYLECSAK	1.42	0.50
731	Q969H4	CNKSR1 Connector enhancer of kinase suppressor of ras 1	CNKSR1	NLLQLCPQSLEALAVR	1.43	0.52
732	O95453	PARN Poly(A)-specific ribonuclease PARN	PARN	CPVTIPEDQK	1.43	0.52
733	P46782	RPS5 40S ribosomal protein S5	RPS5	AQCPIVER	1.44	0.52
734	Q29RF7	PDS5A Sister chromatid cohesion protein PDS5 homolog A	PDS5A	QPTSEANCSAMFGK	1.44	0.52
735	P63241	EIF5A Eukaryotic translation initiation factor 5A-1	EIF5A	YEDICPSTHNMDVPN IK	1.44	0.53
736	P46940	IQGAP1 Ras GTPase-activating-like protein IQGAP1	IQGAP1	QIPAITCIQSQWR	1.44	0.53
737	O43929	ORC4 Origin	ORC4	SNSLIHTECLSQVQR	1.44	0.53

		recognition complex subunit 4				
738	Q16186	ADRM1 Proteasomal ubiquitin receptor ADRM1	ADRM1	VPQCPSGR	1.44	0.53
739	Q9HCY8	S100A14 Protein S100-A14	S100A14	IANLGSCNDSK	1.44	0.53
740	Q9ULV4	CORO1C Coronin-1C	CORO1C	CDLISIPK	1.45	0.53
741	O94979	SEC31A Protein transport protein Sec31A	SEC31A	SCATFSSSHR	1.45	0.54
742	P08559	PDHA1 Pyruvate dehydrogenase E1 component subunit alpha,	PDHA1	VDGMDILCVR	1.45	0.54
743	O94925	GLS Glutaminase kidney isoform, mitochondrial	GLS	CVQSNIVLLTQAFR	1.46	0.54
744	Q92599	SEPT8 Septin-8	8-Sep	QYPWGVVQVENEN HCDFVK	1.46	0.55
745	Q9NUU 7	DDX19A ATP-dependent RNA helicase DDX19A	DDX19A	VLVTTNVCAR	1.46	0.55
746	Q14318	FKBP8 Peptidyl-prolyl cis-trans isomerase FKBP8	FKBP8	CLNNLAASQLK	1.47	0.55
747	Q96T51	RUFY1 RUN and FYVE domain-containing protein 1	RUFY1	HLSCTVGDLQTK	1.47	0.55
748	Q9UJU6	DBNL Drebrin-like protein	DBNL	AEEDVEPECIMEK	1.47	0.55
749	Q5T0N5	FNBP1L Formin-binding protein 1-like	FNBP1L	FTSCVAFFNILNELND YAGQR	1.48	0.56
750	Q9Y5Y2	NUBP2 Cytosolic Fe-S cluster assembly factor NUBP2	NUBP2	VMGIVENMSGFTCP HCTECTSVFSR	1.48	0.57
751	Q96QR8	PURB Transcriptional activator protein Pur-beta	PURB	GGGGGPCGFQPASR	1.48	0.57
752	O60716	CTNND1 Catenin delta-1	CTNND1	TPAILEASAGAIQNLC AGR	1.48	0.57
753	Q14232	EIF2B1 Translation initiation factor eIF-2B subunit alpha	EIF2B1	IGTNQMAVCAK	1.50	0.59
754	Q96PK6	RBM14 RNA-binding protein 14	RBM14	IFVGNVSAACTSQELR	1.51	0.59
755	Q00613	HSF1 Heat shock factor protein 1	HSF1	QECMDSK	1.51	0.59
756	P61247	RPS3A 40S ribosomal protein S3a	RPS3A	NCLTNFHGMDLTR	1.51	0.59
757	Q6UB35	MTHFD1L Monofunctional C1-	MTHFD1L	YTQQGFGNLPICMAK	1.52	0.60

		tetrahydrofolate synthase, mitochondrial				
758	Q9Y3D2	MSRB2 Methionine-R-sulfoxide reductase B2, mitochondrial	MSRB2	YCSGTGWPSFSEAHG TSGSDESHTGILR	1.52	0.60
759	P62249	RPS16 40S ribosomal protein S16	RPS16	TATAVAHCK	1.52	0.61
760	Q99832	CCT7 T-complex protein 1 subunit eta	CCT7	CQVFEETQIGGER	1.53	0.62
761	P62330	ARF6 ADP-ribosylation factor 6	ARF6	NWYVQPSCATSGDG LYEGLTWLTSNYK	1.53	0.62
762	P22102	GART Trifunctional purine biosynthetic protein adenosin	GART	SAGVQCFGPTAEAA QLESSK	1.53	0.62
763	P05386	RPLP1 60S acidic ribosomal protein P1	RPLP1	ALANVNIGSLICNVG AGGPAPAAGAAPAG GPAPSTAAAPAEEK	1.54	0.62
764	P51570	GALK1 Galactokinase	GALK1	GHALLIDCR	1.54	0.63
765	P27797	CALR Calreticulin	CALR	HEQNIDCGGGYVK	1.54	0.63
766	Q6YN16	HSDL2 Hydroxysteroid dehydrogenase-like protein 2	HSDL2	TAIHTAAMDMLGGP GIESQCR	1.55	0.63
767	Q9NXJ5	PGPEP1 Pyroglutamyl-peptidase 1	PGPEP1	YLCDFTYYTSLYQSHG R	1.55	0.63
768	Q7L2J0	MEPCE 7SK snRNA methylphosphate capping enzyme	MEPCE	SCFPASLTASR	1.55	0.63
769	P58107	EPPK1 Epiplakin	EPPK1	TSYAQLLEECPR	1.55	0.63
770	P27707	DCK Deoxycytidine kinase	DCK	SCPSFSASSEGTR	1.55	0.63
771	P05388	RPLP0 60S acidic ribosomal protein P0	RPLP0	AGAIAPCEVTVPAQN TGLGPEK	1.55	0.64
772	Q6AI08	HEATR6 HEAT repeat-containing protein 6	HEATR6	LCALR	1.56	0.64
773	Q9P2J5	LARS Leucine--tRNA ligase, cytoplasmic	LARS	NFEATLGWLQEHAC SR	1.56	0.64
774	Q9NVS9	PNPO Pyridoxine-5-phosphate oxidase	PNPO	LPEEEAECYFHSR	1.56	0.64
775	P40337	VHL von Hippel-Lindau disease tumor suppressor	VHL	EPSQVIFCNR	1.57	0.65
776	P12268	IMPDH2 Inosine-5-monophosphate dehydrogenase 2	IMPDH2	HGFCGIPITDTGR	1.57	0.65
777	P34897	SHMT2 Serine hydroxymethyltransferase, mitochondrial	SHMT2	NTCPGDR	1.57	0.65
778	Q5VZ89	DENND4C DENN domain-containing protein 4C	DENND4C	CANVNNSSTTSQR	1.58	0.66
779	P53618	COPB1 Coatomer	COPB1	ALSGYCGFMAANLYA	1.58	0.66

		subunit beta		R		
780	P15880	RPS2 40S ribosomal protein S2	RPS2	GCTATLGNFAK	1.58	0.66
781	P54136	RARS Arginine--tRNA ligase, cytoplasmic	RARS	NC*GC*LGASPNLEQ LQEENLK	1.58	0.66
782	P34897	SHMT2 Serine hydroxymethyltransfer ase, mitochondrial	SHMT2	AALEALGSCLNNK	1.59	0.67
783	Q96I99	SUCLG2 Succinate--CoA ligase [GDP-forming] subunit beta,	SUCLG2	SCNGPVLVGSPQGG VDIEEVAASNPELIFK	1.59	0.67
784	O60502	MGEA5 Protein O-GlcNAcase	MGEA5	SFVQWLGCR	1.60	0.68
785	Q8TCU6	PREX1 Phosphatidylinositol 3,4,5-trisphosphate-dependent	PREX1	LCVLNEILGTER	1.61	0.68
786	Q9UMS 0	NFU1 Pyro glutamyl iron-sulfur cluster scaffold homolog, mitochondrial	NFU1	LQGSCTSCPSSIITLK	1.61	0.69
787	P62316	SNRPD2 Small nuclear ribonucleoprotein Sm D2	SNRPD2	NNTQVLINCR	1.61	0.69
788	P35914	HMGCL Hydroxymethylglutaryl-CoA lyase, mitochondrial	HMGCL	LLEAGNFICQALNR	1.61	0.69
789	Q9Y2R9	MRPS7 28S ribosomal protein S7, mitochondrial	MRPS7	NCEPMIGLVPILK	1.61	0.69
790	P08559	PDHA1 Pyruvate dehydrogenase E1 component subunit alpha,	PDHA1	FAAAYCR	1.61	0.69
791	P61927	RPL37 60S ribosomal protein L37	RPL37	THTLCR	1.61	0.69
792	P34932	HSPA4 Heat shock 70 kDa protein 4	HSPA4	GCALQCAILSPAFK	1.62	0.69
793	P46776	RPL27A 60S ribosomal protein L27a	RPL27A	NQSFCPTVNLDK	1.62	0.69
794	P05388	RPLP0 60S acidic ribosomal protein P0	RPLP0	CFIVGADNVGSK	1.62	0.70
795	P82912	MRPS11 28S ribosomal protein S11, mitochondrial	MRPS11	ASHNNTQIQVVSASN EPLAFASCGTEGFR	1.62	0.70
796	P68363	TUBA1B Tubulin alpha-1B chain	TUBA1B	YMACCLLYR	1.62	0.70
797	P23396	RPS3 40S ribosomal protein S3	RPS3	GLCAIAQAESLR	1.63	0.70
798	Q13228	SELENBP1 Selenium-binding protein 1	SELENBP1	CGNCGPGYSTPLEA MK	1.63	0.70

799	P50991	CCT4 T-complex protein 1 subunit delta	CCT4	TGCNVLLIQK	1.63	0.71
800	Q27J81	INF2 Inverted formin-2	INF2	AVLLASDAQECTLEEVVER	1.64	0.71
801	Q6P2I3	FAHD2B Fumarylacetoacetate hydrolase domain-containing pr	FAHD2B	TFDTFCPLGPALVTK	1.64	0.71
802	P38606	ATP6V1A V-type proton ATPase catalytic subunit A	ATP6V1A	VLDALFPCVQGGTTAIPGAFGCGK	1.64	0.72
803	P62318	SNRPD3 Small nuclear ribonucleoprotein Sm D3	SNRPD3	VLHEAEGHIVTCETNTGEVYR	1.65	0.72
804	P35914	HMGCL Hydroxymethylglutaryl-CoA lyase, mitochondrial	HMGCL	NINCSIEESFQR	1.65	0.73
805	P17987	TCP1 T-complex protein 1 subunit alpha	TCP1	SLHDALCVVK	1.67	0.74
806	O00148	DDX39A ATP-dependent RNA helicase DDX39A	DDX39A	NCPHVVVGTPGR	1.67	0.74
807	O95833	CLIC3 Chloride intracellular channel protein 3	CLIC3	ASEDGESVGHCPSCQR	1.67	0.74
808	O15020	SPTBN2 Spectrin beta chain, non-erythrocytic 2	SPTBN2	IHCLENVDK	1.67	0.74
809	P49411	TUFM Elongation factor Tu, mitochondrial	TUFM	GDECELLGHSK	1.67	0.74
810	P08134	RHOC Rho-related GTP-binding protein RhoC	RHOC	LVIVGDGACGK	1.67	0.74
811	O15198	SMAD9 Mothers against decapentaplegic homolog 9	SMAD9	FCLGLLSNVNR	1.67	0.74
812	Q96JB5	CDK5RAP3 CDK5 regulatory subunit-associated protein 3	CDK5RAP3	CQQLQQEYSR	1.69	0.75
813	Q1KMD3	HNRNPUL2 Heterogeneous nuclear ribonucleoprotein U-like pro	HNRNPUL2	NFILDQCNVYNSGQR	1.69	0.76
814	P35658	NUP214 Nuclear pore complex protein Nup214	NUP214	ACFQVGTSEEMK	1.69	0.76
815	Q16698	DECR1 2,4-dienoyl-CoA reductase, mitochondrial	DECR1	VHAIQCDVR	1.69	0.76
816	Q92598	HSPH1 Heat shock protein 105 kDa	HSPH1	CTPSVISFGSK	1.69	0.76

817	P34897	SHMT2 Serine hydroxymethyltransferase, mitochondrial	SHMT2	EVCDEVK	1.70	0.77
818	Q05639	EEF1A2 Elongation factor 1-alpha 2	EEF1A2	PMCVESFSQYPPLGR	1.70	0.77
819	P40926	MDH2 Malate dehydrogenase, mitochondrial	MDH2	GYLGPEQLPDCLK	1.70	0.77
820	Q9BTZ2	DHRS4 Dehydrogenase/reductase SDR family member 4	DHRS4	VNCLAPGLIK	1.71	0.77
821	Q96BN8	OTULIN Ubiquitin thioesterase otulin	OTULIN	PEMQCPAEHEEDMYR	1.71	0.77
822	Q15365	PCBP1 Poly(rC)-binding protein 1	PCBP1	VMTIPYQPMPASSPVICAGGQDR	1.71	0.77
823	Q5T440	IBA57 Putative transferase CAF17, mitochondrial	IBA57	VWAVLPSSPEACGAASLQER	1.71	0.77
824	Q9ULA0	DNPEP Aspartyl aminopeptidase	DNPEP	ISASCQHPTAFEEAIPK	1.71	0.78
825	P61006	RAB8A Ras-related protein Rab-8A	RAB8A	CDVNDK	1.71	0.78
826	O43837	IDH3B Isocitrate dehydrogenase [NAD] subunit beta, mitochondrial	IDH3B	LGDGLFLQCCEEVAELYPK	1.71	0.78
827	P24752	ACAT1 Acetyl-CoA acetyltransferase, mitochondrial	ACAT1	IHMGSCAENTAK	1.73	0.79
828	P24752	ACAT1 Acetyl-CoA acetyltransferase, mitochondrial	ACAT1	QAVLGAGLPISTPCTTINK	1.73	0.79
829	Q96BF6	NACC2 Nucleus accumbens-associated protein 2	NACC2	NTLANSCGTGIR	1.73	0.79
830	P21333	FLNA Filamin-A	FLNA	LQVEPAVDTSGVQCYGPGIEGQGVFR	1.74	0.80
831	P29372	MPG DNA-3-methyladenine glycosylase	MPG	AGQPHSSSDAAQAPAEQPHSSSDAAQAPCPR	1.74	0.80
832	P43897	TSFM Elongation factor Ts, mitochondrial	TSFM	FECGEGEEAAETE	1.75	0.80
833	Q96I99	SUCLG2 Succinate--CoA ligase [GDP-forming] subunit beta,	SUCLG2	IDATQVEVNPFGETPEGQVVCFDAK	1.76	0.81
834	P42765	ACAA2 3-ketoacyl-CoA thiolase, mitochondrial	ACAA2	LCGSGFQSIVNGCQEICVK	1.77	0.82
835	O60502	MGEA5 Protein O-GlcNAcase	MGEA5	ANSSVVSVNCK	1.77	0.83
836	Q16822	PCK2 Phosphoenolpyruvate	PCK2	YVAAAFPSACGK	1.78	0.83

		carboxykinase [GTP], mitochond				
837	A0AVT1	UBA6 Ubiquitin-like modifier-activating enzyme 6	UBA6	PNVGCQQDSEELLK	1.78	0.83
838	Q96HY7	DHTKD1 Probable 2-oxoglutarate dehydrogenase E1 component	DHTKD1	VEELCPFPLDSLQQE MSK	1.78	0.83
839	P53597	SUCLG1 Succinate--CoA ligase [ADP/GDP-forming] subunit al	SUCLG1	LIGPNCPGVINPGECK	1.78	0.83
840	P24752	ACAT1 Acetyl-CoA acetyltransferase, mitochondrial	ACAT1	QGEYGLASICNGGGG ASAMLIQK	1.79	0.84
841	P62333	PSMC6 26S proteasome regulatory subunit 10B	PSMC6	DHQPCIIFMDEIDAIG GR	1.79	0.84
842	P36873	PPP1CC Serine/threonine-protein phosphatase PP1-gamma cat	PPP1CC	GNHECASINR	1.80	0.85
843	P62829	RPL23 60S ribosomal protein L23	RPL23	ISLGLPVGAVINCADN TGAK	1.80	0.85
844	Q53H96	PYCR3 Pyrroline-5-carboxylate reductase 3	PYCR3	SDVCTPGGTTIYGLH ALEQGGLR	1.80	0.85
845	P61247	RPS3A 40S ribosomal protein S3a	RPS3A	ACQSIYPLHDVFVR	1.80	0.85
846	Q9NZB2	FAM120A Constitutive coactivator of PPAR-gamma-like protei	FAM120A	GSQMGTVQPIPCLLS MPTR	1.81	0.86
847	P13804	ETFA Electron transfer flavoprotein subunit alpha, mito	ETFA	CDK	1.82	0.86
848	Q00839	HNRNPU Heterogeneous nuclear ribonucleoprotein U	HNRNPU	MCLFAGFQR	1.82	0.86
849	P63244	RACK1 Receptor of activated protein C kinase 1	RACK1	FSPNSSNPIIVSCGWD K	1.82	0.87
850	P62753	RPS6 40S ribosomal protein S6	RPS6	LNISFPATGCQK	1.82	0.87
851	Q96RQ3	MCCC1 Methylcrotonoyl-CoA carboxylase subunit alpha, mitochondrial	MCCC1	ESLCQAALGLILK	1.84	0.88
852	P48735	IDH2 Isocitrate dehydrogenase [NADP], mitochondrial	IDH2	VCVETVESGAMTK	1.85	0.89
853	P42765	ACAA2 3-ketoacyl-CoA thiolase, mitochondrial	ACAA2	EECDK	1.85	0.89
854	Q06587	RING1 E3 ubiquitin-	RING1	FCSDCIVTALR	1.85	0.89

		protein ligase RING1				
855	P35998	PSMC2 26S proteasome regulatory subunit 7	PSMC2	SVCTEAGMFAIR	1.85	0.89
856	P62333	PSMC6 26S proteasome regulatory subunit 10B	PSMC6	NVCTEAGMFAIR	1.86	0.89
857	Q16822	PCK2 Phosphoenolpyruvate carboxykinase [GTP], mitochond	PCK2	LCQPEGIHICDGTEAE NTATLTLLEQQGLIR	1.86	0.89
858	P60709	ACTB Actin, cytoplasmic 1	ACTB	LCYVALDFEQEMATA ASSSSLEK	1.86	0.90
859	P58107	EPPK1 Epiplakin	EPPK1	YLQGTGCIAGLLLPGS QER	1.87	0.90
860	P40926	MDH2 Malate dehydrogenase, mitochondrial	MDH2	GCDVVVIPAGVPR	1.87	0.90
861	P10515	DLAT Dihydrolipoyllysine-residue acetyltransferase comp	DLAT	NFSAIINPPQACILAIG ASEDK	1.88	0.91
862	P27635	RPL10 60S ribosomal protein L10	RPL10	MLSCAGADR	1.89	0.92
863	P62333	PSMC6 26S proteasome regulatory subunit 10B	PSMC6	AVASQLDCNFLK	1.89	0.92
864	O95340	PAPSS2 Bifunctional 3-phosphoadenosine 5-phosphosulfate	PAPSS2	LFADAGLVCITSFISPF AK	1.90	0.92
865	Q12906	ILF3 Interleukin enhancer-binding factor 3	ILF3	CLAALASLR	1.90	0.92
866	Q8TC07	TBC1D15 TBC1 domain family member 15	TBC1D15	TLLVNCQNK	1.91	0.93
867	P51570	GALK1 Galactokinase	GALK1	QCEEVAR	1.91	0.93
868	Q86W42	THOC6 THO complex subunit 6 homolog	THOC6	AQVPGSSPGLLSLSLN QQPAAPECK	1.92	0.94
869	Q6AI08	HEATR6 HEAT repeat-containing protein 6	HEATR6	SSDMDDITFCMLLQN ALK	1.93	0.95
870	Q68CP9	ARID2 AT-rich interactive domain-containing protein 2	ARID2	SCSNAAFALK	1.94	0.95
871	P32322	PYCR1 Pyrroline-5-carboxylate reductase 1, mitochondrial	PYCR1	SLLINAVEASCIR	1.94	0.96
872	Q9Y5Y2	NUBP2 Cytosolic Fe-S cluster assembly factor NUBP2	NUBP2	VGILDVDLCGPSIPR	1.95	0.97
873	P08865	RPSA 40S ribosomal protein SA	RPSA	YVDIAIPCNNK	1.96	0.97
874	Q8NFQ	TOR1AIP2 Torsin-1A-	TOR1AIP2	ISHLVLPVQPVSSIEE	1.97	0.98

	8	interacting protein 2		QGCLF		
875	A6NDG6	PGP Glycerol-3-phosphate phosphatase	PGP	NNQESDCVSK	1.97	0.98
876	P48735	IDH2 Isocitrate dehydrogenase [NADP], mitochondrial	IDH2	CATITPDEAR	1.97	0.98
877	Q00839	HNRNPU Heterogeneous nuclear ribonucleoprotein U	HNRNPU	AVVVCPK	1.98	0.98
878	P51553	IDH3G Isocitrate dehydrogenase [NAD] subunit gamma, mito	IDH3G	LGDGLFLQCCR	1.98	0.99
879	Q9H7X7	IFT22 Intraflagellar transport protein 22 homolog	IFT22	ILFVGPCESGK	1.98	0.99
880	Q6AI08	HEATR6 HEAT repeat-containing protein 6	HEATR6	ACALQVLSAILEGSK	1.99	0.99
881	P48735	IDH2 Isocitrate dehydrogenase [NADP], mitochondrial	IDH2	SSGGFVWACK	1.99	0.99
882	Q13162	PRDX4 Peroxiredoxin-4	PRDX4	EEECHFYAGGQVYPGEASR	1.99	0.99
883	P62280	RPS11 40S ribosomal protein S11	RPS11	CPFTGNVSIR	2.00	1.00
884	P23396	RPS3 40S ribosomal protein S3	RPS3	GCEVVVSGK	2.01	1.01
885	P06865	HEXA Beta-hexosaminidase subunit alpha	HEXA	GVQAQPLNVGFCEQEFEQT	2.01	1.01
886	P42356	PI4KA Phosphatidylinositol 4-kinase alpha	PI4KA	GGGGGGGGGGGCSGSGSSASR	2.01	1.01
887	Q9Y5Y2	NUBP2 Cytosolic Fe-S cluster assembly factor NUBP2	NUBP2	AVHQCDR	2.03	1.02
888	P49327	FASN Fatty acid synthase	FASN	LGMLSPEGTCK	2.03	1.02
889	P13804	ETFA Electron transfer flavoprotein subunit alpha, mito	ETFA	QFNYTHICAGASAFGK	2.03	1.02
890	P50213	IDH3A Isocitrate dehydrogenase [NAD] subunit alpha, mito	IDH3A	PCVSIEGYK	2.03	1.02
891	P08865	RPSA 40S ribosomal protein SA	RPSA	ADHQPLTEASYVNLPTIALCNTDSPLR	2.03	1.02
892	P63244	RACK1 Receptor of activated protein C kinase 1	RACK1	LWNTLGVCK	2.05	1.04
893	P46109	CRKL Crk-like protein	CRKL	VPCAYDK	2.07	1.05
894	P16455	MGMT Methylated-DNA--protein-cysteine	MGMT	VVCSSGAVGNYSGGLAVK	2.07	1.05

		methyltransferase				
895	Q9NR50	EIF2B3 Translation initiation factor eIF-2B subunit gamma	EIF2B3	LLSALCPEEPPVHSSAQIVSK	2.09	1.06
896	P62333	PSMC6 26S proteasome regulatory subunit 10B	PSMC6	GCLLYGPPGTGK	2.09	1.06
897	P04350	TUBB4A Tubulin beta-4A chain	TUBB4A	VSDTVVEPYNATLSVHQLVENTDETYCIDNEALYDICFR	2.10	1.07
898	Q71U36	TUBA1A Tubulin alpha-1A chain	TUBA1A	TIQFVDWCPTGFK	2.10	1.07
899	P62701	RPS4X 40S ribosomal protein S4, X isoform	RPS4X	ECLPLIIFLR	2.11	1.08
900	P26440	IVD Isovaleryl-CoA dehydrogenase, mitochondrial	IVD	ASGAVGLSYGAHSNLCINQLVR	2.14	1.10
901	P38606	ATP6V1A V-type proton ATPase catalytic subunit A	ATP6V1A	WDFTPCK	2.15	1.10
902	P04183	TK1 Thymidine kinase, cytosolic	TK1	YSSSFCTHDR	2.16	1.11
903	Q16822	PCK2 Phosphoenolpyruvate carboxykinase [GTP], mitochond	PCK2	VECVGDDIAWMR	2.17	1.11
904	P28331	NDUFS1 NADH-ubiquinone oxidoreductase 75 kDa subunit, mitochondrial	NDUFS1	VVAACAMPVMK	2.17	1.12
905	P26440	IVD Isovaleryl-CoA dehydrogenase, mitochondrial	IVD	ACDEGHCTAK	2.18	1.12
906	Q16822	PCK2 Phosphoenolpyruvate carboxykinase [GTP], mitochond	PCK2	CLHSVGQPLTGQGEPVSQWPCNPEK	2.19	1.13
907	P43246	MSH2 DNA mismatch repair protein Msh2	MSH2	HVIECAK	2.19	1.13
908	P68363	TUBA1B Tubulin alpha-1B chain	TUBA1B	SIQFVDWCPTGFK	2.22	1.15
909	P53597	SUCLG1 Succinate--CoA ligase [ADP/GDP-forming] subunit al	SUCLG1	IICQGFTGK	2.22	1.15
910	P60709	ACTB Actin, cytoplasmic 1	ACTB	CDVDIR	2.22	1.15
911	Q99714	HSD17B10 3-hydroxyacyl-CoA dehydrogenase type-2	HSD17B10	LGNNCVFAPADVTSEK	2.22	1.15
912	P49411	TUFM Elongation factor Tu, mitochondrial	TUFM	GEETPVIVGSALCALEGR	2.23	1.16
913	P50213	IDH3A Isocitrate	IDH3A	IEAACFATIK	2.24	1.16

		dehydrogenase [NAD] subunit alpha, mito				
914	P17987	TCP1 T-complex protein 1 subunit alpha	TCP1	GANDFMCDEMER	2.24	1.16
915	P49411	TUFM Elongation factor Tu, mitochondrial	TUFM	NMITGTAPLDGCILV VAANDGPMPQTR	2.25	1.17
916	P32969	RPL9 60S ribosomal protein L9	RPL9	TICSHVQNMIK	2.25	1.17
917	Q07020	RPL18 60S ribosomal protein L18	RPL18	GCGTVLLSGPR	2.27	1.18
918	P85037	FOXK1 Forkhead box protein K1	FOXK1	SMVSPVPSPTGTISVP NSCPASPR	2.27	1.18
919	Q9HC84	MUC5B Mucin-5B	MUC5B	AQAACANAR	2.29	1.19
920	Q13347	EIF3I Eukaryotic translation initiation factor 3 subunit	EIF3I	ITSAVWGPLGECIIAG HESGELNQYSAK	2.29	1.20
921	P62879	GNB2 Guanine nucleotide-binding protein G(I)/G(S)/G(T)	GNB2	ELPGHTGYLSCCR	2.31	1.21
922	P11586	MTHFD1 C-1-tetrahydrofolate synthase, cytoplasmic	MTHFD1	GCLELIK	2.32	1.22
923	P25398	RPS12 40S ribosomal protein S12	RPS12	LGEWVGLCK	2.34	1.22
924	P68363	TUBA1B Tubulin alpha-1B chain	TUBA1B	AVCMLSNTTAIAEA WAR	2.34	1.23
925	Q07157	TJP1 Tight junction protein ZO-1	TJP1	CLPGDPNYLVGANCV SVLIDHF	2.37	1.24
926	P16278	GLB1 Beta-galactosidase	GLB1	TVGAALDILCPSGPIK	2.37	1.24
927	P48735	IDH2 Isocitrate dehydrogenase [NADP], mitochondrial	IDH2	DLAGCIHGLSNVK	2.37	1.25
928	Q9BQE3	TUBA1C Tubulin alpha-1C chain	TUBA1C	AVCMLSNTTAVAEA WAR	2.39	1.26
929	P08559	PDHA1 Pyruvate dehydrogenase E1 component subunit alpha,	PDHA1	NFYGGNGIVGAQVPL GAGIALACK	2.40	1.26
930	O95747	OXSR1 Serine/threonine-protein kinase OSR1	OXSR1	TFVGTPCWMAPEV MEQVR	2.40	1.26
931	Q6NXE6	ARMC6 Armadillo repeat-containing protein 6	ARMC6	DCEDVAK	2.43	1.28
932	Q02252	ALDH6A1 Methylmalonate-semialdehyde dehydrogenase	ALDH6A1	AEMDAAIASCK	2.43	1.28
933	O75362	ZNF217 Zinc finger protein 217	ZNF217	QTETAADCR	2.48	1.31
934	P53384	NUBP1 Cytosolic Fe-S	NUBP1	LPIIGVVENMSGFICP	2.50	1.32

		cluster assembly factor NUBP1		K		
935	P04350	TUBB4A Tubulin beta-4A chain	TUBB4A	LTTPTYGDLNHLVSATMSGVTTCLR	2.52	1.34
936	P04350	TUBB4A Tubulin beta-4A chain	TUBB4A	NMMAACDPR	2.55	1.35
937	Q53H96	PYCR3 Pyrroline-5-carboxylate reductase 3	PYCR3	VLPNLPCVVQEGAIVMAR	2.57	1.36
938	P04350	TUBB4A Tubulin beta-4A chain	TUBB4A	TAVCDIPPR	2.57	1.36
939	Q9Y5Q8	GTF3C5 General transcription factor 3C polypeptide 5	GTF3C5	VCTNPVDR	2.61	1.38
940	P13804	ETFA Electron transfer flavoprotein subunit alpha, mito	ETFA	LGGEVSCLVAGTK	2.62	1.39
941	P36578	RPL4 60S ribosomal protein L4	RPL4	SGQGAFGNMCR	2.63	1.39
942	Q5VSL9	STRIP1 Striatin-interacting protein 1	STRIP1	AHSNPDFLPVDNCLQSVLGQR	2.64	1.40
943	P40939	HADHA Trifunctional enzyme subunit alpha, mitochondrial	HADHA	CLAPMMSEVIR	2.65	1.40
944	P13804	ETFA Electron transfer flavoprotein subunit alpha, mito	ETFA	TIYAGNALCTVK	2.71	1.44
945	P62888	RPL30 60S ribosomal protein L30	RPL30	VCTLAIIDPGDSDIIR	2.73	1.45
946	P07858	CTSB Cathepsin B	CTSB	GQDHCGIESEVVAGIPR	2.75	1.46
947	P04406	GAPDH Glyceraldehyde-3-phosphate dehydrogenase	GAPDH	IISNASCTTNCLAPLAK	2.75	1.46
948	P13995	MTHFD2 Bifunctional methylenetetrahydrofolate dehydrogenase	MTHFD2	ICNAVSPDK	2.78	1.48
949	P62913	RPL11 60S ribosomal protein L11	RPL11	IAVHCTVR	2.81	1.49
950	Q96CM8	ACSF2 Acyl-CoA synthetase family member 2, mitochondrial	ACSF2	MVSTPIGGLSYVQGCTK	2.82	1.49
951	P04183	TK1 Thymidine kinase, cytosolic	TK1	NTMEALPACLLR	2.86	1.52
952	Q14790	CASP8 Caspase-8	CASP8	VFFIQACQGDNYQK	2.88	1.52
953	P16278	GLB1 Beta-galactosidase	GLB1	TTLPQDCSNPAPLSSPLNGVHDR	2.92	1.55
954	Q9ULA0	DNPEP Aspartyl aminopeptidase	DNPEP	CPTSGR	2.93	1.55
955	P50914	RPL14 60S ribosomal protein L14	RPL14	ALVDGPCTQVR	2.96	1.56

956	Q16822	PCK2 Phosphoenolpyruvate carboxykinase [GTP], mitochond	PCK2	FPGCMQGR	3.03	1.60
957	P63244	RACK1 Receptor of activated protein C kinase 1	RACK1	AEPPQCTSLAWSAD GQTLFAGYTDNLVR	3.07	1.62
958	Q7L0Y3	TRMT10C Mitochondrial ribonuclease P protein 1	TRMT10C	LNLATECLPLDK	3.07	1.62
959	Q01813	PFKP ATP-dependent 6-phosphofructokinase, platelet type	PFKP	GITNLCVIGGDGSLTG ANLFR	3.10	1.63
960	P68363	TUBA1B Tubulin alpha-1B chain	TUBA1B	AYHEQLSVAEITNACF EPANQMVK	3.12	1.64
961	Q9BQE3	TUBA1C Tubulin alpha-1C chain	TUBA1C	AYHEQLTVAEITNACF EPANQMVK	3.19	1.67
962	Q16822	PCK2 Phosphoenolpyruvate carboxykinase [GTP], mitochond	PCK2	YNNCWLAR	3.25	1.70
963	P50914	RPL14 60S ribosomal protein L14	RPL14	CMQLTDFILK	3.29	1.72
964	Q92947	GCDH Glutaryl-CoA dehydrogenase, mitochondrial	GCDH	ASATGMIIMDGVEVP EENVLPGASSLGGPF GCLNNAR	3.30	1.72
965	P48735	IDH2 Isocitrate dehydrogenase [NADP], mitochondrial	IDH2	EPIICK	3.31	1.73
966	Q92947	GCDH Glutaryl-CoA dehydrogenase, mitochondrial	GCDH	GYGCAGVSSVAYGLL AR	3.44	1.78
967	Q9BT09	CNPY3 Protein canopy homolog 3	CNPY3	NHQEEDLTEFLCANH VLK	3.45	1.79
968	P27797	CALR Calreticulin	CALR	LFPNSLDQTDMHGD SEYNIMFGPDICGPG TK	3.46	1.79
969	Q9BW8 3	IFT27 Intraflagellar transport protein 27 homolog	IFT27	CILAGDPAVGK	3.55	1.83
970	P17858	PFKL ATP-dependent 6-phosphofructokinase, liver type	PFKL	VFANAPDSACVIGLK	3.56	1.83
971	P17858	PFKL ATP-dependent 6-phosphofructokinase, liver type	PFKL	CHDYYTTEFLYNLYSS EGK	3.58	1.84
972	P07858	CTSB Cathepsin B	CTSB	ICEPGYSPTYK	3.62	1.85
973	Q06203	PPAT Amidophosphoribosyltr ansferase	PPAT	CELENCQPFVVETLH GK	3.65	1.87
974	Q7Z4W	DCXR L-xylulose	DCXR	EC*PGIEPVC*VDLG	3.86	1.95

	1	reductase		DWEATER		
975	P09001	MRPL3 39S ribosomal protein L3, mitochondrial	MRPL3	ENCNGK	3.90	1.96
976	Q13347	EIF3I Eukaryotic translation initiation factor 3 subunit	EIF3I	HVLTGSADNSCR	4.15	2.05
977	P22570	FDXR NADPH:adrenodoxin oxidoreductase, mitochondrial	FDXR	AVPTGDMEDLPCGL VLSSIGYK	4.24	2.09
978	P46459	NSF Vesicle-fusing ATPase	NSF	SQLSCVVVDDIER	4.36	2.12
979	P02765	AHSG Alpha-2-HS-glycoprotein	AHSG	CDSSPDSAEDVR	5.32	2.41
980	P58107	EPPK1 Epiplakin	EPPK1	LLDAQLATGGLVCPA R	5.50	2.46
981	P31749	AKT1 RAC-alpha serine/threonine-protein kinase	AKT1	TFCGTPEYLAPEVLED NDYGR	5.61	2.49
982	Q01813	PFKP ATP-dependent 6-phosphofructokinase, platelet type	PFKP	LPLMECVQMTQDVQ K	5.92	2.57
983	P07339	CTSD Cathepsin D	CTSD	AIGAVPLIQGEYMIPC EK	7.95	2.99
984	O00244	ATOX1 Copper transport protein ATOX1	ATOX1	HEFSVDMTCGGCAE AVSR	11.78	3.56
985	P63244	RACK1 Receptor of activated protein C kinase 1	RACK1	YWLCAATGPSIK	20.00	4.32

Table A2-5 Comparing cysteine sensitivity to CoA-SNO, GSNO, and PAPA NONOate. 429 cysteine containing peptides were identified in all 3 datasets with a corresponding *R* value. *R* value is the average heavy:light ratio from two individual datasets.

index	UniProt ID	description	symbol	sequence	CoASNO R value	GSNO R value	PAPA NONOate R value
1	P30044	PRDX5 Peroxiredoxin-5, mitochondrial	PRDX5	ALNVEPDGTG LTCSLAPNIISQ L	0.34	0.41	0.35
2	P31948	STIP1 Stress-induced-phosphoprotein 1	STIP1	ALSVGNIDDAL QCYSEAIK	0.52	0.77	0.78
3	P49591	SARS Serine--tRNA ligase, cytoplasmic	SARS	TICAILENYQTE K	0.55	0.84	0.70
4	P55212	CASP6 Caspase-6	CASP6	GTCADR	0.55	0.66	0.78
5	P22314	UBA1 Ubiquitin-like modifier-activating enzyme 1	UBA1	DNPGVVTCLD EAR	0.56	0.71	0.67
6	O43707	ACTN4 Alpha-actinin-4	ACTN4	ELPPDQAEYCI AR	0.57	0.75	0.69
7	P53041	PPP5C Serine/threonine-protein phosphatase 5	PPP5C	TECYGYALGD ATR	0.59	0.76	0.95
8	P13639	EEF2 Elongation factor 2	EEF2	ETVSEESNVLC LSK	0.59	0.81	0.71
9	P04632	CAPNS1 Calpain small subunit 1	CAPNS1	YSDESGNMDF DNFISCLVR	0.60	0.63	0.76
10	P52788	SMS Spermine synthase	SMS	LYCPVEFSK	0.60	0.75	0.67
11	P51659	HSD17B4 Peroxisomal multifunctional enzyme type 2	HSD17B 4	FIYEGSSDFSCL PTFGVIIGQK	0.61	0.89	0.66
12	P15924	DSP Desmoplakin	DSP	LLEAQACTGGI IHPTTGQK	0.61	0.65	0.63
13	P0DMV 8	HSPA1A Heat shock 70 kDa protein 1A	HSPA1A	ELEQVCNPIIS GLYQGAGGPG PGGFGAQGPK	0.62	0.69	0.76
14	P07237	P4HB Protein disulfide-isomerase	P4HB	EECPAVR	0.63	0.69	0.77
15	Q96FJ2	DYNLL2 Dynein light chain 2, cytoplasmic	DYNLL2	NADMSEDMQ QDAVDCATQ AMEK	0.63	0.72	0.76
16	Q15185	PTGES3 Prostaglandin E synthase 3	PTGES3	LTFSCLGGSDN FK	0.64	0.84	0.70
17	P21266	GSTM3 Glutathione S-transferase Mu 3	GSTM3	LCYSSDHEK	0.64	0.97	0.61

18	P62258	YWHAE 14-3-3 protein epsilon	YWHAE	LICCDILDVLDK	0.64	0.83	0.76
19	Q86SX6	GLRX5 Glutaredoxin-related protein 5, mitochondrial	GLRX5	GTPEQPQCGF SNAVVQILR	0.65	0.80	0.90
20	P78417	GSTO1 Glutathione S-transferase omega-1	GSTO1	LNECVDHTPK	0.65	0.74	0.80
21	P60953	CDC42 Cell division control protein 42 homolog	CDC42	YVECSALTQK	0.65	0.81	0.69
22	P61970	NUTF2 Nuclear transport factor 2	NUTF2	NINDAWVCT NDMFR	0.65	0.74	0.72
23	Q99460	PSMD1 26S proteasome non-ATPase regulatory subunit 1	PSMD1	VLTMPETCR	0.66	1.00	0.80
24	O75874	IDH1 Isocitrate dehydrogenase [NADP] cytoplasmic	IDH1	SEGGFIWACK	0.66	0.79	0.77
25	P04155	TFF1 Trefoil factor 1	TFF1	GVPWCFYPNT IDVPPEEECEF	0.66	0.51	0.59
26	P23528	CFL1 Cofilin-1	CFL1	AVLFCLSEDK	0.67	0.66	0.69
27	Q7L2H7	EIF3M Eukaryotic translation initiation factor 3 subunit	EIF3M	VAASCGAIQYI PTELDQVR	0.67	0.95	0.79
28	Q04917	YWHAH 14-3-3 protein eta	YWHAH	ELETVCNDVLS LLDK	0.67	0.77	1.25
29	O00299	CLIC1 Chloride intracellular channel protein 1	CLIC1	EEFASTCPDDE EIELAYEQVAK	0.68	0.74	0.84
30	P23528	CFL1 Cofilin-1	CFL1	HELQANCYEE VK	0.68	0.60	0.77
31	Q14697	GANAB Neutral alpha-glucosidase AB	GANAB	DGSDYEGWC WPGSAGYPDF TNPTMR	0.68	0.87	0.79
32	P49773	HINT1 Histidine triad nucleotide-binding protein 1	HINT1	CAADLGLNK	0.69	1.37	0.79
33	Q13404	UBE2V1 Ubiquitin-conjugating enzyme E2 variant 1	UBE2V1	LPQPPEGQCY SN	0.69	0.56	0.93
34	O00299	CLIC1 Chloride intracellular channel protein 1	CLIC1	IGNCPFSQR	0.70	0.76	1.30
35	Q15691	MAPRE1 Microtubule-associated protein RP/EB family member	MAPRE1	NIELICQENEG ENDPVLQR	0.70	0.75	0.85

36	P62826	RAN GTP-binding nuclear protein Ran	RAN	VCENIPIVLCG NK	0.70	1.00	0.92
37	Q9NQR 4	NIT2 Omega-amidase NIT2	NIT2	VGLGICYDMR	0.70	0.77	0.96
38	P37802	TAGLN2 Transgelin-2	TAGLN2	DGTVLCELINA LYPEGQAPVK	0.70	0.75	0.78
39	P14625	HSP90B1 Endoplasmin	HSP90B 1	LTESPCALVAS QYGWSGNME R	0.70	0.77	0.64
40	P39687	ANP32A Acidic leucine-rich nuclear phosphoprotein 32 fami	ANP32A	SLDLFNCEVTN LNDYR	0.70	0.73	1.16
41	P26599	PTBP1 Polypyrimidine tract-binding protein 1	PTBP1	LSLDGQNIYNA CCTLR	0.70	0.96	1.20
42	Q9Y696	CLIC4 Chloride intracellular channel protein 4	CLIC4	AGSDGESIGN CPFSQR	0.70	0.96	0.91
43	P63104	YWHAZ 14-3-3 protein zeta/delta	YWHAZ	YDDMAACMK	0.71	0.70	0.72
44	P14678	SNRPB Small nuclear ribonucleoprotein-associated protein	SNRPB	CILQDGR	0.71	0.71	1.09
45	Q9UNH 7	SNX6 Sorting nexin-6	SNX6	IGSSLYALGTQ DSTDICK	0.71	0.92	1.09
46	P00558	PGK1 Phosphoglycerate kinase 1	PGK1	GCITIIGGGDT ATCCAK	0.71	0.68	1.12
47	P62937	PPIA Peptidyl-prolyl cis-trans isomerase A	PPIA	ITIADCGQLE	0.71	0.67	0.74
48	P31947	SFN 14-3-3 protein sigma	SFN	GEELSCEER	0.71	0.76	0.93
49	P60174	TPI1 Triosephosphate isomerase	TPI1	IAVAAQNCYK	0.72	0.75	0.75
50	P13693	TPT1 Translationally-controlled tumor protein	TPT1	EIADGLCLEVE GK	0.72	0.70	0.67
51	Q99873	PRMT1 Protein arginine N-methyltransferase 1	PRMT1	VIGIECSSISDY AVK	0.72	0.99	1.22
52	P55735	SEC13 Protein SEC13 homolog	SEC13	FASGGCDNLIK	0.73	0.95	0.77
53	O95292	VAPB Vesicle-associated membrane protein-associated pro	VAPB	CVFELPAENDK	0.73	0.79	0.78

54	P30086	PEBP1 Phosphatidylethanolamine-binding protein 1	PEBP1	APVAGTCYQAEWDDYVPK	0.73	0.68	0.69
55	Q92598	HSPH1 Heat shock protein 105 kDa	HSPH1	LCGPYEK	0.73	0.81	0.91
56	P25789	PSMA4 Proteasome subunit alpha type-4	PSMA4	YLLQYQEPIPCEQLVTALCDIK	0.73	0.93	0.75
57	P22626	HNRNPA2B1 Heterogeneous nuclear ribonucleoproteins A2/B1	HNRNPA2B1	LTDCVVMR	0.73	1.05	0.74
58	P78406	RAE1 mRNA export factor	RAE1	VFTASCDK	0.73	1.17	1.68
59	P49915	GMPS GMP synthase [glutamine-hydrolyzing]	GMPS	ACTTEEDQEK	0.73	0.82	0.89
60	P22061	PCMT1 Protein-L-isoaspartate(D-aspartate) O-methyltransferase	PCMT1	ALDVGSGSGILTACFAR	0.74	0.77	0.73
61	P21964	COMT Catechol O-methyltransferase	COMT	YLPDTLLLEECGLLR	0.74	0.74	0.74
62	P63104	YWHAZ 14-3-3 protein zeta/delta	YWHAZ	DICNDVLSLLEK	0.74	0.69	0.77
63	P22234	PAICS Multifunctional protein ADE2	PAICS	CGETAFIAPQCEMIPIEWVCR	0.74	0.92	0.98
64	P47756	CAPZB F-actin-capping protein subunit beta	CAPZB	DETVSDCSPHIANIGR	0.75	0.81	0.88
65	P60174	TPI1 Triosephosphate isomerase	TPI1	VPADTEVVCAPPTAYIDFAR	0.75	0.69	0.75
66	O14662	STX16 Syntaxin-16	STX16	ACSEQEGR	0.75	0.88	0.74
67	Q09666	AHNAK Neuroblast differentiation-associated protein AHNA	AHNAK	LEGDLTGPSVDVEVPDVELECPDAK	0.75	0.81	0.80
68	P08238	HSP90AB1 Heat shock protein HSP 90-beta	HSP90AB1	VFIMDSCDELIPEYLNFIR	0.75	0.89	0.87
69	P27348	YWHAQ 14-3-3 protein theta	YWHAQ	YDDMATCMK	0.75	0.71	0.72
70	P30153	PPP2R1A Serine/threonine-protein phosphatase 2A 65 kDa reg	PPP2R1A	LNIISNLDCVNEVIGIR	0.76	0.95	0.83

71	O14561	NDUFAB1 Acyl carrier protein, mitochondrial	NDUFAB1	LMCPQEIVDYIADK	0.76	0.79	0.81
72	A0A075B759	PPIAL4E Peptidyl-prolyl cis-trans isomerase A-like 4E	PPIAL4E	IIPGFMCQGGDFTR	0.76	0.63	0.72
73	Q04726	TLE3 Transducin-like enhancer protein 3	TLE3	SPISQLDCLNR	0.76	2.00	0.79
74	P28074	PSMB5 Proteasome subunit beta type-5	PSMB5	VIEINPYLLGTMAGGAADCSFWER	0.77	0.76	0.81
75	P27348	YWHAQ 14-3-3 protein theta	YWHAQ	DNLTLWTSDSAGEECDAAEGAEN	0.77	0.92	0.80
76	Q5TFE4	NT5DC1 5-nucleotidase domain-containing protein 1	NT5DC1	ENCGIYFPEIK	0.77	0.75	0.89
77	P38646	HSPA9 Stress-70 protein, mitochondrial	HSPA9	CELSSSVQTDINLPYLTMDSSGPK	0.77	0.88	0.99
78	P11940	PABPC1 Polyadenylate-binding protein 1	PABPC1	GFGFVCFSSPEEATK	0.77	0.93	0.78
79	Q04917	YWHAH 14-3-3 protein eta	YWHAH	NCNDFQYESK	0.77	0.79	0.82
80	Q12931	TRAP1 Heat shock protein 75 kDa, mitochondrial	TRAP1	SPAAECLSEK	0.77	0.74	0.77
81	Q09666	AHNAK Neuroblast differentiation-associated protein AHNA	AHNAK	VDVECPDVNIEGPEGK	0.78	0.75	0.73
82	Q15369	ELOC Elongin-C	ELOC	TYGGCEGPDAMYVK	0.78	0.74	0.86
83	P31949	S100A11 Protein S100-A11	S100A11	CIESLIAVFQK	0.78	0.66	0.73
84	Q96FW1	OTUB1 Ubiquitin thioesterase OTUB1	OTUB1	PDGNCFYR	0.78	0.79	0.84
85	Q9Y490	TLN1 Talin-1	TLN1	AGALQCSPSDAYTK	0.78	0.61	0.75
86	Q15149	PLEC Plectin	PLEC	LLEAQACTGGIIDPSTGER	0.78	0.82	0.87
87	P0DMV8	HSPA1A Heat shock 70 kDa protein 1A	HSPA1A	FEELCSDLFR	0.78	0.75	0.81
88	P07737	PFN1 Profilin-1	PFN1	CYEMASHLR	0.79	0.74	0.80
89	O14545	TRAFD1 TRAF-type zinc finger domain-containing protein 1	TRAFD1	AVCEADQSHGGPR	0.79	0.93	0.71

90	O14950	MYL12B Myosin regulatory light chain 12B	MYL12B	NAFACFDEEATGTIQEDYLR	0.79	0.82	0.82
91	Q5TFE4	NT5DC1 5-nucleotidase domain-containing protein 1	NT5DC1	HFLSDTGMACR	0.79	0.84	1.25
92	P49458	SRP9 Signal recognition particle 9 kDa protein	SRP9	VTDDLVCLVYK	0.79	0.82	0.84
93	O75874	IDH1 Isocitrate dehydrogenase [NADP] cytoplasmic	IDH1	DLAACIK	0.79	0.75	0.72
94	P62993	GRB2 Growth factor receptor-bound protein 2	GRB2	VLNEECDQNWYK	0.79	0.99	0.95
95	Q96HE7	ERO1A ERO1-like protein alpha	ERO1A	HDDSSDNFCEADDIQSPEAEYVDLLLNPER	0.80	0.83	0.91
96	Q5RKV6	EXOSC6 Exosome complex component MTR3	EXOSC6	APPGGCEER	0.80	1.13	0.84
97	P21964	COMT Catechol O-methyltransferase	COMT	LITIEINPDCAAITQR	0.80	1.03	0.74
98	P60174	TPI1 Triosephosphate isomerase	TPI1	IIYGGSVTGATCK	0.80	0.68	0.77
99	Q1KMD3	HNRNPUL2 Heterogeneous nuclear ribonucleoprotein U-like pro	HNRNPUL2	LQEALDAEMLEDEAGGGGAGPGGACK	0.80	0.72	0.82
100	Q7Z6Z7	HUWE1 E3 ubiquitin-protein ligase HUWE1	HUWE1	AQCETLSPDGLPEEQPQTTK	0.80	0.97	0.88
101	Q9H993	ARMT1 Protein-glutamate O-methyltransferase	ARMT1	CGADWEEYIK	0.80	0.77	0.81
102	P21266	GSTM3 Glutathione S-transferase Mu 3	GSTM3	YTCGEAPDYDR	0.80	1.02	0.69
103	P49419	ALDH7A1 Alpha-aminoadipic semialdehyde dehydrogenase	ALDH7A1	STCTINYSK	0.81	0.87	0.76
104	P26641	EEF1G Elongation factor 1-gamma	EEF1G	AAAPAPEEEMDECEQALAAEPK	0.81	0.88	0.84
105	Q9H3P7	ACBD3 Golgi resident protein GCP60	ACBD3	QVLMGPYNPDTCPEVGFFDVLGNDR	0.81	0.74	0.86

106	P04075	ALDOA Fructose-bisphosphate aldolase A	ALDOA	YASICQQNGIVPIVEPEILPDGDHDLK	0.81	0.72	0.78
107	P58107	EPPK1 Epiplakin	EPPK1	YLEGTSCIAGVLVPAK	0.81	0.93	0.98
108	P14868	DARS Aspartate--tRNA ligase, cytoplasmic	DARS	LEYCEALAMLR	0.81	0.86	0.85
109	O75663	TIPRL TIP41-like protein	TIPRL	VACAEEWQESR	0.81	0.75	0.89
110	Q9HCC0	MCCC2 Methylcrotonoyl-CoA carboxylase beta chain, mitoch	MCCC2	LPCIYLVDSGGAYLPR	0.81	0.95	0.88
111	Q96EI5	TCEAL4 Transcription elongation factor A protein-like 4	TCEAL4	PEVTCTLEDK	0.82	0.81	0.87
112	Q06323	PSME1 Proteasome activator complex subunit 1	PSME1	GPPCGPVNCNEK	0.82	0.82	0.98
113	P36507	MAP2K2 Dual specificity mitogen-activated protein kinase	MAP2K2	LCDFGVSGQLIDSMANSFVGTR	0.82	0.85	0.96
114	P14866	HNRNPL Heterogeneous nuclear ribonucleoprotein L	HNRNPL	QPAIMPGQSYGLEDGSCSYK	0.82	0.89	0.89
115	P51610	HCFC1 Host cell factor 1	HCFC1	LVIYGGMSGCR	0.82	0.75	0.95
116	P00505	GOT2 Aspartate aminotransferase, mitochondrial	GOT2	EYLPIGGLAEFCK	0.82	0.67	0.77
117	P00492	HPRT1 Hypoxanthine-guanine phosphoribosyltransferase	HPRT1	SYCNDQSTGDIK	0.82	0.77	1.13
118	Q96EY8	MMAB Cob(I)yrinic acid a,c-diamide adenosyltransferase,	MMAB	IQCTLQDVGSALATPCSSAR	0.82	0.77	0.87
119	Q8N806	UBR7 Putative E3 ubiquitin-protein ligase UBR7	UBR7	VEQNSEPCAGSSSESDLQTVFK	0.82	0.82	1.14
120	P63167	DYNLL1 Dynein light chain 1, cytoplasmic	DYNLL1	NADMSEEMQQDSVECATQALEK	0.82	1.02	0.88
121	Q06323	PSME1 Proteasome activator complex subunit 1	PSME1	GPPC*GPVNC*NEK	0.82	1.06	0.77

122	Q9NTK5	OLA1 Obg-like ATPase 1	OLA1	STFFNVLTNSQASAENFPFCTIDPNESR	0.83	0.86	0.88
123	Q3LXA3	TKFC Triokinase/FMN cyclase	TKFC	AAGDGDCGTTHSR	0.83	0.84	0.72
124	Q9NZZ3	CHMP5 Charged multivesicular body protein 5	CHMP5	APPPSLTDCIGTVDSR	0.83	0.71	0.88
125	P07741	APRT Adenine phosphoribosyltransferase	APRT	VVVVDDLLATGGTMNAACELLGR	0.83	0.88	1.17
126	P61158	ACTR3 Actin-related protein 3	ACTR3	YSYVCPDLVK	0.84	0.91	1.01
127	Q15019	SEPT2 Septin-2	2-Sep	LTVVDTPGYGDAINCR	0.84	0.72	1.04
128	Q15149	PLEC Plectin	PLEC	AFCGFEDPR	0.84	0.78	0.93
129	P27348	YWHAQ 14-3-3 protein theta	YWHAQ	YLAEVACGDDR	0.84	0.86	0.87
130	O14980	XPO1 Exportin-1	XPO1	LDINLLDNVVNCLYHGEGAQQR	0.84	0.86	0.88
131	Q14151	SAFB2 Scaffold attachment factor B2	SAFB2	ILDILGETCK	0.84	0.78	0.80
132	P61978	HNRNPK Heterogeneous nuclear ribonucleoprotein K	HNRNPK	GSDFDCELR	0.84	0.79	0.80
133	Q16644	MAPKAPK3 MAP kinase-activated protein kinase 3	MAPKAPK3	QAGSSSASQGCNNQ	0.84	0.72	0.76
134	Q15020	SART3 Squamous cell carcinoma antigen recognized by T-ce	SART3	CAAVDVEPPSK	0.85	1.07	1.06
135	O60701	UGDH UDP-glucose 6-dehydrogenase	UGDH	ASVGFGGSCFQK	0.85	1.42	0.71
136	Q9H773	DCTPP1 dCTP pyrophosphatase 1	DCTPP1	YTELPHGAISEDQAVGPADIPCDSTGQTST	0.85	0.84	0.78
137	O75348	ATP6V1G1 V-type proton ATPase subunit G 1	ATP6V1G1	GSCSTEVEK	0.85	0.84	0.79
138	Q9BV86	NTMT1 N-terminal Xaa-Pro-Lys N-methyltransferase 1	NTMT1	IICSAGLSLLAEER	0.85	0.89	1.03
139	P49327	FASN Fatty acid synthase	FASN	AINCATSGVVGLVNCLR	0.85	0.82	1.09
140	P30041	PRDX6	PRDX6	DFTPVCTTELG	0.85	1.00	0.56

		Peroxiredoxin-6		R			
141	P21291	CSRP1 Cysteine and glycine-rich protein 1	CSRP1	DGEIYCK	0.85	0.77	0.80
142	Q9BYG5	PARD6B Partitioning defective 6 homolog beta	PARD6B	HGAGSGCLGTMEVK	0.86	0.63	1.10
143	P49589	CARS Cysteine--tRNA ligase, cytoplasmic	CARS	VQPQWSPPAGTQPCR	0.86	0.85	0.90
144	P78347	GTF2I General transcription factor II-I	GTF2I	SILSPGGSCGPIK	0.86	0.91	0.89
145	P14618	PKM Pyruvate kinase PKM	PKM	GIFPVLCK	0.86	0.74	0.84
146	P61978	HNRNPK Heterogeneous nuclear ribonucleoprotein K	HNRNPK	IIPTLEEGLQLPSPTATSQLPLESDAVECLNYQHYK	0.86	0.84	0.87
147	Q8N335	GPD1L Glycerol-3-phosphate dehydrogenase 1-like protein	GPD1L	ICDEITGR	0.86	0.95	0.84
148	P33316	DUT Deoxyuridine 5-triphosphate nucleotidohydrolase,	DUT	TDIQIALPSGCYGR	0.86	0.83	0.64
149	P13489	RNH1 Ribonuclease inhibitor	RNH1	ELDLSNNCLGDAGILQLVESVR	0.86	0.99	0.74
150	Q96FW1	OTUB1 Ubiquitin thioesterase OTUB1	OTUB1	QEPLGSDSEGVNCLAYDEAIMAQQDR	0.86	0.87	0.90
151	Q9NVU0	POLR3E DNA-directed RNA polymerase III subunit RPC5	POLR3E	AAGTDSFNGHPPQGCASTPVAR	0.86	0.80	0.92
152	P60981	DSTN Destrin	DSTN	LGGSLIVAFEGCPV	0.86	0.71	0.89
153	P15924	DSP Desmoplakin	DSP	ACGSEIMQK	0.86	0.96	0.82
154	O60361	NME2P1 Putative nucleoside diphosphate kinase	NME2P1	SCAHDWVYE	0.86	0.79	0.69
155	P63208	SKP1 S-phase kinase-associated protein 1	SKP1	ENQWCEEK	0.87	0.91	0.95
156	O60664	PLIN3 Perilipin-3	PLIN3	DIAQQLQATCTSLGSSIQGLPTNVK	0.87	0.77	0.83
157	P18669	PGAM1 Phosphoglycerate mutase 1	PGAM1	YADLTEDQLPSCESLK	0.87	0.78	0.72
158	P37235	HPCAL1 Hippocalcin-like protein 1	HPCAL1	LLQCDPSSASQF	0.87	0.97	1.14

159	P38606	ATP6V1A V-type proton ATPase catalytic subunit A	ATP6V1A	WDFTPCK	0.87	0.99	2.13
160	P04406	GAPDH Glyceraldehyde-3-phosphate dehydrogenase	GAPDH	VPTANVSVVDLTCR	0.88	0.40	0.34
161	P17676	CEBPB CCAAT/enhancer-binding protein beta	CEBPB	APPTACYAGAAPAPSQVK	0.88	1.02	0.93
162	P60981	DSTN Destrin	DSTN	CSTPEEIK	0.88	0.86	0.95
163	Q9HCC0	MCCC2 Methylcrotonoyl-CoA carboxylase beta chain, mitoch	MCCC2	NIAQIAVVMGSCTAGGAYVPAMADENIIVR	0.88	0.88	1.07
164	P21266	GSTM3 Glutathione S-transferase Mu 3	GSTM3	IAAYLQSDQFCK	0.88	1.09	0.53
165	P49419	ALDH7A1 Alpha-aminoadipic semialdehyde dehydrogenase	ALDH7A1	GSDCGIVNVNIPTSGAEIGGAFGGEK	0.88	1.01	0.88
166	P21333	FLNA Filamin-A	FLNA	AHVVPCFDASK	0.88	0.91	0.88
167	P00966	ASS1 Argininosuccinate synthase	ASS1	FELSCYSLAPQIK	0.89	0.84	0.89
168	P33240	CSTF2 Cleavage stimulation factor subunit 2	CSTF2	LCVQNSPQEAR	0.89	0.82	0.79
169	P00338	LDHA L-lactate dehydrogenase A chain	LDHA	VIGSGCNLDSAR	0.89	0.83	0.82
170	Q96RS6	NUDCD1 NudC domain-containing protein 1	NUDCD1	DSAQCAAIAER	0.89	0.92	0.87
171	Q9UNE7	STUB1 E3 ubiquitin-protein ligase CHIP	STUB1	AQQACIEAK	0.89	1.07	1.12
172	Q14103	HNRNPD Heterogeneous nuclear ribonucleoprotein D0	HNRNPD	FGEVVDCTLK	0.89	0.82	0.71
173	P13639	EEF2 Elongation factor 2	EEF2	YVEPIEDVPCGNIVGLVGVDQFLVK	0.89	0.91	0.87
174	Q09666	AHNAK Neuroblast differentiation-associated protein AHNA	AHNAK	GPFVEAEVPDVDLECPDAK	0.89	0.86	0.87
175	Q9P258	RCC2 Protein RCC2	RCC2	AVQDLCGWR	0.89	0.94	1.26

176	P21964	COMT Catechol O-methyltransferase	COMT	IVDAVIQEHQPSVLLELGAYCGYSAVR	0.90	0.95	0.80
177	P30084	ECHS1 Enoyl-CoA hydratase, mitochondrial	ECHS1	ICPVETLVEEAIQCAEK	0.90	0.71	0.69
178	P53004	BLVRA Biliverdin reductase A	BLVRA	MTVCLETEK	0.90	1.00	0.81
179	O00233	PSMD9 26S proteasome non-ATPase regulatory subunit 9	PSMD9	GIGMNEPLVDCEGYPR	0.90	0.96	0.96
180	P38117	ETFB Electron transfer flavoprotein subunit beta	ETFB	EVIAVSCGPAQCQETIR	0.91	0.93	1.18
181	Q08379	GOLGA2 Golgin subfamily A member 2	GOLGA2	CEAPDANQQLQQAMEER	0.91	1.20	1.27
182	Q92879	CELF1 CUGBP Elav-like family member 1	CELF1	AMHQAQTMEGCSSPMVVK	0.91	1.05	0.97
183	Q06323	PSME1 Proteasome activator complex subunit 1	PSME1	EDLCTK	0.91	1.09	1.26
184	P30041	PRDX6 Peroxiredoxin-6	PRDX6	DINAYNCEEPTEK	0.91	0.91	0.74
185	P50395	GDI2 Rab GDP dissociation inhibitor beta	GDI2	TDDYLDQPCYETINR	0.92	0.69	0.80
186	P13639	EEF2 Elongation factor 2	EEF2	IWCFGPDGTGPNILTDITK	0.92	0.82	0.79
187	Q09666	AHNAK Neuroblast differentiation-associated protein AHNA	AHNAK	SSGCDVNLPGVNVK	0.92	0.89	0.89
188	Q09666	AHNAK Neuroblast differentiation-associated protein AHNA	AHNAK	LEGDLTGPSVGVEVPDVELECPDAK	0.92	0.90	0.86
189	P38646	HSPA9 Stress-70 protein, mitochondrial	HSPA9	GAVVGIDLGTTNSCVAVMEGK	0.93	1.31	1.13
190	P31943	HNRNPH1 Heterogeneous nuclear ribonucleoprotein H	HNRNPH1	GLPWSCSADEVQR	0.93	1.18	0.94
191	P20700	LMNB1 Lamin-B1	LMNB1	CQSLTEDLEFR	0.93	0.90	1.02
192	O43865	AHCYL1 S-adenosylhomocysteine hydrolase-like protein 1	AHCYL1	LCVPAMNVNDSVTK	0.93	0.92	1.10

193	Q9HCC0	MCCC2 Methylcrotonoyl-CoA carboxylase beta chain, mitoch	MCCC2	MVAAVACAQVPK	0.93	1.06	1.00
194	P57721	PCBP3 Poly(rC)-binding protein 3	PCBP3	INISEGNCPER	0.93	0.88	0.81
195	O15371	EIF3D Eukaryotic translation initiation factor 3 subunit	EIF3D	FMTPVIQDNPSGWGPCAVPEQFR	0.93	0.83	0.87
196	Q7L1Q6	BZW1 Basic leucine zipper and W2 domain-containing prot	BZW1	FDPTQFQDCIIQGLTETGTDLEAVAK	0.93	0.83	0.83
197	P08134	RHOC Rho-related GTP-binding protein RhoC	RHOC	LVIVGDGACGK	0.93	2.09	1.58
198	O43684	BUB3 Mitotic checkpoint protein BUB3	BUB3	TPCNAGTFSQPEK	0.94	0.92	0.96
199	P51812	RPS6KA3 Ribosomal protein S6 kinase alpha-3	RPS6KA3	AENGLLMTPCYTANFVAPEVLK	0.94	0.97	1.14
200	P51659	HSD17B4 Peroxisomal multifunctional enzyme type 2	HSD17B4	ICDFENASK	0.94	0.92	0.90
201	P60709	ACTB Actin, cytoplasmic 1	ACTB	CPEALFQPSFLGMESCGIHETTFNSIMK	0.94	1.09	1.49
202	Q13526	PIN1 Peptidyl-prolyl cis-trans isomerase NIMA-interacting	PIN1	SGEEDFESLASQFSDCSSAK	0.94	0.73	0.91
203	P30626	SRI Sorcin	SRI	DTAQQGVVNFPYDDFIQCVMSV	0.95	1.08	0.74
204	Q9Y508	RNF114 E3 ubiquitin-protein ligase RNF114	RNF114	DCGGAAQLAGPAAEADPLGR	0.95	0.95	0.97
205	Q15370	ELOB Elongin-B	ELOB	ADDTFEALCIEPFSSPPELPDVMK	0.95	1.01	0.88
206	Q9BQ69	MACROD1 O-acetyl-ADP-ribose deacetylase MACROD1	MACROD1	LEVDAIVNAANSSLLGGGGVDGCIHR	0.95	0.67	1.20
207	Q9ULV4	CORO1C Coronin-1C	CORO1C	DTICNQDER	0.95	1.15	1.04
208	P78371	CCT2 T-complex protein 1 subunit beta	CCT2	TVYGGGCSEMLMAHAVTQLANR	0.95	1.85	1.12

209	Q15365	PCBP1 Poly(rC)-binding protein 1	PCBP1	AITIAGVPQSVTECVK	0.95	0.74	0.78
210	P49327	FASN Fatty acid synthase	FASN	LTPGCEAEAETEAICFFVQQFTDMEHNR	0.95	0.90	1.39
211	O60701	UGDH UDP-glucose 6-dehydrogenase	UGDH	ISSINSISALCEATGADVEEVATAIGMDQR	0.96	0.79	0.71
212	Q01433	AMPD2 AMP deaminase 2	AMPD2	CGVPFTDLLDAAK	0.96	0.90	0.81
213	Q14694	USP10 Ubiquitin carboxyl-terminal hydrolase 10	USP10	SSVELPPYSGTVLCGTQAVDK	0.96	1.06	0.81
214	Q9H8W4	PLEKHF2 Pleckstrin homology domain-containing family F mem	PLEKHF2	ICDFCYDLLSAGDMATCQPAR	0.96	0.93	0.96
215	Q9HCY8	S100A14 Protein S100-A14	S100A14	IANLGSCNDSK	0.96	0.91	1.44
216	P57721	PCBP3 Poly(rC)-binding protein 3	PCBP3	LVVPASQCGSLIGK	0.97	0.97	0.81
217	P33316	DUT Deoxyuridine 5-triphosphate nucleotidohydrolase,	DUT	IAQLICER	0.97	1.86	0.90
218	P52895	AKR1C2 Aldo-keto reductase family 1 member C2	AKR1C2	EEPWVDPNSPVLLEDPVLCALAK	0.97	0.97	0.81
219	Q9C0C9	UBE2O (E3-independent) E2 ubiquitin-conjugating enzyme	UBE2O	CYNEMALIR	0.97	0.81	0.99
220	P20810	CAST Calpastatin	CAST	SECK	0.98	0.95	0.84
221	P38606	ATP6V1A V-type proton ATPase catalytic subunit A	ATP6V1A	VLDALFPCVQGGTTAIPGAFGCGK	0.98	1.24	1.63
222	Q15366	PCBP2 Poly(rC)-binding protein 2	PCBP2	AITIAGIPQSIIECVK	0.99	0.79	0.79
223	Q13185	CBX3 Chromobox protein homolog 3	CBX3	LTWHSCPEDEAQ	1.00	1.23	1.11
224	O15355	PPM1G Protein phosphatase 1G	PPM1G	GTEAGQVGEPGIPTGEAGPSCSSASDK	1.00	1.23	1.06
225	P46109	CRKL Crk-like protein	CRKL	VPCAYDK	1.01	0.81	2.06
226	Q8WVJ2	NUDCD2 NudC domain-containing protein 2	NUDCD2	DAANCWTSLLESEYAADPWVQDQMQR	1.01	0.93	0.88
227	P37837	TALDO1 Transaldolase	TALDO1	ALAGCDFLTISPK	1.01	0.77	0.76

228	Q99832	CCT7 T-complex protein 1 subunit eta	CCT7	EGTDSSQGIP QLVSNISACQV IAEAVR	1.02	1.03	1.01
229	P36954	POLR2I DNA-directed RNA polymerase II subunit RPB9	POLR2I	NCDYQQEAD NSCIYVNK	1.02	0.63	0.81
230	P13639	EEF2 Elongation factor 2	EEF2	CELLYEGPPDD EAAMGIK	1.02	0.80	0.79
231	P58107	EPPK1 Epiplakin	EPPK1	CVPDPDTGLY MLQLAGR	1.02	1.03	0.75
232	P14618	PKM Pyruvate kinase PKM	PKM	AEGSDVANAV LDGADCIMLS GETAK	1.03	0.83	0.76
233	Q04637	EIF4G1 Eukaryotic translation initiation factor 4 gamma 1	EIF4G1	LQGINCGPDF TPSFANLGR	1.03	1.04	0.91
234	P13639	EEF2 Elongation factor 2	EEF2	VTDGALVVVD CVSGVCVQTE TVLR	1.03	0.90	1.47
235	P35658	NUP214 Nuclear pore complex protein Nup214	NUP214	ACFQVGTSEE MK	1.04	1.21	1.48
236	P50991	CCT4 T-complex protein 1 subunit delta	CCT4	AQDIEAGDGT TSVVIIAGSLLD SCTK	1.04	0.93	0.85
237	Q15365	PCBP1 Poly(rC)-binding protein 1	PCBP1	LVVPATQCGSL IGK	1.04	0.92	0.82
238	O43175	PHGDH D-3-phosphoglycerate dehydrogenase	PHGDH	NAGNCLSPAVI VGLLK	1.05	1.17	1.23
239	Q16851	UGP2 UTP--glucose-1-phosphate uridylyltransferase	UGP2	LNGGLGTSMG CK	1.05	1.00	0.81
240	Q8NDH 3	NPEPL1 Probable aminopeptidase NPEPL1	NPEPL1	IVDTPCNEMN TDTFLEEINK	1.05	1.13	1.12
241	P56545	CTBP2 C-terminal-binding protein 2	CTBP2	DCTVEMPILK	1.05	1.20	1.05
242	A6NDG6	PGP Glycerol-3-phosphate phosphatase	PGP	NNQESDCVSK	1.06	1.10	1.95
243	P10599	TXN Thioredoxin	TXN	LVVVDFSATW CGPCK	1.06	0.78	0.87
244	P10809	HSPD1 60 kDa heat shock protein, mitochondrial	HSPD1	CEFQDAYVLLS EK	1.06	1.18	0.95
245	Q9Y5P6	GMPPB Mannose-1-phosphate guanyltransferase beta	GMPPB	LCSGPGIVGNV LVDPSAR	1.06	0.96	0.89

246	P10599	TXN Thioredoxin	TXN	CMPTFQFFK	1.07	0.93	0.86
247	P49327	FASN Fatty acid synthase	FASN	DPETLVGYSMVGCQR	1.07	0.86	1.12
248	O14929	HAT1 Histone acetyltransferase type B catalytic subunit	HAT1	VDENFDCVEADDVEGK	1.07	1.11	1.13
249	P60842	EIF4A1 Eukaryotic initiation factor 4A-I	EIF4A1	VVMALGDYMGASCHACIGGTNVR	1.07	0.98	0.81
250	Q9Y3F4	STRAP Serine-threonine kinase receptor-associated protei	STRAP	IGFPETTEEELEEIASENSDCIFPSAPDVK	1.07	1.18	0.90
251	P08238	HSP90AB1 Heat shock protein HSP 90-beta	HSP90AB1	GFEVVYMTEPIDEYCVQQLK	1.07	0.91	0.86
252	O95671	ASMTL N-acetylserotonin O-methyltransferase-like protein	ASMTL	AEAGEAGQATAEAECHR	1.08	1.15	1.12
253	P42566	EPS15 Epidermal growth factor receptor substrate 15	EPS15	GSDPFASDCFFR	1.08	0.85	0.95
254	Q9Y2Q3	GSTK1 Glutathione S-transferase kappa 1	GSTK1	ETTEAACR	1.08	1.06	0.94
255	Q9NQT5	EXOSC3 Exosome complex component RRP40	EXOSC3	LLAPDCEIIQEVGK	1.08	1.39	1.17
256	Q00765	REEP5 Receptor expression-enhancing protein 5	REEP5	NCMTDLLAK	1.08	1.02	0.99
257	P80404	ABAT 4-aminobutyrate aminotransferase, mitochondrial	ABAT	TMGCLATTHSK	1.08	1.38	0.69
258	Q6PI48	DARS2 Aspartate--tRNA ligase, mitochondrial	DARS2	LICLVTGSPSIR	1.09	1.03	0.92
259	P02795	MT2A Metallothionein-2	MT2A	SCCSCCPVGCAK	1.09	0.80	0.58
260	P62191	PSMC1 26S proteasome regulatory subunit 4	PSMC1	AICTEAGLMALR	1.09	1.28	1.27
261	P49327	FASN Fatty acid synthase	FASN	ADEASELACPTPK	1.09	0.96	1.06
262	P61006	RAB8A Ras-related protein Rab-8A	RAB8A	CDVNDK	1.10	1.35	1.70

263	Q96AE4	FUBP1 Far upstream element-binding protein 1	FUBP1	IQQESGCK	1.10	0.99	1.12
264	Q9HCC0	MCCC2 Methylcrotonoyl-CoA carboxylase beta chain, mitoch	MCCC2	AATGEEVSAEDLGGADLHCR	1.10	1.36	1.14
265	Q16576	RBBP7 Histone-binding protein RBBP7	RBBP7	VHIPNDDAQFDASHCDSDK	1.10	1.22	1.24
266	O95336	PGLS 6-phosphogluconolactonase	PGLS	AACCLAGAR	1.10	0.96	1.18
267	P12004	PCNA Proliferating cell nuclear antigen	PCNA	CAGNEDIITLR	1.12	0.78	0.73
268	P40926	MDH2 Malate dehydrogenase, mitochondrial	MDH2	SQETECTYFSTPLLLGK	1.12	0.74	0.94
269	P14618	PKM Pyruvate kinase PKM	PKM	NTGIICTIGPASR	1.12	0.86	0.80
270	P08134	RHOC Rho-related GTP-binding protein RhoC	RHOC	ISAFGYLECSAK	1.12	2.03	1.06
271	P25398	RPS12 40S ribosomal protein S12	RPS12	QAHLCVLASNCDEPMYVK	1.12	0.83	0.56
272	P67936	TPM4 Tropomyosin alpha-4 chain	TPM4	EENVGLHQTLDQTLNELNCI	1.12	1.21	1.00
273	O95671	ASMTL N-acetylserotonin O-methyltransferase-like protein	ASMTL	LTACQVATAFNLSR	1.13	1.25	1.41
274	Q86VY4	TSPYL5 Testis-specific Y-encoded-like protein 5	TSPYL5	APETCSTAGR	1.13	1.41	1.10
275	Q9P2R7	SUCLA2 Succinate--CoA ligase [ADP-forming] subunit beta,	SUCLA2	ICNQVLVCER	1.14	0.97	0.96
276	Q9BV86	NTMT1 N-terminal Xaa-Pro-Lys N-methyltransferase 1	NTMT1	DNMAQEGVILDDVDSSVCR	1.14	1.63	1.21
277	P60763	RAC3 Ras-related C3 botulinum toxin substrate 3	RAC3	AVLCPPPVK	1.15	1.08	0.94
278	O60361	NME2P1 Putative nucleoside diphosphate kinase	NME2P1	GDFCIQVGR	1.15	0.71	0.85
279	Q9UHD8	SEPT9 Septin-9	9-Sep	SQEATEAAPSCVGDMADTPR	1.15	1.12	0.99
280	P13639	EEF2 Elongation	EEF2	STLTDSLVCK	1.16	1.18	1.08

		factor 2					
281	P38117	ETFB Electron transfer flavoprotein subunit beta	ETFB	EVIAVSC*GPAQC*QETIR	1.17	1.14	1.11
282	Q00610	CLTC Clathrin heavy chain 1	CLTC	VIQCFAETGQVQK	1.18	0.82	1.01
283	P42704	LRPPRC Leucine-rich PPR motif-containing protein, mitochondrial	LRPPRC	SCGSLLPELK	1.19	1.06	1.08
284	P60866	RPS20 40S ribosomal protein S20	RPS20	TPCGEGSK	1.20	0.99	1.38
285	Q9BRA2	TXNDC17 Thioredoxin domain-containing protein 17	TXNDC17	SWCPDCVQAEPVVR	1.20	1.07	0.94
286	P31943	HNRNPH1 Heterogeneous nuclear ribonucleoprotein H	HNRNPH1	DLNYCFSGMSDHR	1.20	1.27	1.31
287	Q8TEX9	IPO4 Importin-4	IPO4	APAALPALCDLLASAADPQIR	1.20	0.97	1.15
288	P21333	FLNA Filamin-A	FLNA	THEAEIVEGENHTYCIR	1.20	1.28	0.91
289	P34932	HSPA4 Heat shock 70 kDa protein 4	HSPA4	CTPACISFGPK	1.21	1.39	1.05
290	P38117	ETFB Electron transfer flavoprotein subunit beta	ETFB	QAIDDDCNQTGQMTAGFLDWPQGTFASQVTLEGDK	1.21	1.42	1.30
291	O60502	MGEA5 Protein O-GlcNAcase	MGEA5	ANSSVVSVNCK	1.21	1.22	1.60
292	Q15631	TSN Translin	TSN	ETAAACVEK	1.21	1.47	1.03
293	Q7Z2W4	ZC3HAV1 Zinc finger CCCH-type antiviral protein 1	ZC3HAV1	NSNVDSSYLESLYQSCPR	1.22	1.24	1.23
294	Q9BRA2	TXNDC17 Thioredoxin domain-containing protein 17	TXNDC17	SWC*PDC*VQAEPVVR	1.22	1.07	0.81
295	Q7Z6Z7	HUWE1 E3 ubiquitin-protein ligase HUWE1	HUWE1	DQSAQCTASK	1.22	0.79	0.98
296	P46782	RPS5 40S ribosomal protein S5	RPS5	AQCPIVER	1.22	1.72	1.39
297	P60981	DSTN Destrin	DSTN	HECQANGPEDLNR	1.23	1.44	0.89
298	P46776	RPL27A 60S ribosomal protein L27a	RPL27A	NQSFCPTVNLDK	1.23	1.65	1.61

299	P25398	RPS12 40S ribosomal protein S12	RPS12	VVGCSCVVVK	1.23	0.90	1.07
300	Q9NQ88	TIGAR Fructose-2,6-bisphosphatase TIGAR	TIGAR	EECPVFTPPGGETLDQVK	1.23	0.81	1.16
301	Q9UN37	VPS4A Vacuolar protein sorting-associated protein 4A	VPS4A	LLEPVVCMSDMLR	1.23	1.36	0.97
302	Q9HA64	FN3KRP Ketosamine-3-kinase	FN3KRP	ATGHSGGGCISQGR	1.24	1.04	1.15
303	O00148	DDX39A ATP-dependent RNA helicase DDX39A	DDX39A	AIVDCGFEHPSEVQHECIPQAILGMDVLCQAK	1.24	1.08	1.11
304	P08708	RPS17 40S ribosomal protein S17	RPS17	VCEEIAIIPSK	1.24	1.24	0.89
305	P07814	EPRS Bifunctional glutamate/proline--tRNA ligase	EPRS	LGVENCYFPMFVSQSALEK	1.26	1.36	1.40
306	Q9NZT2	OGFR Opioid growth factor receptor	OGFR	DCNGDTPNLSFYR	1.27	1.24	1.32
307	Q96QR8	PURB Transcriptional activator protein Pur-beta	PURB	GGGGGPCGFQPASR	1.27	1.52	1.47
308	P30084	ECHS1 Enoyl-CoA hydratase, mitochondrial	ECHS1	ALNALCDGLIDELNQALK	1.28	0.83	0.86
309	Q92879	CELF1 CUGBP Elav-like family member 1	CELF1	GCAFVTFTTR	1.29	0.98	0.79
310	P34897	SHMT2 Serine hydroxymethyltransferase, mitochondrial	SHMT2	AALEALGSCLNNK	1.29	1.44	1.54
311	P34897	SHMT2 Serine hydroxymethyltransferase, mitochondrial	SHMT2	YYGGAEVVDEIELLCQR	1.29	0.97	1.45
312	P58107	EPPK1 Epiplakin	EPPK1	YLCGLGAVGGVR	1.29	1.32	1.23
313	P62195	PSMC5 26S proteasome regulatory subunit 8	PSMC5	NIDINDVTPNCR	1.29	1.17	1.29
314	P48735	IDH2 Isocitrate dehydrogenase [NADP], mitochondrial	IDH2	SSGGFVWACK	1.29	1.96	1.99
315	O15355	PPM1G Protein phosphatase 1G	PPM1G	CSGDGVGAPR	1.30	1.61	1.11
316	P61247	RPS3A 40S ribosomal protein S3a	RPS3A	LFCVGFTK	1.32	1.43	1.07
317	P56192	MARS Methionine--tRNA ligase,	MARS	LFVSDGVPGCLPVLAAAGR	1.32	1.58	1.07

		cytoplasmic					
318	P48735	IDH2 Isocitrate dehydrogenase [NADP], mitochondrial	IDH2	VCVETVESGAMTK	1.33	1.80	1.90
319	P54886	ALDH18A1 Delta-1-pyrroline-5-carboxylate synthase	ALDH18A1	GDECGLALGR	1.33	1.31	1.37
320	P24752	ACAT1 Acetyl-CoA acetyltransferase, mitochondrial	ACAT1	QGEYGLASICNGGGGASAMLIQK	1.35	0.79	1.77
321	P09622	DLD Dihydrolipoyl dehydrogenase, mitochondrial	DLD	NETLGGTCLNVGCIPSK	1.35	1.01	6.68
322	P46782	RPS5 40S ribosomal protein S5	RPS5	TIAECLADELINAAK	1.35	1.43	1.30
323	Q9NR46	SH3GLB2 Endophilin-B2	SH3GLB2	SQTTYYAQCYR	1.36	0.91	1.14
324	P43897	TSFM Elongation factor Ts, mitochondrial	TSFM	FECGEGEEAAETE	1.36	1.91	1.73
325	P10809	HSPD1 60 kDa heat shock protein, mitochondrial	HSPD1	CIPALDSLTPANEDQK	1.36	1.40	0.97
326	O94979	SEC31A Protein transport protein Sec31A	SEC31A	SCATFSSSHR	1.37	1.29	1.44
327	Q06587	RING1 E3 ubiquitin-protein ligase RING1	RING1	FCSDCIVTALR	1.37	0.83	1.84
328	P55769	SNU13 NHP2-like protein 1	SNU13	LLDLVQQSCNYK	1.38	1.28	1.22
329	Q27J81	INF2 Inverted formin-2	INF2	LGPQDSDPTEANLESADPELCIR	1.39	1.86	1.08
330	P48735	IDH2 Isocitrate dehydrogenase [NADP], mitochondrial	IDH2	CATITPDEAR	1.40	2.02	1.96
331	P09110	ACAA1 3-ketoacyl-CoA thiolase, peroxisomal	ACAA1	DCLIPMGITSENVAER	1.41	0.76	0.81
332	Q99832	CCT7 T-complex protein 1 subunit eta	CCT7	QLCDNAGFDATNILNK	1.42	1.25	1.58
333	P46782	RPS5 40S ribosomal protein S5	RPS5	VNQAIWLLCTGAR	1.43	1.29	1.16
334	P29401	TKT Transketolase	TKT	QAFTDVATGSLGQGLGAACGMAYTGK	1.43	0.85	1.05

335	P12532	CKMT1A Creatine kinase U-type, mitochondrial	CKMT1A	LGYILTCPSNLGTGLR	1.43	0.87	1.31
336	P53597	SUCLG1 Succinate--CoA ligase [ADP/GDP-forming] subunit al	SUCLG1	LIGPNCPGVINPGECK	1.44	1.49	1.81
337	P68104	EEF1A1 Elongation factor 1-alpha 1	EEF1A1	PMCVESFSDYPPLGR	1.44	1.95	1.44
338	O75934	BCAS2 Pre-mRNA-splicing factor SPF27	BCAS2	NDITAWQECVNNSMAQLEHQAVR	1.44	1.65	1.14
339	Q9H0C8	ILKAP Integrin-linked kinase-associated serine/threonine	ILKAP	CGVTSVPDIR	1.45	1.25	0.86
340	Q7RTV0	PHF5A PHD finger-like domain-containing protein 5A	PHF5A	PCTLVR	1.46	1.03	1.00
341	O00244	ATOX1 Copper transport protein ATOX1	ATOX1	VCIESEHSMDTLLATLK	1.46	1.70	1.43
342	P62280	RPS11 40S ribosomal protein S11	RPS11	CPFTGNVSIR	1.46	2.04	1.63
343	Q16822	PCK2 Phosphoenolpyruvate carboxykinase [GTP], mitochond	PCK2	QCPIMDPAWEAPEGVPIDAIIFGGR	1.46	1.39	1.20
344	P08865	RPSA 40S ribosomal protein SA	RPSA	YVDIAIPCNNK	1.46	1.87	2.13
345	Q96I99	SUCLG2 Succinate--CoA ligase [GDP-forming] subunit beta,	SUCLG2	SCNGPVLVGSPQGGVDIEEVAASNPELIFK	1.47	1.58	1.58
346	Q14C86	GAPVD1 GTPase-activating protein and VPS9 domain-containing	GAPVD1	FSLCSDNLEGISEGPSNR	1.48	0.91	1.22
347	Q27J81	INF2 Inverted formin-2	INF2	CPASEPGLDATTASESR	1.48	1.40	1.25
348	Q1KMD3	HNRNPUL2 Heterogeneous nuclear ribonucleoprotein U-like pro	HNRNPUL2	NFILDQCNVYNSGQR	1.49	1.60	1.68
349	Q8TAQ2	SMARCC2 SWI/SNF complex subunit SMARCC2	SMARCC2	NLAGDVCAIMR	1.50	1.58	1.16
350	Q14980	NUMA1 Nuclear mitotic apparatus protein 1	NUMA1	HLCQQLQAEQAAAEK	1.52	0.93	1.14

351	P05388	RPLP0 60S acidic ribosomal protein P0	RPLP0	CFIVGADNVGSK	1.52	1.62	1.61
352	P62333	PSMC6 26S proteasome regulatory subunit 10B	PSMC6	GCLLYGPPGTGK	1.53	2.39	2.08
353	P26641	EEF1G Elongation factor 1-gamma	EEF1G	FPEELTQTFMSCNLITGMFQR	1.53	1.56	1.80
354	P05388	RPLP0 60S acidic ribosomal protein P0	RPLP0	AGAIAPCEVTVPAQNTGLGPEK	1.53	1.61	1.54
355	Q9UL25	RAB21 Ras-related protein Rab-21	RAB21	VVLLGEGCVGK	1.54	1.40	1.04
356	P62857	RPS28 40S ribosomal protein S28	RPS28	TGSQGQCTQVR	1.55	1.69	0.97
357	P40926	MDH2 Malate dehydrogenase, mitochondrial	MDH2	TIIPLISQCTPK	1.55	0.84	1.20
358	P62879	GNB2 Guanine nucleotide-binding protein G(I)/G(S)/G(T)	GNB2	ELPGHTGYLSCCR	1.55	1.68	2.30
359	Q6PKG0	LARP1 La-related protein 1	LARP1	TASISSSPSEGTPTVGSYGCTPQSLPK	1.57	1.83	1.15
360	P08559	PDHA1 Pyruvate dehydrogenase E1 component subunit alpha,	PDHA1	VDGMDILCVR	1.57	1.38	1.44
361	P27797	CALR Calreticulin	CALR	HEQNIDCGGGYVK	1.57	1.82	1.54
362	P10809	HSPD1 60 kDa heat shock protein, mitochondrial	HSPD1	AAVEEGIVLGGGCALLR	1.58	1.63	1.04
363	P02795	MT2A Metallothionein-2	MT2A	CAQGCICK	1.58	0.65	0.57
364	P60709	ACTB Actin, cytoplasmic 1	ACTB	LCYVALDFEQEMATAASSSSLEK	1.59	1.60	1.89
365	P62333	PSMC6 26S proteasome regulatory subunit 10B	PSMC6	NVCTEAGMFAIR	1.59	1.62	1.84
366	P63241	EIF5A Eukaryotic translation initiation factor 5A-1	EIF5A	YEDICPSTHNMDVPNIK	1.60	1.90	1.43
367	Q00613	HSF1 Heat shock factor protein 1	HSF1	QECMDSK	1.61	0.84	1.50
368	P62333	PSMC6 26S proteasome regulatory subunit	PSMC6	AVASQLDCNFLK	1.61	1.58	1.88

		10B					
369	P27635	RPL10 60S ribosomal protein L10	RPL10	MLSCAGADR	1.62	1.71	1.88
370	P49327	FASN Fatty acid synthase	FASN	AFDTAGNGYCR	1.63	1.14	1.33
371	Q05639	EEF1A2 Elongation factor 1-alpha 2	EEF1A2	PMCVESFSQYPPLGR	1.66	1.84	1.70
372	Q7L0Y3	TRMT10C Mitochondrial ribonuclease P protein 1	TRMT10C	LNLATECLPLDK	1.67	1.81	3.05
373	P50914	RPL14 60S ribosomal protein L14	RPL14	ALVDGPCTQVR	1.70	2.06	2.87
374	Q86W42	THOC6 THO complex subunit 6 homolog	THOC6	AQVPGSSPGLLSLSLNQQPAAPECK	1.73	1.74	1.90
375	O95833	CLIC3 Chloride intracellular channel protein 3	CLIC3	ASEDGESVGHCPSCQR	1.73	1.58	1.66
376	P30084	ECHS1 Enoyl-CoA hydratase, mitochondrial	ECHS1	EMQNLSFQDCYSSK	1.74	0.87	0.68
377	P16455	MGMT Methylated-DNA--protein-cysteine methyltransferase	MGMT	VVCSSGAVGNYSGGLAVK	1.77	1.24	1.92
378	P15924	DSP Desmoplakin	DSP	YQAECSQFK	1.77	1.73	1.56
379	P48735	IDH2 Isocitrate dehydrogenase [NADP], mitochondrial	IDH2	NYDGDVQSDILAQGFGSLGLMTSVLVCPDGK	1.79	1.81	2.84
380	P54646	PRKAA2 5-AMP-activated protein kinase catalytic subunit	PRKAA2	TSCGSPNYAAPEVISGR	1.81	1.72	1.21
381	P35998	PSMC2 26S proteasome regulatory subunit 7	PSMC2	SVCTEAGMFAIR	1.86	1.73	1.84
382	P13804	ETFA Electron transfer flavoprotein subunit alpha, mito	ETFA	TIYAGNALCTVK	1.87	2.55	2.67
383	P50213	IDH3A Isocitrate dehydrogenase [NAD] subunit alpha, mito	IDH3A	IEAACFATIK	1.88	1.82	2.12
384	P58107	EPPK1 Epiplakin	EPPK1	YLQGTGCIAGLLLPGSQER	1.89	2.44	1.76
385	P68363	TUBA1B Tubulin alpha-1B chain	TUBA1B	YMACCLLYR	1.90	1.58	1.61

386	P49411	TUFM Elongation factor Tu, mitochondrial	TUFM	GEETPVIVGSALCALEGR	1.92	2.77	1.83
387	Q13748	TUBA3C Tubulin alpha-3C/D chain	TUBA3C	TIQFVDWCPTGFK	1.96	1.59	2.12
388	P27707	DCK Deoxycytidine kinase	DCK	SCPSFSASSEGTR	1.96	1.99	1.54
389	P40926	MDH2 Malate dehydrogenase, mitochondrial	MDH2	GYLGPEQLPDCLK	1.99	1.08	1.69
390	P15924	DSP Desmoplakin	DSP	GVITDQNSDGYCQTGTMSR	2.01	1.65	1.80
391	P62280	RPS11 40S ribosomal protein S11	RPS11	DVQIGDIVTVGECR	2.04	2.49	2.61
392	Q02252	ALDH6A1 Methylmalonate-semialdehyde dehydrogenase	ALDH6A1	AEMDAAIASCK	2.04	1.83	2.33
393	P13639	EEF2 Elongation factor 2	EEF2	DLEEDHACIPIK	2.05	2.15	1.36
394	P68363	TUBA1B Tubulin alpha-1B chain	TUBA1B	SIQFVDWCPTGFK	2.06	1.84	2.22
395	Q8TCU6	PREX1 Phosphatidylinositol 3,4,5-trisphosphate-dependent	PREX1	LCVLNEILGTER	2.07	1.56	1.60
396	A6NNZ2	cimageipi-sp|A6NNZ2|TBB8L_HUMAN Tubulin beta-8 chain-like protein LOC260334	cimageipi-sp|A6NNZ2|TBB8L_HUMAN	TAVCDIPPR	2.09	2.11	2.56
397	Q06203	PPAT Amidophosphoribosyltransferase	PPAT	CELENCQPFVVETLHGK	2.12	1.07	3.62
398	Q15365	PCBP1 Poly(rC)-binding protein 1	PCBP1	VMTIPYQPMPASSPVICAGGQDR	2.12	2.45	1.70
399	Q9BQE3	TUBA1C Tubulin alpha-1C chain	TUBA1C	AVCMLSNTTAVAEAWAR	2.14	2.13	1.71
400	P35270	SPR Sepiapterin reductase	SPR	TVVNISSLCALQPFK	2.21	0.89	0.92
401	P32322	PYCR1 Pyrroline-5-carboxylate reductase 1, mitochondrial	PYCR1	SLLINAVEASCIR	2.27	1.21	1.62
402	A6NNZ2	TBB8L Tubulin beta-8 chain-like protein	TBB8L	NMMAACDPR	2.29	2.10	2.53

403	Q9Y5Y2	NUBP2 Cytosolic Fe-S cluster assembly factor NUBP2	NUBP2	VGILDVDLCGPSIPR	2.30	2.22	1.95
404	O00244	ATOX1 Copper transport protein ATOX1	ATOX1	HEFSVDMTCGGCAEAVSR	2.32	3.63	11.71
405	P68363	TUBA1B Tubulin alpha-1B chain	TUBA1B	AVCMLSNTTAIAEAWAR	2.34	2.10	2.34
406	P50213	IDH3A Isocitrate dehydrogenase [NAD] subunit alpha, mito	IDH3A	CSDFTEEICR	2.38	3.28	2.45
407	P21333	FLNA Filamin-A	FLNA	LQVEPAVDTSGVQCYGPGIEGQGVFR	2.42	1.80	1.73
408	P19367	HK1 Hexokinase-1	HK1	TVCGVVSR	2.50	1.47	0.58
409	P63244	RACK1 Receptor of activated protein C kinase 1	RACK1	AEPPQCTSLAWSADGQTLFAGYTDNLVR	2.51	2.72	2.89
410	P17987	TCP1 T-complex protein 1 subunit alpha	TCP1	GANDFMCDEMER	2.60	1.38	2.23
411	P49411	TUFM Elongation factor Tu, mitochondrial	TUFM	NMITGTAPLDGCILVVAANDGPMPQTR	2.60	2.47	2.24
412	P26440	IVD Isovaleryl-CoA dehydrogenase, mitochondrial	IVD	ACDEGHCTAK	2.67	2.13	2.17
413	Q16822	PCK2 Phosphoenolpyruvate carboxykinase [GTP], mitochond	PCK2	VECVGDDIAWMR	2.71	2.09	2.15
414	P13804	ETFA Electron transfer flavoprotein subunit alpha, mito	ETFA	LGGEVSCLVAGTK	2.75	2.62	2.63
415	P17858	PFKL ATP-dependent 6-phosphofructokinase, liver type	PFKL	VFANAPDSACVIGLK	2.81	3.33	3.54
416	Q99714	HSD17B10 3-hydroxyacyl-CoA dehydrogenase type-2	HSD17B10	VDVAVNCAGIAVASK	2.84	1.89	1.48
417	Q96I99	SUCLG2 Succinate--CoA ligase [GDP-forming] subunit beta,	SUCLG2	IDATQVEVNPFGETPEGQVVCFDAK	2.89	2.71	1.80
418	Q01813	PFKP ATP-dependent phosphofructokinase, platelet type	PFKP	LPLMECVQMTQDVQK	3.06	2.82	5.89

419	Q9BQE3	TUBA1C Tubulin alpha-1C chain	TUBA1C	AYHEQLTVAEITNACFEPANQMVK	3.07	2.65	3.17
420	Q99714	HSD17B10 3-hydroxyacyl-CoA dehydrogenase type-2	HSD17B10	LGNNCVFAPADVTSEK	3.08	2.72	2.21
421	P04350	TUBB4A Tubulin beta-4A chain	TUBB4A	LTTPTYGDLNHLVSATMSGVTTCLR	3.11	1.94	2.46
422	Q92947	GCDH Glutaryl-CoA dehydrogenase, mitochondrial	GCDH	GYGCAGVSSVAYGLLAR	3.14	1.62	3.43
423	P68363	TUBA1B Tubulin alpha-1B chain	TUBA1B	AYHEQLSVAEITNACFEPANQMVK	3.17	2.68	3.12
424	P25398	RPS12 40S ribosomal protein S12	RPS12	LGEWVGLCK	4.10	4.34	2.32
425	Q96DV4	MRPL38 39S ribosomal protein L38, mitochondrial	MRPL38	VAEGQVTCPYLPPFPAR	4.12	0.74	0.86
426	P62888	RPL30 60S ribosomal protein L30	RPL30	VCTLAIIDPGDSDIIR	4.14	1.35	2.71
427	P31749	AKT1 RAC-alpha serine/threonine-protein kinase	AKT1	TFCGTPEYLAPEVLEDNDYGR	4.46	3.09	5.57
428	P07339	CTSD Cathepsin D	CTSD	AIGAVPLIQGEYMIPCEK	4.60	5.52	7.92
429	P53396	ACLY ATP-citrate synthase	ACLY	PASFMTSICDER	9.93	1.04	1.17

Table A3-1 Protiens identified with OAT immunoprecipitation. *R* values indicate light:heavy ReDiMe ratios normalized to the reported OAT *R* value and averaged across two datasets. Considered peptides were required to have a SEM < 30%.

index	Symbol	Protein	Cellular Component	*R* value (log2)
1	CCDC124	Coiled-coil domain-containing protein 124	cytoplasm;cytoskeleton	-7.68
2	RPS15	40S ribosomal protein S15	cytosol;membrane;nucleus;ribosome	-6.07
3	EIF4A1	Eukaryotic initiation factor 4A-I	cytoplasm;cytosol;membrane;nucleus	-4.73
4	C1QBP	Complement component 1 Q subcomponent-binding protein, mitochondrial	cell surface;cytoplasm;cytosol;extracellular;membrane;mitochondrion;nucleus	-4.37
5	ATPIF1	ATPase inhibitor, mitochondrial	cell surface;mitochondrion	-4.21
6	WDR61	WD repeat-containing protein 61	cytoplasm;cytosol;nucleus	-4.16
7	KRT9	Keratin, type I cytoskeletal 9	cytosol;membrane;nucleus	-4.05
8	EIF3CL	eukaryotic translation initiation factor 3 subunit C-like protein	cytoplasm	-3.96
9	RPLP2	60S acidic ribosomal protein P2	cytosol;membrane;ribosome	-3.87
10	PPIB	peptidyl-prolyl cis-trans isomerase B	endoplasmic reticulum;membrane;nucleus;organelle lumen	-3.84
11	PTMA	Prothymosin alpha	cytosol;nucleus	-3.76
12	KRT1	Keratin, type II cytoskeletal 1	cytoskeleton;cytosol;extracellular;membrane;nucleus	-3.48
13	PTER	Phosphotriesterase-related protein		-3.37
14	KRT2	Keratin, type II cytoskeletal 2 epidermal	cytoskeleton;cytosol;membrane;nucleus	-3.35
15	HSPH1	Heat shock protein 105 kDa	cytoplasm;cytosol;extracellular;nucleus;organelle lumen	-3.32
16	PPIA	peptidyl-prolyl cis-trans isomerase A	cytoplasm;cytosol;extracellular;membrane;nucleus;organelle lumen	-3.25
17	ENO1	alpha-enolase	cell surface;cytoplasm;cytosol;membrane;nucleus	-3.24
18	NUDT5	ADP-sugar pyrophosphatase	cytosol;nucleus	-3.22
19	RPL7A	60S ribosomal protein L7a	cytoplasm;cytosol;membrane;nucleus;ribosome	-3.17
20	RPS26	40S ribosomal protein S26	cytosol;membrane;ribosome	-3.12
21	HNRNPC	Heterogeneous nuclear ribonucleoproteins C1/C2	cytoskeleton;cytosol;extracellular;membrane;nucleus;spliceosomal complex	-3.08
22	KRT10	Keratin, type I cytoskeletal 10	cytoplasm;cytoskeleton;cytosol;membrane;nucleus	-2.99
23	IMPDH2	inosine-5'-monophosphate dehydrogenase 2	cytoplasm;cytosol;extracellular;membrane;nucleus;organelle lumen	-2.94
24	HNRNPH1	Heterogeneous nuclear ribonucleoprotein H	cytosol;membrane;nucleus;spliceosomal complex	-2.94
25	RCN2	Reticulocalbin-2	endoplasmic reticulum;organelle	-2.91

			lumen	
26	RPL23	60S ribosomal protein L23	cytoplasm;cytosol;membrane;ribosome	-2.86
27	SRSF2	serine/arginine-rich splicing factor 2	cytosol;nucleus;spliceosomal complex	-2.85
28	FKBP3	peptidyl-prolyl cis-trans isomerase FKBP3	cytoplasm;nucleus	-2.82
29	EIF1AX	Eukaryotic translation initiation factor 1A, X-chromosomal	cytosol	-2.80
30	BTF3	Isoform 2 of Transcription factor BTF3	cytosol;nucleus	-2.76
31	ACTR1A	Alpha-centractin	cytoplasm;cytoskeleton;cytosol	-2.75
32	HNRNPU	Heterogeneous nuclear ribonucleoprotein U	cell surface;chromosome;cytoplasm;membrane;nucleus;spliceosomal complex	-2.73
33	SFPQ	splicing factor, proline- and glutamine-rich	chromosome;cytoplasm;nucleus	-2.70
34	SSBP1	Single-stranded DNA-binding protein, mitochondrial	mitochondrion;nucleus;organelle lumen	-2.66
35	MIS18A	protein Mis18-alpha	chromosome;cytosol;nucleus	-2.65
36	ECH1	Delta(3,5)-Delta(2,4)-dienoyl-CoA isomerase, mitochondrial	membrane;mitochondrion	-2.65
37	EIF3H	Eukaryotic translation initiation factor 3 subunit H	cytoplasm;cytosol;membrane	-2.60
38	HERC2	E3 ubiquitin-protein ligase HERC2	cytoplasm;cytoskeleton;membrane;nucleus	-2.58
39	BCAP31	B-cell receptor-associated protein 31	cytosol;endoplasmic reticulum;membrane;mitochondrion	-2.54
40	ATP5A1	ATP synthase subunit alpha, mitochondrial	membrane;mitochondrion;organelle lumen	-2.53
41	RPS23	40S ribosomal protein S23	cytosol;membrane;ribosome	-2.52
42	SSRP1	FACT complex subunit SSRP1	chromosome;nucleus	-2.48
43	SNRPB	Small nuclear ribonucleoprotein-associated proteins B and B'	cytoplasm;cytosol;nucleus;spliceosomal complex	-2.48
44	GNE	bifunctional UDP-N-acetylglucosamine 2-epimerase/N-acetylmannosamine kinase	cytoplasm;cytosol	-2.48
45	SNRNP40	U5 small nuclear ribonucleoprotein 40 kDa protein	cytosol;nucleus;spliceosomal complex	-2.47
46	YWHAZ	14-3-3 protein zeta/delta	cytoplasm;cytosol;membrane;mitochondrion;nucleus	-2.47
47	HIST1H4A	histone H4	chromosome;extracellular;membrane;nucleus	-2.44
48	RPL14	60S ribosomal protein L14	cytosol;membrane;ribosome	-2.43
49	SRSF7	serine/arginine-rich splicing factor 7 ""	cytoplasm;nucleus	-2.42
50	RPL10	60S ribosomal protein L10	cytosol;endoplasmic	-2.41

			reticulum;membrane;nucleus;ribosom e	
51	CCT5	T-complex protein 1 subunit epsilon	cytoplasm;cytoskeleton;cytosol	-2.39
52	CALU	Calumenin	endoplasmic reticulum;extracellular;Golgi;membran e;organelle lumen	-2.37
53	LUC7L2	Putative RNA-binding protein Luc7-like 2	nucleus;spliceosomal complex	-2.33
54	SSB	Lupus La protein	cytoplasm;nucleus	-2.33
55	RPS11	40S ribosomal protein S11	cytoplasm;cytosol;membrane;ribosom e	-2.33
56	HSPA4	Heat shock 70 kDa protein 4	cytoplasm;cytosol	-2.32
57	NEURL4	Neuralized-like protein 4	cytoplasm;cytoskeleton	-2.31
58	PRKACA	cAMP-dependent protein kinase catalytic subunit alpha	cytoplasm;cytosol;membrane;mitocho ndrion;nucleus	-2.30
59	OXSM	3-oxoacyl-[acyl-carrier-protein] synthase, mitochondrial	cytosol;mitochondrion	-2.30
60	SUB1	Activated RNA polymerase II transcriptional coactivator p15	nucleus	-2.29
61	DDX21	Nucleolar RNA helicase 2	cytoplasm;membrane;nucleus	-2.28
62	RPS28	40S ribosomal protein S28	cytosol;ribosome	-2.21
63	COPG1	Coatomer subunit gamma-1	cytoplasm;cytosol;Golgi;membrane	-2.21
64	GAPDH	glyceraldehyde-3-phosphate dehydrogenase	cytoplasm;cytoskeleton;cytosol;membr ane;nucleus	-2.19
65	PYCR2	Pyrroline-5-carboxylate reductase 2	cytoplasm;mitochondrion;organelle lumen	-2.16
66	PRKAR1 B	cAMP-dependent protein kinase type I-beta regulatory subunit	cytosol;membrane	-2.15
67	IGKV2-29	Immunoglobulin kappa variable 2-29	extracellular;membrane	-2.14
68	HIST2H2 AC	Histone H2A type 2-C	chromosome;nucleus	-2.13
69	PSMB3	proteasome subunit beta type-3	cytoplasm;cytosol;nucleus;proteasome	-2.12
70	PYCR1	Pyrroline-5-carboxylate reductase 1, mitochondrial	mitochondrion;organelle lumen	-2.10
71	RPS18	40S ribosomal protein S18	cytoplasm;cytosol;membrane;nucleus; ribosome	-2.09
72	CCT3	T-complex protein 1 subunit gamma	cytoplasm;cytoskeleton;cytosol;membr ane	-2.07
73	PGAM1	Phosphoglycerate mutase 1	cytoplasm;cytosol;extracellular;membr ane;organelle lumen	-2.06
74	EEF1A1	Elongation factor 1-alpha 1	cytoplasm;cytoskeleton;cytosol;extrac ellular;membrane;nucleus;organelle lumen	-2.06
75	DDX5	probable ATP-dependent RNA helicase DDX5	cytoplasm;membrane;nucleus;spliceos omal complex	-2.02
76	ALDOA	fructose-bisphosphate aldolase A	cytoplasm;cytoskeleton;cytosol;extrac ellular;membrane;nucleus;organelle lumen	-2.01

77	RCN1	Reticulocalbin-1	endoplasmic reticulum;organelle lumen	-2.01
78	CCT4	T-complex protein 1 subunit delta	cytoplasm;cytoskeleton;cytosol	-1.99
79	SERBP1	Plasminogen activator inhibitor 1 RNA-binding protein	cytoplasm;cytosol;membrane;nucleus	-1.98
80	YWHAB	14-3-3 protein beta/alpha	cytoplasm;cytosol;membrane;mitochondrion;nucleus	-1.98
81	HSP90AA1	Heat shock protein HSP 90-alpha	cytoplasm;cytosol;extracellular;membrane;nucleus;organelle lumen	-1.95
82	PHGDH	D-3-phosphoglycerate dehydrogenase	cytosol	-1.93
83	HSPD1	60 kDa heat shock protein, mitochondrial	cell surface;cytoplasm;cytosol;endosome;membrane;mitochondrion;organelle lumen	-1.89
84	PSMB2	proteasome subunit beta type-2	cytoplasm;cytosol;membrane;nucleus;proteasome	-1.89
85	SRSF3	Serine/arginine-rich splicing factor 3	cytoplasm;nucleus	-1.87
86	RPS14	40S ribosomal protein S14	cytosol;membrane;mitochondrion;ribosome	-1.86
87	ACTB	Actin, cytoplasmic 1	cytoplasm;cytoskeleton;cytosol;membrane;nucleus	-1.85
88	HDAC1	histone deacetylase 1	chromosome;cytoplasm;cytosol;nucleus	-1.85
89	HNRNPM	Heterogeneous nuclear ribonucleoprotein M	membrane;nucleus;spliceosomal complex	-1.84
90	ERH	Enhancer of rudimentary homolog		-1.83
91	TRA2B	transformer-2 protein homolog beta	membrane;nucleus;spliceosomal complex	-1.83
92	PSMA3	Proteasome subunit alpha type-3	cytoplasm;cytosol;nucleus;proteasome	-1.82
93	PSMB4	Proteasome subunit beta type-4	cytoplasm;cytosol;nucleus;proteasome	-1.81
94	CDK2AP1	Cyclin-dependent kinase 2-associated protein 1	cytosol;nucleus	-1.77
95	HSPA1A	heat shock 70 kDa protein 1A	cytoplasm;cytoskeleton;cytosol;endoplasmic reticulum;extracellular;mitochondrion;nucleus	-1.77
96	RPL19	60S ribosomal protein L19	cytosol;membrane;ribosome	-1.75
97	PCBP1	Poly(RC)-binding protein 1	cytoplasm;cytosol;membrane;nucleus	-1.73
98	NSRP1	Nuclear speckle splicing regulatory protein 1	nucleus	-1.72
99	RPS7	40S ribosomal protein S7	cytoplasm;cytoskeleton;cytosol;membrane;nucleus;ribosome	-1.71
100	HSP90AB1	Heat shock protein HSP 90-beta	cell surface;cytoplasm;cytosol;extracellular;membrane;mitochondrion;nucleus;organelle lumen	-1.70

101	TUBA1B	Tubulin alpha-1B chain	cytoplasm;cytoskeleton;membrane	-1.70
102	DDX46	probable ATP-dependent RNA helicase DDX46	cytoplasm;membrane;nucleus	-1.67
103	CCT2	T-complex protein 1 subunit beta	cytoplasm;cytosol;extracellular;organelle lumen	-1.63
104	HNRNPK	Heterogeneous nuclear ribonucleoprotein K	cytoplasm;membrane;nucleus;spliceosomal complex	-1.60
105	HIST2H2BF	Histone H2B type 2-F	chromosome;cytosol;nucleus	-1.59
106	PSMD7	26S proteasome non-ATPase regulatory subunit 7	cytosol;extracellular;membrane;nucleus;organelle lumen;proteasome	-1.57
107	PLOD1	Procollagen-lysine,2-oxoglutarate 5-dioxygenase 1	endoplasmic reticulum;membrane	-1.57
108	GIT2	ARF GTPase-activating protein GIT2		-1.56
109	TIMM50	Mitochondrial import inner membrane translocase subunit TIM50	membrane;mitochondrion;nucleus	-1.56
110	TCP1	T-complex protein 1 subunit alpha	cytoplasm;cytoskeleton;cytosol;Golgi	-1.56
111	TUBB	tubulin beta chain	cytoplasm;cytoskeleton;extracellular;membrane;nucleus;organelle lumen	-1.55
112	KLC1	Isoform J of Kinesin light chain 1	cytosol;membrane	-1.55
113	NPM1	Nucleophosmin	cytoplasm;cytoskeleton;cytosol;membrane;nucleus	-1.55
114	HIST3H3	histone H3.1t	chromosome;nucleus	-1.54
115	PAICS	multifunctional protein ADE2	cytoplasm;cytosol;membrane	-1.51
116	CHD4	Isoform 2 of Chromodomain-helicase-DNA-binding protein 4	cytoplasm;membrane;nucleus	-1.51
117	TRAP1	heat shock protein 75 kDa, mitochondrial	membrane;mitochondrion;organelle lumen	-1.50
118	EEF1G	elongation factor 1-gamma	cytoplasm;cytosol;endoplasmic reticulum;membrane;nucleus	-1.49
119	PSMB7	Proteasome subunit beta type-7	cytoplasm;cytosol;extracellular;nucleus;organelle lumen;proteasome	-1.46
120	EEF2	Elongation factor 2	cytoplasm;cytosol;extracellular;membrane;nucleus;organelle lumen;ribosome	-1.43
121	EIF3F	Eukaryotic translation initiation factor 3 subunit F	cytoplasm;cytosol;membrane	-1.43
122	PRPF8	Pre-mRNA-processing-splicing factor 8	membrane;nucleus;spliceosomal complex	-1.42
123	RPL6	60S ribosomal protein L6	cytosol;membrane;nucleus;ribosome	-1.42
124	RPL4	60S ribosomal protein L4	cytoplasm;cytosol;endoplasmic reticulum;membrane;nucleus;ribosome	-1.42
125	SRRT	serrate RNA effector molecule homolog	cytoplasm;nucleus	-1.42
126	RPL23A	60S ribosomal protein L23a	cytoplasm;cytosol;nucleus;ribosome	-1.42
127	PSMC2	26S proteasome regulatory subunit 7	cytoplasm;cytosol;extracellular;membrane;nucleus;organelle	-1.41

			lumen;proteasome	
128	SF3A1	splicing factor 3A subunit 1	nucleus;spliceosomal complex	-1.41
129	RPS3A	40S ribosomal protein S3a	cytoplasm;cytosol;endoplasmic reticulum;nucleus;ribosome	-1.41
130	DDX23	Probable ATP-dependent RNA helicase DDX23	cytoplasm;nucleus;spliceosomal complex	-1.41
131	PSMA4	Proteasome subunit alpha type-4	cytoplasm;cytosol;nucleus;proteasome	-1.41
132	RPL7	60S ribosomal protein L7	cytoplasm;cytosol;membrane;nucleus;ribosome	-1.40
133	ARHGEF7	Isoform 1 of Rho guanine nucleotide exchange factor 7	cytosol;membrane;vacuole	-1.39
134	PSMD4	26S proteasome non-ATPase regulatory subunit 4	cytoplasm;cytosol;nucleus;proteasome	-1.39
135	PRPF19	Pre-mRNA-processing factor 19	cytoplasm;cytoskeleton;membrane;nucleus;spliceosomal complex	-1.37
136	PSMC5	26S proteasome regulatory subunit 8	cytoplasm;cytosol;membrane;nucleus;proteasome	-1.36
137	MCM4	DNA replication licensing factor MCM4	membrane;nucleus	-1.35
138	CCT6A	T-complex protein 1 subunit zeta	cytoplasm;cytosol;membrane	-1.34
139	GLO1	lactoylglutathione lyase	cytoplasm;cytosol;membrane;nucleus	-1.34
140	AVEN	Cell death regulator Aven	membrane	-1.34
141	PSMD2	26S proteasome non-ATPase regulatory subunit 2	cytoplasm;cytosol;extracellular;membrane;nucleus;organelle lumen;proteasome	-1.34
142	RPS19	40S ribosomal protein S19	cytoplasm;cytosol;membrane;nucleus;ribosome	-1.33
143	HSPA8	Heat shock cognate 71 kDa protein	cytoplasm;cytosol;endosome;extracellular;membrane;nucleus;organelle lumen;spliceosomal complex	-1.33
144	PSMD12	26s proteasome non-atpase regulatory subunit 12	cytoplasm;cytosol;extracellular;membrane;organelle lumen;proteasome	-1.33
145	DCTN2	dynactin subunit 2	chromosome;cytoplasm;cytoskeleton;cytosol;membrane	-1.33
146	CAPZB	F-actin-capping protein subunit beta	cytoplasm;cytoskeleton;cytosol	-1.33
147	EIF3A	Eukaryotic translation initiation factor 3 subunit A	cytoplasm;cytosol;membrane;nucleus	-1.30
148	SUPT16H	FACT complex subunit SPT16	chromosome;nucleus	-1.30
149	RPS15A	40S ribosomal protein S15a	cytoplasm;cytosol;membrane;mitochondrion;ribosome	-1.30
150	MTA3	Metastasis-associated protein MTA3	cytoplasm;nucleus	-1.29
151	COPE	coatomer subunit epsilon	cytoplasm;cytosol;Golgi;membrane	-1.29
152	RPS17; RPS17L	40S ribosomal protein S17	cytosol;membrane;ribosome	-1.28
153	VPS26A	Vacuolar protein sorting-associated protein 26A	cytoplasm;cytosol;endosome;membrane;vacuole	-1.27

154	HSPA5	78 kDa glucose-regulated protein	cell surface;cytoplasm;endoplasmic reticulum;membrane;mitochondrion;nucleus;organelle lumen	-1.26
155	NCL	Nucleolin	cytoplasm;membrane;nucleus	-1.26
156	TJP1	Tight junction protein ZO-1	cytoplasm;cytosol;membrane	-1.25
157	DOCK11	dedicator of cytokinesis protein 11	cytosol	-1.25
158	MTA2	Metastasis-associated protein MTA2	membrane;nucleus	-1.25
159	RPL31	60S ribosomal protein L31	cytosol;membrane;ribosome	-1.25
160	RBBP7	Histone-binding protein RBBP7	cytosol;nucleus	-1.24
161	PSMD1	26S proteasome non-ATPase regulatory subunit 1	cytosol;extracellular;membrane;nucleus;organelle lumen;proteasome	-1.23
162	PSMB1	proteasome subunit beta type-1	cytoplasm;cytosol;extracellular;nucleus;organelle lumen;proteasome	-1.23
163	PSMA7	Proteasome subunit alpha type-7	cytoplasm;cytosol;nucleus;proteasome	-1.22
164	ALDH7A1	Alpha-aminoadipic semialdehyde dehydrogenase	cytoplasm;cytosol;mitochondrion;nucleus;organelle lumen	-1.21
165	RPL8	60S ribosomal protein L8	cytoplasm;cytosol;membrane;ribosome	-1.21
166	KIF5B	Kinesin-1 heavy chain	cytoplasm;cytoskeleton;cytosol;membrane	-1.21
167	TROVE2	60 kDa SS-A/Ro ribonucleoprotein	cytoplasm;cytosol;nucleus	-1.21
168	RPL17	60S ribosomal protein L17	cytosol;nucleus;ribosome	-1.20
169	SNRNP200	U5 small nuclear ribonucleoprotein 200 kDa helicase	membrane;nucleus;spliceosomal complex	-1.20
170	RPS13	40S ribosomal protein S13	cytosol;membrane;nucleus;ribosome	-1.20
171	UBE3A	Ubiquitin-protein ligase E3A	cytoplasm;cytosol;nucleus;proteasome	-1.20
172	LUC7L3	Luc7-like protein 3	nucleus;spliceosomal complex	-1.19
173	TACC2	Transforming acidic coiled-coil-containing protein 2	cytoplasm;cytoskeleton;cytosol;membrane;nucleus	-1.19
174	TACC3	Transforming acidic coiled-coil-containing protein 3	cytoplasm;cytoskeleton	-1.18
175	CAPZA1	F-actin-capping protein subunit alpha-1	cytoplasm;cytoskeleton;cytosol;extracellular	-1.18
176	SLC25A5	ADP/ATP translocase 2	membrane;mitochondrion;nucleus	-1.18
177	RBBP4	Histone-binding protein RBBP4	cytosol;nucleus	-1.18
178	HDAC2	Histone deacetylase 2	chromosome;cytoplasm;nucleus	-1.17
179	HNRNPA1	Heterogeneous nuclear ribonucleoprotein A1	cytoplasm;membrane;nucleus;spliceosomal complex	-1.16
180	CHD1	Chromodomain-helicase-DNA-binding protein 1	cytoplasm;nucleus	-1.15
181	SF3B2	Splicing factor 3b subunit 2	nucleus;spliceosomal complex	-1.14
182	RPL26	60S ribosomal protein L26	cytoplasm;cytosol;membrane;ribosome	-1.14
183	ECD	Protein ecdysoneless homolog	cytoplasm;cytosol;nucleus	-1.13

184	PRDX1	peroxiredoxin-1	cytoplasm;cytosol;mitochondrion;nucleus	-1.13
185	GIT1	ARF GTPase-activating protein GIT1	cytoplasm;cytosol;membrane	-1.11
186	DHX15	Pre-mRNA-splicing factor ATP-dependent RNA helicase DHX15	cytoplasm;nucleus;spliceosomal complex	-1.11
187	PSMB5	proteasome subunit beta type-5	cytoplasm;cytosol;nucleus;proteasome	-1.11
188	PSMA2	Proteasome subunit alpha type-2	cytoplasm;cytosol;extracellular;nucleus;organelle lumen;proteasome	-1.10
189	THRAP3	Thyroid hormone receptor-associated protein 3	nucleus	-1.09
190	MTA1	Isoform 3 of Metastasis-associated protein MTA1	cytoplasm;cytosol;nucleus	-1.08
191	IGF2BP1	Insulin-like growth factor 2 mRNA-binding protein 1	cytoplasm;cytosol;nucleus	-1.08
192	MBD3	methyl-CpG-binding domain protein 3	chromosome;cytoplasm;nucleus	-1.06
193	PSMA6	Proteasome subunit alpha type-6	cytoplasm;cytosol;nucleus;proteasome	-1.05
194	HSPA9	Stress-70 protein, mitochondrial	cytoplasm;mitochondrion;nucleus;organelle lumen	-1.05
195	RPL15	60S ribosomal protein L15	cytosol;membrane;nucleus;ribosome	-1.05
196	PSMA1	Proteasome subunit alpha type-1	cytoplasm;cytosol;nucleus;proteasome	-1.05
197	SNRPF	Small nuclear ribonucleoprotein F	cytoplasm;cytosol;nucleus;spliceosomal complex	-1.04
198	LRRFIP2	Isoform 4 of Leucine-rich repeat flightless-interacting protein 2		-1.03
199	PRPF6	Pre-mRNA-processing factor 6	membrane;nucleus;spliceosomal complex	-1.03
200	CHERP	Calcium homeostasis endoplasmic reticulum protein	cytoplasm;endoplasmic reticulum;membrane	-1.02
201	DDX17	Isoform 2 of Probable ATP-dependent RNA helicase DDX17	cytoplasm;cytosol;membrane;nucleus	-1.02
202	PSMD3	26S proteasome non-ATPase regulatory subunit 3	cytosol;extracellular;membrane;nucleus;organelle lumen;proteasome	-1.02
203	FOCAD	focadhesin	membrane	-1.02
204	HNRNPA2B1	heterogeneous nuclear ribonucleoproteins A2/B1	cytoplasm;extracellular;membrane;nucleus;spliceosomal complex	-1.01
205	PRKAR1A	cAMP-dependent protein kinase type I-alpha regulatory subunit	cytoplasm;cytosol;membrane	-1.00
206	RBM22	Pre-mRNA-splicing factor RBM22	cytoplasm;nucleus;spliceosomal complex	-1.00
207	EEF1B2	Elongation factor 1-beta	cytoplasm;cytosol;endoplasmic reticulum;nucleus	-0.99
208	SNRPD3	small nuclear ribonucleoprotein sm d3	cytoplasm;cytosol;nucleus;spliceosomal complex	-0.98
209	ATP5B	ATP synthase subunit beta, mitochondrial	cell surface;membrane;mitochondrion;nucleus;organelle lumen	-0.98
210	CSNK2A	Casein kinase II subunit alpha	chromosome;cytoplasm;cytosol;memb	-0.98

	1		rane;nucleus	
211	ATRX	transcriptional regulator ATRX	chromosome;nucleus	-0.98
212	DCTN1	Dynactin subunit 1	chromosome;cytoplasm;cytoskeleton;cytosol;membrane;nucleus	-0.98
213	RBM39	RNA-binding protein 39	cytoskeleton;nucleus	-0.97
214	CCT7	T-complex protein 1 subunit eta	cytoplasm;cytosol;mitochondrion	-0.97
215	GATAD2A	Transcriptional repressor p66-alpha	nucleus	-0.96
216	UBA52	Ubiquitin-60S ribosomal protein L40	cytoplasm;cytosol;endoplasmic reticulum;membrane;nucleus;ribosome	-0.95
217	RPS10	40S ribosomal protein S10	cytoplasm;cytosol;membrane;nucleus;ribosome	-0.95
218	SF3A3	splicing factor 3a subunit 3	nucleus;spliceosomal complex	-0.94
219	MATR3	Matrin-3	membrane;nucleus	-0.94
220	EIF4B	eukaryotic translation initiation factor 4B	cytosol	-0.93
221	EIF3B	Eukaryotic translation initiation factor 3 subunit B	cytoplasm;cytosol	-0.93
222	EFTUD2	116 kDa U5 small nuclear ribonucleoprotein component	cytosol;membrane;nucleus;spliceosomal complex	-0.92
223	SRRM2	serine/arginine repetitive matrix protein 2	nucleus;spliceosomal complex	-0.92
224	RPS3	40S ribosomal protein S3	cytoplasm;cytoskeleton;cytosol;endoplasmic reticulum;membrane;mitochondrion;nucleus;organelle lumen;ribosome	-0.91
225	HTRA2	Serine protease HTRA2, mitochondrial	chromosome;cytoskeleton;cytosol;endoplasmic reticulum;membrane;mitochondrion;nucleus	-0.91
226	RPS6	40S RIBOSOMAL PROTEIN S6	cytoplasm;cytosol;membrane;nucleus;ribosome	-0.90
227	RPS4X	40S ribosomal protein S4, X isoform	cytoplasm;cytosol;membrane;ribosome	-0.89
228	NAP1L1	Nucleosome assembly protein 1-like 1	membrane;nucleus	-0.88
229	HIST1H1D	Histone H1.3	chromosome;nucleus	-0.88
230	CD2BP2	CD2 antigen cytoplasmic tail-binding protein 2	cytoplasm;cytosol;nucleus	-0.87
231	CCAR1	Cell division cycle and apoptosis regulator protein 1	cytoplasm	-0.87
232	RPL3	60S ribosomal protein L3	cytoplasm;cytosol;nucleus;ribosome	-0.84
233	TPR	Nucleoprotein TPR	chromosome;cytoplasm;cytoskeleton;membrane;nucleus	-0.84
234	PSMC3	26S proteasome regulatory subunit 6A	cytoplasm;cytosol;extracellular;membrane;nucleus;organelle lumen;proteasome	-0.83
235	HABP4	Intracellular hyaluronan-binding	cytoplasm;cytosol;extracellular;nucleus	-0.83

		protein 4		
236	PSMD11	26S proteasome non-ATPase regulatory subunit 11	cytoplasm;cytosol;extracellular;membrane;nucleus;organelle lumen;proteasome	-0.83
237	EAPP	e2f-associated phosphoprotein	cytoplasm;nucleus	-0.82
238	GATAD2B	Transcriptional repressor p66-beta	nucleus	-0.81
239	HSPB1	Heat shock protein beta-1	cytoplasm;cytoskeleton;cytosol;membrane;nucleus;proteasome	-0.81
240	PSMB6	Proteasome subunit beta type-6	cytoplasm;cytosol;nucleus;proteasome	-0.81
241	SNRNP70	U1 small nuclear ribonucleoprotein 70 kDa	cytoplasm;nucleus;spliceosomal complex	-0.81
242	RPL13	60S ribosomal protein L13	cytosol;membrane;nucleus;ribosome	-0.79
243	RPS12	40S ribosomal protein S12	cytoplasm;cytosol;membrane;ribosome	-0.78
244	ERGIC1	Endoplasmic reticulum-Golgi intermediate compartment protein 1	endoplasmic reticulum;Golgi;membrane	-0.77
245	DNAJA1	DnaJ homolog subfamily A member 1	cytoplasm;cytoskeleton;cytosol;endoplasmic reticulum;membrane;mitochondrion;nucleus	-0.77
246	MRE11A	Double-strand break repair protein MRE11	chromosome;cytoplasm;cytosol;nucleus	-0.74
247	RUVBL2	RuvB-like 2	cytoplasm;cytosol;membrane;nucleus	-0.72
248	BCLAF1	Bcl-2-associated transcription factor 1	cytoplasm;nucleus	-0.71
249	SMU1	WD40 repeat-containing protein SMU1	cytoplasm;nucleus;spliceosomal complex	-0.71
250	TSSC4	Protein TSSC4		-0.71
251	NME2; NME1-NME2	nucleoside diphosphate kinase b	cytoplasm;cytosol;extracellular;membrane;nucleus;organelle lumen	-0.67
252	VPS35	Vacuolar protein sorting-associated protein 35	cytoplasm;cytosol;endosome;membrane;mitochondrion;vacuole	-0.65
253	GSS	glutathione synthetase	cytosol	-0.65
254	CSNK2B	Casein kinase II subunit beta	chromosome;cytoplasm;cytosol;extracellular;membrane;nucleus;organelle lumen	-0.63
255	KLC2	Kinesin light chain 2	cytoplasm;cytoskeleton;cytosol;membrane	-0.63
256	BCAS2	Pre-mRNA-splicing factor spf27	nucleus;spliceosomal complex	-0.61
257	HTATSF1	HIV Tat-specific factor 1	nucleus;spliceosomal complex	-0.61
258	AP3D1	AP-3 complex subunit delta-1	cytoplasm;Golgi;membrane	-0.61
259	RPSA	40S ribosomal protein SA	cytoplasm;cytosol;membrane;nucleus;ribosome	-0.61
260	IRS4	insulin receptor substrate 4	cytosol;membrane	-0.60
261	PSMC4	26S proteasome regulatory subunit 6B	cytoplasm;cytosol;membrane;nucleus;proteasome	-0.59

262	HDLBP	Vigilin	cytoplasm;cytosol;membrane;nucleus	-0.59
263	MYL6	Myosin light polypeptide 6	cytosol;membrane	-0.58
264	PSMC1	26S proteasome regulatory subunit 4	cytoplasm;cytosol;membrane;nucleus; proteasome	-0.56
265	PHB	Prohibitin	cell surface;cytoplasm;endosome;membrane;mitochondrion;nucleus	-0.54
266	PRRC2C	Protein Prrc2c	membrane	-0.52
267	EIF3I	Eukaryotic translation initiation factor 3 subunit I	cytoplasm;cytosol	-0.52
268	PSMD13	26S proteasome non-ATPase regulatory subunit 13	cytosol;extracellular;membrane;nucleus;organelle lumen;proteasome	-0.50
269	TRIM21	E3 ubiquitin-protein ligase TRIM21	cytoplasm;cytosol;nucleus;vacuole	-0.49
270	GCFC1; PAXBP1	PAX3- and PAX7-binding protein 1	cytosol;nucleus	-0.48
271	RPS8	40S ribosomal protein S8	cytoplasm;cytosol;endoplasmic reticulum;membrane;nucleus;ribosome	-0.48
272	MBD2	Methyl-CpG-binding domain protein 2	chromosome;cytoplasm;cytosol;nucleus	-0.41
273	MCM3	DNA replication licensing factor mcm3	cytoplasm;membrane;nucleus	-0.35
274	LARP1	La-related protein 1	cytoplasm;membrane	-0.27
275	AKAP8L	A-kinase anchor protein 8-like	chromosome;cytoplasm;nucleus	-0.25
276	PSMC6	26S proteasome regulatory subunit 10B	cytoplasm;cytosol;membrane;nucleus; proteasome	-0.25
277	SNRPD1	Small nuclear ribonucleoprotein Sm D1	cytoplasm;cytosol;nucleus;spliceosomal complex	-0.25
278	RPS21	40S ribosomal protein S21	cytosol;ribosome	-0.21
279	PSMA5	Proteasome subunit alpha type-5	cytoplasm;cytosol;extracellular;nucleus;organelle lumen;proteasome	-0.10
280	OAT	Ornithine aminotransferase, mitochondrial	cytoplasm;mitochondrion;organelle lumen	0.00
281	SNRPG	Small nuclear ribonucleoprotein G	cytoplasm;cytosol;nucleus;spliceosomal complex	0.03
282	PRPS1L1	Ribose-phosphate pyrophosphokinase 3		0.04
283	RPL34	60S ribosomal protein L34	cytosol;mitochondrion;ribosome	0.05
284	PCMT1	protein-L-isoaspartate(D-aspartate) O-methyltransferase	cytoplasm;cytosol	0.25

Table A5-1 Reactive cysteines in *T. gondii*. Displayed are mean isoTOP-ABPP R values ±RSD for 1018 IA-alkyne labelled peptides averaged across 2/2 MS runs with RSD < 50%. (*) indicates probe-modified residue within the peptide sequence.

Index	Gene ID	Description	sequence	*R* value	RSD
1	TGGT1_268835	hypothetical protein	TPAPC*EGAEK	0.61	1.17
2	TGGT1_258970	hypothetical protein	SPAAGC*HER	0.68	28.28
3	TGGT1_249630	glutathione S-transferase, N-terminal domain-containing	ATTVPTLFQYTVC*PYC*TATR	0.77	0.00
4	TGGT1_311030	hypothetical protein	GVGSSSTASC*SSAR	0.83	23.14
5	TGGT1_222160	aldehyde dehydrogenase	AAMTAFYGLFPNSGQC*C*VASSR	0.86	14.06
6	TGGT1_215775	rhoptry protein ROP8	VVSTVC*R	0.93	2.29
7	TGGT1_290890	putative carbonyl reductase 1	IISVASMC*GK	0.95	1.49
8	TGGT1_218200	UDP-sugar pyrophospharylase	VVLAPSWGISQDC*MR	1.06	0.67
9	TGGT1_233170	hypothetical protein	VIDYLLPAPC*SR	1.07	9.96
10	TGGT1_300140	putative elongation factor 1-gamma	C*ELDLLPEPTMDLNEWK	1.11	1.27
11	TGGT1_217900	hypothetical protein	YC*DSVANTTC*AR	1.12	7.58
12	TGGT1_223070	hypothetical protein	VDCMC*QLGIEYIR	1.14	2.48
13	TGGT1_286630	redoxin domain-containing protein	MIPDGNGC*FTSK	1.36	9.92
14	TGGT1_317720	putative eukaryotic translation initiation factor	AC*DFTFHVQQR	1.37	49.21
15	TGGT1_290670	leucyl aminopeptidase LAP	TVAVVLPTC*QK	1.49	1.43
16	TGGT1_226430	reticulon protein	MC*AAPVC*AC*VSPYIQEAQDFC*SR	1.63	5.66
17	TGGT1_248320	carrier superfamily protein	TNVQAGC*QQIEPHAR	1.66	7.67
18	TGGT1_266450	lysine decarboxylase family protein	MLC*EYLEAR	1.67	16.09
19	TGGT1_263300	eukaryotic porin protein	VC*DYVSATIGSQIDVSK	1.75	7.70
20	TGGT1_230450	bifunctional GMP synthase/glutamine aminotransferase	C*VDGEEAEGEK	1.78	0.79
21	TGGT1_312110	apicoplast-associated thioredoxin family protein A	TAVSC*PAAK	1.79	4.36
22	TGGT1_233000	KOW motif domain-containing protein	ILLPSNSALC*ATAAQLASK	1.79	0.79
23	TGGT1_263660	hypothetical protein	C*AFLDNPVYK	1.81	4.31

24	TGGT1_272030 B	kelch repeat-containing protein	GPC*GEETAPR	1.82	20.98
25	TGGT1_297420	putative beta-tubulin cofactor D	SHSGGNEIQC*PVER	1.88	0.38
26	TGGT1_321420	kelch repeat-containing protein	ATPVC*TFAYLGQAQTENR	1.91	4.08
27	TGGT1_278870	myosin F	LVC*ATSGR	1.91	10.02
28	TGGT1_236570	lysine decarboxylase family protein	IEWMC*PYWQK	1.91	5.92
29	TGGT1_270240	MAG1 protein (MAG1)	AC*QDMAPIEEALC*HK	1.95	4.35
30	TGGT1_230070	BolA family protein	SC*GCGAAYDCVIVSDAFDGK	1.97	9.72
31	TGGT1_258070	hypothetical protein	AAGC*PDEDASAPLLALPQR	1.98	3.22
32	TGGT1_251620	putative flap structure-specific endonuclease 1	DGNSFGNFTNDAGDC*TSHIAGML NR	2.01	2.47
33	TGGT1_271888	putative 3-ketoacyl-CoA reductase	MDLFSC*GC*IK	2.05	2.42
34	TGGT1_248100	synaptobrevin protein	GEASPSGEGAC*AGSSR	2.13	9.96
35	TGGT1_256970	putative vacuolar ATP synthase subunit A	TC*ISQALSK	2.14	0.66
36	TGGT1_284560	ribosomal protein RPL9	VEMWYGTC*TDLSC*IR	2.18	1.30
37	TGGT1_236570	lysine decarboxylase family protein	EIPAPVGGSGHQYSAGDVAAVTDLS EPC*PVAIC*TGGGPGMMEAGNSG AASVAGGR	2.19	1.94
38	TGGT1_242330	ribosomal protein RPS5	AMC*PIVER	2.25	7.87
39	TGGT1_215470	ribosomal protein RPL10A	VC*VMGDAVHC*EQAK	2.26	1.57
40	TGGT1_215740	putative notchless	LWC*LNTETPLR	2.26	13.14
41	TGGT1_306960	phenylalanine--tRNA ligase, beta subunit protein	SYMLTGDALNC*LSEK	2.28	5.28
42	TGGT1_226710	hypothetical protein	EPPLC*SLEGASADAAVQMVK	2.28	3.72
43	TGGT1_300270	hypothetical protein	C*PENIWVFR	2.29	33.11
44	TGGT1_202820	ubiquitin-conjugating enzyme subfamily protein	DC*PSGC*SVGLDDEAGGDFFVWR	2.36	17.98
45	TGGT1_232060	hypothetical protein	VGEC*AGFAPR	2.37	5.08
46	TGGT1_306000	AP2 domain transcription factor AP2IX-8	ASWVC*ATSGK	2.38	35.43
47	TGGT1_260260	ribosomal protein RPP1	ALQGQNIADLISNAGAC*AAAAPAA AAPVAGGDAGAAPAK	2.38	0.59

48	TGGT1_216450	peptidase, T1 family protein	GELYCVETSGC*C*SK	2.39	7.69
49	TGGT1_237820	IMC sub-compartment protein ISP2	LTQGNSAIELSC*ER	2.42	2.34
50	TGGT1_312820	hypothetical protein	C*PAEPWCLYSVVR	2.43	21.53
51	TGGT1_263530	putative chaperonin	TGEFIPPC*VQVGQTVVVPEYGGMK	2.46	3.45
52	TGGT1_236970	SWI2/SNF2-containing PHD finger protein	GVDSAVQSGFAGAC*TANAPFAGPGFK	2.46	28.74
53	TGGT1_217555	hypothetical protein	VGGCPFAGMMSTGVC*PVTGK	2.46	31.62
54	TGGT1_226430	reticulon protein	C*YENVNC*VLESVR	2.47	6.60
55	TGGT1_291640	aspartate carbamoyltransferase	DAAAC*PGTLSETSVQNGC*SEGAWCQLLQGK	2.47	6.60
56	TGGT1_257680	myosin light chain MLC1	C*PVC*YQK	2.48	36.86
57	TGGT1_258820	hypothetical protein	GHGCC*SQNAGSSEEPQQQAEGSHYAK	2.55	4.17
58	TGGT1_202870	SAP domain-containing protein	AAC*GAPAGSTEK	2.55	5.55
59	TGGT1_229210	putative small nuclear ribonucleoprotein polypeptide	SLILC*NNR	2.56	4.15
60	TGGT1_226960	phosphofructokinase PFKII	SEACGAAAC*R	2.57	6.34
61	TGGT1_310640	phosphorylase family protein	GLNC*SAETFFAC*QGR	2.58	1.92
62	TGGT1_265870B	pantoate-beta-alanine ligase	SAGVAAPETCC*TR	2.58	10.96
63	TGGT1_309120	ribosomal protein RPL4	NIPGVELC*K	2.63	0.27
64	TGGT1_256970	putative vacuolar ATP synthase subunit A	VLDSLFPTVQGGTCAIPGAFGC*GK	2.66	7.97
65	TGGT1_306030	glutathione s-transferase, n-terminal domain containing	LYEFEGC*PFCR	2.67	4.24
66	TGGT1_244390	coatomer epsilon subunit protein	AFQQAPQDC*DTLVNLIC*C*CR	2.67	15.36
67	TGGT1_219850	prolyl-tRNA synthetase (ProRS)	LNQWC*SVVR	2.68	1.32
68	TGGT1_227420	4-hydroxy-3-methylbut-2-enyl diphosphate reductase	QLQVVDATC*PLVTK	2.70	10.48
69	TGGT1_209950	putative thioredoxin	DGC*SEC*QSLLDGEFNTLAK	2.73	1.82
70	TGGT1_214290	DJ-1 family protein	AVAYPC*FMDQFPADMR	2.73	3.63
71	TGGT1_255420	hypothetical protein	C*MLLENFEATGAPQVR	2.73	11.91

72	TGGT1_269190	glyceraldehyde-3-phosphate dehydrogenase GAPDH2	VVSC*ASC*TTNGLAPLVK	2.74	2.84
73	TGGT1_233140	putative deoxyuridine 5-triphosphate nucleotidohy	GEGGFGSTTC*PAGEPEMK	2.77	0.26
74	TGGT1_266460	putative small ubiquitin family modifier	LMQAYC*NR	2.77	23.78
75	TGGT1_313400	DnaJ domain-containing protein	C*YYEVLGVAK	2.78	9.43
76	TGGT1_226970	ribosomal protein RPS11	C*PFTGNVSIR	2.78	3.82
77	TGGT1_249250	ribosomal protein RPL35A	VNQYPSC*SLLQLEGVNDR	2.79	2.29
78	TGGT1_272660	hypothetical protein	AGTAGDGETC*TETPVISFLPVSGPE HPAGGSQR	2.80	1.01
79	TGGT1_288650	dense granule protein GRA12	GLDC*MLGSR	2.81	5.80
80	TGGT1_249900	putative adenine nucleotide translocator	GEQEIQYTGTADC*WK	2.82	0.75
81	TGGT1_312090	ribosomal protein RPL23	VTLGLPVGALINC*C*DNSGAK	2.82	5.28
82	TGGT1_264080	acyl carrier protein ACP	YGTC*PNMSSGVCATPSTASLGTLG QPAGTVAR	2.82	4.77
83	TGGT1_300000	ribosomal protein RPL18	AGGEC*LTFDQLALR	2.82	3.01
84	TGGT1_232300	ribosomal protein RPS3	GLC*AMAQAESLR	2.83	2.00
85	TGGT1_290890	putative carbonyl reductase 1	GMFVACCCPGWC*R	2.83	3.50
86	TGGT1_313270	hypothetical protein	APAAPGAGGFC*DDPSR	2.84	14.72
87	TGGT1_299200	putative Bet3 transport protein	TGMGGCDC*FR	2.85	7.21
88	TGGT1_220240	hypothetical protein	VPADTQSPCC*GAK	2.87	3.21
89	TGGT1_243570	ribosomal protein RPS26	QCYC*VSC*AIHSR	2.87	0.99
90	TGGT1_238010	ribosomal protein RPL23A	C*YEAATC*TFPK	2.87	4.93
91	TGGT1_228210	26S proteasome regulatory subunit	AMASNMNC*NFMK	2.91	24.79
92	TGGT1_217030	hypothetical protein	SGAASGEC*SAHANEK	2.93	3.86
93	TGGT1_266990	beta-COP	WTC*ELAFR	2.95	4.08
94	TGGT1_263420	ubiquitin-specific protease USP4	LLVPSGFC*AQEAQK	2.95	6.71
95	TGGT1_310040	putative ubiquitin conjugating enzyme E2	IYC*VSINC*GPSYPDEPPEVC*FR	2.96	9.81

96	TGGT1_306960	phenylalanine--tRNA ligase, beta subunit protein	C*QGEASLQNGSASMNGWVFPR	2.97	8.35
97	TGGT1_243730	rhoptry protein ROP9	ANC*VNFCR	2.97	3.81
98	TGGT1_233110	IMP dehydrogenase (IMPDH)	IGMGSGSIC*TTQVVC*AVGR	2.97	11.43
99	TGGT1_223620	putative SNARE protein	MEC*IFEGEK	2.97	16.19
100	TGGT1_276110	cytochrome b5 family heme/steroid binding domain-c	NC*C*TSATATK	2.98	9.75
101	TGGT1_248390	ribosomal protein RPL26	IMTAPLC*K	2.98	3.32
102	TGGT1_207460 B	Rab5B protein	GPANCC*IAVAANK	2.99	16.35
103	TGGT1_206510	toxolysin TLN4	C*GLPGLSPSASPSAEVR	3.01	23.96
104	TGGT1_259980	DnaJ domain-containing protein	C*YYQTLGVDR	3.03	2.10
105	TGGT1_219520	histone arginine methyltransferase PRMT1	HVYGIEC*SEIVNIAR	3.03	8.87
106	TGGT1_269180	MIF4G domain-containing protein	SPVC*SGTGAVPEATK	3.05	1.63
107	TGGT1_305780	putative 5-3 exoribonuclease	SGEFC*PNLR	3.05	29.96
108	TGGT1_410360	putative transmembrane protein	SVEDPEVLPEEDEASSSLPPPPPPSPPPPPPVEDPLSPESQTVDLSC*LSGTTVR	3.06	0.69
109	TGGT1_279390	putative proliferation-associated protein 2G4	VIC*GC*VPGADVYALC*K	3.07	3.46
110	TGGT1_232350	lactate dehydrogenase LDH1	VMC*EASGVPTNMIC*GMAC*MLDSGR	3.10	0.69
111	TGGT1_249910	putative mitochondria-associated granulocyte macro	ILGLDSSGSSSAPLC*R	3.11	1.36
112	TGGT1_305290	putative vacuolar atp synthase subunit e	YLPPPPSADNDGMSC*C*GGVVLMTR	3.12	1.59
113	TGGT1_319510	hypothetical protein	AC*PLTAAAASVASATAEASLR	3.12	17.22
114	TGGT1_268950	hypothetical protein	MC*MAEFLQK	3.14	29.10
115	TGGT1_266060	ribosomal protein RPSA	ESAYANVPVIALC*DTDSPLEHVDICIPCNNK	3.14	1.35
116	TGGT1_292130	ribosomal protein RPL13A	VVVIDC*QGHLLGR	3.15	8.53
117	TGGT1_225930	triose-phosphate isomerase TPI-I	C*NGTVGSITDLCGEFGK	3.16	8.29
118	TGGT1_324600	heat shock protein	ISC*IQTHEK	3.16	0.90
119	TGGT1_265450	hexokinase	IC*LR	3.16	1.34

120	TGGT1_208790	putative MC family transporter	TALASC*GAAGWR	3.17	3.35
121	TGGT1_232710	ribosomal protein RPS3A	LC*C*EDIQGR	3.19	4.43
122	TGGT1_319560	microneme protein MIC3	C*EK	3.21	30.67
123	TGGT1_245460	ribosomal protein RPS8	HTLC*LQNK	3.21	0.88
124	TGGT1_209260	putative cytochrome c oxidase subunit	MWNC*NEYVR	3.21	7.05
125	TGGT1_262910	putative NADH-cytochrome b5 reductase 1	LEC*PSQSLGLPVGK	3.22	6.38
126	TGGT1_269885B	rhoptry metalloprotease toxolysin TLN1	GAC*SGTGC*QK	3.23	23.46
127	TGGT1_240860	acyltransferase domain-containing protein	DC*MQK	3.24	4.59
128	TGGT1_243580	putative Hit family protein involved in cell-cycle	AVQQATGC*EGVNVLQNNGK	3.24	4.36
129	TGGT1_259660	orotate phosphoribosyltransferase	GIPIVAC*TAMSLNR	3.24	27.94
130	TGGT1_214790	glycoprotein	MGVDPELC*DFIDR	3.25	21.32
131	TGGT1_292130	ribosomal protein RPL13A	C*EDINISGSLHR	3.26	41.65
132	TGGT1_314970	root hair defective 3 gtp-binding protein (rhd3) p	YQSEVC*QR	3.27	44.11
133	TGGT1_256770	putative eukaryotic translation initiation factor	TC*VFC*LGC*LQCIDPK	3.29	11.18
134	TGGT1_277500	putative 26S proteasome regulatory subunit 7	TDAC*FIC*VIGSELVQK	3.30	2.36
135	TGGT1_300000	ribosomal protein RPL18	LTVC*ALR	3.30	5.36
136	TGGT1_319560	microneme protein MIC3	EFGISASSC*K	3.30	6.65
137	TGGT1_273460	eukaryotic translation initiation factor 3 subunit	DC*DVWK	3.30	8.37
138	TGGT1_233190	SKIP/SNW domain-containing protein	YTPAQQGTGHNSGC*AQR	3.31	28.03
139	TGGT1_285220	CAP-Gly domain-containing protein	LSSLSLC*GTR	3.31	2.56
140	TGGT1_239490	dehydrogenase E1 component family protein	DHLFC*QYR	3.31	4.27

141	TGGT1_217540	RNA recognition motif-containing protein	TVSGAGYC*FLEYADPR	3.32	5.96
142	TGGT1_312090	ribosomal protein RPL23	GWGSC*LNR	3.33	4.47
143	TGGT1_214150	putative mitochondrial inner membrane translocase	LNAILNGC*SDYAPK	3.33	7.64
144	TGGT1_288650	dense granule protein GRA12	WDQVGTSVC*R	3.34	4.03
145	TGGT1_268730	glutaredoxin-related protein	APMC*GFSAR	3.35	2.96
146	TGGT1_231910	ATP synthase F1 gamma subunit	GLC*GGVNSFVAK	3.36	15.81
147	TGGT1_267060	ribosomal protein RPL14	LC*VVQYGPDAGK	3.37	5.67
148	TGGT1_232350	lactate dehydrogenase LDH1	VIPC*SVYC*NGEYGLK	3.37	7.97
149	TGGT1_320050	ribosomal protein RPL5	IIC*QVVYSTIEGDR	3.38	3.56
150	TGGT1_211030	hypothetical protein	VEDQDLLPFVGYC*R	3.38	5.44
151	TGGT1_293390	putative cytochrome C-type heme lyase	ALGSAAGNDAC*PFR	3.39	8.15
152	TGGT1_270640	RNA recognition motif-containing protein	NLC*FETSPDR	3.40	3.96
153	TGGT1_306400	hypothetical protein	GDTPGC*APR	3.40	8.54
154	TGGT1_216880	guanine nucleotide-binding protein	SGAPWC*TSLNWSHDGR	3.40	16.64
155	TGGT1_289360	hypothetical protein	SLEFC*TGK	3.40	23.71
156	TGGT1_274060	2-oxoglutarate/malate translocase OMT	NFC*DAVVK	3.41	8.10
157	TGGT1_207440	ribosomal protein RPS4	TDQC*YPAGFMDVISIEK	3.41	4.15
158	TGGT1_289690	glyceraldehyde-3-phosphate dehydrogenase GAPDH1	SSDVIVSNASC*TTNC*LAPLAK	3.41	4.15
159	TGGT1_226970	ribosomal protein RPS11	NVTCHLSPC*FEQVK	3.42	2.69
160	TGGT1_202830	putative Elicitor-responsive protein	SPC*WNQAFK	3.42	1.65
161	TGGT1_236540	RNA recognition motif-containing protein	GLPWSC*SENEIVR	3.42	3.72
162	TGGT1_313380	hypothetical protein	AELNEFGVNTGGLC*C*GSSLTLEDFK	3.43	0.00
163	TGGT1_203490	GNL3L/Grn1 GTPase	LENPQEVATGVAAWCC*SETLQR	3.44	11.32
164	TGGT1_226860	SAG-related sequence SRS67	C*C*NDFGAIC*TPGNVESEYQGMFPLAGK	3.44	2.47
165	TGGT1_213410	putative small nuclear ribonucleoprotein f	C*NNVLYLR	3.44	30.42
166	TGGT1_286790	nuclear factor NF2	AMC*TELDTSEPR	3.44	29.19

167	TGGT1_242330	ribosomal protein RPS5	TIAEC*LADEIMNC*AK	3.45	2.87
168	TGGT1_217820	PCI domain-containing protein	IENVEQAGQAAGTLC*SVFR	3.45	4.51
169	TGGT1_267330	fumarate hydratase	VFPGC*QDTGTAIVLGK	3.47	2.65
170	TGGT1_256970	putative vacuolar ATP synthase subunit A	EDFLQQNAFSDYDYMC*PLYK	3.47	5.51
171	TGGT1_300140	putative elongation factor 1-gamma	QLVADFWC*AC*DDIQGR	3.48	5.49
172	TGGT1_288720	ribosomal protein RPL10	MLSC*AGADR	3.48	41.71
173	TGGT1_230160	hypothetical protein	C*FILNITPGVSER	3.49	4.26
174	TGGT1_202530	aspartate-tRNA ligase	EAGC*PNIPEDLSEFDLSTEQEK	3.49	1.42
175	TGGT1_273460	eukaryotic translation initiation factor 3 subunit	LQQENDETYC*DLFTWAC*PK	3.49	0.81
176	TGGT1_202680	putative peptidase M16, alpha subunit	EHLVYSAEC*LR	3.50	29.09
177	TGGT1_310860	U5 snRNP-specific protein	VFAGC*LDNTIR	3.51	7.06
178	TGGT1_248340	GTP-binding nuclear protein ran/tc4	VC*ENIPIVLVGNK	3.51	0.00
179	TGGT1_310490	ribosomal protein RPL27A	NQYTC*PTVNVDK	3.51	5.24
180	TGGT1_311240	putative DnaJ family chaperone	ISLLESLC*GFK	3.51	13.70
181	TGGT1_315620	putative vacuolar ATP synthase subunit C	NALC*DEACLLDIPHLK	3.53	3.41
182	TGGT1_306670	hypothetical protein	AIFGNWC*TR	3.53	5.01
183	TGGT1_276930	hypothetical protein	TAVEFNGEC*R	3.53	8.22
184	TGGT1_289210	prefoldin subunit protein	IGEC*FASADSDTIEEELDR	3.53	10.63
185	TGGT1_230520	putative cyclophilin 1	IIPSFMC*QGGDFTR	3.53	23.07
186	TGGT1_219800	putative vacuolar ATP synthase subunit b	VLAEEFLDINGC*PINPQC*R	3.54	6.20
187	TGGT1_271810	putative lanp	LEGEEAC*EGAEGELEGK	3.54	15.40
188	TGGT1_239100	ribosomal protein RPS7	C*LFDIETSSQSDLK	3.54	9.59
189	TGGT1_214290	DJ-1 family protein	LISAVENETYDC*IAIPGGMPGAER	3.55	18.55
190	TGGT1_214575	hypothetical protein	VSFNC*PYSENC*R	3.56	14.52
191	TGGT1_411430	rhoptry protein ROP5	ELIGYC*R	3.57	4.17
192	TGGT1_254900	putative proteasome subunit beta type 2	LGC*AAAANFTR	3.57	4.56
193	TGGT1_282180	hypothetical protein	IFGDC*ASTIK	3.57	15.45
194	TGGT1_280730	putative cytosolic fe-s cluster assembling factor	SC*PFQTALIR	3.58	3.36

195	TGGT1_216580	hypothetical protein	ASSPC*GASAAASGGGSAGALVAR	3.58	14.83
196	TGGT1_309820	ribosomal protein RPL11	IAC*YVTVR	3.58	22.12
197	TGGT1_295630	hypothetical protein	PASGSNGPLC*ASSEETASAGDGDSQQPGK	3.59	18.34
198	TGGT1_264760	Oxysterol-binding protein	ALLNC*TR	3.60	3.54
199	TGGT1_217570	ribosomal protein RPS27	LTEGC*SFR	3.61	0.20
200	TGGT1_263040	ribosomal protein RPS16	VNGC*PLEHLQPEALK	3.61	1.96
201	TGGT1_319530	splicing factor SF2	C*AR	3.63	10.34
202	TGGT1_229360	transaldolase	NIGEIIALAGC*DR	3.65	3.49
203	TGGT1_312090	ribosomal protein RPL23	LPAC*SLGDLVLATVK	3.66	3.86
204	TGGT1_244560	putative heat shock protein 90	LVEAPC*AVVASEWGYSAQMEK	3.66	6.96
205	TGGT1_245680	ribosomal protein RPL21	C*NELFLR	3.67	12.15
206	TGGT1_217900	hypothetical protein	YC*DSVANTTC*AR	3.67	23.89
207	TGGT1_234450	ribosomal protein RPS15A	C*GVISPR	3.68	5.20
208	TGGT1_202820	ubiquitin-conjugating enzyme subfamily protein	VC*ISILHPPGDDVFNEQEK	3.69	3.83
209	TGGT1_250330	hypothetical protein	C*ALESMIAAPPEAEQQCGGDNGR	3.70	32.34
210	TGGT1_272010	Gar1 protein RNA binding region protein	FYIDC*QQTLPLSR	3.70	4.97
211	TGGT1_231410	hypothetical protein	C*LDYLSTFR	3.70	7.26
212	TGGT1_247220	nudix -type motif 9 isoform a family protein	C*CASPEGPGSDAR	3.70	8.79
213	TGGT1_309120	ribosomal protein RPL4	NHAVLC*R	3.71	27.29
214	TGGT1_309120	ribosomal protein RPL4	FC*LYTASAFK	3.71	4.96
215	TGGT1_221620	putative beta-tubulin	EAEGC*DC*LQGFQITHSLGGGTGSGMGTLLISK	3.72	7.60
216	TGGT1_202460	diacylglycerol kinase accessory domain (presumed)	TVQVLAAPC*DK	3.73	2.85
217	TGGT1_229930	p25-alpha family protein	GQAAGLGPSGATAQISLADIC*DR	3.74	2.65
218	TGGT1_310030	putative cyclase-associated protein	LC*VNSLISGAEFVNC*R	3.75	6.23
219	TGGT1_216670	FUSE-binding protein 2 / KH-type splicing regulator	AC*LDESLR	3.76	1.13
220	TGGT1_248810	nuclear factor NF7	VALESSQHC*K	3.77	2.44

221	TGGT1_288630	putative nucleosome assembly protein (NAP)	GSGC*C*C*SSEEAAALLQPHMK	3.77	2.44
222	TGGT1_220400	actin depolymerizing factor ADF	GALPANDC*R	3.77	4.70
223	TGGT1_263040	ribosomal protein RPS16	NAVAVALC*TQGK	3.78	2.24
224	TGGT1_261570	ribosomal protein RPL7A	NC*PVLAIDNVR	3.78	3.74
225	TGGT1_203630	ribosomal protein RPL44	C*KSFELGAEK	3.79	15.13
226	TGGT1_223940	GAP45 protein (GAP45)	SVVGYTVTPC*DMAAIDETAK	3.79	8.21
227	TGGT1_221522	adaptor complexes medium subunit family protein	LVEHAGADHTYVESDC*AR	3.79	9.33
228	TGGT1_261010	putative tat-binding family protein	VIMC*TNR	3.79	10.82
229	TGGT1_308090	rhoptry protein ROP5	EEELIGYC*R	3.80	6.70
230	TGGT1_249180	bifunctional dihydrofolate reductase-thymidylates	STAAQAAAPAESVFVPFC*PELGR	3.80	7.44
231	TGGT1_229000	kelch repeat-containing protein	LAPVC*TTFSVLDVR	3.80	14.14
232	TGGT1_205510	putative nucleolar protein 5	AAEEVASPALSEPTVAISC*R	3.81	3.16
233	TGGT1_306060	rhoptry neck protein RON8	QEC*ALLGNVLK	3.82	0.93
234	TGGT1_258780	OTU family cysteine protease	AC*QSLLEQR	3.82	7.97
235	TGGT1_237470	glycine cleavage T-protein (aminomethyl transferase	TPQPATPAVC*AGDER	3.82	13.90
236	TGGT1_313270	hypothetical protein	NQAPC*AETTGR	3.83	4.06
237	TGGT1_251690	putative seryl-tRNA synthetase, cytoplasmic	CLC*CILENYQTPLGVK	3.84	23.57
238	TGGT1_311470	rhoptry neck protein RON5	AGSHVVLSAC*K	3.85	3.67
239	TGGT1_295350	putative nucleoside diphosphate kinase	GDFC*IDVGR	3.85	9.55
240	TGGT1_315270	hypothetical protein	PAAGGASVTGAAPGAC*TPSSSSPGER	3.85	13.22
241	TGGT1_314042	putative cytochrome c1 heme lyase	SSC*PYGMGEGGEGTQGSNVEVPAGLSDVR	3.86	5.69
242	TGGT1_311470	rhoptry neck protein RON5	YATLQAPAAPAPSFYGITSSGC*R	3.86	13.02
243	TGGT1_214930	hypothetical protein	ALPQYLNC*R	3.86	5.50
244	TGGT1_309120	ribosomal protein RPL4	AGQAAFGNMC*R	3.87	4.57
245	TGGT1_273905	hypothetical protein	ALTALAC*QMR	3.87	5.31
246	TGGT1_257680	myosin light chain	VGEYDGACESPSC*R	3.88	0.55

		MLC1			
247	TGGT1_201780	microneme protein MIC2	SMC*GC*SGTSDDDSPC*PLYLR	3.88	8.58
248	TGGT1_227600	ribosomal protein RPL34	C*VK	3.88	8.02
249	TGGT1_205470	putative translation elongation factor 2 family pr	YVEHVQDVPC*GNTC*C*LVGVDQYLLK	3.89	6.01
250	TGGT1_202370	putative T-complex protein 1, epsilon subunit (TCP	TENYPYFGLDC*MLK	3.89	0.36
251	TGGT1_266760	isocitrate dehydrogenase	SSGGFVWAC*K	3.89	4.00
252	TGGT1_211060	hypothetical protein	AYC*APVPSAFASQQPNGLGGEAGVR	3.90	15.07
253	TGGT1_269980	putative preprotein translocase Sec61	PVMC*ILPEVQAPDR	3.90	19.06
254	TGGT1_260810	hypothetical protein	WPGDYPEGLLAC*VTEQVK	3.90	26.32
255	TGGT1_316400B	alpha tubulin TUBA1	YMAC*C*LMYR	3.91	0.54
256	TGGT1_319560	microneme protein MIC3	C*DNGYSGSASATSHHGK	3.91	1.45
257	TGGT1_280440	putative ubiquitin conjugating enzyme E2	TGAVC*LNILR	3.92	0.90
258	TGGT1_212960B	hypothetical protein	AC*HDVASNR	3.92	6.68
259	TGGT1_263300	eukaryotic porin protein	SAELAAEVDC*NLLDGR	3.92	39.55
260	TGGT1_232230	ribosomal protein RPL30	LIIISNNC*PALR	3.92	1.08
261	TGGT1_209140	anti-silencing protein, ASF1 family protein	VVYVGSAEC*EK	3.92	4.33
262	TGGT1_258410	photosensitized INA-labeled protein PHIL1	VDPC*EC*GYPEETYTPYEVAR	3.93	1.98
263	TGGT1_251500	putative eukaryotic initiation factor-3, subunit 3	ENYPTPVNGQLLGIDC*R	3.93	2.34
264	TGGT1_318720	pyridoxal phosphate enzyme, YggS family protein	GETETPC*GDSEVR	3.93	29.87
265	TGGT1_254440	ribosomal protein RPL12	MLDDGEIDC*PEA	3.93	8.28
266	TGGT1_312400	putative exosomal 3-5 exoribonuclease complex su	ASPELGAELTCIDPNC*K	3.93	21.59
267	TGGT1_310030	putative cyclase-associated protein	VSELYSC*	3.94	2.15
268	TGGT1_232710	ribosomal protein RPS3A	STC*YAQTSQIR	3.94	3.95

269	TGGT1_233720	DNA-directed RNA polymerase II RPBABC8	TEEC*SSER	3.94	3.23
270	TGGT1_254440	ribosomal protein RPL12	EILGTCNSVGC*TVDGK	3.95	1.61
271	TGGT1_262620	RNA recognition motif-containing protein	GC*GIVEYTNVEDAQK	3.95	3.22
272	TGGT1_207680	putative suppressor of kinetochore protein 1	TMVEEDSDC*QESIPLPNVDTC*ILK	3.95	31.86
273	TGGT1_205700	cyclophilin precursor	IIPQFMC*QGGDFTR	3.96	0.18
274	TGGT1_232710	ribosomal protein RPS3A	NC*LTDFHGMDMTR	3.96	6.26
275	TGGT1_230420	sarco/endoplasmic reticulum Ca2+-ATPase	C*GDK	3.96	8.05
276	TGGT1_228470	ribosomal protein RPL15	C*TQSTR	3.96	7.14
277	TGGT1_290660	RNA recognition motif-containing protein	NIYDGC*NTLQIQPSR	3.96	13.57
278	TGGT1_222910	phosphoglycerate mutase	PSSPDETSQAAEEASSSTC*EATQK	3.97	16.23
279	TGGT1_233030	gliding-associated protein GAP70 (GAP70)	SVTGNTC*QR	3.98	9.43
280	TGGT1_254410	putative protein phosphatase 2C	LLFEEC*MR	3.99	16.86
281	TGGT1_221620	putative beta-tubulin	EIVHIQAGQC*GNQIGAK	3.99	6.38
282	TGGT1_273905	hypothetical protein	LGALQPC*LR	4.00	7.26
283	TGGT1_300140	putative elongation factor 1-gamma	LPLLESEVGGVC*LFESNAICR	4.00	32.39
284	TGGT1_305510	hypothetical protein	LC*ATPQSR	4.01	2.30
285	TGGT1_236040	fructose-1,6-bisphosphate aldolase	YAAIC*QANR	4.01	1.06
286	TGGT1_249900	putative adenine nucleotide translocator	YTGIVDC*FR	4.01	3.88
287	TGGT1_223050	ribosomal protein RPS20	SPC*GEGTNTWDR	4.02	4.05
288	TGGT1_249850	GAP40 protein	TFC*AYDVIMNAADVEAAR	4.02	3.52
289	TGGT1_277500	putative 26S proteasome regulatory subunit 7	LC*PNSTGADIR	4.03	3.34
290	TGGT1_311680	FUN14 family protein	NLSSYTLAC*K	4.03	3.69
291	TGGT1_215040	HEAT repeat-containing protein	ALLQASSPLC*LEEVVPR	4.03	9.31
292	TGGT1_203450	DUF3228 domain-containing protein	DAGIEFFQGYAPFC*R	4.03	9.66
293	TGGT1_206590	calcium-dependent protein kinase CDPK2A	IIDFGLSC*R	4.05	2.62
294	TGGT1_249780	hypothetical protein	ILASVPLC*R	4.05	6.12

295	TGGT1_239530	alanine-glyoxylate aminotransferase	VDLAYSC*SQK	4.05	6.47
296	TGGT1_213900	regulator of chromosome condensation RCC1	LALSGPAETGGEGHAC*PLAQGVAP EAPSVYTPASGDSSR	4.05	0.70
297	TGGT1_201780	microneme protein MIC2	TEVSAPQPGTPTC*PDC*PAPMGR	4.06	1.74
298	TGGT1_232300	ribosomal protein RPS3	AC*YGVLR	4.06	3.48
299	TGGT1_249990	hypothetical protein	NFHTEASSVMQQIDTC*SAK	4.06	8.01
300	TGGT1_274060	2-oxoglutarate/malate translocase OMT	VQPFAVGGLSGC*VATTC*VQPID MIK	4.06	19.85
301	TGGT1_282055	protein phosphatase PP2C-hn	TVC*ASATSR	4.07	7.13
302	TGGT1_250330	hypothetical protein	DLVPAC*NR	4.08	2.26
303	TGGT1_251780	heat shock protein	GDVVGIDLGTTNSC*VAVMEGSQP K	4.09	2.94
304	TGGT1_201380	putative chorismate synthase	HDPC*VLPR	4.09	10.56
305	TGGT1_297060	phosphoglycerate mutase PGMII	AVVTC*WTVLK	4.10	1.55
306	TGGT1_318230	phosphoglycerate kinase PGKI	VTFVEDC*VGPK	4.10	2.07
307	TGGT1_272290	pyruvate dehydrogenase complex subunit PD-HE1Beta	IVAC*STPYNAR	4.10	4.83
308	TGGT1_209600	hypothetical protein	EAADTNPPATLC*AVVDLPQNR	4.10	5.86
309	TGGT1_245680	ribosomal protein RPL21	GDYVDIVC*DPSVQK	4.11	7.23
310	TGGT1_236550	hypothetical protein	VNGNTQLC*EDSW	4.12	0.86
311	TGGT1_300260	threonyl-tRNA synthetase family protein	VLYEQPSAESEAITAADDEEEEEAEC *PCGEHAEESPAEK	4.12	14.61
312	TGGT1_310330	hypothetical protein	TDTTC*DSR	4.12	1.03
313	TGGT1_224205	putative ER lumen protein retaining receptor	C*LTSGVPVQFMLSENV	4.13	7.37
314	TGGT1_226970	ribosomal protein RPS11	EGDIVTAGQC*R	4.13	6.51
315	TGGT1_219080	putative edge expressed protein	ETLQAVELC*R	4.13	7.19
316	TGGT1_234450	ribosomal protein RPS15A	IEQFC*SNLLPSR	4.13	8.22
317	TGGT1_290200	NAD/NADP octopine/nopaline dehydrogenase, alpha-he	GYAGC*R	4.14	7.35

318	TGGT1_294220	hypothetical protein	TLFDC*SSQGGAFDIAQGDLPAYSS DSPTGR	4.15	16.21
319	TGGT1_227360	ribosomal protein RPL3	AIC*HTQPSK	4.15	2.04
320	TGGT1_240600	putative chaperonin cpn60	AEMTC*DGDDPVGAAAEVVDEME GEIELQK	4.15	2.39
321	TGGT1_311430	fibrillarin	ANC*VDSTAK	4.15	11.93
322	TGGT1_228190	putative eukaryotic initiation factor-3, subunit 5	DAC*FQFQELPLELFASSSDR	4.17	8.32
323	TGGT1_249530	putative exportin 1	ASQSIC*ENNMR	4.17	11.71
324	TGGT1_205320	hypothetical protein	ETC*QK	4.17	23.26
325	TGGT1_263300	eukaryotic porin protein	SC*ADLLTK	4.17	11.53
326	TGGT1_313270	hypothetical protein	GC*QDSGDAHAYPGEGR	4.17	17.30
327	TGGT1_239760	ribosomal protein RPL22	FTVDC*QK	4.18	4.57
328	TGGT1_233400	TAF9 RNA polymerase II, TATA box binding protein (	ENVEC*EIFR	4.18	14.06
329	TGGT1_234520	U2 snRNP auxilliary factor, large subunit, splicin	VVC*AAFFPEEK	4.18	38.45
330	TGGT1_236650	DEAD (Asp-Glu-Ala-Asp) box polypeptide 17	GAEIC*VAC*PGR	4.18	10.33
331	TGGT1_262050	rhoptry kinase family protein ROP39	MGGASDC*QVTNEMQAAEVVQK	4.18	4.40
332	TGGT1_210980	putative alternative splicing type 3 and	VCAVCGALQSAGDALC*R	4.19	0.17
333	TGGT1_269840	proteasome regulatory subunit	VVIDC*FR	4.19	1.01
334	TGGT1_247510	fructose-bisphospatase II	FLEEC*HDDK	4.19	29.70
335	TGGT1_246100	putative phosducin	EVGC*FSSSHPESR	4.20	1.68
336	TGGT1_235020	putative COPI protein	DPGSAC*SGYGVER	4.21	6.05
337	TGGT1_227030	hypothetical protein	VDVVGVIPVDC*SEFDC*K	4.21	10.41
338	TGGT1_318430	malate dehydrogenase MDH	C*LDLYQLTPISGVDVR	4.21	17.13
339	TGGT1_261950	ATP synthase beta subunit ATP-B	IMNVIGEPVDEC*GPVPAK	4.22	1.51
340	TGGT1_288650	dense granule protein GRA12	LDHGAC*FVGK	4.22	2.52
341	TGGT1_260810	hypothetical protein	C*ETLNLFR	4.22	21.98
342	TGGT1_247470	putative nucleolar protein	GWDQIAQDTDAVQEAC*LDFAR	4.22	6.70
343	TGGT1_306630	tRNA methyltransferase complex GCD14 subunit	FVNFSPC*VEQVQR	4.22	17.76

		prote			
344	TGGT1_288860	RuvB family 2 protein	AAGLVC*K	4.23	2.51
345	TGGT1_249900	putative adenine nucleotide translocator	EFTGLVDC*LGK	4.23	8.20
346	TGGT1_292130	ribosomal protein RPL13A	GQQIIC*VR	4.23	12.89
347	TGGT1_318430	malate dehydrogenase MDH	VLPC*AAYLNGEYGVK	4.23	1.00
348	TGGT1_273370	putative coatomer gamma 2-subunit protein	NPLAEC*LLIR	4.23	1.67
349	TGGT1_232410	PDI family protein	EAQFLPIC*SGLEEGDR	4.25	0.17
350	TGGT1_209030	actin ACT1	C*DVDIR	4.25	1.50
351	TGGT1_233460	SAG-related sequence SRS29B (SAG1)	QIC*PAGTTSSC*TSK	4.25	4.50
352	TGGT1_319920	2-oxo acid dehydrogenases acyltransferase (catalyt	HC*DGATVAR	4.25	3.33
353	TGGT1_225540	hypothetical protein	GSVDC*AHLDK	4.25	3.66
354	TGGT1_318430	malate dehydrogenase MDH	DMYVGVPC*VIGAGGVEK	4.25	17.97
355	TGGT1_221320	acetyl-CoA carboxylase ACC1	DLC*PTVPSLIELNR	4.25	34.61
356	TGGT1_312050	putative small GTPase Rab2	C*GPVNAYGSR	4.26	0.17
357	TGGT1_209108	hypothetical protein	VTC*PTTGQQR	4.26	2.49
358	TGGT1_238180	putative 26s proteasome regulatory complex subunit	DFMSLLC*PIAR	4.26	10.80
359	TGGT1_227960	PCI domain-containing protein	ELALC*HK	4.26	28.75
360	TGGT1_214180	ENTH domain-containing protein	C*SFNC*TDYLQIMK	4.26	3.65
361	TGGT1_262620	RNA recognition motif-containing protein	EGTASTEPTC*R	4.27	0.17
362	TGGT1_254940	MIF4G domain-containing protein	DPAQGQDSAC*LGLGDNGDSTASAR	4.27	19.07
363	TGGT1_293180	NADP-specific glutamate dehydrogenase	NLSVVTPPELVTDDPGDMPDC*K	4.28	12.74
364	TGGT1_251810	putative translation initiation factor eIF-5A	SVLVTVLQAC*GK	4.28	26.63
365	TGGT1_265330	putative cell-cycle-associated protein kinase GSK	C*VDTGEVVAIK	4.28	7.93
366	TGGT1_233100	SPFH domain / Band 7 family protein	DLQMVNITC*R	4.28	5.29
367	TGGT1_251810	putative translation initiation factor eIF-5A	YEDVC*PTSHNMEVPNVK	4.28	8.26

368	TGGT1_311500	ThiF family protein	FPVC*TLR	4.29	18.46
369	TGGT1_272030A	kelch repeat-containing protein	SSSLATAPSSPAGVSADAVAQGSPGVHTPQAPQQGTAC*DR	4.29	31.32
370	TGGT1_231440	LsmAD domain-containing protein	SSSSC*GADSGVGGGAR	4.30	16.30
371	TGGT1_256030	hypothetical protein	PC*LPAK	4.30	16.12
372	TGGT1_260440	nuclear factor NF3	ANASTFDVSNGVC*SLK	4.30	17.76
373	TGGT1_218520	microneme protein MIC6	QESGC*EENGCGPPDAVQSC*R	4.30	3.62
374	TGGT1_207770	PCI domain-containing protein	TYQSYHLSQC*R	4.31	2.14
375	TGGT1_321520	hypothetical protein	EC*EGEK	4.31	6.41
376	TGGT1_320570	putative elongation factor Tu	ALSC*PAAQAPAASLGTAPK	4.31	0.33
377	TGGT1_238940	putative GDP mannose 4,6-dehydratase	C*STFNTER	4.32	12.62
378	TGGT1_270830	small nuclear ribonucleoprotein	DNSQVLINC*R	4.32	5.89
379	TGGT1_228400	WD domain, G-beta repeat-containing protein	C*ALSGDDIMGPR	4.32	18.66
380	TGGT1_220400	actin depolymerizing factor ADF	FGVYDC*GNK	4.33	4.09
381	TGGT1_269180	MIF4G domain-containing protein	SSHAEC*ATPSR	4.33	13.24
382	TGGT1_223668	LYAR-type C2HC zinc finger protein	SSPGSQADQC*ER	4.33	3.59
383	TGGT1_309120	ribosomal protein RPL4	ILETLGC*TAELER	4.33	4.57
384	TGGT1_222220	alveolin domain containing intermediate filament I	MVNYIFEC*PAR	4.34	0.49
385	TGGT1_300040	ubiquitin-conjugating enzyme subfamily protein	QC*DFTK	4.34	20.39
386	TGGT1_223960	ubiquitin interaction motif family protein	C*GGDSDFVR	4.35	1.46
387	TGGT1_248500	hypothetical protein	SADPQNC*LIVPVQGVQELSAR	4.35	15.13
388	TGGT1_218940	hypothetical protein	AGAGAFHTSGSTGGC*PIPTDF	4.36	5.19
389	TGGT1_237220	putative DNA replication licensing factor Mcm7	LAQALAC*LR	4.36	8.76
390	TGGT1_219790B	pre-mRNA processing factor PRP3	IWAAQPPSVEPWDAC*ILK	4.36	13.30
391	TGGT1_218590	protein phosphatase 2C domain-containing	AMSGQSSSFSGGLPEQGSDPC*QLAAPNR	4.37	1.29

		protein			
392	TGGT1_290040	putative macrophage migration inhibitory factor	VASIGGITSSTNC*K	4.39	0.32
393	TGGT1_279390	putative proliferation-associated protein 2G4	TGDTYIVEAC*SK	4.39	7.09
394	TGGT1_214210	rRNA pseudouridine synthase	LC*GSEETENGEATEAAVK	4.40	8.53
395	TGGT1_217740	3-ketoacyl-(acyl-carrier-protein) reductase	PLSTTSC*SAYK	4.40	33.63
396	TGGT1_256840	hypothetical protein	IVFDSPVC*NAR	4.41	6.41
397	TGGT1_320120	diadenosine tetraphosphatase family protein	SLPSSSVSSSC*PSVSSPAEYVDWQR	4.41	16.03
398	TGGT1_236650	DEAD (Asp-Glu-Ala-Asp) box polypeptide 17	GC*AYTFFTPDK	4.42	0.48
399	TGGT1_232030	hypothetical protein	SAPAVGDSSYC*SQPSLLC*R	4.42	0.48
400	TGGT1_218810	histidyl-tRNA synthetase	DAVAQEAHNSSPPSSAC*LTAHATTGEGK	4.42	10.09
401	TGGT1_245620	ribosomal-ubiquitin protein RPS27A	C*GLTYILNAEE	4.42	21.44
402	TGGT1_247930	SNARE domain-containing protein	C*DQLLQQNAQR	4.44	3.03
403	TGGT1_279380	hypothetical protein	SMSC*VDTSNEK	4.45	15.43
404	TGGT1_226980	hypothetical protein	LMDDLFSGC*ER	4.45	1.27
405	TGGT1_202370	putative T-complex protein 1, epsilon subunit (TCP	SMHDALC*VVR	4.46	24.60
406	TGGT1_216880	guanine nucleotide-binding protein	YTIVDDQHNDWVSC*VR	4.46	0.00
407	TGGT1_280710	putative 20S proteasome subunit beta 7	TMDMGLAGC*AW	4.46	18.39
408	TGGT1_202760	hypothetical protein	VTTC*GASAGNAK	4.47	0.16
409	TGGT1_359490	elongation factor 1-alpha	MDSC*NYSEDR	4.47	5.38
410	TGGT1_243960	nuclear transport factor 2 (ntf2) domain-containing	VGSDAC*ASPTVK	4.47	20.88
411	TGGT1_269190	glyceraldehyde-3-phosphate dehydrogenase GAPDH2	GADYVC*ESTGVFC*TTEAAAK	4.48	34.92
412	TGGT1_256840	hypothetical protein	AADCVSDEGTGC*AAAASR	4.48	31.76

413	TGGT1_291140	CCR4-Not complex component, Not1 protein	APMTGSPTAGGVSC*SAASAGEAD GVSLR	4.48	1.89
414	TGGT1_283780	glucose-6-phosphate isomerase GPI	APHESGQSELC*SSTR	4.48	4.74
415	TGGT1_210730	putative ATP-dependent hsl protease ATP-binding su	EIAPNNLLLIGPSGC*GK	4.49	4.57
416	TGGT1_293400	hypothetical protein	SDPC*AAALPLSR	4.49	24.44
417	TGGT1_236560	hypothetical protein	GQMPSSPASGC*PSSTPFDSEPHQP R	4.49	40.83
418	TGGT1_277500	putative 26S proteasome regulatory subunit 7	SVC*TEAGILAIR	4.49	0.31
419	TGGT1_257310	hypothetical protein	C*GFLPSANFASPSGEEPQR	4.49	0.63
420	TGGT1_249690	hypothetical protein	VTSAAAC*GGSDVASSSPHGSSVTT SSAIEQAPLR	4.49	5.04
421	TGGT1_274060	2-oxoglutarate/malate translocase OMT	IQLAGEAGGSTNPFTVC*R	4.49	12.60
422	TGGT1_313070	hypothetical protein	DC*AGSGVCAPK	4.50	20.61
423	TGGT1_313270	hypothetical protein	SDEGAATC*STGGGAAGPEGPHVG LAPEPVVHGAAGDK	4.50	6.60
424	TGGT1_257040	TB2/DP1, HVA22 family protein	GNAPSSMGAEEC*PSIQVAGFDLQ R	4.51	18.05
425	TGGT1_247460	proliferating cell nuclear antigen PCNA1	SLGLNLASVC*K	4.51	5.64
426	TGGT1_251690	putative seryl-tRNA synthetase, cytoplasmic	DC*WGIFR	4.52	2.50
427	TGGT1_288380	heat shock protein HSP90	PEDVTWEEYC*AFYK	4.52	23.15
428	TGGT1_298610	GYF domain-containing protein	C*GALVNSTGAGTGPAADESSK	4.53	2.66
429	TGGT1_242330	ribosomal protein RPS5	VNQAIYLIC*TGAR	4.53	2.66
430	TGGT1_205340	ribosomal protein RPS12	AQVC*FLSESC*SEPAYK	4.53	8.91
431	TGGT1_318440	helicase associated domain (ha2) protein	C*SASAAGTR	4.53	6.56
432	TGGT1_216860	DEAD (Asp-Glu-Ala-Asp) box polypeptide DDX39	VAHFVLDEC*DK	4.53	13.11
433	TGGT1_254690	phospholipase/carboxyl esterase	VVDATC*ER	4.54	0.47
434	TGGT1_219150	zinc finger, zz type domain-containing protein	HEEGC*ASAMK	4.54	16.68

435	TGGT1_244650	putative eukaryotic initiation factor-5	FFGC*ELGAMAK	4.55	1.71
436	TGGT1_244560	putative heat shock protein 90	LGC*YEDDTNR	4.55	9.80
437	TGGT1_206320	hypothetical protein	EIEVSPPQHMYC*ANTMTPEQFADR	4.55	4.04
438	TGGT1_258500	hypothetical protein	SEQEHC*YR	4.55	9.32
439	TGGT1_221660	DEAD/DEAH box helicase domain-containing protein	C*PNTGNFVDEFEINDYPQIAR	4.55	9.32
440	TGGT1_232350	lactate dehydrogenase LDH1	DVQATVIGTHGDC*MVPLVR	4.55	3.11
441	TGGT1_206670	hypothetical protein	ASALC*AQSR	4.56	49.21
442	TGGT1_277720	GDA1/CD39 (nucleoside phosphatase) family protein	IEC*MATR	4.56	7.44
443	TGGT1_220270	alveolin domain containing intermediate filament I	VPVNSGGFFGQC*C*GPAQVGSDSSPETYDR	4.57	10.21
444	TGGT1_266990	beta-COP	AVHSCC*TR	4.58	6.96
445	TGGT1_258720	putative Ubiquitin family protein	LVAAQC*GTR	4.58	8.81
446	TGGT1_232710	ribosomal protein RPS3A	MFC*IAFTK	4.58	4.94
447	TGGT1_305520	ribosomal protein RPS2	AFVAVGDSNGHC*GLGVK	4.59	5.71
448	TGGT1_311720	chaperonin protein BiP	DVEAVC*NPIISK	4.59	16.81
449	TGGT1_211290	rhoptry protein ROP15	SSGTEIPSTLAC*PSSSPLK	4.59	3.39
450	TGGT1_223680	ubiquitin family protein	C*ATQTEIPVQAQR	4.59	10.78
451	TGGT1_205130	hypothetical protein	SGC*AANSSPSSSSSNLR	4.60	2.62
452	TGGT1_212210	hypothetical protein	SLTQESSAVATEAC*AETQEK	4.60	14.00
453	TGGT1_231850	serine-threonine phosophatase 2C (PP2C)	MC*EQLNK	4.60	15.54
454	TGGT1_263090	14-3-3 protein	NLVENC*LDEQQPK	4.60	6.00
455	TGGT1_201400	Sin3-associated polypeptide SAP18	AVESC*EGIQTDSK	4.61	4.15
456	TGGT1_237150	putative minor histocompatibility antigen h13	EAYEASC*MHR	4.61	4.76
457	TGGT1_218570	Nin one binding (NOB1) Zn-ribbon family protein	AETSPSSAPTLC*HFAR	4.62	26.33
458	TGGT1_205558	NAC domain-containing protein	DVDLVMSQVEC*SR	4.64	1.37

459	TGGT1_311470	rhoptry neck protein RON5	NDLC*DVTASDAQIFPSAPADEGLQGFPR	4.64	0.30
460	TGGT1_262040	SAC3/GANP family protein	VC*MATLLK	4.64	2.13
461	TGGT1_273520	PCI domain-containing protein	IGEEC*DSDFFLQPLK	4.64	16.15
462	TGGT1_218220	putative cell-cycle-associated protein kinase CDK	LLDVC*DGGLEPSTTK	4.65	2.28
463	TGGT1_305820	SGS domain-containing protein	SAPC*NLSQPVK	4.65	9.59
464	TGGT1_311010	hypothetical protein	SGTC*EHSEK	4.65	25.12
465	TGGT1_265180	hypothetical protein	TQESC*GEGLHGTGETAAGYSFFSR	4.65	49.17
466	TGGT1_306650	hypothetical protein	ETGC*TAHSETK	4.66	17.47
467	TGGT1_250700	hypothetical protein	AFAC*LAQPPSEEDER	4.66	37.33
468	TGGT1_234450	ribosomal protein RPS15A	MNVLADC*LK	4.67	3.18
469	TGGT1_216860	DEAD (Asp-Glu-Ala-Asp) box polypeptide DDX39	C*LEK	4.67	13.49
470	TGGT1_290720	putative vacuolar proton translocating ATPase subunit	SLASEDSALPSPPLAFSVSQGPC*DGR	4.67	14.10
471	TGGT1_263300	eukaryotic porin protein	YC*VSDVTTEVK	4.67	6.66
472	TGGT1_313380	hypothetical protein	ILDC*HADDQAVWMAK	4.67	24.53
473	TGGT1_306400	hypothetical protein	VC*LSPAVGTQR	4.68	0.15
474	TGGT1_305030	kinase, pfkB family protein	C*GDSDK	4.68	4.08
475	TGGT1_275650	hypothetical protein	IC*SSFEEWSSSAQMHK	4.68	11.34
476	TGGT1_251690	putative seryl-tRNA synthetase, cytoplasmic	YAGYSSC*FR	4.68	0.45
477	TGGT1_309752	putative succinate-Coenzyme A ligase, beta subunit	LEAAC*QC*IR	4.68	16.79
478	TGGT1_222952	phosphohistidine phosphatase	VC*VEEGVQK	4.69	4.52
479	TGGT1_258930	peptidylprolyl isomerase	QENFAQLANQYSDC*GSFQK	4.70	1.05
480	TGGT1_267330	fumarate hydratase	HGASCPVGIGVSC*SADR	4.70	7.82
481	TGGT1_310430A	Hsp90 domain-containing protein	STC*GQTFTLEK	4.70	10.23
482	TGGT1_223050	ribosomal protein RPS20	VC*TELINGAK	4.72	1.65
483	TGGT1_268890	citrate synthase I	SVC*GGLSNAEAR	4.73	10.33

484	TGGT1_216790	putative ATP-binding cassette sub-family E member	VIVYEGEPGVEC*VAR	4.73	0.60
485	TGGT1_310070	putative methyltransferase	ILVLGC*GTSR	4.73	5.98
486	TGGT1_233460	SAG-related sequence SRS29B (SAG1)	C*SYGADSTLGPVK	4.73	8.37
487	TGGT1_222952	phosphohistidine phosphatase	LQQASVSC*ASHPSGDSSGK	4.74	6.86
488	TGGT1_249780	hypothetical protein	PFQC*IYAR	4.75	2.38
489	TGGT1_313100	signal recognition particle SRP54 protein	VALVC*ADTFR	4.75	5.66
490	TGGT1_286630	redoxin domain-containing protein	AVGSVPLGSAASSGGMC*SSVSGG PASVFSSSALK	4.76	15.91
491	TGGT1_276930	hypothetical protein	C*GDMAVSSATHPESIDR	4.76	0.30
492	TGGT1_212270	hypothetical protein	EVSNVPC*R	4.76	13.37
493	TGGT1_298020	DEAD-family helicase	QEASIC*PR	4.76	13.37
494	TGGT1_271820	lipoyltransferase and lipoate-protein ligase	IEGTESC*MR	4.77	8.46
495	TGGT1_232800	hypothetical protein	AGPSDPHTTYAC*R	4.77	11.72
496	TGGT1_252290	putative importin alpha	NATWTLSNLC*R	4.79	2.51
497	TGGT1_278960	hypothetical protein	GNVTDPASFLVC*VR	4.80	9.00
498	TGGT1_299670	hypothetical protein	C*SNMPVPAGASNAPPQSAAR	4.80	3.24
499	TGGT1_202680	putative peptidase M16, alpha subunit	VISPQEFC*TAIDAVTEADIK	4.81	32.82
500	TGGT1_295360	hypothetical protein	LC*ER	4.81	46.36
501	TGGT1_249390	glutamate/leucine/phenylalanine/valine dehydrogenase	MQYIMQPC*K	4.82	6.61
502	TGGT1_219540	cytosolic tRNA-Ala synthetase	DGSLTPLPAPC*VDTGMGLER	4.82	13.95
503	TGGT1_256050	signal recognition particle 14kd protein	THPTTNC*PEAK	4.82	0.59
504	TGGT1_291140	CCR4-Not complex component, Not1 protein	TLFFEC*R	4.83	3.51
505	TGGT1_223140	tRNA binding domain-containing protein	YVQPC*LLQR	4.83	3.81
506	TGGT1_204400	putative ATPase synthase subunit alpha	C*VDALVPVGR	4.84	0.44
507	TGGT1_232250	catalase	AIGLPTAAC*YPAK	4.84	0.88
508	TGGT1_271935	hypothetical protein	PIQYSC*PQPAK	4.84	2.63
509	TGGT1_316400 B	alpha tubulin TUBA1	TIQFVDWC*PTGFK	4.84	4.09

510	TGGT1_246090	hypothetical protein	AEEATGTQEC*EK	4.84	16.07
511	TGGT1_273520	PCI domain-containing protein	C*INVDMIAK	4.85	10.36
512	TGGT1_273905	hypothetical protein	LLTTC*SAVHAPEESR	4.85	11.24
513	TGGT1_271930	hypothetical protein	INC*PSVSVTISADDTPLPQGLGEVK	4.86	0.73
514	TGGT1_223000	dynein light chain DLC	NADMPEDLQQDAIDC*ANQALEK	4.86	11.21
515	TGGT1_232030	hypothetical protein	WLAC*LHGSGNDDTR	4.86	13.97
516	TGGT1_261440	ARM repeats containing protein	LQDC*K	4.87	5.38
517	TGGT1_288630	putative nucleosome assembly protein (NAP)	NNAEAAAC*QK	4.87	11.48
518	TGGT1_217890	putative alkyl hydroperoxide reductase/ Thiol spec	GC*QLLGVSVDSK	4.87	11.62
519	TGGT1_287500	putative T complex chaperonin	VMVLGC*GLEC*STTEAK	4.87	2.03
520	TGGT1_321620	dynamin-related protein DRPB	IC*VVGTQSAGK	4.87	4.65
521	TGGT1_267080	putative 26S protease regulatory subunit 4	ATC*TEAGLLALR	4.87	4.94
522	TGGT1_318430	malate dehydrogenase MDH	VC*GMAGVLDSAR	4.88	0.44
523	TGGT1_217510	hypothetical protein	MGEIC*PGTVSSYVDVPNFGR	4.88	12.04
524	TGGT1_222380	importin-beta N-terminal domain-containing protein	INAANQLSELC*TSK	4.88	32.06
525	TGGT1_263070	CMGC kinase, CK2 family	FVNSENQHLAC*ADAIDLIDK	4.88	2.03
526	TGGT1_273960	chaperonin GroS protein	QPGSVAPTSLHC*AGSDSGGEGFVR	4.88	17.97
527	TGGT1_290040	putative macrophage migration inhibitory factor	FGGSSDPC*AFIR	4.89	2.75
528	TGGT1_224205	putative ER lumen protein retaining receptor	TSGSPPGFSGGVESTTTAPAVC*SFPGSSSSTFSIK	4.90	7.66
529	TGGT1_290200	NAD/NADP octopine/nopaline dehydrogenase, alpha-he	LFNEDIPFGLC*VLK	4.90	11.26
530	TGGT1_243920	putative DNA replication licensing factor MCM5	C*AVLAAANPSFGSFDDTQDSSEQHEFK	4.91	2.45
531	TGGT1_269650	FFD and TFG box motifs protein	GVEC*GEELGGEK	4.92	2.45
532	TGGT1_316540	IMC sub-compartment protein ISP3	NPC*VVGFR	4.92	12.52

533	TGGT1_209030	actin ACT1	C*PEALFQPSFLGK	4.92	3.74
534	TGGT1_243410	tetratricopeptide repeat-containing protein	QFEGGNADNPFASLFEC*R	4.92	14.66
535	TGGT1_240280	S1/P1nuclease	VEMEC*MK	4.93	4.88
536	TGGT1_286800	hypothetical protein	HAQADAC*EVAR	4.93	20.65
537	TGGT1_262040	SAC3/GANP family protein	YDPSSLTLLC*QYTEEQVAK	4.94	3.01
538	TGGT1_292920	putative heat shock protein 75	GVIDC*DDIPLNVSR	4.94	12.60
539	TGGT1_232300	ribosomal protein RPS3	GC*EVVVSGK	4.94	14.60
540	TGGT1_237820	IMC sub-compartment protein ISP2	VDC*SAGISK	4.95	10.00
541	TGGT1_275802	SRP72 RNA-binding domain-containing protein	SGGC*TLDDAIK	4.95	1.43
542	TGGT1_222860	putative eukaryotic translation initiation factor	DC*SVLVYNGHR	4.97	11.95
543	TGGT1_288830	NADH dehydrogenase (NDH2-II)	LLNQPNVYALGDC*AAIAPPR	4.97	25.89
544	TGGT1_305520	ribosomal protein RPS2	EYQIIDHFFQPGNC*AAPLK	4.97	27.32
545	TGGT1_268850	enolase 2	GNPTVEVDLLTDGGC*FR	4.97	6.83
546	TGGT1_288740	putative L-asparaginase	AC*SSAPHLTESR	4.98	0.99
547	TGGT1_290040	putative macrophage migration inhibitory factor	C*MIFC*PVAATPAQQDALLK	4.98	0.99
548	TGGT1_252290	putative importin alpha	EAC*WTISNITAGNR	4.98	38.34
549	TGGT1_204530	microneme protein MIC11	GEVQQTC*EELADLAAR	5.00	10.90
550	TGGT1_306970	thymidylate kinase	TAEAVAASTAATGAPVDATFC*R	5.00	7.07
551	TGGT1_206510	toxolysin TLN4	C*AADQNAADAK	5.01	9.75
552	TGGT1_314750	hypothetical protein	IPGC*PVSPALLK	5.01	2.54
553	TGGT1_211390	hypothetical protein	HEGGPAAAAC*EQSPTLLK	5.01	21.74
554	TGGT1_240600	putative chaperonin cpn60	LILADEC*R	5.02	10.71
555	TGGT1_202390	S15 sporozoite-expressed protein	SGLC*GGGNSK	5.03	39.82
556	TGGT1_314422	rhodanese family domain-containing protein	EPAELQTLGC*IPGAVNIPLGR	5.03	10.12
557	TGGT1_206680	hypothetical protein	AAAAC*PFFK	5.04	9.69
558	TGGT1_245650	hypothetical protein	AGATASC*ALESDNALQTENLNGLPK	5.04	33.28

559	TGGT1_248320	carrier superfamily protein	DTPGASSSLSPSSPAAAASC*SHSSSASK	5.04	2.81
560	TGGT1_219270	multi-pass transmembrane protein	DINTDIMPTEGSQQAATC*ASPTGTGYYGTNQTIGSAPGAVYQPLQTGLSPDALGR	5.04	7.86
561	TGGT1_259240	ribosomal protein RPS21	C*SATGR	5.05	0.84
562	TGGT1_289690	glyceraldehyde-3-phosphate dehydrogenase GAPDH1	GIISYTDEEVVSSDFVHC*K	5.06	2.94
563	TGGT1_254690	phospholipase/carboxylesterase	SVHDLPLSVTPADAAAMC*SSGASESVLPK	5.06	13.29
564	TGGT1_249590	putative proteasome subunit alpha type 5-2	LNC*NNVEVACVK	5.06	2.24
565	TGGT1_216030A	hypothetical protein	LLTGSQSC*NPGVATDPQLHR	5.06	11.18
566	TGGT1_257350	putative eukaryotic translation initiation factor	C*IIQDTLDMR	5.06	13.14
567	TGGT1_244150	glycerate kinase	AAEEAC*ASVEK	5.07	16.74
568	TGGT1_263080	hypothetical protein	PTAGSC*AAGTAVVNPEDPTK	5.08	9.06
569	TGGT1_313270	hypothetical protein	GPETGPQGDSQAPVAC*GDSGPQGAETTFVK	5.09	22.67
570	TGGT1_293360	hypothetical protein	C*EDGSC*PQPLSSFLPDSPFITK	5.10	2.64
571	TGGT1_232710	ribosomal protein RPS3A	DIENAC*K	5.10	0.83
572	TGGT1_308860	hypothetical protein	AAC*PADEVLGR	5.10	35.49
573	TGGT1_290670	leucyl aminopeptidase LAP	VC*PSAEGQR	5.11	2.91
574	TGGT1_305340	corepressor complex CRC230	C*EEER	5.11	0.28
575	TGGT1_219540	cytosolic tRNA-Ala synthetase	C*LTAAIADGAEPSNEGR	5.13	9.92
576	TGGT1_224350A	putative aminopeptidase N	SGALLVTQC*EAEGFR	5.13	17.09
577	TGGT1_311230	hypothetical protein	QLAATASAGTLPC*QASSVAPK	5.14	1.24
578	TGGT1_202760	hypothetical protein	C*VSAAK	5.14	13.63
579	TGGT1_283510	hypothetical protein	IGLSDSDLLDFHSDDEMPVAPAAQC*HR	5.14	4.68
580	TGGT1_273370	putative coatomer gamma 2-subunit protein	SDDVSVC*EAVLQGFE	5.14	34.39
581	TGGT1_202370	putative T-complex protein 1, epsilon	MQVEHQC*AR	5.15	1.37

		subunit (TCP			
582	TGGT1_265390	hypothetical protein	VPLEC*ALR	5.15	17.03
583	TGGT1_251620	putative flap structure-specific endonuclease 1	VPDGFC*FQEAR	5.15	18.12
584	TGGT1_239490	dehydrogenase E1 component family protein	SQTLFVC*R	5.16	6.17
585	TGGT1_201700	WD domain, G-beta repeat-containing protein	LLASC*SEDGTVK	5.16	7.27
586	TGGT1_290890	putative carbonyl reductase 1	TVPC*QQWLSTPVA	5.16	5.62
587	TGGT1_310630	hypothetical protein	VADWLLC*R	5.16	12.33
588	TGGT1_247510	fructose-bisphospatase II	VDALMVEHSPEC*R	5.17	2.87
589	TGGT1_267800	dynamin-related protein DRPA	QIQQLETPSLQC*VEQVYEELQK	5.17	3.83
590	TGGT1_248320	carrier superfamily protein	MQASIGMPGQC*QTIR	5.18	6.55
591	TGGT1_305820	SGS domain-containing protein	LNNVIVPETC*SYR	5.19	1.77
592	TGGT1_233460	SAG-related sequence SRS29B (SAG1)	LSAEGPTTMTLVC*GK	5.19	2.86
593	TGGT1_205100	hypothetical protein	ETFGC*R	5.19	6.27
594	TGGT1_215950	hypothetical protein	AETETVC*GEGR	5.20	25.45
595	TGGT1_218780	putative phosphoserine aminotransferase	GC*GMSVLEMSHR	5.20	37.80
596	TGGT1_268730	glutaredoxin-related protein	GSEC*AAVQPAGGHSK	5.21	15.47
597	TGGT1_263520	microtubule associated protein SPM1	SEQAEPDYSAC*C*K	5.21	18.73
598	TGGT1_216880	guanine nucleotide-binding protein	VWNLSNC*K	5.22	0.14
599	TGGT1_277270	NTPase II	VTNEMQC*R	5.22	2.17
600	TGGT1_312090	ribosomal protein RPL23	EC*AELWPK	5.23	10.15
601	TGGT1_256840	hypothetical protein	DAVANQPLTAC*IAK	5.23	12.04
602	TGGT1_259550	dihydropteroate synthase	PLPTPEDMEAALNDC*TSSGEATNE DVPGQGNK	5.24	5.00
603	TGGT1_222270	hypothetical protein	LLQFAC*AGQLR	5.24	33.63
604	TGGT1_289690	glyceraldehyde-3-phosphate dehydrogenase GAPDH1	VPVPDVSVVDLTC*K	5.24	5.94
605	TGGT1_248360	hypothetical protein	SNEIEGYEVPINDC*QYDISMDQVR	5.25	0.81
606	TGGT1_259240	ribosomal protein	GESDAC*LNR	5.26	3.50

		RPS21			
607	TGGT1_250770	putative eukaryotic initiation factor-4A	CHAC*VGGTVVR	5.26	38.98
608	TGGT1_229990	putative T-complex protein 1 subunit alpha	SVHDALC*AVSR	5.27	2.55
609	TGGT1_266960	beta-tubulin	EIVHVQGGQC*GNQIGAK	5.27	3.09
610	TGGT1_208200	PHD-finger domain-containing protein	TGTAC*SVPSVSATPTPAYAAQR	5.28	9.79
611	TGGT1_313640	hypothetical protein	SAGEESC*GTGNK	5.30	3.34
612	TGGT1_216000	alveolin domain containing intermediate filament I	VNASAMSC*TPWASPAVQER	5.30	4.67
613	TGGT1_268200	RNA recognition motif-containing protein	MASLAAADAC*IR	5.30	0.53
614	TGGT1_313380	hypothetical protein	C*FVYPAAATPYGAC*ASAGAQEPTR	5.30	10.41
615	TGGT1_306540	phosphotransferase enzyme family protein	AGEHC*CAAENCR	5.31	11.19
616	TGGT1_321620	dynamin-related protein DRPB	GSDQC*EDIEMLTR	5.31	11.98
617	TGGT1_257310	hypothetical protein	TPATDGTGAGADAC*PTPESR	5.31	14.91
618	TGGT1_268200	RNA recognition motif-containing protein	ETGC*AHLGAQGPK	5.32	2.79
619	TGGT1_293360	hypothetical protein	ASSETSMDC*FENQNFYR	5.32	3.86
620	TGGT1_257350	putative eukaryotic translation initiation factor	VTGAPPGNAC*ASAVPLSPAPEVAR	5.32	2.39
621	TGGT1_249850	GAP40 protein	PFLQAIQEDGGENYADVC*DDEAHSS	5.33	2.52
622	TGGT1_226250	DEAD (Asp-Glu-Ala-Asp) box polypeptide DDX3X	C*PILVATDVAAR	5.33	1.06
623	TGGT1_216880	guanine nucleotide-binding protein	GVLEGHTDC*VTAISTPSLK	5.33	1.59
624	TGGT1_256760	pyruvate kinase PyK1	MIDAGMNVC*R	5.34	2.91
625	TGGT1_294200	glucose-6-phosphate 1-dehydrogenase	NC*STHNGWTR	5.34	10.86
626	TGGT1_318440	helicase associated domain (ha2) protein	C*PVVPNYGAR	5.35	0.40
627	TGGT1_226250	DEAD (Asp-Glu-Ala-Asp) box polypeptide DDX3X	QDIPSFLPPLVLSC*TSSSSR	5.35	9.66
628	TGGT1_205470	putative translation elongation factor 2 family pr	VLYAC*QLASAPR	5.35	3.17
629	TGGT1_205340	ribosomal protein RPS12	LVQGLC*K	5.36	9.90

630	TGGT1_266630	hypothetical protein	YPC*EER	5.36	5.28
631	TGGT1_316400 B	alpha tubulin TUBA1	C*VFLDLEPTVVDEVR	5.36	3.17
632	TGGT1_231640	alveolin domain containing intermediate filament I	DCADPC*SDC*C*QPAEQQR	5.36	10.03
633	TGGT1_220900	hypothetical protein	VFMQQPLVC*R	5.38	4.34
634	TGGT1_232230	ribosomal protein RPL30	VSC*LAVTDPGDSDIIR	5.38	14.60
635	TGGT1_263520	microtubule associated protein SPM1	SNPIC*PVSK	5.38	1.05
636	TGGT1_206510	toxolysin TLN4	FGTGDFDTLC*K	5.38	3.15
637	TGGT1_313140	isocitrate dehydrogenase	SEGGFVWAC*K	5.38	36.80
638	TGGT1_236840	putative zinc finger (C-x8-C-x5-C-x3-H)-2	IAEDSC*TVGTYDPK	5.39	4.07
639	TGGT1_312600	heat shock protein HSP21	APGTESEAC*GHR	5.39	0.79
640	TGGT1_202530	aspartate-tRNA ligase	DAC*LAQSPQLYK	5.39	6.30
641	TGGT1_246740	hypothetical protein	EPLSLMSDLDC*LR	5.40	0.66
642	TGGT1_203080	RNA recognition motif-containing protein	GGPSMAPAPSSGTC*AAPNLLDDI	5.41	0.65
643	TGGT1_298020	DEAD-family helicase	LGYSAC*SLHGGK	5.41	1.44
644	TGGT1_318410	putative TCP-1 chaperonin	STAALAANC*NAAK	5.42	5.88
645	TGGT1_211020	RNA recognition motif-containing protein	DLPAVC*SGGSDSALR	5.43	7.17
646	TGGT1_233890	hypothetical protein	APAETPGTC*GSAEPGQAPGQQTA QDMVER	5.43	28.81
647	TGGT1_251690	putative seryl-tRNA synthetase, cytoplasmic	VEQFC*ITTPEESWK	5.43	13.80
648	TGGT1_222160	aldehyde dehydrogenase	DIGMAYHC*ANR	5.43	17.19
649	TGGT1_247550	heat shock protein HSP60	NQMLAGC*NR	5.44	5.59
650	TGGT1_286580	hypothetical protein	YEDTVEGLC*LGSVTSHSGESAHENS EAR	5.44	11.32
651	TGGT1_288360	tryptophanyl-tRNA synthetase (TrpRS2)	C*LIPQAIDQDPYFR	5.44	11.44
652	TGGT1_209030	actin ACT1	DC*YVGDEAQSK	5.45	3.51
653	TGGT1_247030	hypothetical protein	FVGGAAC*VFR	5.45	25.43
654	TGGT1_235160	hypothetical protein	C*SSLDAQAFAPPEAR	5.46	15.94
655	TGGT1_235930	domain K- type RNA binding proteins family protein	LSHVC*GADLNILER	5.46	23.46
656	TGGT1_210840	arginyl-tRNA synthetase family protein	LIC*DVSR	5.46	29.42
657	TGGT1_223940	GAP45 protein (GAP45)	C*GC*DLGDQHDENECPICR	5.47	26.11

658	TGGT1_268850	enolase 2	NEWGWC*K	5.48	8.39
659	TGGT1_208030	microneme protein MIC4	NDVDGVVSGPYTFC*DNGENLQVLEAK	5.48	7.23
660	TGGT1_320100	RNA recognition motif-containing protein	ALDSSEHPASLLPVSALVAPGGTC*PGDR	5.48	9.29
661	TGGT1_294620	putative eukaryotic initiation factor-3, subunit 8	NVEC*TPEQER	5.49	10.18
662	TGGT1_253470	alveolin domain containing intermediate filament I	C*NGHSSPGFEK	5.49	2.06
663	TGGT1_240220	hypothetical protein	FQASASALSDTLAC*FPR	5.49	27.56
664	TGGT1_244110	nucleosome assembly protein (nap) protein	DSANPSAQAGTPAVPAFWMNC*LK	5.50	43.45
665	TGGT1_236650	DEAD (Asp-Glu-Ala-Asp) box polypeptide 17	EEPVHINVGSLDLQAC*QNIK	5.51	1.16
666	TGGT1_312622	DUF803 domain-containing protein	C*ALLDDEDSTQQQALGR	5.51	15.91
667	TGGT1_239820	D-3-phosphoglycerate dehydrogenase	EALLGGLPQSAVNLQC*VR	5.52	2.18
668	TGGT1_222220	alveolin domain containing intermediate filament I	AQELATQMDC*PVPSR	5.52	10.39
669	TGGT1_215980	hypothetical protein	HWNDTTSIC*R	5.53	7.04
670	TGGT1_288860	RuvB family 2 protein	FVQC*PEGELQK	5.53	7.81
671	TGGT1_290600	succinyl-CoA-synthetase alpha SCSA	VIC*QGLTGK	5.53	0.77
672	TGGT1_291680	Sec23/Sec24 trunk domain-containing protein	YVQC*NSGGSQAR	5.53	7.16
673	TGGT1_210980	putative alternative splicing type 3 and	AHGGDGC*EK	5.54	6.77
674	TGGT1_263130	putative citrate synthase	IC*EETDPADSVAAHFLK	5.55	6.37
675	TGGT1_240810	hypothetical protein	LHSCAGGEESSGQC*LEK	5.56	17.69
676	TGGT1_313580	cytochrome b5 family heme/steroid binding domain-c	VFFEPSSASAC*APASSGPLC*GR	5.56	0.76
677	TGGT1_288360	tryptophanyl-tRNA synthetase (TrpRS2)	FGC*SSITPELISR	5.57	8.12
678	TGGT1_204050	subtilisin SUB1	VPPC*SSSPR	5.59	2.15
679	TGGT1_233460	SAG-related sequence SRS29B (SAG1)	SVIIGC*TGGSPEK	5.60	32.58
680	TGGT1_233110	IMP dehydrogenase (IMPDH)	VAQGVSGC*VVDK	5.61	3.41
681	TGGT1_313380	hypothetical protein	FSDSEGC*LDANQIR	5.61	0.76

682	TGGT1_215590	flavoprotein subunit of succinate dehydrogenase	TIADEC*K	5.62	7.43
683	TGGT1_228200	vacuolar (h+)-atpase g subunit protein	SC*ASQFPTTR	5.62	12.22
684	TGGT1_265330	putative cell-cycle-associated protein kinase GSK	LC*DFGSAK	5.63	13.95
685	TGGT1_233480	SAG-related sequence SRS29C (SRS2)	FTC*R	5.63	21.24
686	TGGT1_217910	DNA polymerase (pol2) superfamily protein	VHVSC*PGENSSLPER	5.63	49.74
687	TGGT1_205040	PGAP1 family protein	NTQETC*ETR	5.64	5.14
688	TGGT1_207640	isoleucyl-tRNA synthetase family protein	SHQTVC*R	5.64	10.16
689	TGGT1_314090	proteasome beta subunit	DC*VGIASDTR	5.64	0.00
690	TGGT1_289600	heat shock protein HSP29	SVPVTTTTSSFAASSC*GTTTGPTTSATDFAFDDLK	5.64	0.50
691	TGGT1_205470	putative translation elongation factor 2 family pr	NC*DPNAPLMMYVSK	5.65	3.50
692	TGGT1_259550	dihydropteroate synthase	TNSETSGDHIAC*SHR	5.65	3.75
693	TGGT1_287500	putative T complex chaperonin	PLC*TEGR	5.66	3.88
694	TGGT1_220860	DEAD/DEAH box helicase	GC*ATPDAR	5.66	4.38
695	TGGT1_288460	hypothetical protein	ALAEQLAPSC*SALETAYQQAVEQVR	5.69	0.12
696	TGGT1_268850	enolase 2	IEESLGSDC*QYAGAGFR	5.69	1.62
697	TGGT1_210960	putative replication factor C subunit 4	VC*DNPPPEAVR	5.69	16.40
698	TGGT1_278050	putative proteasome subunit alpha type 1	NLYDTDC*ITWSPQGR	5.69	19.88
699	TGGT1_209170	hypothetical protein	C*QGTQNDVK	5.69	22.37
700	TGGT1_280610	signal recognition particle receptor alpha subunit	C*LQVPLFER	5.71	20.45
701	TGGT1_270710	WW domain binding protein 11	YYNPALC*NAGIFR	5.71	8.67
702	TGGT1_209280	hypothetical protein	QTPVSSSSC*ATTR	5.71	25.76
703	TGGT1_292080	leucyl-tRNA synthetase	YFC*SFPYPYMNGK	5.72	36.99
704	TGGT1_247470	putative nucleolar protein	SQAAVGVC*DPALGK	5.72	2.97
705	TGGT1_291640	aspartate carbamoyltransferase	C*SFEAATLR	5.74	3.58

706	TGGT1_205470	putative translation elongation factor 2 family pr	GAGQIMPTC*R	5.74	1.23
707	TGGT1_273370	putative coatomer gamma 2-subunit protein	C*SQIITK	5.76	2.58
708	TGGT1_225050	putative adenosylhomocysteinase	FDNVYGC*R	5.77	0.49
709	TGGT1_293690	profilin PRF	DDHEEDTIGEDGNAC*GK	5.77	2.94
710	TGGT1_306960	phenylalanine--tRNA ligase, beta subunit protein	AGC*EHASAHAAEQLQR	5.77	8.33
711	TGGT1_298610	GYF domain-containing protein	SAQVC*IGGAATGHR	5.77	12.01
712	TGGT1_243540	WD domain, G-beta repeat-containing protein	NC*AGLASSAK	5.78	2.57
713	TGGT1_222020	phosphoglycerate kinase PGKII	C*AADAQTAVVPVTEIPEGWMGLDNGPQTTAR	5.78	20.80
714	TGGT1_206590	calcium-dependent protein kinase CDPK2A	C*VPSPGAGAAAAR	5.78	19.57
715	TGGT1_225050	putative adenosylhomocysteinase	VVIC*GFGDVGK	5.79	0.61
716	TGGT1_221620	putative beta-tubulin	SAVC*DIPPK	5.79	18.46
717	TGGT1_206690	glideosome-associated protein with multiple-membra	C*LTGEFR	5.80	9.27
718	TGGT1_258410	photosensitized INA-labeled protein PHIL1	GDC*QSEWSNAFVSR	5.84	0.12
719	TGGT1_221620	putative beta-tubulin	YLTAC*ALFR	5.84	4.48
720	TGGT1_266960	beta-tubulin	FWEVISDEHGIDPTGTYC*GDSDLQLER	5.84	7.51
721	TGGT1_272910	T-complex protein 1 delta subunit	TLPGVQQLC*VR	5.85	3.51
722	TGGT1_235160	hypothetical protein	YFVVEC*ASPAAAGIGGDSAR	5.85	14.75
723	TGGT1_233470	hypothetical protein	MMLSGPPVVTQPGEGVAASC*QSNSR	5.86	10.38
724	TGGT1_304760	RNA recognition motif-containing protein	LDHGPEVPC*VGR	5.86	16.41
725	TGGT1_214840	AP2 domain transcription factor AP2X-7	FC*GENPQSSLSTPQDVDAHGQSTEATPASSVHASGER	5.88	1.08
726	TGGT1_217890	putative alkyl hydroperoxide reductase/ Thiol spec	MLDALQHVEQYGEVC*PANWK	5.88	1.81

727	TGGT1_252290	putative importin alpha	LQDC*ANQDIYEK	5.88	4.69
728	TGGT1_269180	MIF4G domain-containing protein	SAANGPVSAQGSGNAC*AGLYSK	5.88	8.18
729	TGGT1_261400	hypothetical protein	TC*PVSGSPNNLLTLK	5.88	28.38
730	TGGT1_222400	hypothetical protein	HAC*SAGTQENVK	5.89	4.45
731	TGGT1_264650	phosphoacetylglucosamine mutase	TC*DEGDGQK	5.89	11.90
732	TGGT1_201780	microneme protein MIC2	C*VCPMGYQAR	5.89	17.66
733	TGGT1_220900	hypothetical protein	LC*YAPTEYSLEIEK	5.89	3.84
734	TGGT1_253430	putative asparagine synthetase	FQEC*IDQSGR	5.89	4.32
735	TGGT1_249390	glutamate/leucine/phenylalanine/valine dehydrogenase	SDSLWQDDELVSC*VLLK	5.89	5.76
736	TGGT1_299210	CTP synthase	SVAGVVC*PGGFGDR	5.89	7.44
737	TGGT1_277270	NTPase II	LNSLNFDLC*K	5.90	1.56
738	TGGT1_206470	pyruvate dehydrogenase complex subunit PDH-E3II	TC*VSHPTLSEAVK	5.90	4.68
739	TGGT1_205130	hypothetical protein	TTHLSPQESLC*SR	5.90	18.11
740	TGGT1_271350	bifunctional protein FolC subfamily protein	C*VTPVAVETGSEK	5.90	18.83
741	TGGT1_226250	DEAD (Asp-Glu-Ala-Asp) box polypeptide DDX3X	DLMAC*AQTGSGK	5.92	10.40
742	TGGT1_258470	hypothetical protein	TETTMSTTWC*ASEK	5.92	14.70
743	TGGT1_216900	cytokine induced apoptosis inhibitor 1 family prot	SALQAFAQAVC*R	5.92	40.13
744	TGGT1_224050	AP2 domain transcription factor AP2X-4	SGGIDC*VLSYLFEEDQEESPALSGQAEEAPTVK	5.93	8.95
745	TGGT1_264770	hypothetical protein	C*GADEADGQGNQR	5.93	23.51
746	TGGT1_205470	putative translation elongation factor 2 family pr	ETVSAPSHMTC*LSK	5.93	3.82
747	TGGT1_243710	t-complex protein beta subunit	LQEISFGC*EDDGLR	5.93	4.53
748	TGGT1_359490	elongation factor 1-alpha	AGMVLTFAPVGLTTEC*K	5.93	8.35
749	TGGT1_293570	putative translocation protein sec62	VMDVVLNC*TIR	5.95	39.37
750	TGGT1_260500	putative COPI associated protein	LC*ADVTGGR	5.95	44.60

751	TGGT1_202680	putative peptidase M16, alpha subunit	SSIFMNLEC*R	5.95	2.14
752	TGGT1_229950	putative 26S proteasome regulatory subunit 6b	VSAADIAAIC*QEAGMQAVR	5.96	8.67
753	TGGT1_227650	putative microtubule-associated protein RP/EB fami	TGGAC*ATHAQGSR	5.96	9.02
754	TGGT1_286590	microtubule associated protein SPM2	GPTAYSC*TALR	5.97	2.25
755	TGGT1_217740	3-ketoacyl-(acyl-carrier-protein) reductase	AIADALAEGGVSHLIC*VAR	5.97	46.59
756	TGGT1_270010	hypothetical protein	IAAPGSVTATENC*MQAPLPDPR	5.97	2.13
757	TGGT1_211250	hypothetical protein	GEAATSAASSSAGC*QGSTR	5.98	3.91
758	TGGT1_229950	putative 26S proteasome regulatory subunit 6b	TGC*SVALHR	5.99	4.14
759	TGGT1_235470	myosin A	C*IK	6.00	1.77
760	TGGT1_222380	importin-beta N-terminal domain-containing protein	ADC*LSQLILGTSR	6.00	5.89
761	TGGT1_231640	alveolin domain containing intermediate filament I	WTNEVYEVEC*IK	6.01	14.72
762	TGGT1_266960	beta-tubulin	SSVC*DIPPK	6.02	11.17
763	TGGT1_237560	iron-sulfur cluster protein ISCU	VHC*SLLAEDAVR	6.03	4.46
764	TGGT1_309752	putative succinate-Coenzyme A ligase, beta subunit	VLVC*DAK	6.05	1.17
765	TGGT1_270120	thioredoxin-like protein TLP1	VTDSEEDC*SVK	6.07	3.73
766	TGGT1_243910	Cof family hydrolase subfamily protein	C*VQPIPR	6.08	1.40
767	TGGT1_225790	PDI family protein	C*AQIVPVVR	6.08	19.77
768	TGGT1_233190	SKIP/SNW domain-containing protein	VVYC*TPGSAEGVDALR	6.09	5.69
769	TGGT1_313580	cytochrome b5 family heme/steroid binding domain-c	SAGLAVPPGC*GVGSQSR	6.09	2.09
770	TGGT1_232340	protein phosphatase 2C domain-containing protein	ITLYGGC*EDK	6.09	15.79
771	TGGT1_273760	heat shock protein HSP70	FEELC*MDYFR	6.10	15.30
772	TGGT1_205710	lysine-tRNA ligase	LLDALCGEYVEC*QAR	6.11	10.08

773	TGGT1_219790 B	pre-mRNA processing factor PRP3	PAGDGAHADAQC*SAPAAGSPVQK	6.12	1.73
774	TGGT1_212260	Sjogrens syndrome/scleroderma autoantigen 1 (Auto	C*GVLPASER	6.12	2.89
775	TGGT1_243200	hypothetical protein	LPAAC*QIDATAQGSNADSK	6.12	4.85
776	TGGT1_305340	corepressor complex CRC230	GC*ALETTTAQQSLEEEK	6.13	24.36
777	TGGT1_219850	prolyl-tRNA synthetase (ProRS)	GSVTPLAAMC*DEK	6.13	20.99
778	TGGT1_278870	myosin F	VSAQDPLGAC*ISGR	6.14	0.12
779	TGGT1_293180	NADP-specific glutamate dehydrogenase	C*QSEASEVADPEEVDAFVK	6.15	9.09
780	TGGT1_243930	hypothetical protein	EMCAPLSGSQPVC*R	6.15	15.53
781	TGGT1_275802	SRP72 RNA-binding domain-containing protein	LQSMSEDC*PEK	6.17	19.38
782	TGGT1_219850	prolyl-tRNA synthetase (ProRS)	WYEEC*LAVPVIK	6.18	19.68
783	TGGT1_277270	NTPase II	GFQQSC*SAGEVEVR	6.19	0.23
784	TGGT1_235470	myosin A	AC*GLLFLDAER	6.19	2.97
785	TGGT1_269190	glyceraldehyde-3-phosphate dehydrogenase GAPDH2	VPTLDVSVVDLTC*R	6.19	4.57
786	TGGT1_310490	ribosomal protein RPL27A	AAGGAC*VLTG	6.19	30.61
787	TGGT1_264780	UTP-glucose-1-phosphate uridylyltransferase	GC*VPSYVTLPFALEN	6.20	40.29
788	TGGT1_244390	coatomer epsilon subunit protein	C*GVTHVTGTLAQQEK	6.21	6.50
789	TGGT1_263180	myosin D	IVC*QDK	6.22	6.82
790	TGGT1_222270	hypothetical protein	SPALGAAPGC*TDTGNDAEATPLA MTLR	6.24	7.14
791	TGGT1_247550	heat shock protein HSP60	IQDALC*ATK	6.24	13.95
792	TGGT1_273090	cell division protein CDC48CY	LDEVGYDDIGGC*R	6.24	24.84
793	TGGT1_273090	cell division protein CDC48CY	AASPC*VLFFDELDSIGTQR	6.24	13.82
794	TGGT1_321620	dynamin-related protein DRPB	IQAPVIEC*LDR	6.25	7.24
795	TGGT1_301120	acetyl-CoA acetyltransferase	AGIEGSQVDQVIVGQALQAGC*GQ APQR	6.27	6.88
796	TGGT1_280600	putative histidyl-tRNA synthetase (HisRS)	AYFC*QHGTTLER	6.27	10.72

797	TGGT1_213030	hypothetical protein	QPQLSSGSGGYEDVSSSVYSQNDYG C*LNGVR	6.27	12.18
798	TGGT1_297500	T-complex protein 1 eta subunit	C*AQTTLNSK	6.28	1.58
799	TGGT1_226250	DEAD (Asp-Glu-Ala-Asp) box polypeptide DDX3X	FSC*LGAGGAR	6.28	3.15
800	TGGT1_228210	26S proteasome regulatory subunit	NVC*TEAGMFAIR	6.28	13.74
801	TGGT1_275650	hypothetical protein	DSIC*EPTSVK	6.28	7.66
802	TGGT1_289600	heat shock protein HSP29	LGQDC*NNIIK	6.29	3.94
803	TGGT1_311470	rhoptry neck protein RON5	GDDSHC*WATR	6.30	5.95
804	TGGT1_305980	pyruvate dehydrogenase complex subunit PDH-E3I	TAVVSGGDPGGTC*VNR	6.30	6.73
805	TGGT1_291140	CCR4-Not complex component, Not1 protein	C*VLEAIR	6.32	1.01
806	TGGT1_295360	hypothetical protein	C*AAPPLDAK	6.32	17.01
807	TGGT1_270530	ubiquitin fusion degradation protein UFD1CY	C*AEYDELVR	6.36	31.71
808	TGGT1_268835	hypothetical protein	ALWVSC*SNPPVWK	6.36	40.02
809	TGGT1_267390	DNA-directed RNA polymerase I RPAC1	LVC*AAEGPR	6.36	45.36
810	TGGT1_269190	glyceraldehyde-3-phosphate dehydrogenase GAPDH2	DLFFGAC*DATVSPDDLPSVPEALEK	6.37	25.53
811	TGGT1_280600	putative histidyl-tRNA synthetase (HisRS)	PGSVTPLPSESLESMC*PDAGLSR	6.38	1.89
812	TGGT1_290040	putative macrophage migration inhibitory factor	IAAALSAAC*ER	6.38	4.88
813	TGGT1_212310	vacuolar ATP synthetase	VDGLC*SSYK	6.41	36.18
814	TGGT1_218300	zinc finger (CCCH type) motif-containing protein	AGGNVPTSPVYEQLAAC*GAGVTT PVVNAADR	6.42	4.19
815	TGGT1_221970	hypothetical protein	LEC*LSAR	6.42	10.79
816	TGGT1_273370	putative coatomer gamma 2-subunit protein	PQFTPYDC*DK	6.43	7.70
817	TGGT1_212250	XPG N-terminal domain-containing protein	NC*MGIVMK	6.44	9.22

818	TGGT1_293180	NADP-specific glutamate dehydrogenase	VADC*VIDQGYI	6.45	1.65
819	TGGT1_280610	signal recognition particle receptor alpha subunit	SGSC*SATLSPYTLQWK	6.45	2.96
820	TGGT1_269190	glyceraldehyde-3-phosphate dehydrogenase GAPDH2	QQTPETFSSSAFAEPSPESTPGAC*PLSSNDGELSLQQAEALLR	6.45	33.33
821	TGGT1_231480	putative GCN1	NSVDAPSLALVC*PIAIR	6.46	9.31
822	TGGT1_294898	tetratricopeptide repeat-containing protein	HLPQVYAELPAGVC*TPESGDEEGEVK	6.46	1.31
823	TGGT1_312090	ribosomal protein RPL23	ISAAATAIC*	6.47	16.95
824	TGGT1_207620	pyridine nucleotide-disulfide oxidoreductase	IVMIC*EESVPPYDR	6.48	5.35
825	TGGT1_244690	hypothetical protein	GGASHPASAESVDAAAC*EASAGSSDLGDGSR	6.48	23.57
826	TGGT1_305520	ribosomal protein RPS2	C*AK	6.49	12.32
827	TGGT1_205440	CCT chaperonin gamma subunit	TLAQNC*GTNVVK	6.51	8.26
828	TGGT1_202370	putative T-complex protein 1, epsilon subunit (TCP	SNILAAC*AVADTLR	6.57	4.42
829	TGGT1_252290	putative importin alpha	EQQQLAENPFC*ELIEQADGITVIEK	6.58	2.58
830	TGGT1_266990	beta-COP	ALC*GLMTGLEK	6.58	23.00
831	TGGT1_305800	6-pyruvoyl tetrahydrobiopterin synthase	SGVLGLGPAPNSNC*C*LGGNATGDASR	6.60	16.50
832	TGGT1_272910	T-complex protein 1 delta subunit	SLHDALC*VVR	6.61	5.25
833	TGGT1_321640	cell division protein CDC48AP	AAAPC*VIFFDEMDSIAK	6.61	29.10
834	TGGT1_272910	T-complex protein 1 delta subunit	IDDIVMC*R	6.62	21.49
835	TGGT1_212260	Sjogrens syndrome/scleroderma autoantigen 1 (Auto	AVSFQATC*SVAGR	6.63	11.31
836	TGGT1_240890	6-phosphofructokinase	STSHC*LGSR	6.64	3.30
837	TGGT1_201760	hypothetical protein	AHAAANTSTC*PQR	6.64	7.24
838	TGGT1_203380	DnaJ domain-containing protein	TAGSGGGGAC*FASSTR	6.65	48.91
839	TGGT1_201760	hypothetical protein	SAGQHC*MLNASGGSER	6.65	19.57

840	TGGT1_207620	pyridine nucleotide-disulfide oxidoreductase	LLLC*TGSEAR	6.66	0.96
841	TGGT1_218780	putative phosphoserine aminotransferase	IYDAIEESDFFVC*PVAR	6.68	19.60
842	TGGT1_318310	transketolase	VTVLSLC*R	6.68	3.92
843	TGGT1_250330	hypothetical protein	EEC*PGVATAVGALTAAR	6.68	16.42
844	TGGT1_209210	hypothetical protein	LLGVC*GER	6.69	13.86
845	TGGT1_253440	putative cell-cycle-associated protein kinase SRPK	PDEEQFGSPC*SR	6.69	15.97
846	TGGT1_205440	CCT chaperonin gamma subunit	HASC*SGDSTK	6.69	4.86
847	TGGT1_210840	arginyl-tRNA synthetase family protein	FGDFQC*NSAMALFK	6.69	38.26
848	TGGT1_222160	aldehyde dehydrogenase	VAPALTC*GCTVVMK	6.70	18.91
849	TGGT1_294340	hypothetical protein	C*QESHAFPTK	6.70	15.83
850	TGGT1_245670	pyruvate dehydrogenase complex subunit PDH-E1Alpha	SC*LSPQQQHR	6.71	0.00
851	TGGT1_261410	protein-tyrosine-phosphatase	SPLPSSVSPQPVC*SR	6.71	18.97
852	TGGT1_262040	SAC3/GANP family protein	NTYDQEAC*LAVLK	6.74	19.42
853	TGGT1_227030	hypothetical protein	YFQGIC*AFLK	6.75	14.78
854	TGGT1_234280	AMP deaminase	C*GETGAGGGDNGATEK	6.75	45.46
855	TGGT1_316400 B	alpha tubulin TUBA1	C*GINYQPPTVVPGGDLAK	6.77	3.13
856	TGGT1_293590	putative 3-oxoacyl-acyl-carrier protein synthase I	VLETGIVPPTINQEETDPEC*DLNYV PNK	6.79	14.58
857	TGGT1_299970	tetratricopeptide repeat-containing protein	SEDGSTSLPSLPPLTPALLEQEGNSN C*PR	6.81	1.45
858	TGGT1_263070	CMGC kinase, CK2 family	MLIYDHC*QR	6.82	21.27
859	TGGT1_249390	glutamate/leucine/phenylalanine/valine dehydrogena	GSADLFNPC*GGR	6.83	7.98
860	TGGT1_253700	transporter, major facilitator family protein	STC*STTGGPR	6.84	4.03
861	TGGT1_295410	transcription initiation factor TFIID complex	THGYC*SVSR	6.86	16.90

862	TGGT1_213870	UBA/TS-N domain-containing protein	STYLSSAVDC*QDSAK	6.86	25.36
863	TGGT1_268200	RNA recognition motif-containing protein	HVFDEC*TR	6.87	12.67
864	TGGT1_225050	putative adenosylhomocysteinase	ELLFPAINVNDC*VTK	6.93	5.41
865	TGGT1_269700	NLI interacting factor family phosphatase	DSHHDSGSASVC*PTGDR	6.93	6.43
866	TGGT1_214940	MIC2-associated protein M2AP	LYASSGLTAINDDPSLGC*K	6.93	1.84
867	TGGT1_220100	phosphoribosylpyrophosphate synthetase	LGDALLFC*GNSNEPLAR	6.93	6.73
868	TGGT1_305820	SGS domain-containing protein	IAHLEC*SEADFSER	6.94	7.04
869	TGGT1_306195	hypothetical protein	QPPQSPTSSSSPSDQPC*SLAASSVTK	6.94	28.04
870	TGGT1_309752	putative succinate-Coenzyme A ligase, beta subunit	DC*TQIEVNPLVETHDGR	6.96	4.27
871	TGGT1_249390	glutamate/leucine/phenylalanine/valine dehydrogena	C*DLTDVLSAK	6.96	7.11
872	TGGT1_268850	enolase 2	VNQIGTVSESIEAC*QLAQK	6.97	5.79
873	TGGT1_257150	NOT2 / NOT3 / NOT5 family protein	MC*LEEMLYETSQR	6.97	31.37
874	TGGT1_294640	ribonucleoside-diphosphate reductase large chain	IEPVAPVC*R	6.99	4.76
875	TGGT1_235160	hypothetical protein	GTHASC*PAR	7.03	6.95
876	TGGT1_202530	aspartate-tRNA ligase	LIGGASEGGASC*FTLK	7.03	7.15
877	TGGT1_273760	heat shock protein HSP70	EVESVC*TPIITK	7.03	21.24
878	TGGT1_262380	putative elongation factor Tu	TLDDAQAGDQVGC*LLK	7.03	38.95
879	TGGT1_242570	hypothetical protein	SC*QPQDLDEMAPLPLLQLR	7.07	40.61
880	TGGT1_256990	glycyl-tRNA synthetase	C*GIADSGLR	7.11	14.23
881	TGGT1_301340	DnaJ domain-containing protein	AAEEGAAC*SR	7.13	12.10
882	TGGT1_288500	FAD Malate-dehydrogenase (MDH-FAD)	NNSQTIHC*GDIETNYTVEK	7.15	23.65
883	TGGT1_223540	importin-beta N-terminal domain-containing protein	AC*VLQVAK	7.16	17.49
884	TGGT1_318230	phosphoglycerate	GSIAFC*GAVAK	7.17	47.67

		kinase PGKI			
885	TGGT1_243710	t-complex protein beta subunit	GEAC*TIVLR	7.18	17.64
886	TGGT1_235690	hypothetical protein	LEHC*VVGNPQVGAEGAQR	7.20	1.67
887	TGGT1_269010	AP2 domain transcription factor AP2VIII-7	NAC*GSLSTGAAAAASDR	7.20	22.59
888	TGGT1_214140	hypothetical protein	SVGTPSVGPAGPPPVC*GDSEANAS GEGAGGGGPR	7.23	44.73
889	TGGT1_273760	heat shock protein HSP70	EPC*R	7.24	7.03
890	TGGT1_222160	aldehyde dehydrogenase	AC*TQGPLVDK	7.25	5.46
891	TGGT1_305810	hypothetical protein	PQDNGTVTVPGNSATESTPESPTC* VQVPPATGAR	7.26	37.52
892	TGGT1_297500	T-complex protein 1 eta subunit	ALEC*IPR	7.26	0.58
893	TGGT1_212260	Sjogrens syndrome/scleroderma autoantigen 1 (Auto	ASADATTPQVHC*TPIAGR	7.28	14.96
894	TGGT1_217740	3-ketoacyl-(acyl-carrier-protein) reductase	QQAAC*DEAAADLR	7.29	8.06
895	TGGT1_239630	cytidine and deoxycytidylate deaminase zinc-binding	DQPDTAC*AGAAPEDNAQMANK	7.32	13.14
896	TGGT1_273760	heat shock protein HSP70	LVDFC*VQDFK	7.36	13.64
897	TGGT1_266990	beta-COP	FSAAC*AGLDEAER	7.37	14.39
898	TGGT1_297500	T-complex protein 1 eta subunit	GQIISNINAC*QVIADIVR	7.38	27.59
899	TGGT1_202890	hypothetical protein	VPAEWLEGPC*GIPNGIASK	7.39	41.72
900	TGGT1_225690	hypothetical protein	LPC*VSSFAVK	7.45	6.26
901	TGGT1_282070	hypothetical protein	SC*SPGPSGPANGGVR	7.48	12.01
902	TGGT1_222160	aldehyde dehydrogenase	TIPVDNPDEVFC*YTR	7.48	26.28
903	TGGT1_275802	SRP72 RNA-binding domain-containing protein	QDVTAC*APR	7.48	9.08
904	TGGT1_203490	GNL3L/Grn1 GTPase	C*SSYALGAPALLR	7.49	7.65
905	TGGT1_207370	hypothetical protein	IC*GLGSIVAR	7.49	19.45
906	TGGT1_239820	D-3-phosphoglycerate dehydrogenase	C*DHIVNFVNVK	7.56	3.84
907	TGGT1_273090	cell division protein CDC48CY	TAGFSGADLAELC*QR	7.57	11.31
908	TGGT1_253430	putative asparagine	TASDC*QPLPSLFK	7.59	11.37

		synthetase			
909	TGGT1_209080	transport protein particle (trapp) component, bet3	DLLAGC*TYTGVPTTR	7.65	16.19
910	TGGT1_219520	histone arginine methyltransferase PRMT1	GPAGFSATVLPC*DEATK	7.70	2.30
911	TGGT1_283780	glucose-6-phosphate isomerase GPI	VIPAEFIGFC*K	7.73	35.24
912	TGGT1_223140	tRNA binding domain-containing protein	SGELHVNGDC*R	7.77	14.84
913	TGGT1_286590	microtubule associated protein SPM2	VAAYLQQQC*K	7.81	19.30
914	TGGT1_270510	asparaginyl-tRNA synthetase (NOB+tRNA synthase)	SFTPGHLEDQVPTSC*K	7.82	1.27
915	TGGT1_264830	hypothetical protein	LLQAFSAPGAPEASC*AEAASSPSAASSNSQR	7.82	3.07
916	TGGT1_203600	hypothetical protein	GEAAALGMEHSSC*GER	7.83	16.90
917	TGGT1_220100	phosphoribosylpyrophosphate synthetase	PEVAEC*PR	7.83	16.54
918	TGGT1_294640	ribonucleoside-diphosphate reductase large chain	VACGIHC*GDVEK	7.84	41.67
919	TGGT1_316400B	alpha tubulin TUBA1	AVC*MISNSTAIAEVFSR	7.85	47.86
920	TGGT1_232660	Hsp70 interacting protein HIP	EEASAAC*EAGNSER	7.99	40.00
921	TGGT1_280610	signal recognition particle receptor alpha subunit	MIDAIC*AFSR	8.01	8.83
922	TGGT1_313410	proteasome 26S regulatory subunit	IQAVVEQC*R	8.05	16.69
923	TGGT1_270510	asparaginyl-tRNA synthetase (NOB+tRNA synthase)	ETPVTVC*GWSR	8.11	3.58
924	TGGT1_268980	hypothetical protein	MQEADAC*SSTQK	8.11	14.82
925	TGGT1_272520	hypothetical protein	AC*FTNMPLQQDALPR	8.13	2.26
926	TGGT1_239530	alanine-glyoxylate aminotransferase	VVAAEGISTC*WK	8.19	23.93
927	TGGT1_237890	calcium-dependent protein kinase CDPK4	VALPSPC*QALLTPSGAEAEAQSPSR	8.24	30.89
928	TGGT1_233340	hypothetical protein	VC*FFNPAVDR	8.26	17.39
929	TGGT1_205440	CCT chaperonin gamma subunit	QVVDAC*LNTK	8.28	12.90
930	TGGT1_311230	hypothetical protein	PGEAETSC*R	8.28	9.14
931	TGGT1_299070	pyruvate kinase PyKII	C*ASTGTSALR	8.30	21.91
932	TGGT1_277270	NTPase II	C*MIDEYGVK	8.31	20.59

933	TGGT1_293390	putative cytochrome C-type heme lyase	SLPVSAPSSC*AASCAPGAASTC*TG SPSGR	8.33	26.42
934	TGGT1_205470	putative translation elongation factor 2 family pr	C*ITIK	8.33	49.74
935	TGGT1_217510	hypothetical protein	ANTSPSTPAAPISDSVVYC*EPLQTA EPQPLLDK	8.37	6.85
936	TGGT1_305490	programmed cell death protein 2, c-terminal domain	AC*EISQLGGK	8.39	5.99
937	TGGT1_286600	hypothetical protein	GSTGC*PAGQTPLYPAVR	8.41	13.54
938	TGGT1_230850	hypothetical protein	TYC*ADLTPVQLLPMR	8.67	1.63
939	TGGT1_310030	putative cyclase-associated protein	VNSVIIDNC*DNLR	8.68	27.31
940	TGGT1_238050	nuclease and tudor domain-containing protein	IQSGSLGLTEC*GAQLSQAMR	8.68	29.16
941	TGGT1_243410	tetratricopeptide repeat-containing protein	TEENTASPSPAC*GR	8.70	3.74
942	TGGT1_236110	putative autophagy-related protein 3 atg3	LNAEC*GHELR	8.75	22.72
943	TGGT1_270510	asparaginyl-tRNA synthetase (NOB+tRNA synthase)	QAIPVFGC*GSTR	8.86	2.55
944	TGGT1_225000	hypothetical protein	DPGC*PYTASGPK	8.98	8.19
945	TGGT1_292080	leucyl-tRNA synthetase	AEQDC*GENGEK	9.04	30.98
946	TGGT1_288380	heat shock protein HSP90	ITDSPC*VLVTSEYGWSANMER	9.04	48.03
947	TGGT1_252290	putative importin alpha	EQAVWALGNIAGDSPQC*R	9.12	25.74
948	TGGT1_205710	lysine-tRNA ligase	ELC*NAYTELNDPVR	9.14	8.44
949	TGGT1_318410	putative TCP-1 chaperonin	C*LEVLDQLK	9.14	5.19
950	TGGT1_275350	TBC domain-containing protein	LSAAC*GTSPLGQGSSSSPSYVPEK	9.20	8.23
951	TGGT1_246720	hypothetical protein	C*VYTPELTDAIR	9.28	15.78
952	TGGT1_258050	actin like protein ALP2a	ALLSC*FAVGR	9.37	11.77
953	TGGT1_305980	pyruvate dehydrogenase complex subunit PDH-E3I	IYPDAC*LIATGR	9.38	5.13
954	TGGT1_204400	putative ATPase synthase subunit alpha	HC*VIIYDDLSK	9.45	3.67
955	TGGT1_309752	putative succinate-Coenzyme A ligase, beta subunit	ENGYQGGVQVC*ESPR	9.84	44.07
956	TGGT1_266990	beta-COP	LQEC*VQR	9.90	12.71

957	TGGT1_214840	AP2 domain transcription factor AP2X-7	FGAPQGTLAEGTSSSC*LFSTAGTPSR	10.10	41.68
958	TGGT1_259690	orotidine-5-phosphate decarboxylase/orotate	VC*ALIPDDVPILLDAK	10.12	43.27
959	TGGT1_251590	hypothetical protein	PGDAGGC*VAAR	10.21	20.02
960	TGGT1_244460	hypothetical protein	GETSAC*ADSDQAR	10.23	35.94
961	TGGT1_245670	pyruvate dehydrogenase complex subunit PDH-E1Alpha	MVEDAC*AR	10.37	6.89
962	TGGT1_286750	MA3 domain-containing protein	VWTGTDPDNAEAC*EFK	10.37	5.32
963	TGGT1_311230	hypothetical protein	VPAETGVSSC*VFR	10.45	31.07
964	TGGT1_249390	glutamate/leucine/phenylalanine/valine dehydrogena	DIQC*LDSPDAPPILLK	10.83	26.06
965	TGGT1_219250	acetyltransferase, GNAT family protein	GGPIDSPASLHAAAGSEATAC*SR	10.85	36.63
966	TGGT1_244460	hypothetical protein	DLPQTGC*FLALDTPR	11.55	14.20
967	TGGT1_293590	putative 3-oxoacyl-acyl-carrier protein synthase I	C*LENAIADANIDK	11.73	12.85
968	TGGT1_311230	hypothetical protein	VSMSPAGVSVSPAGVATC*PTGSTGR	11.83	27.57
969	TGGT1_277000	putative transport protein Sec24	AVVQSVQGEHLC*NAMR	12.31	1.09
970	TGGT1_311400	WD domain, G-beta repeat-containing protein	TAVSFC*DPTHR	12.95	31.23
971	TGGT1_215040	HEAT repeat-containing protein	C*LSAFTSR	14.82	29.39
972	TGGT1_231010	general transcription factor IIE polypeptide 1 GTF	APSASEASSGHSQAVDC*VAAAHPAK	14.94	47.90
973	TGGT1_239630	cytidine and deoxycytidylate deaminase zinc-binding	AYC*PYSEFPVGAAVLTDK	14.98	47.46
974	TGGT1_202750	3 exoribonuclease family, domain 1 domain-contain	EAAGEC*FPVEDIPIIVTVGEIANR	15.20	44.72
975	TGGT1_214840	AP2 domain transcription factor AP2X-7	DGNMVVLGNPIAGTPGC*LLSGSASGDGTTSAEK	15.27	43.81
976	TGGT1_228120	hypothetical protein	SEFELLC*AADPLAVAAQEAAR	15.64	39.48
977	TGGT1_246040	MIF4G domain-containing protein	VFQSLC*EALQNAR	15.87	36.86

978	TGGT1_316490	hypothetical protein	SFATYGANLNC*GLNLASQR	16.22	33.01
979	TGGT1_297230	Vps53 family protein	SSNPFATGATC*AGEQSSFSPFVED ADEALLDSEQR	16.31	32.05
980	TGGT1_265530	RNA recognition motif-containing protein	GFC*FVTMGSEEAK	16.32	21.58
981	TGGT1_258980	hypothetical protein	VLLDDVGLSYIC*ATAER	16.42	30.83
982	TGGT1_289690	glyceraldehyde-3-phosphate dehydrogenase GAPDH1	SSDVIVSNASC*TTNC*LAPLAK	16.58	5.97
983	TGGT1_247760	AMP-binding enzyme domain-containing protein	PAC*ADGEVPATGQK	16.65	28.45
984	TGGT1_211730	histone lysine methyltransferase SET8	TGQDDGAFC*LETWLAGAGDDAA GGER	16.75	27.44
985	TGGT1_280600	putative histidyl-tRNA synthetase (HisRS)	ESFTDVLVC*SVGDNMLK	16.81	26.89
986	TGGT1_247300	hypothetical protein	TAQHTLDLC*GAVAEEETAK	16.89	26.09
987	TGGT1_222160	aldehyde dehydrogenase	AGNVFINC*YNTTDIAAPFGGFK	16.92	25.74
988	TGGT1_201780	microneme protein MIC2	NVEYEPCSYPAC*GASC*TYVWSD WNK	17.52	20.02
989	TGGT1_230850	hypothetical protein	EVDHFTAVC*TVPGPAYDLR	17.80	17.52
990	TGGT1_230420	sarco/endoplasmic reticulum Ca2+-ATPase	LGC*TDSTLNAR	17.82	17.35
991	TGGT1_214140	hypothetical protein	TPLSLEC*LAR	17.96	16.06
992	TGGT1_232710	ribosomal protein RPS3A	LC*C*EDIQGR	18.00	15.71
993	TGGT1_244200	putative 2-oxoglutarate dehydrogenase e1 component	SQMFENFC*GQK	18.88	8.39
994	TGGT1_257960	GDP-D-mannose pyrophosphorylase	IGEDC*LIGPDVTIDR	19.35	4.75
995	TGGT1_236530	DUF298 domain-containing protein	SGVC*TVAALR	19.80	1.46
996	TGGT1_312660	hypothetical protein	GAAGC*FVPASSPATSQATASDGAA SSR	20.00	0.04
997	TGGT1_243440	histone lysine acetyltransferase GCN5-B	ALELSPVC*FSPAYAASLR	20.00	0.00
998	TGGT1_232710	ribosomal protein RPS3A	C*QLR	20.00	0.00
999	TGGT1_239820	D-3-phosphoglycerate dehydrogenase	DAC*IINASR	20.00	0.00

1000	TGGT1_225870	hypothetical protein	DC*LMQMPGSR	20.00	0.00
1001	TGGT1_213900	regulator of chromosome condensation RCC1	DEALVSPQGGEC*ALADK	20.00	0.00
1002	TGGT1_233890	hypothetical protein	DTTEQPLSPAVDTSSSSC*R	20.00	0.00
1003	TGGT1_203610	putative 3-5 exoribonuclease csl4	EGGQLQPVTC*TLMR	20.00	0.00
1004	TGGT1_306660	RNA pseudouridine synthase superfamily protein	ELLGLGDSGVVPFPTC*GTLASR	20.00	0.00
1005	TGGT1_292080	leucyl-tRNA synthetase	GFYDGVLLVGPC*AGQK	20.00	0.00
1006	TGGT1_244650	putative eukaryotic initiation factor-5	GGTAMTSFPYC*LQK	20.00	0.00
1007	TGGT1_262935	hypothetical protein	GIADHAAPC*DVEQGK	20.00	0.00
1008	TGGT1_240450	Maf family protein	ILEGQGC*PC*GVISPDIDEK	20.00	0.00
1009	TGGT1_289300	methionyl-tRNA synthetase	LC*VSNDQYIR	20.00	0.00
1010	TGGT1_307570	putative glycerol-3-phosphate dehydrogenase (gpdh)	LNIVEC*AALSGANVANDVAR	20.00	0.00
1011	TGGT1_263420	ubiquitin-specific protease USP4	PSPEAAC*HR	20.00	0.00
1012	TGGT1_243460	hypothetical protein	SGAC*GGGNGPDGVATGPGEAR	20.00	0.00
1013	TGGT1_216220	AP2 domain transcription factor AP2XI-5	SLFVNGGC*PGGYGSGGVDPTQR	20.00	0.00
1014	TGGT1_201780	microneme protein MIC2	SMC*GC*SGTSDDDSPC*PLYLR	20.00	0.00
1015	TGGT1_203760	hypothetical protein	SPSGSAQC*AGDR	20.00	0.00
1016	TGGT1_226910	Amylo-alpha-1,6-glucosidase	SQLPAGVPEVAPLC*MK	20.00	0.00
1017	TGGT1_267580	cyclin2 related protein	SSTVC*AAASSR	20.00	0.00
1018	TGGT1_296010	phosphatidylinositol 3- and 4-kinase	WSATSSSSVPSAAATSTAC*ASR	20.00	0.00

Table A5-2 Highly reactive cysteines identified in T. gondii. Shown are final isoTOP-ABPP ratios for 102 peptides with R values < 3, representing 130 modified cysteines. Labeled cysteines are indicated by asterisks (*) within the grouped peptide sequence

Index	*Toxo*DB ID	Uniprot ID	*Toxo*DB annotation	*R* value	peptide sequence	Labeled cysteine position(s)
1	TGGT1_268835	S7V493	hypothetical protein	0.61	TPAPC*EGAEK	240
2	TGGT1_258970	S7UZ14	hypothetical protein	0.68	SPAAGC*HER	2645
3	TGGT1_249630	S7V075	glutathione S-transferase, N-terminal domain-containing	0.77	ATTVPTLFQYTVC*PYC*TATR	124, 127
4	TGGT1_311030	B6KAG9	hypothetical protein	0.83	GVGSSSTASC*SSAR	26
5	TGGT1_222160	S8FE58	aldehyde dehydrogenase	0.86	AAMTAFYGLFPNSGQC*C*VASSR	290, 291
6	TGGT1_215775	A0A125YM30	rhoptry protein ROP8	0.93	VVSTVC*R	456
7	TGGT1_290890	S7W4F8	putative carbonyl reductase 1	0.95	IISVASMC*GK	251
8	TGGT1_218200	S7WA78	UDP-sugar pyrophospharylase	1.06	VVLAPSWGISQDC*MR	522
9	TGGT1_233170	S7WJC3	hypothetical protein	1.07	VIDYLLPAPC*SR	133
10	TGGT1_300140	B9Q2T3	putative elongation factor 1-gamma	1.11	C*ELDLLPEPTMDLNEWK	236
11	TGGT1_217900	S7V1B7	hypothetical protein	1.12	YC*DSVANTTC*AR	90, 98
12	TGGT1_223070	S7VTV4	hypothetical protein	1.14	VDCMC*QLGIEYIR	95
13	TGGT1_286630	B6KN66	redoxin domain-containing protein	1.36	MIPDGNGC*FTSK	221
14	TGGT1_317720	S7UGQ9	putative eukaryotic translation initiation factor	1.37	AC*DFTFHVQQR	69
15	TGGT1_290670	S7UP88	leucyl aminopeptidase LAP	1.49	TVAVVLPTC*QK	384
16	TGGT1_226430	S8F0X6	reticulon protein	1.63	MC*AAPVC*AC*VSPYIQEAQDFC*SR	162, 167, 169, 181
17	TGGT1_248320	B6KH56	carrier superfamily protein	1.66	TNVQAGC*QQIEPHAR	285
18	TGGT1_266450	B9Q1Y2	lysine decarboxylase family protein	1.67	MLC*EYLEAR	52
19	TGGT1_263300	B9Q0Q9	eukaryotic porin protein	1.75	VC*DYVSATIGSQIDVSKPSNPDAVK	257
20	TGGT1_230450	B6KJD3	bifunctional GMP synthase/glutamine amidotransferase	1.78	C*VDGEEAEGEK	155
21	TGGT1_	S7UTI6	apicoplast-associated	1.79	TAVSC*PAAK	309

	312110		thioredoxin family protein A			
22	TGGT1_233000	S7V342	KOW motif domain-containing protein	1.79	ILLPSNSALC*ATAAQLASK	664
23	TGGT1_263660	S7UXS3	hypothetical protein	1.81	C*AFLDNPVYK	210
24	TGGT1_272030B	S7V3S1	kelch repeat-containing protein	1.82	GPC*GEETAPR	157/177/207
25	TGGT1_297420	S7UKY2	putative beta-tubulin cofactor D	1.88	SHSGGNEIQC*PVER	2006
26	TGGT1_321420	S8FEK9	kelch repeat-containing protein	1.91	ATPVC*TFAYLGQAQTENR	395
27	TGGT1_278870	Q286V9	myosin F	1.91	LVC*ATSGR	1746
28	TGGT1_236570	S8G4S4	lysine decarboxylase family protein	1.91	IEWMC*PYWQK	141
29	TGGT1_270240	S8F4K6	MAG1 protein (MAG1)	1.95	AC*QDMAPIEEALC*HK	297, 308
30	TGGT1_230070	S7WBE0	BolA family protein	1.97	SC*GCGAAYDCVIVSDAFDGK	34
31	TGGT1_258070	S7UYW4	hypothetical protein	1.98	AAGC*PDEDASAPLLALPQR	587
32	TGGT1_251620	B6KHT0	putative flap structure-specific endonuclease 1	2.01	DGNSFGNFTNDAGDC*TSHIAGMLNR	62
33	TGGT1_271888	A0A125YR36	putative 3-ketoacyl-CoA reductase	2.05	MDLFSC*GC*IK	6, 8
34	TGGT1_248100	S7V159	synaptobrevin protein	2.13	GEASPSGEGAC*AGSSR	16
35	TGGT1_256970	B6KAW0	putative vacuolar ATP synthase subunit A	2.14	TC*ISQALSK	257
36	TGGT1_284560	B9PT01	ribosomal protein RPL9	2.18	VEMWYGTC*TDLSC*IR	63, 68
37	TGGT1_236570	S7W5X6	lysine decarboxylase family protein	2.19	EIPAPVGGSGHQYSAGDVAAVTDLSEPC*PVAIC*TGGGPGMMEAGNSGAASVAGGR	200, 205
38	TGGT1_242330	B9PPE8	ribosomal protein RPS5	2.25	AMC*PIVER	54
39	TGGT1_215470	B9PZT4	ribosomal protein RPL10A	2.26	VC*VMGDAVHC*EQAK	65, 73
40	TGGT1_215740	S8G472	putative notchless	2.26	LWC*LNTETPLR	171
41	TGGT1_306960	S8EZ50	phenylalanine--tRNA ligase, beta subunit protein	2.28	SYMLTGDALNC*LSEK	407
42	TGGT1_226710	S8F0Z6	hypothetical protein	2.28	REPPLC*SLEGASADAAVQMVK	280
43	TGGT1_300270	S8ET39	hypothetical protein	2.29	C*PENIWVFR	94

44	TGGT1_202820	S7UV33	ubiquitin-conjugating enzyme subfamily protein	2.36	DC*PSGC*SVGLDDEAGGDFFVWR	20, 24
45	TGGT1_232060	B6KJQ4	hypothetical protein	2.37	VGEC*AGFAPR	286
46	TGGT1_306000	S8EVH8	AP2 domain transcription factor AP2IX-8	2.38	ASWVC*ATSGK	502
47	TGGT1_260260	B9PKQ4	ribosomal protein RPP1	2.38	ALQGQNIADLISNAGAC*AAAAPAAAAPVAGGDAGAAPAK	137
48	TGGT1_216450	B6KT24	peptidase, T1 family protein	2.39	GELYCVETSGC*C*SK	166, 167
49	TGGT1_237820	B9Q3R2	IMC sub-compartment protein ISP2	2.42	LTQGNSAIELSC*ER	80
50	TGGT1_312820	S7W8D0	hypothetical protein	2.43	C*PAEPWCLYSVVR	111
51	TGGT1_263530	S7UXE3	putative chaperonin	2.46	TGEFIPPC*VQVGQTVVVPEYGGMK	89
52	TGGT1_236970	S8EW83	SWI2/SNF2-containing PHD finger protein	2.46	GVDSAVQSGFAGAC*TANAPFAGPGFK	2400
53	TGGT1_217555	S7V1I5	hypothetical protein	2.46	VGGCPFAGMMSTGVC*PVTGK	101
54	TGGT1_226430	A0A125YHI4	reticulon protein	2.47	C*YENVNC*VLESVR	99, 105
55	TGGT1_291640	B6KKZ3	aspartate carbamoyltransferase	2.47	DAAAC*PGTLSETSVQNGC*SEGAWCQLLQGK	73, 86
56	TGGT1_257680	Q95UJ7	myosin light chain MLC1	2.48	C*PVC*YQK	8, 11
57	TGGT1_258820	B6KBB2	hypothetical protein	2.55	GHGCC*SQNAGSSEEPQQQAEGSHYAK	102
58	TGGT1_202870	S7W3P9	SAP domain-containing protein	2.55	AAC*GAPAGSTEK	236
59	TGGT1_229210	B9PHV0	putative small nuclear ribonucleoprotein polypeptide	2.56	SLILC*NNR	71
60	TGGT1_226960	B9Q857	phosphofructokinase PFKII	2.57	SEACGAAAC*R	1222
61	TGGT1_310640	Q2HXR1	phosphorylase family protein	2.58	GLNCSAETFFAC*QGR	198
62	TGGT1_265870B	S7VW35	pantoate-beta-alanine ligase	2.58	SAGVAAPETCC*TR	77
63	TGGT1_309120	A0A125YTR1	ribosomal protein RPL4	2.63	NIPGVELC*K	231
64	TGGT1_256970	S7WF08	putative vacuolar ATP synthase subunit A	2.66	VLDSLFPTVQGGTCAIPGAFGC*GK	253
65	TGGT1_306030	B9PZA9	glutathione s-transferase, n-terminal domain containing	2.67	LYEFEGC*PFCR	94

66	TGGT1_244390	S7VTV8	coatomer epsilon subunit protein	2.67	AFQQAPQDC*DTLVNLIC*C*CR	246, 254, 255
67	TGGT1_219850	S7V2A6	prolyl-tRNA synthetase (ProRS)	2.68	LNQWC*SVVR	466
68	TGGT1_227420	S7WDA3	4-hydroxy-3-methylbut-2-enyl diphosphate reductase	2.70	QLQVVDATC*PLVTK	478
69	TGGT1_209950	B6KPH1	putative thioredoxin	2.73	DGC*SECQSLLDGEFNTLAK DGCSEC*QSLLDGEFNTLAK	65, 68
70	TGGT1_255420	B6KAN6	hypothetical protein	2.73	C*MLLENFEATGAPQVR	189
71	TGGT1_214290	S8EW18	DJ-1 family protein	2.73	AVAYPC*FMDQFPADMR	198
72	TGGT1_269190	S7WDK9	glyceraldehyde-3-phosphate dehydrogenase GAPDH2	2.74	VVSC*ASC*TTNGLAPLVK	795, 797
73	TGGT1_266460	B9Q1Y1	putative small ubiquitin family modifier	2.77	LMQAYC*NR	45
74	TGGT1_233140	B6KK00	putative deoxyuridine 5-triphosphate nucleotidohy	2.77	GEGGFGSTTC*PAGEPEMK	154
75	TGGT1_313400	S7W1G5	DnaJ domain-containing protein	2.78	C*YYEVLGVAK	10
76	TGGT1_226970	B9PMU7	ribosomal protein RPS11	2.78	C*PFTGNVSIR	60
77	TGGT1_249250	B9PR43	ribosomal protein RPL35A	2.79	VNQYPSC*SLLQLEGVNDR	32
78	TGGT1_272660	B1NF34	hypothetical protein	2.80	AGTAGDGETC*TETPVISFLPVSGPEHPAGGSQR	45
79	TGGT1_288650	S8GHD8	dense granule protein GRA12	2.81	GLDC*MLGSR	289
80	TGGT1_312090	B9PK53	ribosomal protein RPL23	2.82	VTLGLPVGALINC*C*DNSGAK	27, 28
81	TGGT1_249900	B9PRA8	putative adenine nucleotide translocator	2.82	GEQEIQYTGTADC*WK	276
82	TGGT1_264080	O77470	acyl carrier protein ACP	2.82	YGTC*PNMSSGVCATPSTASLGTLGQPAGTVAR	45
83	TGGT1_300000	B6KV50	ribosomal protein RPL18	2.82	AGGEC*LTFDQLALR	119
84	TGGT1_232300	S7V3B5	ribosomal protein RPS3	2.83	GLC*AMAQAESLR	119
85	TGGT1_290890	S7W4F8	putative carbonyl reductase 1	2.83	GMFVACCCPGWC*R	344
86	TGGT1_313270	S7USI3	hypothetical protein	2.84	APAAPGAGGFC*DDPSRPASSGGR	1229
87	TGGT1_299200	B9Q377	putative Bet3 transport protein	2.85	TGMGGCDC*FR	76
88	TGGT1_220240	S8GRB2	hypothetical protein	2.87	VPADTQSPCC*GAK	250

89	TGGT1_238010	S7W653	ribosomal protein RPL23A	2.87	C*YEAATC*TFPK	68, 74
90	TGGT1_243570	B9PP49	ribosomal protein RPS26	2.87	QCYC*VSC*AIHSR	74, 77
91	TGGT1_228210	S8G6I9	26S proteasome regulatory subunit	2.91	AMASNMNC*NFMK	203
92	TGGT1_217030	B6KSV6	hypothetical protein	2.93	SGAASGEC*SAHANEK	153
93	TGGT1_266990	S8GGL3	beta-COP	2.95	WTC*ELAFR	945
94	TGGT1_263420	S7UXP7	ubiquitin-specific protease USP4	2.95	LLVPSGFC*AQEAQK	887
95	TGGT1_310040	S8GCV6	putative ubiquitin conjugating enzyme E2	2.96	IYC*VSINC*GPSYPDEPPEVC*FR	121, 126, 138
96	TGGT1_306960	S7USY3	phenylalanine--tRNA ligase, beta subunit protein	2.97	C*QGEASLQNGSASMNGWVFPR	293
97	TGGT1_243730	S8F3X8	rhoptry protein ROP9	2.97	ILLLDDDRANC*VNFCR	318
98	TGGT1_223620	B9PLX3	putative SNARE protein	2.97	MEC*IFEGEK	81
99	TGGT1_233110	B6KJZ7	IMP dehydrogenase (IMPDH)	2.97	IGMGSGSIC*TTQVVC*AVGR	315, 321
100	TGGT1_276110	S8F7T0	cytochrome b5 family heme/steroid binding domain-c	2.98	NC*C*TSATATK	105, 106
101	TGGT1_248390	B6KH63	ribosomal protein RPL26	2.98	IMTAPLC*K	35
102	TGGT1_207460B	Q1JSY8	Rab5B protein	2.99	GPANCC*IAVAANK	146